

## REPORT DOCUMENTATION PAGE

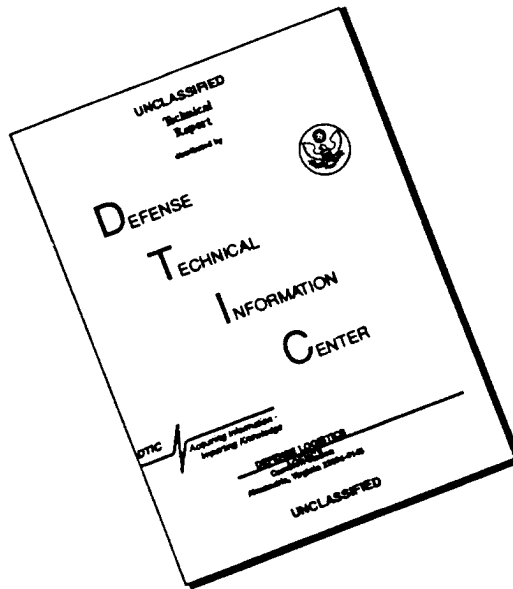
Form Approved  
OMB No. 0704-0188

Public reporting burden for this collection of information is estimated to average 1 hour per response, including the time for reviewing instructions, searching existing data sources, gathering and maintaining the data needed, and completing and reviewing the collection of information. Send comments regarding this burden estimate or any other aspect of the collection of information, including suggestions for reducing this burden, to Washington Headquarters Services, Directorate for Information Operations and Reports, 1215 Jefferson Davis Highway, Suite 1204, Arlington, VA 22202-4302, and to the Office of Management and Budget, Paperwork Reduction Project (0704-0188), Washington, DC 20503.

1. AGENCY USE ONLY (Leave blank)		2. REPORT DATE March 1996	3. REPORT TYPE AND DATES COVERED Final Report June 1992-October 1995
4. TITLE AND SUBTITLE Undrained Creep Behavior of Clayey Soils			5. FUNDING NUMBERS G F49620-92 J-0294
6. AUTHOR(S) Miguel Picornell & Soheil Nazarian			AFOSR-TR-96  0298
7. PERFORMING ORGANIZATION NAME(S) AND ADDRESS(ES) Center for Geotechnical and Highway Materials Research University of Texas at El Paso			
8. SPONSORING/MONITORING AGENCY NAME(S) AND ADDRESS(ES) Air Force Office of Scientific Research Bldg. 410 Bolling AFB, DC 20032-6448  NA			9. SPONSORING/MONITORING AGENCY REPORT NUMBER  92-J-0294
10. SUPPLEMENTARY NOTES			
11a. DISTRIBUTION/AVAILABILITY STATEMENT  Unlimited		11b. DISTRIBUTION STATEMENT  Approved for public release, distribution unlimited  19960625 203	
12. ABSTRACT (Maximum 200 words)  Clayey soils were used to prepare specimens possessing controlled pore solution chemistry. Specimens were consolidated and equilibrated at four different soil suction levels. Various specimens were subjected to creep/recovery tests under drained and undrained conditions in conventional triaxial cells. The results were used to make comparisons with the behaviors predicted by a nonlinear viscoelastic model, based on power law, previously recommended by the parent project. Specimens of identical characteristics were subjected to high strain rates using a dynamic triaxial test system. Each test consisted of a series of stress controlled pulses of 50 msec duration. The pulse involved a ramp-up to a peak deviatoric stress and a ramp-down to zero. The peak stress was increased for the successive pulses. The response of the specimen, and the strain time history, was recorded. With the power laws developed and fitted to the creep/recovery data, in conjunction with the modified superposition principle, the response of specimens during dynamic testing has been predicted. Closer predictions were obtained by using the model developed for undrained testing conditions.			
13. SUBJECT TERMS Unsaturated Clayey Soils, Creep, Soil Suction, High Strain Rates			14. NUMBER OF PAGES 332
			15. PRICE CODE
16. SECURITY CLASSIFICATION OF REPORT Unclassified	17. SECURITY CLASSIFICATION OF THIS PAGE Unclassified	18. SECURITY CLASSIFICATION OF ABSTRACT Unclassified	19. LIMITATION OF ABSTRACT UL

DTIC QUALITY INSPECTED 1

# DISCLAIMER NOTICE



THIS DOCUMENT IS BEST QUALITY AVAILABLE. THE COPY FURNISHED TO DTIC CONTAINED A SIGNIFICANT NUMBER OF PAGES WHICH DO NOT REPRODUCE LEGIBLY.

AIR FORCE OF THE UNITED STATES (AFSC)  
SERVICE :  
THIS IS  
PHOTOGRAPH  
1970-  
1980-  
1990-  
2000-  
2010-  
2020-  
2030-  
2040-  
2050-  
2060-  
2070-  
2080-  
2090-  
2100-  
2110-  
2120-  
2130-  
2140-  
2150-  
2160-  
2170-  
2180-  
2190-  
2200-  
2210-  
2220-  
2230-  
2240-  
2250-  
2260-  
2270-  
2280-  
2290-  
2300-  
2310-  
2320-  
2330-  
2340-  
2350-  
2360-  
2370-  
2380-  
2390-  
2400-  
2410-  
2420-  
2430-  
2440-  
2450-  
2460-  
2470-  
2480-  
2490-  
2500-  
2510-  
2520-  
2530-  
2540-  
2550-  
2560-  
2570-  
2580-  
2590-  
2600-  
2610-  
2620-  
2630-  
2640-  
2650-  
2660-  
2670-  
2680-  
2690-  
2700-  
2710-  
2720-  
2730-  
2740-  
2750-  
2760-  
2770-  
2780-  
2790-  
2800-  
2810-  
2820-  
2830-  
2840-  
2850-  
2860-  
2870-  
2880-  
2890-  
2900-  
2910-  
2920-  
2930-  
2940-  
2950-  
2960-  
2970-  
2980-  
2990-  
3000-  
3010-  
3020-  
3030-  
3040-  
3050-  
3060-  
3070-  
3080-  
3090-  
3100-  
3110-  
3120-  
3130-  
3140-  
3150-  
3160-  
3170-  
3180-  
3190-  
3200-  
3210-  
3220-  
3230-  
3240-  
3250-  
3260-  
3270-  
3280-  
3290-  
3300-  
3310-  
3320-  
3330-  
3340-  
3350-  
3360-  
3370-  
3380-  
3390-  
3400-  
3410-  
3420-  
3430-  
3440-  
3450-  
3460-  
3470-  
3480-  
3490-  
3500-  
3510-  
3520-  
3530-  
3540-  
3550-  
3560-  
3570-  
3580-  
3590-  
3600-  
3610-  
3620-  
3630-  
3640-  
3650-  
3660-  
3670-  
3680-  
3690-  
3700-  
3710-  
3720-  
3730-  
3740-  
3750-  
3760-  
3770-  
3780-  
3790-  
3800-  
3810-  
3820-  
3830-  
3840-  
3850-  
3860-  
3870-  
3880-  
3890-  
3900-  
3910-  
3920-  
3930-  
3940-  
3950-  
3960-  
3970-  
3980-  
3990-  
4000-  
4010-  
4020-  
4030-  
4040-  
4050-  
4060-  
4070-  
4080-  
4090-  
4100-  
4110-  
4120-  
4130-  
4140-  
4150-  
4160-  
4170-  
4180-  
4190-  
4200-  
4210-  
4220-  
4230-  
4240-  
4250-  
4260-  
4270-  
4280-  
4290-  
4300-  
4310-  
4320-  
4330-  
4340-  
4350-  
4360-  
4370-  
4380-  
4390-  
4400-  
4410-  
4420-  
4430-  
4440-  
4450-  
4460-  
4470-  
4480-  
4490-  
4500-  
4510-  
4520-  
4530-  
4540-  
4550-  
4560-  
4570-  
4580-  
4590-  
4600-  
4610-  
4620-  
4630-  
4640-  
4650-  
4660-  
4670-  
4680-  
4690-  
4700-  
4710-  
4720-  
4730-  
4740-  
4750-  
4760-  
4770-  
4780-  
4790-  
4800-  
4810-  
4820-  
4830-  
4840-  
4850-  
4860-  
4870-  
4880-  
4890-  
4900-  
4910-  
4920-  
4930-  
4940-  
4950-  
4960-  
4970-  
4980-  
4990-  
5000-  
5010-  
5020-  
5030-  
5040-  
5050-  
5060-  
5070-  
5080-  
5090-  
5100-  
5110-  
5120-  
5130-  
5140-  
5150-  
5160-  
5170-  
5180-  
5190-  
5200-  
5210-  
5220-  
5230-  
5240-  
5250-  
5260-  
5270-  
5280-  
5290-  
5300-  
5310-  
5320-  
5330-  
5340-  
5350-  
5360-  
5370-  
5380-  
5390-  
5400-  
5410-  
5420-  
5430-  
5440-  
5450-  
5460-  
5470-  
5480-  
5490-  
5500-  
5510-  
5520-  
5530-  
5540-  
5550-  
5560-  
5570-  
5580-  
5590-  
5600-  
5610-  
5620-  
5630-  
5640-  
5650-  
5660-  
5670-  
5680-  
5690-  
5700-  
5710-  
5720-  
5730-  
5740-  
5750-  
5760-  
5770-  
5780-  
5790-  
5800-  
5810-  
5820-  
5830-  
5840-  
5850-  
5860-  
5870-  
5880-  
5890-  
5900-  
5910-  
5920-  
5930-  
5940-  
5950-  
5960-  
5970-  
5980-  
5990-  
6000-  
6010-  
6020-  
6030-  
6040-  
6050-  
6060-  
6070-  
6080-  
6090-  
6100-  
6110-  
6120-  
6130-  
6140-  
6150-  
6160-  
6170-  
6180-  
6190-  
6200-  
6210-  
6220-  
6230-  
6240-  
6250-  
6260-  
6270-  
6280-  
6290-  
6300-  
6310-  
6320-  
6330-  
6340-  
6350-  
6360-  
6370-  
6380-  
6390-  
6400-  
6410-  
6420-  
6430-  
6440-  
6450-  
6460-  
6470-  
6480-  
6490-  
6500-  
6510-  
6520-  
6530-  
6540-  
6550-  
6560-  
6570-  
6580-  
6590-  
6600-  
6610-  
6620-  
6630-  
6640-  
6650-  
6660-  
6670-  
6680-  
6690-  
6700-  
6710-  
6720-  
6730-  
6740-  
6750-  
6760-  
6770-  
6780-  
6790-  
6800-  
6810-  
6820-  
6830-  
6840-  
6850-  
6860-  
6870-  
6880-  
6890-  
6900-  
6910-  
6920-  
6930-  
6940-  
6950-  
6960-  
6970-  
6980-  
6990-  
7000-  
7010-  
7020-  
7030-  
7040-  
7050

for  
The Air Force Office of Scientific Research  
Building 410  
Bolling AFB, DC 20032-6448

Approved for public release,  
distribution unlimited

By  
M. Picornell and S. Nazarian  
Center for Geotechnical and Highway Materials Research  
The University of Texas at El Paso  
El Paso, Texas 79968-0516  
915/747-5664

## ABSTRACT

The present research project was conceived as an extension of a parent project, "Behavior of Unsaturated Clayey Soils at High Strain Rates." The soil used in both projects had been collected from the flood plain of the Rio Grande and subjected to engineering and physicochemical characterization tests. Soluble components and organic matter were also removed from it at that time. Furthermore, the soil suspension stock, with the precisely known and controlled chemistry of the pore solution, was prepared for this study too. This stock provided soil for the preparation of specimens to be tested during this study.

The preparation of specimens consisted in consolidating a well mixed soil cake under 50 psi confining pressure, constant temperature, and for a fixed length of time. The cake was obtained and prepared by initially centrifugating the soil suspension to reduce water content and reduce the volume changes that the suspension would experiment during consolidation. Then, the cake was extracted from the centrifuge bottles and placed on a glass plate where it was prepared for consolidation by thoroughly mixing it.

Each consolidated specimen was trimmed to a 1.4 inch diameter. The specimens were placed inside a triaxial cell over a high air entry porous stone to equilibrate them to predetermined soil suction levels of 15 psi, 30 psi, 40 psi, and 70

psi. Specimens to be tested under undrained conditions had a special loading cap installed during the assembly of the cell. After reaching an equilibrium point, some were used for creep recovery testing and the rest for dynamic tests at high strain rates.

The creep tests were performed at several deviatoric stress levels and at the suction levels previously mentioned. The results of these tests were used to make comparisons with the model suggested in the parent project. A nonlinear viscoelastic model, based on power laws, helped to explain the observed behavior.

The specimens for the dynamic tests, identically prepared as for creep tests, were placed inside a dynamic triaxial cell and tested by applying on them consecutive load pulses. Each pulse was of larger peak intensity than the previous. At each load pulse, the load-time and strain-time histories were recorded. The suggested model was used to make predictions of the strain-time histories and comparisons were made with the laboratory results. The suggested model, a power law of time with the coefficient and exponent being functions of the deviatoric stress and soil suction levels, offered a satisfactory comparison when used in conjunction with a modified superposition principle.

The predictions from dynamic tests, at the peak, are larger than the measured strain levels for drained conditions, but they over impose in a much closer manner for undrained conditions according to the results of this study. The observed

discrepancies among laboratory data and predictions seem to be caused because of the inaccurate records of the load-time history applied to the specimen and to limitations of the model, as suggested by the parent project. The friction between the push rod and the bushing of the triaxial cell seem to be of no major concern as previously believed to be.

Summarizing, this study indicates that for undrained conditions the model predictions of the peak strains are much closer to data values. Additionally, the model can explain the plastic strain remaining for specimens after load pulse application on both drainage conditions. Finally the records of the transient creep phase, similarly to the results of the parent project, can be advantageously used to model soil behavior at high strain rates. Continuing this research could provide more assurance to the above conclusions as well as additional information on the model applicability.

## TABLE OF CONTENTS

	<u>PAGE NO.</u>
ABSTRACT.....	ii
TABLE OF CONTENTS.....	v
LIST OF TABLES.....	ix
LIST OF FIGURES.....	xi

### CHAPTER ONE - INTRODUCTION

1.1 Problem Statement.....	1
1.2 Objectives and Approach.....	2
1.3 Organization.....	2

### CHAPTER TWO - BACKGROUND

2.1 Introduction.....	4
2.2 The Mechanics of Unsaturated Soils.....	4
2.3 The Behavior of Stress-Strain-Time for Soils.....	9
2.4 Rate Process Theory Applied to Soil Deformation.....	12
2.5 Nonlinear Viscoelastic Models.....	16
2.6 Review of Contemporary Literature.....	25

### CHAPTER THREE - PREPARATION OF SPECIMENS

3.1 Introduction.....	40
3.2 Preparation of Specimens.....	40

## **CHAPTER FOUR - CREEP RECOVERY TESTING**

4.1	Introduction.....	66
4.2	Description of Testing Procedures.....	66
4.3	Discussion of Results.....	67
4.4	Repeated Tests for Verification Purposes.....	85

## **CHAPTER FIVE - INDEX PROPERTIES**

5.1	Introduction.....	87
5.2	Index Properties of the Soil Stock.....	87
5.3	Index Properties of Specimens.....	92
5.4	Water Contents of the Specimens.....	94

## **CHAPTER SIX - MODEL FOR CREEP AND RECOVERY**

6.1	Introduction.....	102
6.2	Initial Power Law .....	102
6.3	Recovery Power Law.....	114

## **CHAPTER SEVEN - HIGH STRAIN RATE EQUIPMENT**

7.1	Introduction.....	126
7.2	Test Equipment.....	126
7.3	Triaxial Cell Calibration.....	128



## CHAPTER EIGHT-HIGH STRAIN RATE TESTING

8.1 Introduction.....	136
8.2 Specimen Preparation.....	136
8.3 Methodology for Conducting Tests.....	137
8.4 Procedures for Data Reduction.....	139
8.5 Results of Scheduled Tests.....	140

## CHAPTER NINE - PREDICTED AND MEASURED DYNAMIC BEHAVIOR

9.1 Introduction.....	146
9.2 Methodology for Predicting the Specimen Response.....	147
9.3 Results and Discussion.....	150

## CHAPTER TEN - CONCLUSIONS AND RECOMMENDATIONS

10.1 Summary .....	158
10.2 Conclusions.....	161
10.3 Recommendations.....	163

REFERENCES.....	165
-----------------	-----

APPENDICES: .....	167
-------------------	-----

"A" RECORDS OF CONSOLIDATION OF SLURRY.....	167
"B" RECORDS OF EQUILIBRATION TO SPECIFIED SOIL SUCTION.....	202
"C" RECORDS OF CREEP/RECOVERY TESTS.....	237
"D" RESULTS OF GRAIN SIZE ANALYSIS.....	269

"E" DATA OF EXTERNAL VERSUS INTERNAL LOAD CELL READINGS FOR SYNTHETIC SPECIMENS.....	275
"F" FORTRAN LISTING OF PROGRAM "HSTRAIN" .....	291
"G" SELECTED RESULTS OF DYNAMIC TESTS ON SPECIMENS AT 15 PSI SOIL SUCTION.....	300
"H" SELECTED RESULTS OF DYNAMIC TESTS ON SPECIMENS AT 40 PSI SOIL SUCTION.....	307
"I" SELECTED RESULTS OF DYNAMIC TESTS ON SPECIMENS AT 70 PSI SOIL SUCTION.....	316

## LIST OF TABLES

<u>TABLE NO.</u>	<u>PAGE NO.</u>
3.1	Records of Electrical Conductivity Readings.....42
3.2	Conditions and Results of Consolidated Specimens.....47
3.3	Characteristics of High Air Entry Porous Disks.....56
3.4	Conditions During Specimen Equilibration Phase.....58
3.5	Equations for Calculating Necessary Load to Balance Cell Pressure and Friction.....65
4.1	Summary of Conditions and Results of Creep/Recovery Tests.....68
5.1	Tests on Soil Stock and Specimens.....88
5.2	Atterberg Limits of the Soil Stock Saturated With Lithium Chloride.....91
5.3	Atterberg Limits of the Soil Stock Saturated With Aluminum Chloride.....91
5.4	Cation Exchange Capacity Measurements.....92
5.5	Specific Gravity of the Solids.....93
5.6	Water Content Before and After Creep/Recovery Tests.....96
6.1	Values of Parameters $\alpha$ and $\beta$ for Different Soil Suction Levels.....106
6.2	Values of Parameters $\alpha_1$ and $\alpha_2$ for Different Soil Suction Levels.....111
6.3	Regression Values of Recovery Phase.....118
6.4	Values of $\alpha_{R1}$ and $\alpha_{R2}$ for Different Soil Suction Levels.....122
7.1	Conditions of Dynamic Tests on Synthetic Specimens.....130

8.1	Load Pulses Applied to the Specimen During a Time Span of 50 msec.....	138
8.2	Results of Dynamic Tests for Specimens Equilibrated at 15 psi.....	142
8.3	Results of Dynamic Tests for Specimen Equilibrated at 30 psi.....	143
8.4	Results of Dynamic Tests for Specimens Equilibrated at 40 psi.....	144
8.5	Results of Dynamic Tests for Specimens Equilibrated at 70 psi.....	145

## LIST OF FIGURES

<u>FIGURE NO.</u>	<u>PAGE NO.</u>
2.1 Regina Clay Showing its Total Matric and Osmotic Suctions with Respect to Water Content.....	7
2.2 Unsaturated Soil Extended Mohr-Coulomb Strength Relationship.....	10
2.3 Common Stages of Creep.....	11
2.4 Energy Barriers and Activation Energy.....	14
2.5 Ideal Creep Curve.....	18
2.6 Recovery Stage with the Modified Superposition Principle Applied.....	20
2.7 Murayama and Shibata Proposed Rheological Model for Clays.....	26
2.8 Flow Strain and Time Relationship.....	28
2.9 Rheological Development by Christensen and Wu.....	29
2.10 Rheological Developed Model by Abdel-Hady and Herrin.....	31
2.11 Rheological Model Suggested by Komamura and Huang.....	34
2.12 Model Proposed by Komamura and Huang for Visco-Elastic Case with Small Stress Levels.....	36
2.13 Visco-Plastic Model by Komamura and Huang for Water Content Above the Visco-Plastic Limit Case.....	37
2.14 Komamura and Huang Viscous Model for Water Contents Higher Than	

	Liquid Limit.....	39
3.1	Schematic of Consolidation Apparatus.....	46
3.2	Specimen Before Trimming.....	50
3.3	Specimen After Trimming.....	51
3.4	Schematic of Set-up for Equilibrium Process on a Specimen to be Subjected to Creep/Recovery Under Drained Conditions.....	52
3.5	Schematic of Set-up for Equilibrium Process on a Specimen to be Subjected to Creep/Recovery Under Undrained Conditions.....	53
3.6	Schematic of Loading Cap for Undrained Testing Conditions.....	54
3.7	Apparatus Set-up for Creep/Recovery Testing Under Drained Conditions.....	62
3.8	Apparatus Set-up for Creep/Recovery Testing Under Undrained Conditions.....	63
4.1	Comparison of Drained Versus Undrained Creep Tests.....	73
4.2	Drained Versus Undrained Creep Tests for 15 psi Soil Suction.....	75
4.3	Drained Versus Undrained Creep Tests for 30 psi Soil Suction.....	76
4.4	Drained Versus Undrained Creep Tests for 40 psi Soil Suction.....	78
4.5	Drained Versus Undrained Creep Tests for 70 psi Soil Suction.....	79
4.6	Evaluation of Secondary Creep Stage for 15 psi Soil Suction.....	81
4.7	Evaluation of Secondary Creep stage for 30 psi Soil Suction.....	82

4.8	Evaluation of Secondary Creep stage for 40 psi Soil Suction.....	83
4.9	Evaluation of Secondary Creep stage for 70 psi Soil Suction.....	84
5.1	Results of Hydrometer Tests on the Soil Stock.....	90
5.2	Comparison of the Grain Size Distribution for Soil Stock and for Specimens.....	95
6.1	Initial Creep Phase for Undrained Conditions of Specimens Equilibrated at 70 psi.....	104
6.2	Initial Creep Phase for Drained Conditions of Specimens Equilibrated at 70 psi.....	105
6.3	Power Relationship Between Parameter $\alpha$ and the Deviatoric Stress for Three Soil Suction Levels at Drained Conditions.....	109
6.4	Power Relationship Between Parameter $\alpha$ and the Deviatoric Stress for Four Soil Suction Levels at Undrained Conditions.....	110
6.5	Comparison of Laboratory Data Versus Model Prediction for Creep Phase.....	113
6.6	Drained Recovery Phase for Specimens Equilibrated at 70 psi Soil Suction.....	115
6.7	Undrained Recovery Phase for Specimens Equilibrated at 70 psi Soil Suction.....	116
6.8	Power Law Regression Between Parameter $\alpha_R$ and Deviatoric Stress for	

	Drained Condition.....	120
6.9	Power Law Regression Between Parameter $\alpha_R$ and Deviatoric Stress for Undrained Condition.....	121
6.10	Comparison of Laboratory Data Versus Model Prediction for Recovery Phase.....	124
7.1	Comparison of Load Values Obtained by Equation and Load Cell for Soft Synthetic Specimen.....	131
7.2	Comparison of Load Values Obtained by Equation and Load Cell for Medium Synthetic Specimen.....	132
7.3	Comparison of Load Values Obtained by Equation and Load Cell for Hard Synthetic Specimen.....	133
7.4	Comparison of Stresses Recorded by Internal and External Load Cells.....	135
9.1	Example of the Approximation of the Load Pulse Used in the Predictions.....	148
9.2	Comparison of Predicted Versus Measured Strain for Drained Conditions.....	151
9.3	Comparison of Predicted Versus Measured Strain for Undrained Conditions.....	152
9.4	Comparisons of Strains for Drained and Undrained Conditions at 15 psi Soil Suction.....	153



9.5	Comparisons of Strains for Drained and Undrained Conditions at 40 psi Soil Suction.....	154
9.6	Comparisons of Strains for Drained and Undrained Conditions at 70 psi Soil Suction.....	155

## CHAPTER ONE

### INTRODUCTION

#### 1.1 PROBLEM STATEMENT

To evaluate the survivability of military and security structures after a conventional or nuclear attack, it is necessary to understand and accurately model the soil-structure interaction under extreme loading conditions. A realistic prediction of the soil response could be possible by developing appropriate constitutive equations. The equations would have to: 1) account for the high strain rates imposed on the soil, 2) include the effects of the soil suction, and 3) consider the soil saturation state since many of these structures are surrounded by, or rest on, soils which are in unsaturated conditions.

Since the strength and behavior of soils, more pronounced for clayey than for other type, have a strain-rate dependency; there is interest in determining the extent of influence of soil suction on the constitutive behavior of clayey soils, mostly those that are unsaturated. Thus, with the investigations performed at small strain-rates and directed towards the behavior of saturated clayey soils, this problem will be addressed considering the work done by the previous researchers and their suggestions.

## **1.2 OBJECTIVES AND APPROACHES**

This thesis has essentially been dedicated to investigate the applicability of low strain rate tests and a mathematical model suggested by the parent project, for the prediction of the behavior of unsaturated clayey soils at high strain rates. The approach for this study consisted in performing creep/ recovery tests under drained and undrained conditions. The results were compared with the model to determine whether the soil behavior at low strain rates could be explained. A secondary phase of the study was the testing of identical specimens under high strain rates. For this, a dynamic soil testing facility, MTS, was utilized. The obtained results were compared with the predictions of the model used for creep/recovery results, with a modified superposition principle. The model applicability was investigated by comparing predictions and actual measurements for various soil suction and deviatoric stress combinations.

## **1.3 ORGANIZATION**

This thesis is composed of ten chapters. Chapter two contains documentation about the mechanics of unsaturated soils. It also includes the information upon which the creep and recovery tests are based on. Chapter three contains the details of the test set-up, and, specimen preparation. Chapter four discusses the creep/recovery tests and reduction of data. Chapter five contains the

description of the properties of the material used on this study. Chapter six is information about the suggested model. Chapter seven describes the testing facility for dynamic tests and the procedures for performing such tests. Chapter eight discusses the high strain rate testing phase of this study. Chapter nine includes the comparison of predicted and measured dynamic behavior as well as an evaluation of the capabilities of the model. Chapter ten summarizes this study, and offers conclusions and recommendations for further studies. Each test is individually documented in the appendices.

## CHAPTER TWO

### BACKGROUND

#### 2.1 INTRODUCTION

This chapter is intended to describe and discuss the basic aspects of the mechanics of unsaturated soils, aspects of the existing rheological models, and of the behavior of such soils with time dependent stresses and strains.

#### 2.2 THE MECHANICS OF UNSATURATED SOILS

As it is known, pore air pressure is usually taken as zero for atmospheric pressure. Thus, below atmospheric pressure the pore pressure becomes negative and above atmospheric pressure the pore pressure becomes positive. These indications are applicable to the conditions experienced by unsaturated soils which have a composition of solid, liquid, and gaseous phases.

When the pore pressure becomes negative, which is when the water table is drawn below the ground surface, the pore water pressure decreases and evapotranspiration results in the larger air bubbles of the pore space. This causes an increment in the gaseous phase. Oppositely, when the pore pressure is positive in the liquid phase, any gaseous phase present within the soil is possible only as

trapped gas at a higher pressure than the atmospheric. Thus, the gas tends to diffuse out of the soil system and the soil pore spaces are completely filled with water causing an increment in the liquid phase.

The magnitude of the negative pressure, commonly known as soil suction of the pore-water in soil science, is a measure of the affinity of soil for water. Soil suction is therefore a usual term associated with the concepts of unsaturated soil. It is defined as a thermodynamic variable by the soil science. By the International Society of Soil Sciences the definition is: soil suction,  $(h)$ , is the negative pressure to which a pool of pure and free water at the same elevation and temperature must be subjected in order to be in equilibrium with the soil water. Such negative pressure being in relation to the external gas pressure acting on the soil water, normally known as atmospheric pressure.

For measuring purposes of soil suction, the relative humidity of air, in the thermodynamic equilibrium with soil water, is the basis. For such purposes, a useful relationship is:

$$h_t = -(RT/v_w) \ln(p/p_o) \quad (2.1)$$

where

$h_t$  = total suction

$R$  = universal gas constant

$T$  = absolute temperature

$v_w$  = volume of a mole of liquid water

$p/p_o$  = relative humidity

$p$  = partial pressure of water vapor

$p_o$  = partial pressure of saturated water vapor

In addition to this relationship, the soil suction, or total suction, is represented by the algebraic sum of matric and osmotic suctions. Osmotic suction results from the presence of soluble salts in the pore water. Matric suction is related to the negative pore water pressure, also known as capillary stress in soil. Some particularities of osmotic suction are that its gradients don't affect water flow unless a semipermeable barrier prevents the movement of the electrolyte; also, its changes with water content are small relative to matric suction, as indicated by Figure 2.1. And a final third particularity, as also shown in the figure, is that the results of Fredlund in 1979 suggest that approximately the total suction gradients can be substituted by matric suction gradients.

The above mentioned relationship and particularities are considered by the following expressions:

$$h_t = h_m + h_s, \quad (2.2)$$

$$h_m = u_a - u_w, \quad (2.3)$$

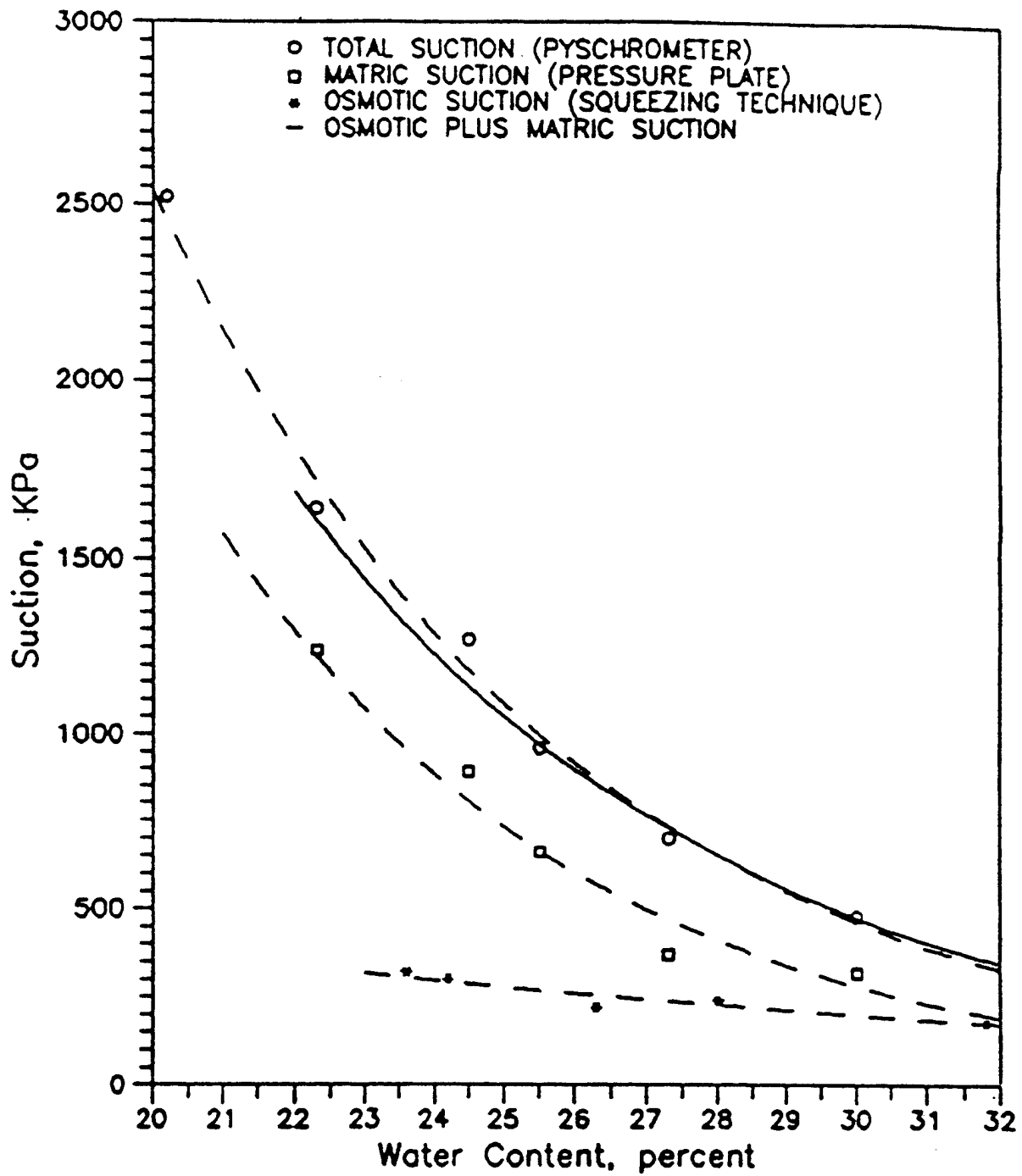


Figure 2.1 Regina Clay Showing its Total Matric and Osmotic Suctions with Respect to Water Content (Fredlund, 1979)



where

$h_t$  = total suction

$h_m$  = matric suction

$h_s$  = osmotic or solute suction

$u_a$  = pore air pressure

$u_w$  = pore water pressure

Furthermore, for unsaturated soils, a Mohr-Coulomb strength relation conceptually proposed by Fredlund was that the shear strength of unsaturated soil could be expressed in the form of an extended or three dimensional manner. This was possible because in recent time he suggested that the unsaturated soil was composed of a system with four phases that included solids, water, air, and air water interface; assuming that the air phase becomes continuous at degrees of saturation less than 85% to 90%; a fact supported by a stress analysis consistent with multiphase continuum mechanics. Thus, Fredlund suggested relationship is:

$$\tau = c' + (\sigma - u_a)\tan\phi' + (u_a - u_w)\tan\phi^b \quad (2.4)$$

where

$\tau$  = shear strength

$c'$  = cohesion intercept when the two stress state variables are zero

$\sigma - u_a$  = stress state variable, applied stress

$u_a - u_w$  = stress state variable, applied matrix suction

$\phi'$  = angle of friction with respect to applied stress

$\phi^b$  = angle of friction with respect to matric suction

and it is illustrated by Figure 2.2. The relationship proposes two independent stress tensors,  $\sigma - u_a$  and  $u_a - u_w$ , and as the degree of saturation approaches 100%; the pore air pressure reaches up to the pore water pressure. Consequently, the pore air term in the first stress tensor becomes the pore water pressure since the matric suction term goes to zero.

### 2.3 THE BEHAVIOR OF STRESS-STRAIN-TIME FOR SOILS

There are several factors which affect the behavior of soil when this is experiencing creep. In particular geotechnical problems requiring long term behavior analysis, major factors of interest for this time-dependent deformation include stress history, drainage conditions, and type of stress system. As a result of the dependency of the creep behavior on the mentioned factors, the strain pattern of a tested soil specimen is also affected. In many situations, the constant applied stress upon a specimen would cause the strain phases shown by Figure 2.3. The stages are the following:

- (1) Initial instantaneous stage. An initial elastic strain occurs immediately upon loading. If the applied stress exceeds the yield stress, an initial plastic strain also occurs.

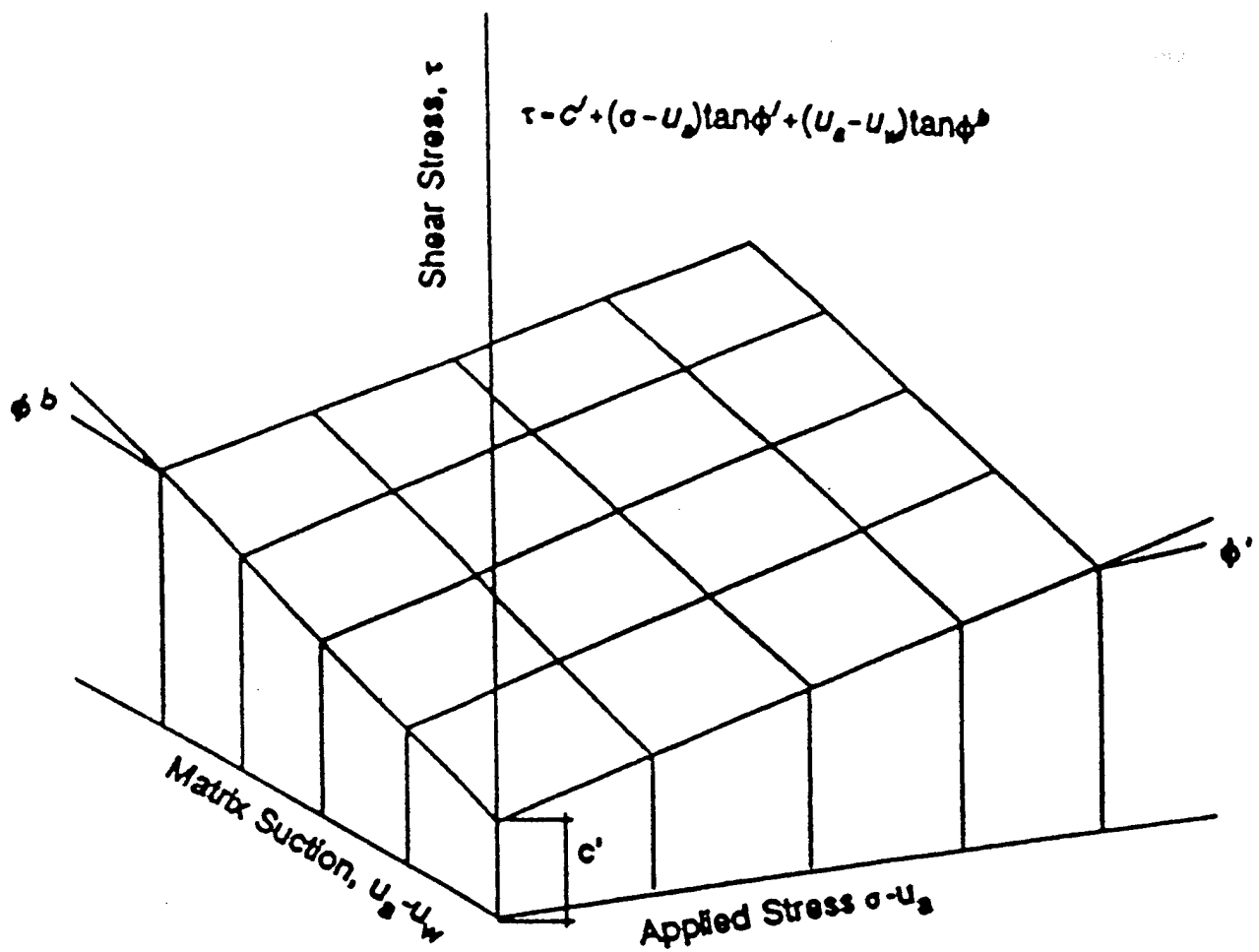


Figure 2.2 Unsaturated Soil Extended Mohr-Coulomb Strength Relationship  
(Fredlund, 1979)

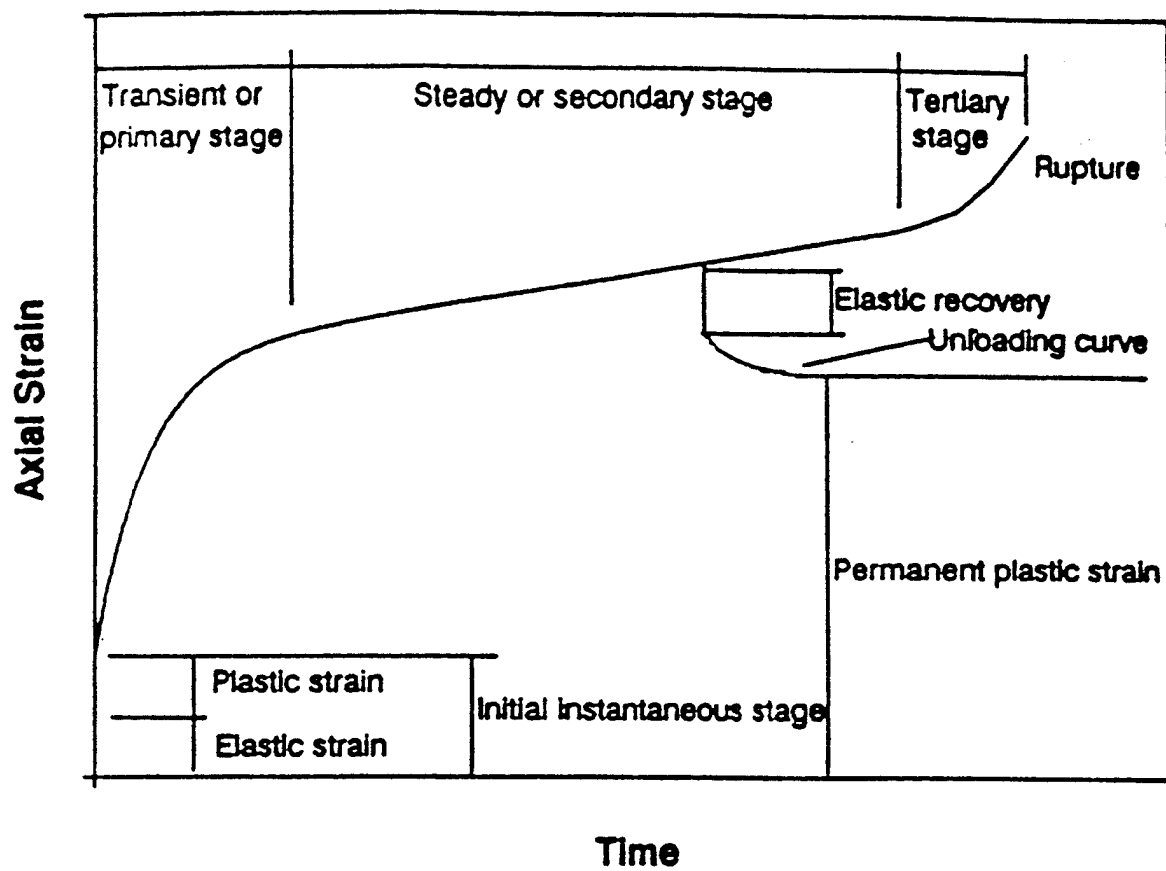


Figure 2.3 Common Stages of Creep

- (2) Transient or primary stage. Here the rate of creep strain decreases with time as a result of strain hardening.
- (3) Steady or secondary creep stage. The creep strain rate is essentially constant in this region. In certain instances it is actually slowly decreasing but not noticed because the data is frequently being nicely approximated by a straight line.
- (4) Tertiary is the final stage. The creep strain rate increases leading to failure of the specimen.

A peculiarity of this behavior is that all of the elastic strain will be recovered, plus some of the creep strain, over an interval of time if the load is removed.

#### 2.4 RATE PROCESS THEORY APPLIED TO SOIL DEFORMATION

To study the creep behavior of soil specimens, Mitchell and Singh (1968), as well as Christensen and Wu (1964), applied the rate process theory that Glasstone, Laidler, and Eyring (1941) had proposed for the time-dependent rearrangement of matter and polymers. With such studies, the nature of soil strength along with the functional forms for the influence of some variables on soil behavior were provided. Thus, in 1968 Mitchell, Campanella, and Singh developed for most soil deformation problems the expression which used the concept behind the rate process theory. Since the theory is based on the fact that atoms, molecules, and/or particles participate in a time dependent flow of deformation process as "flow units", such units are

constrained from movement relative to each other by virtue of energy barriers separating adjacent equilibrium positions as observed in Figure 2.4. The concept was that the displacement of flow units to new positions requires the introduction of sufficient energy to surmount the barrier, which is referred to as the activation energy,  $\Delta F$ . The value of the activation energy depends on the material and type of process and is supplied by thermal energy and various applied potentials. The developed equation for the rate of strain in soil is the following:

$$\dot{\epsilon} = X \frac{kT}{h} \exp\left(-\frac{\Delta F}{RT}\right) \exp\left(\frac{f\lambda N}{2RT}\right) \quad (2.4)$$

where

$\dot{\epsilon}$  = rate of creep strain

$X$  = parameter may be both, time and structure dependent

$k$  = Boltzman's constant ( $1.38 \times 10^{-16} \text{ erg} \cdot \text{K}^{-1}$ )

$T$  = absolute temperature (K)

$h$  = Planck's constant ( $6.625 \times 10^{-27} \text{ erg Sec}^{-1}$ )

$\Delta F$  = activative energy (erg)

$R$  = universal gas constant ( $1.98 \text{ cal K}^{-1} \text{ mole}^{-1}$ )

$N$  = Avogadro's number ( $6.02 \times 10^{23}$ )

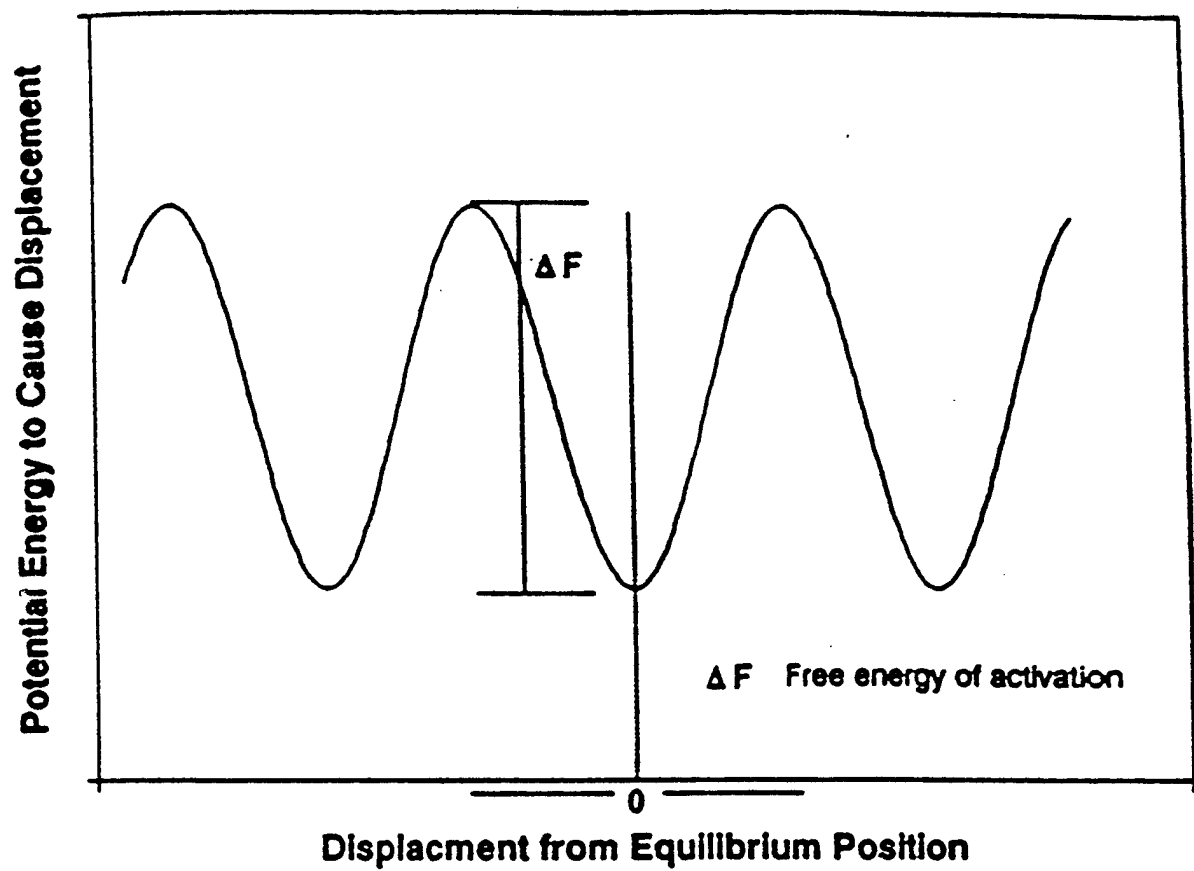


Figure 2.4 Energy Barriers and Activation Energy (Mitchell, 1964)

$\lambda$  = distance between successive equilibrium positions (A)

$f$  = force acting on the flow unit ( $\text{g/cm}^2$ )

It implies that the creep rate, among other factors, was related to axial load and temperature. With basis on the mentioned theory, Singh and Mitchell proposed additional equations for the description of creep deformation over the range of stresses of engineering interest for various types of clayey soils. Such functions were for strain-stress-time relationships of the following form:

$$\dot{\epsilon} = Ae^{-\alpha D} \left( \frac{t_1}{t} \right)^m \quad (2.5)$$

where

$\dot{\epsilon}$  = creep strain rate

$t$  = time

$D$  = stress intensity which is the ratio of the deviatoric stress to ultimate axial strength

$A$  = strain rate at time  $t$  and  $D = 0.0$

$\alpha$  = value of the slope of the mid-range linear portion of a plot of logarithmic strain rate versus deviatoric stress, all points corresponding to the same time after load application

$m$  = slope of a logarithmic strain rate versus logarithmic time straight line



$t_1$  = reference line

Taking  $t_1$  as unity, equation (2.5) becomes:

$$\dot{\epsilon} = Ae^{-\alpha D} \left(\frac{1}{t}\right)^m \quad (2.6)$$

Integration of equation (2.6) yields:

$$\epsilon = \epsilon_1 + \frac{A}{1-m} e^{-\alpha D} (t^{1-m} - 1), \quad m \neq 1 \quad (2.7)$$

$$\epsilon = \epsilon_1 + Ae^{-\alpha D} \ln(t), \quad m = 1 \text{ and } t = 1 \quad (2.8)$$

where  $\epsilon_1$  is creep strain at unit time.

## 2.5 NONLINEAR VISCOELASTIC MODELS

### 2.5.1 General Concepts

Viscoelasticity is concerned with materials which exhibit strain rate effects in response to applied stress. These effects are manifested by the phenomena of creep under constant stress and stress relaxation under constant strain. Viscoelasticity combines elasticity (spring) and viscosity (dashpot or viscous flow).

The strain of nonlinear viscoelastic materials exhibit a highly nonlinear dependence on stress. Still under development, Shames and Cozzarelli (1992) summarized this nonlinear viscoelastic theory as shown by Figure 2.5. The figure presents the three periods of deformation which characterize the development of creep strain under a uniaxial stress. The periods are: Instantaneous response, decreasing strain rate, and constant strain rate. Tertiary was omitted since it isn't pertinent to the purpose of this study.

The superposition of three components,

$$\epsilon(t) = \epsilon_1 + \epsilon_s(t) + \epsilon_i(t), \quad t \geq 0 \quad (2.9)$$

expresses the creep strain due to constant uniaxial stress under constant temperature. Considering: (1) that  $\epsilon_1$  is independent of time, all elastic at the elastic part, and has some plastic response; (2) that  $\epsilon_i(t)$  is a function of time starting from zero at  $t = 0$  and the derivative approaching zero as time approaches zero; and (3) that  $\epsilon_s(t)$  is linear with time, giving a constant steady creep strain rate; The previous equation can also be expressed as:

$$\epsilon(t) = f_1(\sigma) + f_s(\sigma)t + f_i(\sigma)g(t) \quad (2.10)$$

where  $f_1(\sigma)$ ,  $f_s(\sigma)$ , and  $f_i(\sigma)$  are stress functions and  $g(t)$  is a transient time function

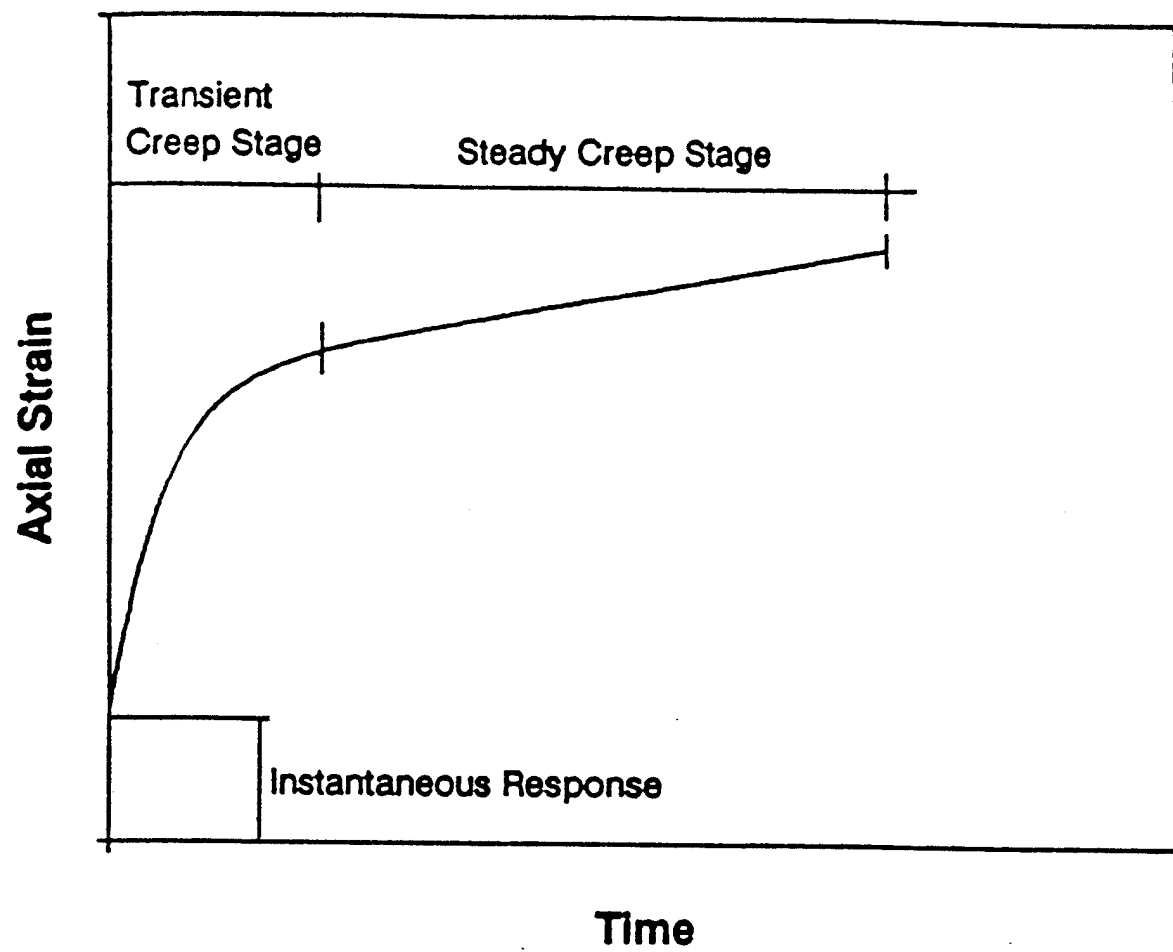


Figure 2.5 Ideal Creep Curve

needing to satisfy the following additional requirement:

$$g(0) = 0 \qquad \lim_{t \rightarrow \infty} \frac{dg}{dt} = 0. \qquad (2.11)$$

To describe nonlinear behavior of the recovery stage, the modified superposition method proposed by Findlay et al (1968) is useful and gives the strain during recovery at zero stress by:

$$\epsilon_r(t) = f(\sigma, t-t_0) - f(\sigma_0, t-t_1), \quad t > t_1 \qquad (2.12)$$

where

$\epsilon_r(t)$  = strain after removal of load

$\sigma_0$  = constant applied stress during creep stage

$t_0$  = time of application of  $\sigma_0$

$t_1$  = time of removal of  $\sigma_0$

Figure 2.6 illustrates the application of this equation.

### 2.5.2 Constant Uniaxial Stress Applied on Models

For relatively large stress applied, the expression of stress function is obtained from test data, as a combination of elastic and plastic strains.

For relatively small applied stress, the instantaneous stress function,  $f_1(\sigma_0)$ ,

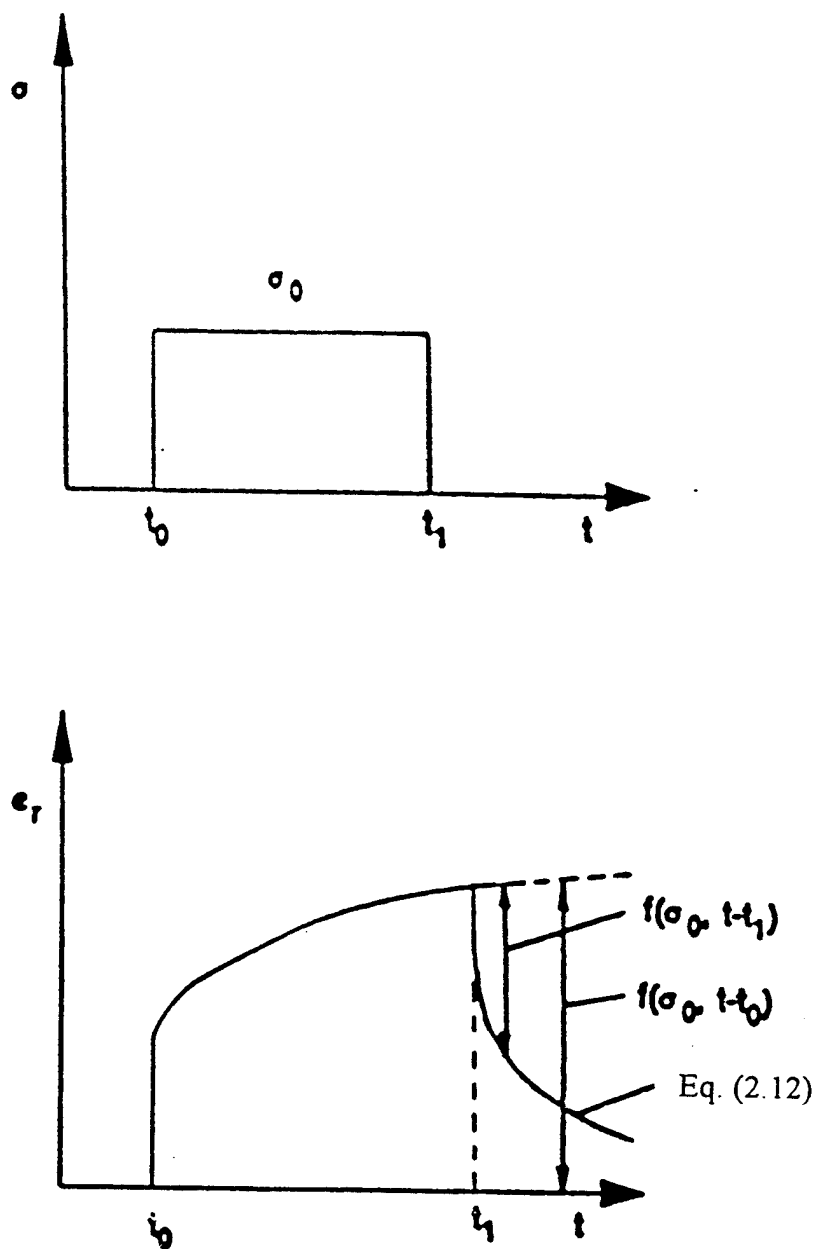


Figure 2.6 Recovery Stage with the Modified Superposition Principle Applied

is linear and assumed as:

$$f_1(\sigma_o) = (\sigma_o)/E \quad (2.13)$$

E is Young's Modulus of material.

Two forms of stress function for the steady creep are used for soil creep behavior. For this study, the relationship used is the following:

$$f_s(\sigma_o) = A\sigma_o^n \quad (2.14)$$

where A, and n are material constants. Based on this function the stress power law for steady creep component is:

$$\epsilon_s(t) = A\sigma_o^n t \quad (2.15)$$

similarly, the function for transient creep is the following:

$$f_t(\sigma_o) = C\sigma_o^m \quad (2.16)$$

where C and m are material constants. To satisfy the requirement listed in (2.11), the time power function,

$$g(t) = t^q, \quad 0 < q < 1 \quad (2.17)$$

is commonly used. Thus the transient strain component can be represented by the

following expression:

$$\epsilon_i(t) = C \sigma_o^m t^q, \quad 0 < q < 1 \quad (2.18)$$

Thus the total creep strain for constant stress is represented by the following expression:

$$\epsilon_i(t) = f_i(\sigma_o) + A \sigma_o^n t + C \sigma_o^m t^q \quad (2.19)$$

### 2.5.3 Variable Uniaxial Stress Applied on Models

The behavior of nonlinear viscoelastic materials under variable stress requires for its analysis the employment of the strain-hardening hypothesis and the time-hardening hypothesis. The first hypothesis assumes that the creep strain rate is function of the stress and accumulated creep strain.

$$\dot{\epsilon}(t) = f[\epsilon(t), \sigma(t)] \quad (2.20)$$

where  $\epsilon(t)$  refers either to total creep strain or to each component of creep strain and normally excluding the elastic strain. The second hypothesis assumes that creep strain rate is a function of stress and time in the following manner:

$$\dot{\epsilon}(t) = f[\sigma(t), t] \quad (2.21)$$

The strain-hardening hypothesis implies that the creep model acquired from a particular stress, such as a constant stress  $\sigma_o$ , is still valid for any stress variation  $\sigma(t)$ . This hypothesis works well for materials experiencing relatively minor changes in microscopic structure during deformation by creep.

The time-hardening hypothesis works well for materials experiencing significant microscopic change, thus the creep model for an aging material is manipulated into the form of equation (2.21) and the creep model becomes also valid for any stress function  $\sigma(t)$ .

Both hypothesis are discussed further in the next sections.

#### 2.5.3.1 Transient Creep Component From Strain-Hardening Hypothesis

The time power transient creep component under constant uniaxial stress given by equation (2.20) can be rearranged into:

$$[\epsilon_i(t)]^{1/q} = [C \sigma_o^m]^{1/q} t, \quad (2.22)$$

differentiated with respect to time,

$$\frac{\partial [\epsilon_i(t)]^{1/q}}{\partial t} = [C \sigma_o^m]^{1/q} \quad (2.23)$$



which can also be written as:

$$\dot{\epsilon}(t) = q [C \sigma_0^m]^{-\frac{1}{q}} [\epsilon_t(t)]^{1-\frac{1}{q}}, \quad 0 < q < 1 \quad (2.24)$$

Equation (2.24) indicates that the strain rate decreases as the strain increases, satisfying the strain-hardening hypothesis. Therefore,  $\sigma_0$  can be replaced by  $\sigma(t)$ . Equation (2.23) becomes:

$$\frac{\partial [\epsilon_t(t)]^{\frac{1}{q}}}{\partial t} = [C \sigma(t)^m]^{-\frac{1}{q}} \quad (2.25)$$

which integrated gives:

$$\epsilon_t(t) = \left[ \int_0^t [C \sigma(t)^m]^{-\frac{1}{q}} dt \right]^q \quad (2.26)$$

which is the integral form of time power transient creep strain component.

#### 2.5.3.2 Transient Creep Component From Time-Hardening Hypothesis

The time power transient creep component under constant stress  $\sigma_0$  given by equation (2.21) can be differentiated to obtain the following expression for the strain

rate:

$$\dot{\epsilon}(t) = Cq \sigma_0^m t^{q-1} \quad (2.27)$$

which is in the form required by the time-hardening hypothesis. So, the general expression is:

$$\epsilon_r(t) = \int_0^t Cq [\sigma(t)]^m t^{q-1} dt \quad (2.28)$$

## 2.6 REVIEW OF CONTEMPORARY LITERATURE

The stress-strain-time behavior of soils has been attempted to model. For this purpose several rheological models have been proposed and they are composed of a combination of linear springs with linear and nonlinear dashpots and sliders. Some of such models include the Murayama and Shibata developed mechanical model in 1956; the proposed model by Christensen and Wu similar to the Kelvin-Maxwell model in 1964; the five element model introduced by Abdel-Hady and Herrin in 1966; and the new model for soil behavior by Komamura and Huang in 1974.

The model developed by Murayama and Shibata explained viscosity, elasticity, and internal resistance of clay, as Figure 2.7 presents it. The composition is of a spring element in series with a modified Voight element ( $\epsilon_2, \sigma_0, n_2$ ). The

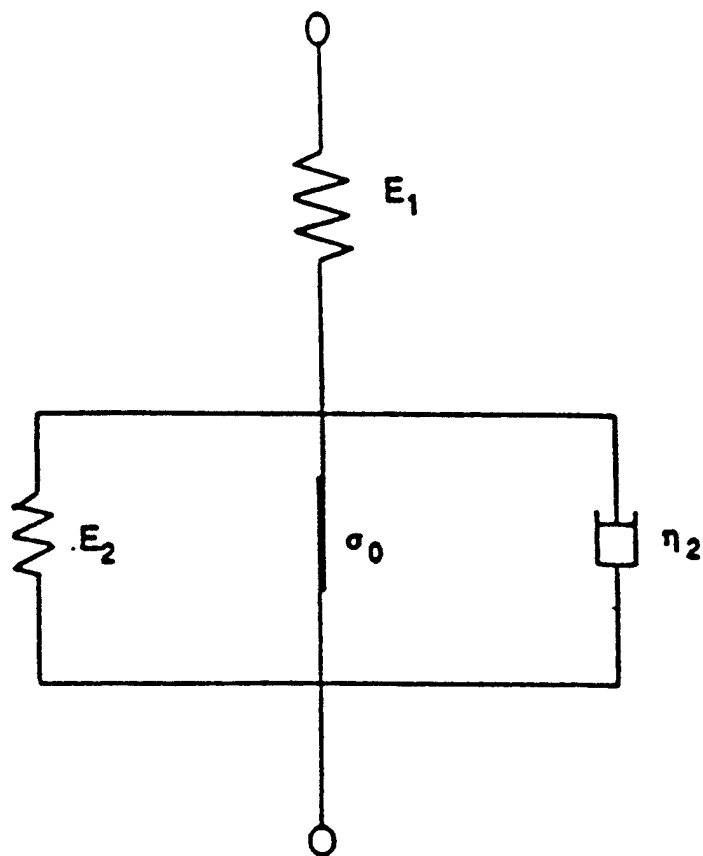


Figure 2.7 Murayama and Shibata Proposed Rheological Model for Clays  
(1956)

relationship among total strain  $\epsilon$  and time  $t$ , given by:

$$\epsilon = \frac{\sigma}{E_1} + \frac{(\sigma - \sigma_0)}{E_2} \log\left(\frac{A_2}{2} B_2 E_2 t\right), \quad 0 < \epsilon_2 < \frac{(\sigma - \sigma_0)}{2B_2 E_2} (2B_2 - 1) \quad (2.29)$$

$$\epsilon = \frac{\sigma}{E_2} + \frac{(\sigma - \sigma_0)}{E_2}, \quad \epsilon_2 > \frac{(\sigma - \sigma_0)}{2B_2 E_2} (2B_2 - 1) \quad (2.30)$$

were  $A_2$  and  $B_2$  are material constants determined by rate process.  $E_1$ ,  $E_2$ ,  $n_2$ , and  $\sigma_0$  can be appreciated in Figure 2.7. Initially the flow of clay strain is proportional to the logarithm of time, equation 2.29, but for the time approaching infinity, Figure 2.8, the flow of clay strain approaches the asymptotic value of equation 2.30.

The Christensen and Wu model, Figure 2.9, proposed a spring  $k_2$  representing the nonflow stress effect. Spring  $k_1$  and dashpot  $\beta$  represented the response from the particle structure of the flow stress. The total strain, in terms of the rate process theory could be obtained by the following expression:

$$\gamma = \frac{1}{k_1} \tau + \frac{1}{\alpha k_2} \ln \tanh \left[ \frac{1}{2} \alpha \beta \frac{k_1 k_2}{k_1 + k_2} t + \tanh^{-1} e^{\left( \frac{\alpha k_1 \tau}{k_1 + k_2} \right)} \right] \quad (2.31)$$

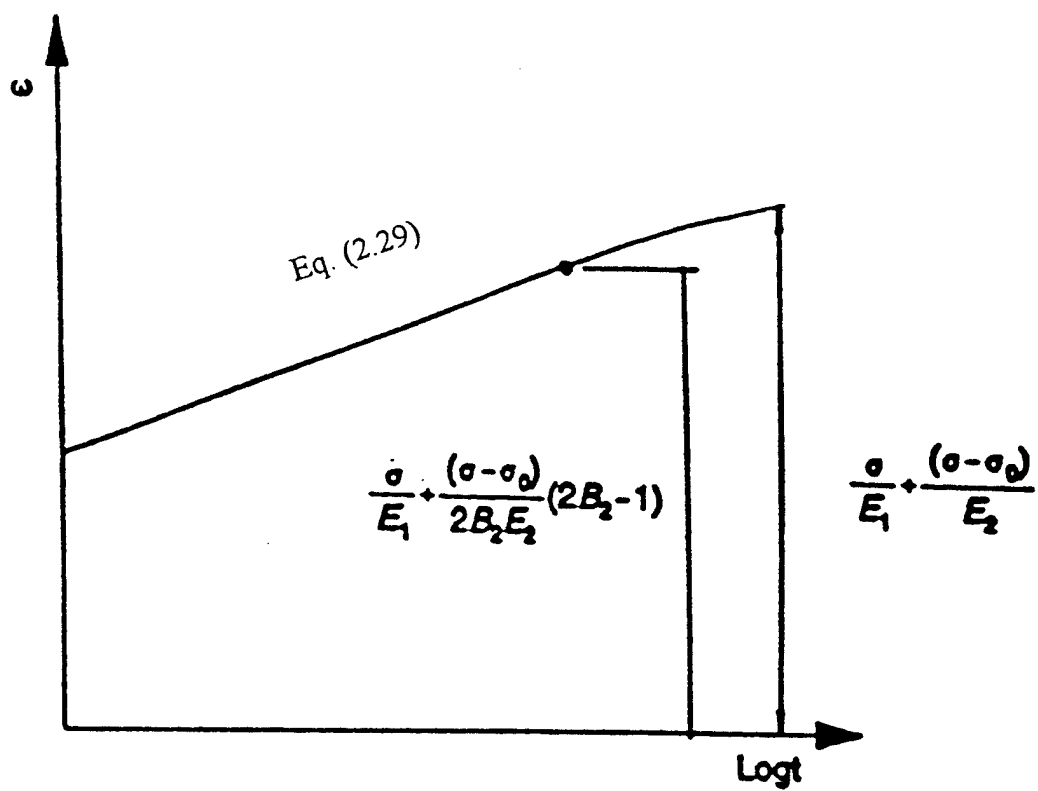


Figure 2.8 Flow Strain and Time Relationship (Murayama and Shibata, 1956)

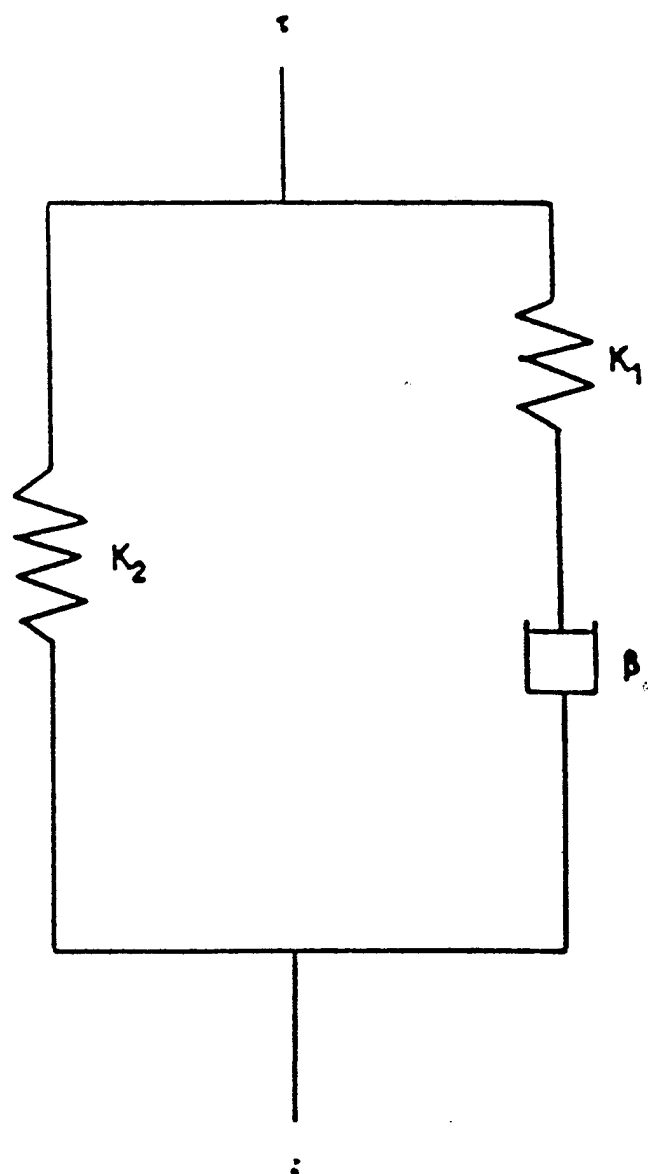


Figure 2.9 Rheological Development by Christensen and Wu (1956)

The Abdel-Hady and Herrin model, illustrated by Figure 2.10, describes the behavior of compacted soil-asphalt mixtures. The total creep strain at any time was the superposition of four deformation components, based on the typical creep curve. The total creep expression is the following:

$$\epsilon = \epsilon_0 + \epsilon_i + \epsilon_d + \epsilon_p \quad (2.32)$$

where:

$\epsilon$  = total strain at any time

$\epsilon_0$  = instantaneous elastic strain

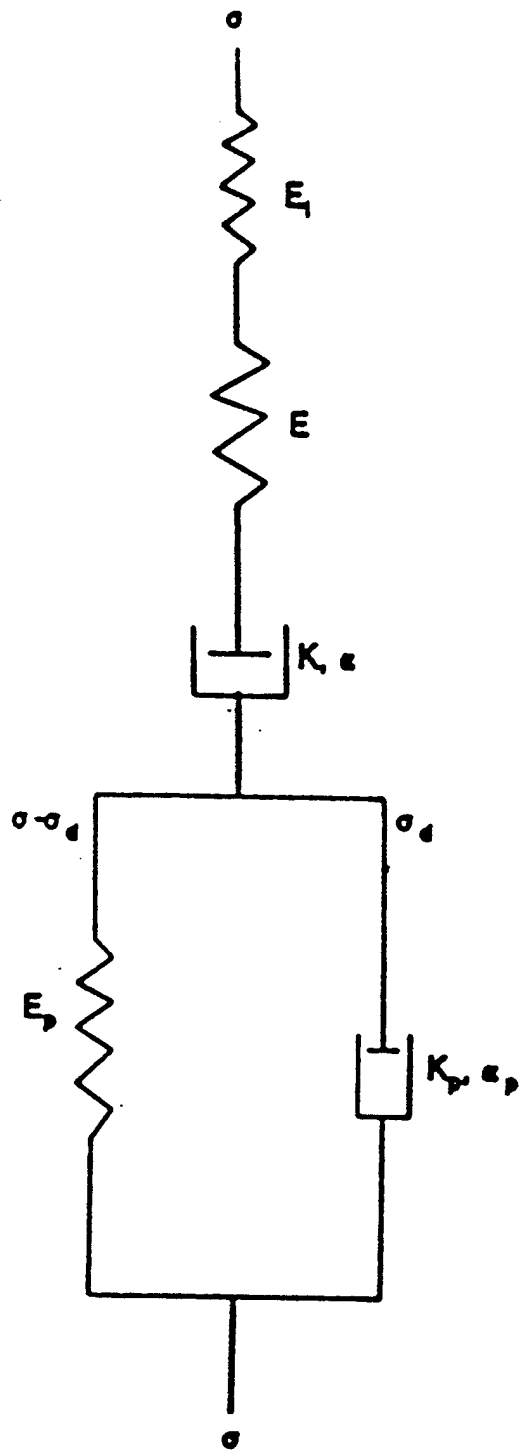
$\epsilon_i$  = instantaneous plastic strain

$\epsilon_d$  = transient creep strain

$\epsilon_p$  = secondary (constant) creep strain

The instantaneous strain,  $\epsilon_0 + \epsilon_i$ , upon the application of load is represented by the elastic elongation of spring  $E$  and the irrecoverable elongation of the spring  $E_1$ . Transient creep strain  $\epsilon_p$  and secondary creep strain  $\epsilon_d$  are represented by the action dashpot,  $k$ ,  $\alpha$ , in series with the parallel unit composed of the spring  $E_p$  and the dashpot  $k_p$ ,  $\alpha_p$ .

Instantaneous strains due to applied stress  $\sigma$  are represented by the following





expression:

$$\epsilon_0 = \frac{\sigma}{E}, \quad \epsilon_1 = \frac{\sigma}{E_1} \quad (2.33)$$

where

$\sigma$  = stress applied on the fine-element model

$E$  = spring modulus

$E_1$  = constant for response of spring element with irrecoverable deformation

From strain-time curves on different stress level obtained experimentally; the strains: total instantaneous, instantaneous recovery, and instantaneous irrecoverable; can be evaluated and the mean value of  $E+E_1$  be obtained by the previous equation (2.33).

Transient and secondary creep strains are respectively obtained, in terms of the rate process theory, by:

$$\ln(\dot{\epsilon}_d) = \ln\left(\frac{k}{2}\right) + \alpha \sigma \quad (2.34)$$

$$\dot{\epsilon}_p = K_p \sinh(\alpha_p \sigma_d) \quad (2.35)$$

where:

$\dot{\epsilon}_d$  = rate of transient creep strain

$\dot{\epsilon}_p$  = rate of secondary creep strain

$K$  = constant specifying the rate flow of the dashpot,  $\text{sec}^{-1}$

$\alpha$  = constant specifying the response as the resistance of the dashpot to force, in  $\text{psi}^{-1}$

$\sigma$  = stress applied to the five-element model, in psi

$K_p, \alpha_p$  = properties of the parallel spring and dashpot

$\sigma_d$  = stress acting on the parallel viscous element

Using the rate process theory,  $K_p$  and  $\alpha_p$  can be obtained from experimental data of a single strain-time curve; the values of  $K$  and  $\alpha$  can be obtained from the constant creep rate versus stress level curve.

The Komamura and Huang model describes the deformation behavior of soil when it is subjected to stress and water content conditions of different intensity. The model was suggested because there were cases on which water contents were below the visco-plastic limit for applied stresses larger than the critical stresses. The visco-plastic-elastic model is composed of Voight and Bingham elements in series, Figure 2.11. The relationship is expressed as follows:

$$\epsilon = \frac{1}{\eta_1}(\sigma - \sigma_0)t + \frac{\sigma}{E}\left(1 - e^{-\frac{E}{\eta_2}t}\right), \quad \sigma > \sigma_0 \quad (2.36)$$

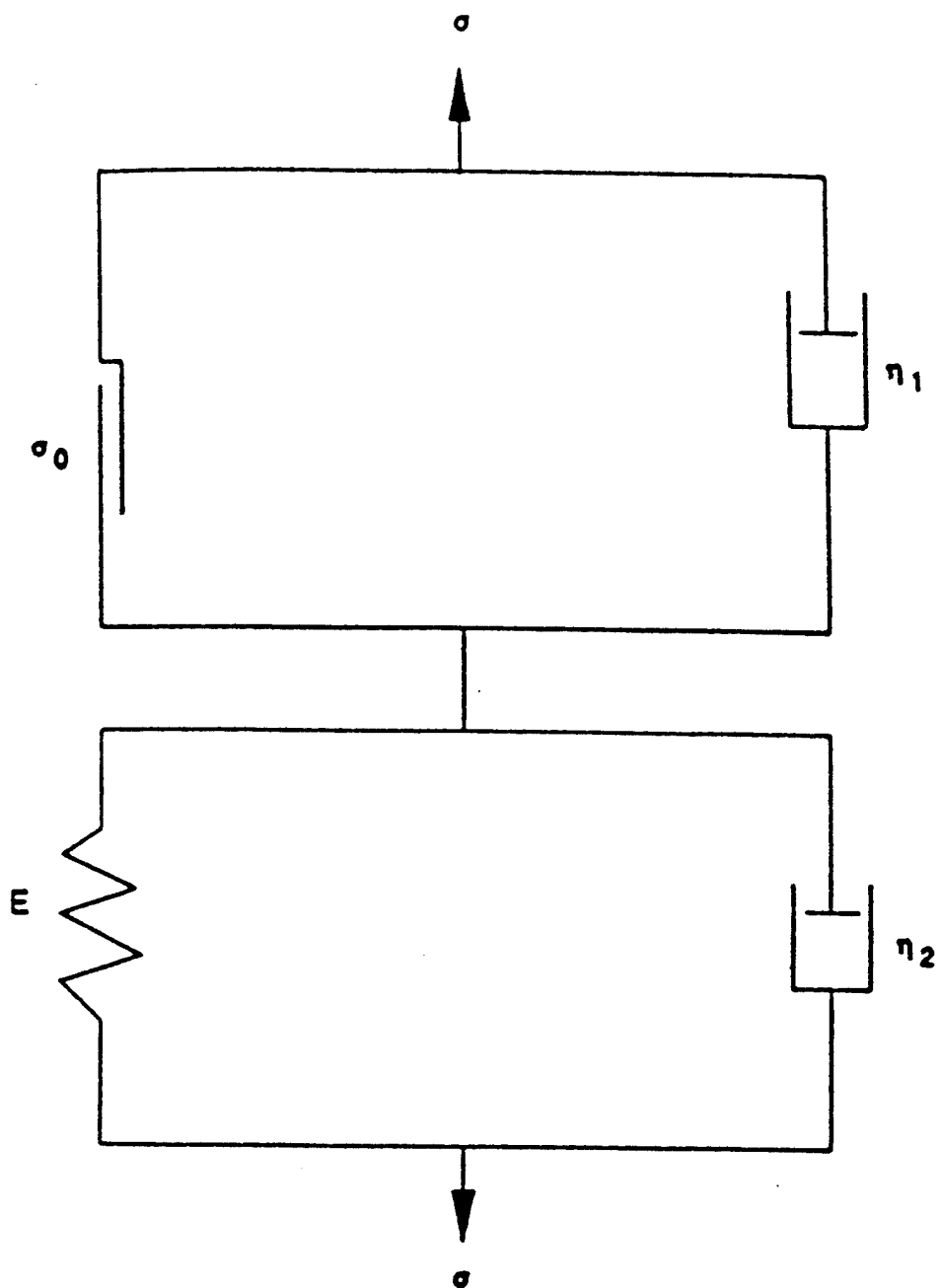


Figure 2.11 Rheological Model Suggested by Komamura and Huang (1974)

where:

$\epsilon$  = axial strain

$t$  = time

$\sigma$  = stress level,  $\sigma > \sigma_0$

$\sigma_0$  = critical stress

$\eta_1$  = Bingham viscosity

$\eta_2$  = Voight viscosity

$E$  = modulus of elasticity, spring constant for rheological model

Only the Voight model should be applied, Figure 2.12, if there is a case where the stress level applied is below the critical stress,  $\sigma_0$ , and the maximum slider element resistance exceeds the applied stress. The strain-stress-time relationship becomes:

$$\epsilon = \frac{\sigma}{E} (1 - e^{-\frac{E}{\eta_2} t}), \quad \sigma < \sigma_0 \quad (2.37)$$

if the case is when the water content is higher than the visco-plastic limit, a value of zero is given to the modulus of elasticity of the spring in the Voight unit. The model becomes as shown by Figure 2.13. The relationship is the following:

$$\epsilon = \frac{\sigma - \sigma_0}{\eta_1} t + \frac{\sigma}{\eta_2} t \quad (2.38)$$

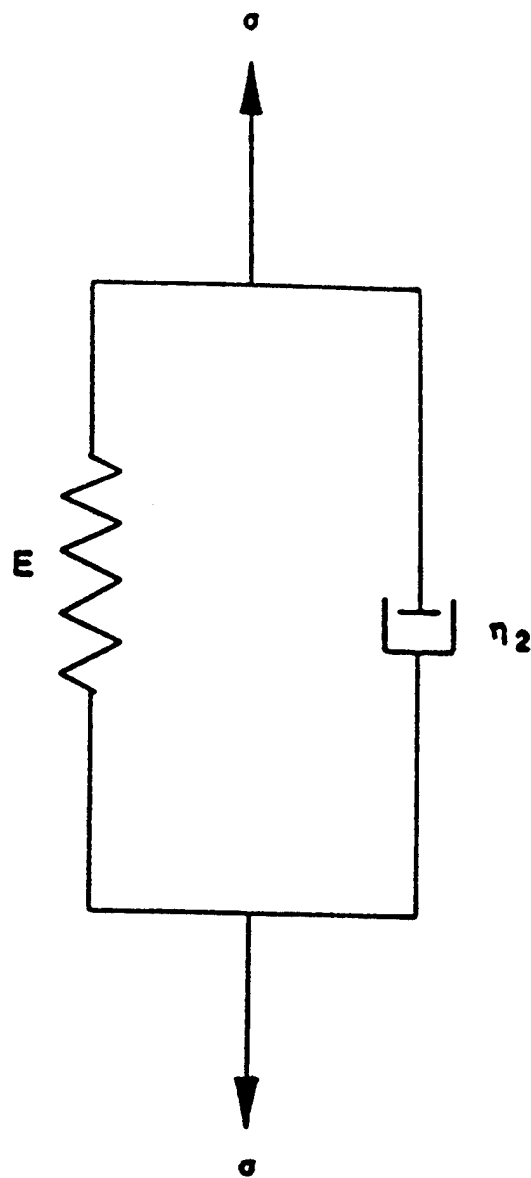


Figure 2.12 Model Proposed by Komamura and Huang for Visco-Elastic Case  
With Small Stress Levels (1974)

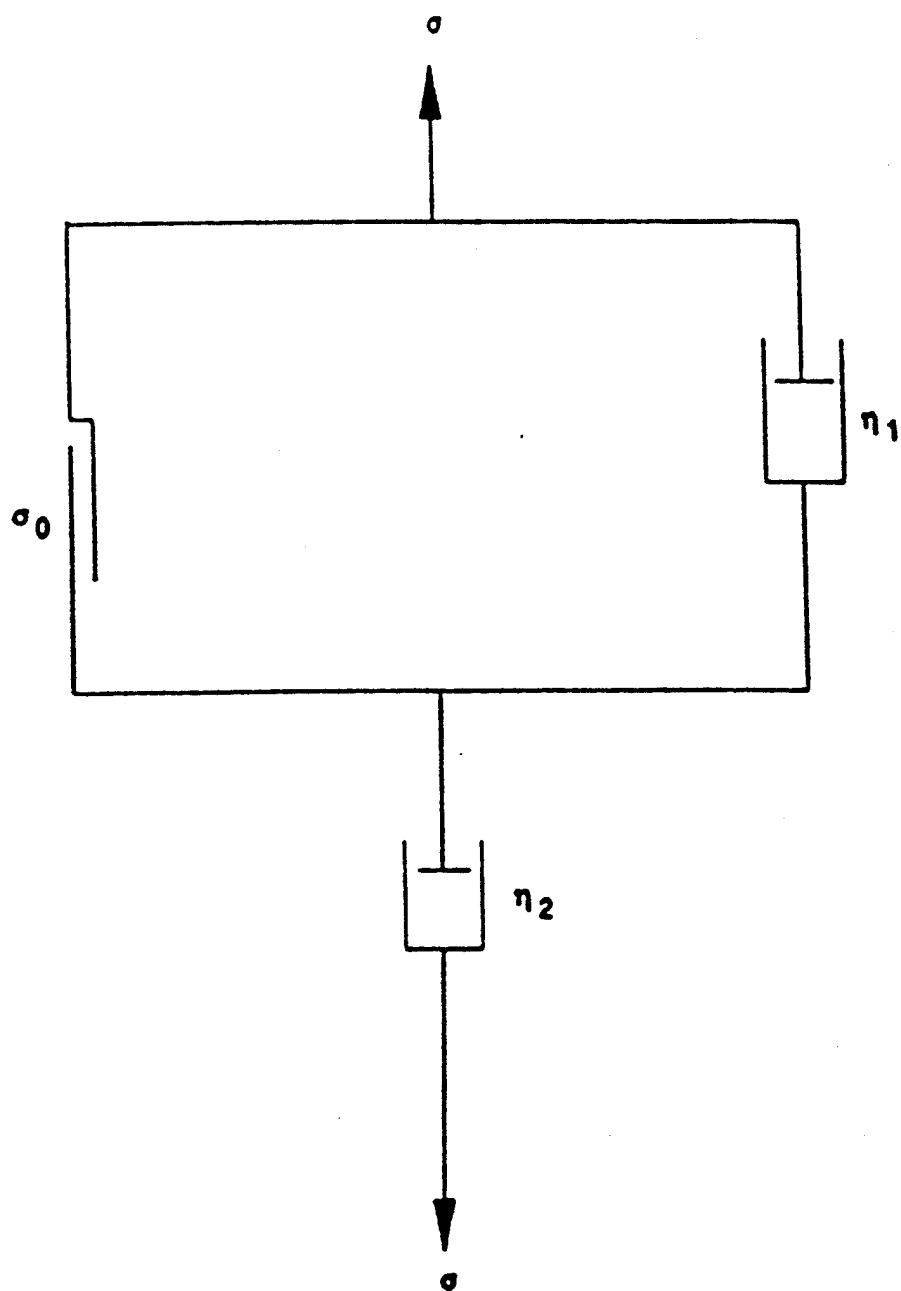


Figure 2.13 Visco-Plastic Model by Komamura and Huang for Water Content  
Above the Visco-Plastic Limit Case (1974)

when the case presents water contents higher than the liquid limit, the rheological model becomes the viscous model presented in Figure 2.14. The relationship is the following:

$$\epsilon = \left( \frac{1}{\eta_1} + \frac{1}{\eta_2} \right) \sigma t \quad (2.39)$$

The rheological coefficients of soil in all the above models vary accordingly to the water content of a particular case.

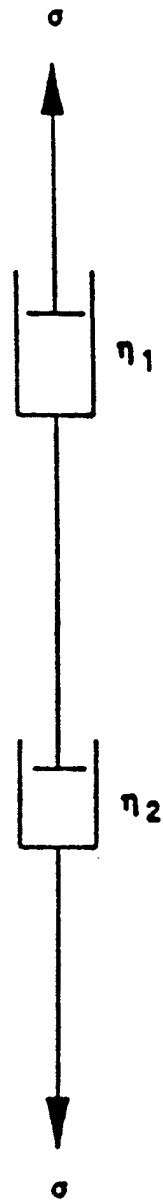


Figure 2.14 Komamura and Huang Viscous Model for Water Contents Higher Than Liquid Limit (1974)



## CHAPTER THREE

### PREPARATION OF SPECIMENS

#### 3.1 INTRODUCTION

In this chapter the preparation of specimens and the test set-up are described. Preparation of samples was conducted in a constant room temperature at 20° C and under controlled moisture conditions. Conventional triaxial cells were the main part of the test set-up.

#### 3.2 PREPARATION OF SPECIMENS

##### 3.2.1 Soil Stock Preparation

This study used the recycled soil previously employed by the parent project. Such soil was subjected to treatment during that time. All soluble matter had been removed and a strict control of the chemical make-up of the pore fluid was established. This process is explained in detail in pages 57, 58, and 59 of final report for the parent project.

The preparation of new soil stock was performed by placing the recycled chips in a recipient to oven dry them. The dry soil was washed with fresh salt solution, 0.01 molal calcium chloride, of 1900 micromhos/cm electrical conductivity. This process consisted in dispersing the soil into a container using the solution, and allowing the

soil suspension to flocculate and sediment at the bottom. The clean supernatant was decanted and the process repeated until its electrical conductivity approached 1900 micromhos/cm. Table 3.1 presents the records of the various stock batches for this study. When the desired electrical conductivity was obtained by the supernatant, the remaining soil suspension was placed in centrifuge bottles and centrifugated during 15 minutes at 2000 rpm. The centrifuge created a segregated soil cake which was recovered from each bottle and placed on a glass plate. With the use of a spatula, the soil slurry was thoroughly mixed until a homogeneous condition existed. At such condition, soil moisture in the suspension has been reduced allowing for a shorter consolidation time and a better control of specimen volume changes while being consolidated.

### 3.2.2 Consolidation of Specimens

Using a conventional triaxial cell of 2.8 inch diameter pedestals, top and bottom, an appropriate rubber membrane was fixed with a rubber string at the bottom pedestal and the slurry was placed inside the membrane, over a filter paper and corundum porous stone. When the membrane was filled-up with slurry to an approximate height of five inches, a filter paper, corundum stone, and top cap were placed inside. The cap, having the lower portion inside the membrane, was secured

Table 3.1

## Record of Electrical Conductivity Readings

Soil Stock Preparation #	Date	Conductivity micro-siemmens	Cycle of Wash #
1	2/27/93	2330	1
1	3/1/93	2310	2
1	3/3/93	2300	3
1	3/7/93	2150	4
1	3/8/93	2100	5
1	3/9/93	2070	6
1	3/10/93	1984	7
1	3/11/93	1905	8
1	3/12/93	1901	9
2	8/3/93	2600	1
2	8/6/93	2300	2
2	8/8/93	2100	3
2	8/9/93	2100	4
2	8/11/93	2030	5
2	8/12/93	2000	6
2	8/15/93	1985	7

Notes:

Electrical conductivity of 0.01M calcium chloride solution is 1900 micro-siemmens.

Continuation of Table 3.1

Record of Electrical Conductivity Readings

Soil Stock Preparation #	Date	Conductivity micro-siemmens	Cycle of Wash #
2	8/16/93	1930	8
2	8/18/93	1910	9
3	3/17/94	-	1
3	3/20/94	2300	2
3	3/23/94	2100	3
3	3/24/94	2100	4
3	3/25/94	1984	5
3	3/26/94	1985	6
3	3/27/94	1930	7
3	3/28/94	1905	-
4	8/31/94	-	1
4	9/1/94	2300	2
4	9/2/94	-	3
4	9/6/94	2400	4
4	9/7/94	1900	-
4	9/8/94	1900	5

Notes:

Electrical conductivity of 0.01M calcium chloride solution is 1900 micro-siemmens.

Continuation of Table 3.1

Record of Electrical Conductivity Readings

Soil Stock Preparation #	Date	Conductivity micro-siemmens	Cycle of Wash #
4	9/9/94	1900	-
5	3/22/95	-	1
5	3/23/95	2410	2
5	3/25/95	2215	3
5	3/27/95	2005	4
5	3/28/95	2010	-
5	3/29/95	1981	-
5	3/29/95	1981	-
5	3/30/95	1910	-

Notes:

Electrical conductivity of 0.01M calcium chloride solution is 1900 micro-siemmens.

in the same manner as the bottom pedestal, using rubber strings which pressed the membrane against the acrylic surface of the top cap. Next, the cell was assembled and completely filled with tap water through the top opening for the pressure application. When filled, the cell was taken to the temperature room which already

had a permanent 20°C temperature. Inside the room the cell was connected, from its top opening to the pressure supply using a polyethylene line, and from the bottom polyethylene line to a burette for monitoring the specimen's expelled water. The burette had a closed valve at the bottom and was also partially filled with distilled water. When all line connections were secured, 50 psi air pressure was applied and the burette valve opened in a simultaneous manner. Thus, the consolidation was started at 50 psi cell pressure and with the outflow of the specimen directed towards the burette; where a record was kept of the volume of water expelled from the specimen versus time. Figure 3.1 presents the consolidation set-up.

Appendix A contains the records of monitored volume of fluid expelled for each specimen. The results of sixty eight consolidated specimens are included. Also, a summary of the conditions and results during the consolidation phase of all specimens is presented in Table 3.2. The results indicate that the full consolidation phase required a period of time of about two weeks (20,000 to 25,000 minutes). From the appendix it is noticed that a primary 100% consolidation was achieved during the initial 2,000 to 3,000 minutes. The results of Table 3.2 suggest that the specimens were not exactly the same with respect to the initial water content of the slurry specimen before starting to consolidate. Such differences were caused because of the supernatant left after the stock preparation was not always the same for all

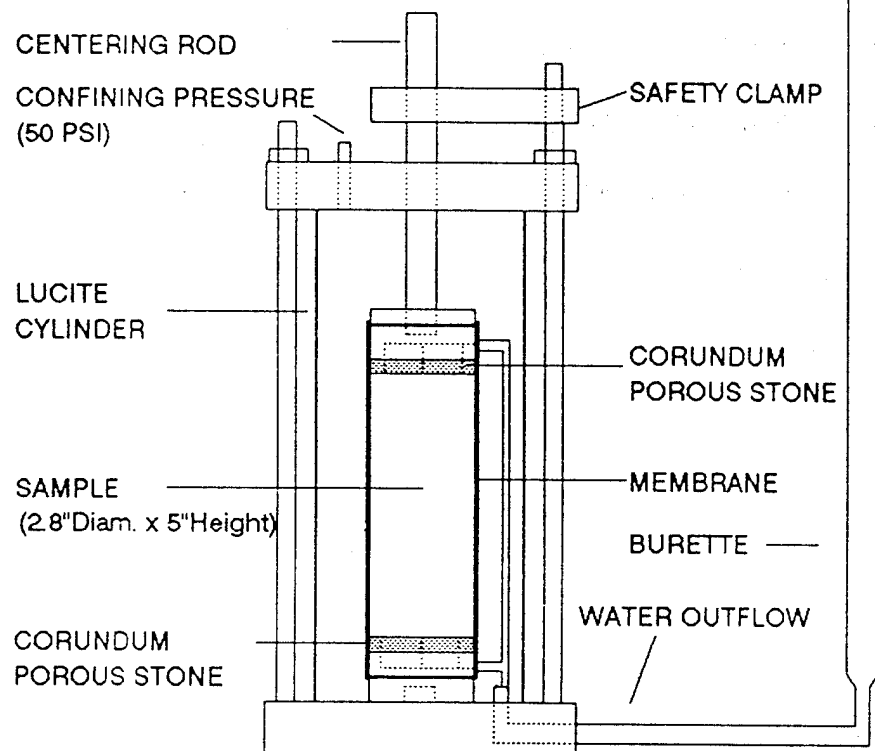


Figure 3.1 Schematic of Consolidation Apparatus

Table 3.2

## Conditions and Results of Consolidated Specimens

Specimen No.	Consolida- tion Time, hrs.	Water Outflow, ml	Specimen No.	Consolida- tion Time, hrs.	Water Outflow, ml
1	340	138	20	339	174
2	355	143	21	348	160
3	333	126	22	404	178
4	355	200	23	335	181
5	339	166	24	342	194
6	339	194	25	415	168
7	409	132	26	336	190
8	410	172	27	359	172
9	339	162	28	360	174
10	332	117	29	348	171
11	435	191	30	339	185
12	409	118	31	415	168
13	338	245	32	344	166
14	338	99	33	344	169
15	334	151	34	371	83
16	336	261	35	334	162
17	384	145	36	336	187
18	337	131	37	383	165
19	359	315	38	335	491



Continuation of Table 3.2  
Conditions and Results of Consolidated Specimens

Specimen No.	Consolida- tion Time, hrs.	Water Outflow, ml	Specimen No.	Consolida- tion Time, hrs.	Water Outflow, ml
39	383	165	54	309	87
40	380	86	55	289	153
41	318	120	56	360	159
42	313	118	57	289	140
43	313	136	58	336	85
44	405	136	59	311	113
45	337	111	60	361	150
46	357	130	61	315	133
47	310	87	62	355	135
48	335	140	63	308	145
49	334	158	64	331	115
50	335	135	65	316	146
51	332	163	66	291	109
52	393	185	67	334	93
53	335	140	68	379	96

batches, and also because during the mixing of slurry on the glass plate some water loss occurred. But fortunately, the consolidation process was controlled by the length of time for reaching the 100% primary consolidation and not by the total amount of

fluid expelled. Thus, the differences in amounts of expelled water between specimens did not affect the purpose of this study. Typical volumes of expelled water ranged from 85 ml to 415 ml.

### 3.2.3 Specimen Equilibration

After the consolidation process was completed, the cell was disassembled and the specimen removed and trimmed to a final diameter of 1.4 inches and 3.0 inches in length. Figures 3.2 and 3.3 show the specimen before and after trimming, respectively. The shavings produced in this trimming process were used to determine the water content of the specimen after the consolidation phase. Water content values are presented in Chapter 5. The trimmed specimen was enclosed with an appropriate rubber membrane and placed inside a triaxial cell. Figures 3.4 and 3.5 show a schematic of the apparatus set-up used for the equilibrium process. The triaxial cell contained a top acrylic pedestal suitable for the drainage condition upon which the creep\recovery testing would be conducted at the end of this equilibration process.

For drained conditions, the top loading pedestal was simply a 1.4 inch in diameter solid cylindrical acrylic with two openings for pore-air pressure application, but for undrained condition, the loading cap of Figure 3.6 was designed. It consisted of two acrylic pieces separated by a rubber membrane and held together by four screws. Its main features were the air outlet located below the rubber membrane labeled "Air Outlet" in the side view of Figure 3.6. and the air inlet located on the

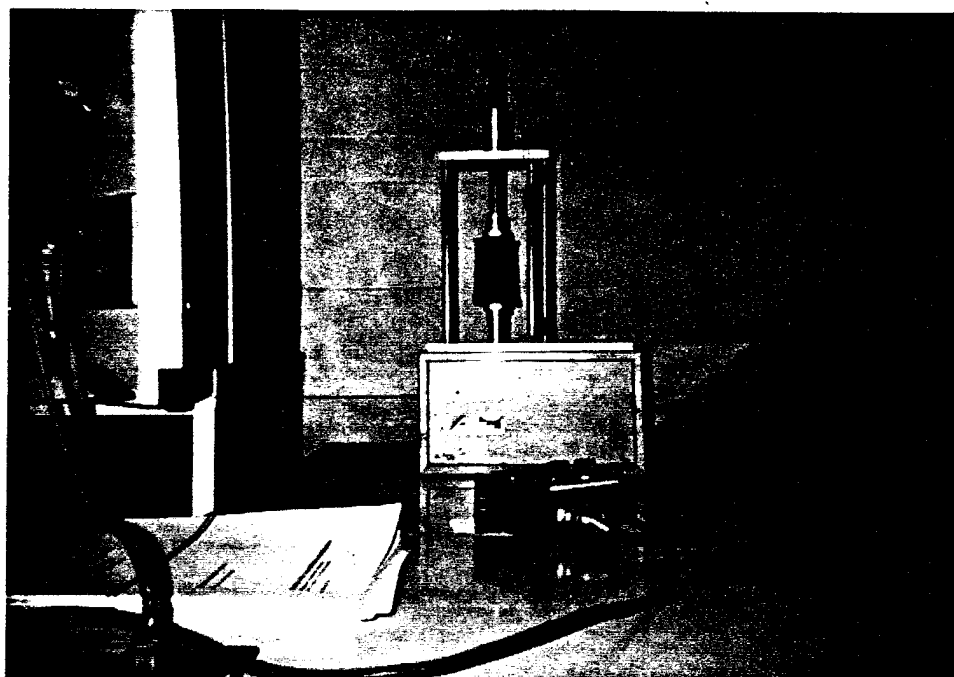


Figure 3.2 Specimen Before Trimming

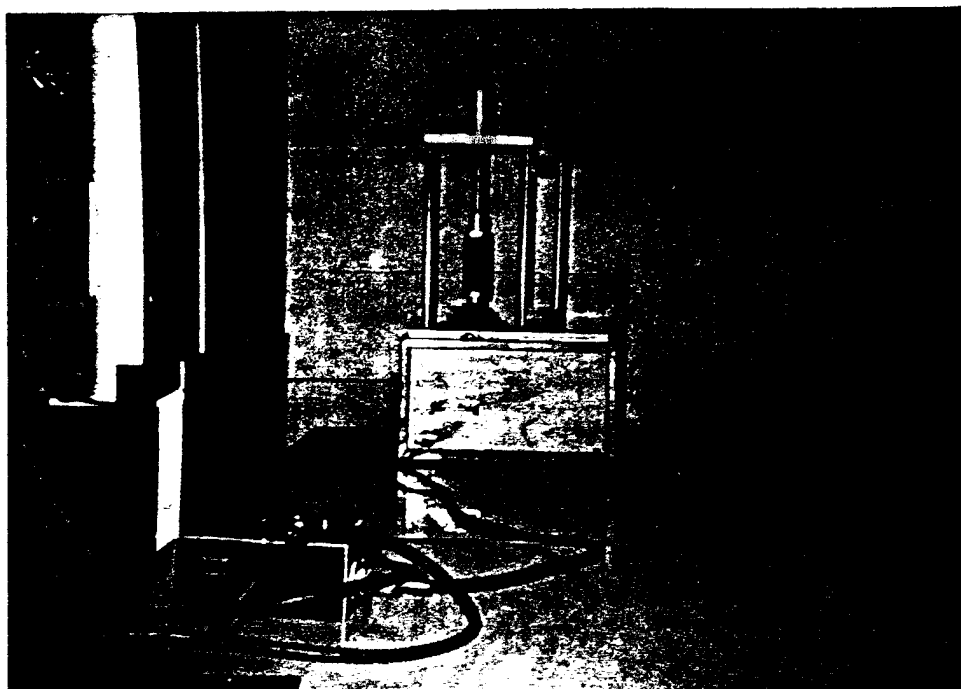


Figure 3.3 Specimen After Trimming

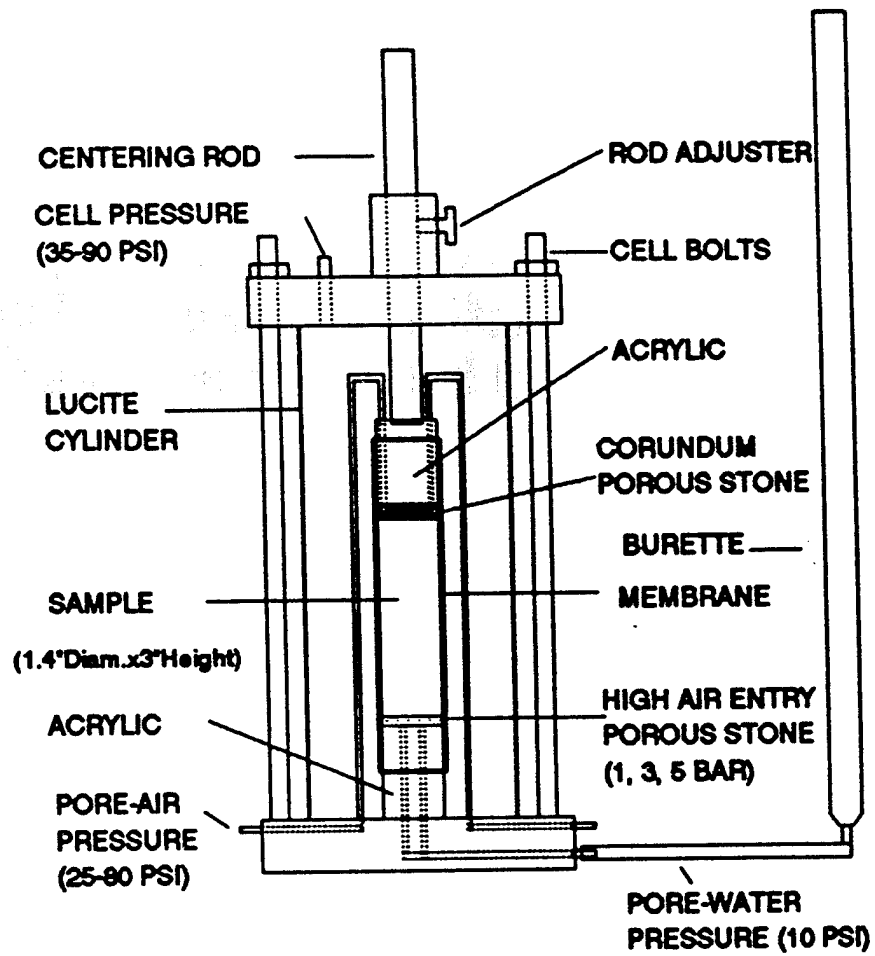


Figure 3.4 Schematic of Set-up For Equilibrium Process on a Specimen to be Subjected to Creep/Recovery Under Drained Conditions

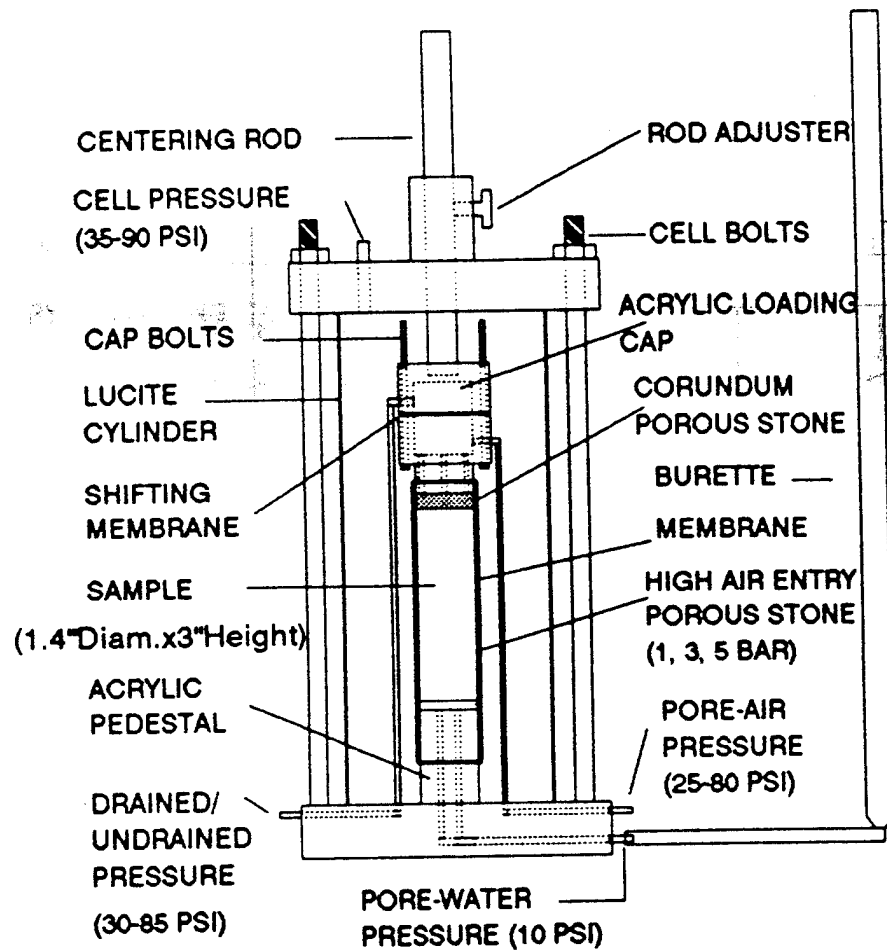
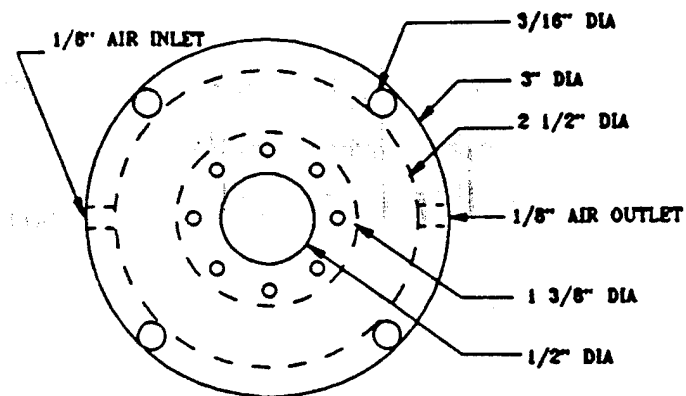
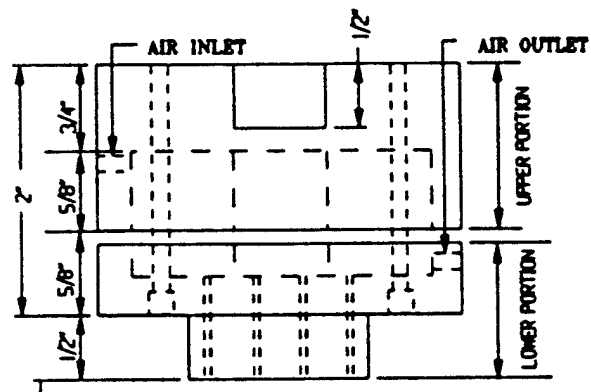


Figure 3.5      Schematic of Set-up For Equilibrium Process on a Specimen to be Subjected to Creep/Recovery Under Undrained Conditions



TOP VIEW



SIDE VIEW

Figure 3.6 Schematic of Loading Cap For Undrained Testing Conditions

other side of the rubber membrane, that is above the membrane, and labelled "Air inlet" in the side view of Figure 3.6. Maintenance of the cap required its disassemblance and installation of a new membrane, every time a new specimen required to be tested. Operation process of the cap required that during the equilibration phase, pore air pressure was to be applied through "Air Outlet" of Figure 3.6, while the "Air Inlet" was opened to atmospheric pressure. Upon completion of the equilibration phase, air pressure exceeding the pore air pressure by about 10 psi was applied at "Air Inlet". Consequently, the excess air pressure applied on top of the membrane caused it to stretch downwards shutting the connections of "Air Outlet". The transparency of the cap allowed the user to observe the membrane actually switching position at the time of switching drainage conditions.

The bottom pedestal of the cell contained a high air entry porous disk made of ceramic which replaced the usual corundum porous stone. In order to equilibrate the specimen to predetermined soil suctions of 15 psi, 30 psi, 40 psi, and 70 psi; the disk was used to control independently the pore water pressure and pore air pressure in the specimen. It allowed the slow passage of water but not the flow of free air as long as the difference between air and water pressures did not exceed the air entry value of the disk. Table 3.3 presents the disks used during this study. With the disk, a continuous column of water would be obtained from the specimen to the water below the disk. To obtain the continuous water flow, the disk was saturated with distilled water.



Table 3.3

## Characteristics of High Air Entry Porous Disks

Air Entry Value	Diameter, in	Thickness, in
1 bar (14.7 psi)	1.125	0.28
3 bar (44.7 psi)	1.175	0.35
5 bar (73.5 psi)	1.115	0.31

With the peculiarities of both acrylic pedestals, the specimen enclosed by the membrane, and with a filter paper between the specimen and the disk, was fixed at the bottom using rubber strings while at the top a filter paper and corundum porous stone were installed between specimen and acrylic before securing the membrane with rubber strings. Once the specimen was secured, the cell was assembled and filled with tap water using the top valve of the cell. Then, it was placed inside the temperature room, which had a 20 °C temperature already set, and connected to the air pressure supply and to a burette. The pore air pressure was applied on the top of the specimen through a bottom valve of the cell and the confining cell pressure was applied through the top valve of the cell. The pore water pressure was controlled through the bottom disk using the burette which monitored the pore fluid being expelled or imbibed. The burette was connected from the top to a 10 psi air pressure source. With all the proper connections ready and the burette partially filled with distilled water, the pressures were applied, first the confining and then the pore air. The valve at the bottom of the burette was opened and the fluid movement monitored.

Appendix B contains the individual records of volume of pore fluid expelled or imbibed with respect to time for each specimen. A summary of the conditions imposed in all the equilibrated specimens is presented in Table 3.4. From the table, the volume of pore fluid expelled during the equilibration phase ranged from fractions of a milliliter, to 45 ml, which was the case for specimen eleven equilibrated at 70 psi suction. The imbibed volume ranged from 0.2 ml to 6 ml depending on the soil suction. In general, there is a large volume of pore fluid expelled when the applied soil suction exceeded the cell pressure in the consolidation cell of 50 psi. For soil suction levels lower than this cell pressure, the volume of fluid expelled was expected to be small as it occurred for all the specimens with only two exceptions: specimens number 2 and 11. Specimen five never reached equilibrium, even after more than a month in process. This specimen was discarded since it appeared that the membrane had a pore that allowed the transfer of water from the cell to the specimen. Specimen 64 was broken while trimming it.

For most of the specimens, the time necessary to reach equilibrium ranged from 10,000 min. (one week) to more than 20,000 min. (two weeks). In general, poor correlation was observed between the volume of fluid expelled during the equilibration phase and the time necessary to reach equilibrium. Thus the criteria used to stop the equilibration phase was to make sure that the movement of water, in or out of the specimen, had leveled off.

Table 3.4

## Conditions During Specimen Equilibration Phase

Specimen No.	Pore-water Pressure psi	Pore-air Pressure psi	Soil Suction psi	Cell Pressure psi	Equilibra- tion Time hrs.	Pore-water Movement ml
1	10	80	70	90	316	1.90
2	10	25	15	35	353	19.50
3	10	25	15	35	329	0.40
4	10	50	40	60	340	4.06
5	10	80	70	90	865	18.70
6	10	80	70	90	571	18.65
7	10	40	30	50	320	0.50
8	10	80	70	90	370	10.50
9	10	40	30	50	436	-0.25
10	10	40	30	50	432	10.80
11	10	80	70	90	408	45.10
12	10	40	30	50	400	0.80
13	10	80	70	90	406	1.20
14	10	80	70	90	455	13.30
15	10	80	70	90	388	-0.84
16	10	80	70	90	388	6.40
17	10	50	40	60	350	14.30
18	10	50	40	60	335	11.70
19	10	50	40	60	337	7.90

Continuation of Table 3.4

Conditions During Specimen Equilibration Phase

Specimen No.	Pore-water Pressure psi	Pore-air Pressure psi	Soil Suction psi	Cell Pressure psi	Equilibra- tion Time hrs.	Pore-water Movement ml
20	10	80	70	90	464	10.75
21	10	80	70	90	458	0.49
22	10	25	15	35	110	0.20
23	10	50	40	60	431	0.67
24	10	50	40	60	430	3.93
25	10	80	70	90	400	5.92
26	10	80	70	90	492	4.97
27	10	25	15	35	284	0.54
28	10	25	15	35	333	-0.08
29	10	25	15	35	333	0.79
30	10	50	40	60	391	6.32
31	10	50	40	60	383	1.32
32	10	80	70	90	284	36.06
33	10	25	15	25	287	0.44
34	10	50	40	60	336	0.07
35	10	50	40	60	336	-0.20
36	10	50	40	60	410	10.70
37	10	80	70	90	408	11.95
38	10	80	70	90	407	3.40

Continuation of Table 3.4

Conditions During Specimen Equilibration Phase

Specimen No.	Pore-water Pressure psi	Pore-air Pressure psi	Soil Suction psi	Cell Pressure psi	Equilibra- tion Time hrs	Pore-water Movement ml
39	10	25	15	35	287	0.44
40	10	80	70	90	406	-0.62
41	10	40	30	50	404	5.52
42	10	40	30	50	337	-5.20
43	10	40	30	50	357	-2.87
44	10	40	30	50	357	-4.92
45	10	80	70	90	357	0.50
46	10	40	30	50	336	2.89
47	10	40	30	50	330	1.49
48	10	80	70	90	332	3.03
49	10	25	15	35	335	3.95
50	10	80	70	90	335	5.20
51	10	25	15	35	334	-0.35
52	10	50	40	60	358	2.25
53	10	40	30	50	332	3.03
54	10	50	40	60	316	3.42
55	10	80	70	90	335	6.60
56	10	50	40	60	310	14.00
57	10	50	40	60	333	2.80

Continuation of Table 3.4

Conditions During Specimen Equilibration Phase

Specimen No.	Pore-water Pressure psi	Pore-air Pressure psi	Soil Suction psi	Cell Pressure psi	Equilibra- tion Time hrs.	Pore-water Movement ml
58	10	80	70	90	332	-0.70
59	10	40	30	50	310	3.55
60	10	25	15	35	272	1.25
61	10	50	40	60	311	4.80
62	10	25	15	35	312	1.20
63	10	40	30	50	217	-4.40
64	*	*	*	*	*	*
65	10	25	15	35	375	1.70
66	10	50	40	60	377	1.47
67	10	80	70	90	304	7.00
68	10	25	15	35	336	7.40

Notes:

(\*) = Specimen broken during trimming.

### 3.3 TEST SET UP

A schematic of the apparatus for performing the testing is shown by Figures 3.7 and 3.8. The same triaxial cell used for equilibration was also used for the

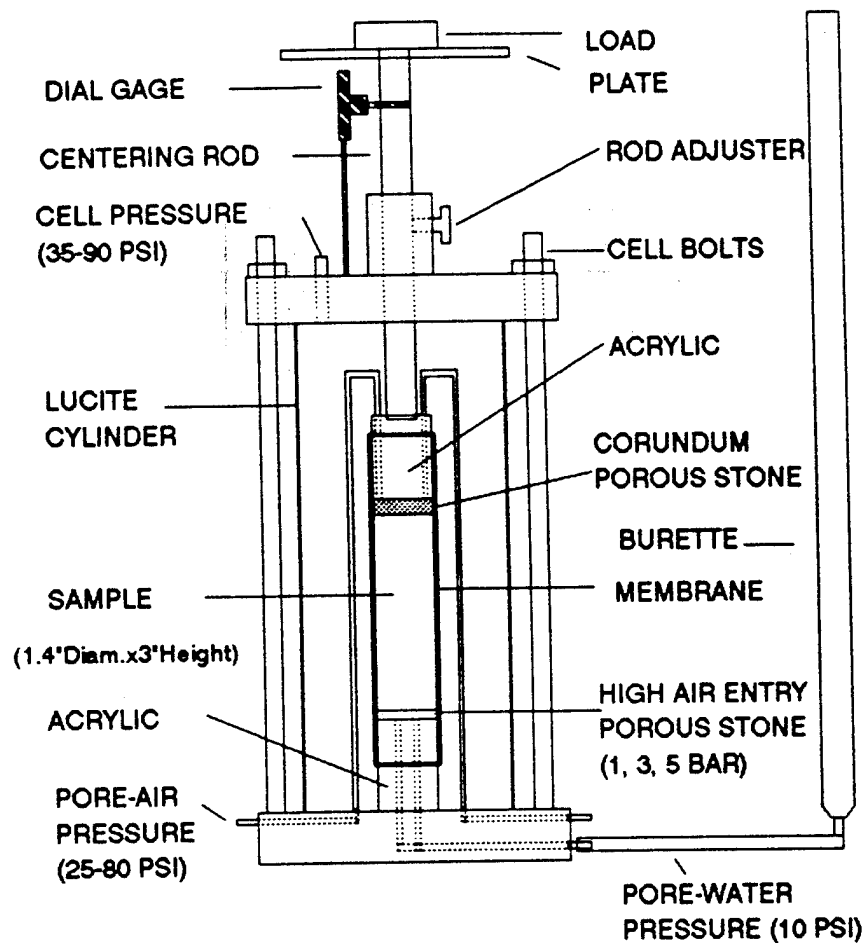


Figure 3.7      Apparatus Set-up For Creep/recovery Testing Under Drained Conditions

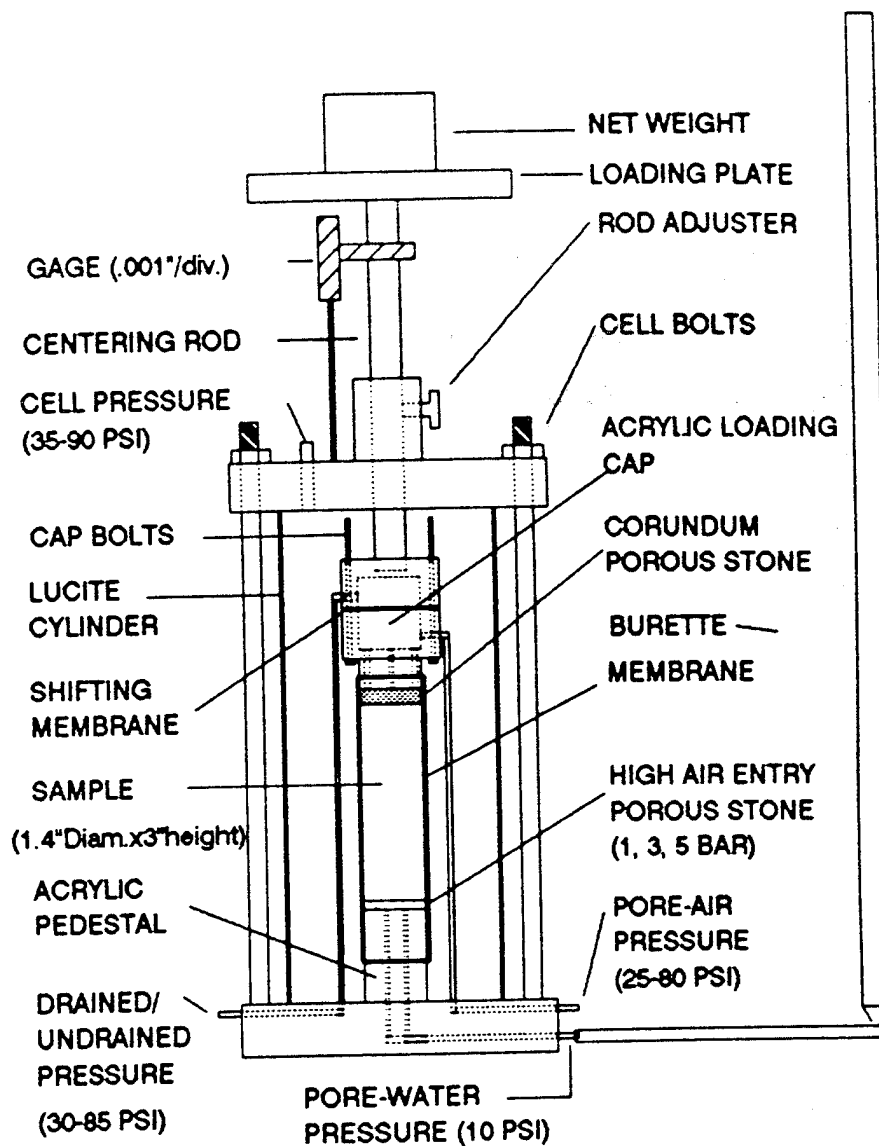


Figure 3.8 Apparatus Set-up For Creep/recovery Testing Under Undrained Conditions



creep/recovery testing. Without unloading the cell or altering the pressures and any other connection, the loading rod was tightened. A 0.0001 in dial gage was attached to the rod and a loading plate fixed at the top of the rod. The desired load was placed on the plate. For tests under undrained conditions, the line connected to the top chamber of the loading cap was connected to a pressure supply which was 10 psi more than the pore-air pressure being applied. Consequently, the shifting membrane moved down and completely sealed the upper end of the specimen. Immediately, the bottom valve of the triaxial cell upon which the burette was connected was also closed and the lower end of the specimen was completely sealed. The maneuvers made the undrained condition possible. Basically, that was the composition of the test set-up and four triaxial cells were available for setting up simultaneous tests. Since the cell pressure and the friction between the rod and cell bushings affected the load transmitted by the rod to the specimen under testing, the four cells were calibrated. Table 3.5 summarizes the four linear regression equations obtained to calculate the loads to account for cell pressure and friction effects. These same equations were used for this study.

Table 3.5

Equations For Calculating Necessary Load To Balance Cell Pressure and Friction

Cell No.	Regression Equation
1	$Y = 0.10052X - 1.663494$
2	$Y = 0.10182X - 1.985027$
3	$Y = 0.09133X - 1.546964$
4	$Y = 0.09093X - 1.393695$

Notes:

X = Cell pressure, psi.

Y = Balanced load, kg.

## CHAPTER FOUR

### CREEP AND RECOVERY TESTING

#### 4.1 INTRODUCTION

The creep and recovery tests performed, along with the results, are described and discussed in this chapter. The tests were performed in conventional triaxial cells previously used for equilibrium to evaluate the strain-stress-time behavior of unsaturated clayey specimens. Undrained and drained conditions during testing were practiced. All testing was conducted at constant room temperature of 20 degrees Celsius.

#### 4.2 DESCRIPTION OF TESTING PROCEDURES

When the equilibrium phase was ended and the set-up was ready for creep, the desired gross load was applied on the loading platform, recall Figures 3.7 and 3.8.

At this point initial readings at gage, and burette for the drained condition cases, were recorded. The rod tightener was loosed and the displacements were recorded using the dial gage. Specimens were monitored until the "steady state" creep had been reached.

After this, the gross load was removed and the recovery experienced by the specimen was similarly monitored by the dial gage until a steady state was also

reached. After all testing was completed, the sample was removed and its moisture content determined. Chapter five contains the information.

#### 4.3 DISCUSSION OF RESULTS

Appendix C presents the records of each creep and recovery test performed. The conditions of such conducted tests along with the obtained results are summarized in Table 4.1. Creep tests were completed for the series of 70 psi, 40 psi, and 15 psi. For 30 psi suction, drained tests with deviatoric stresses of 17.19 psi, 22.91 psi, 28.64 psi, and 34.37 psi were not performed due to time limitation and termination of this project.

Most of the specimens exhibited the general creep development discussed in Chapter 2. For most specimens, the steady state creep was reached after about 5000 minutes (3.5 days). Furthermore, no tertiary phase was ever observed.

With the results, it is possible to compare the effects of drained versus undrained conditions upon tests. For illustration purposes, Figure 4.1 presents the results of tests on specimens fifteen (drained) and thirteen (undrained) which clearly indicate the higher axial strain change that occurs when drained conditions exists. The illustration allows to notice how this condition has significant influence during the

Table 4.1

## Summary of Conditions and Results of Creep/Recovery Tests

Specimen No.	Soil Suction psi	Cell Pressure psi	Deviatoric Stress psi	Asymptotic Strain %	Time for Creep hrs.	Time for Recovery hrs.
1 U	70	90	40.10	2.50	115	*
2 D	15	35	5.73	3.75	335	*
3 U	15	35	5.73	11.20	334	*
4 D	40	60	34.37	8.50	573	96
5 +	70	90	17.19	none	none	none
6 U	70	90	5.73	6.75	307	*
7 U	30	50	11.46	15.00	405	*
8 U	70	90	5.73	1.50	389	100
9 U	30	50	11.46	0.95	415	*
10 U+	30	50	11.46	0.35	2	none
11 U+	70	90	5.73	0.40	1.5	none
12 D	30	50	11.46	0.71	337	126
13 U	70	90	51.56	11.98	502	212
14 D	70	90	51.56	16.00	476	17
15 D	70	90	51.56	16.50	351	46

Notes:

D = Drained condition.

U = Undrained condition.

+ = Specimens presenting problems during testing.

\* = Specimen failure, recovery not done.

Continuation of Table 4.1

Summary of Conditions and Results of Creep/Recovery Tests

Specimen No.	Soil Suction psi	Cell Pressure psi	Deviatoric Stress psi	Asymptotic Strain %	Time for Creep hrs.	Time for Recovery hrs.
16 D	70	90	40.10	7.30	350	46
17 U	40	60	34.37	4.25	335	120
18 D	40	60	28.64	5.40	15	*
19 U	40	60	28.64	1.13	409	44
20 D	70	90	11.46	0.62	414	42
21 D	70	90	5.73	7.70	391	95
22 D	15	35	5.73	4.40	335	149
23 D	40	60	28.64	7.70	457	26
24 D	40	60	22.91	4.40	525	90
25 D	70	90	28.64	2.64	497	49
26 D	70	90	17.19	1.13	425	*
27 D	15	35	22.91	1.85	574	79
28 D	15	35	17.19	1.96	456	170
29 D	15	35	11.46	0.95	481	141
30 D	40	60	11.46	1.72	333	122
31D	40	60	5.73	1.21	335	165

Notes:

D = Drained condition.

U = Undrained condition.

\* = Specimen failure, recovery not done.

Continuation of Table 4.1

Summary of Conditions and Results of Creep/Recovery Tests

Specimen No.	Soil Suction psi	Cell Pressure psi	Deviatoric Stress psi	Asymptotic Strain %	Time for Creep hrs.	Time for Recovery hrs.
32 D	70	90	22.91	2.16	332	69
33 D	15	35	28.64	12.02	358	21
34 U	40	60	22.91	3.04	431	167
35 D	40	60	51.56	8.41	385	*
36 U	40	60	5.76	1.66	343	68
37 U	70	90	17.19	1.23	342	120
38 U	70	90	22.91	2.43	340	4
39 U	15	35	5.73	0.23	367	none
40U	70	90	34.37	6.25	478	143
41U	30	50	40.10	21.75	498	136
42U	30	50	34.37	8.47	385	*
43U	30	50	28.65	4.02	453	116
44U	30	50	22.92	3.50	482	145
45U	70	90	28.65	2.62	479	95
46U	30	50	11.46	2.07	476	72
47U	30	50	5.73	2.23	490	154

Notes:

D = Drained condition.

U = Undrained condition.

\* = Specimen failure, recovery not done.

Continuation of Table 4.1

Summary of Conditions and Results of Creep/Recovery Tests

Specimen	Soil	Cell	Deviatoric	Asymptotic	Time for	Time for
No.	Suction	Pressure	Stress	Strain	Creep	Recovery
	psi	psi	psi	%	hrs.	hrs.
48U	70	90	11.46	0.33	335	152
49U	15	35	28.65	18.77	358	*
50D	70	90	34.37	6.75	336	none
51U	15	35	22.92	3.77	405	73
52D	40	60	17.19	1.36	354	123
53D	30	50	40.10	6.50	316	none
54U	40	60	51.56	8.96	336	none
55U\$	70	90	-	-	-	-
56U	40	60	17.19	10.37	310	172
57U	40	60	11.46	6.40	349	60
58U\$	70	90	-	-	-	-
59D	30	50	5.73	3.85	409	none
60U	15	35	11.46	0.430	307	none
61U\$	40	60	-	-	-	-
62U	15	35	17.19	5.60	311	none

Notes:

D = Drained condition.

U = Undrained condition.

\$ = Specimen used for dynamic test.



Continuation of Table 4.1

Summary of Conditions and Results of Creep/Recovery Tests

Specimen No.	Soil Suction psi	Cell Pressure psi	Deviatoric Stress psi	Asymptotic Strain %	Time for Creep hrs.	Time for Recovery hrs.
63U\$	30	50	-	-	-	-
64D+	30	50	11.46	none	none	none
65U\$	15	35	-	-	-	-
66U\$	40	60	-	-	-	-
67U\$	70	90	-	-	-	-
68U\$	15	35	-	-	-	-

Notes:

D = Drained condition.

U = Undrained condition.

\$ = Specimen used for dynamic test.

+ = Specimens presenting problems during testing.

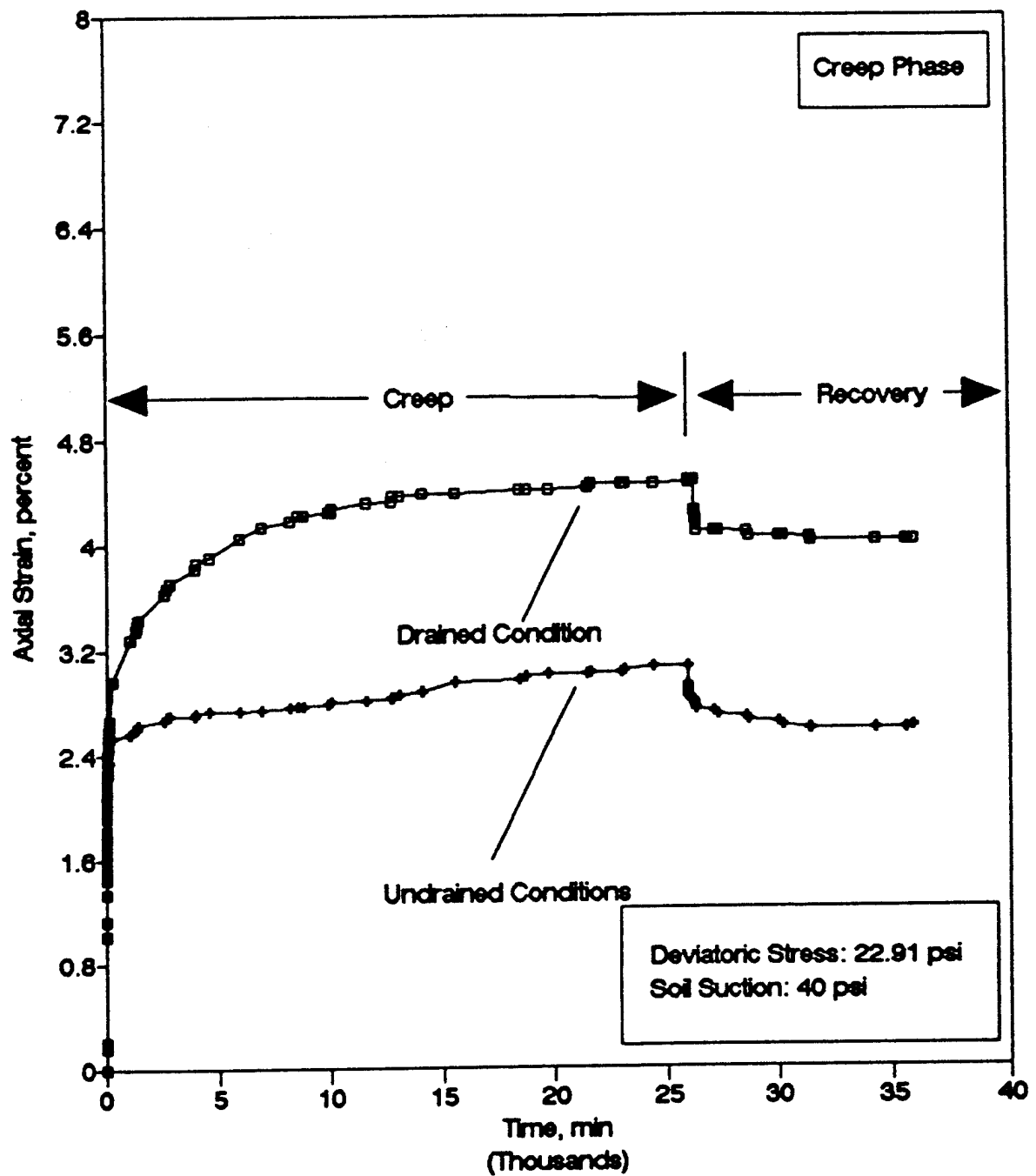


Figure 4.1 Comparison of Drained Versus Undrained Creep Tests

whole testing process. First, it is observed that the primary creep stage terminates for drained tests after a duration of approximately ten thousand minutes while for undrained tests it requires four thousand minutes. Then, it is noticed that, for this particular case, the secondary creep occurs on drained tests with a continuous slope of  $2.01 \times 10^{-5} \%/min$ , while for undrained tests the axial strain rate is of  $8.10 \times 10^{-6}/min$  and remained constant with this slope. Similar behavior was obtained with the rest of the specimens tested, with some exceptions which allow for further analysis. A more detailed analysis follows and discusses the effects of drainage condition upon asymptotic strain values and upon the secondary creep stage.

#### 4.3.1 Effects of Drainage Condition Upon Asymptotic Strain

With a suction of 15 psi, the lowest level applied, samples tested under drained conditions follow an increasing asymptotic slope as the deviatoric stress applied to them is increased. This pattern is represented by selected samples (29, 28, 27, and 33) which have given the expected results. Regarding the undrained tests, only samples number 39 and 60 seem to provide the results which support the fact that a drained test will have higher asymptotic strain value than an undrained test. The above samples are presented in Figure 4.2. Figure 4.3 shows tests results for a suction of 30 psi. Only samples 12, 10 (drained and undrained, respectively) and 59, 47 (drained and undrained, respectively) can be used for comparison purposes. Asymptotic strain for the drained sample was higher by 0.36% more 11.46 psi

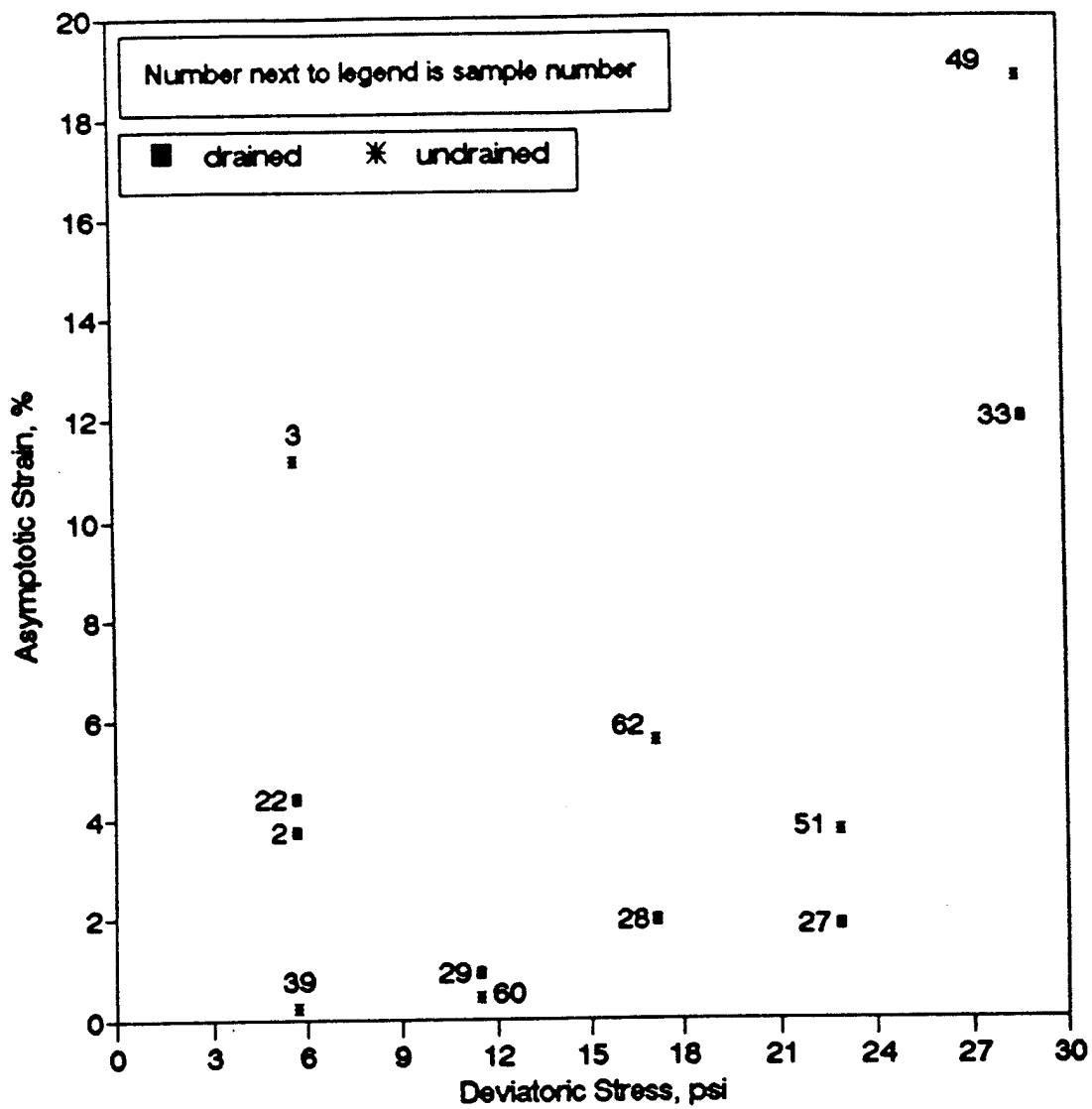


Figure 4.2 Drained Versus Undrained Creep Tests For 15 psi Soil Suction

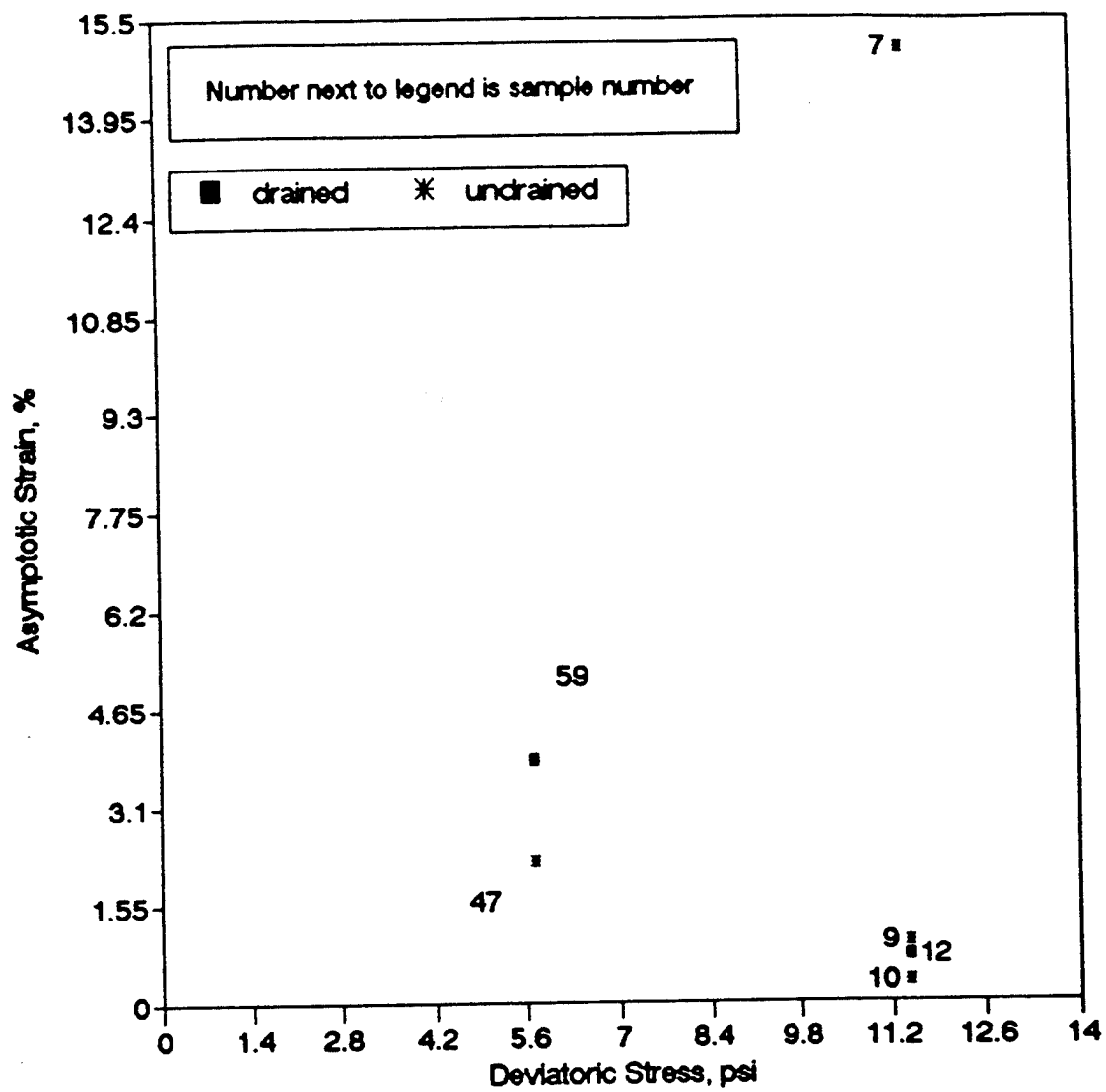


Figure 4.3 Drained Versus Undrained Creep Tests For 30 psi Soil Suction

deviatoric stress and 1.62% more for 5.73 psi deviatoric stress. Figure 4.4 contains the results of tests under 40 psi suction. Representing selected drained tests are samples 31, 30, 24, 18, and 4. They follow the same slope pattern observed in Figures 4.2 and 4.3. Undrained samples (34 and 17) also follow the expected behavior. Samples 24 and 34 demonstrate the effect of drainage condition by having asymptotic strains of 4.40% and 3.04%, respectively, when they were tested under the same deviatoric stress, 22.91 psi. Such is the case too for samples tested under higher stresses but with the particularity of having strain value differences among them which tend to increase as the deviatoric stress applied is being increased. Samples 4 and 17, each with strain value of 8.50% and 4.25% respectively, have a difference of asymptotic strain of 4.25% while 24 and 34 have a difference of 1.36%. Figure 4.5 illustrates samples tested at the highest suction level. The increasing asymptotic slope pattern observed for suction levels of 15 and 40 is also noticed here. Drained tests with more consistent results are on samples number 20, 26, 32, 25, 16, 14, and 15. The best tests for undrained condition are on samples number 11, 37, 38, 1, and 13. One particularity on these results is the smaller difference in asymptotic strain values for drained versus undrained tests under same deviatoric stress. The higher suction applied to these tests has caused them to be almost superimposed when the deviatoric stress is lower than 27.5 psi. Samples 13 and 15 with asymptotic strain values of 11.98% and 16.50% respectively, have a strain difference of 4.52% at the highest stress applied.

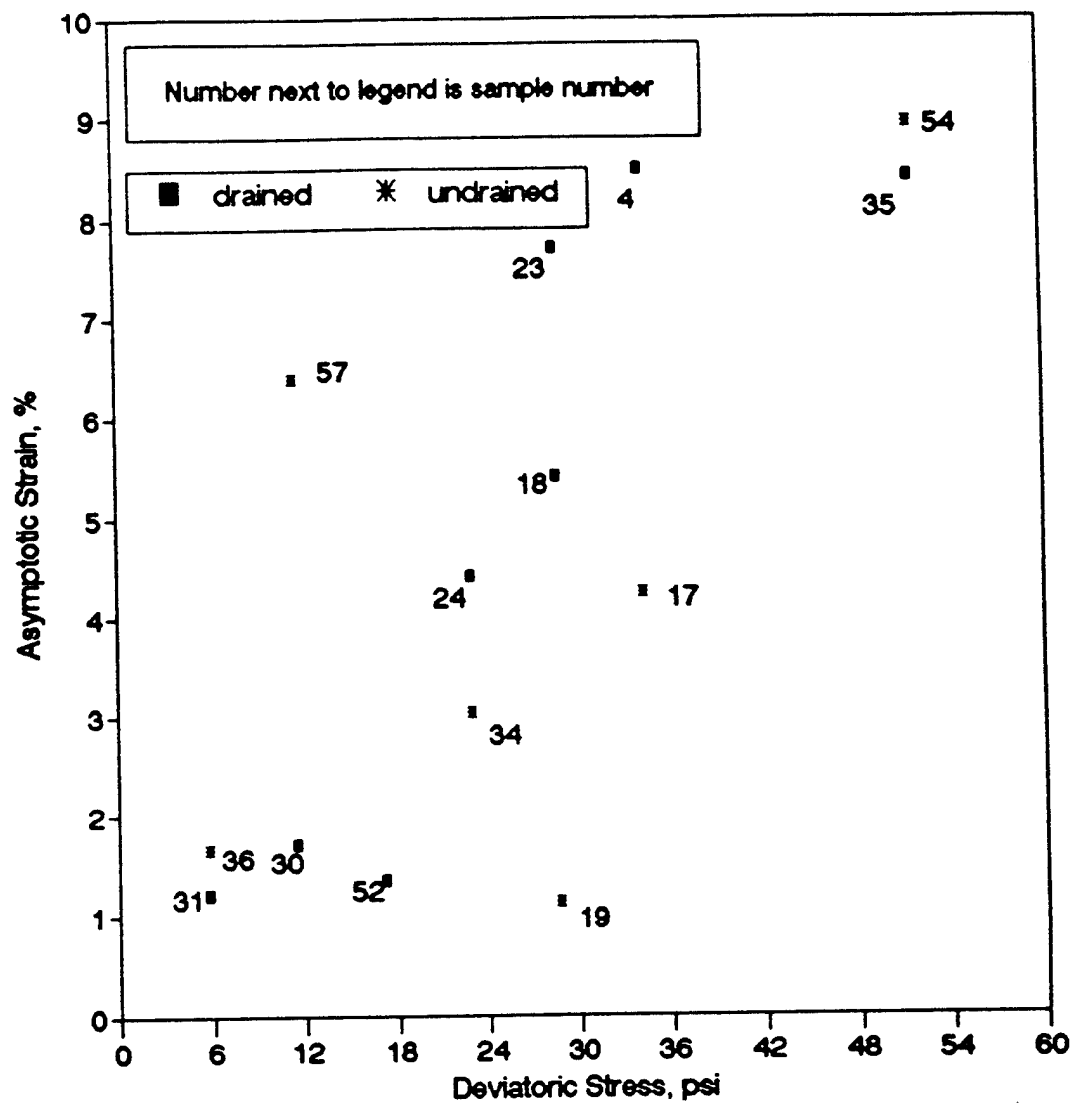


Figure 4.4 Drained Versus Undrained Creep Tests For 40 psi Soil Suction

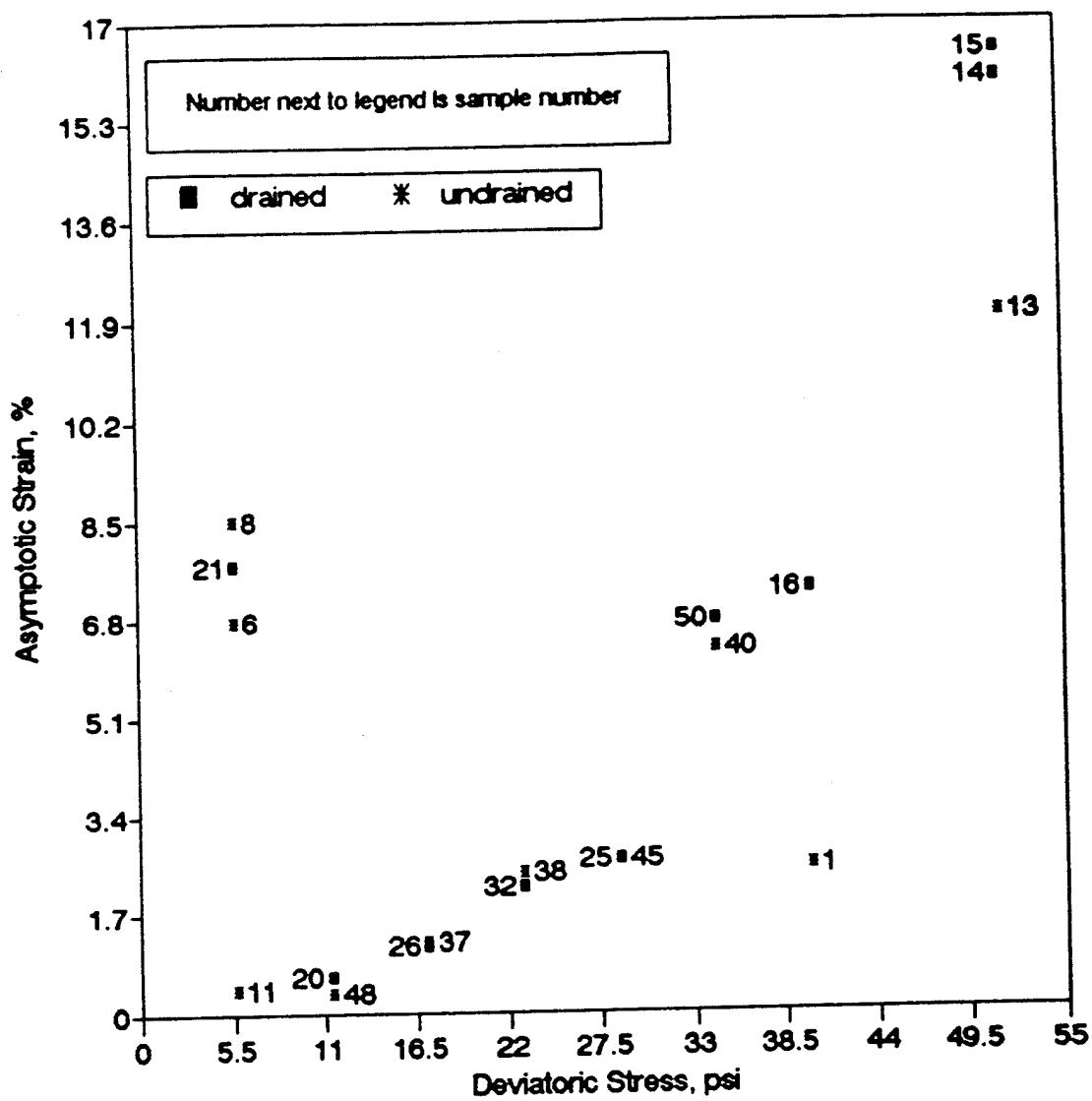


Figure 4.5 Drained Versus Undrained Creep Tests For 70 psi Soil Suction



#### 4.3.2 Effects of Drainage Condition Upon The Secondary Creep Stage

To determine the effect of drainage condition on the secondary creep stage, a detailed evaluation follows in terms of deviatoric stress (psi units) versus axial strain rate (%/min. units), the slope of this portion of the creep curve. The evaluation has been separated by suction levels and the results of the selected samples mentioned above in section 4.3.1 are the only ones considered. In Figure 4.6, a suction of 15 psi, it is noticeable that the rate is much higher for drained samples than for undrained samples. The same conclusion applies to Figures 4.8 and 4.9, but not to Figure 4.7 because it does not have enough test results for an evaluation due to limited specimens tested under suction levels of 30 psi and drained conditions. Also, in Figure 4.6 the asymptotic negative slope pattern of drained tests (22, 29, 27, and 33) indicates how the slope of the secondary creep is being reduced as the deviatoric stress applied is also being increased. Consider sample 22, tested under a deviatoric stress of 5.73 psi, and number 33, tested under a deviatoric stress of 28.64 psi, as examples. They had axial strain rates, or slopes, of  $1.26 \cdot 10^{-5} \% / \text{min.}$  and  $1.36 \cdot 10^{-6} \% / \text{min.}$  respectively; while the intermediate values of  $6.62 \cdot 10^{-6} \% / \text{min.}$  and  $2.81 \cdot 10^{-6} \% / \text{min.}$  for samples 29 and 27 correspondingly, yield the pattern previously mentioned. Figure 4.8 illustrates a similar pattern for drained samples. Specimens 30, 24, 23, 4, and 35 follow a declining sequence in axial strain rate values which indicates a reduction on the slope of the secondary creep. Undrained specimens, 34 and 19, seem to start following the same sequence but with lower

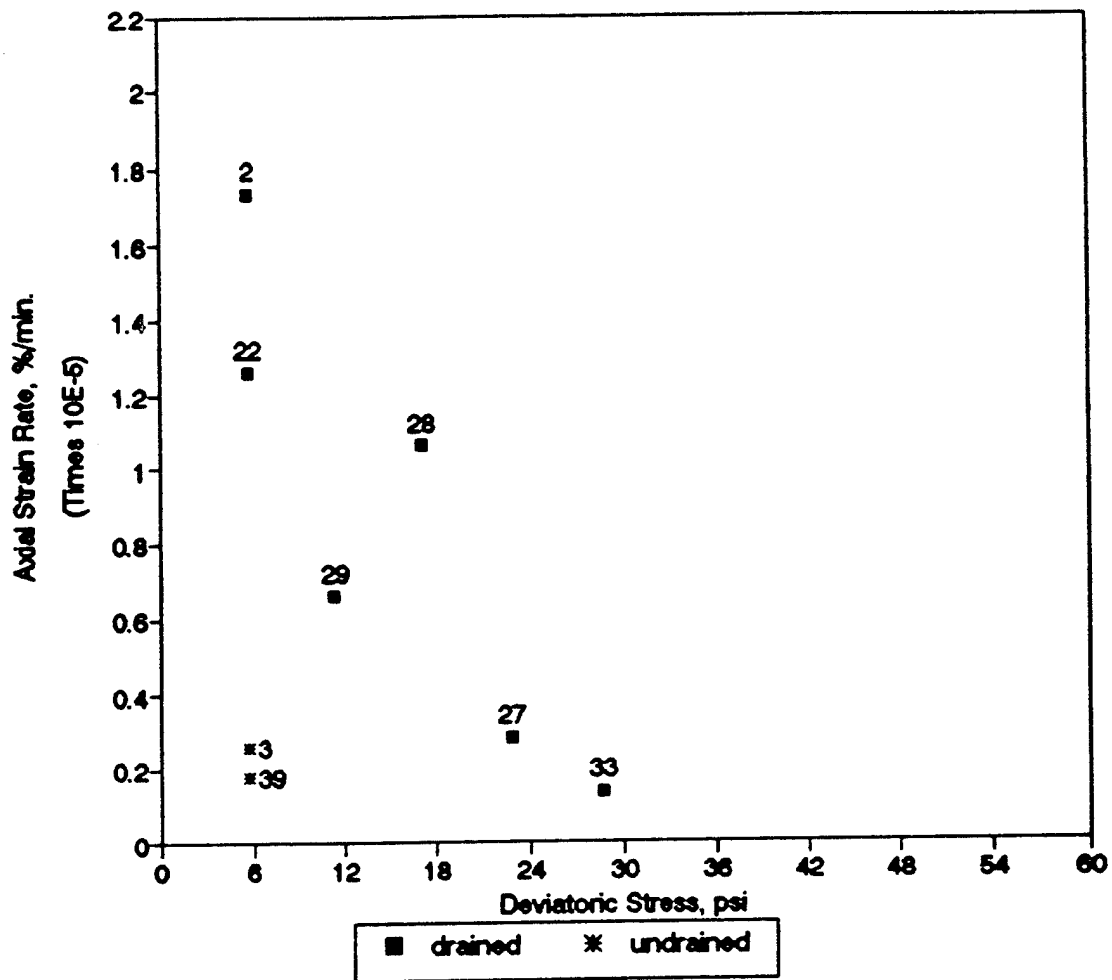


Figure 4.6 Evaluation of Secondary Creep Stage For 15 psi Soil Suction

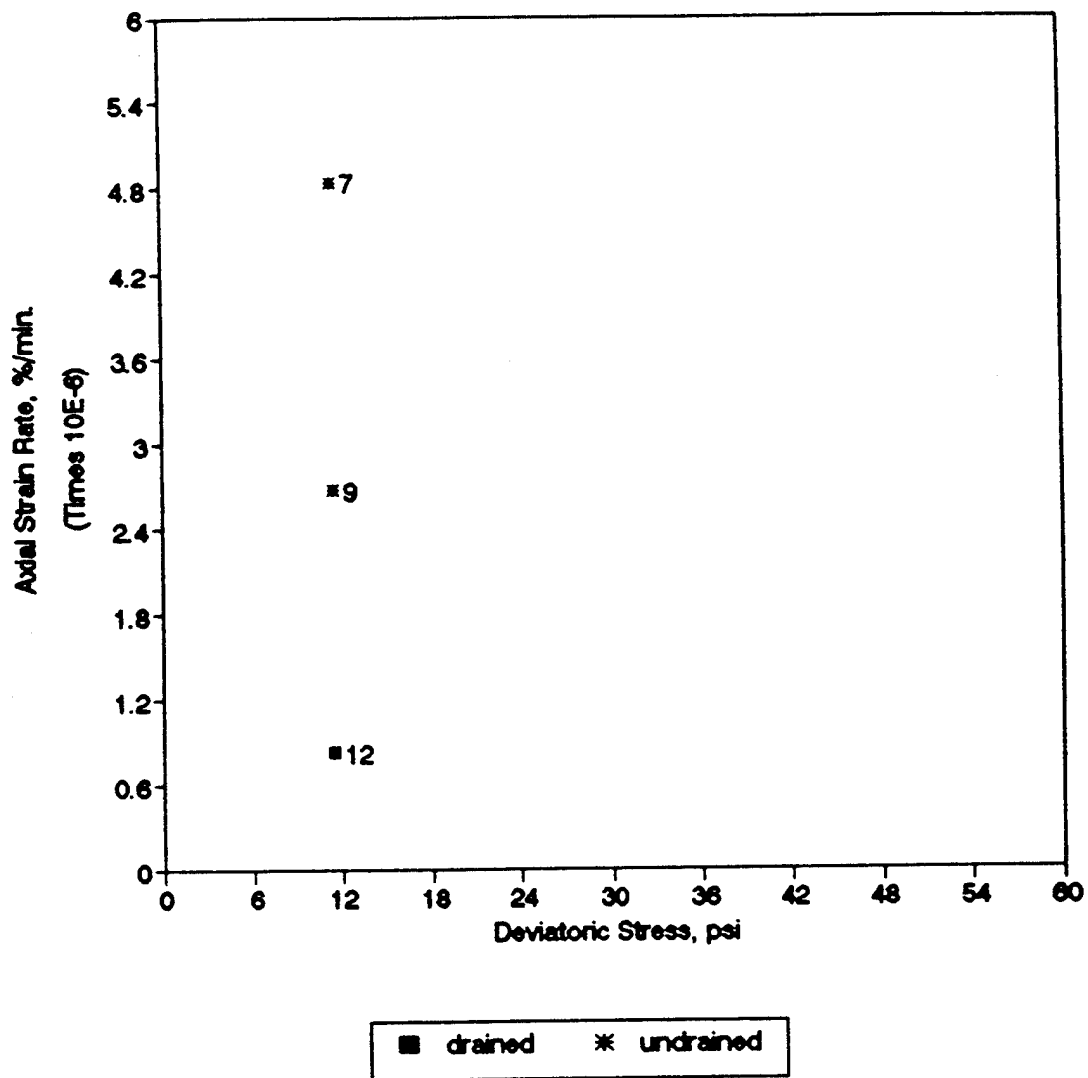


Figure 4.7 Evaluation of Secondary Creep Stage For 30 psi Soil Suction

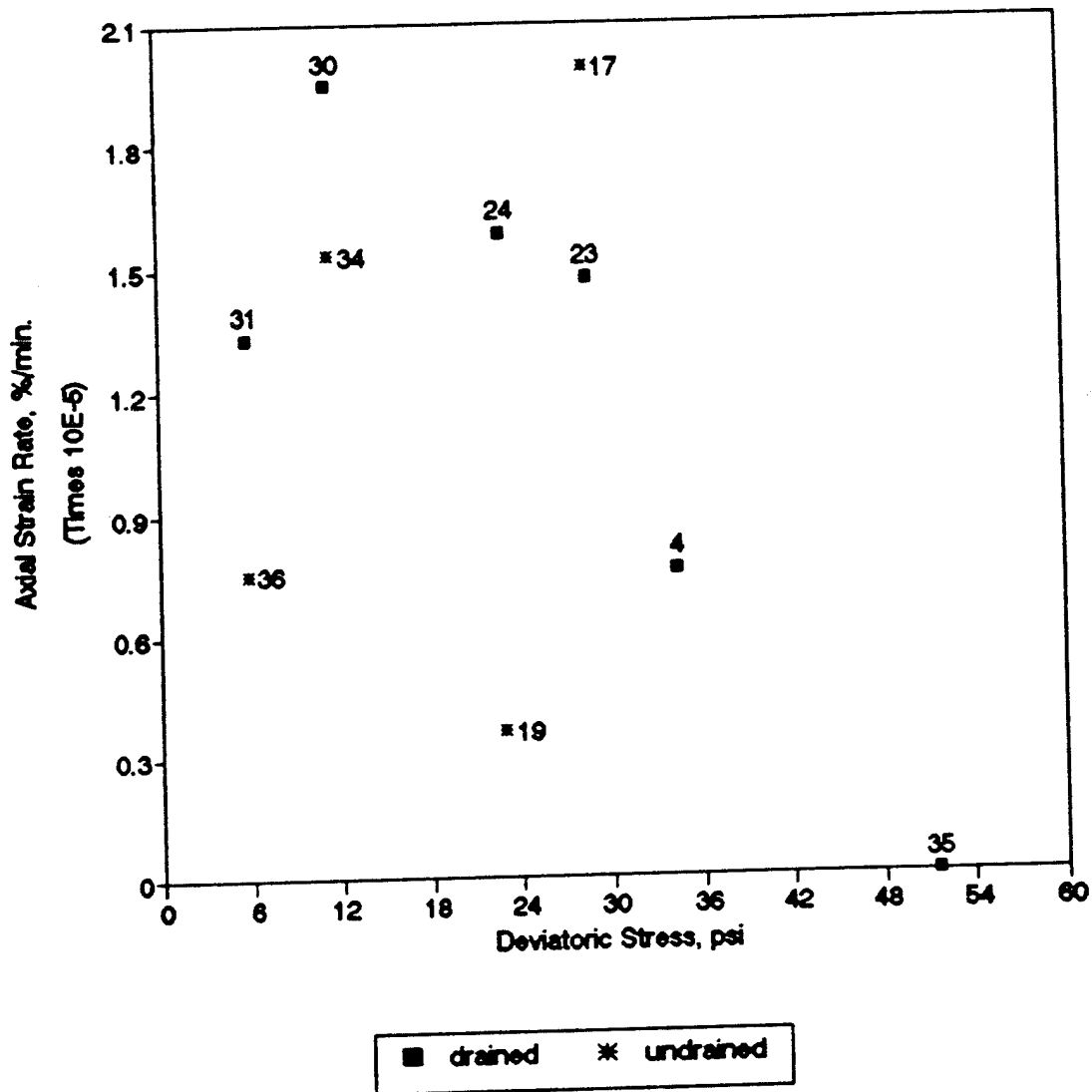


Figure 4.8 Evaluation of Secondary Creep Stage For 40 psi Soil Suction

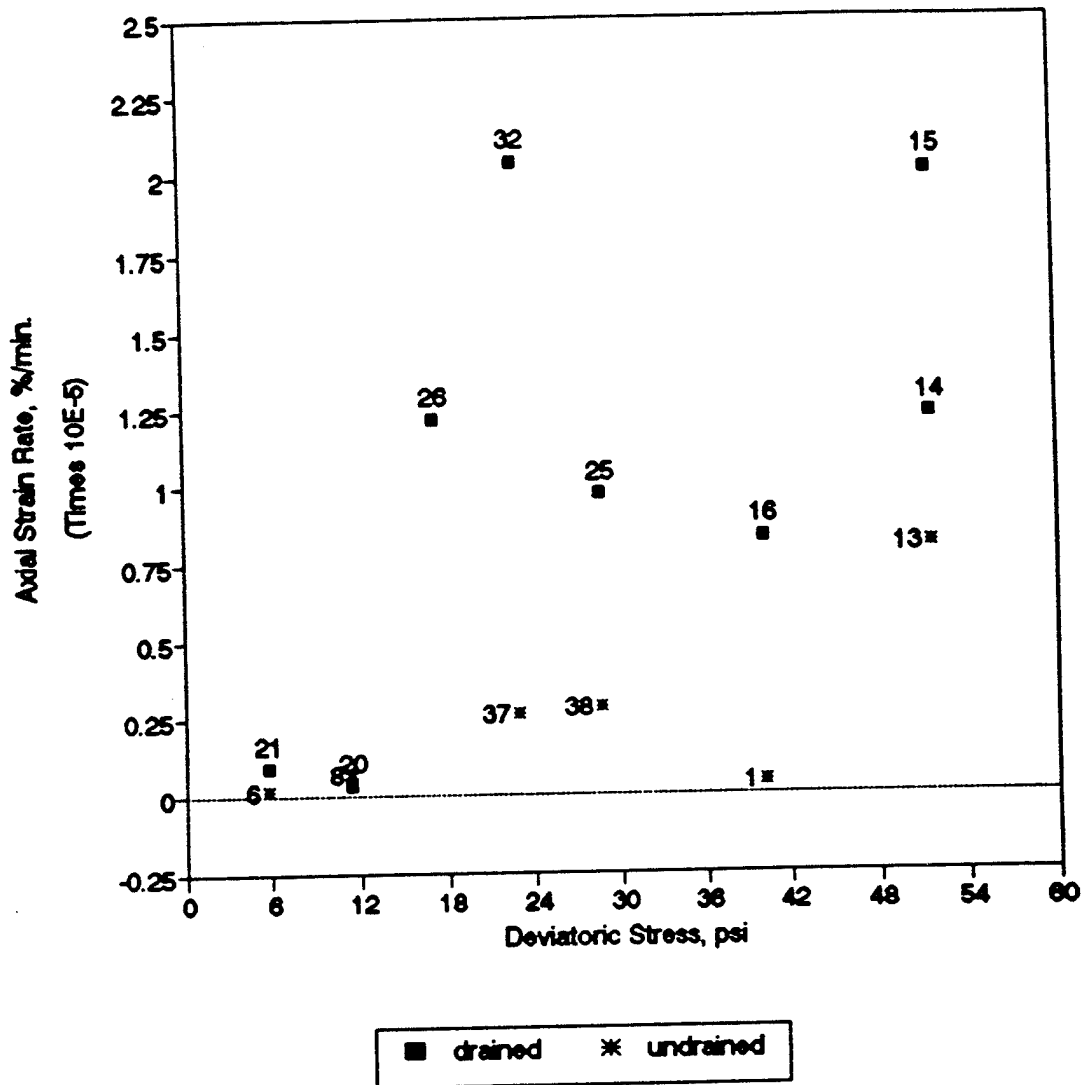


Figure 4.9 Evaluation of Secondary Creep Stage For 70 psi Soil Suction

values of axial strain rate. For this 40 psi suction, the asymptotic shape does not appear. Samples 30 and 35, tested under stresses of 11.46 psi and 51.56 psi correspondingly, had strain rate values of  $1.95 \times 10^{-5} \% / \text{min.}$  and  $1 \times 10^{-11} \% / \text{min.}$  respectively, but the intermediate value of sample 24 was  $1.58 \times 10^{-5} \% / \text{min.}$  for axial strain rate while it was subjected to a deviatoric stress of 22.91 psi. The evaluation of secondary creep for a suction level of 70 psi, Figure 4.9, is difficult to perform in regard to the features presented by the slopes or axial strain rate values. Their arrangement on the figure is very random, although drained samples such as 26, 25, and 16 follow an approximate resemblance similar to that of Figure 4.8. Undrained samples such as 1, 37, and 38 seem to start following the negative slope pattern.

Based on the samples mentioned, drained and undrained, the descending slope appearance which represents how the secondary stage of the creep curve is sloping for each particular test seems to be more horizontal. This suggests the possibility of having an influence from the suction level towards the behavior of specimens when they are at the secondary creep stage of their testing.

#### 4.4 REPEATED TESTS FOR VERIFICATION PURPOSES

Duplicates of tests were performed on specimens two, three, five, six, seven, fourteen, eighteen, and fifty-five. The duplicates, previously listed on Table 4.1, are represented by the results of tests on specimens twenty-two, thirty-nine, twenty-six, eight and eleven, nine and ten, fifteen, twenty-three, and fifty-seven; respectively.

Although there is need for several repetitions for each soil suction and deviatoric stress combination in order to properly characterize average values and variability of the creep\recovery tests, this was not possible to be achieved in the present study due to the large number of tests scheduled and the long duration of each test.

## CHAPTER FIVE

### INDEX PROPERTIES

#### 5.1 INTRODUCTION

In this study, a few tests on the soil stock, as well as on specimens which had already been tested, were performed in order to verify results of similar tests performed during the parent project. Results of new and previous tests are summarized in this chapter. They are also listed in Table 5.1.

#### 5.2 INDEX PROPERTIES OF THE SOIL STOCK

##### 5.2.1 Specific Gravity of Solids

The 2.75 average value obtained from tests performed upon already tested specimens was assumed to be that of the soil. Thus, no further testing was done on the soil stock. The details of these tests are discussed on section 5.3.

##### 5.2.2 Grain Size Distribution

The grain size Analysis tests were performed with the hydrometer test because the soil stock had already been sieved through sieve no. 200. The performance was done according to ASTM test designation D422-63 method. Four



Table 5.1

Tests on Soil Stock and Specimens

Name of Test	Result of Test
Gs	2.75
Hydrometer Analysis	33 % Clay Particles 67 % Silt Particles
Plasticity Index:  - exchange complex saturated with Lithium  - exchange complex saturated with Aluminum	  37.5 %  34.2 %
Cation Exchange Capacity	48.68 Meq/100grams
Clay Mineral Identification	Minerals Identified:  1) Kaolinites  2) Chlorites  3) Micas  4) Quartz  5) Some Smectites

specimens of the soil stock were analyzed and the results are presented in Figure 5.1. The results for all four specimens are very close indicating that 53% of the stock soil are clay size particles (less than 2 microns) and the remaining 47% are silt size particles.

### 5.2.3 Soil Plasticity Characteristics

These Characteristics were determined during the parent project. The Atterberg limits determinations obtained were assumed by this study as those of the soil stock currently used. For reference purposes, Table 5.2 summarizes the results of the determinations on the specimens with the exchange complex saturated with Lithium Chloride; and Table 5.3 summarizes the results of the determinations on the specimens with the exchange complex saturated with Aluminum Chloride. The average PI ranged from 37.5% with Lithium on the exchange complex to 34.2% with Aluminum on the exchange complex.

### 5.2.4 Cation Exchange Capacity

These determinations were conducted during the parent project and they were assumed to be that of the soil stock being used during this study. The results are presented by Table 5.4 for reference information. Three specimens of soil stock were subjected to cation exchange capacity measurements and the average measurement

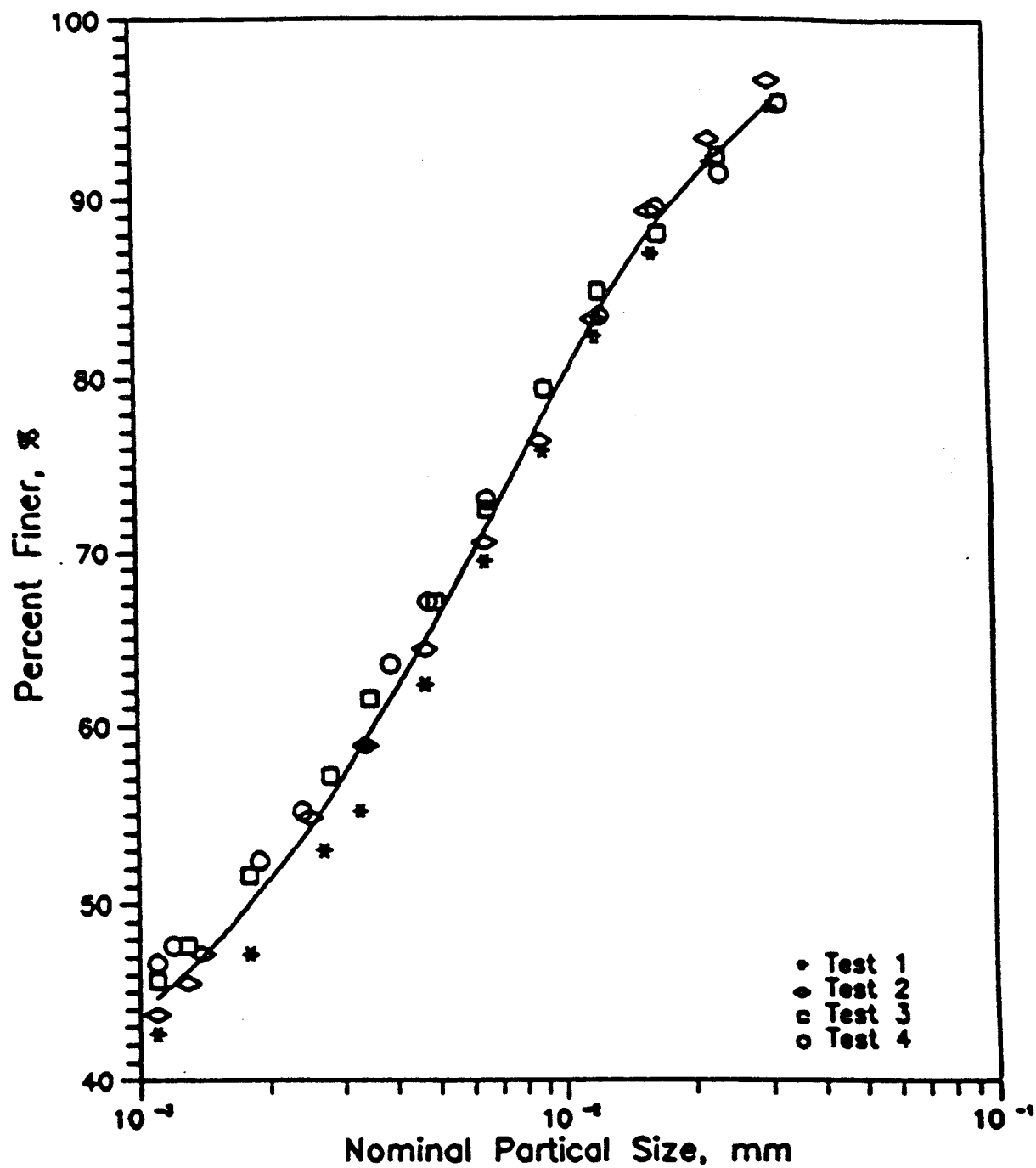


Figure 5.1 Results of Hydrometer Tests on the Soil Stock

Table 5.2

Atterberg Limits of The Soil Stock Saturated With Lithium Chloride

Test No.	Liquid Limit %	Plastic Limit %	Plasticity Index %
1	63.7	24.6	39.1
2	61.1	21.4	39.7
3	60.8	27.8	33.0
4	61.3	23.8	37.5
5	60.7	23.5	37.2
6	61.8	23.1	38.7

Table 5.3

Atterberg Limits of The Soil Stock Saturated With Aluminum Chloride

Test No.	Liquid Limit %	Plastic Limit %	Plasticity Index %
1	58.7	25.6	33.1
2	60.7	25.1	35.6
3	58.3	25.9	32.4
4	61.9	25.0	36.9
5	58.6	25.4	33.2
6	59.4	25.5	33.9

Table 5.4  
Cation Exchange Capacity Measurements

Test No.	Capacity (Meq /100 grams)
1	47.54
2	52.22
3	46.29

for this soil was found to be 48.68 Meq/100grams.

#### 5.2.5 Clay Mineral Identification

The identification obtained during the parent project was used by this study as the mineral composition of the soil stock used by this project. In summary, the x-ray analysis and the cation exchange capacity indicated that the minerals making up the soil stock were: kaolinites, chlorites, micas, quartz, and to some extent smectites.

### 5.3 INDEX PROPERTIES OF SPECIMENS

#### 5.3.1 Specific Gravity of the Solids

Measured specific gravities on already tested specimens are presented in Table 5.5. An average value of 2.75 is observed and was assumed to be the basic

Table 5.5  
Specific Gravity of the Solids

Specimen	Specific Gravity	Specimen	Specific Gravity
1 *	2.78	19 *	2.75
2 *	2.75	20 *	2.76
3 *	2.75	21 *	2.80
4 *	2.75	22 *	2.79
5 *	2.64	23 *	2.80
6 *	2.75	24 *	2.75
7 *	2.65	25 *	2.74
8 *	2.61	26 *	2.73
9 *	2.63	27 *	2.77
10 *	2.67	20 +	2.61
11 *	2.95	21 +	2.95
12 *	2.61	22 +	2.76
13 *	2.88	25 +	2.75
14 *	2.75	27 +	2.80
15 *	2.67	28 +	2.80
16 *	2.77	29 +	2.76
17 *	2.77	32 +	2.67
18 *	2.82	33 +	2.75

Notes:

\* = Values of tests performed during parent project.

+ = Values of tests performed during this study.

index properties of the soil.

### 5.3.2 Grain Size Distribution

During the parent project, some sixteen specimens were used, after the creep phase and dynamic tests, for hydrometer analysis. For verification purposes, during this study, nine specimens were analyzed after being tested and their grain size distributions are included in Appendix D. The results of the parent project and of this study are very close. Figure 5.2 considers the results of the tests performed on already tested specimens. The percentage of clay sizes appears to be several percentage points lower for the specimens, this difference is possibly due to the 0.01M  $\text{CaCl}_2$  pore solution present in the specimens while the soil stock is essentially electrolyte free. Thus, result on the soil stock are more reliable and give a more representative percentage of clay sizes.

## 5.4 WATER CONTENTS OF THE SPECIMENS

Specimens were subjected to determination of moisture content using the trimmings left over when the consolidated samples were trimmed. Determination of moisture content was also done after the completion of the creep/recovery tests or dynamic tests. These water contents, along with the corresponding suction level imposed on the specimen, are presented by Table 5.6.

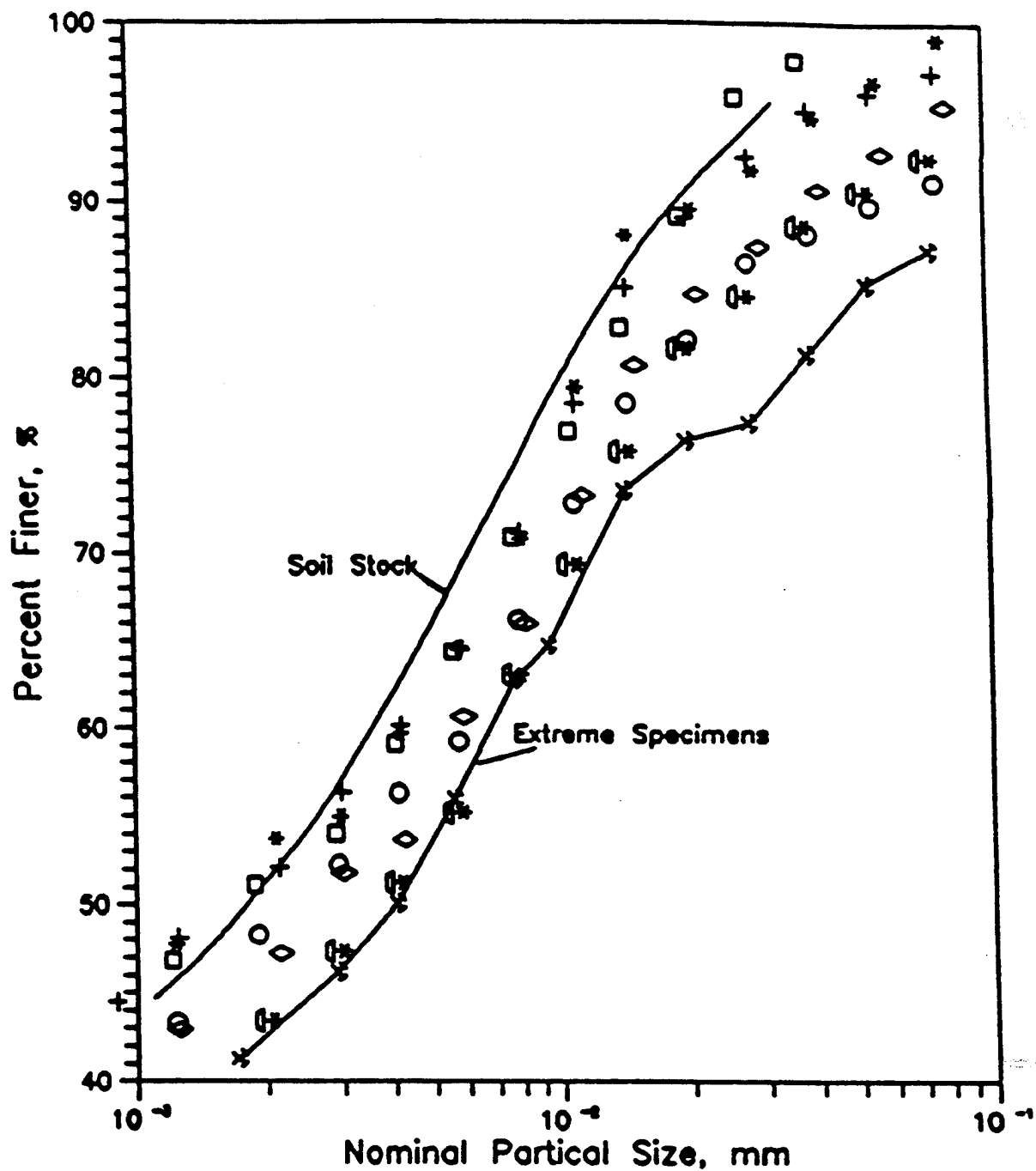


Figure 5.2 Comparison of the Grain Size Distribution for Soil Stock and for Specimens



Table 5.6

## Water Content Before and After Creep/Recovery Tests

Specimen Number  #	Water Content After Consolidation  %	Water Content After Creep  %	Soil Suction  psi	Drainage Condition
1	21.58	20.17	70	undrained
2	14.50	16.32	15	drained
3	14.59	14.47	15	undrained
4	28.85	28.19	40	drained
5	27.79	+	70	drained
6	27.80	25.12	70	drained
7	21.50	21.47	30	undrained
8	24.46	22.27	70	undrained
9	28.45	28.27	30	undrained
10	26.38	*	30	undrained
11	29.14	*	70	undrained
12	26.29	25.27	30	drained
13	23.31	24.25	70	undrained
14	36.42	22.11	70	drained
15	24.51	16.54	70	drained

Notes:

+ = Specimen presented problems with membrane.

\* = Problems with temperature room.

Continuation of Table 5.6

Water Content Before and After Creep/Recovery Tests

Specimen Number	Water Content After Consolidation	Water Content After Creep	Soil Suction	Drainage Condition
#	%	%	psi	
16	25.33	15.93	70	drained
17	24.70	24.71	40	undrained
18	24.16	23.01	40	drained
19	22.15	22.46	40	undrained
20	31.20	28.20	70	drained
21	30.54	35.78	70	drained
22	29.53	31.30	15	drained
23	29.28	28.10	40	drained
24	30.23	27.98	40	drained
25	32.38	23.34	70	drained
26	30.21	25.39	70	drained
27	30.26	30.26	15	drained
28	29.86	30.15	15	drained
29	32.26	31.30	15	drained
30	29.71	28.00	40	drained

Notes:

+ = Specimen presented problems with membrane.

\* = Problems with temperature room.

Continuation of Table 5.6

Water Content Before and After Creep/Recovery Tests

Specimen Number	Water Content After Consolidation	Water Content After Creep	Soil Suction	Drainage Condition
#	%	%	psi	
31	29.74	28.03	40	drained
32	31.18	24.42	70	drained
33	29.78	30.32	15	drained
34	20.92	22.05	40	undrained
35	26.84	26.82	40	drained
36	22.46	24.57	40	undrained
37	32.71	24.86	70	undrained
38	19.91	23.80	70	undrained
39	29.79	29.78	15	undrained
40	26.32	22.70	70	undrained
41	25.42	25.56	30	undrained
42	26.41	25.10	30	undrained
43	24.57	25.07	30	undrained
44	26.14	26.52	30	undrained
45	24.26	23.81	70	undrained

Notes:

+ = Specimen presented problems with membrane.

\* = Problems with temperature room.

Continuation of Table 5.6

Water Content Before and After Creep/Recovery Tests

Specimen Number	Water Content After Consolidation	Water Content After Creep	Soil Suction	Drainage Condition
#	%	%	psi	
46	24.78	24.78	70	undrained
47	29.26	26.88	30	undrained
48	24.88	24.76	70	undrained
49	22.39	31.42	15	undrained
50	29.90	24.10	70	drained
51	26.37	25.46	15	undrained
52	30.32	27.80	40	drained
53	24.88	24.76	30	drained
54	29.26	26.88	40	undrained
55	32.38	32.38	70	undrained
56	29.06	22.80	40	undrained
57	25.55	27.58	40	undrained
58	25.46	25.90	70	undrained
59	25.80	36.21	30	drained
60	25.50	29.77	15	undrained

Notes:

+ = Specimen presented problems with membrane.

\* = Problems with temperature room.

Continuation of Table 5.6

Water Content Before and After Creep/Recovery Tests

Specimen No.	Water Content After Consolidation %	Water Content After Creep %	Soil Suction psi	Drainage Condition
61	26.99	31.79	15	undrained
62	26.36	28.18	30	undrained
63	25.58	30.72	30	undrained
64	23.75	\$	30	drained
65	31.18	30.00	15	undrained
66	30.72	28.07	40	undrained
67	29.21	25.80	70	undrained
68	19.83	30.00	15	undrained

Notes:

\$ = Specimen broken during trimming.

Before the equilibrium phase, the moisture contents varied between 19.83% and 36.42%, with average value of 26.65. After the creep/recovery or dynamic test, the results show that the specimens tested under undrained conditions generally experienced smaller changes in water content. By way of contrast, the specimens tested at drained conditions experienced much larger changes. A few exceptions to this observation were noticed.

## CHAPTER SIX

### MODEL FOR CREEP AND RECOVERY TESTING

#### 6.1 INTRODUCTION

The series of tests to be performed during the entire project was designed to investigate the effects that the deviatoric stress, soil suction level, and drainage condition; had on the creep/recovery testing of specimens. The results of performed tests were used to make comparisons with the behaviors suggested by non-linear viscoelastic model, based on power law, that was recommended by the parent project.

#### 6.2 INITIAL POWER LAW

##### 6.2.1 Suggested Model

The main interest of the study was to have as much accuracy as possible at very early time of the creep phase. This suggested model was previously been observed, during the parent project, to improve the approximation of the initial part(first sixty minutes) of the phase. Thus, such power law model was fitted to the laboratory data of this study,

$$\epsilon(t) = \alpha t^{\beta} \quad (6.1)$$

where

$\epsilon$  = initial creep strain, percent

$\alpha, \beta$  = functions of the deviatoric stress and soil suction

$t$  = elapsed time, min.

The power law does fit the experimental data in a satisfactory fashion. To illustrate this effect, the initial creep curves at 70 psi suction level for undrained and drained conditions are plotted in Figures 6.1 and 6.2. The figures show the linear trend clearly seen in the data. However, the exponent of the power seems to be a function of the deviatoric stress level. Therefore equation 6.1 is modified by taking natural logarithms and yielding:

$$\ln[\epsilon(t)] = \beta \ln(t) + \ln \alpha \quad (6.2)$$

where  $\ln[\epsilon(t)]$  and  $\ln[t]$  can be obtained from the results of the creep tests during the first 60 minutes and  $\alpha$  and  $\beta$  can be obtained from linear regression analysis. As illustrated by Table 6.1, a linear regression was performed for each suction level using equation 6.2. In evaluating the data, parameter  $\beta$  was found to be independent of soil suction and only slightly dependent of deviatoric stress. Furthermore, the average values for each deviatoric stress level were found to be in a fairly narrow range. This peculiarity made possible to approximate  $\beta$  with linear regression by the following



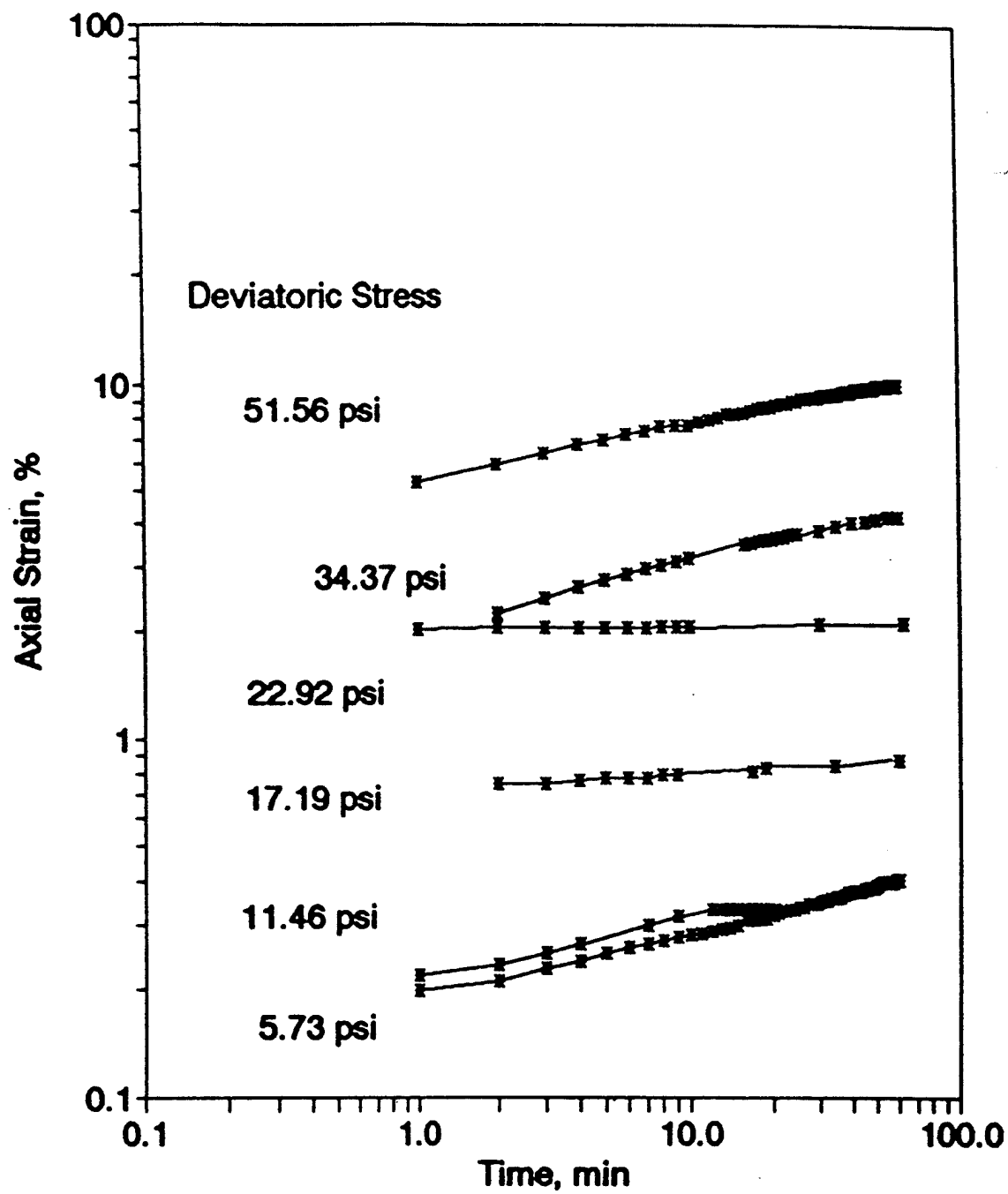


Figure 6.1 Initial Creep Phase For Undrained Conditions of Specimens  
Equilibrated at 70 psi

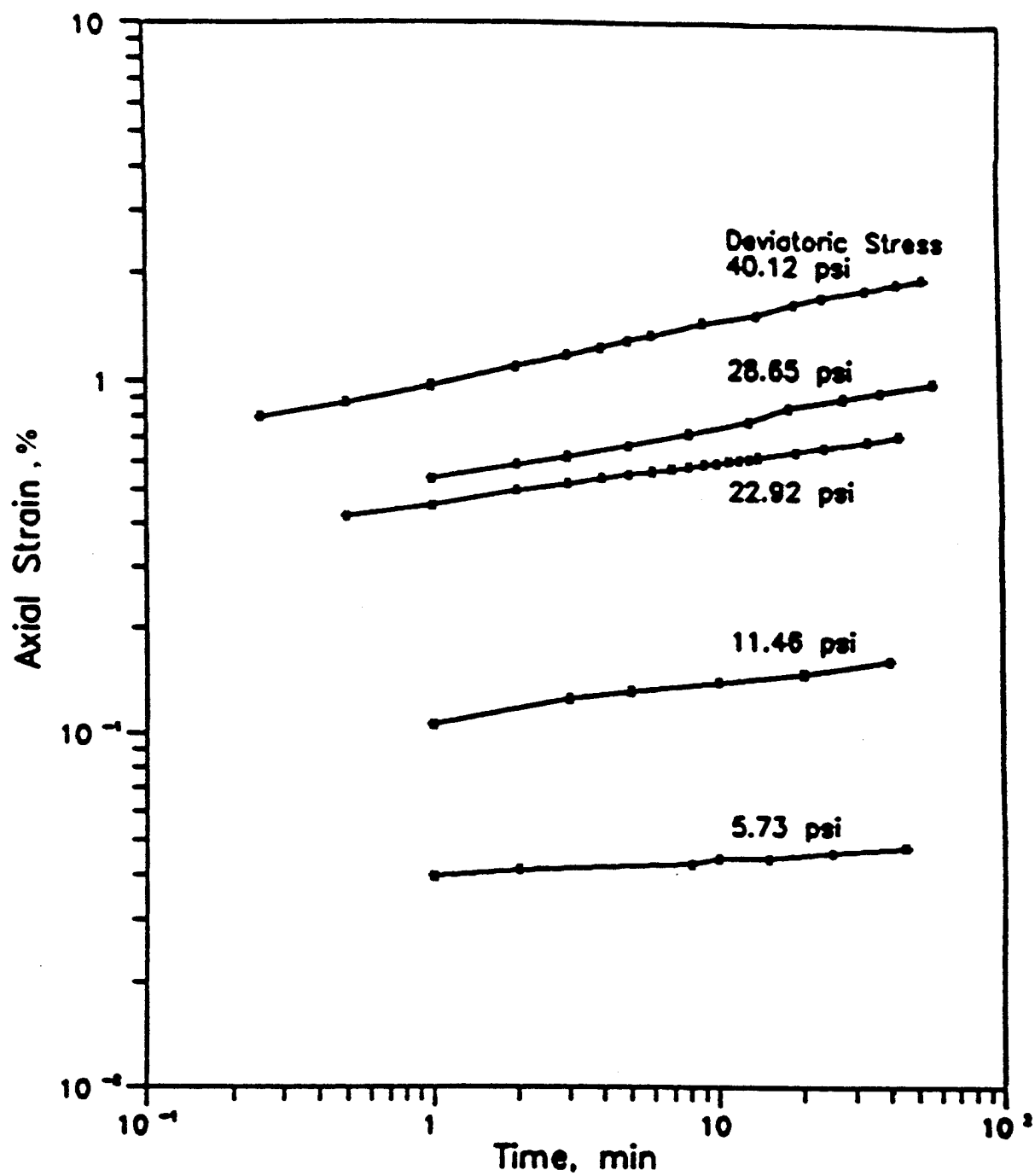


Figure 6.2 Initial Creep Phase For Drained Conditions of Specimens Equilibrated at 70 psi

Table 6.1

Values of Parameters  $\alpha$  and  $\beta$  for Different Soil Suction Levels

Deviatoric Stress, psi	$\alpha$		$\beta$	
	D	U	D	U
15 psi				
5.73	0.0989	0.0074	0.0486	0.0009
11.46	0.1714	0.0981	0.1103	0.0013
14.30	0.2038	0.8853	0.2462	0.0103
17.19	0.4119	0.8853	0.1457	0.0103
22.92	1.1854	1.3003	0.1803	0.0470
28.65	6.3960	17.2491	0.1803	0.03351
30 psi				
11.46	*	0.2649	*	0.0016
22.92	*	1.7185	*	0.0167
28.65	*	1.9250	*	0.1800
34.37	*	8.0034	*	0.0101
40.10	*	20.8158	*	0.0317
40 psi				
5.73	0.0876	*	0.1664	*
11.46	0.1404	0.4205	0.0965	0.0034
17.19	0.2738	0.6253	0.1117	0.0016

D = Drained

U = Undrained

\* = Results not available

Continuation of Table 6.1

Values of Parameters  $\alpha$  and  $\beta$  for Different Soil Suction Levels

Deviatoric Stress, psi	$\alpha$		$\beta$	
	D	U	D	U
40 psi				
22.92	0.6584	1.5895	0.1314	0.0173
28.65	0.9098	*	0.1806	*
34.37	*	3.6299	*	0.0059
51.56	*	8.9600	*	$-1.3 \times 10^{-16}$
70 psi				
5.73	0.04	0.2334	0.0475	0.0033
11.46	0.1095	0.2752	0.1098	0.0014
17.19	*	0.6682	*	0.0052
22.92	0.4607	1.8249	0.1179	0.008
28.65	0.5324	*	0.1581	*
34.37	*	2.5625	*	0.0377
40.12	0.992	*	0.1709	*
51.56	*	6.7253	*	0.0699
51.56	*	8.9600	*	$-1.3 \times 10^{-16}$

D = Drained

U = Undrained

\* = Results not available

relationships:

$$\beta = 0.003623 \sigma_d + 0.055131 \quad (6.3)$$

for drained, and for undrained:

$$\beta = 0.000837 \sigma_d + (-0.00319) \quad (6.4)$$

Parameter  $\alpha$  was observed to increase with the deviatoric stress. The form of the dependence is shown in Figures 6.3 and 6.4. In the Figures the variation was fitted with a power law of the deviatoric stress of the following form:

$$\alpha = \alpha_1 \sigma_d^{\alpha_2} \quad (6.5)$$

The parameters  $\alpha_1$  and  $\alpha_2$  were obtained from regression analysis for each appropriate suction level. Table 6.2 shows the values of these parameters for all soil suctions.

Thus, the two proposed models fitted to the creep data of the initial 60 minutes are represented by the following analytical expressions:

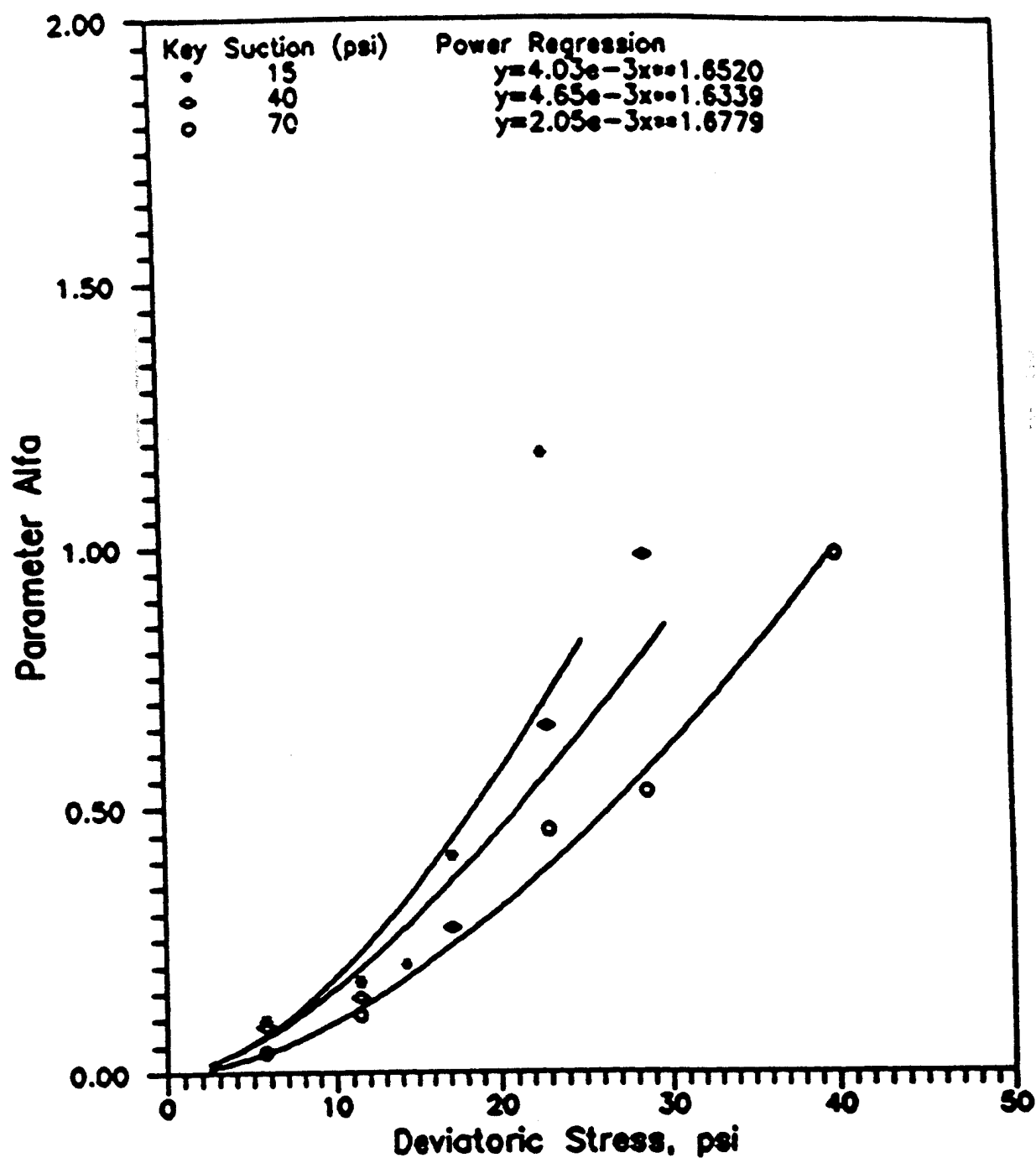


Figure 6.3      Power Relationship Between Parameter  $\alpha$  and the Deviatoric Stress  
For Three Soil Suction Levels at Drained Conditions

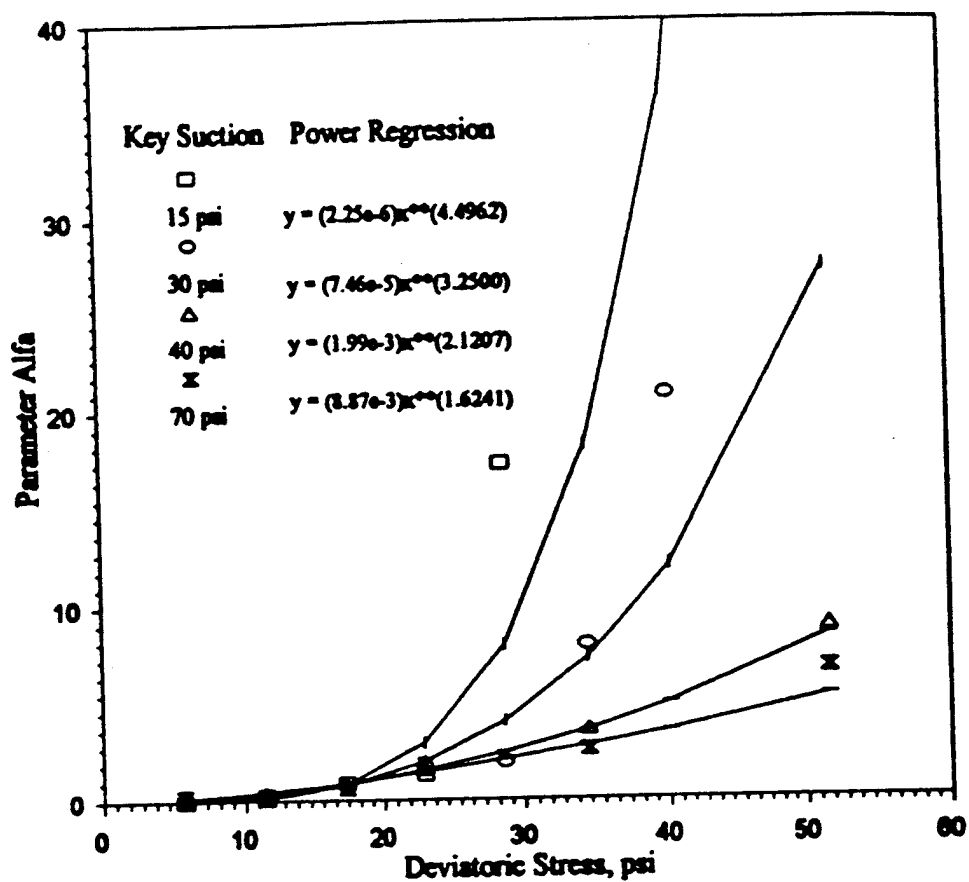


Figure 6.4    Power Relationship Between Parameter  $\alpha$  and the Deviatoric Stress  
For Four Soil Suction Levels at Undrained Conditions

Table 6.2

Values of Parameters  $\alpha_1$  and  $\alpha_2$  for Different Soil Suction Levels

$\alpha_1$		$\alpha_2$	
D	U	D	U
15 psi			
$4.030 \times 10^{-3}$	$0.00226 \times 10^{-3}$	1.6520	2.1206
30 psi			
*	$0.0746 \times 10^{-3}$	*	3.2500
40 psi			
$4.659 \times 10^{-3}$	$1.990 \times 10^{-3}$	1.6339	2.1206
70 psi			
$2.051 \times 10^{-3}$	$8.870 \times 10^{-3}$	1.6779	1.6241

D = Drained

U = Undrained

\* = Results not available



$$\epsilon_f(t) = \alpha_1 \sigma_d^{\alpha_2} t^{(0.003623\sigma_d + 0.055131)} \quad (6.6)$$

for drained, and for undrained;

$$\epsilon_f(t) = \alpha_1 \sigma_d^{\alpha_2} t^{(0.000837\sigma_d + (-0.00319))} \quad (6.7)$$

### 6.2.2 Model Capabilities

Figure 6.5 presents an example of the adequacy of the power law for predicting the creep at the actual test conditions used in the laboratory. From the figure it is noticed the closeness in shape pattern and magnitude of both curves. Unfortunately, some cases had a clear difference; but this disagreement could be overcome by improving the stress function in its explaining of the variation of creep with deviatoric stress. For such improvements the data base would require to be augmented, specifically more repetitions, to check whether the results already obtained include significant testing errors. Unfortunately this is not possible due to time limitations and to the scheduled tests for this project. Despite of this problem it is felt that the model is definitely closely fitting the measured creep data.

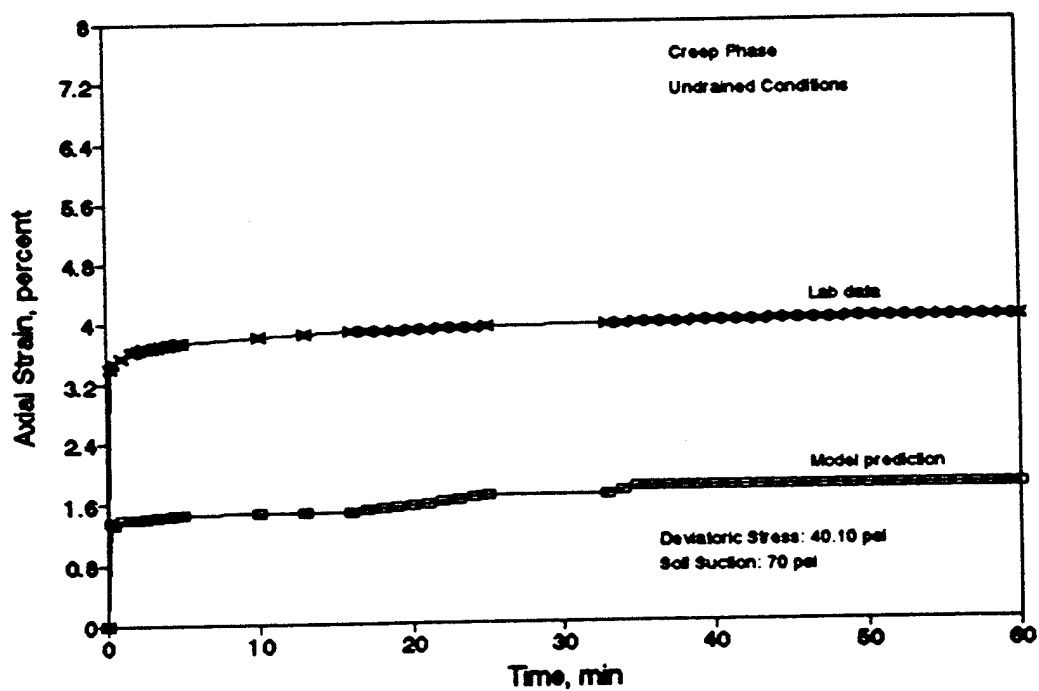
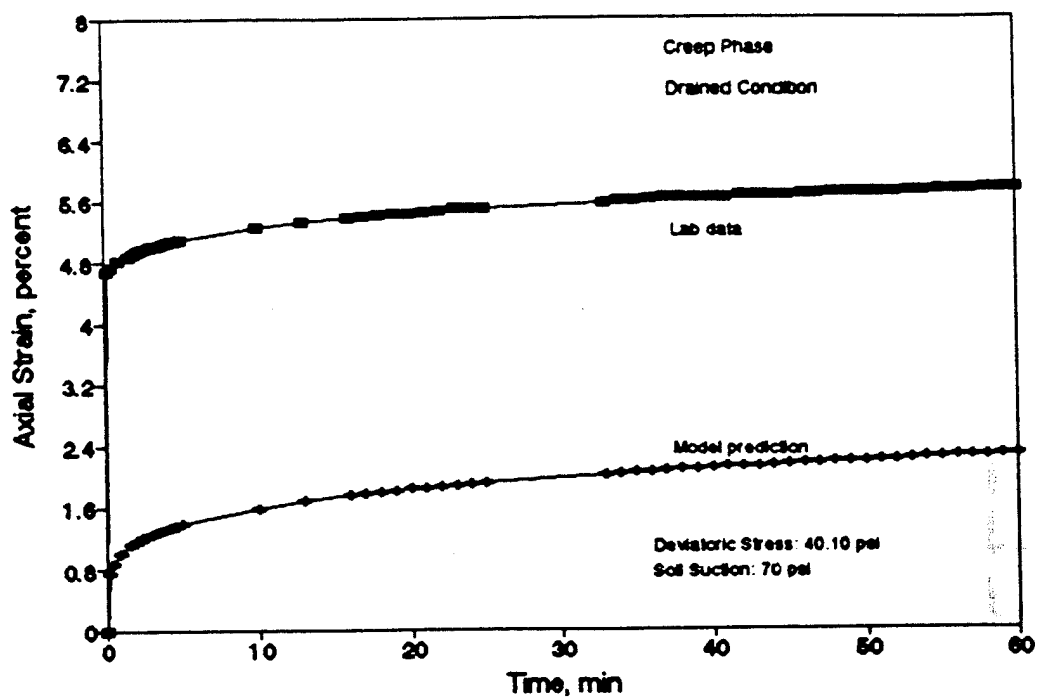


Figure 6.5 Comparison of Laboratory Data Versus Model Prediction For Creep Phase

### 6.3 RECOVERY POWER LAW

#### 6.3.1 Suggested Model

To make a more complete analysis, test data recorded during the recovery phase was also considered by this model. For this purpose, the data was transformed by changing the strain and time origin. Consequently, the time zero was set at the beginning of the unloading and the strain at such time was set to zero. The strains experienced during the recovery became negative.

The power law of time was noticed to fit well the experimental data. For illustrative purposes Figures 6.6 and 6.7 present the recovery curve at 70 psi soil suction which indicates the linear trend of the transformed data.

The observed strains have been fitted with the following expression:

$$\epsilon_R(t) = -\alpha_R t^{\beta_R} \quad (6.8)$$

where:

$\epsilon_R(t)$  = recovery strain that occurs during the time of unloading, percent

$t$  = elapsed time from the time of unloading, minutes

$\alpha_R$  = parameter

$\beta_R$  = parameter

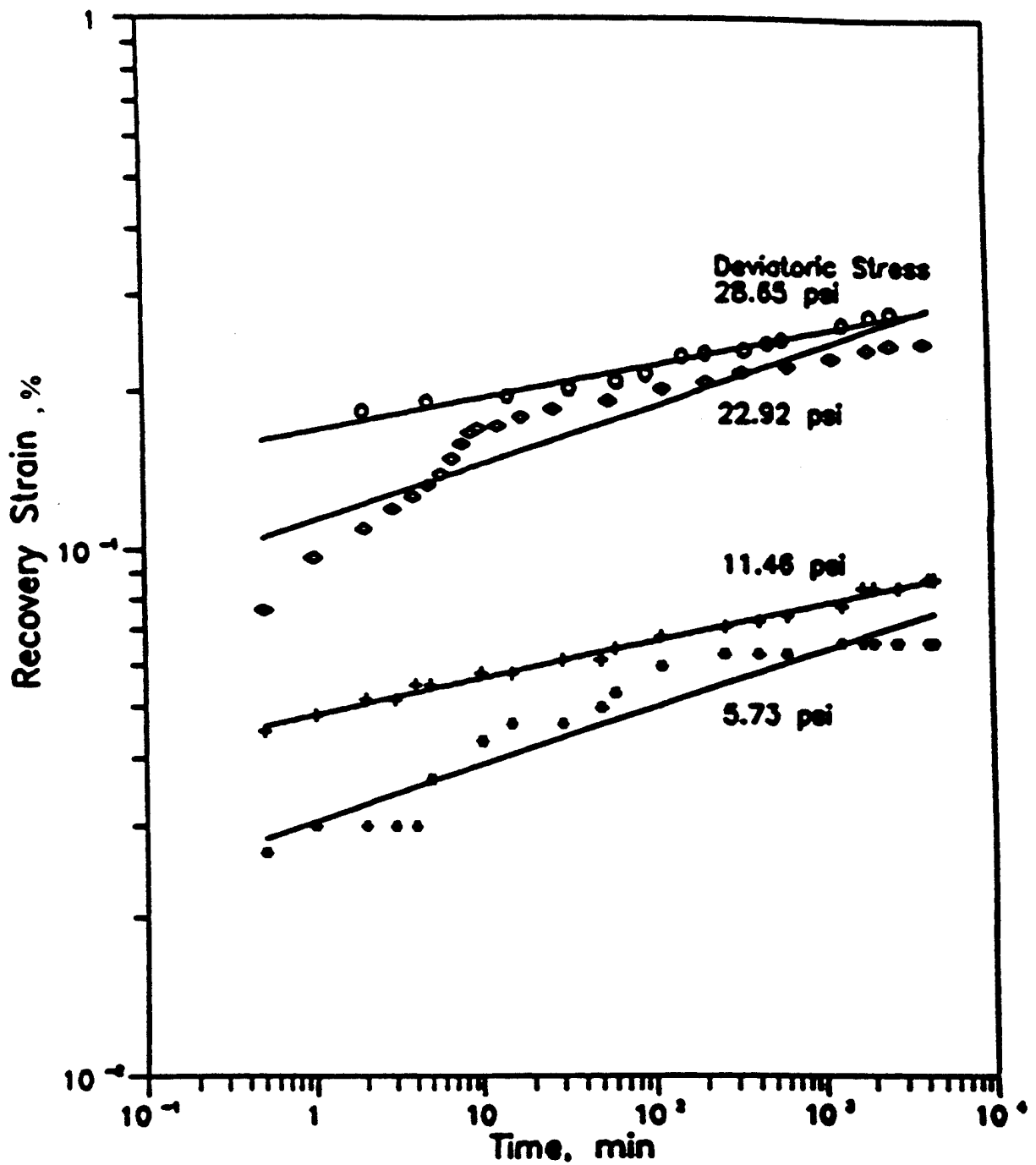


Figure 6.6 Drained Recovery Phase for Specimens Equilibrated at 70 psi Soil

Suction

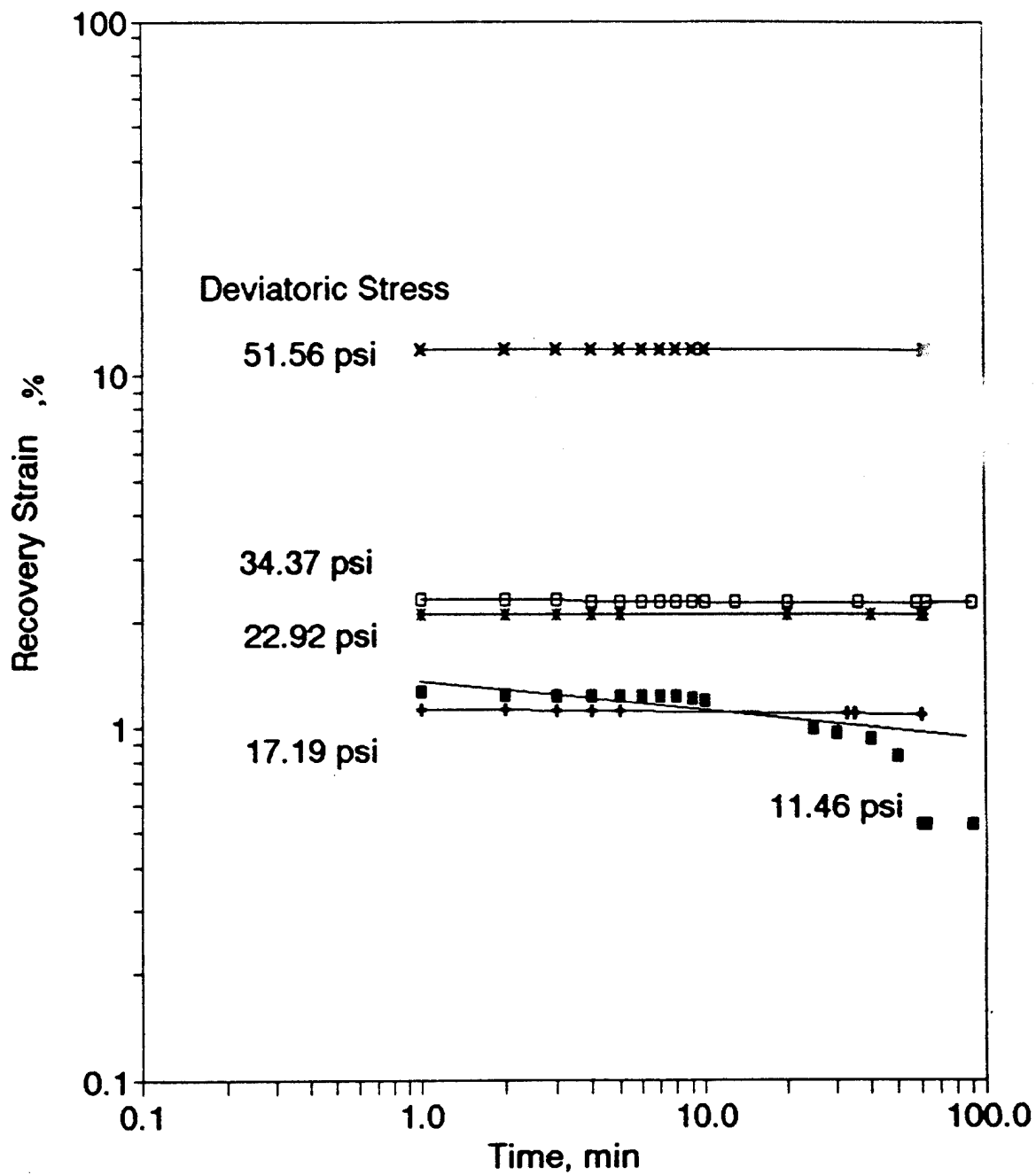


Figure 6.7 Undrained Recovery Phase for Specimens Equilibrated at 70 psi Soil Suction

taking logarithms,

$$\ln|\epsilon_R(t)| = \ln \alpha_R + \beta_R \ln t \quad (6.9)$$

where  $\alpha_R$  and  $\beta_R$  values are obtained from linear regression using the same procedure as for creep model parameters. Table 6.3 contains such values and it can be observed that deviatoric stress has an influence on the value of parameter  $\alpha_R$ . Figures 6.8 and 6.9 present such influence. The results have been fitted with a power law of the deviatoric stress. The actual analytical function for drained and undrained condition is:

$$\alpha_R = \alpha_{R1} \sigma_d^{\alpha_{R2}} \quad (6.10)$$

where  $\alpha_{R1}$  and  $\alpha_{R2}$  are function of soil suction level. These parameters were calculated by regression analysis for each suction level and are summarized in Table 6.4.

The value of  $\beta_R$  for each drainage condition, was assumed to be constant and equal to the average of all results presented by Table 6.3. This is done because of the observed variability which appears to be random and covering a very narrow range. Furthermore, the results appear to indicate that the parameter  $\beta_R$  is independent of

Table 6.3

## Regression Values of Recovery Phase

Deviatoric Stress, psi	$\alpha_R$		$\beta_R$	
	D	U	D	U
15 psi				
5.73	0.0398	*	0.0526	*
11.46	0.0644	*	0.0904	*
14.30	0.0766	*	0.1063	*
17.19	0.0734	*	0.1204	*
22.92	0.2108	3.5321	0.0835	0.00556
28.65	1.5629	*	0.0254	*
30 psi				
5.73	*	2.1980	*	0.00204
22.92	*	3.3230	*	0.01518
28.65	*	3.6910	*	0.01432
40 psi				
5.73	*	1.6475	*	0.00318
11.46	0.0519	1.8120	0.0755	0.00966
17.19	0.0782	10.3024	0.0531	0.00095

Notes:

D = Drained.

U = Undrained.

\* = Phase not performed.

Continuation of Table 6.3

Regression Values of Recovery Phase

Deviatoric Stress, psi	$\alpha_R$		$\beta_R$	
	D	U	D	U
40 psi				
22.92	0.1568	2.9221	0.0831	0.00855
28.65	0.2258	0.7289	0.0708	0.03321
34.37	*	4.1226	*	0.00313
70 psi				
5.73	0.0306	1.4167	0.1081	3.57E-17
11.46	0.0484	1.6822	0.0713	0.21807
17.19	*	1.1349	*	0.00905
22.92	0.1135	2.1060	0.1094	0.00089
28.65	0.1691	0.1919	0.0614	0.10317
34.37	*	2.3131	*	0.00322
40.12	*	22.0828	*	0.00127
51.56	*	11.8587	*	0.00027

Notes:

D = Drained.

U = Undrained.

\* = Phase not performed.



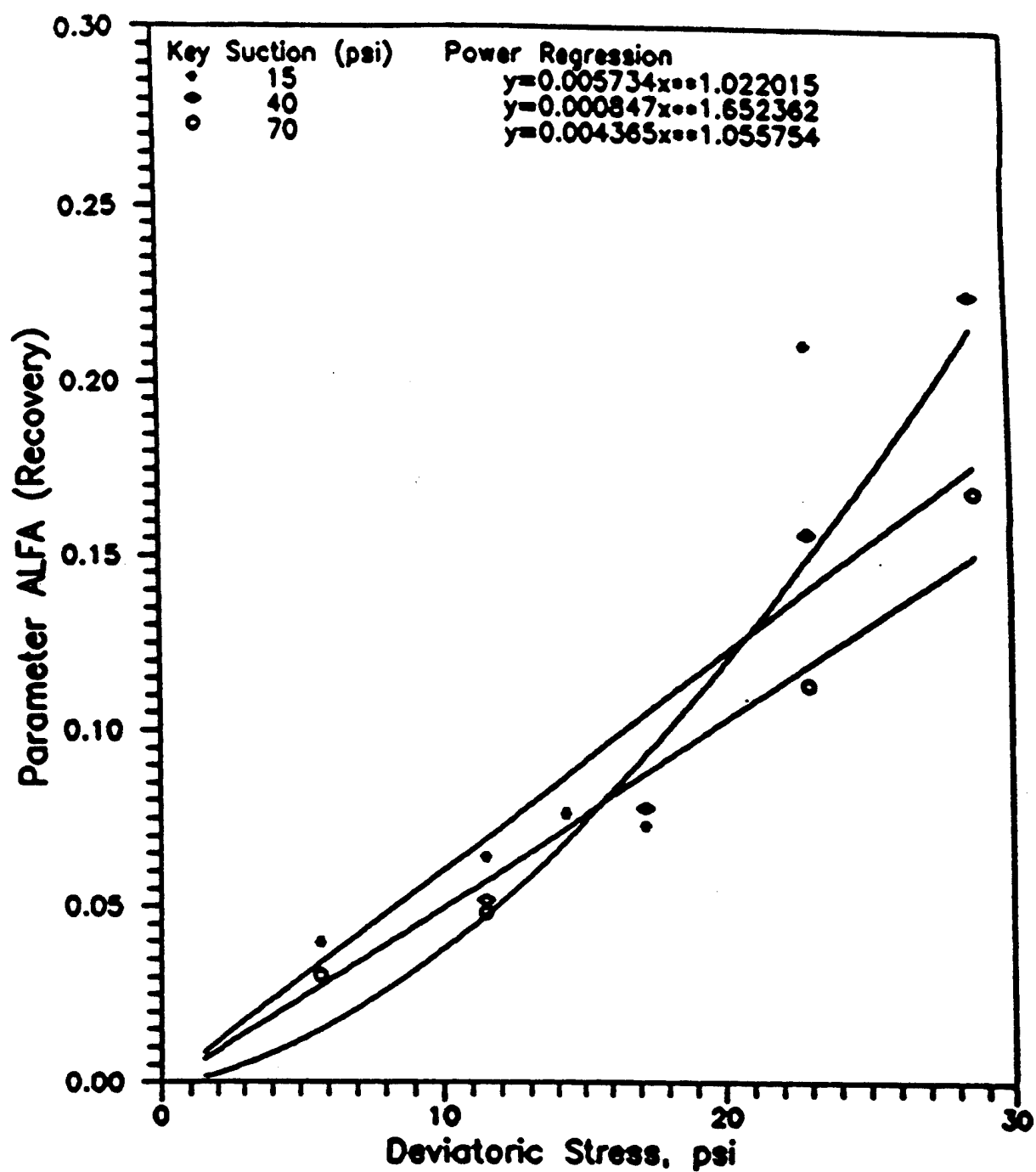


Figure 6.8      Power Law Regression between Parameter  $\alpha_R$  and Deviatoric Stress  
For Drained Condition (Cheng Chang, 1992)

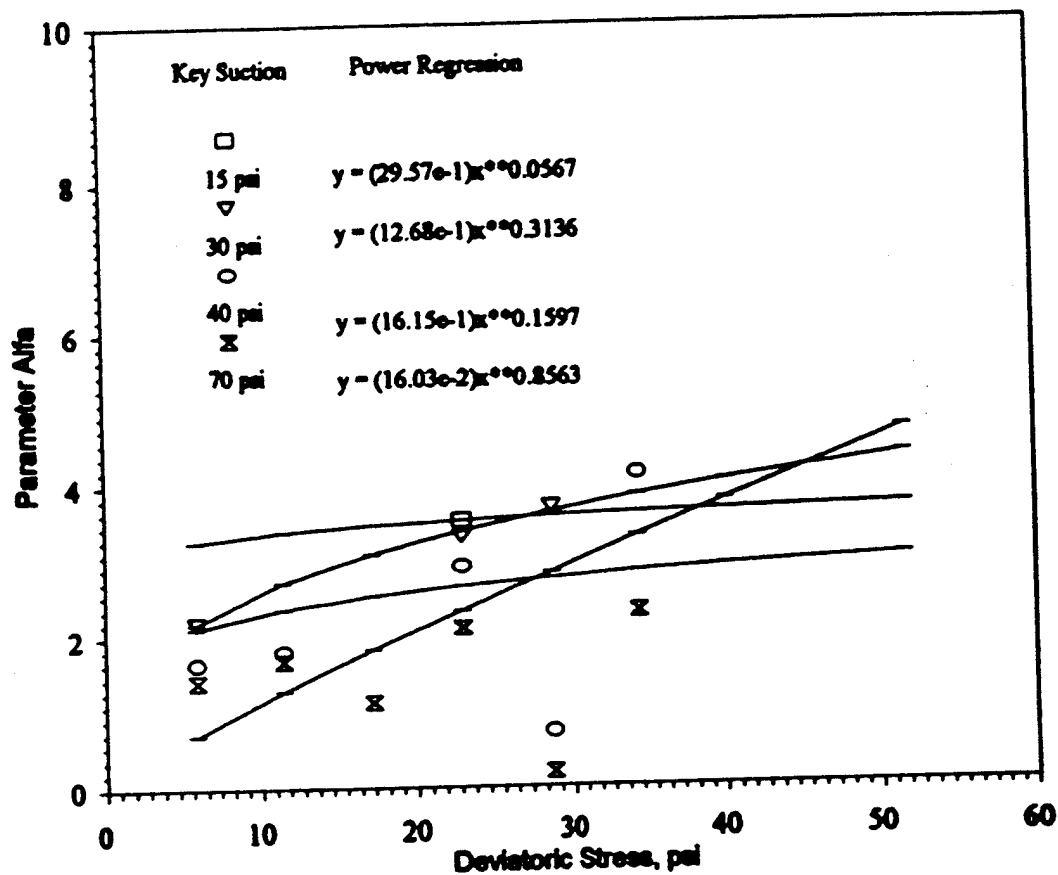


Figure 6.9 Power Law Regression between Parameter  $\alpha_R$  and Deviatoric Stress  
For Undrained Condition

Table 6.4

Values of  $\alpha_{R1}$  and  $\alpha_{R2}$  For Different Soil Suction Levels

$\alpha_{R1}$		$\alpha_{R2}$	
D	U	D	U
15 psi			
$5.73 \times 10^{-3}$	$29.57 \times 10^{-1}$	1.022	0.0567
30 psi			
*	$12.68 \times 10^{-1}$	*	0.3136
40 psi			
$8.47 \times 10^{-4}$	$16.15 \times 10^{-1}$	1.6524	0.1597
70 psi			
$4.37 \times 10^{-3}$	$16.03 \times 10^{-2}$	1.0558	0.8563

D = Drained.

U = Undrained.

\* = Results not available.

deviatoric stress and soil suction.

Thus, the proposed models for the unloading phase are represented by the following relationships:

$$\epsilon_{R(t)} = \alpha_{R1} \sigma_d^{\alpha_{R2}} t^{0.076} \quad (6.11)$$

for drained, and for undrained;

$$\epsilon_{R(t)} = \alpha_{R1} \sigma_d^{\alpha_{R2}} t^{0.024} \quad (6.12)$$

where the coefficient of these power laws is found to be function of the deviatoric stress and soil suction, being the model a power law of time with a constant exponent.

### 6.3.2 Model Capabilities

To model the soil unloading, the recovery model needs to be applied since the parameters of creep suggest certain model and the parameters of recovery suggest other different model. Thus, Figure 6.10 offers the comparison of the lab data and the model prediction; evaluating in this manner the capabilities of the fitted model to the recovery phase.

Specimens subjected to excessively large deviatoric stresses had plastic deformations causing unfavorable comparisons.

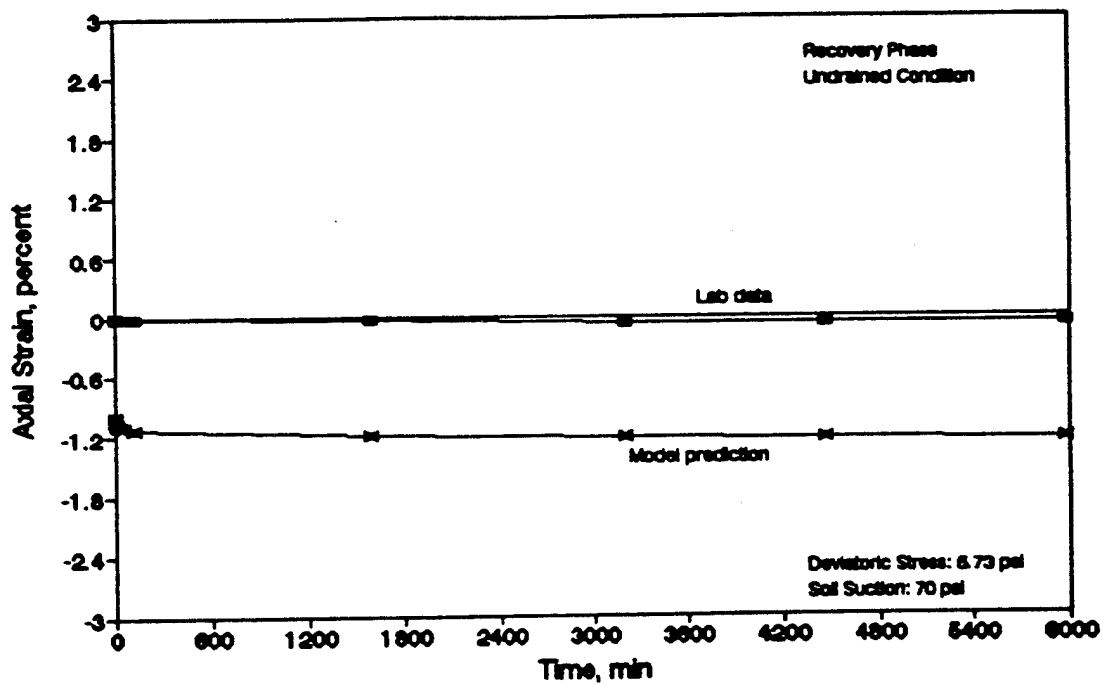
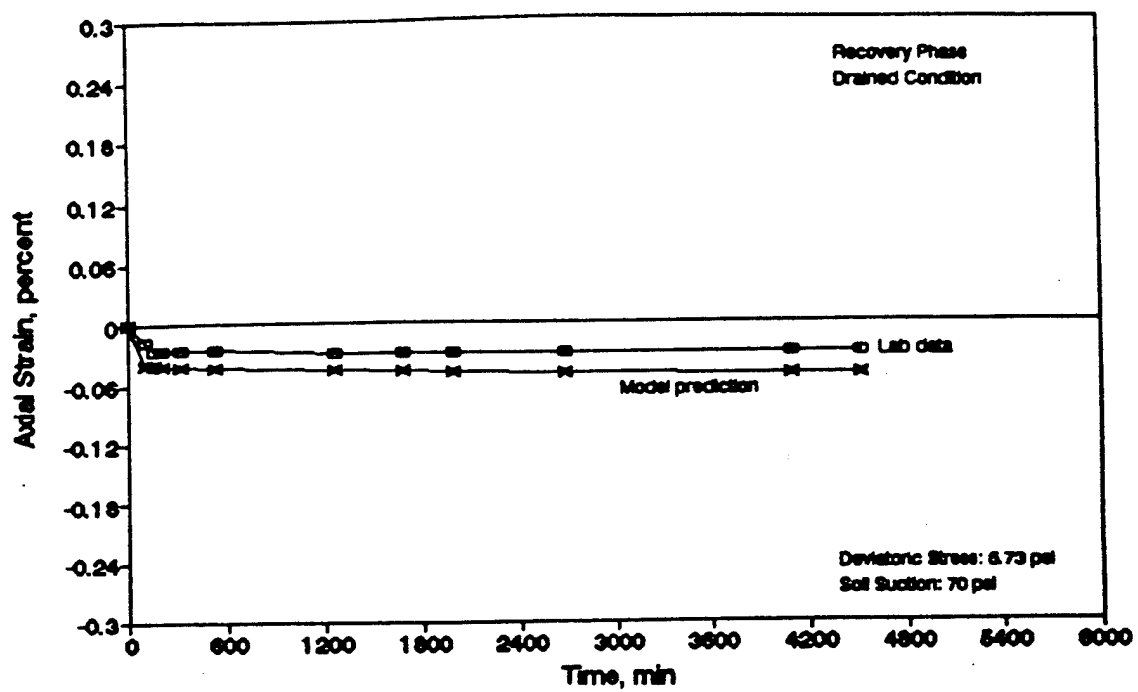


Figure 6.10 Comparison of Laboratory Data Versus Model Prediction For Recovery Phase

For a much better indication of the variation of model parameters with soil suction and deviatoric stress, as also suggested for the creep model, the range and number of test conditions needs to be incremented.

## CHAPTER SEVEN

### HIGH STRAIN RATE EQUIPMENT

#### 7.1 INTRODUCTION

A closed-loop servovalve MTS test system was utilized for performing dynamic tests. This chapter describes the testing equipment and calibration of MTS triaxial cell.

#### 7.2 TEST EQUIPMENT

The system, manufactured by MTS, Inc., consists of several interacting units that can be grouped into four main components: 1) Load Unit, 2) Controller, 3) MicroProfiler, and 4) Hydraulic Power Supply.

The Load Unit consists of two stiff columns that join two stiff structural members; i.e. a movable crosshead and a fixed platen. The crosshead is vertically adjustable to accommodate specimens of varying lengths. The vertical load is applied to the specimen using a hydraulic actuator. The actuator is mounted on the crosshead.

The triaxial cell is fixed to the lower platen. The triaxial cell push-rod is rigidly mounted to the actuator via a load cell. The position of the push-rod is monitored by a linear variable differential transformed (LVDT). A shut-off valve

manifold at the base of the triaxial cell provides control for the soil suction levels. The cell pressure is applied through a shut-off valve on the top plate of the cell.

An additional service manifold is attached to the load frame to accommodate reservoirs for the confining fluid and the pore fluid. Compressed air (obtained from an external air compressor) applied on the water in the pore fluid reservoir causes the water to flow into the specimen through the high-entry porous stone. In this study, the pore fluid reservoir was used as a source of pore water pressure. Pore air pressure was applied from a tubing connected to the valve for the confining pressure reservoir. A valve and a pressure gage are provided to control the pore water and pore air pressures respectively.

The controller consists of a MicroConsole that controls and monitors the operation of the load unit. It also provides chassis connections for functional plug-in modules. Jacks on the rear panel are provided for transducers, servo valves, hydraulic service manifold, etc.

Three plug-in modules are provided: an AC controller, a DC controller, and an Auxiliary Span Control. The Auxiliary Span Control was not used in this study. Either the AC controller or the DC controller can be used to operate the actuator mounted at the top of the load frame. The AC controller and DC controller control the movement of and the load applied by the actuator rod, respectively. Depending on the selected active controller, the test can be run in strain- or stress- controlled mode.



The MicroProfiler on the front panel of the Controller, is a microprocessor based, single output precision wave form generation device, which command the AC or DC controllers for tests in stress, strain, temperature and other test control parameters. Unique wave forms can be programmed with the front panel controls or from a personal computer using an RS232 serial interface. The MicroProfiler creates a wave form by linking together a series of programmed segments which include ramp, haversine and hold time segments. Segments can also be linked together to form a block. A block allows a sequence of segments to be programmed and blocks to be repeated a specific number of times or continuously. The wave form used in the present study was preprogrammed in the MicroProfiler as a ramp-up lasting 25 milliseconds followed by a ramp-down also lasting 25 milliseconds.

The Hydraulic Power Supply provides the high pressure fluid required for the operation of the system. The high pressure fluid is applied to one side of the actuator piston, causing it to move. A servovalve controls the movement of the actuator, by opening or closing in response to the Controller. The valve can be opened in either of two directions allowing the high pressure fluid to flow into the cylinder on either side of the piston. This causes movement of the piston in either of two directions.

### 7.3 TRIAXIAL CELL CALIBRATION

The calibration was done through the analysis of the friction among the push rod and o-ring of the cell. First, a load cell was placed inside the triaxial cell directly

resting on the top pedestal of the specimen. This approach eliminated the friction on the rod, reduced inertia forces due to the mass of rod and its attachments, and since the capacity of the load cell was smaller the noise levels were also considerably reduced.

With this internal cell installed dynamic tests were performed at high strain rates upon three synthetic specimens of different Young's modulus and at the conditions listed on Table 7.1. During testing, load values recorded by the external cell were read directly from the MicroProfiler display while those by the internal cell were read from the display of a separate unit amplifier.

A total of 360 data values were analyzed by the SAS-software (Statistical Analysis Software) yielding equation 7.1 which is a function in terms of confining pressure ( $\sigma_3$ ), and displayed load by MicroProfiler from the recorded load of the external load cell ( $P_{ext}$ ). The dependent variable being the expected load to be recorded by the internal cell ( $P_{int}$ ).

$$P_{int} = 0.0706 + 0.02642103(\sigma_3) + 0.96627432(P_{ext}). \quad (7.1)$$

Figures 7.1, 7.2, and 7.3 demonstrate the acceptable application of equation 7.1 to closely estimate the actual load applied to the specimen. The figures show the pattern of data values recorded by the internal load cell to coincide with the equation line. The line is where the data is expected to fall for each particular condition. After

Table 7.1

## Conditions of Dynamic Tests on Synthetic Specimens

Young Modulus (psi)	Confining Pressure (psi)	Programmed Load Pulse (lb)
2430	0	20
		40
		60
10070	50	80
		100
		150
52000	100	200
		250
		300
		350
		400
	150	450
	200	

Notes:

The above conditions allow for a total of 180 different combinations.

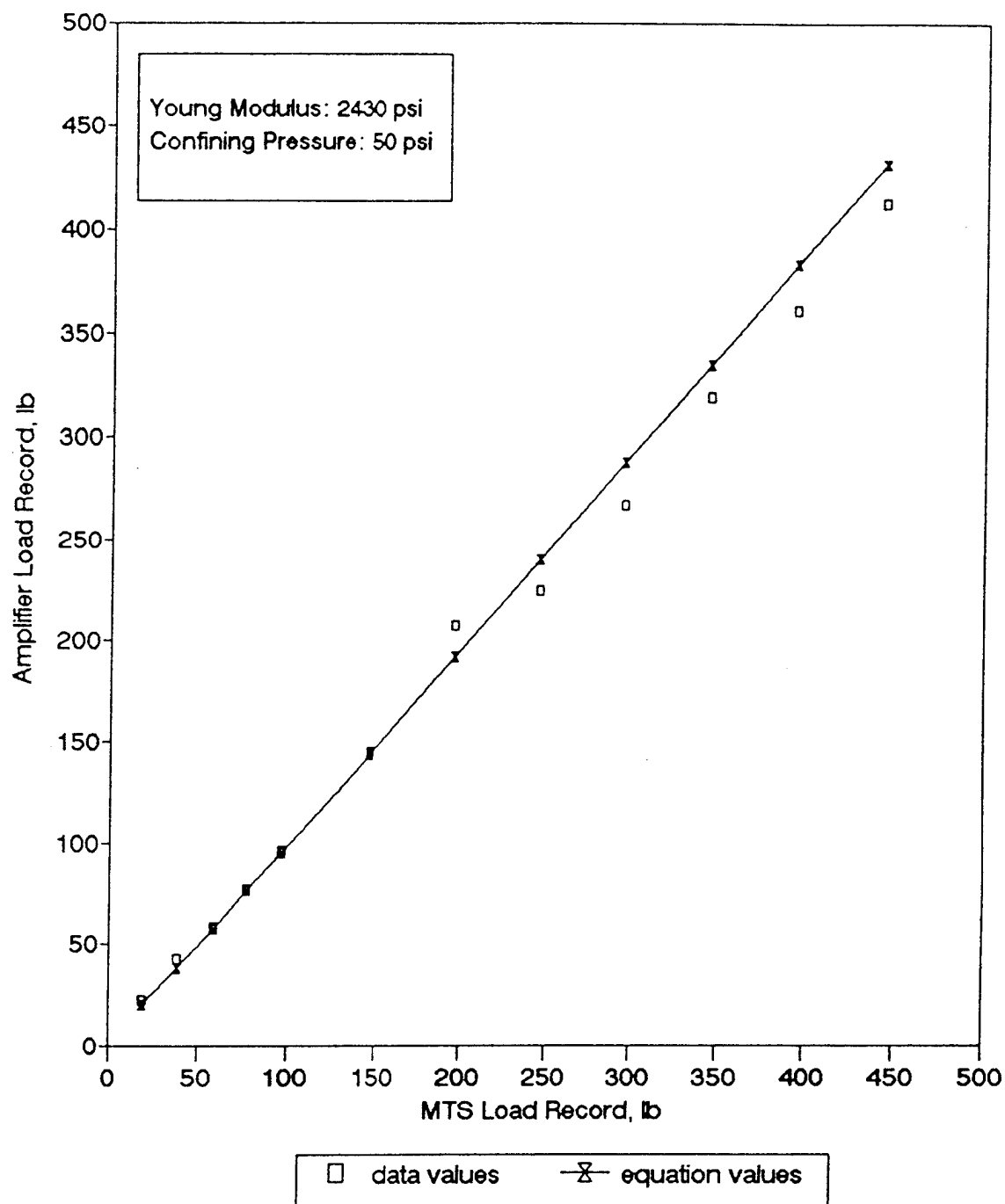


Figure 7.1 Comparison of Load Values Obtained by Equation and Load Cell  
for Soft Synthetic Specimen

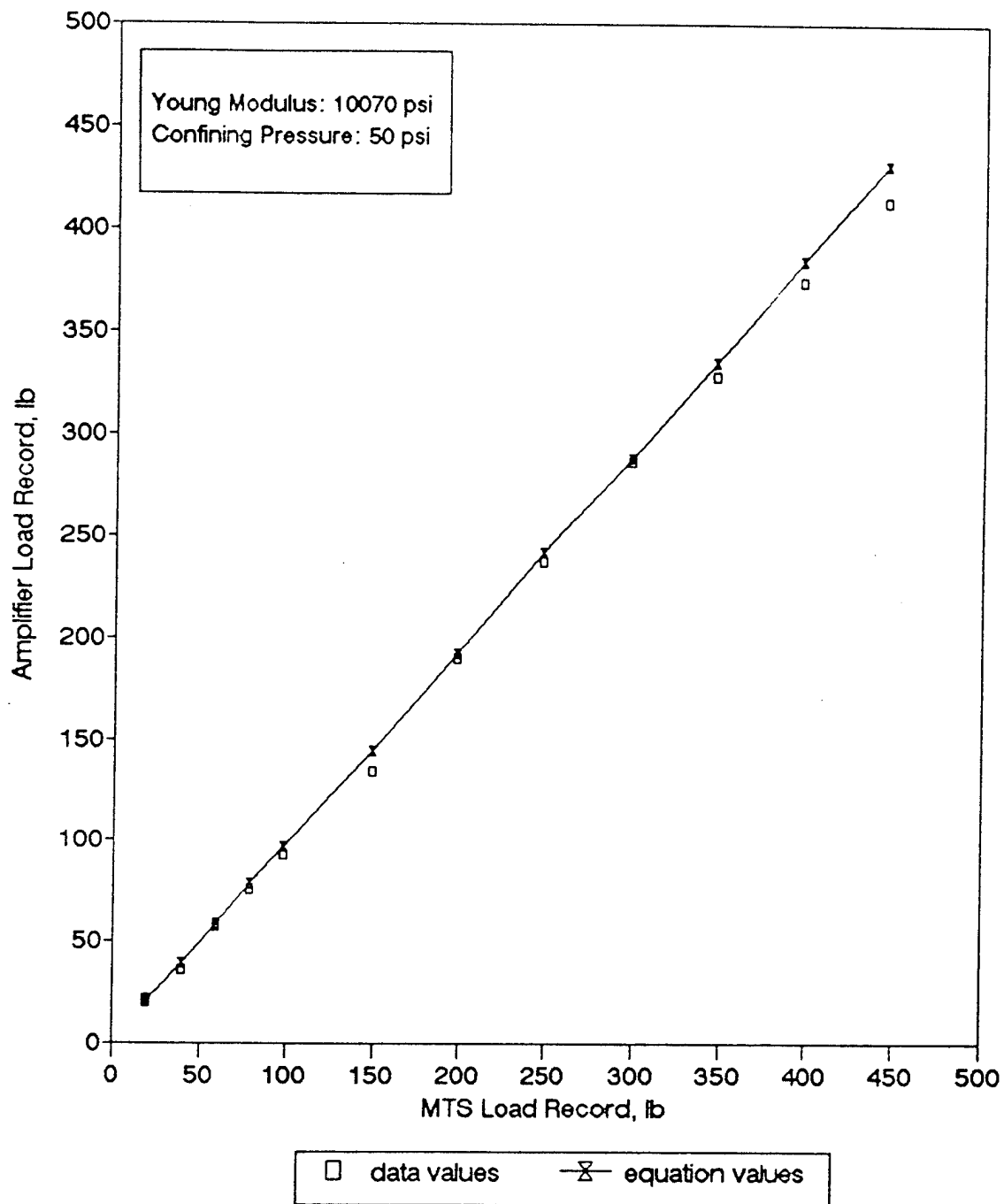


Figure 7.2 Comparison of Load Values Obtained by Equation and Load Cell  
for Medium Synthetic Specimen

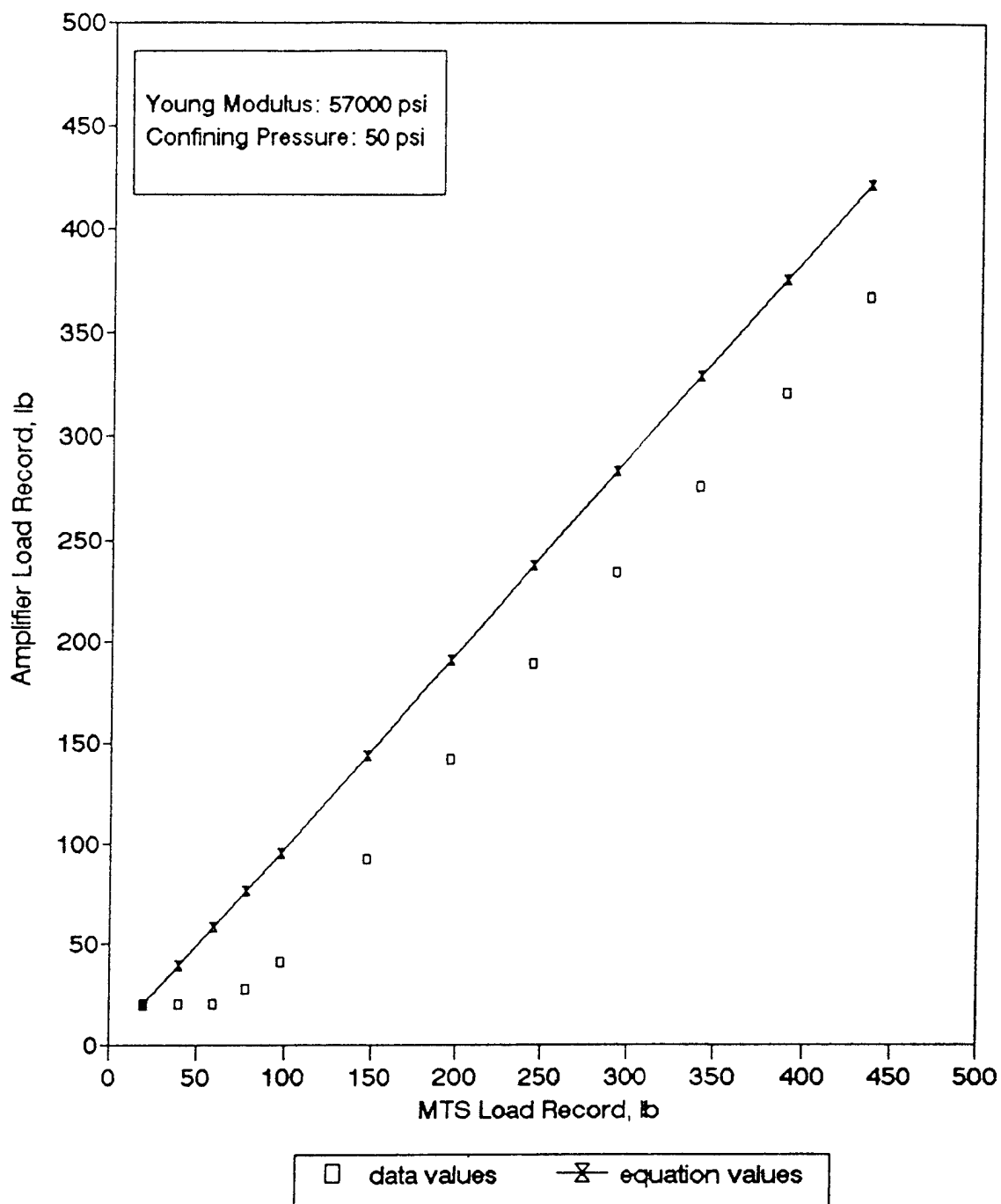


Figure 7.3 Comparison of Load Values Obtained by Equation and Load Cell for Hard Synthetic Specimen.

verifying the validity of equation 7.1, the difference in load recorded by the external load cell and the internal load cell was assumed to be that corresponding to the friction experienced by the push rod at the bushing. Appendix E shows the amount of friction to be expected for each confining pressure (from equation 7.1) and the actual friction experienced by the rod during testing (laboratory data). At the previous figures it is noticed that the friction increases as the confining pressure increases too; which was expected. Also, from the appendix, that as the applied load increased, the friction started to be constant. This was because the difference in recorded loads by the external and internal cells was not as significant for large loads (200->450 lb) as it was for small loads (20->80 lb).

By means of the developed equation (equation 7.1); the actual deviatoric stress experienced by the specimen was recalculated. Figure 7.4 is an example which compares the stresses recorded by the external and internal load cells. As a further step during the calibration process, the predicted strain was possible to be recalculated by the model equation using the deviatoric stresses that were recalculated with equation 7.1.

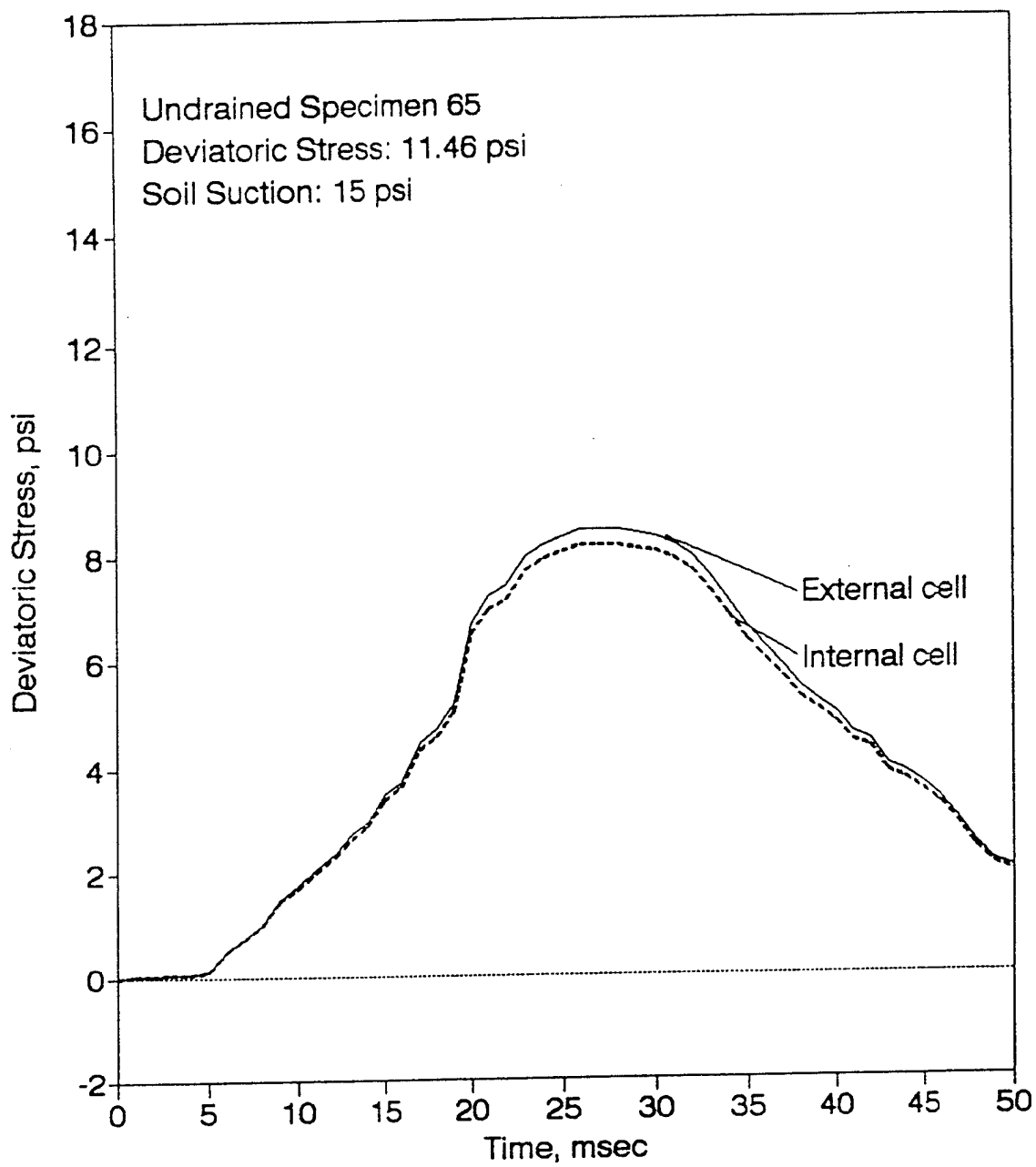


Figure 7.4 Comparison of Stresses Recorded by External and Internal Load Cells



## CHAPTER EIGHT

### HIGH STRAIN RATE TESTING

#### 8.1 INTRODUCTION

Dynamic tests were performed on specimens equilibrated at four suction levels. Thus, specimens of identical characteristics to those used for creep/recovery tests were subjected to high strain rates with concurrent variation in the deviatoric stress. Each test consisted of several pulses being applied on the specimen under controlled conditions. Each pulse lasting 50 milliseconds and consisting of a ramp-up loading to a peak stress and a ramp-down unloading to zero stress. The peak stress being increased from a pulse to the next. This chapter discusses the specimen preparation, the methodology for conducting the tests, the procedures for data reduction, and the results of the scheduled tests.

#### 8.2 SPECIMEN PREPARATION

With the same procedure employed for creep specimens, dynamic tests specimens were consolidated from slurry. After fully reaching this phase, the specimens were trimmed and placed inside the triaxial cell used for the MTS facility for their equilibration. After the equilibration process was completed, all cell valves were closed and pressure lines removed. Immediately, the cell, with the specimen

inside, was moved from the constant temperature room to the MTS facility where it was reconnected to the water and air pressure lines. All initial pressure conditions were established again and the cell was allowed to stabilize during a couple of minutes. Then, testing proceeded rapidly to prevent temperature effects on the specimen, with the advantage of being the specimen temporarily insulated by the same water surrounding it during the equilibrium phase.

### 8.3 METHODOLOGY FOR CONDUCTING TESTS

When the equilibrium process was finalized, the triaxial cell containing the specimen was taken to the MTS test facility room where it was fixed to the base platen of the loading unit. Air and water pressures were reconnected and stabilization time of approximately 2 minutes was allowed. During this time the controller was kept on in a strain-controlled mode. The push rod of the triaxial cell was connected firmly to the load cell of the loading cross head. Next, the out-put of the DC-transducer was adjusted to zero so that the net programmed stress would be the stress received by the specimen. After this, the controller was changed to stress-controlled mode and the output of the AC module was adjusted to zero for proper strain measurements initialized at zero. The load cycles were applied at this point. The MicroProfiler was used for applying the stress pulses listed by Table 8.1. Each pulse was separately programmed into the memory of the MicroProfiler and it consisted of a ramp-up to the peak deviatoric stress in a time period of 25 msec, and a ramp-down

Table 8.1

Load Pulses Applied to the Specimen During a Time Span of 50 msec

Load Pulse No.	Peak Deviatoric Stress psi	Rate psi/min
1	5.73	13752
2	11.46	27504
3	17.19	41256
4	22.92	55008
5	28.65	68760
6	34.38	82512
7	40.12	96288
8	45.85	110040
9	51.58	130992
10	57.31	137544
11	63.04	151296
12	68.77	165048
13	74.50	178800
14	80.24	192576
15	85.97	306328

back to zero psi in a time period of 25 msec. After each load pulse or termination of a program, the AC controller was readjusted to zero so that the next pulse displacement recording would also start from zero.

During each pulse, the data was collected with an analyzer by means of three channels. One channel for the load cell data, a second channel for the LVDT or displacement data, and a third for the MicroProfiler output signal. The analyzer was triggered in advanced, before the stress pulse was applied, so that the entire pulse phase could be fully recorded. For each programmed stress pulse, a total of 4000 data points per channel were collected and saved in a personal computer memory. After the specimen received the last stress pulse, it was removed from the triaxial cell for water content determination.

#### 8.4 PROCEDURES FOR DATA REDUCTION

Each test provided extensive amounts of data which required appropriate reduction. Thus, data reduction was done by the means of the same computer program used during the parent project. The program would automatically provide the strain-time and stress-time relationships. For reference purposes, the program is presented in Appendix F. The program, written in FORTRAN 77 and named "hstrain," would perform in the following sequence:

- 1) The voltage data is smoothed. This is performed by replacing the

value of the voltage at a certain time with the average voltage between the replaced voltage and the voltage at the previous time.

- 2) The next step is to convert the voltage to stresses and strains. The voltage from the load cell is first transformed to load, and this load divided into the undeformed cross section area of the specimen providing the stress. The voltage from the LVDT is first transformed to displacement, and this displacement divided into the initial length of the specimen providing the strain.
- 3) The third step is to identify time zero when the wave form was initialized. This is accomplished scanning the stress and strain time series data.
- 4) The program forms two files. One with the stress-time history detected by the load cell and the second with the strain-time history detected by the LVDT of the push rod.

The output file contains the information on the loading sequence such as desired peak stress, peak deviatoric stress actually measured by the load cell, peak strain for each loading step, and stress-time and strain-time histories for each pulse of stress applied on the specimen.

## 8.5 RESULTS OF SCHEDULED TESTS

Scheduled tests for each soil suction level have been performed along with

three repetitions for the cases of 15 psi, 40 psi, and 70 psi. For the case of 30 psi a repetition was not possible due to time limitations. Table 8.2 presents the tests for specimens equilibrated at 15 psi soil suction; Table 8.3 presents the results for specimens equilibrated at 30 psi soil suction; Table 8.4 presents the results of specimens equilibrated at 40 psi soil suction; and Table 8.6 presents the results of specimens equilibrated at 70 psi soil suction. Also, a graphical appreciation of each individual test for each combination of soil suction and deviatoric stress level is available in Appendices G, H, and I. Notice that specimen 55 was not properly listed on a table because of problems with the equipment operation during its testing. Also, Table 8.3 does not present any results since only noise was recorded by the system during testing of specimen 63; consequently no appendix is included for test results.

Table 8.2

## Results of Dynamic Tests for Specimens Equilibrated at 15 psi

Load Pulse No.	Desired Peak Stress psi	Measured Peak Stress psi			Measured Peak Strain %		
		Drained	Undrained		Drained	Undrained	
		25	68	65	25	68	65
1	5.73	4.28	none	none	0.026	none	none
2	11.46	7.62		8.44	0.061		0.137
3	17.19	10.79		12.11	0.111		0.167
4	22.92	15.59		16.25	0.193		0.628
5	28.65	17.33		none	0.266		none
6	34.38	21.66			0.353		
7	40.12	25.02			0.459		
8	45.85	26.30			0.573		
9	51.58	29.08			0.702		
10	57.31	29.48			0.851		
11	63.04	none			none		
12	68.77	none			none		
13	74.50	none			none		
14	80.24	none			none		
15	85.97	none			none		

Notes:

Drained specimens were selected from results of parent project.

Table 8.3

Results of Dynamic Tests for Specimens Equilibrated at 30 psi

Load Pulse No.	Desired Peak Stress psi	Measured Peak Stress psi			Measured Peak Strain %		
		Drained	Undrained		Drained	Undrained	
		none	63	none	none	63	none
1	5.73		*			*	
2	11.46		*			*	
3	17.19		*			*	
4	22.92		*			*	
5	28.65		*			*	
6	34.38		*			*	
7	40.12		*			*	
8	45.85		*			*	
9	51.58		*			*	
10	57.31		*			*	
11	63.04		none			none	
12	68.77						
13	74.50						
14	80.24						
15	85.97						

Notes:

(\*) Only noise was detected by the system at this load pulse.



Table 8.4

Results of Dynamic Tests for Specimens Equilibrated at 40 psi

Load Pulse No.	Desired Peak Stress psi	Measured Peak Stress psi			Measured Peak Strain %		
		Drained	Undrained		Drained	Undrained	
			61	66		61	66
		41	61	66	41	61	66
1	5.73	4.81	none	3.14	0.022	none	0.031
2	11.46	9.04		5.64	0.052		0.078
3	17.19	12.35		7.28	0.087		0.134
4	22.92	19.42		9.48	0.152		0.235
5	28.65	21.17		none	0.195		none
6	34.38	24.82			0.258		
7	40.12	28.95			0.338		
8	45.85	33.41			0.409		
9	51.58	34.91			0.504		
10	57.31	41.43			0.609		
11	63.04	40.51			0.740		
12	68.77	42.38			0.861		
13	74.50	42.35			1.015		
14	80.24	42.07			1.132		
15	85.97	43.14			1.279		

Notes:

Drained specimens were selected from results of parent project.

Table 8.5

Results of Dynamic Tests for Specimens Equilibrated at 70 psi

Load Pulse No.	Desired Peak  Stress  psi	Measured Peak  Stress  psi			Measured Peak  Strain  %				
		Drained	Undrained		Drained	Undrained			
			31	58		67	31	58	67
1	5.73	4.53	none	4.17	0.013	none	0.093		
2	11.46	9.17		6.36	0.034		0.175		
3	17.19	12.92		5.58	0.061		0.147		
4	22.92	16.65		6.30	0.092		0.179		
5	28.65	21.92		none	0.142		none		
6	34.38	21.49			0.135				
7	40.12	25.80			0.191				
8	45.85	28.11			0.242				
9	51.58	30.61			0.299				
10	57.31	33.93			0.384				
11	63.04	37.05			0.462				
12	68.77	38.97			0.553				
13	74.50	41.15			0.651				
14	80.24	42.47			0.745				
15	85.97	44.02			0.858				

Notes:

Drained specimens were selected from results of parent project.

## CHAPTER NINE

### PREDICTED AND MEASURED DYNAMIC BEHAVIOR

#### 9.1 INTRODUCTION

With the power laws developed and fitted to the creep and recovery data, the response of the specimens during the application of load pulses during dynamic testing has been predicted.

The application was based on the observations and conclusions of the parent project which influenced the belief that the initial part of the transient creep phase would be the model with the most possibilities of explaining the dynamic test behavior.

Thus, in this study the initial power model was used in conjunction with the modified superposition principle (Findley et al, 1976) and the indirect methods proposed by Shames and Cozarelli (1991) which are based on strain hardening hypothesis.

This chapter contains the comparisons obtained using the modified superposition and the initial power law. It also explains the procedure for predicting the specimen response.

## 9.2 METHODOLOGY FOR PREDICTING THE SPECIMEN RESPONSE

This part of the study consisted in arranging the data of the dynamic tests so that it could be used as the input to predict the specimen response. First, the recorded load pulse was approximated by a step like function of constant stress during every millisecond of the 50 msec. duration of the load pulse. For times beyond 50 msec. , the noise recorded from the load cell was neglected and the deviatoric stress was fixed at zero. An example of a load pulse recorded with the step-like approximation superimposed is shown in Figure 9.1.

To predict the strain to be experienced by a specimen during a dynamic test; the modified superposition principle as described by Findley et al (1976) was used. For reference purposes, Findley's method suggests that for N step-wise changes of stress input from  $\sigma_{i-1}$  to  $\sigma_i$  at  $t=t_i$  , the corresponding creep strain at  $t>t_N$  is represented by the following form:

$$\epsilon(t) = \sum_{i=0}^N [f(\sigma_i, t-t_i) - f(\sigma_{i-1}, t-t_i)] \quad t > t_N \quad (9.1)$$

where  $f(\sigma, t)$  is the nonlinear viscoelastic stress-strain-time relationship. In this approach every step is added in full at the beginning of the step (that is from zero to the full value of the deviatoric stress) and subtracted in full at the end of the step. The response at any time is the result of the superposition of all the additions and subtractions from previous steps. In algebraic form, a step-like function of the

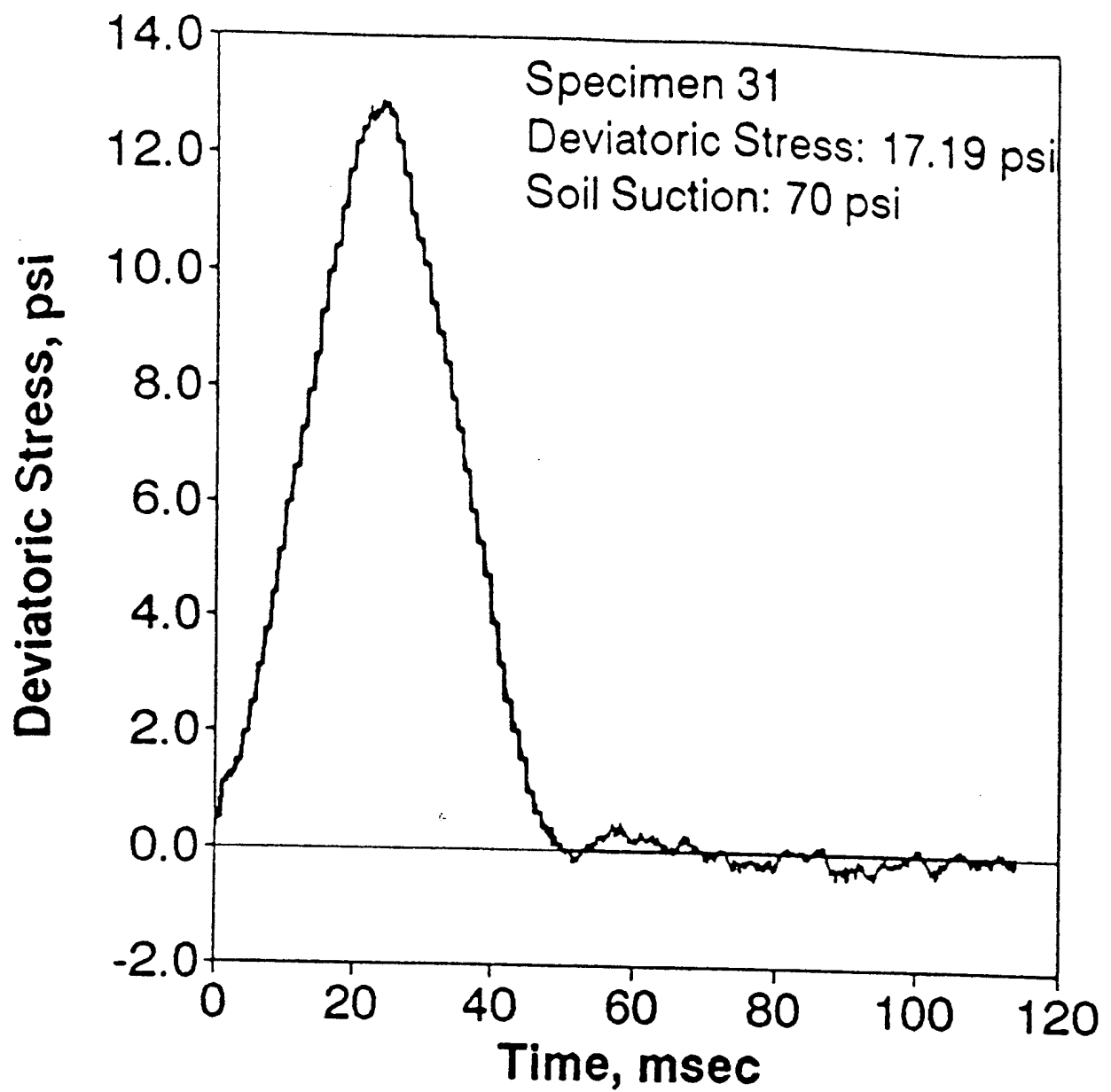


Figure 9.1 Example of The Approximation of The Load Pulse Used in The Predictions (Cheng Chang, 1992)

following type:

- 1)  $\sigma_1$  from  $t_1 / t_2$
- 2)  $\sigma_2$  from  $t_2 / t_3$
- .....
- 3)  $\sigma_N$  from  $t_n / t_{n+1}$

and being used in combination with the initial power law with a power stress function:

$$\epsilon(t) = \alpha_1 \sigma_d^{\alpha_2} t^\beta \quad (9.2)$$

Then the modified superposition principle would become the following relationship:

$$\begin{aligned} \epsilon_p(t) = & \alpha_1(\sigma_1)^{\alpha_2} (t - t_1)^\beta + \sum_{i=1}^N [-\alpha_1(\sigma_i)^{\alpha_2} (t - t_{i+1})^\beta + \\ & \alpha_1(\sigma_{i+1})^{\alpha_2} (t - t_{i+1})^\beta], \text{ for } t_{n-1} \leq t \leq t_{n+2} \end{aligned} \quad (9.3)$$

The modelling consisted in reading the deviatoric stress-time history and forming the step-like function by averaging the stress readings within one millisecond, for the first 50 milliseconds; and using this stress function in conjunction with equation 9.3 to predict the strain-time history for the specimen.

### 9.3 RESULTS AND DISCUSSION

The response of all the specimens tested in dynamic tests was predicted by the initial power model with power stress function, as it was suggested by the parent project. Examples which offer comparison of measured versus predicted strain histories, refer to Appendices G, H, I, and J. For demonstration purposes, results of tests on specimen 41 of the parent project are presented in Figure 9.2. The results indicate that the model predicts quite approximately, for drained conditions, the behavior of the specimens at low deviatoric stress levels, and specially can explain the plastic strain remaining for the specimens after the application of a load pulse. The main shortcoming of the model was its over prediction, for drained conditions, of the peak strains in the vicinity of the peak of the stress pulse. For undrained conditions, Figure 9.3, peak predictions were observed to be much closer. Thus, soil saturation conditions have some effect on the predictions of strain. Comparison of measured versus predicted strain histories for specimens equilibrated at soil suction levels of 15 psi, 40 psi, and 70 psi are presented by Figures 9.4, 9.5, and 9.6, respectively. For 30 psi a comparison is not presented because it was not possible to perform a drained test due to time limitations.

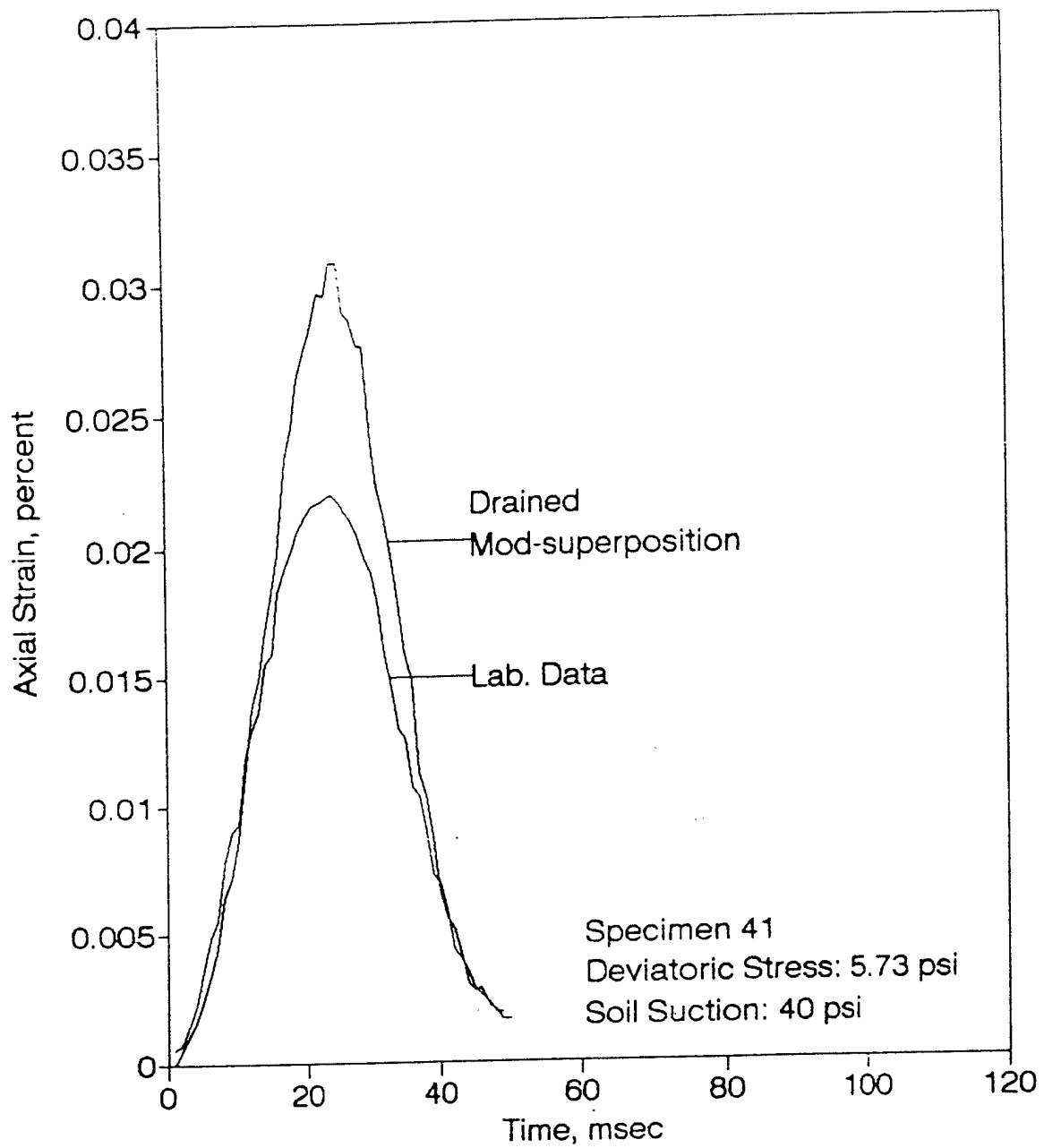


Figure 9.2 Comparison of Predicted Versus Measured Strain For Drained Conditions (Cheng Chang, 1992)



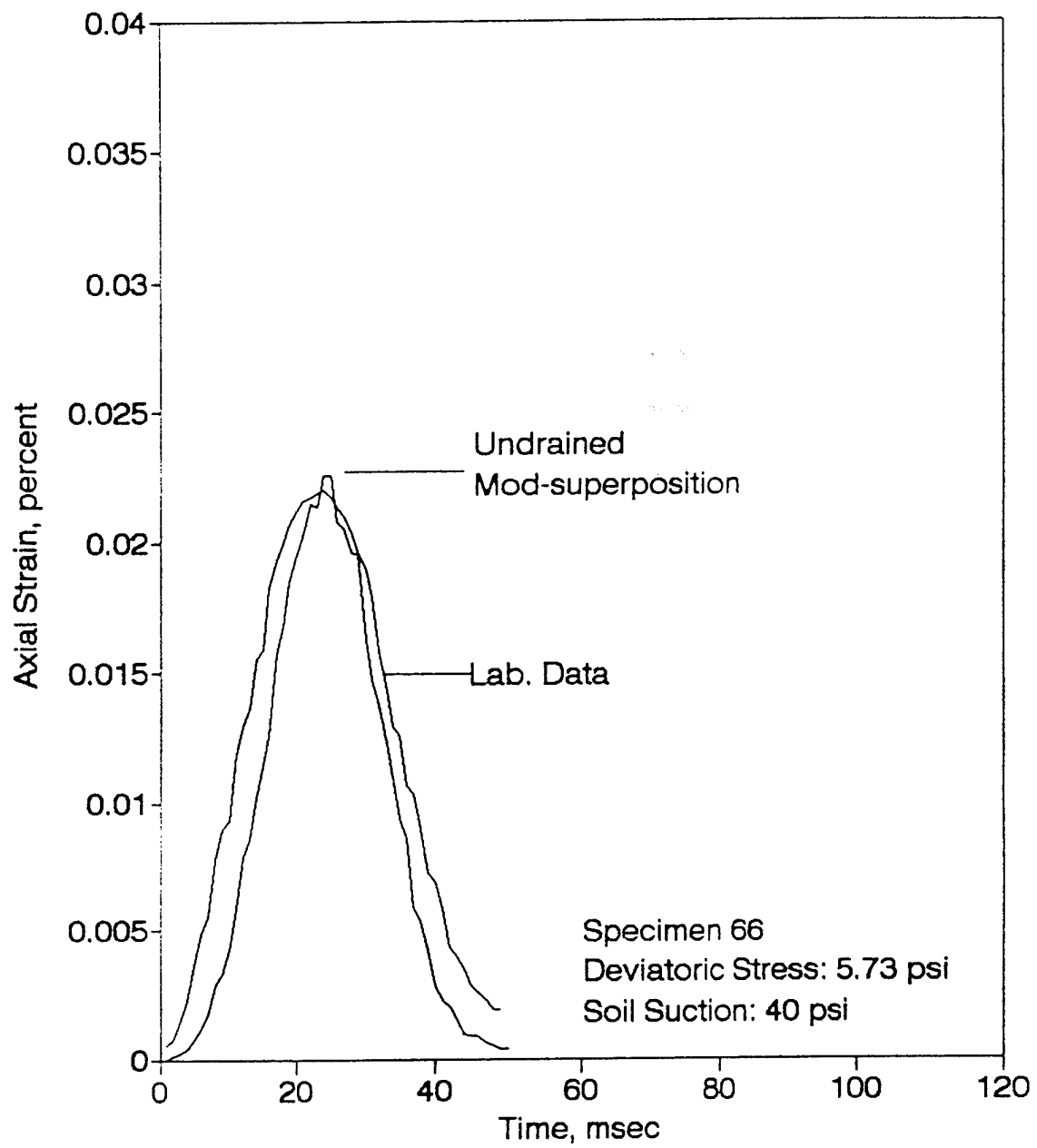


Figure 9.3 Comparison of Predicted Versus Measured Strain For Undrained Conditions

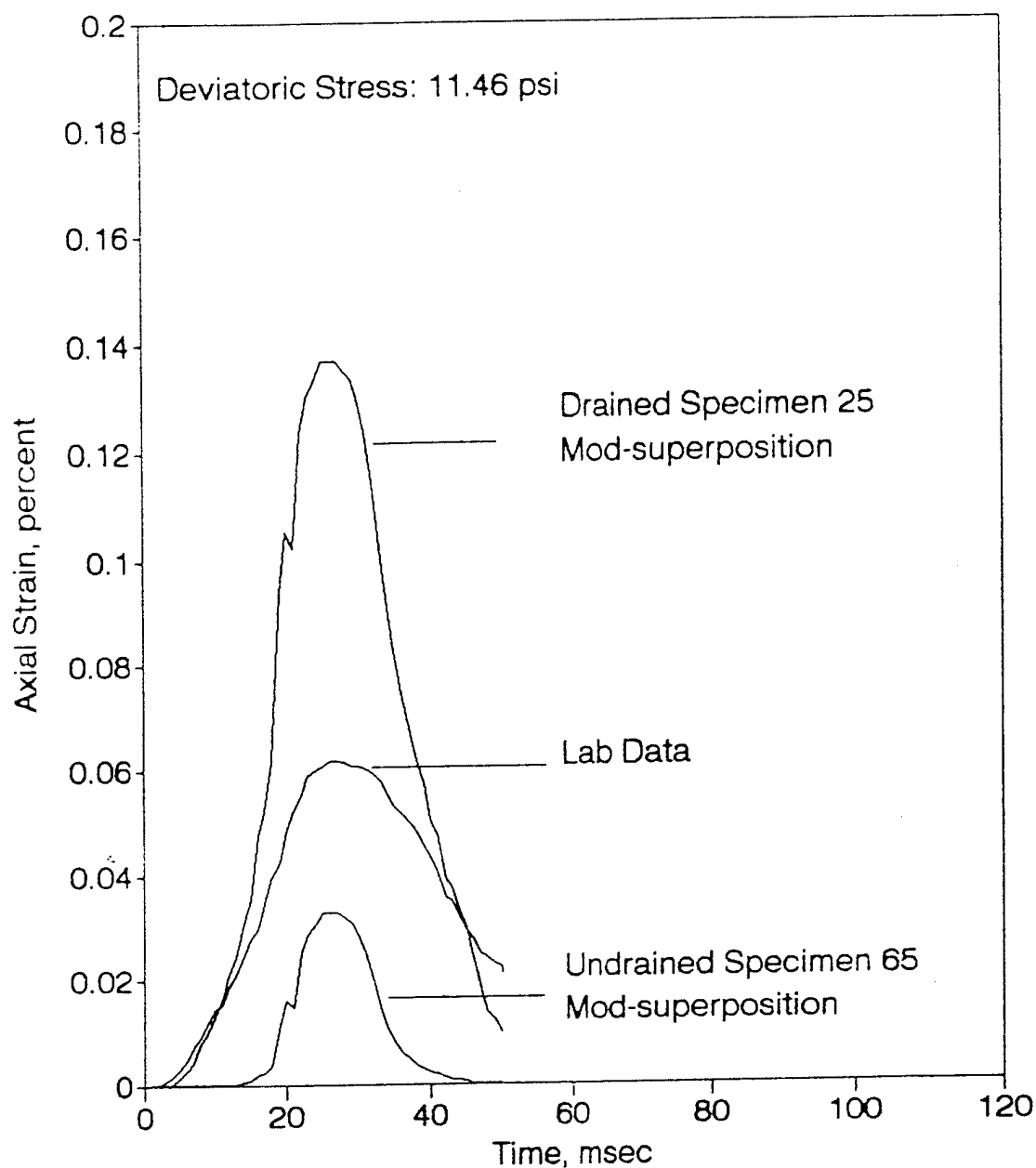


Figure 9.4 Comparison of Strains For Drained (Cheng Chang, 1992) and Undrained Conditions at 15 psi Soil Suction

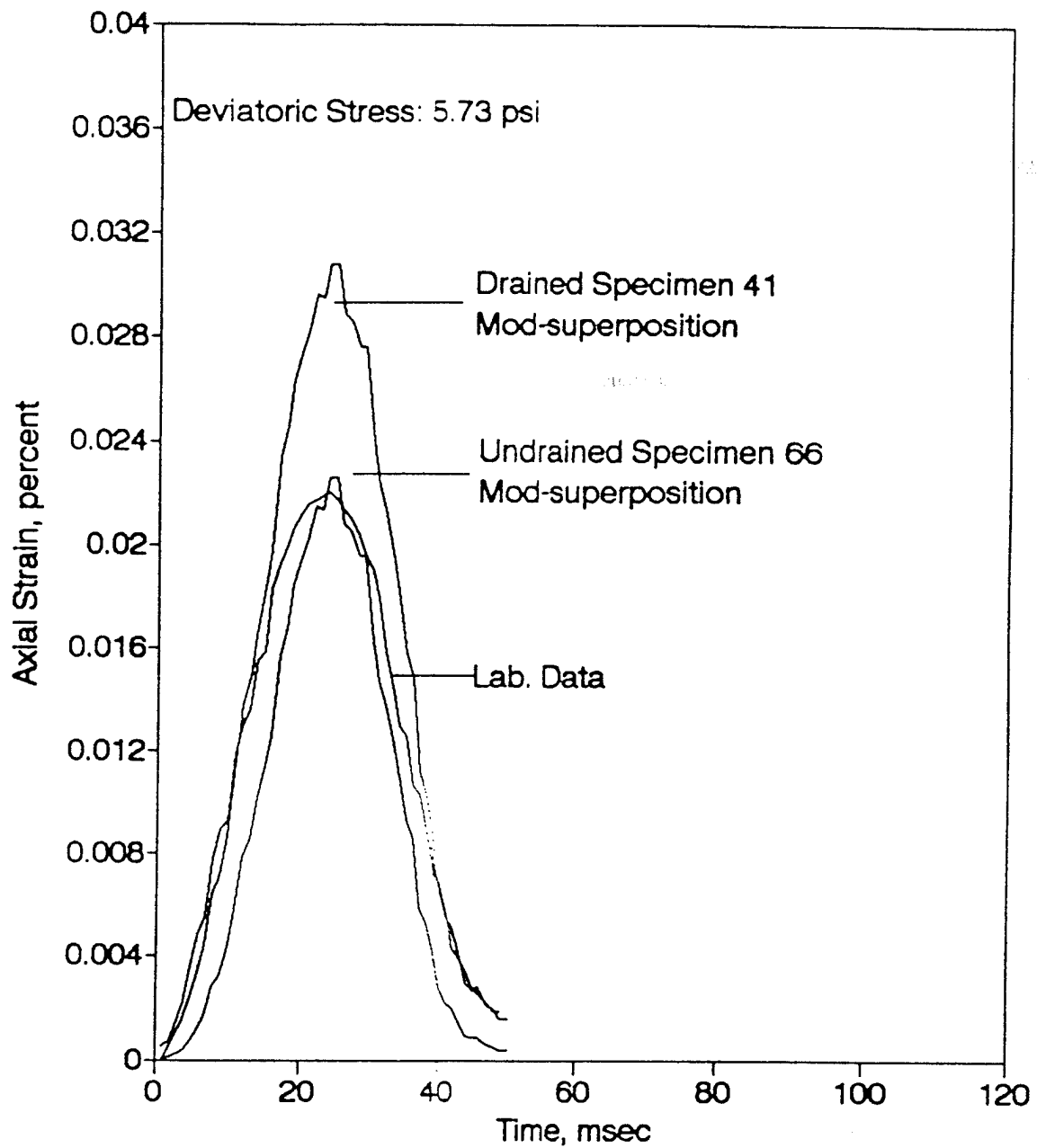


Figure 9.5 Comparison of Strains For Drained (Cheng Chang, 1992) and Undrained Conditions at 40 psi Soil Suction

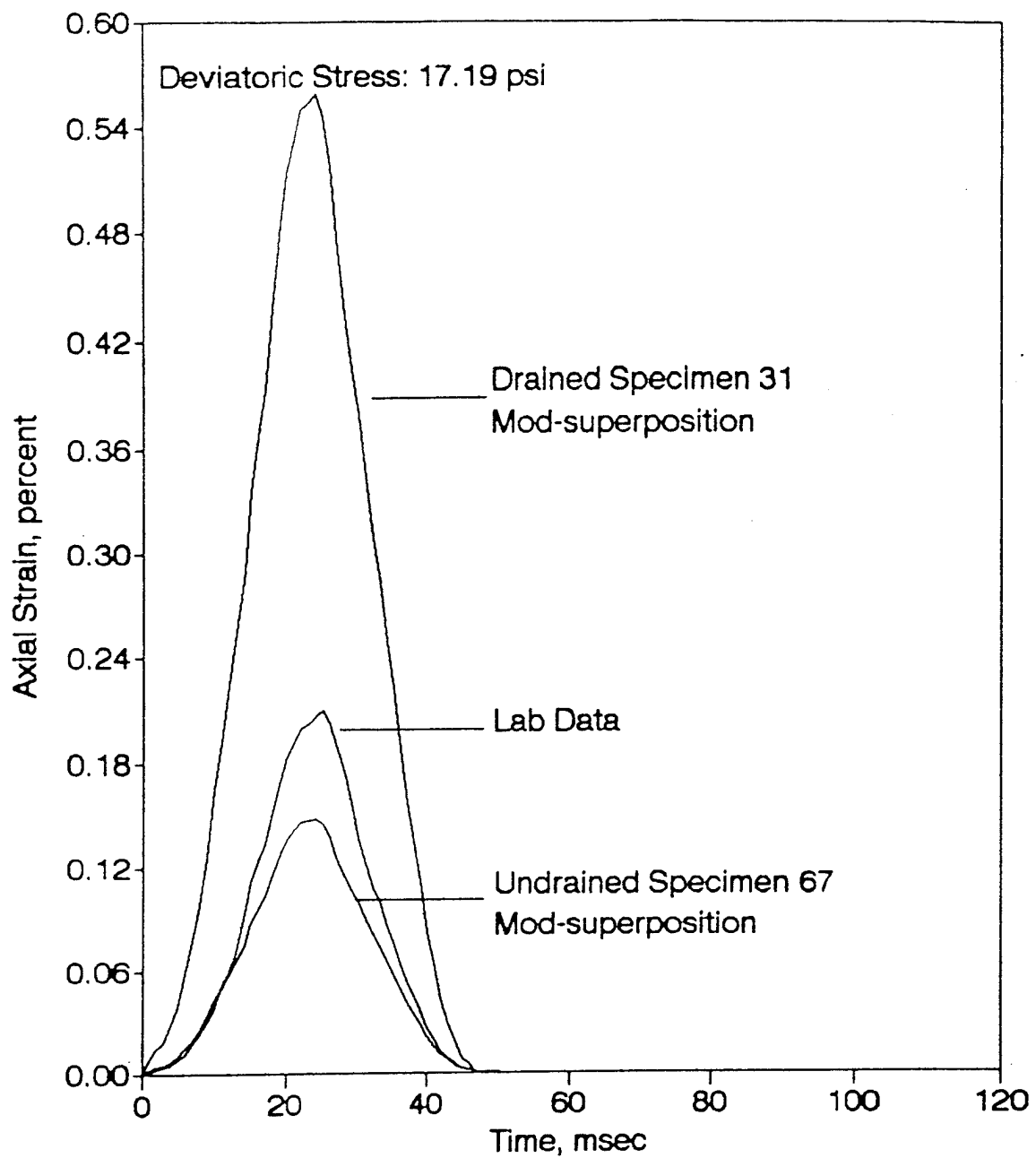


Figure 9.6 Comparison of Strains For Drained (Cheng Chang, 1992) and Undrained Conditions at 70 psi Soil Suction

### 9.3.1 Sources of Error

A probable source of error which explains the observed discrepancies among predicted and measured strain histories for drained and undrained conditions is believed to be due to shortcomings of the initial power law model. During the development of the model, the values of the parameters could be improved by incrementing the number of testing conditions and repetitions which could reduce the variability that was observed during comparisons of model predictions and creep/recovery tests. Thus, by such increment the model would be improved.

Another possibility is the differences in loads programmed and measured during the dynamic testing. Such differences were related to the calibration of the MTS system which consequently caused errors in the stress-time histories recorded. Furthermore, some of the load programmed was balanced by the cell pressure reducing the stress and strain to be experienced by the specimen. Thus, these situations caused differences among predicted and measured strain histories.

A final possibility causing differences on predicted and measured strains was due to the differences in loads, those registered by the load cell versus those experienced by the specimen, as a result of the inertia of the push rod and its attachments. Between the external load cell and the specimen, the total mass of the rod and attachments was of 3.5 kilograms. Such mass subjected to acceleration changes and reversals in time periods of less than a millisecond caused the load cell to experience an incremented load, or a reduced load depending on the movement of

the piston, to be recorded. Thus, when inertia force is experienced, such additional force increment is simultaneously subtracted of the specimen's experienced stress; oppositely, when it is subtracted, the specimen experiences an additional stress.

The appendices present some cases of both drainage conditions which clearly indicate the need of testing repetitions which would improve the approaching to a better representative value of the parameters. For example, the parameters of the model for undrained condition and 70 psi soil suction require verification since it is believed the predictions could be closer to the laboratory data results if the values of the parameters are further investigated and determined.

## CHAPTER TEN

### CONCLUSIONS AND RECOMMENDATIONS

#### 10.1 SUMMARY

Since the study was a continuation of the parent project "Behavior of Unsaturated Clayey Soils at High Strain Rates," the same overall approach was adopted with very minor alterations. The preparation of specimens began by forming a soil suspension with the recycled trimmings, the tested specimens, and a 0.01 molal solution of calcium chloride. This first step consisted in dispersing the soil into a container, flushing it repeatedly with the solution, allowing the solution to flocculate and sediment in the container, and decanting the clean supernatant. The flushing, sedimentation, and decanting continued until the electrical conductivity of the supernatant was 1900 micromhos/cm. The finished soil suspension was sampled and the samples were centrifugated at 2000 rpm for 15 minutes. The clear supernatant was discarded, the soil cake left was placed on a glass plate and thoroughly mixed to homogenize the soil slurry.

The second step was the slurry consolidation under 50 psi cell pressure in a conventional triaxial cell. The slurry was placed inside a rubber membrane on a 2.8 inch in diameter pedestal and top cap. The specimen's initial height was 5 inches. During consolidation, the outflow from the specimen was directed towards a burette

and the volume of expelled water recorded. Volume of water expelled ranged from 85 ml to 475 ml and the time necessary to reach a steady state on the consolidation curve ranged from 10 to 14 days.

The third step of the process was the trimming of the consolidated sample to a size of 3 inch high and 1.4 inch in diameter. The trimmed cylindrical specimen was enclosed by a rubber membrane and placed in a triaxial cell over a high air entry ceramic porous stone to equilibrate it to a predetermined soil suction. The soil suction levels used were 15 psi, 30 psi, 40 psi, and 70 psi. Under this condition, the specimen was allowed to equilibrate while the volume of pore fluid being expelled or imbibed was monitored. The volume of pore water expelled ranged from fractions of a milliliter to 45 ml, and the imbibed volume from 0.2 ml to 6 ml, this depending on the applied soil suction level. The equilibration phase stopped when the movement of pore water in or out of the specimen had leveled off. This was normally not more than 14 days.

The fourth step was the application of the desired load. For drained conditions, this was done by loading the platform, removing the rod adjuster, and monitoring the displacements using a dial gage of 0.0001 inches readability. The monitoring of the specimen's deformation was performed until the secondary creep phase was reached. The time for this was normally not more than 14 days. After the equilibration step was completed the drainage condition was adjusted, the load application started, and displacement monitored.



The fifth step was fitting of the creep curve in the power law model using the initial part of the creep phase and the values of parameters  $\alpha$  and  $\beta$  obtained from linear regression analysis. Since parameter  $\beta$  was found to be independent of soil suction, dependent of deviatoric stress, and the average values for each deviatoric stress level seemed to be in a fairly narrow range; it was approximated with a linear regression. Parameter  $\alpha$  was observed to increase with the deviatoric stress and the variation was fitted with a power law of the deviatoric stress. The parameters  $\alpha_1$  and  $\alpha_2$  were obtained from regression analysis for each appropriate suction level. Two proposed models, one for each drainage condition, were fitted to the creep data of the initial 60 minutes.

The sixth step was the dynamic testing of specimens equilibrated to the same soil suction levels, performed in a closed-loop servo valve MTS test system. Each test consisting of several pulses being applied on the specimen under stress controlled conditions. Each pulse lasting 50 milliseconds and consisting of a ramp-up loading to a peak stress and a ramp-down unloading. The peak stress being increased from a pulse to the next. The specimen preparation was identical to that of specimens for creep tests. After completing the high strain rate test, the data collected was reduced and the strain-time and stress-time relationships were obtained and plotted.

The last step, was the comparison of predicted versus measured dynamic behavior. The prediction was performed using the modified superposition principle (Findley et al, 1976) with the power law model of the initial transient creep strain.

The prediction methodology consisted in using the actually recorded load pulse as the input to predict the specimen's response. The load pulse data was approximated by step like functions of constant stress during every millisecond of the 50 msec duration of the load pulse. The predicted strain-time history was plotted and compared with the laboratory measured data. Allowing for comparisons of the measured versus predicted strain histories and observe the effects of soil saturation conditions while subjected to high strain rates.

## 10.2 CONCLUSIONS

The soil suspension used for the preparation of specimens was composed of 53% clay size particles and 47% silt size particles. The soil has a liquid limit of 60% and plasticity index of 35%. Cation exchange capacity of soil averaged 48.7 meq/100gr. The soil has a mineral composition that includes smectite, mica, quartz, and kaolinite. The hydrometer analysis revealed a particle make up variability which yielded a difference of about 4 % to be shown in the grain size distribution curve; such results indicated that the preparation of replicate specimens was a major problem and thus, results could not be taken at face value.

The consolidation process at a cell pressure of 50 psi yielded preliminary specimens with water contents that ranged from 19.83% to 36.42%. Although the majority of the specimens fell in a narrow range of moisture contents, the differences are attributed to the amount of water content and to the differences in particle make

up of slurry. Thus, final conditions of all soil stock batches require the same moisture content; the amount of moisture content at each soil suspension sample for centrifugation also needs to be the same; and the centrifuged cakes require a better mixing operation since non-homogeneous slurry causes larger percentages of clay particles resulting in a soil with larger affinity for water.

The equilibrium process at the four soil suction levels of 15 psi, 30 psi, 40 psi, and 70 psi; yielded final specimens for testing after expelling or imbibing pore fluid in accordance to their applied suction level. Thus the water content of the specimens was altered after this process. The movement of the pore fluid, as illustrated by Appendix B, was observed to be not consistent to a specific pattern; but such particularity did not affect the purpose of this study which intended to perform this process for obtaining completely homogeneous specimens for each particular suction.

The nonlinear viscoelastic model suggested at the parent project provided a satisfactory and close fit of the initial part of the transient creep phase. The model, a power law of time with a coefficient being a power law of the deviatoric stress level, was applied to both drainage conditions where it was observed that the parameters were to some extent dependent on soil suction, although this should not be generalized since a much larger data base needs to be developed. At this stage only the exponent has definitely been assumed to depend directly on the deviatoric stress level. Furthermore the coefficient too, but by means of a power law of deviatoric stress with exponential function of deviatoric stress level.

The predictions were possible by using the modified superposition principle in conjunction with the developed model. Such combination predicts quite approximately the behavior of the specimens at low deviatoric stress levels as well as the plastic strain remaining for the specimens after the application of a load pulse during dynamic testing. But the model presented some limitations which mainly were related to over predictions, for drained conditions, of the peak strains in the vicinity of the peak of the stress pulse. This was not the case for undrained conditions, with a few exceptional cases, as presented by the appendices. Performing undrained creep tests resulted in closer approximations of the dynamic behavior. Thus, drainage during creep was found to have significant implications even for very early stages of creep test.

In result, with some limitations, as it was the case for the parent project; the results of undrained creep tests can be of substantial and valuable assistance during the study of the behavior of unsaturated clayey soils subjected to high strain rates, specifically while intending to predict such behavior.

### 10.3 RECOMMENDATIONS

The soil stock preparation needs to be done with a stricter control to obtain all final soil stock batches of same moisture content, and consequently have all the samples of the soil suspension for centrifugation with the same initial moisture content. Additional, the suspension needs to be completely agitated and thoroughly

rod-mixed while it still remains at the container, so that collection of homogeneous samples for centrifugation would be possible.

The results of this study strongly suggest the necessity for several repetitions of tests at each combination of testing condition so that the model parameters would have a value of higher level of confidence. Furthermore, soil suction levels under which research needs to be done should be incremented so that a better relationship among the model parameters and soil suction levels can be established. With these two additional suggestions better predictions could be obtained.

In regard to the dynamic testing equipment, the results could be improved if the system becomes more stable. In this manner, the programmed stress would be the stress received by the specimen after a particular loading cycle is terminated. To overcome this problem, it is recommended that a larger servovalve permitting a larger flow rate towards the actuator allowing for better response and stability of the system be adapted. Additionally, for a cleaner data, of reduced noise levels recording, a load cell of smaller capacity is suggested along with the corresponding cartridge of proper limits for the DC-Controller.

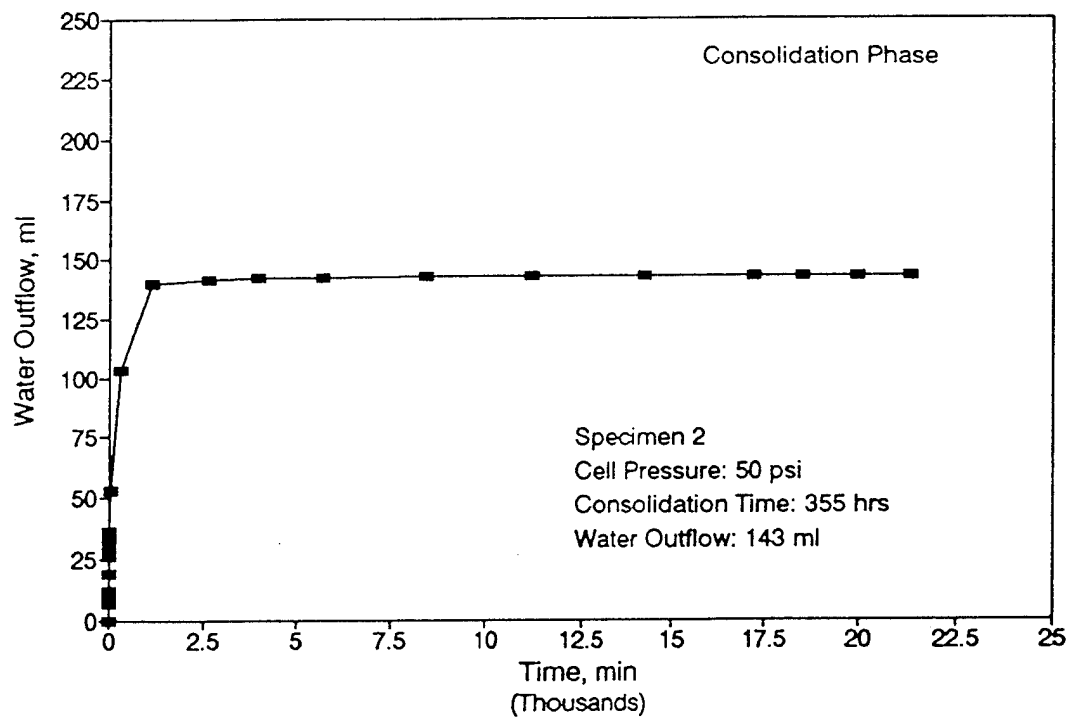
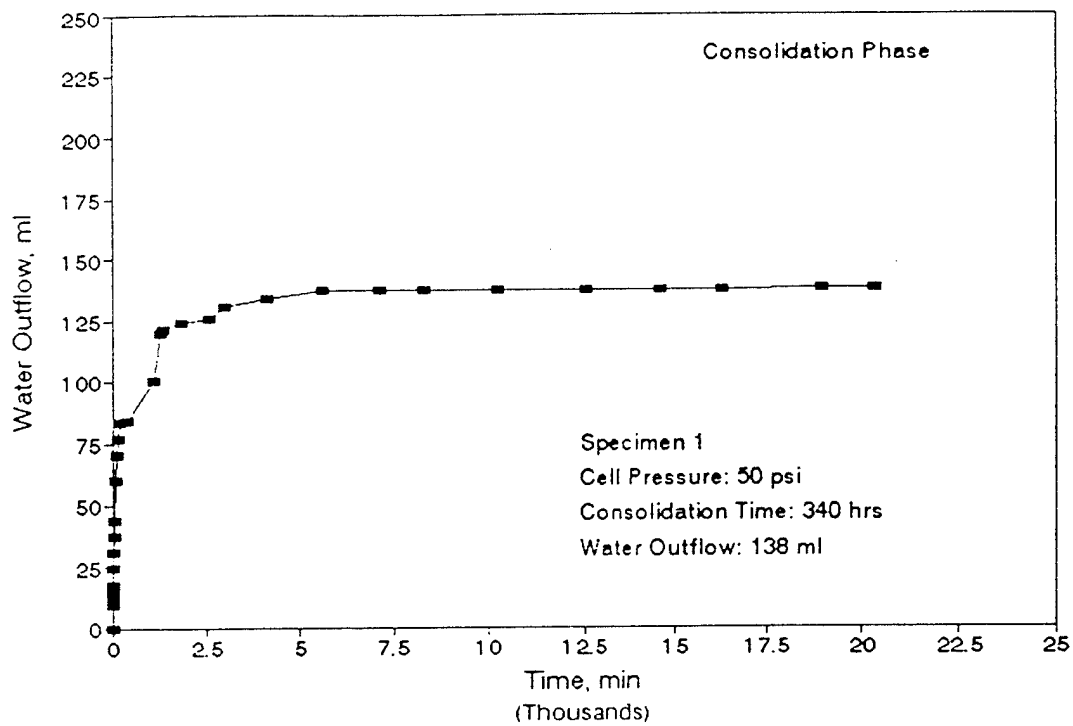
## REFERENCES

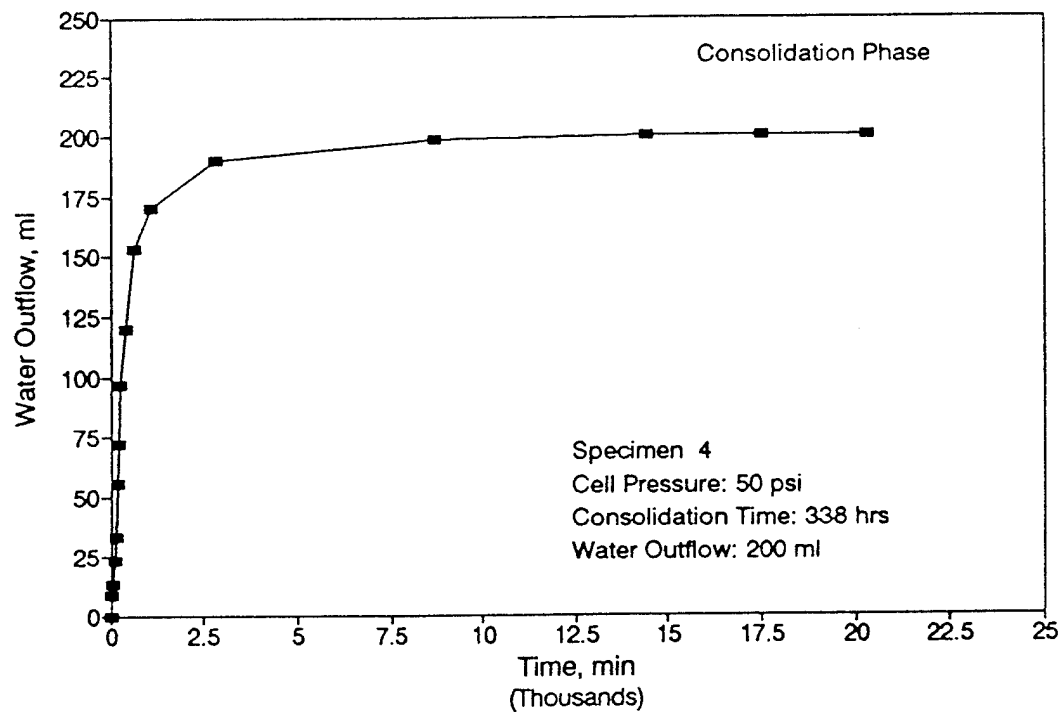
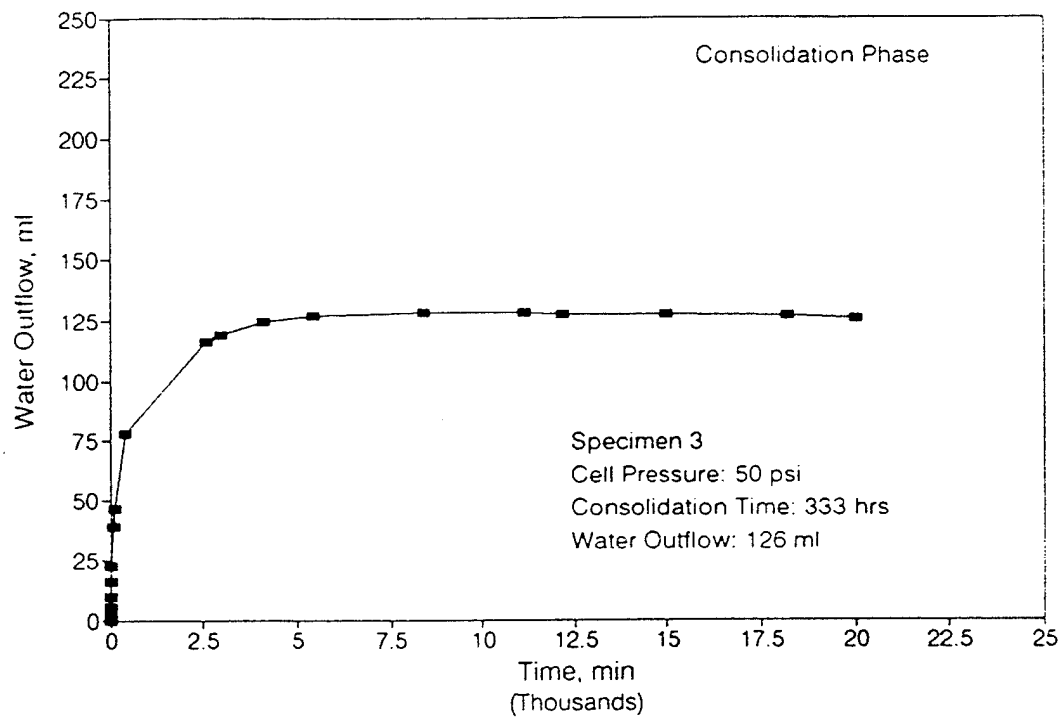
- (1) Abdel-Hady, M. and Herrin, M., "Characteristics of Soil-Asphalt as a Rate Process," *Journal of the Highway Division, Proceedings of the American Society of Civil Engineers*, Vol. 92, No. HW1, March 1966, pp.40-70.
- (2) Cheng, C., "Behavior of Unsaturated Clayey Soils," Thesis, presented to The University of Texas AT El Paso in partial fulfillment of the requirements for the degree of Master of Science, 1992.
- (3) Christensen, R.W. and Wu, T.H., "Analysis of Clay Deformation as a Rate Process, " *Journal of the Soil Mechanics and Foundations Division, Proceedings of the American Society of Civil Engineers*, Vol. 90, No. SM6, November 1964, pp. 125-160.
- (4) Findley, W.N., Lai, J.S. and Onaran, K., "Creep and Relaxation of Nonlinear Viscoelastic Materials," North-Holland Publishing Company, 1976.
- (5) Fredlund, D.G., "Appropriate Concepts and Technology for Unsaturated Soils," *Second Canadian Geotechnical Colloquium, Canadian Geotechnical Journal*, Vol. 16, No. 1, 1979, pp120-140.
- (6) Komamura, F. and Huang, R.J., "New Rheological Model for Soil Behavior," *Journal of the Geotechnical Engineering Division, Proceedings of the American Society of Civil Engineers*, Vol. 100, No. GT7, July 1974, pp. 800-825.

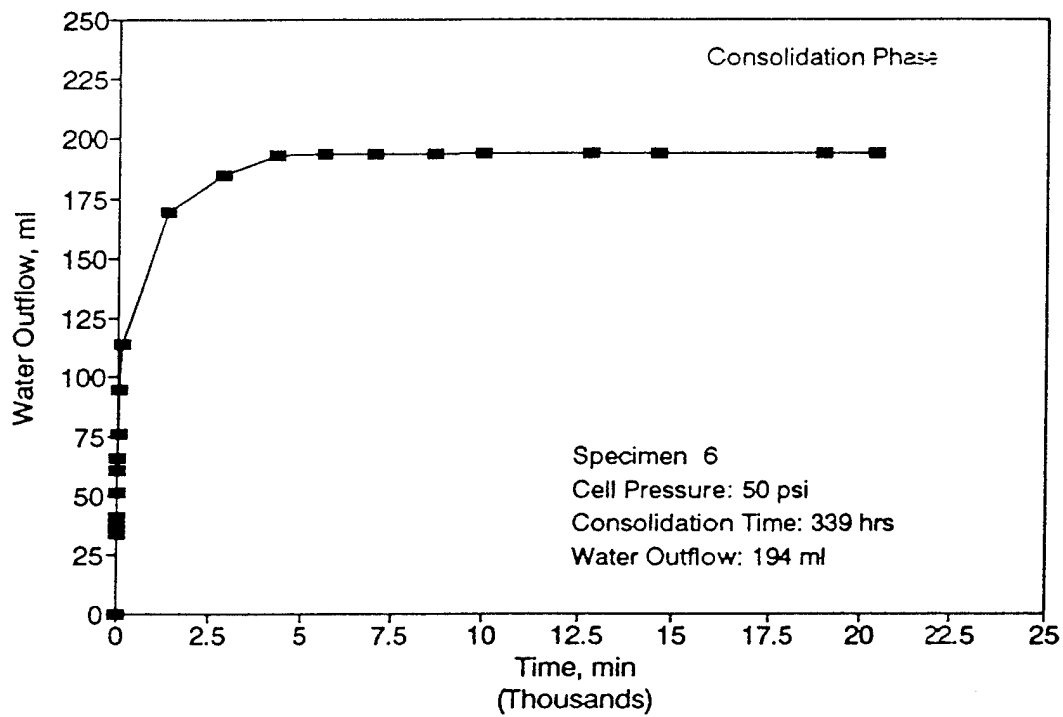
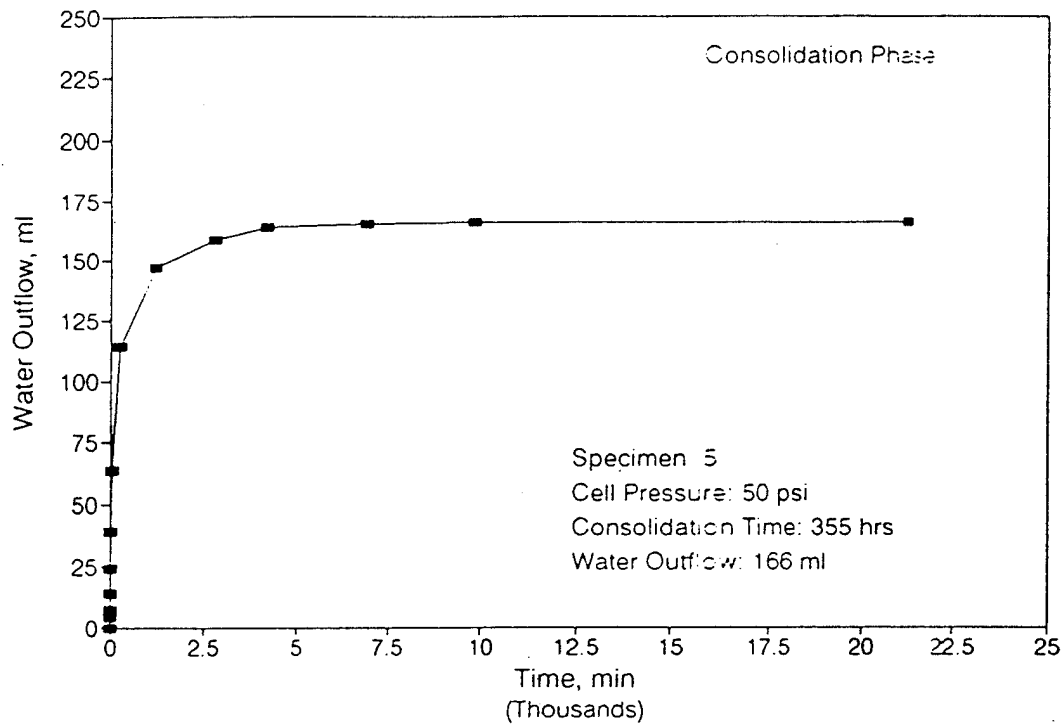
- (7) Mitchell, J.K., Campanella, R.G. and Singh, A., "Soil Creep as a Rate Process," Journal of the Soil Mechanics and Foundation Division, Proceedings of the American Society of Civil Engineers, Vol. 94, No. SM1, January 1968, pp. 231-253.
- (8) Murayama, S. and Shibata, T., "On the Rheological Characteristic of Clay, Part I," Bulletin No. 26, Disaster Prevention Research Institute, Kyoto University, Japan, 1958.
- (9) Murayama, S. and Shibata, T., "Rheological Properties of Clays," Proceedings, 5th International Congress on Soil Mechanics and Foundations, Paris, 1961, pp. 269-275.
- (10) Murayama, S. and Shibata, T., "Flow and Stress Relaxation of Clays (Theoretical Studies on the Rheological Properties of Clay-Part I)," Proceedings, Rheology and Soil Mechanics Symposium of the International Union of Rheological and Applied Mechanics, Grenoble, France, April, 1964.
- (11) Shames, I.H. and Cozzarelli, F.A., "Elastic and Inelastic Stress Analysis," Prentice Hall, New Jersey, 1991.

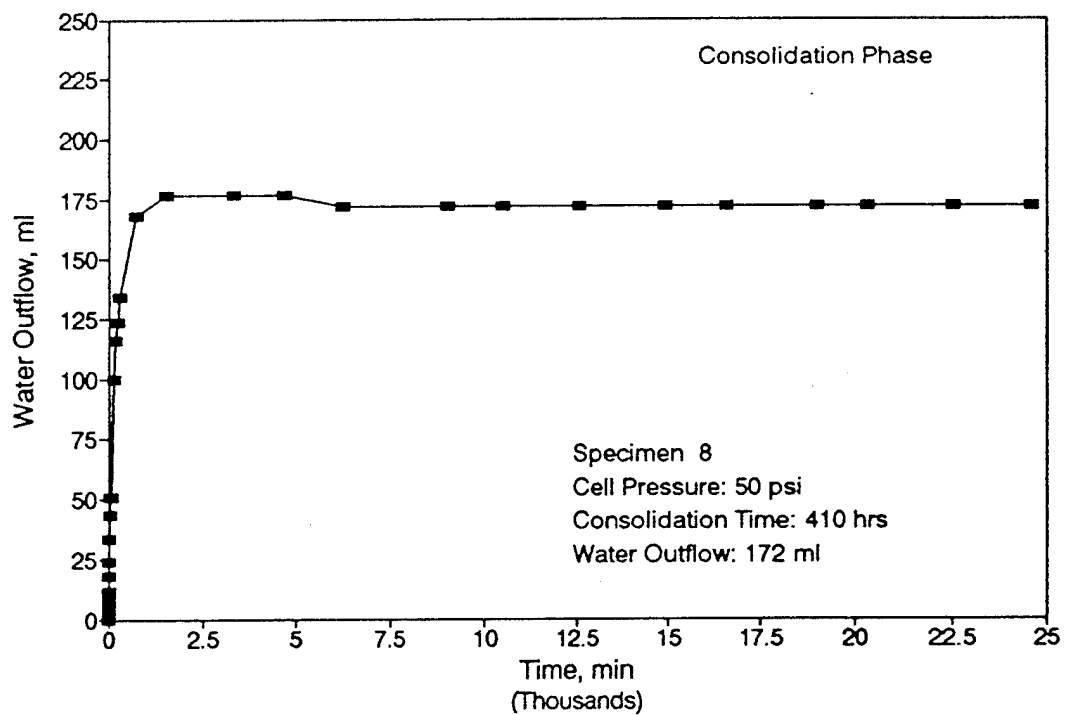
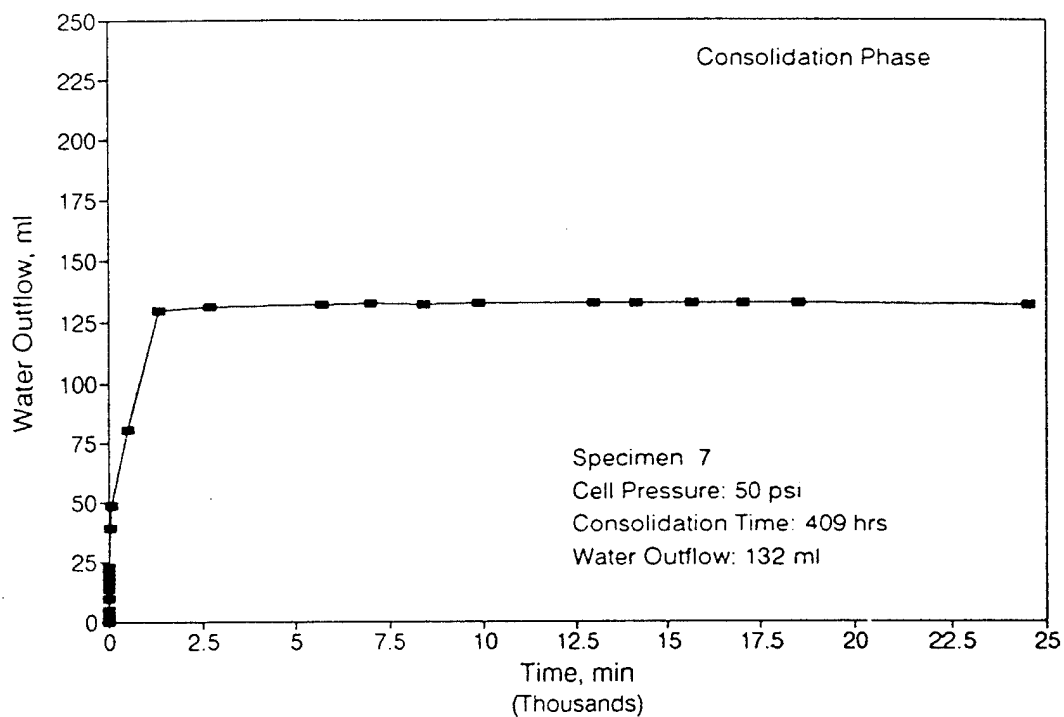
**APPENDIX A**  
**RECORDS OF CONSOLIDATION OF SLURRY**

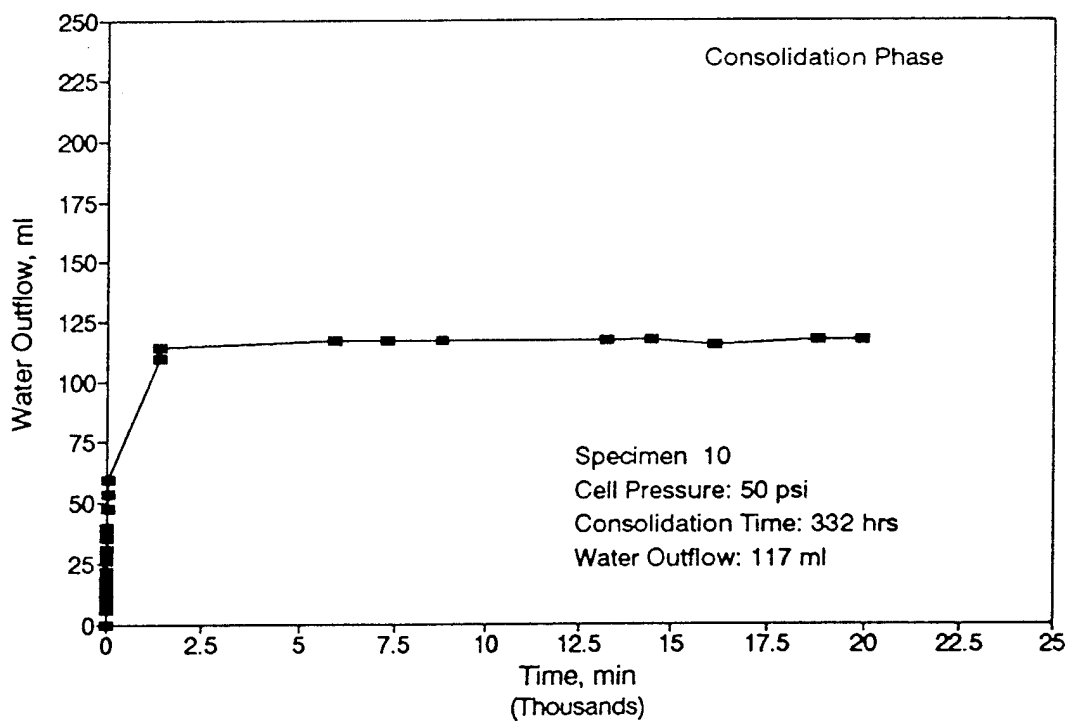
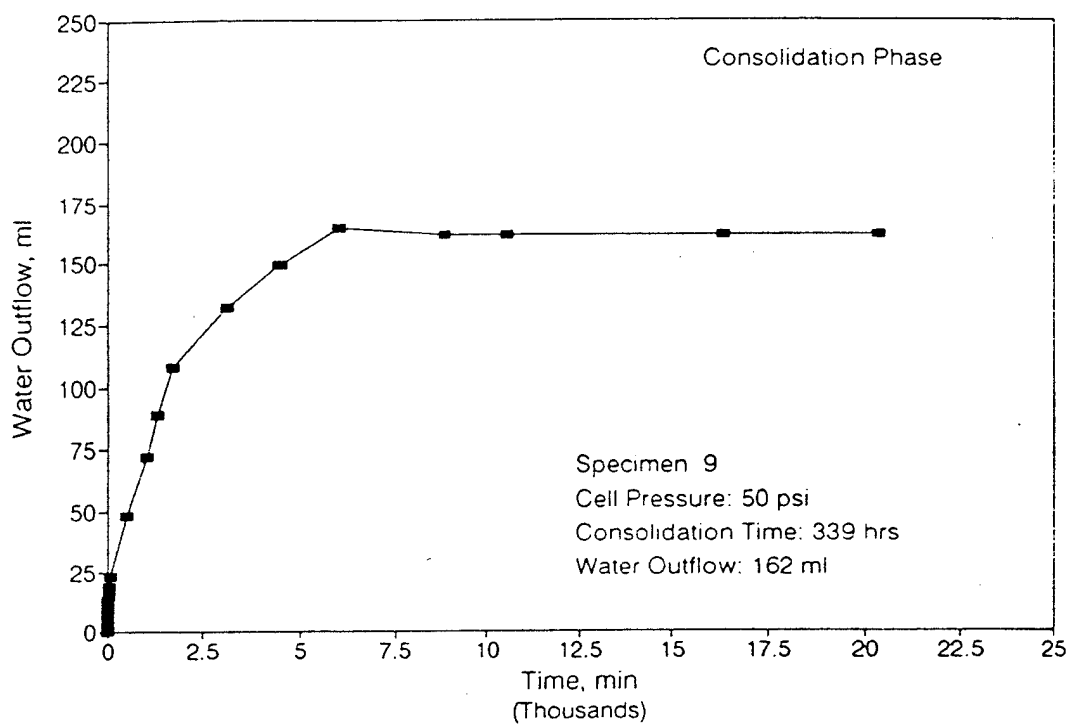


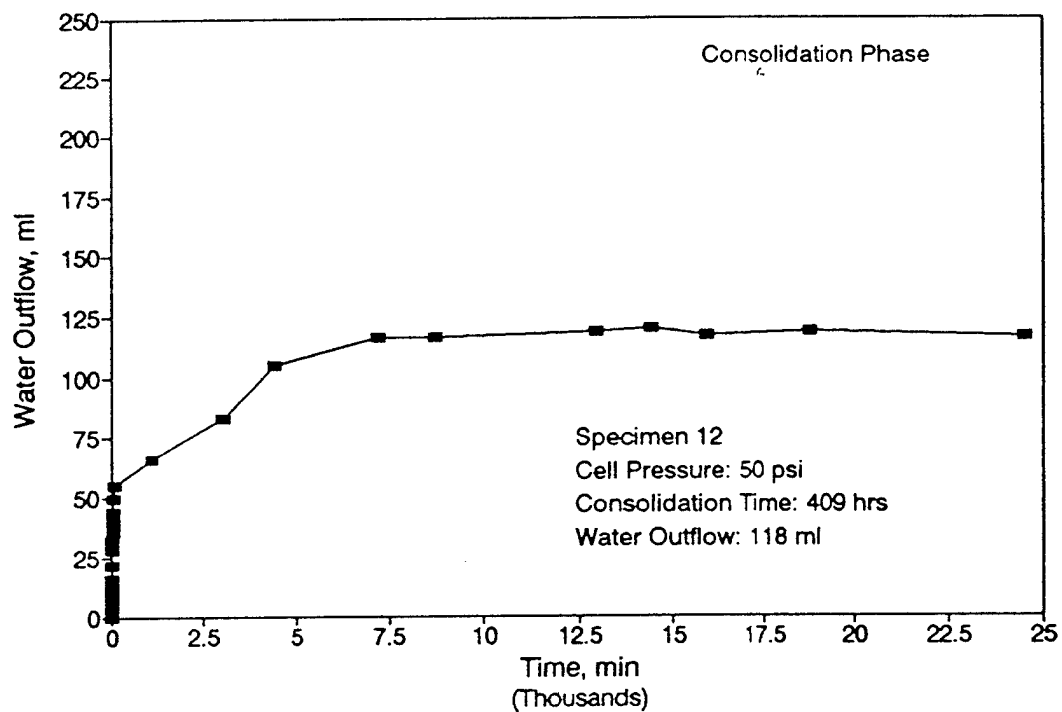
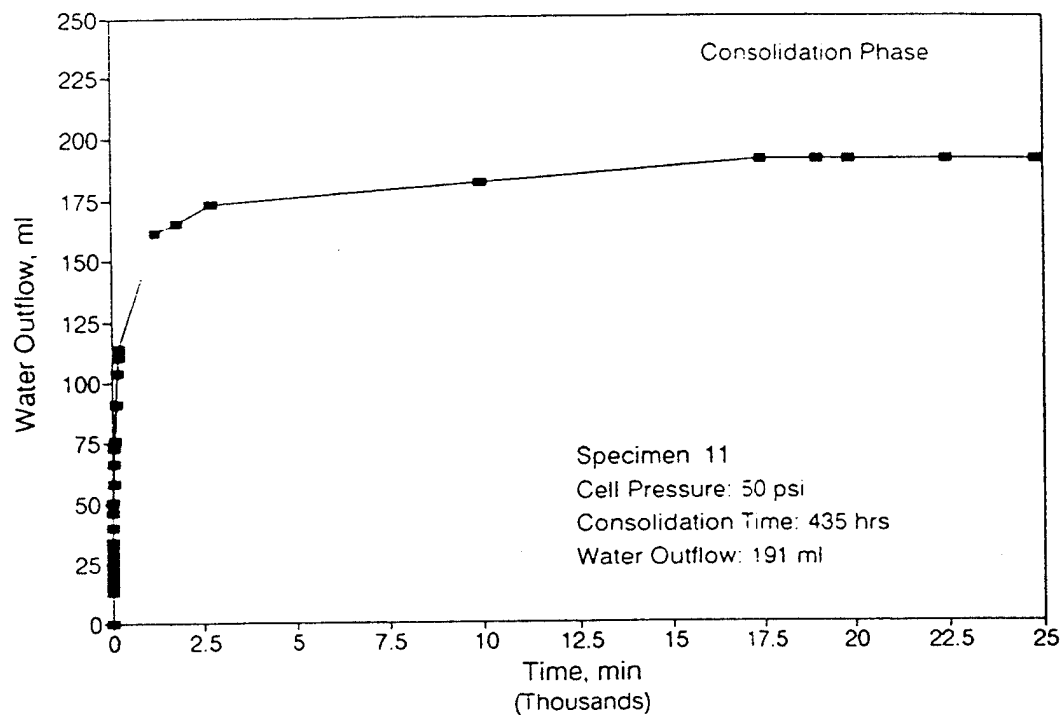


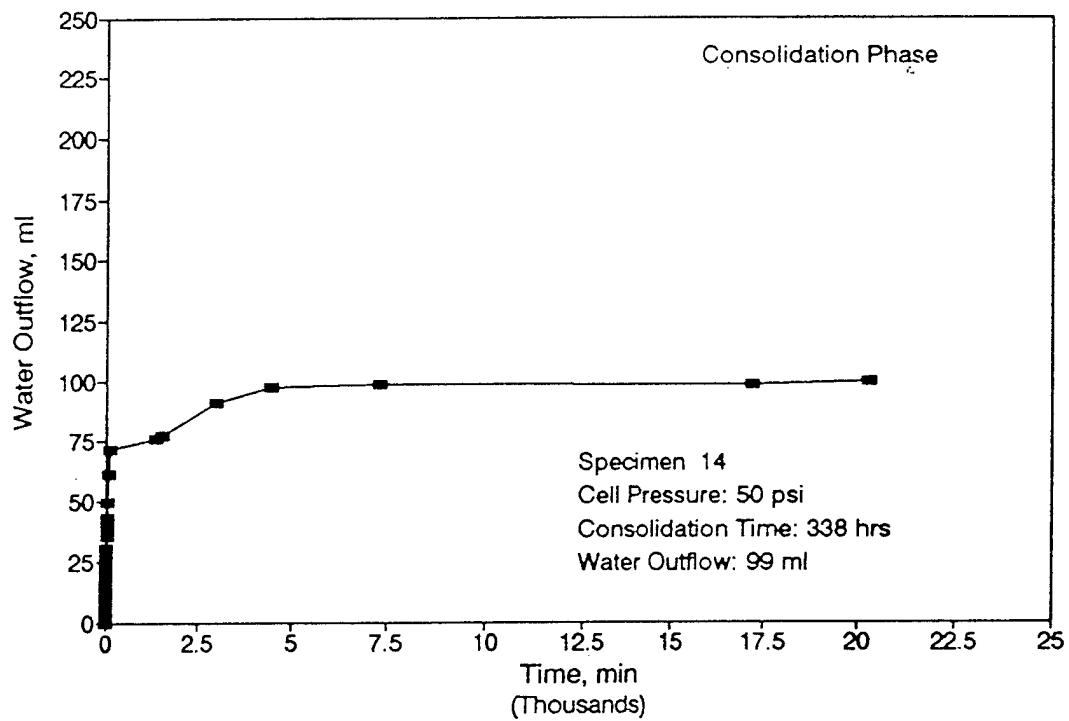
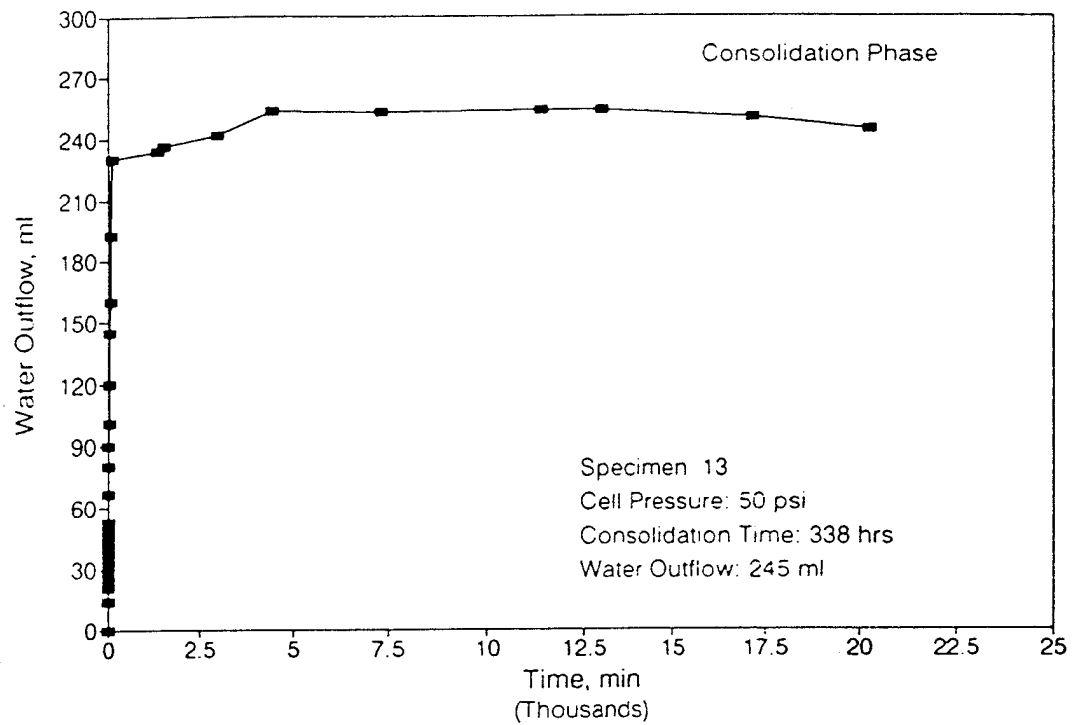


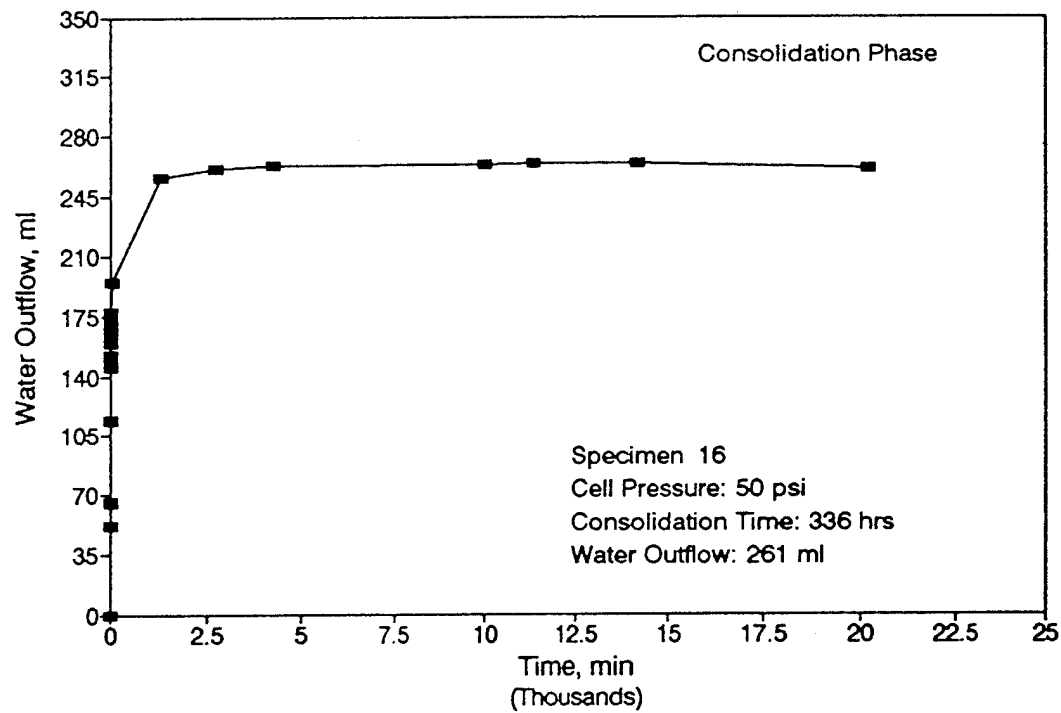
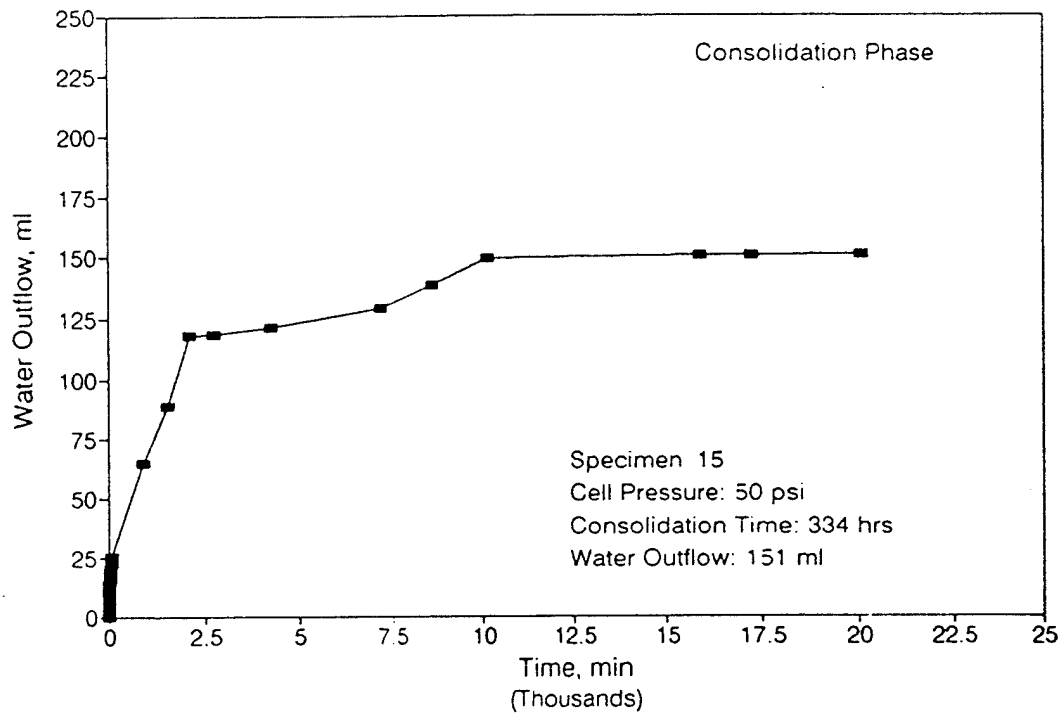




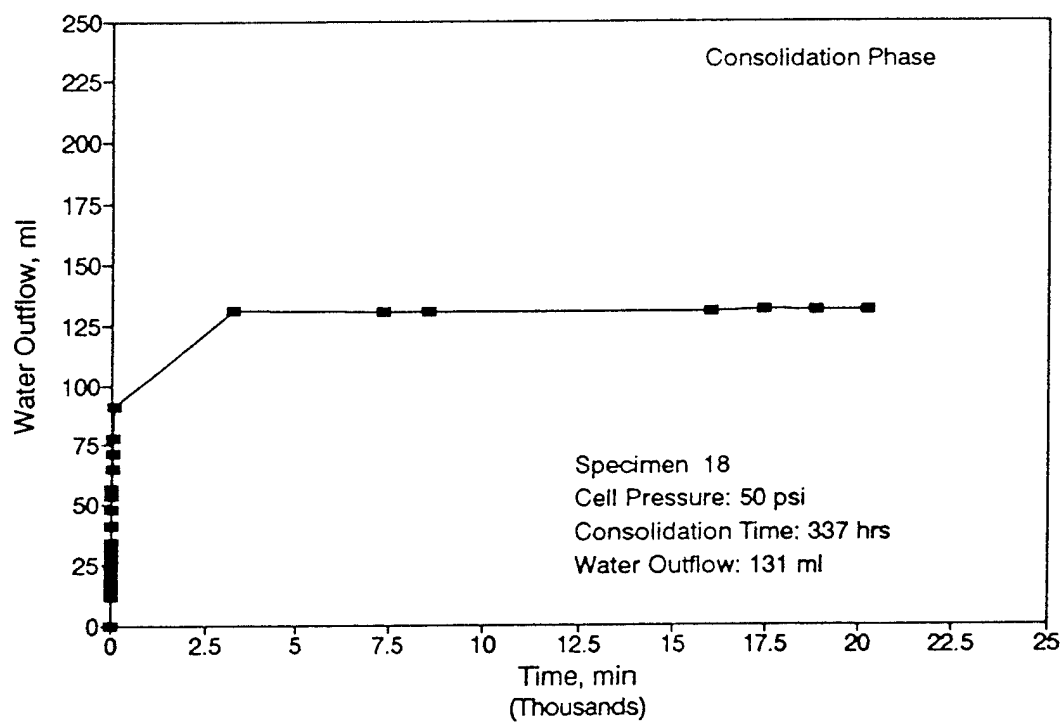
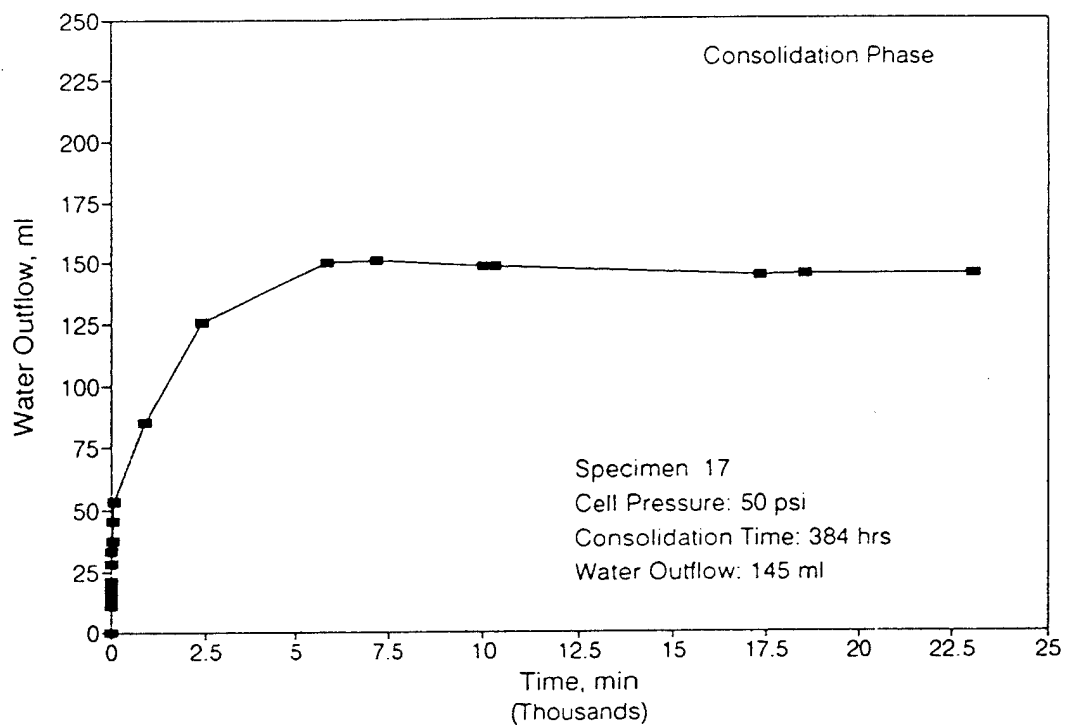


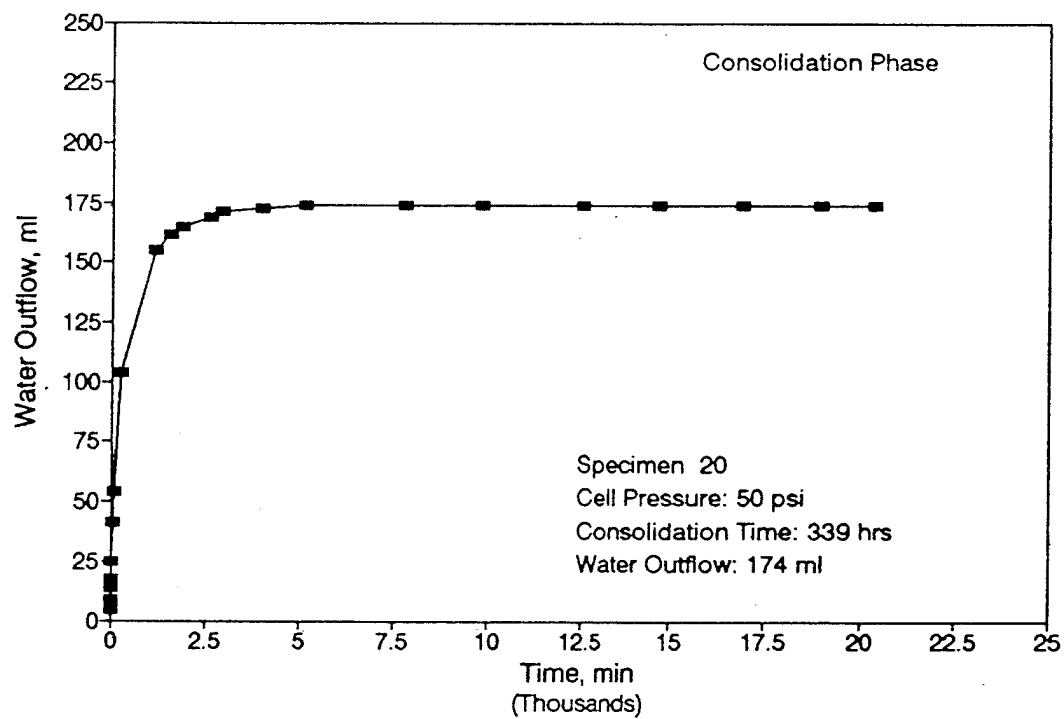
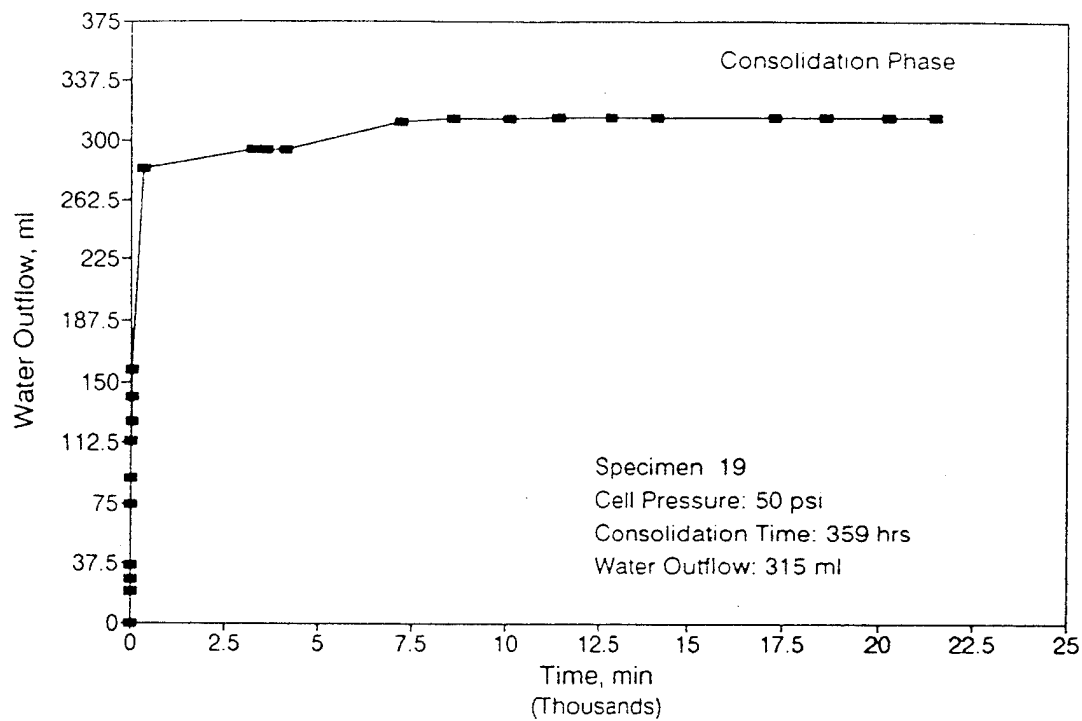


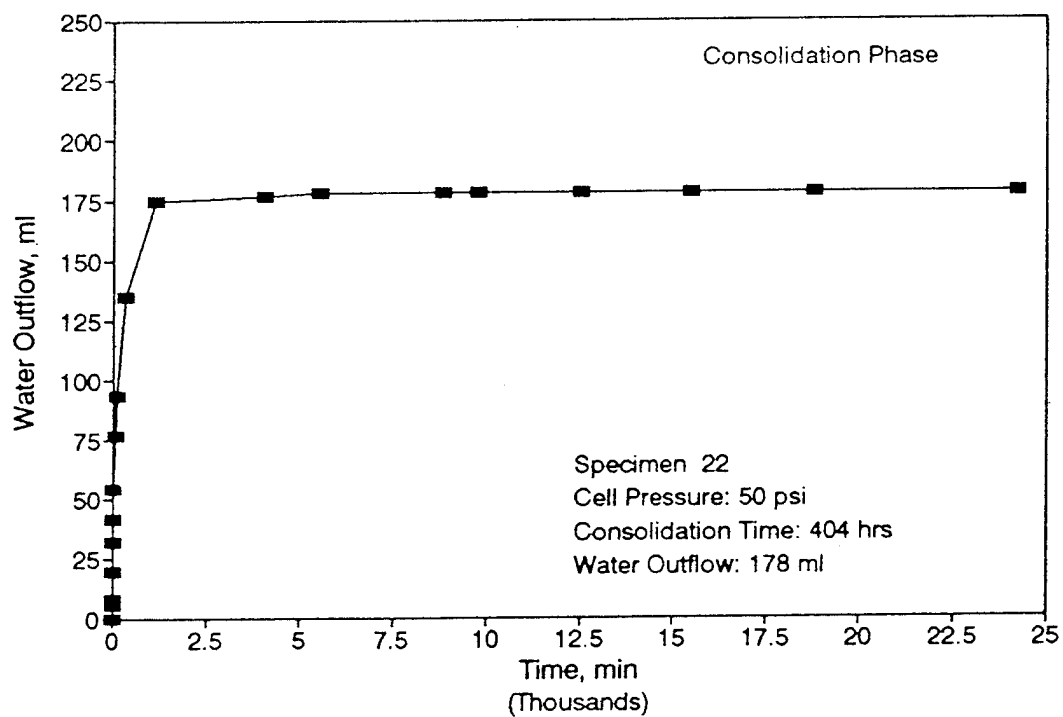
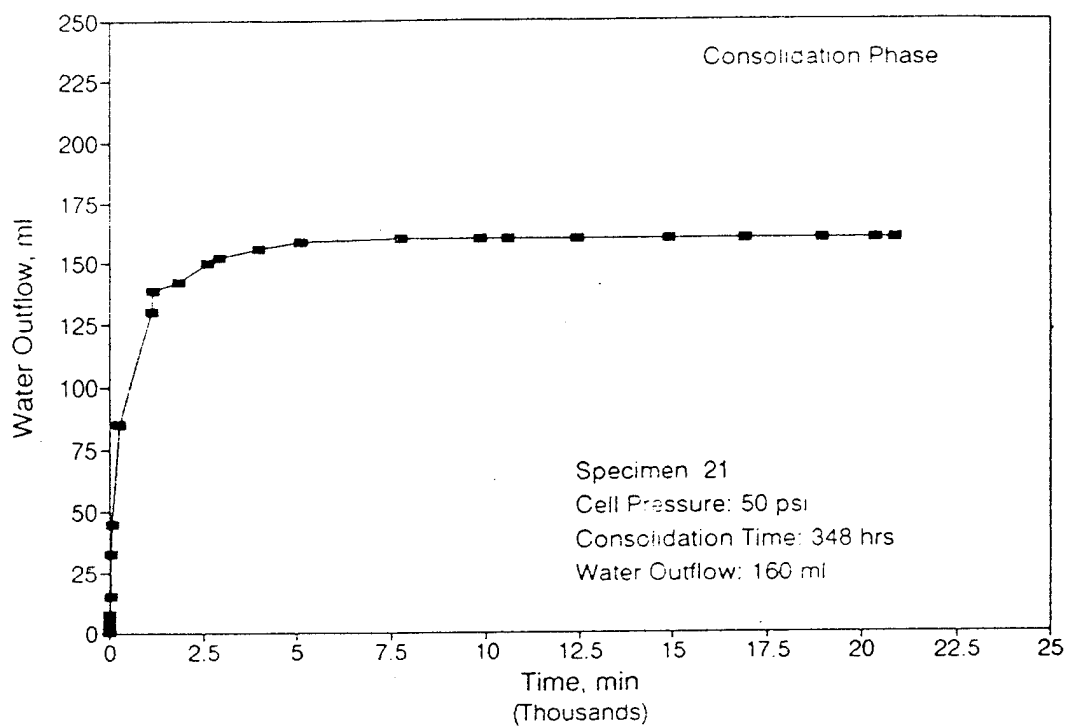


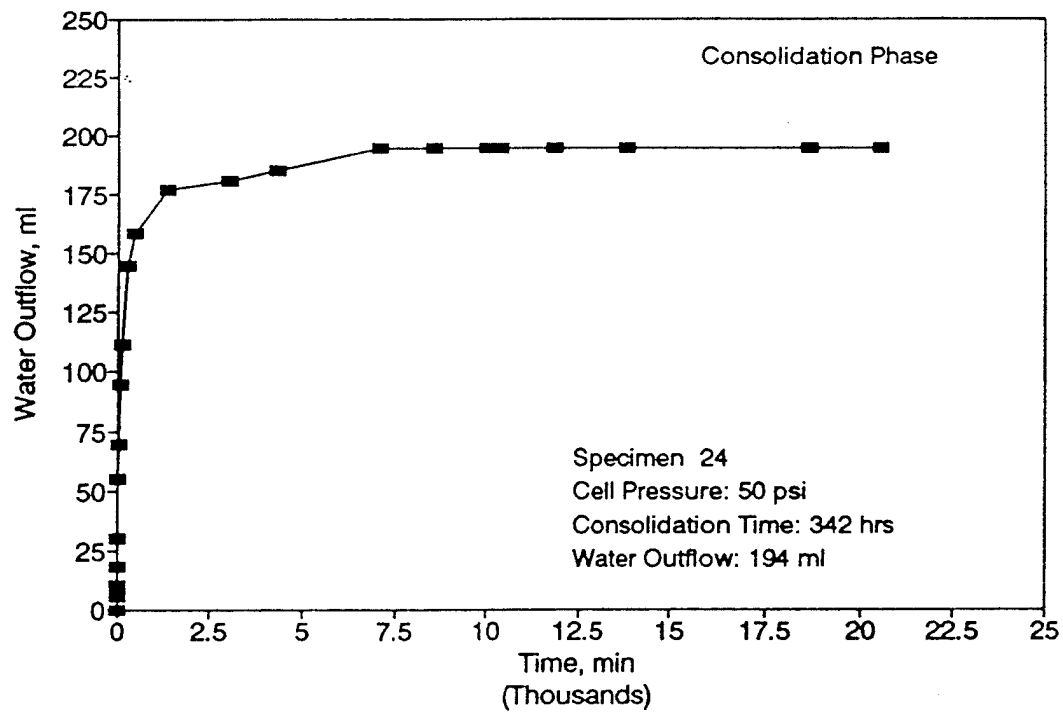
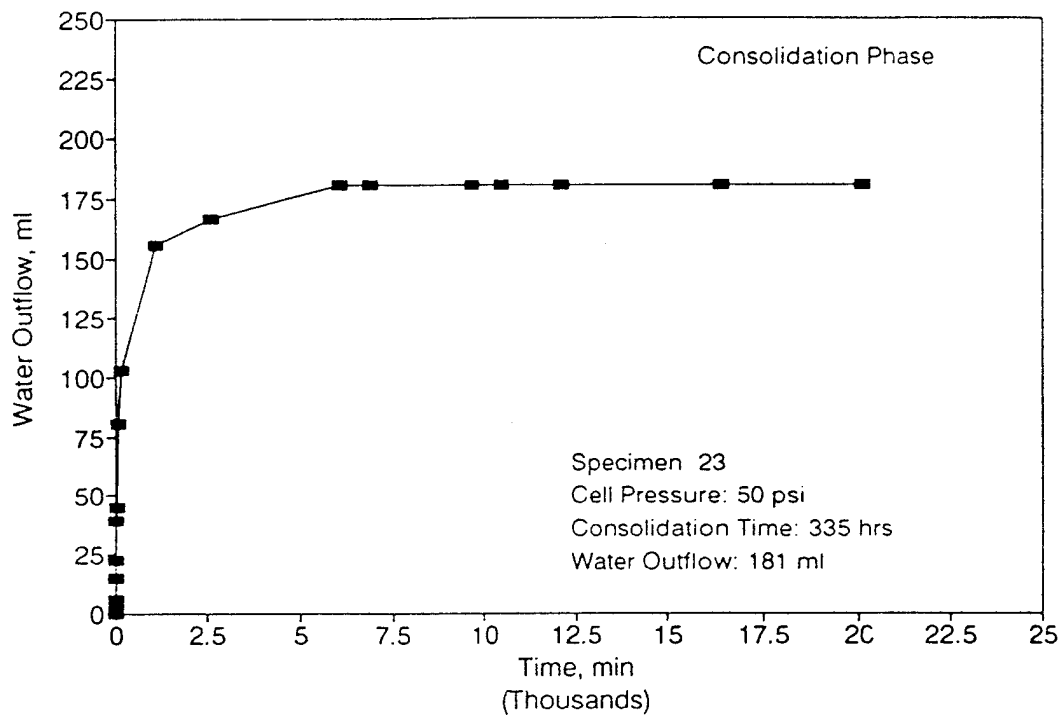


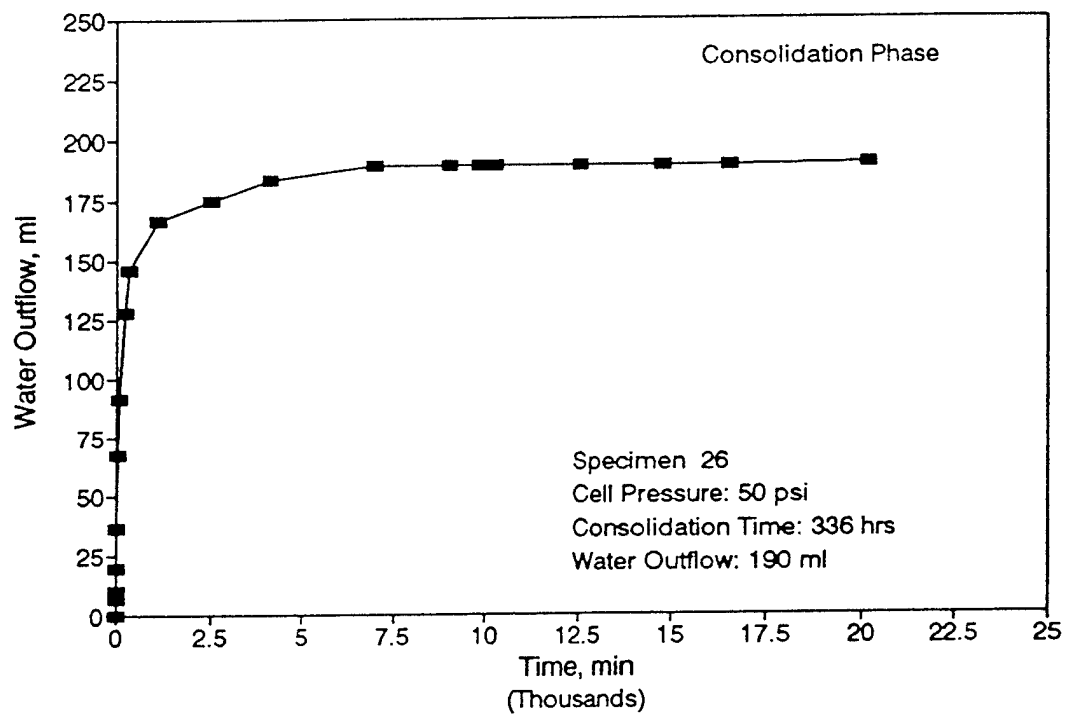
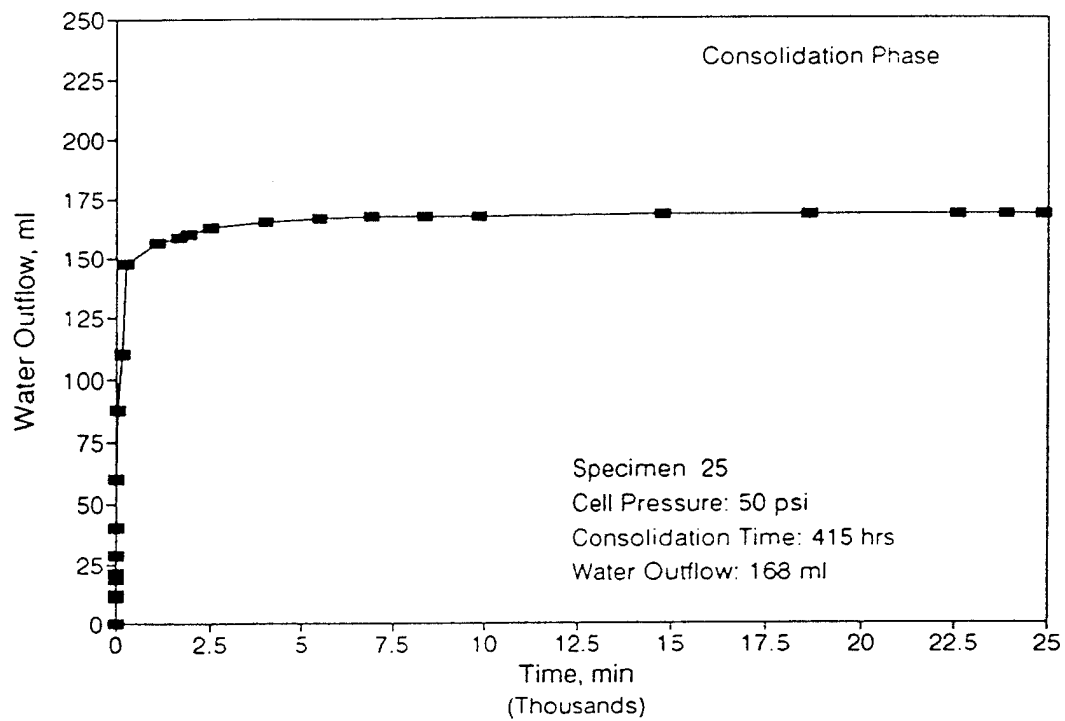


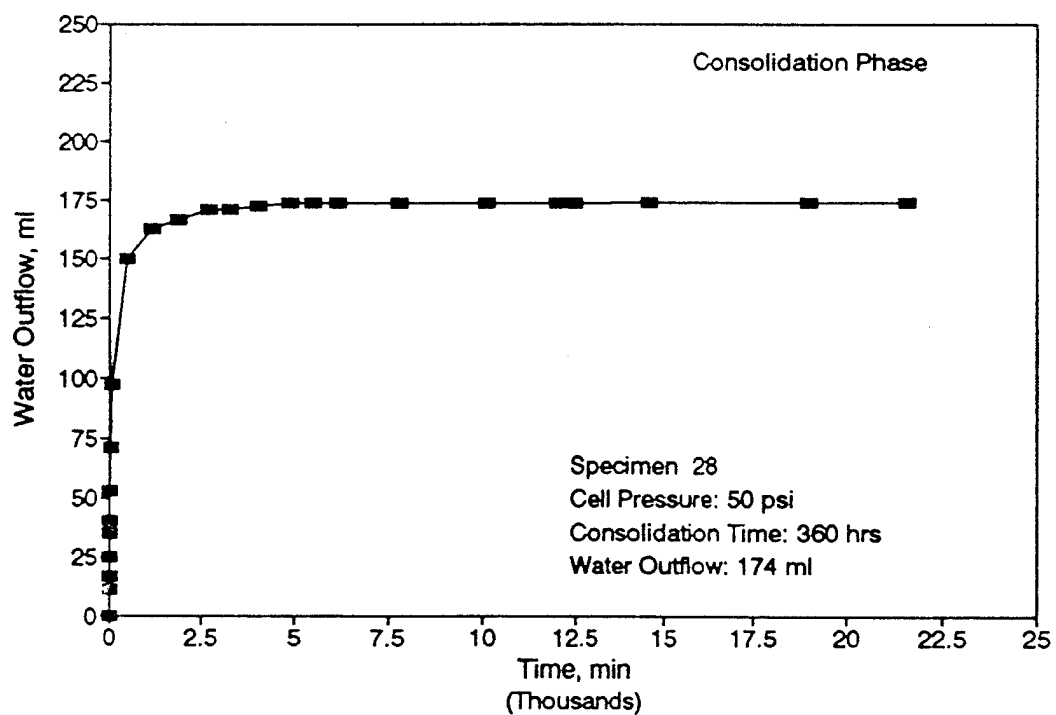
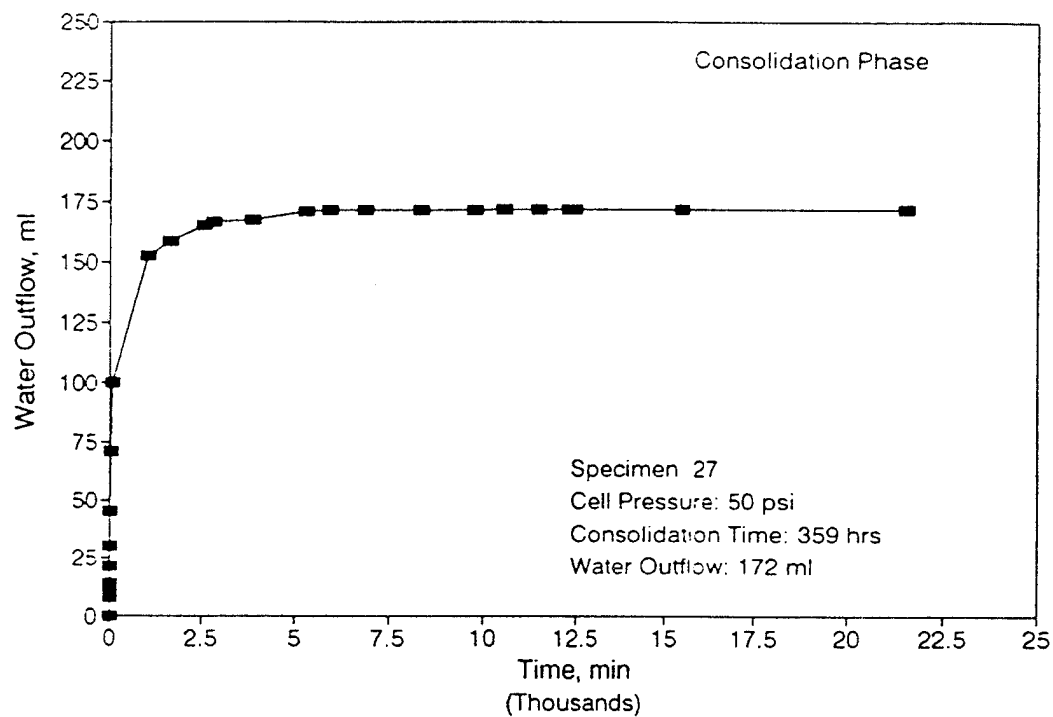


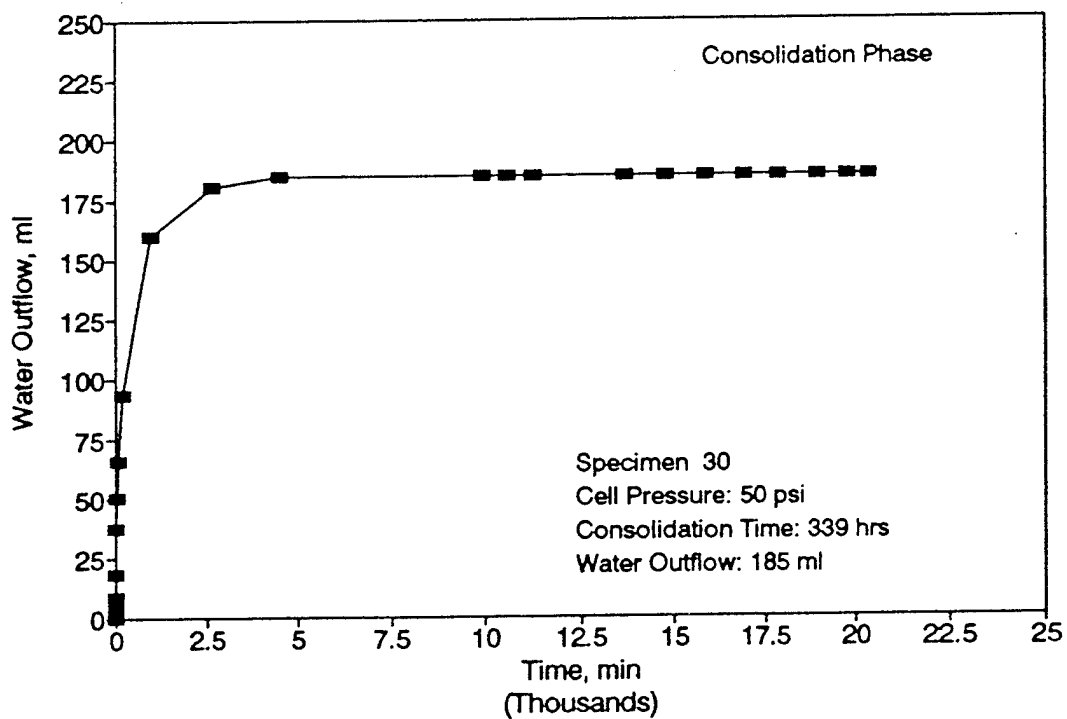
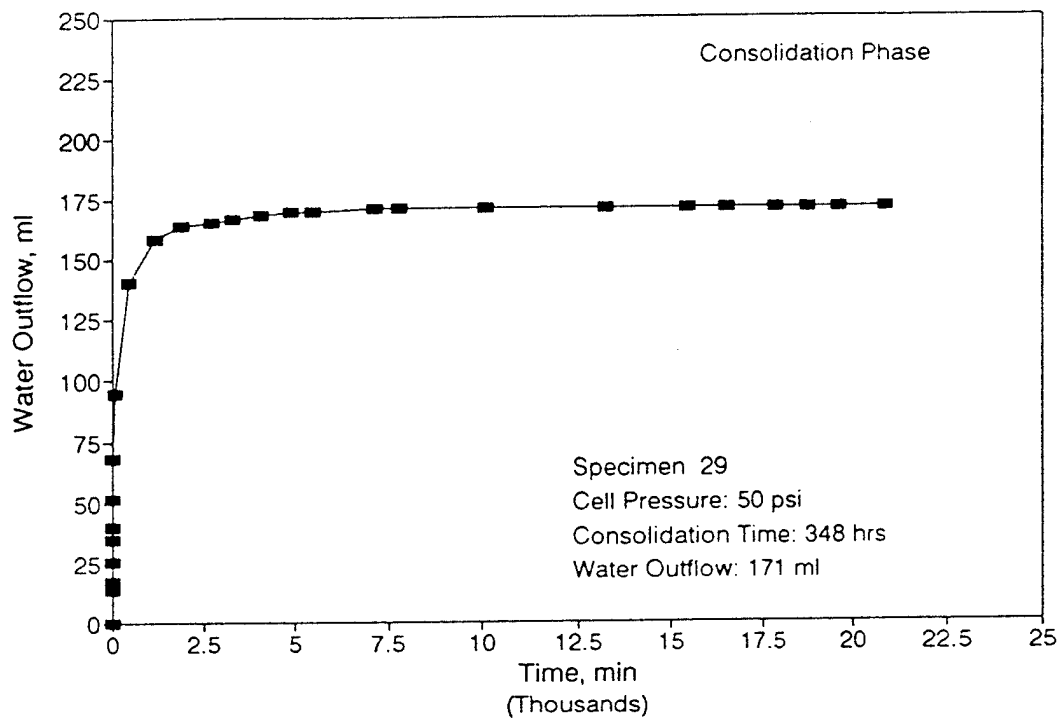


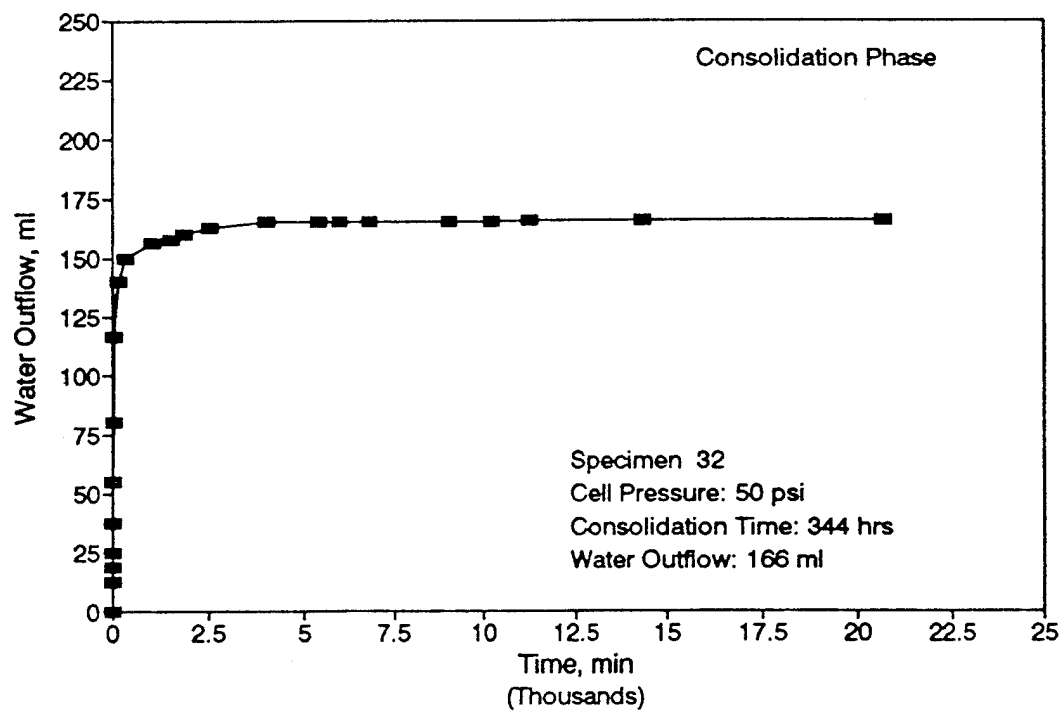
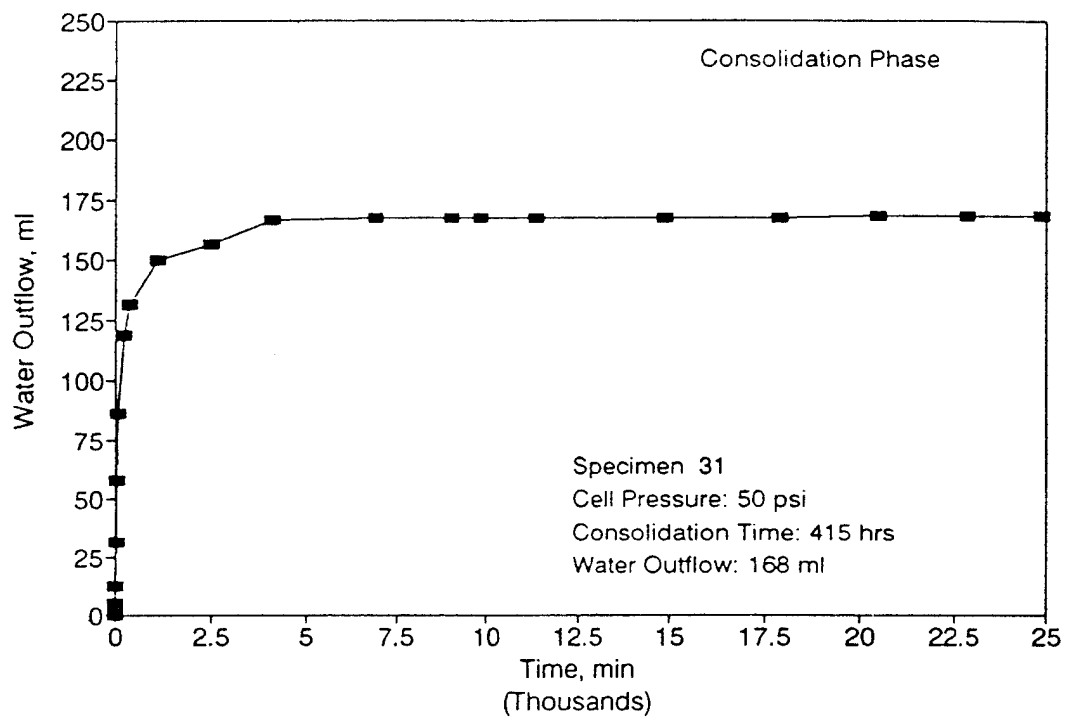




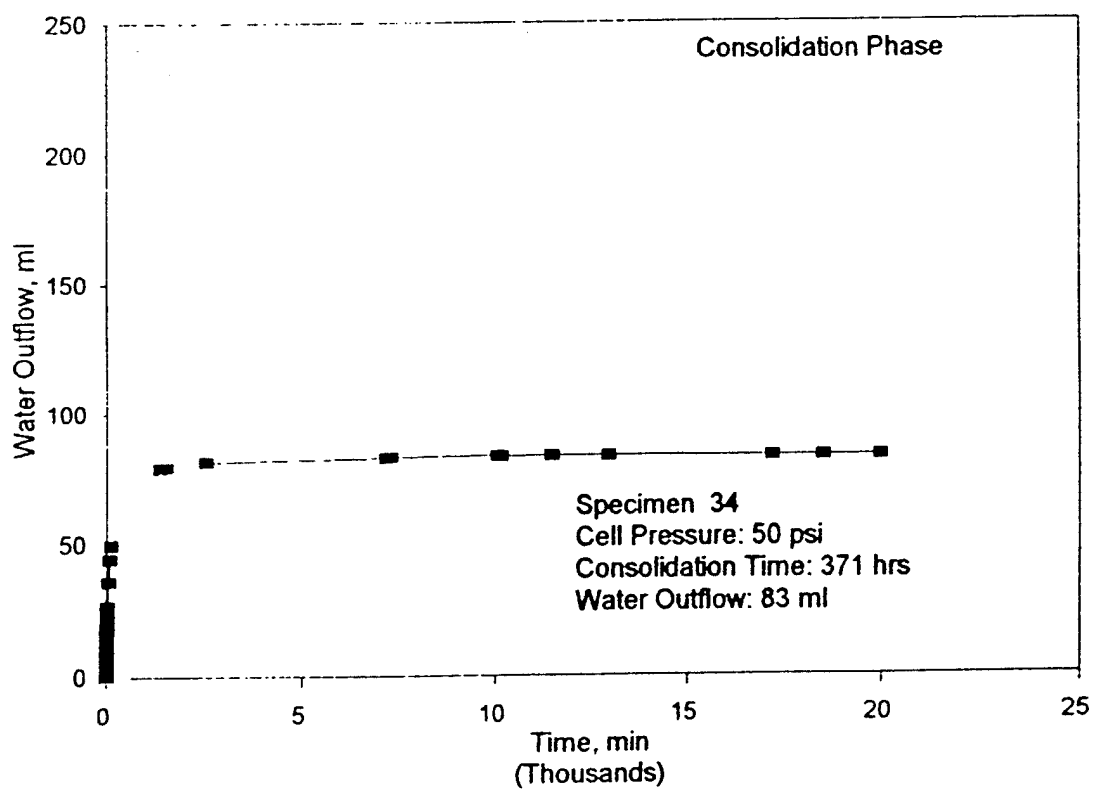
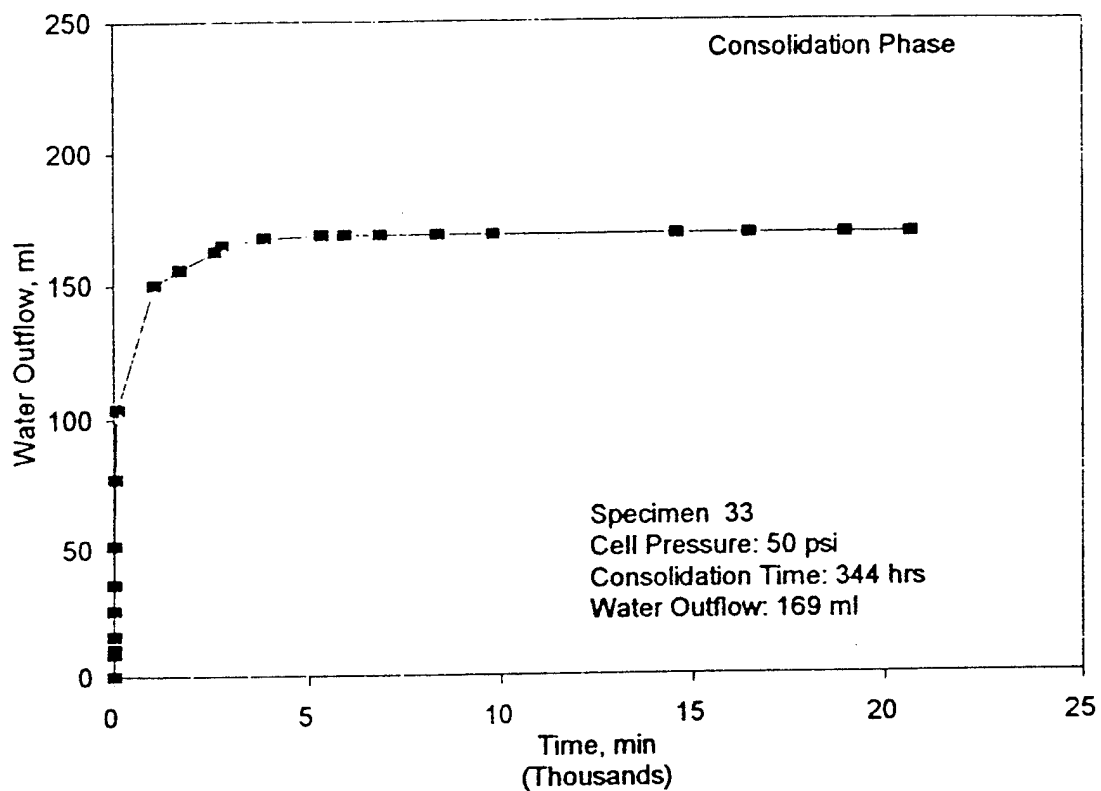


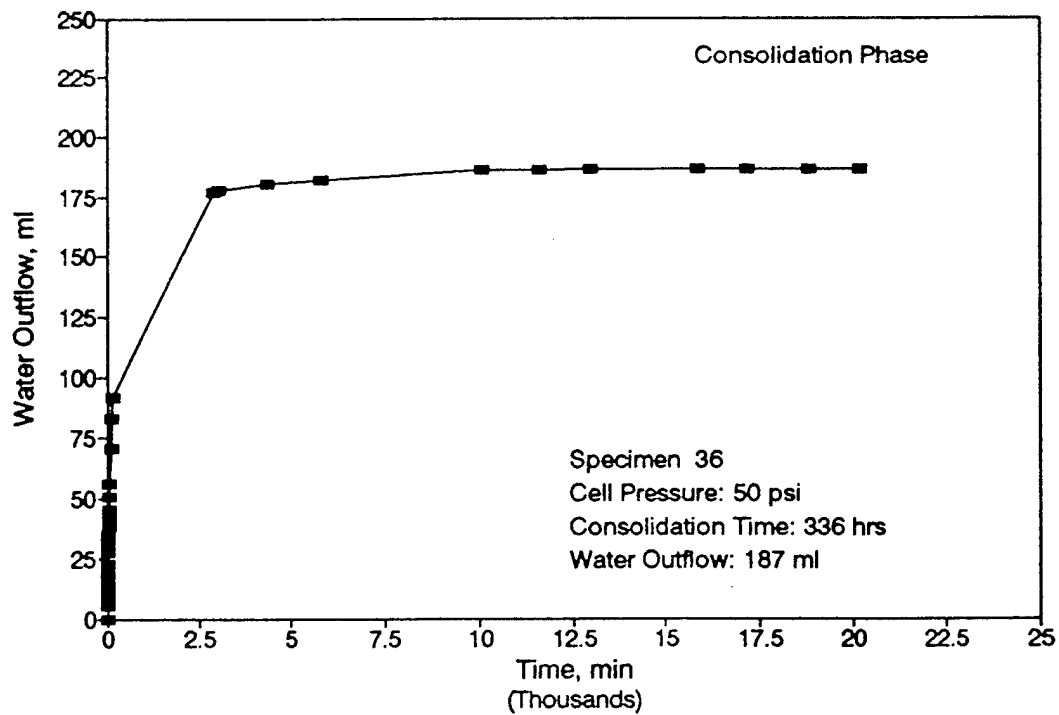
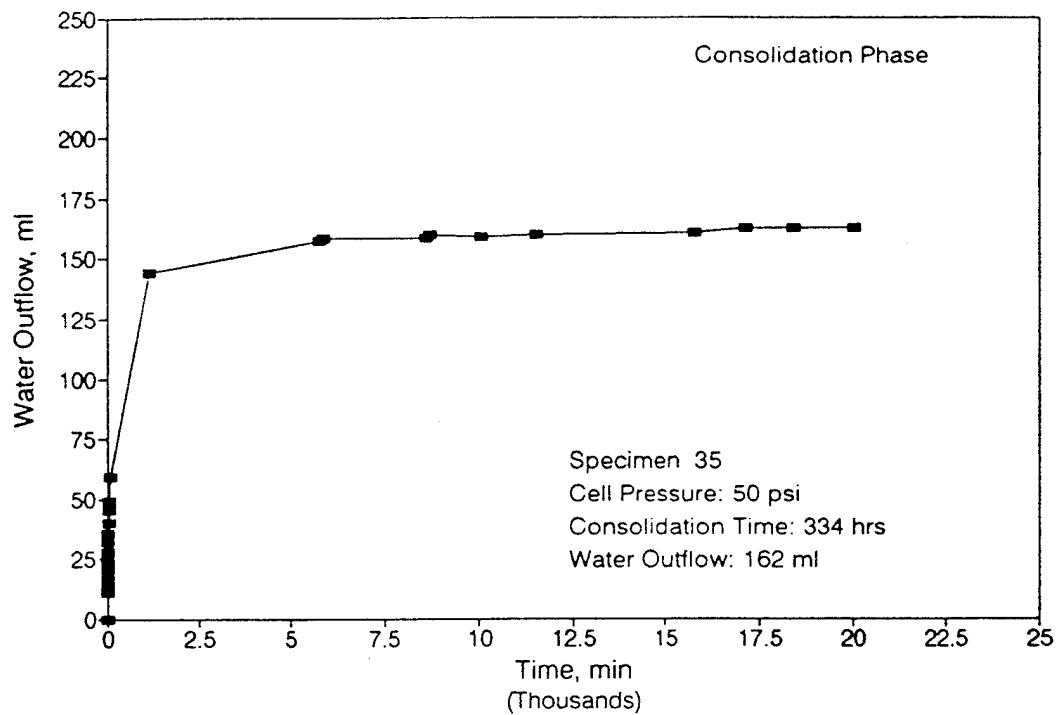


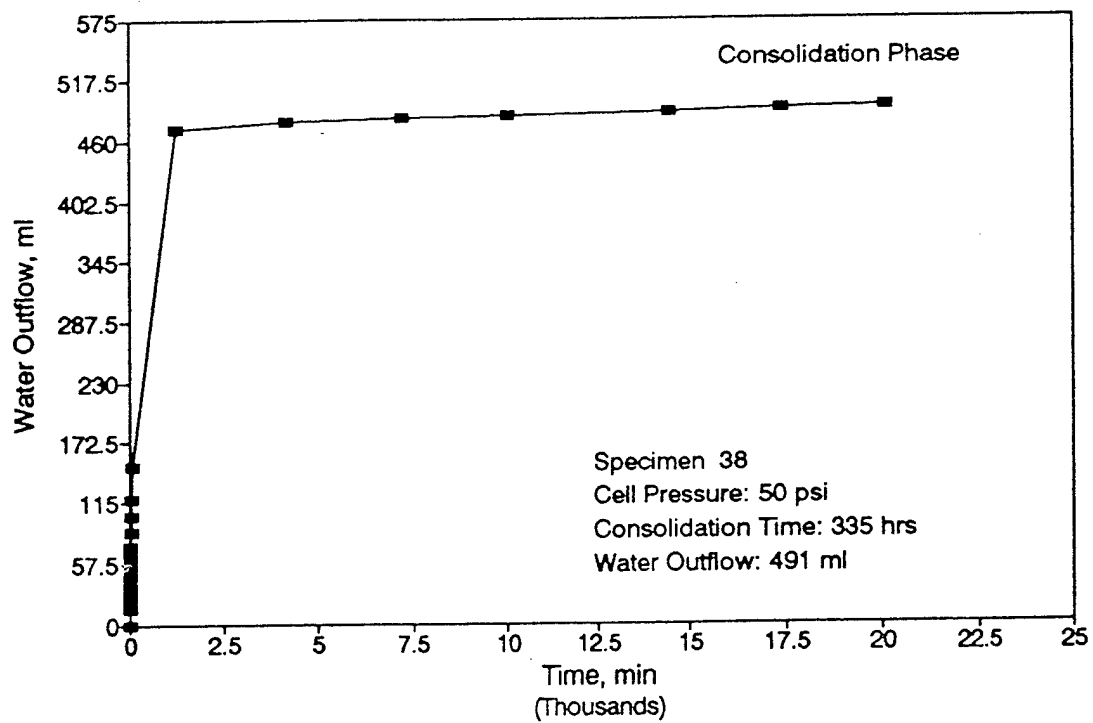
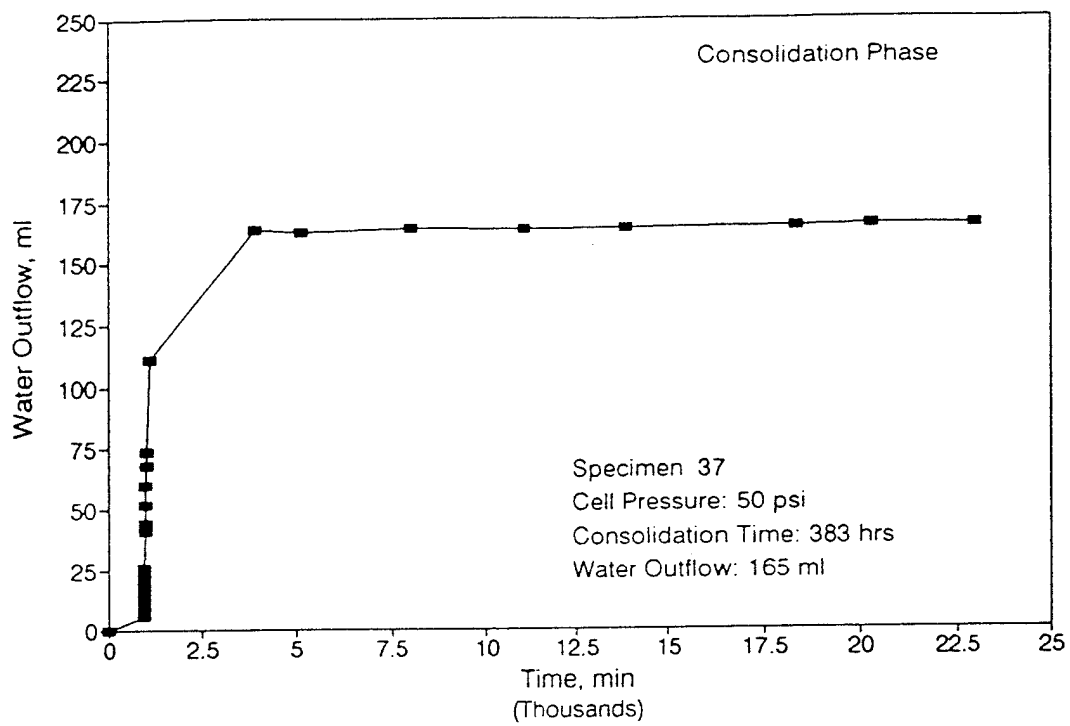


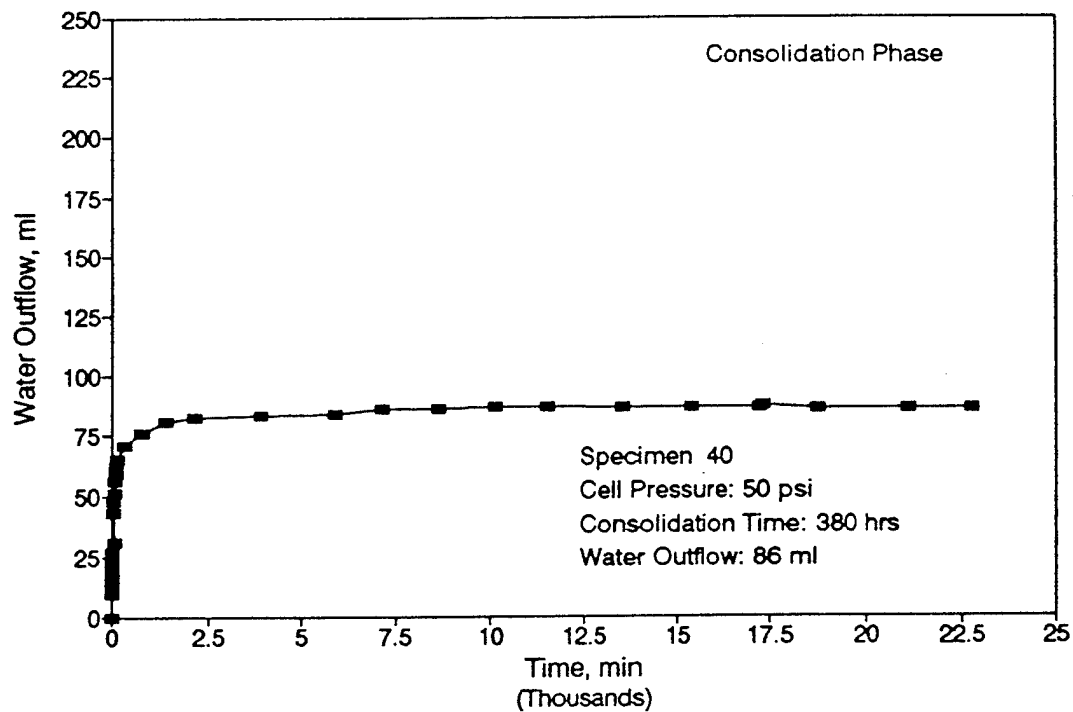
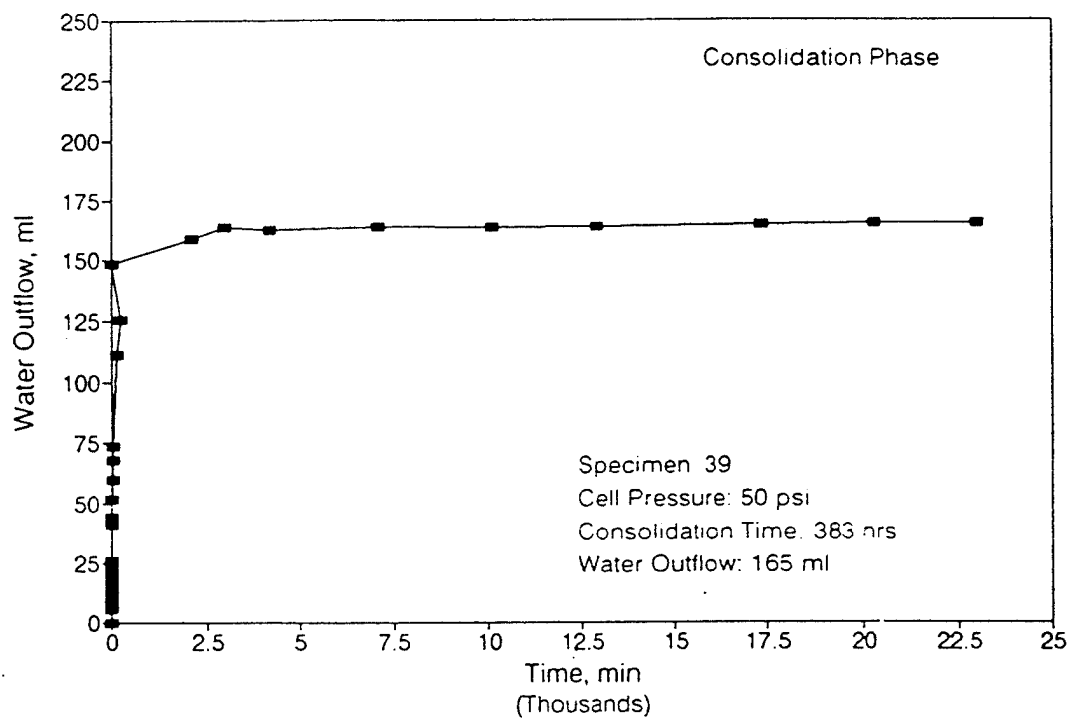


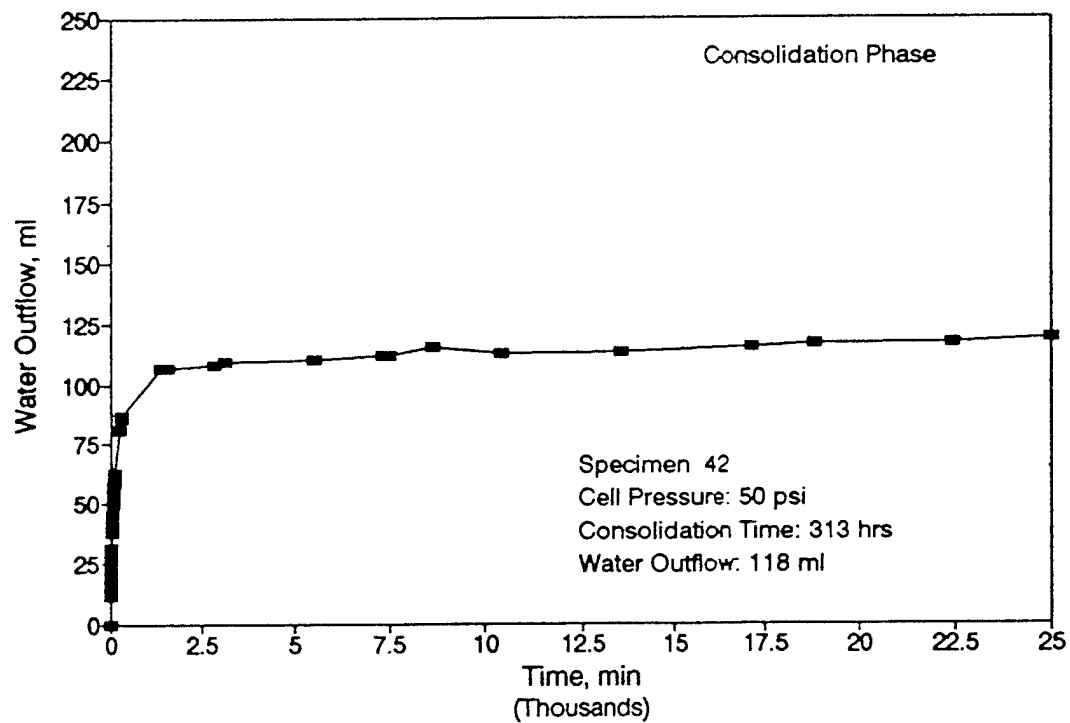
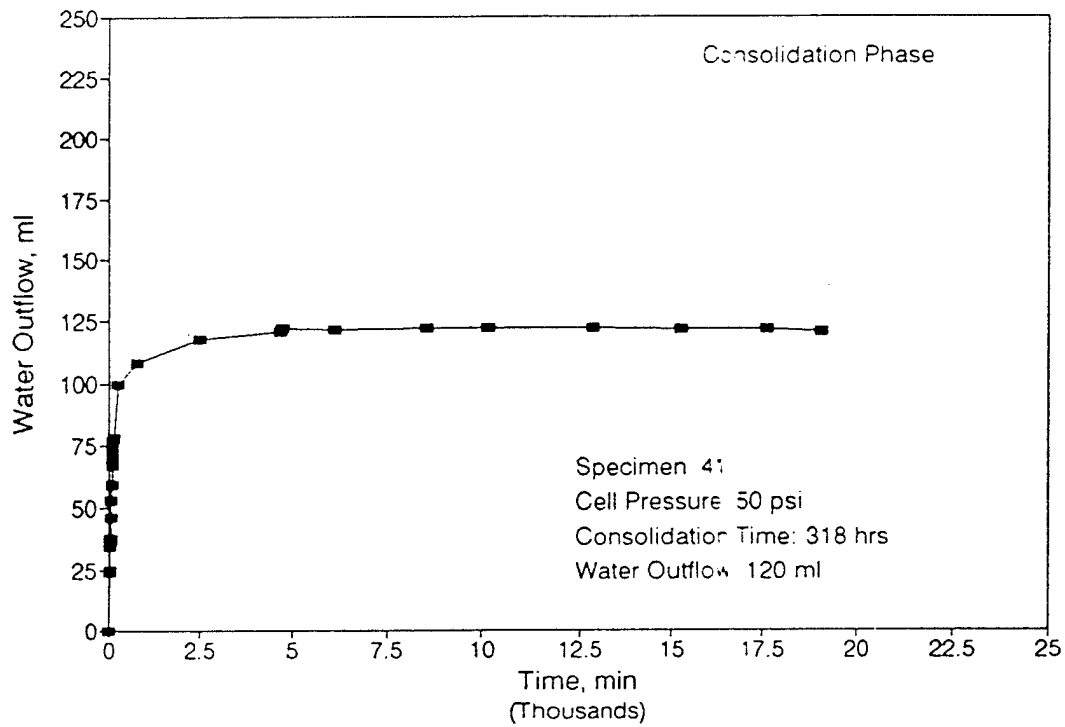


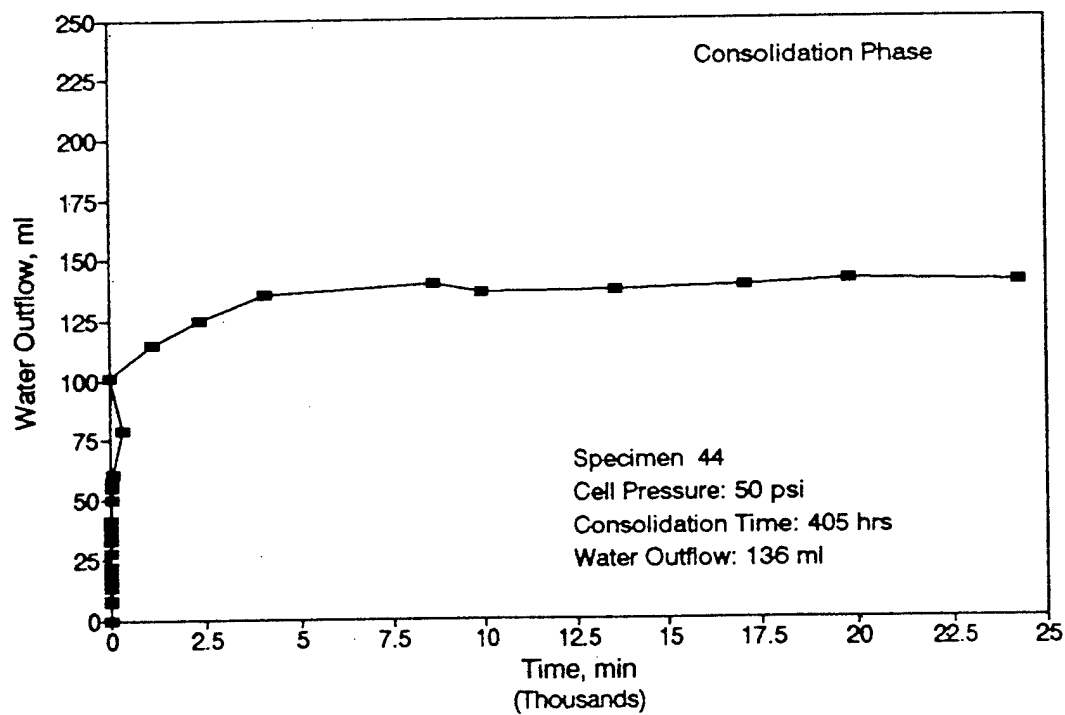
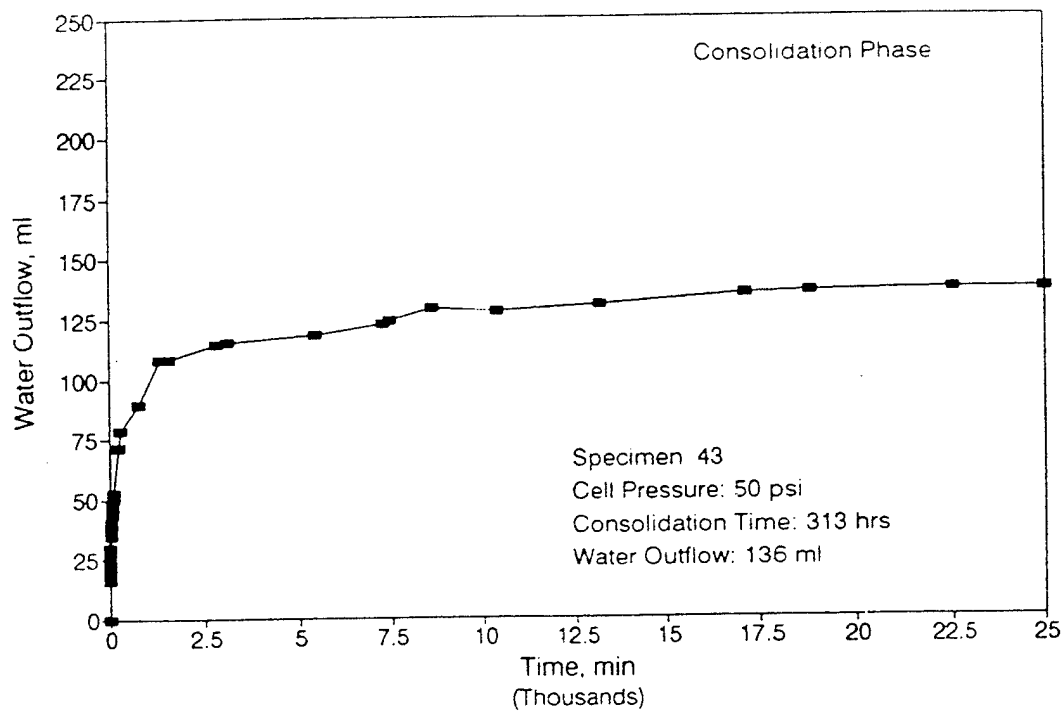


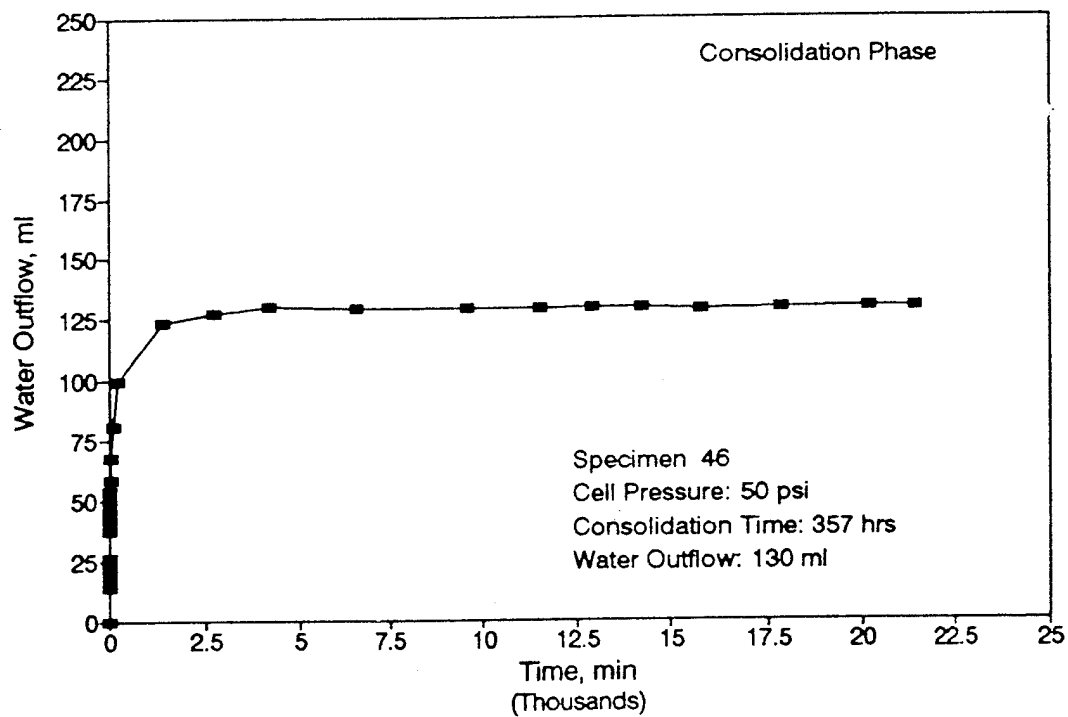
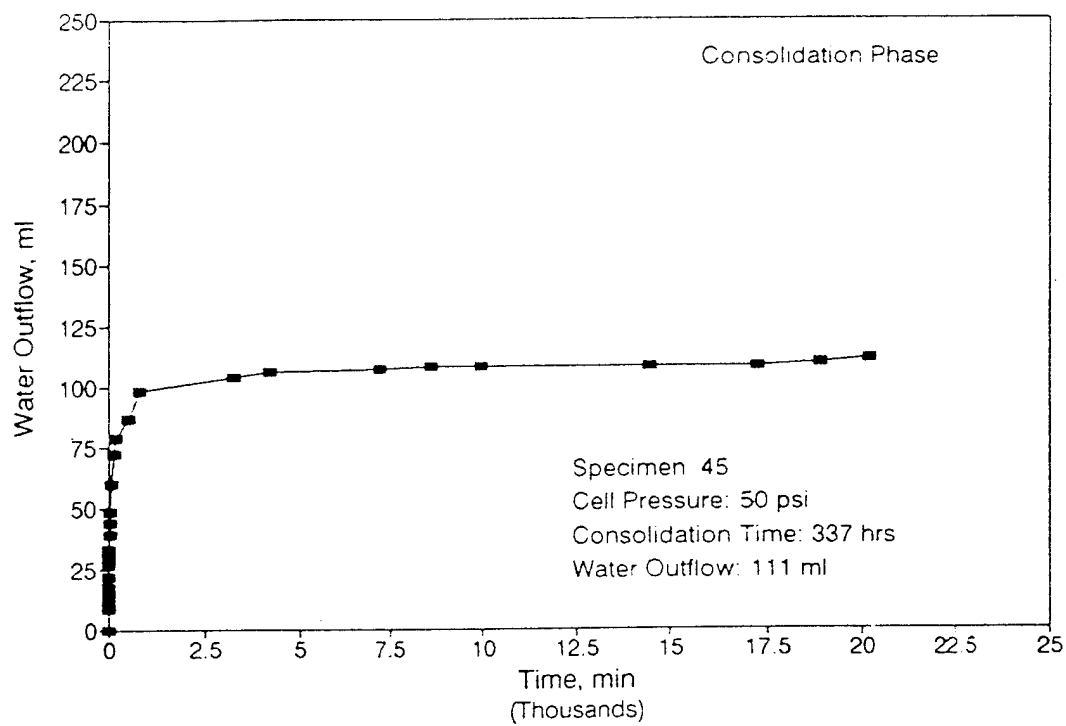


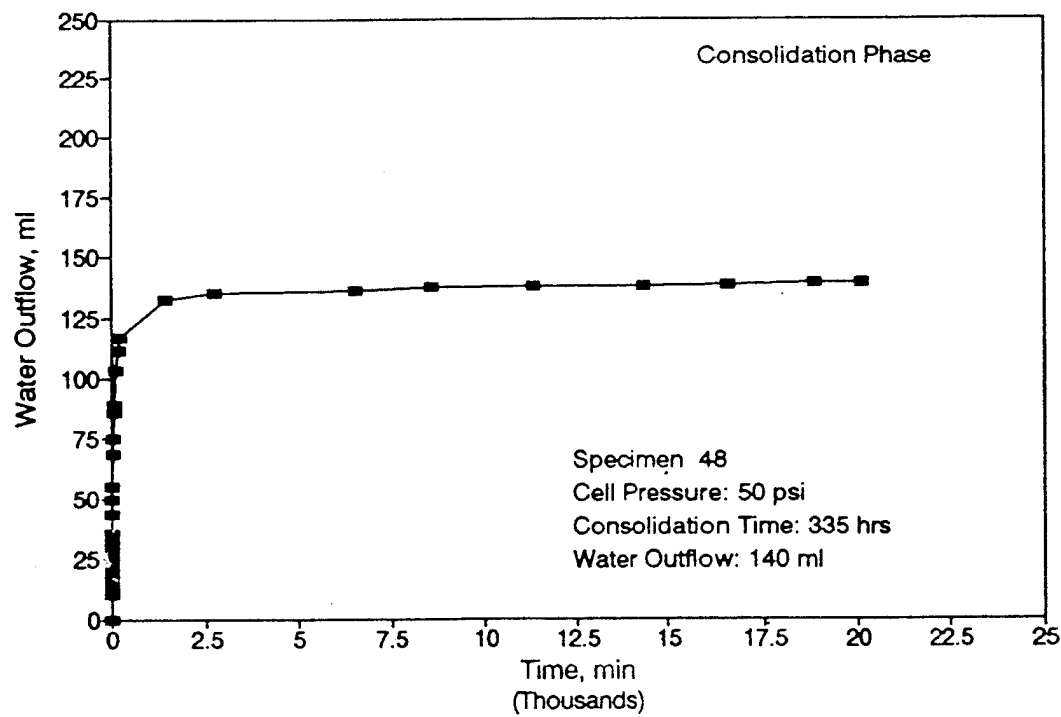
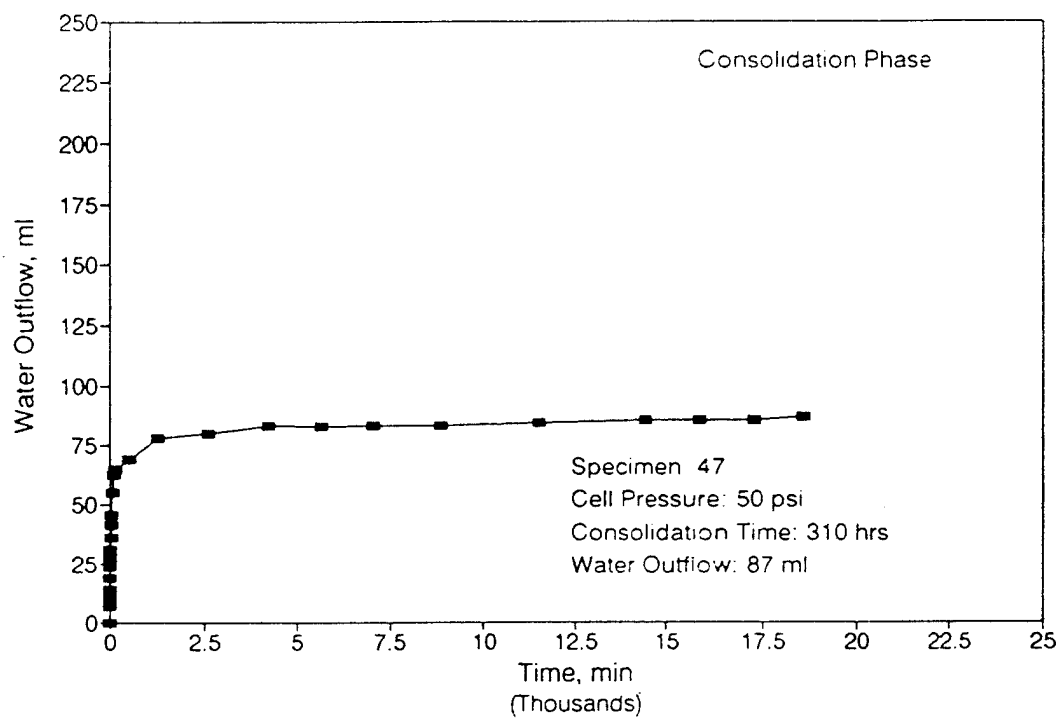




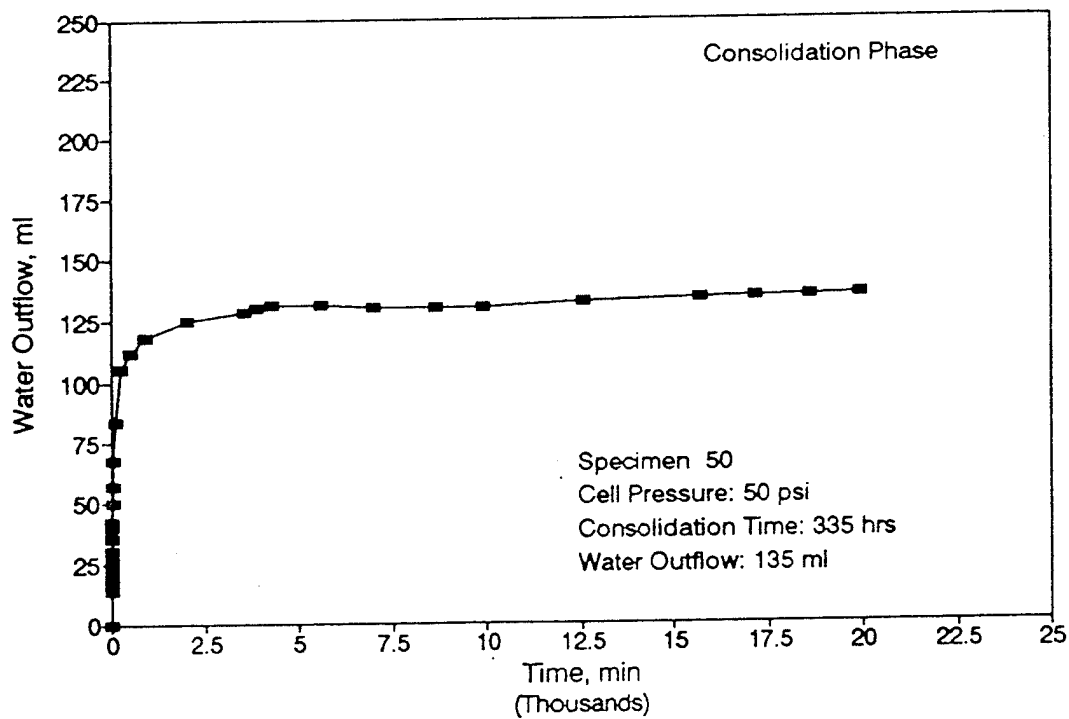
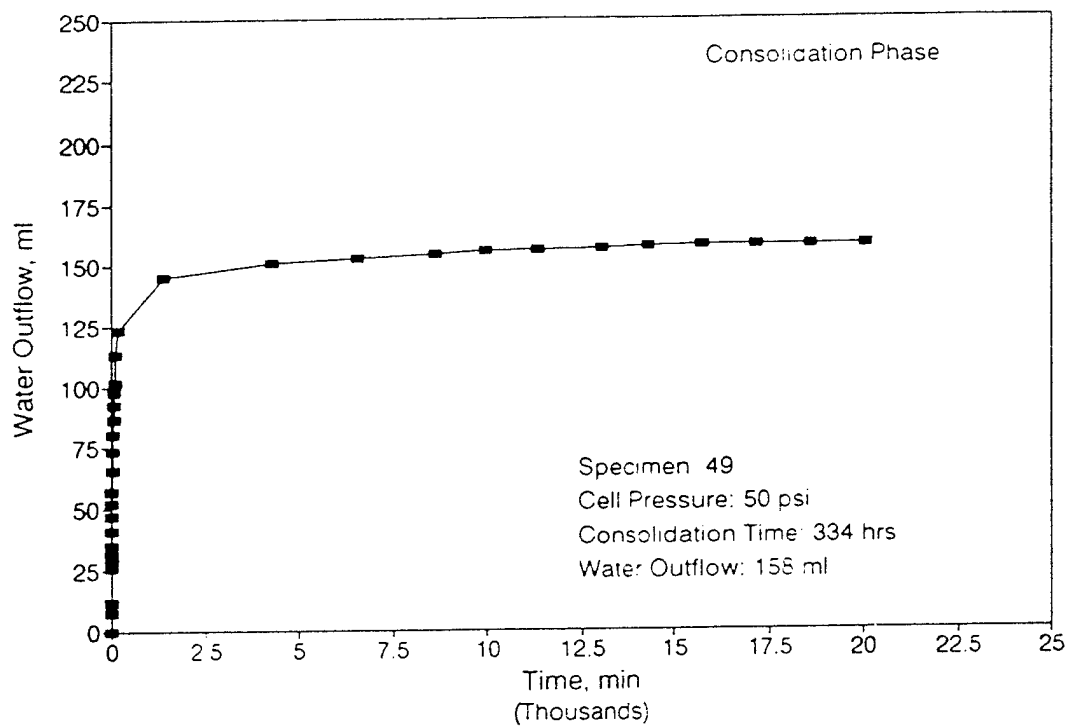


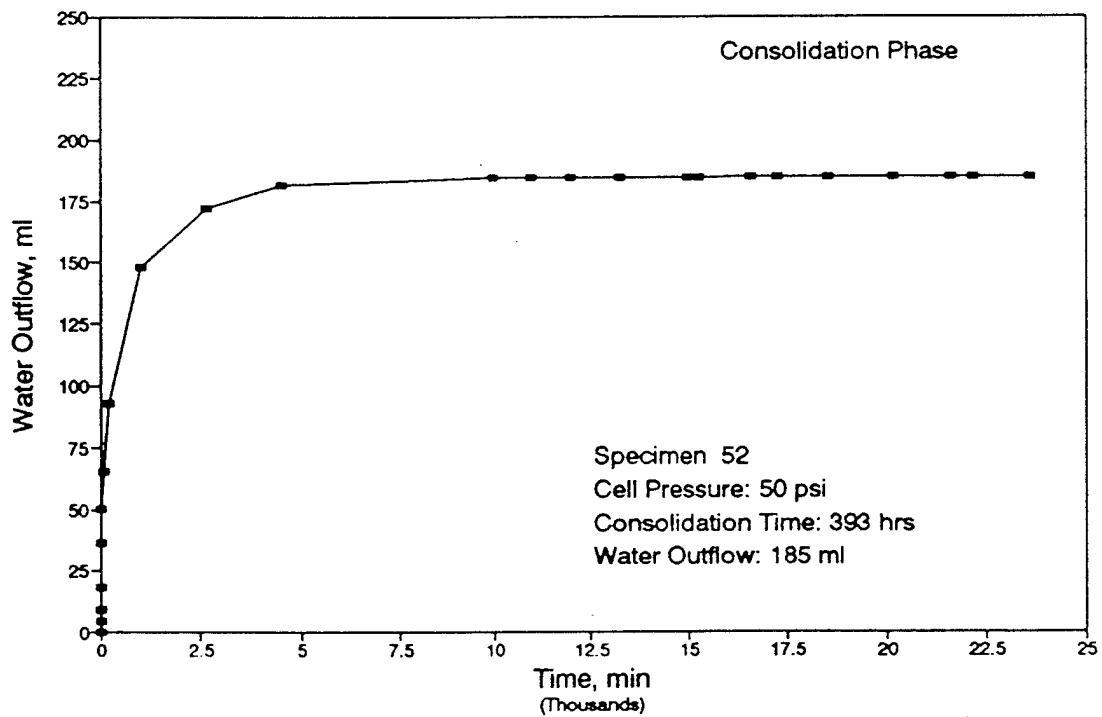
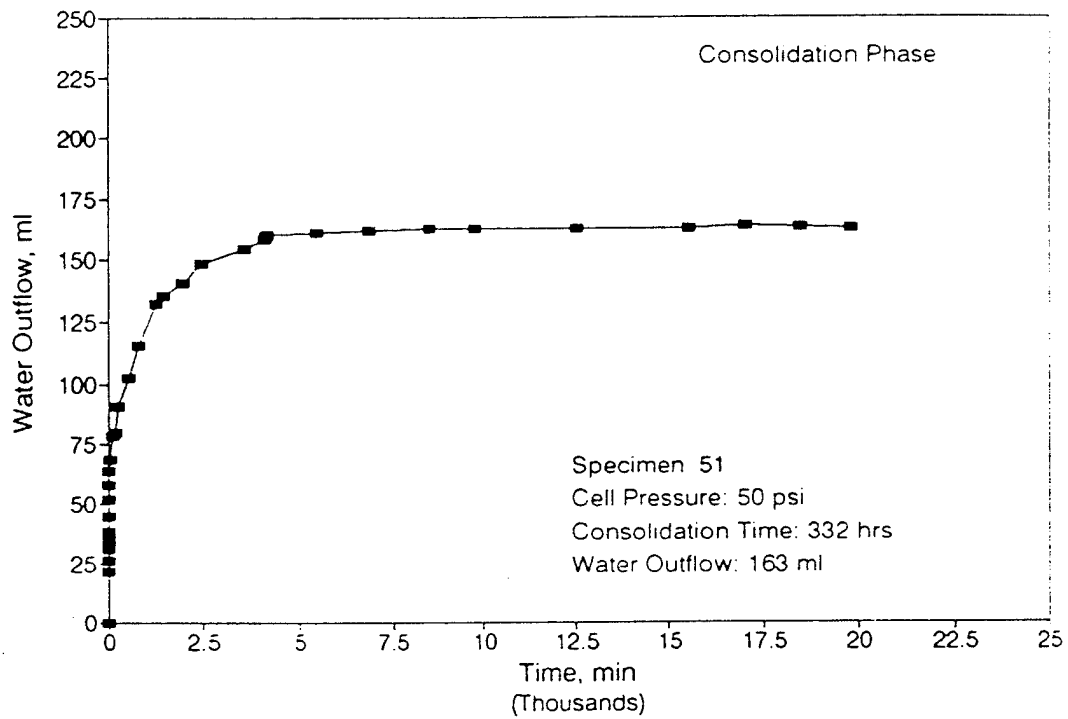


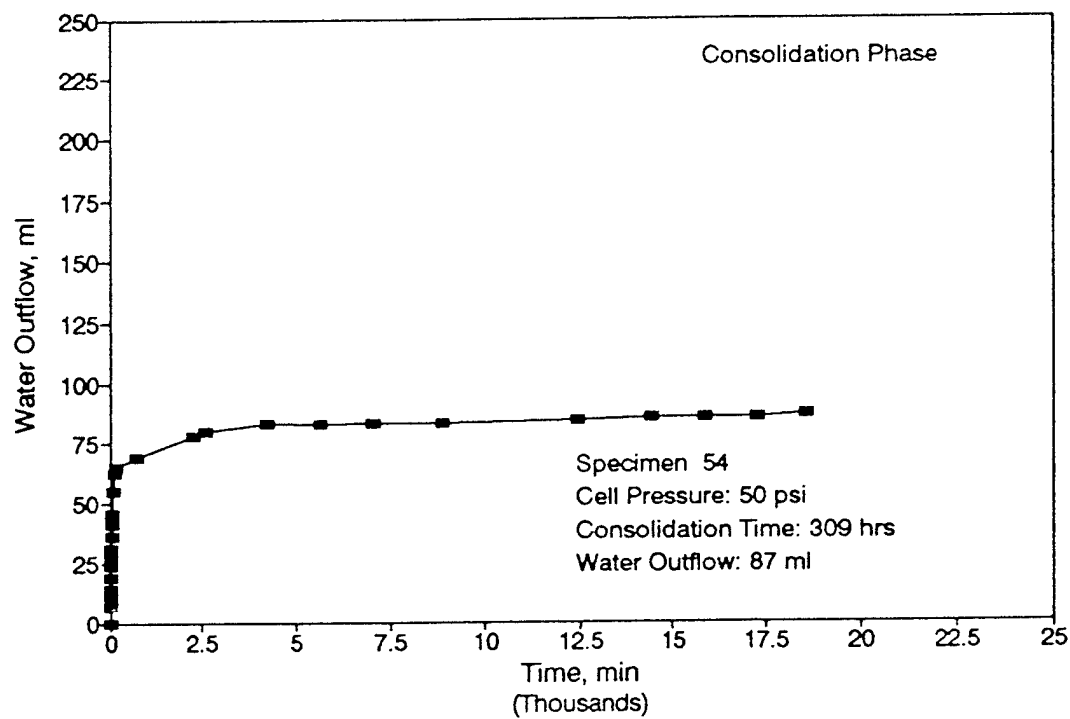
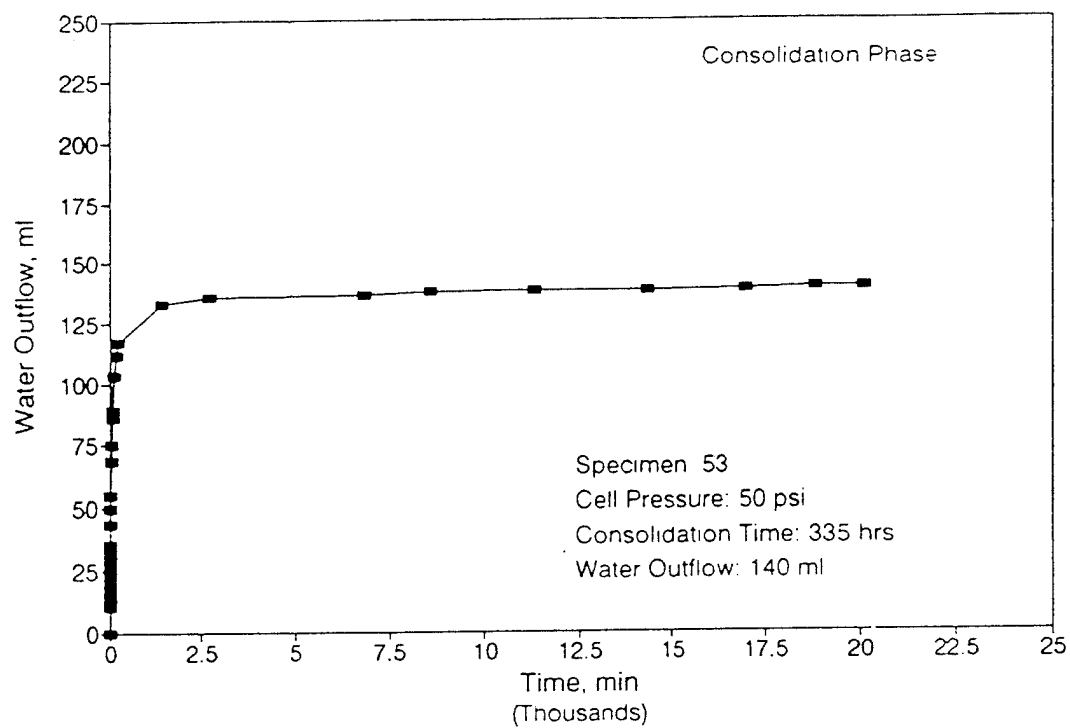


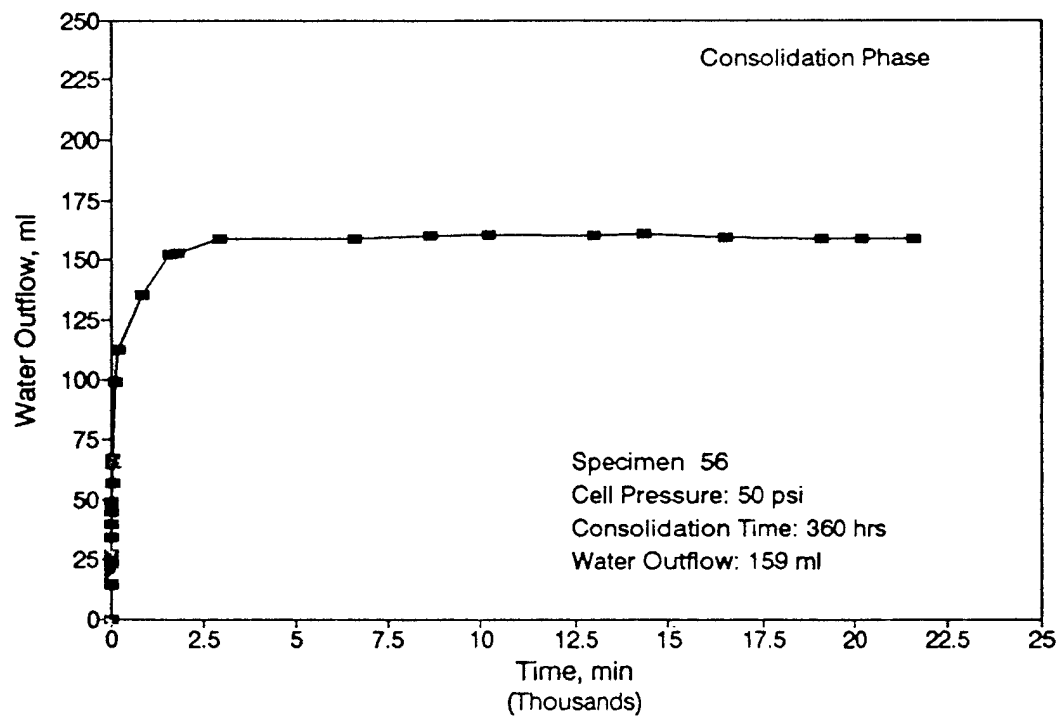
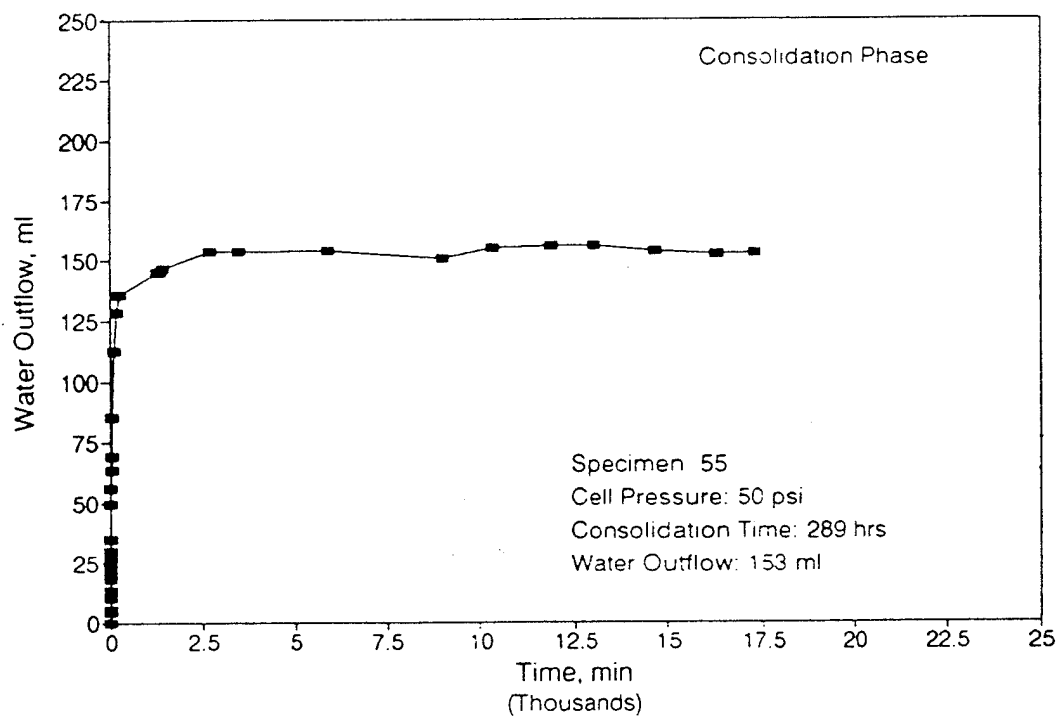


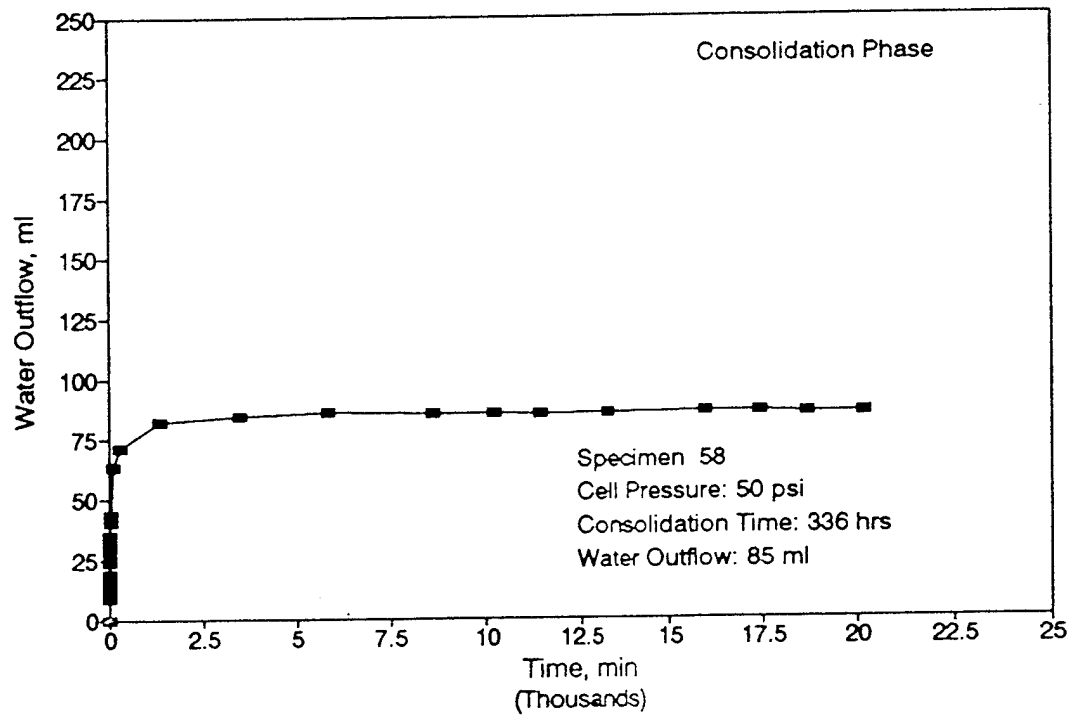
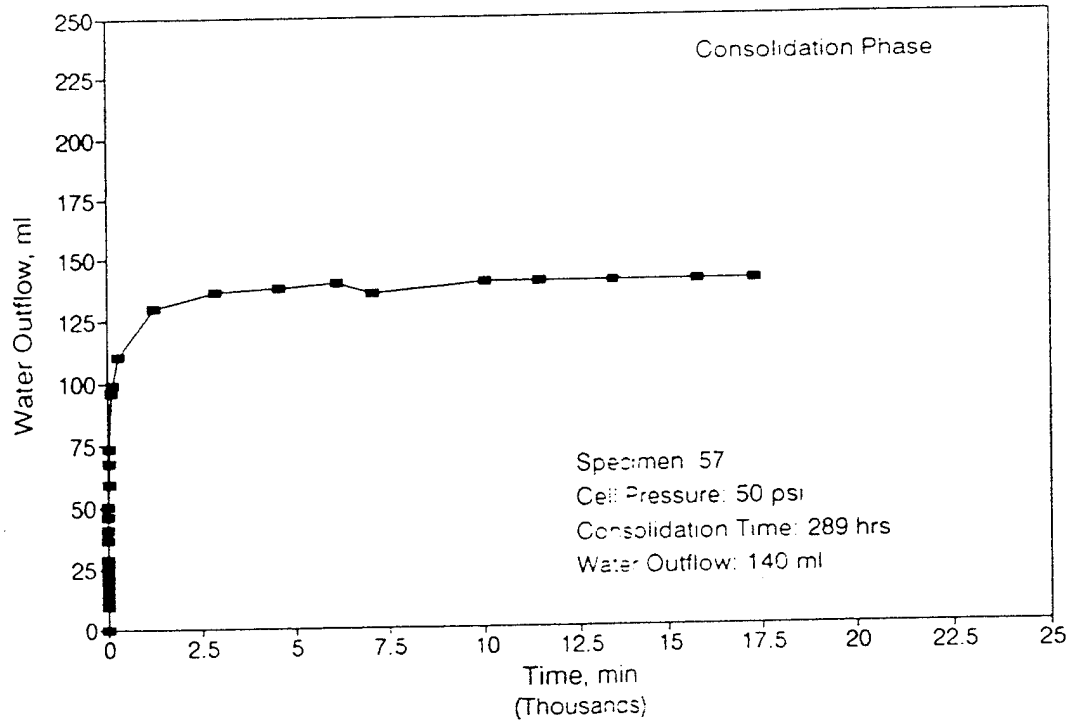


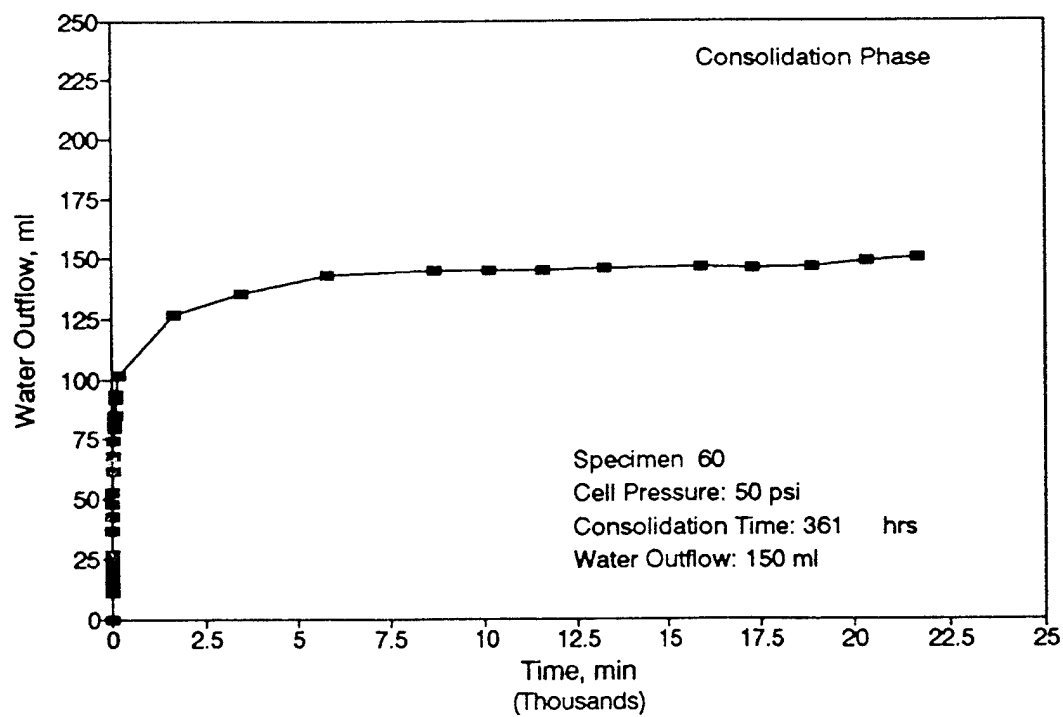
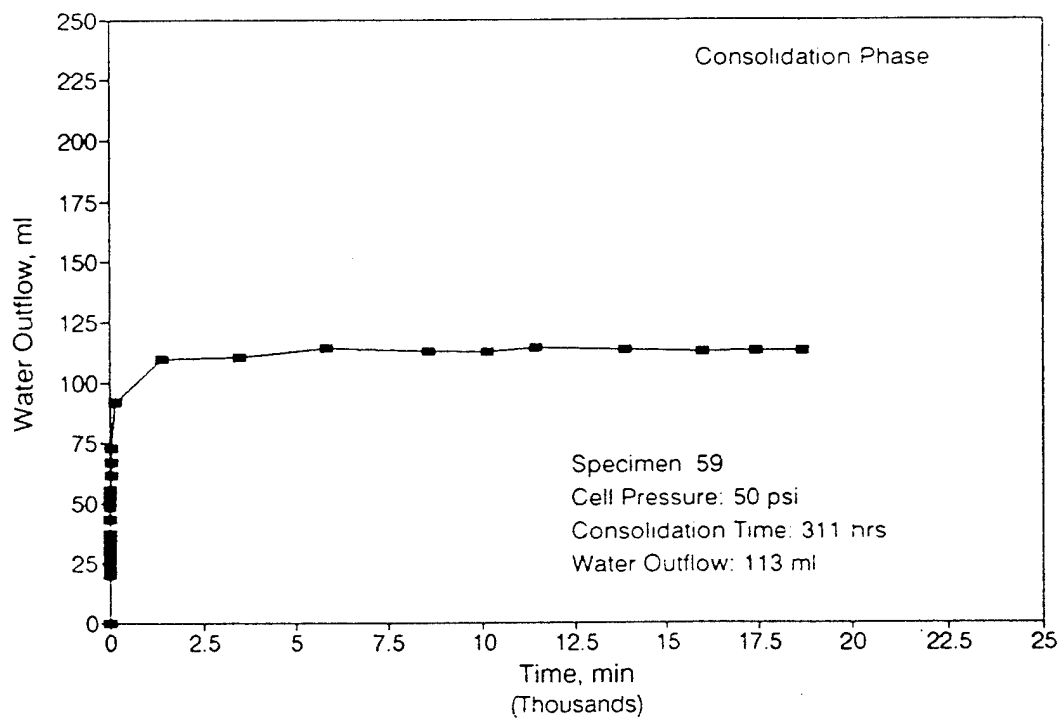


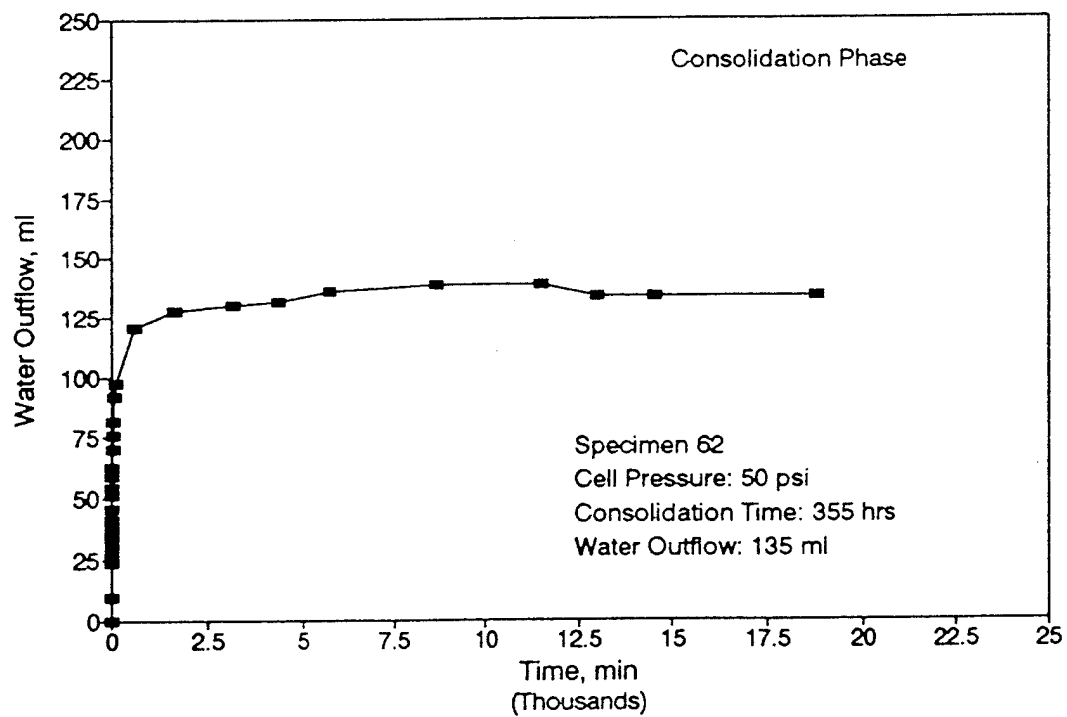
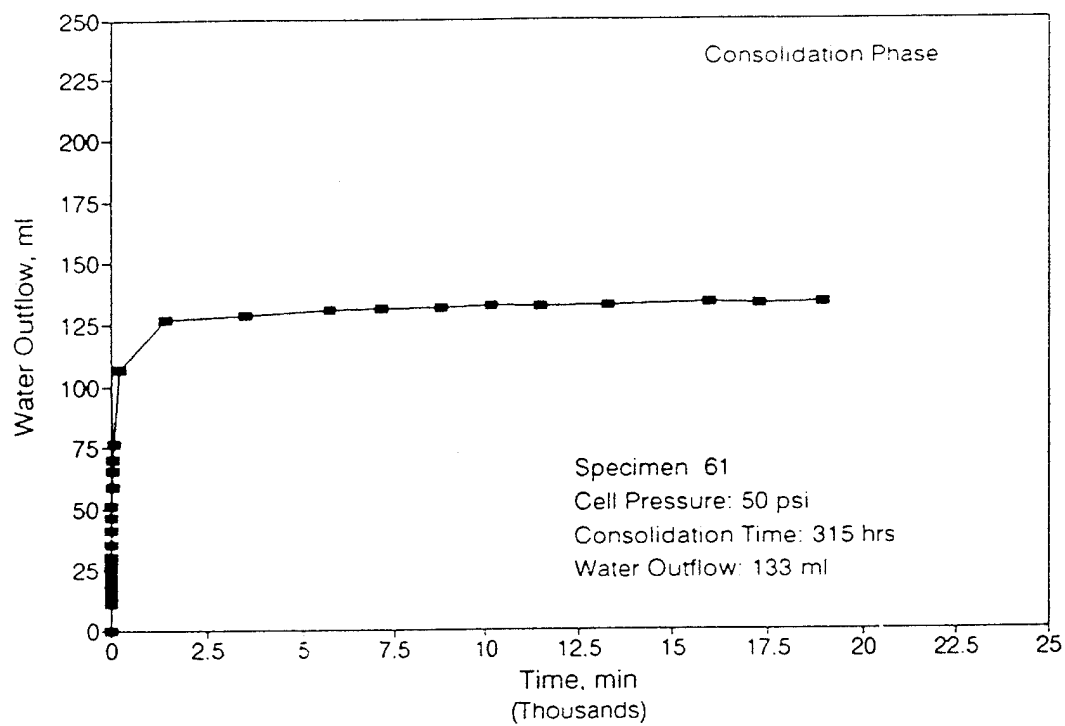


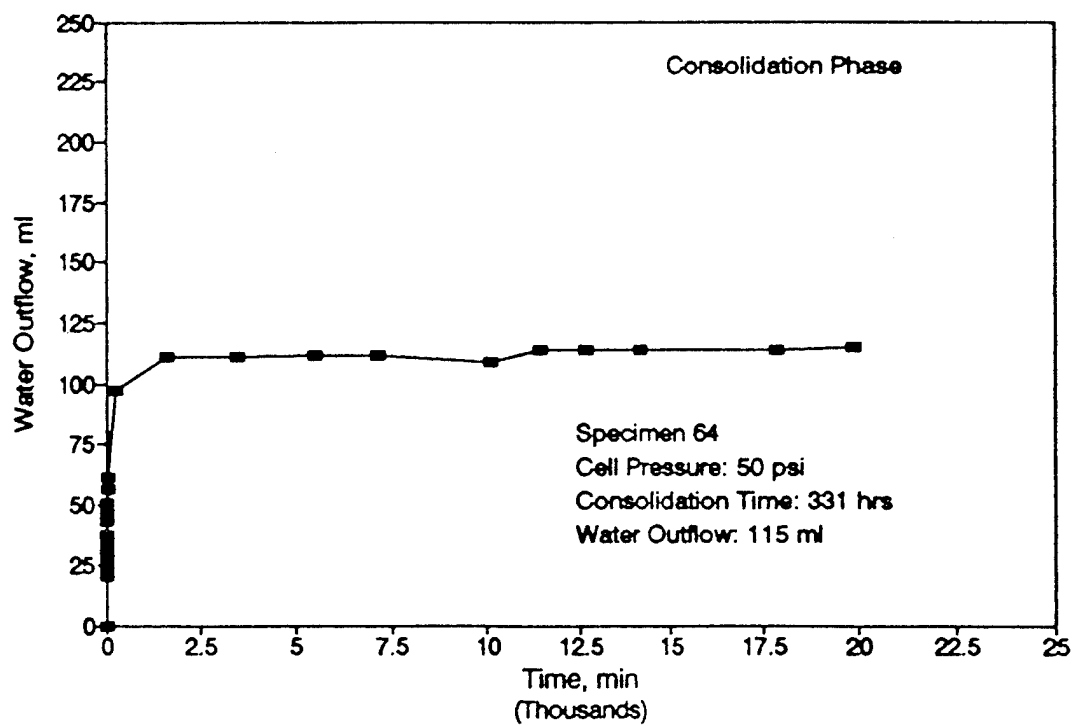
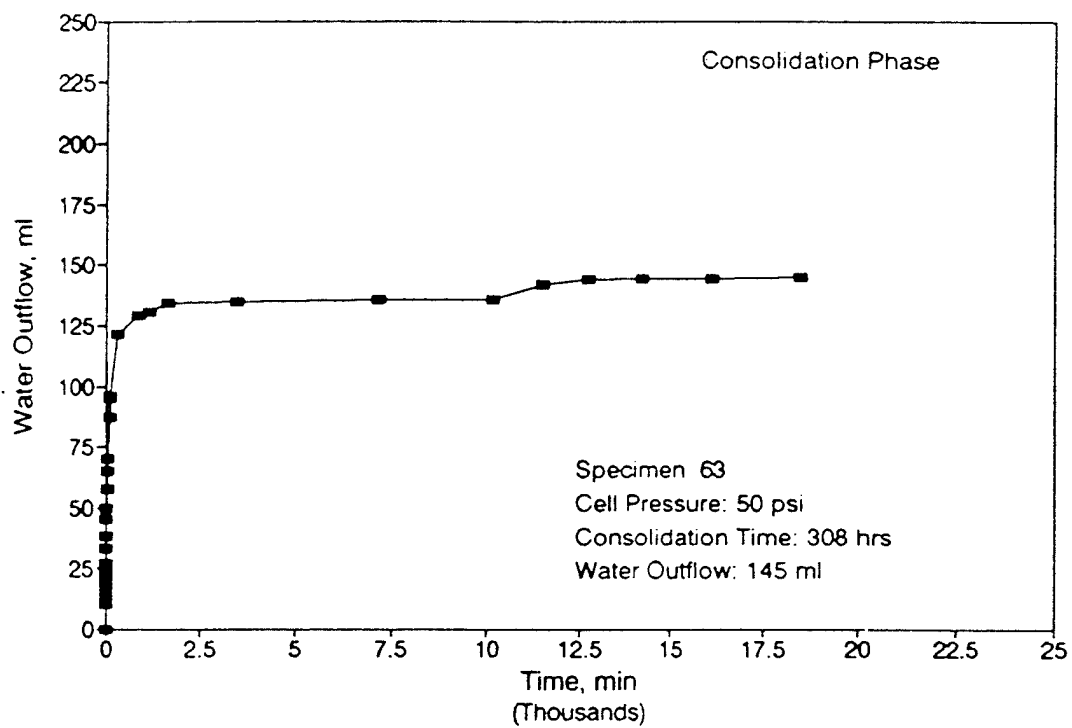




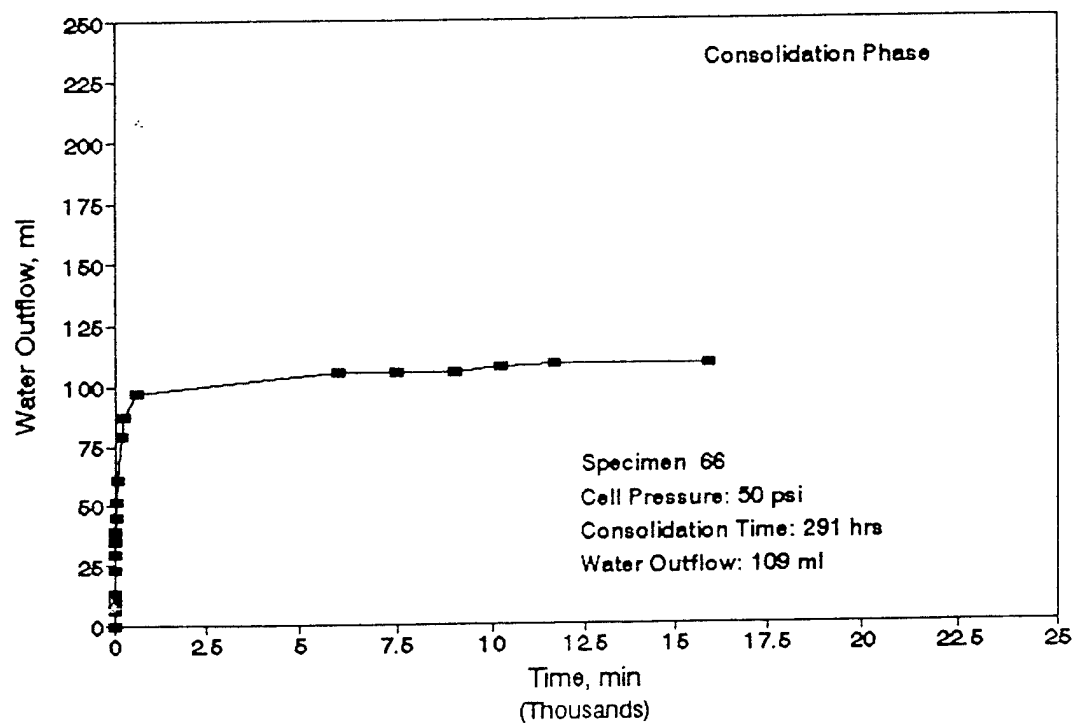
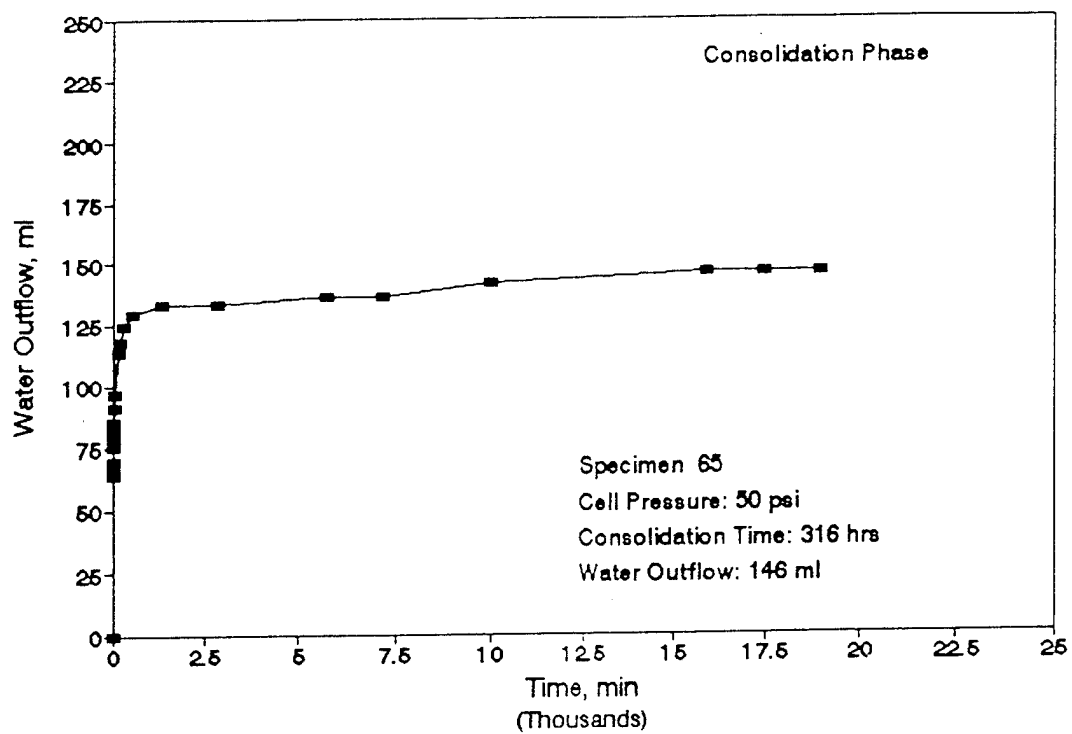


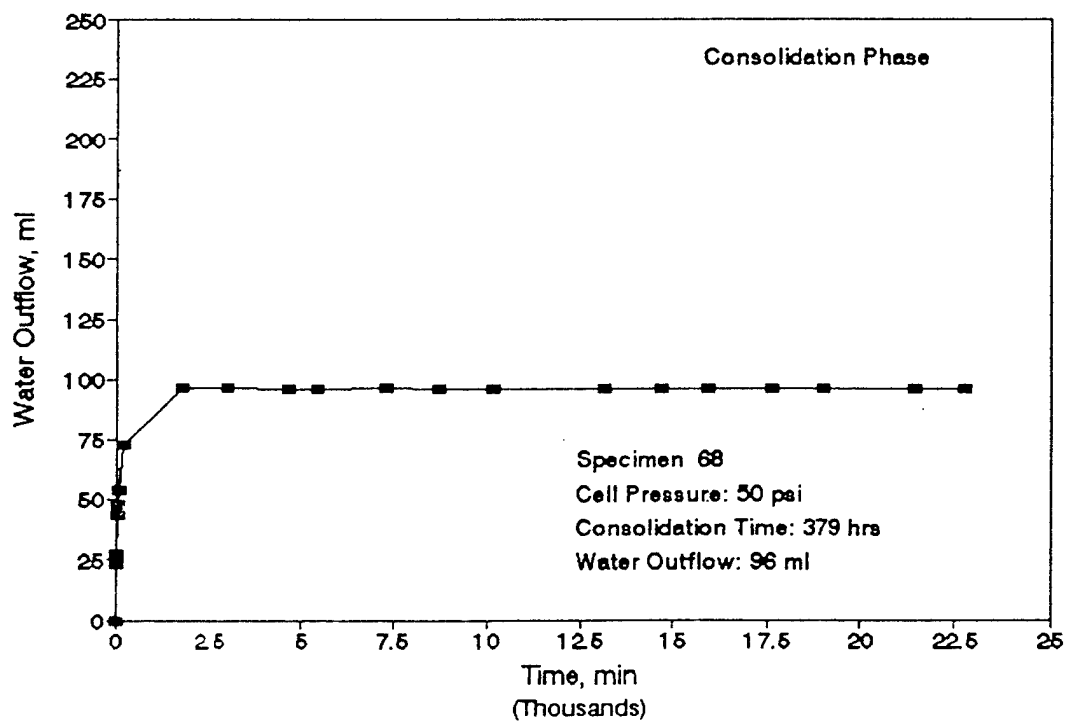
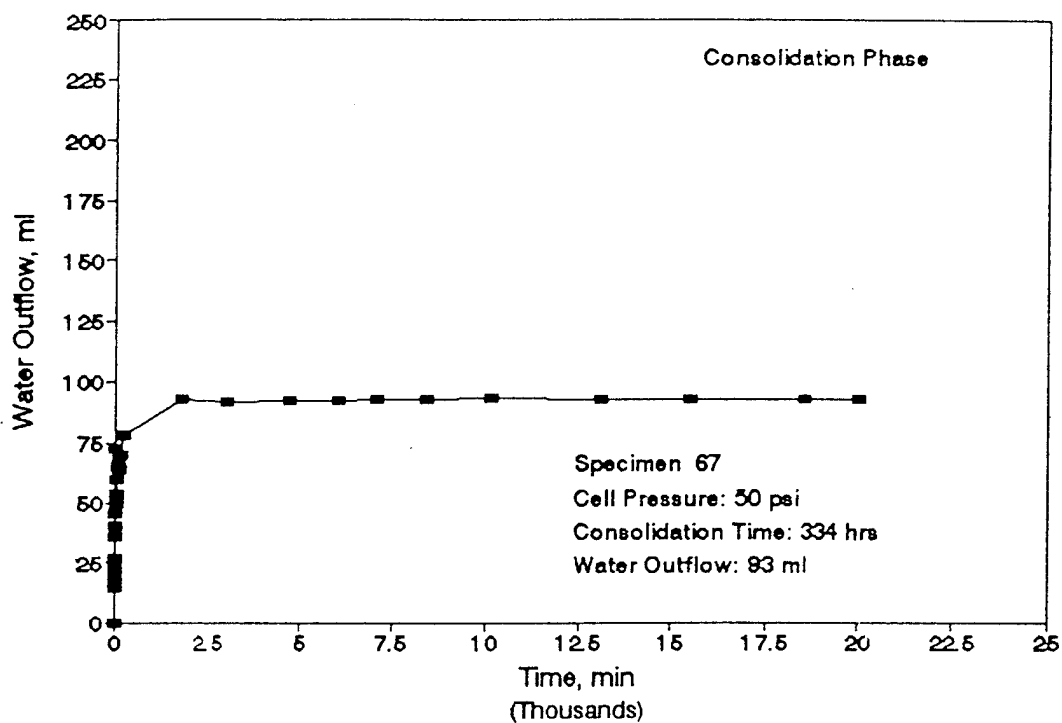




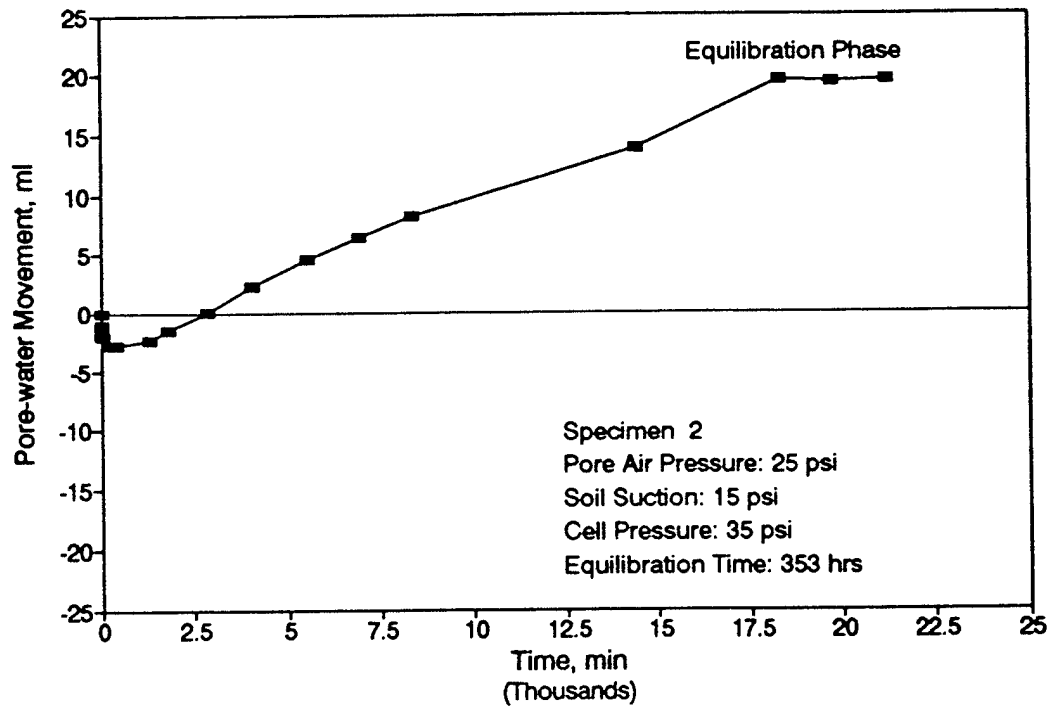
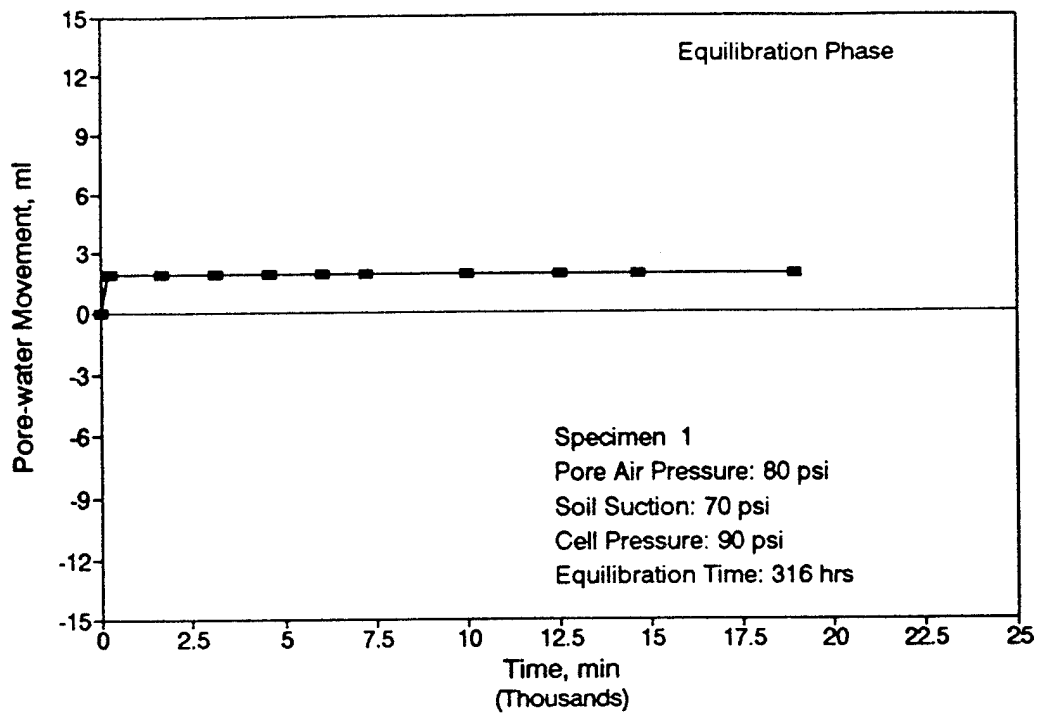


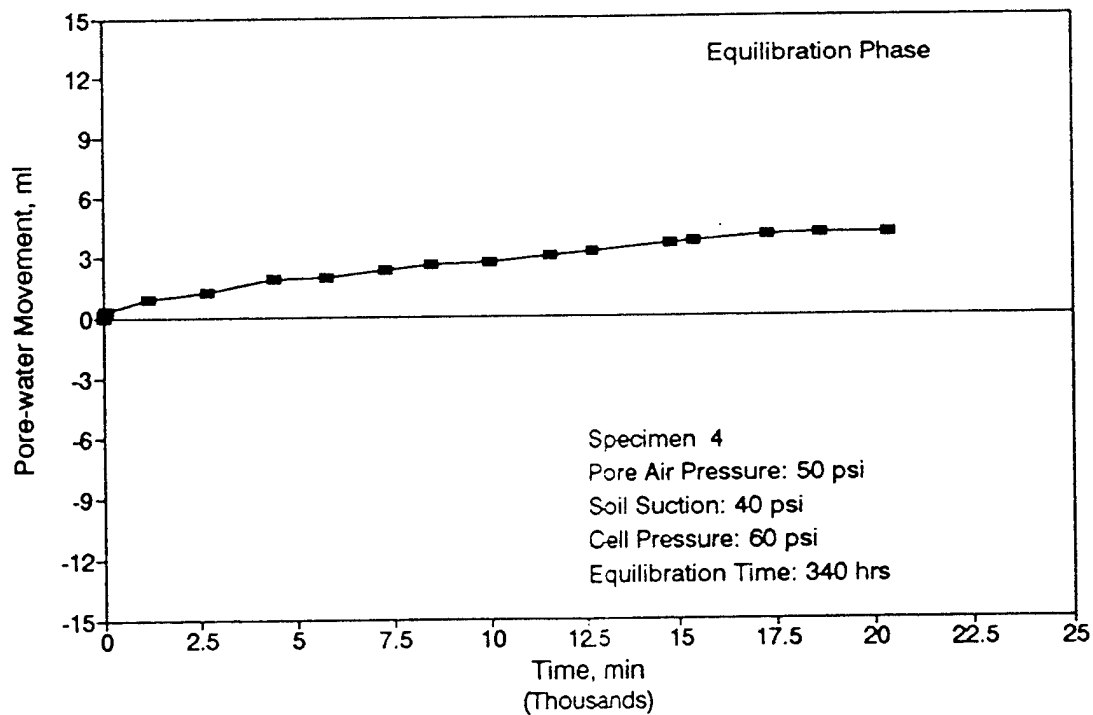
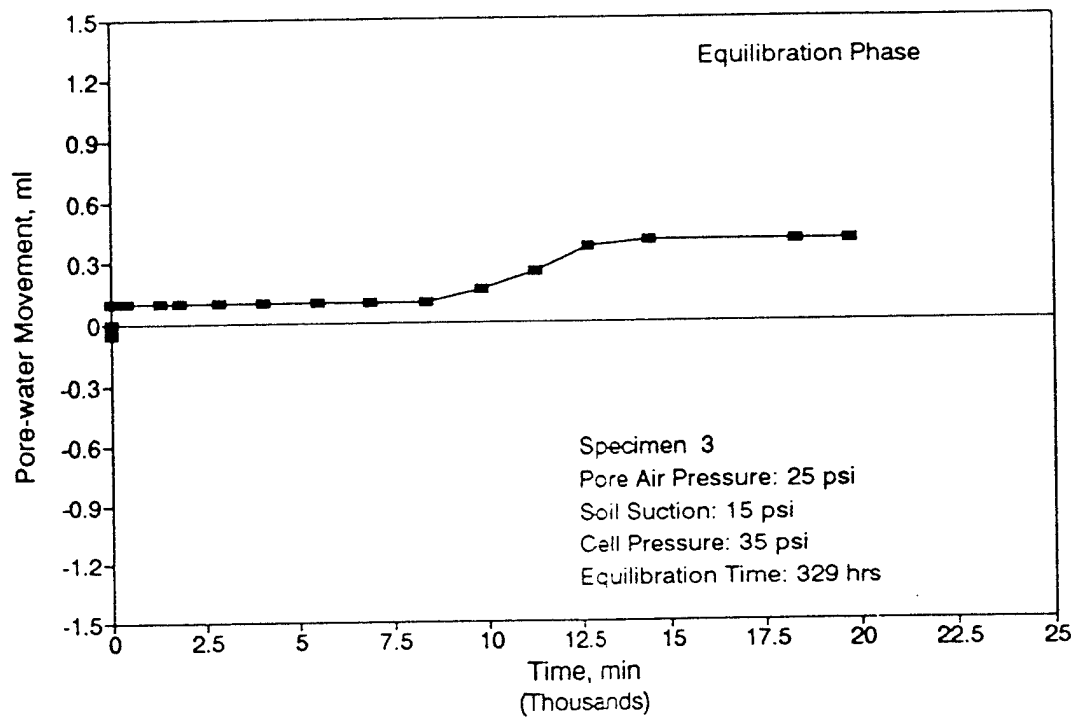


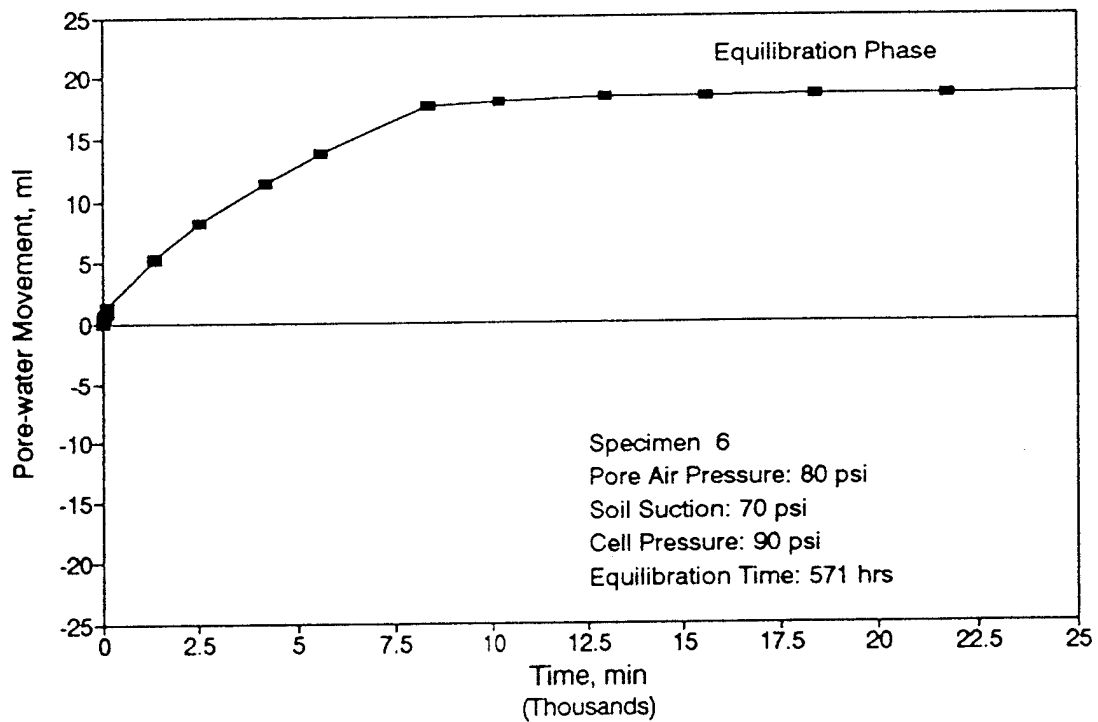
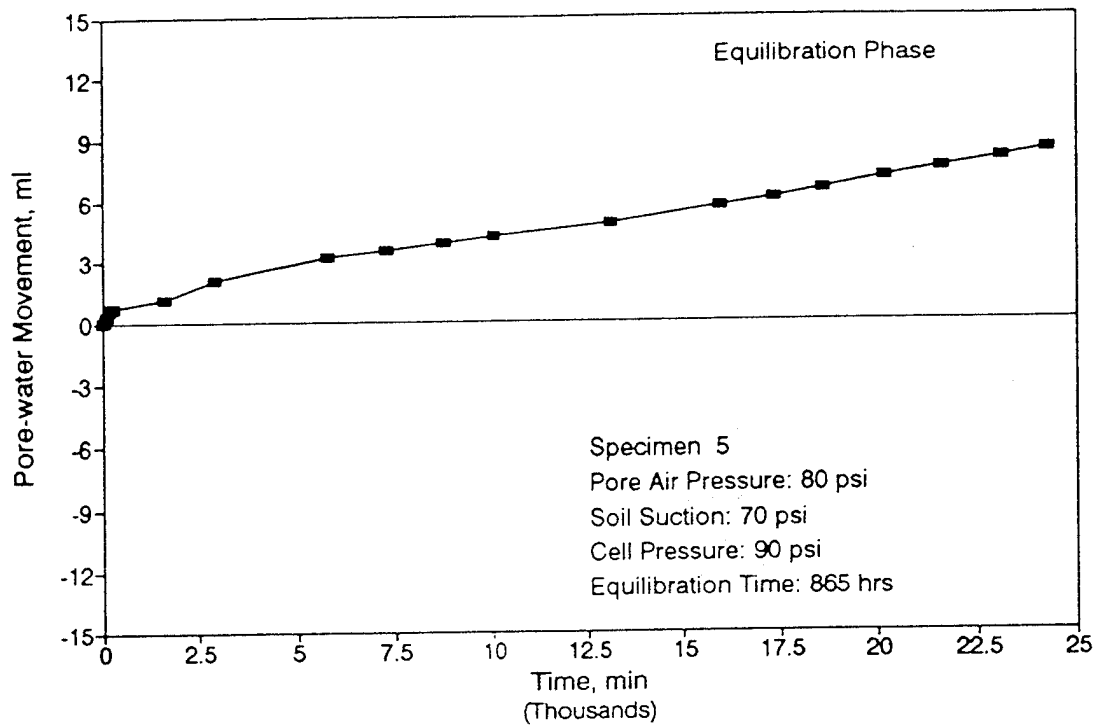


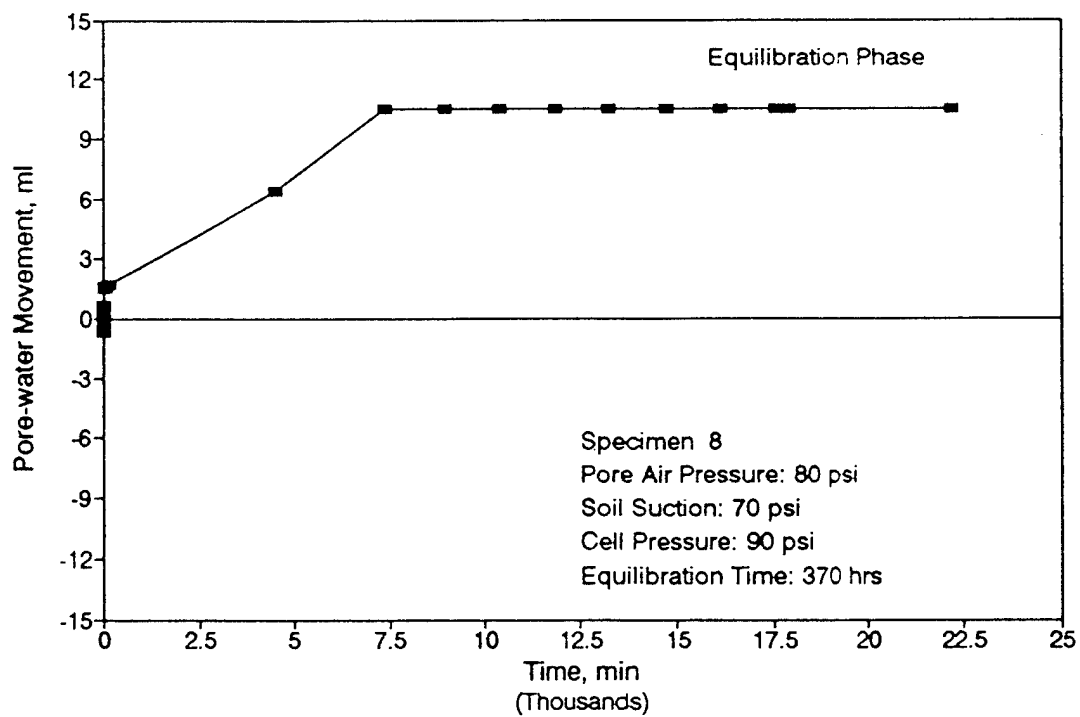
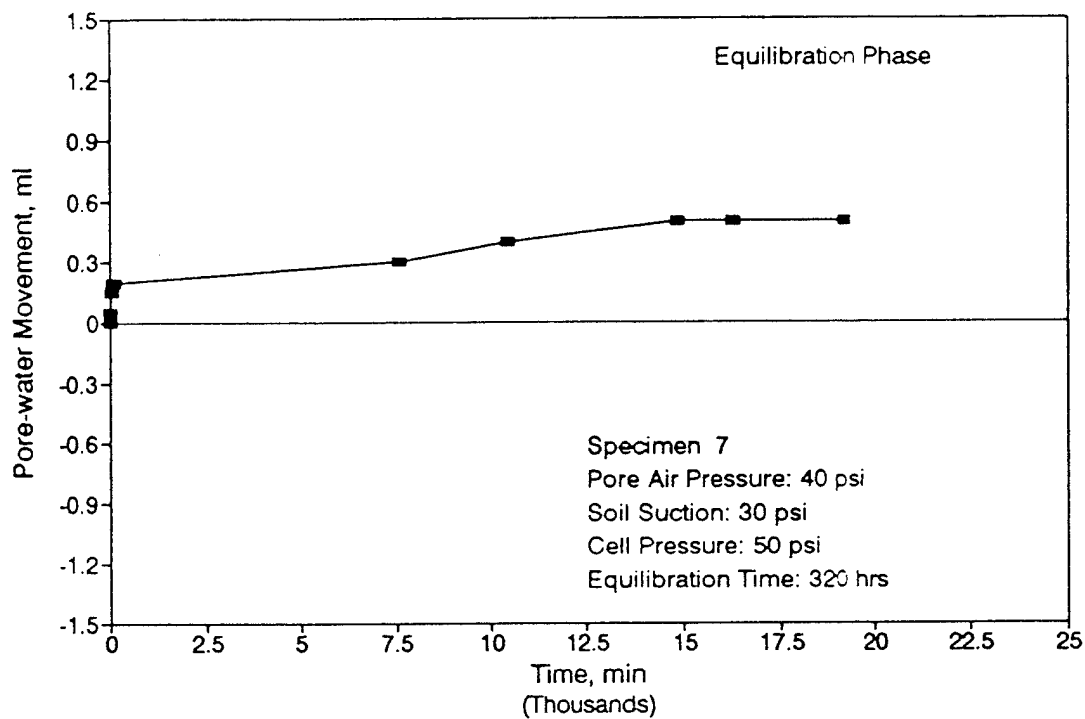


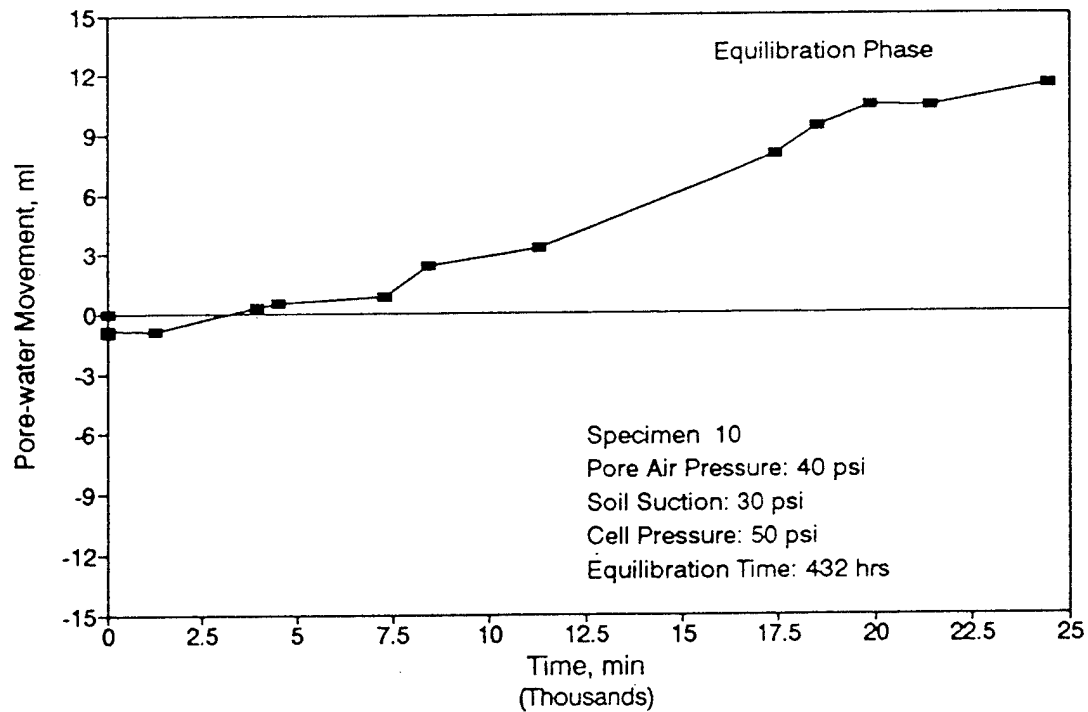
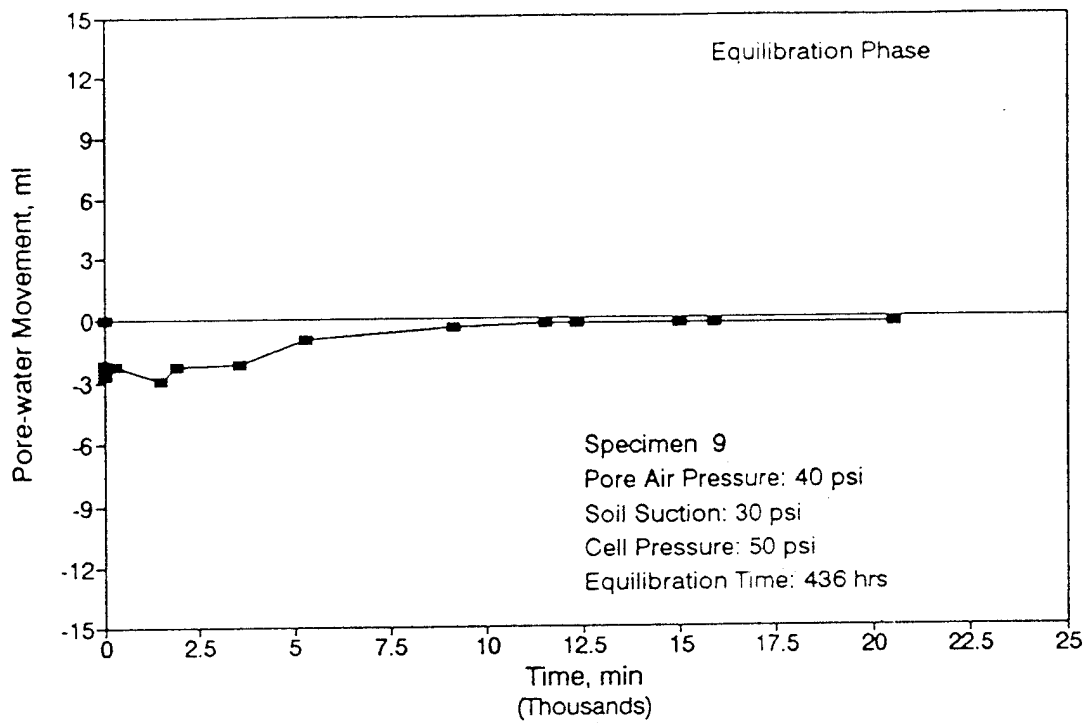
**APPENDIX B**  
**RECORDS OF EQUILIBRATION TO SPECIFIED SOIL SUCTION**



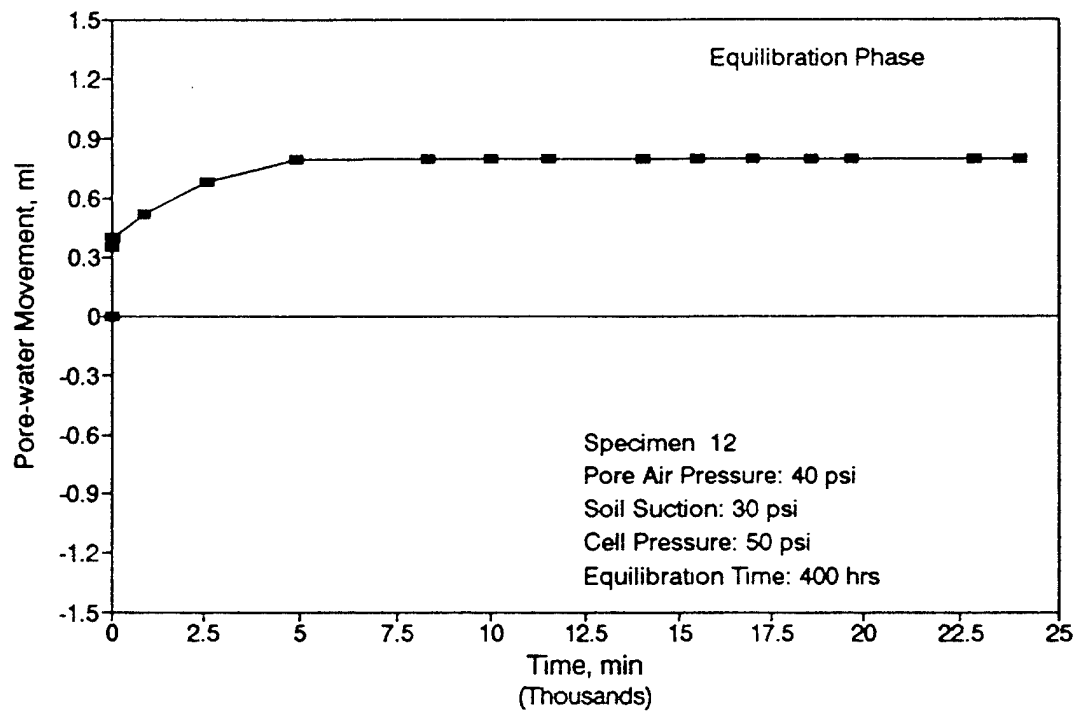
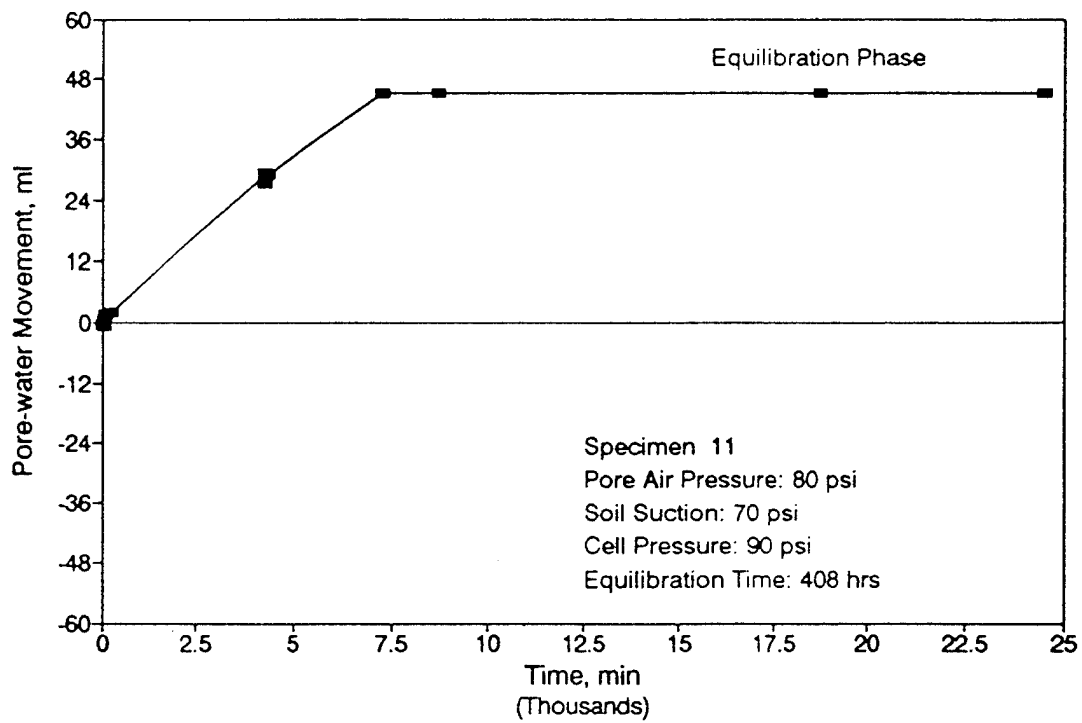


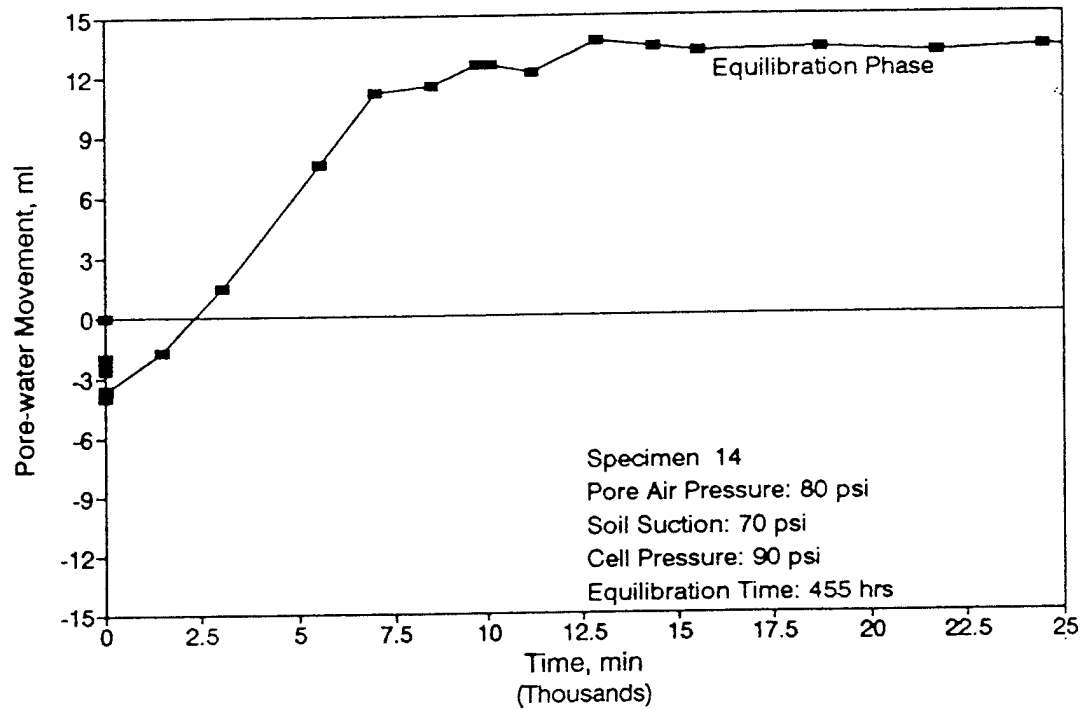
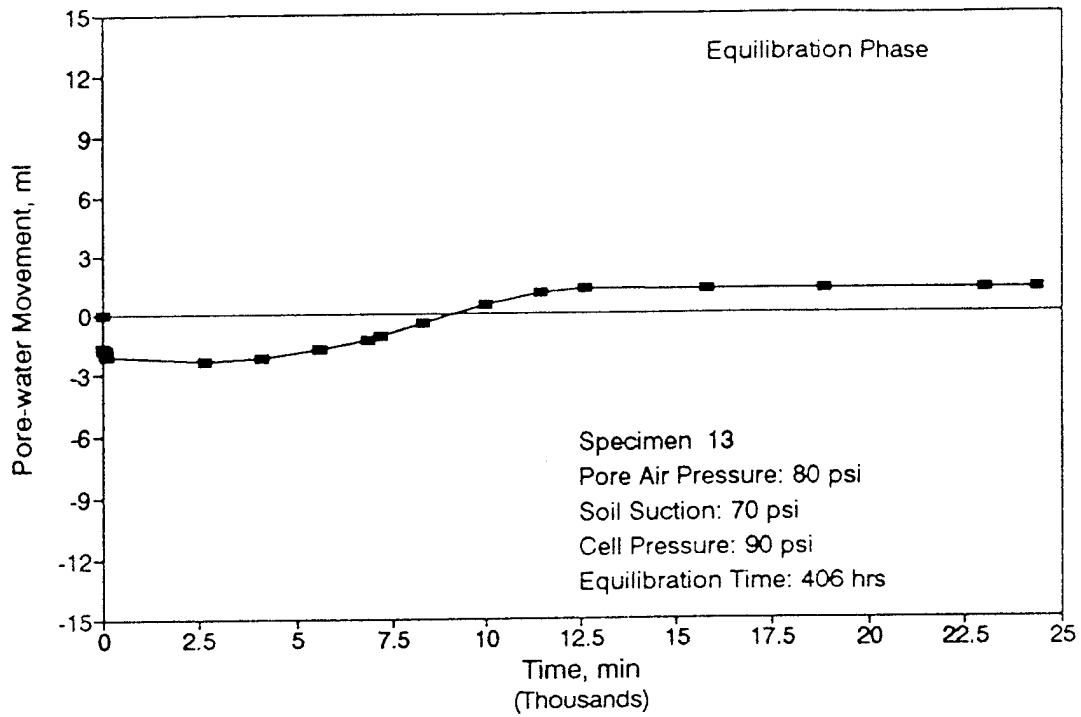


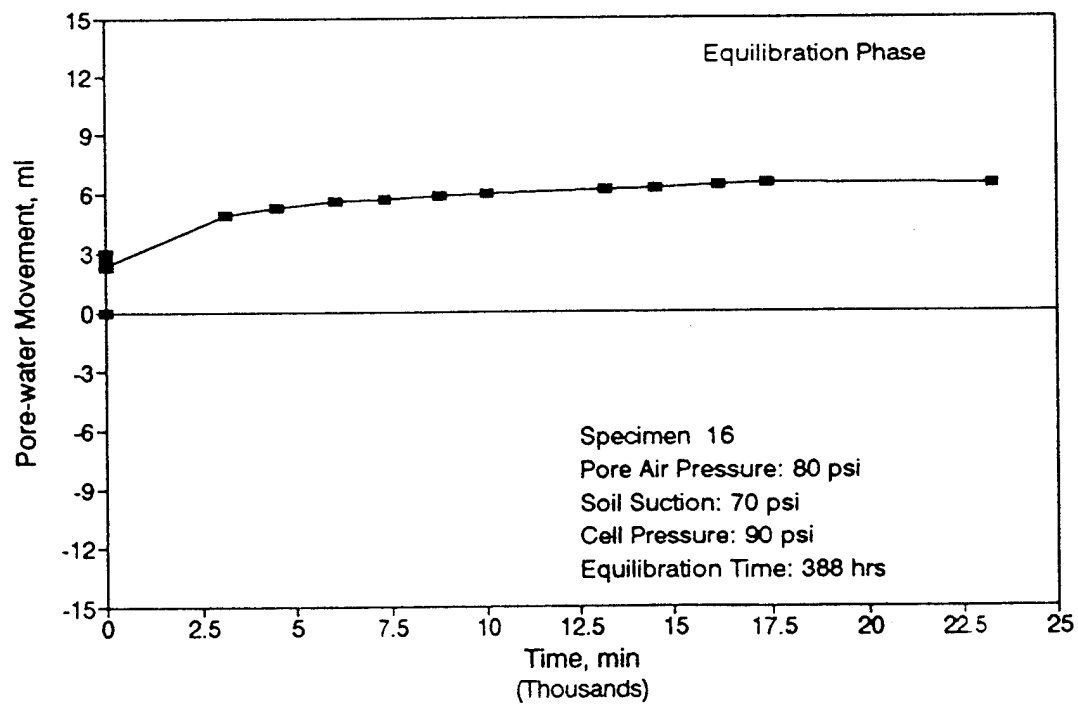
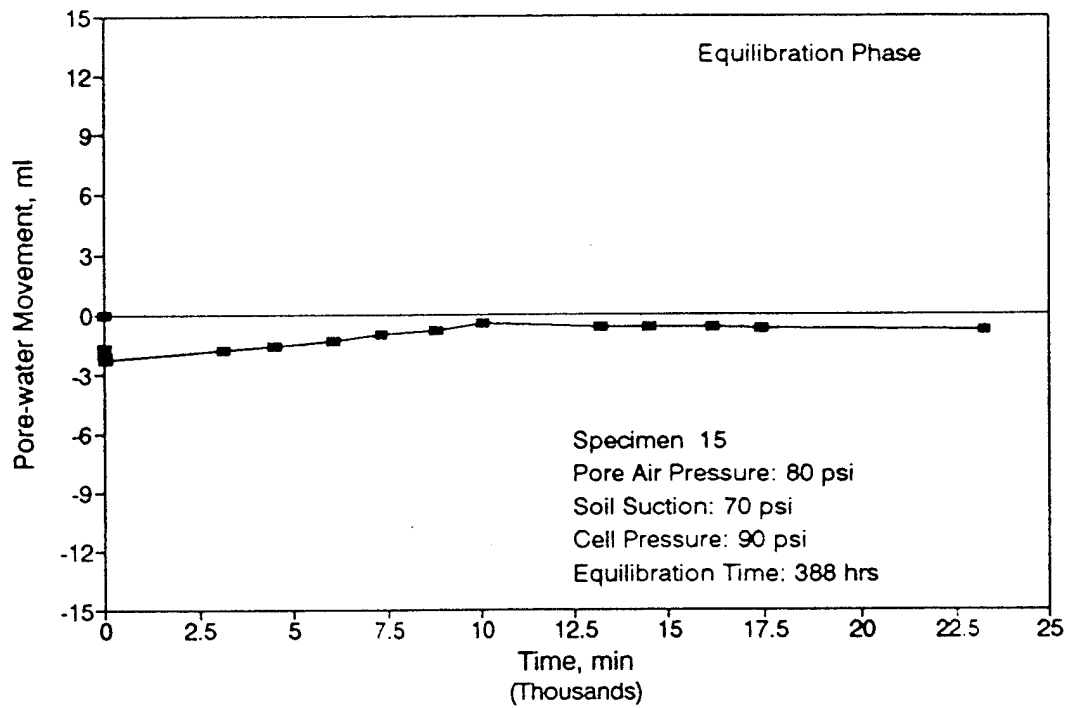


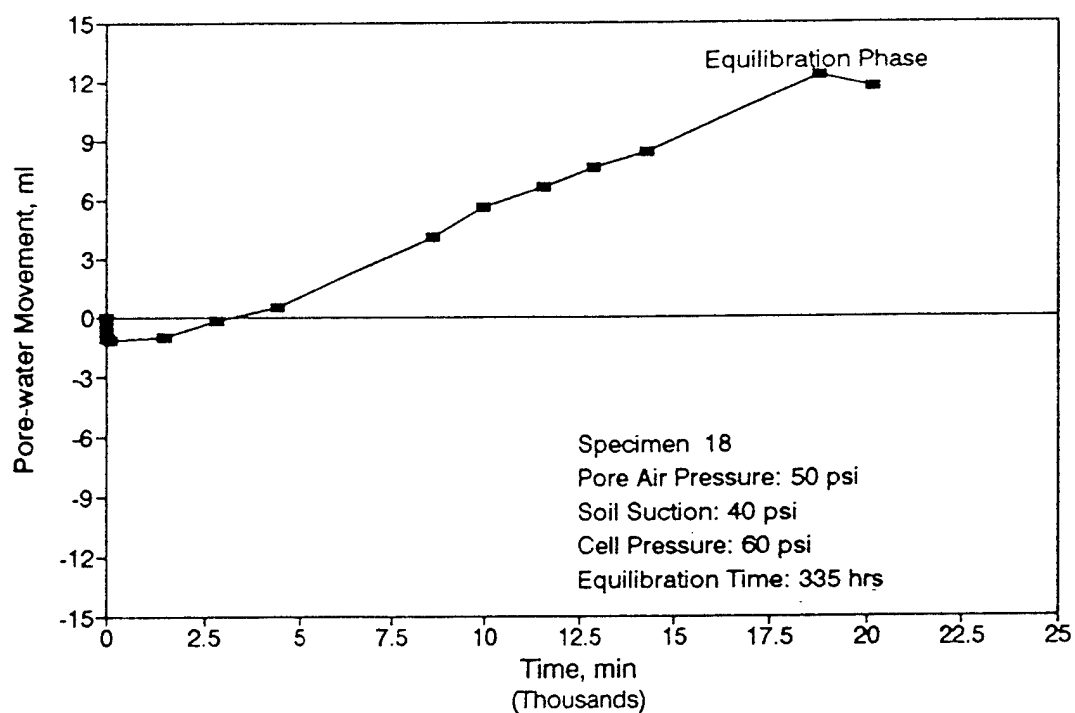
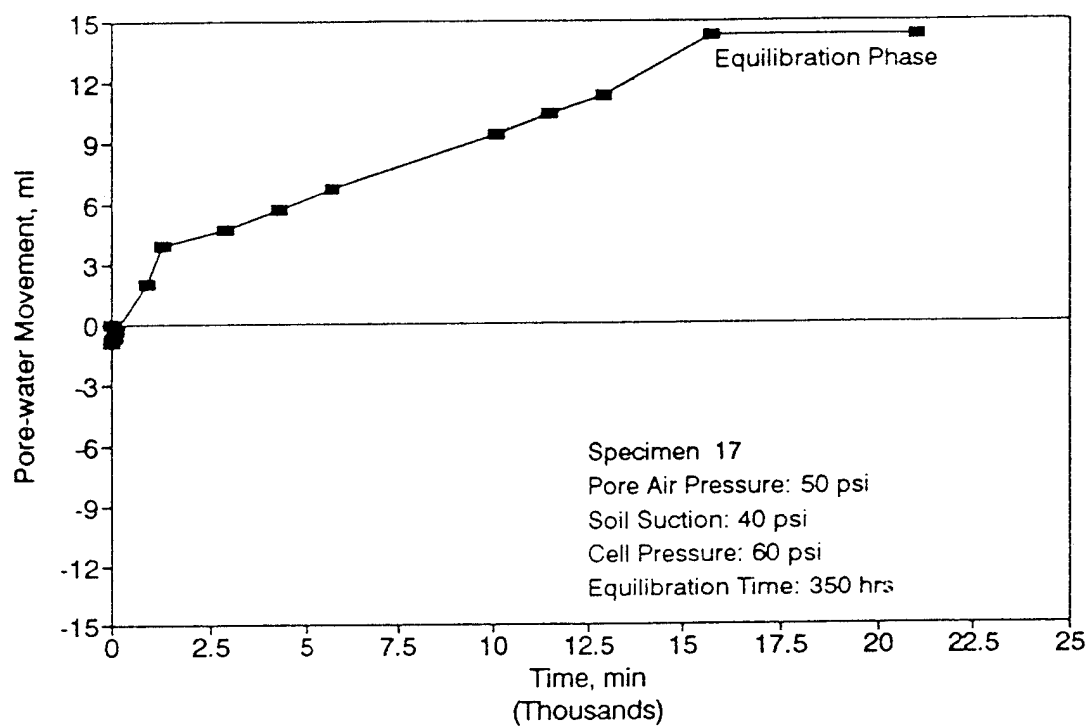


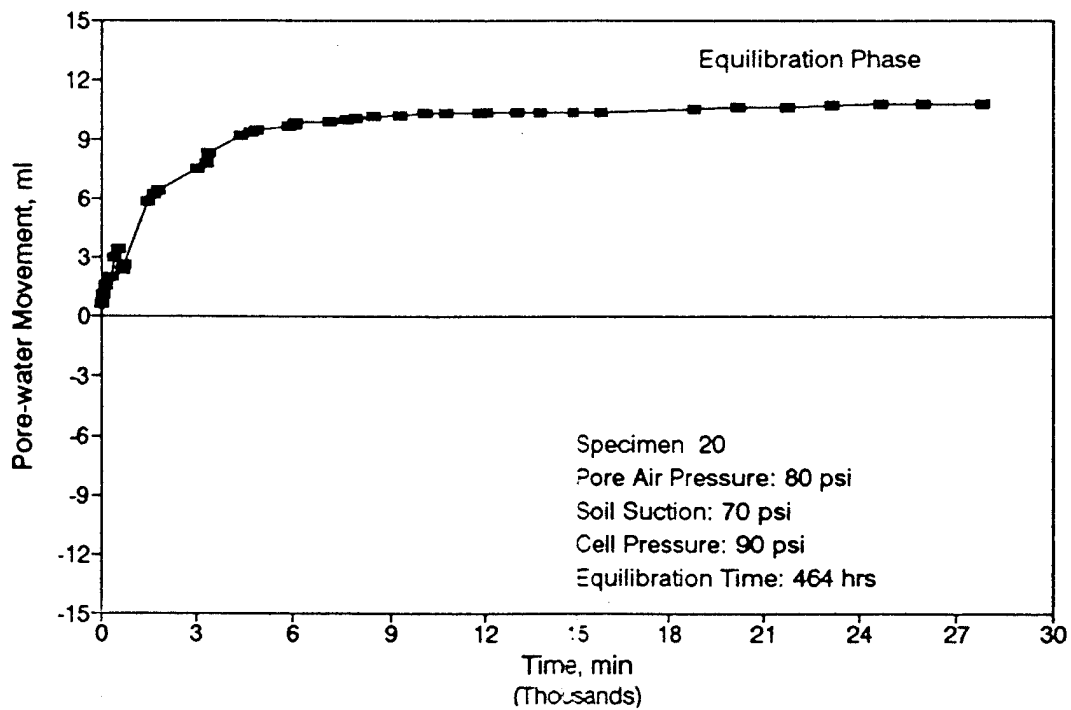
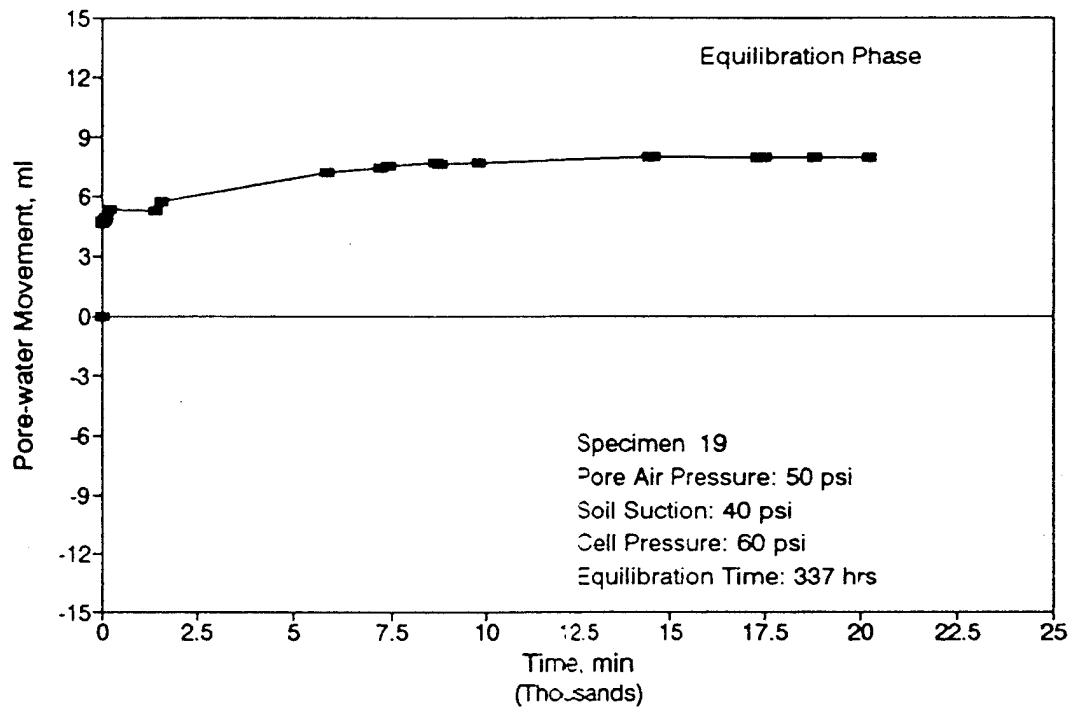


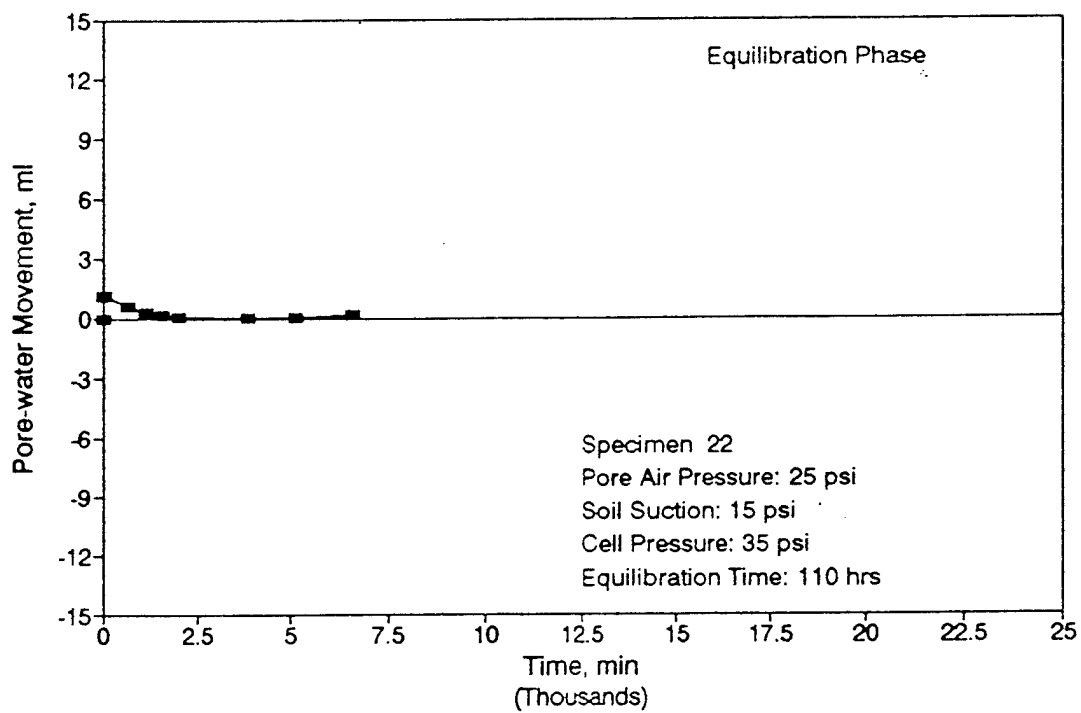
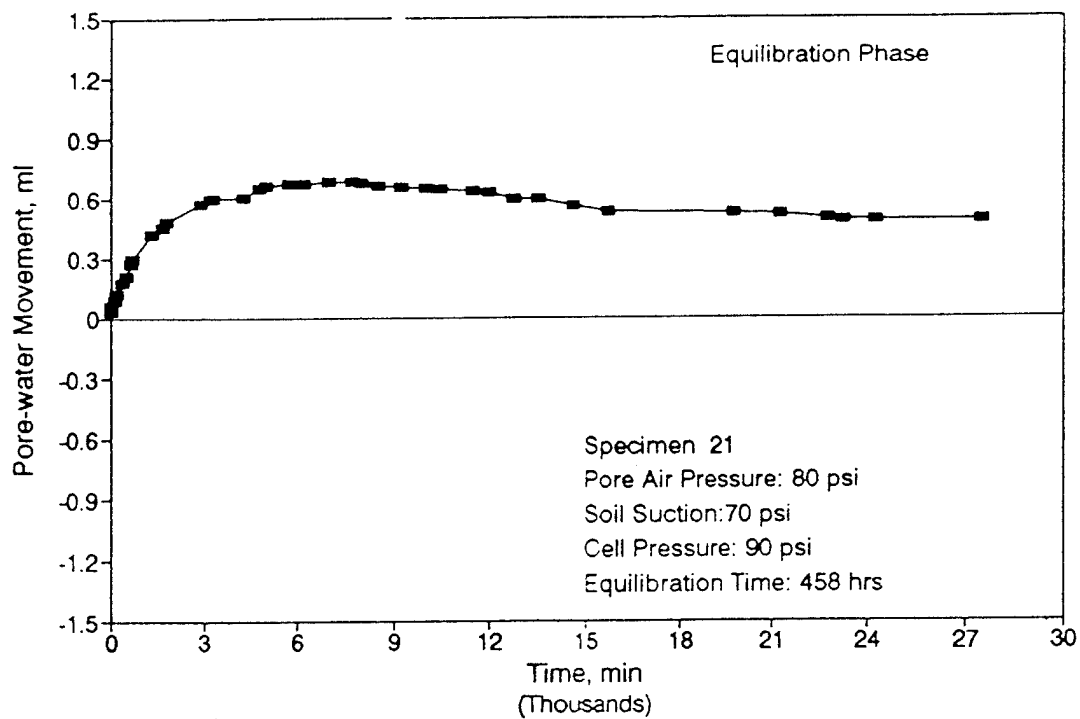


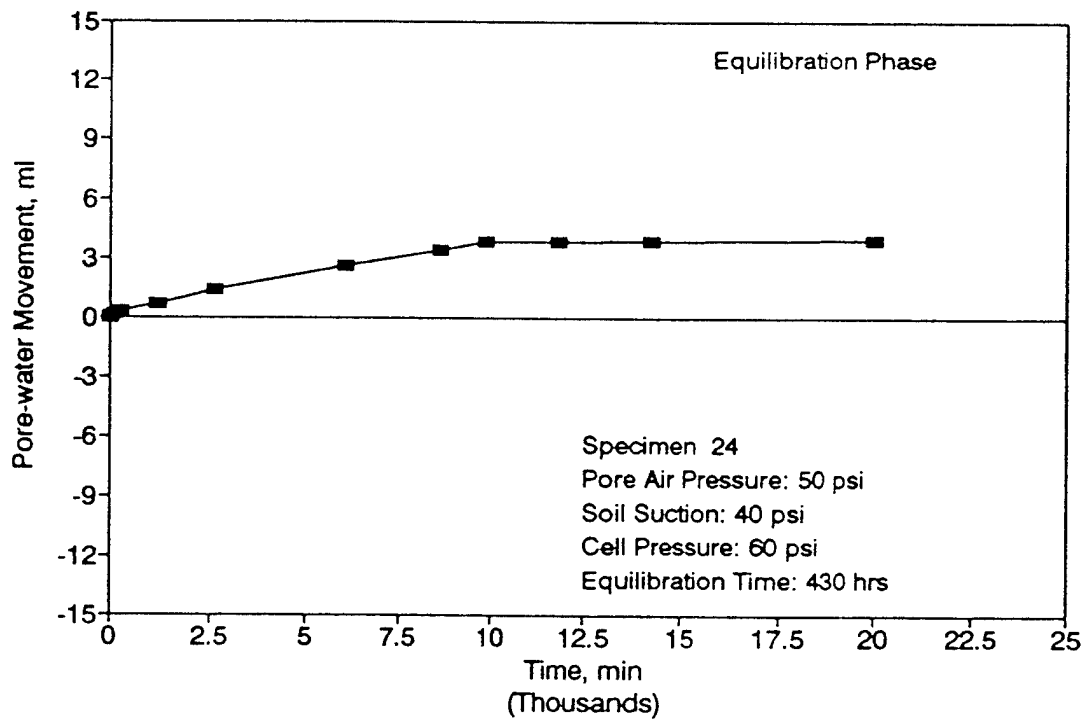
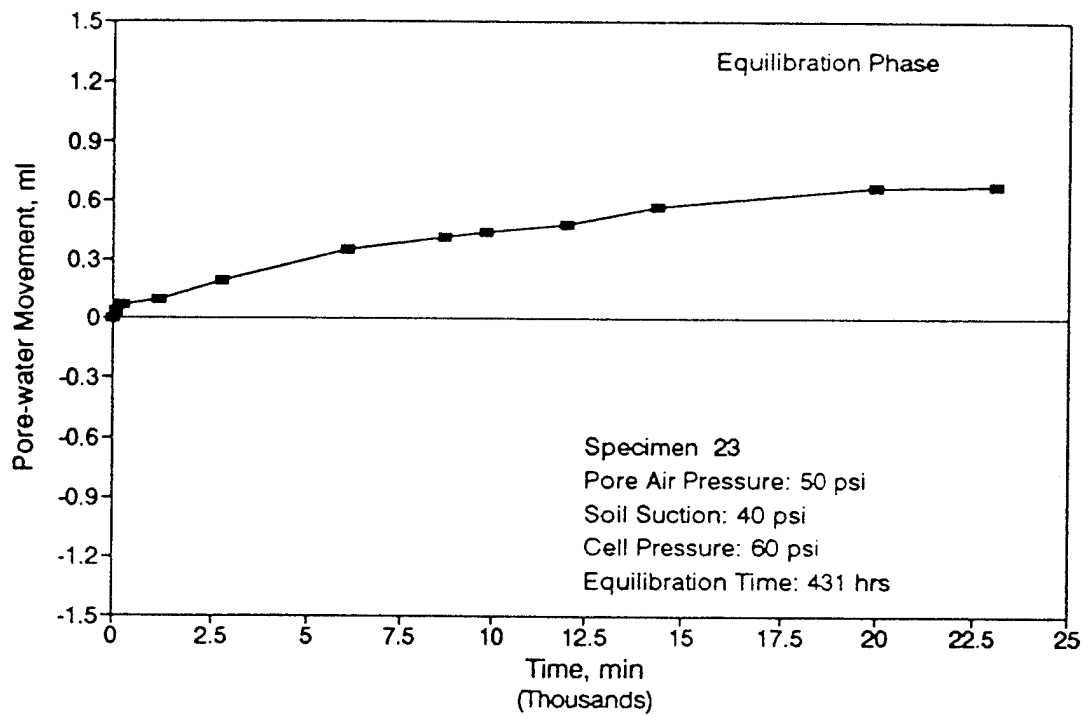


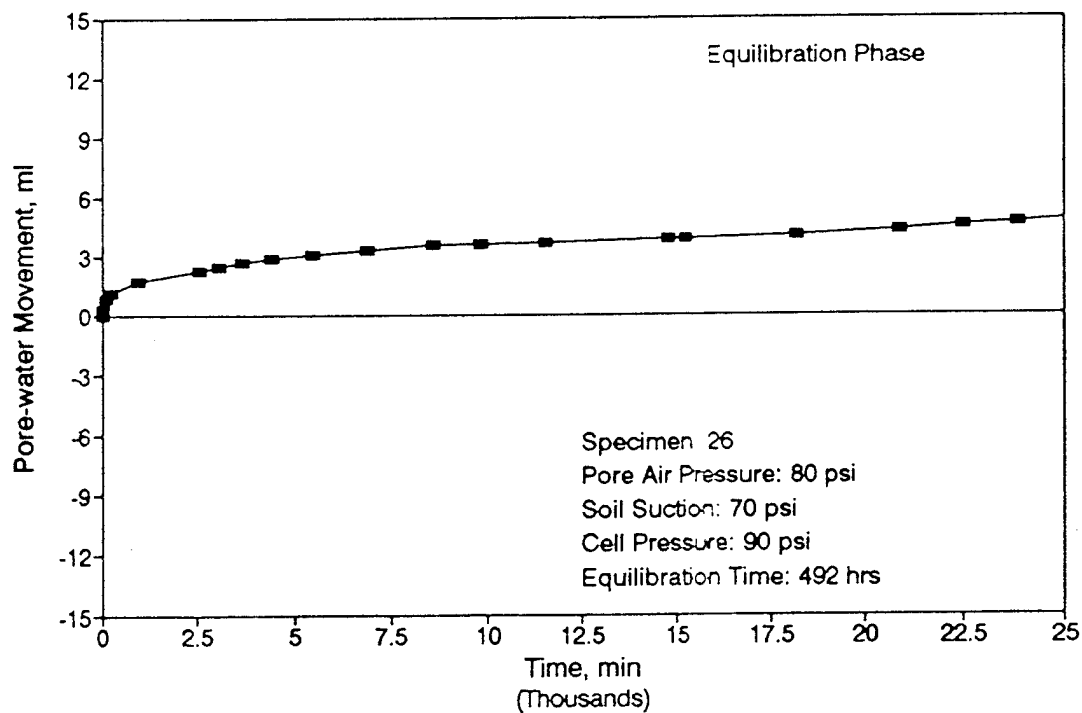
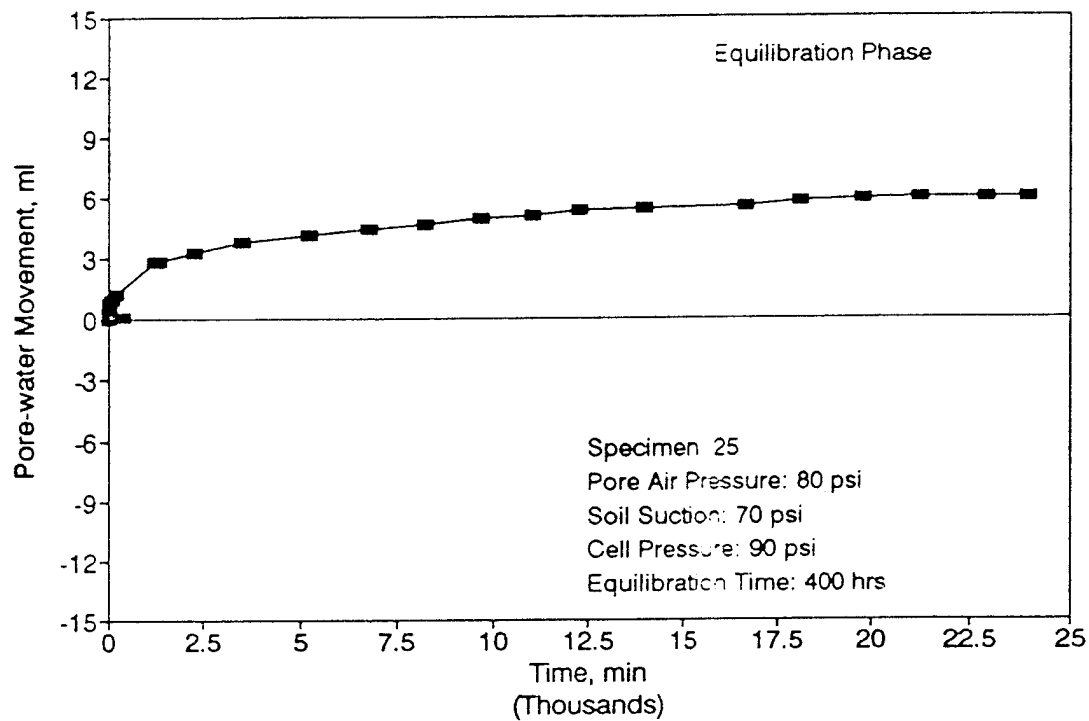




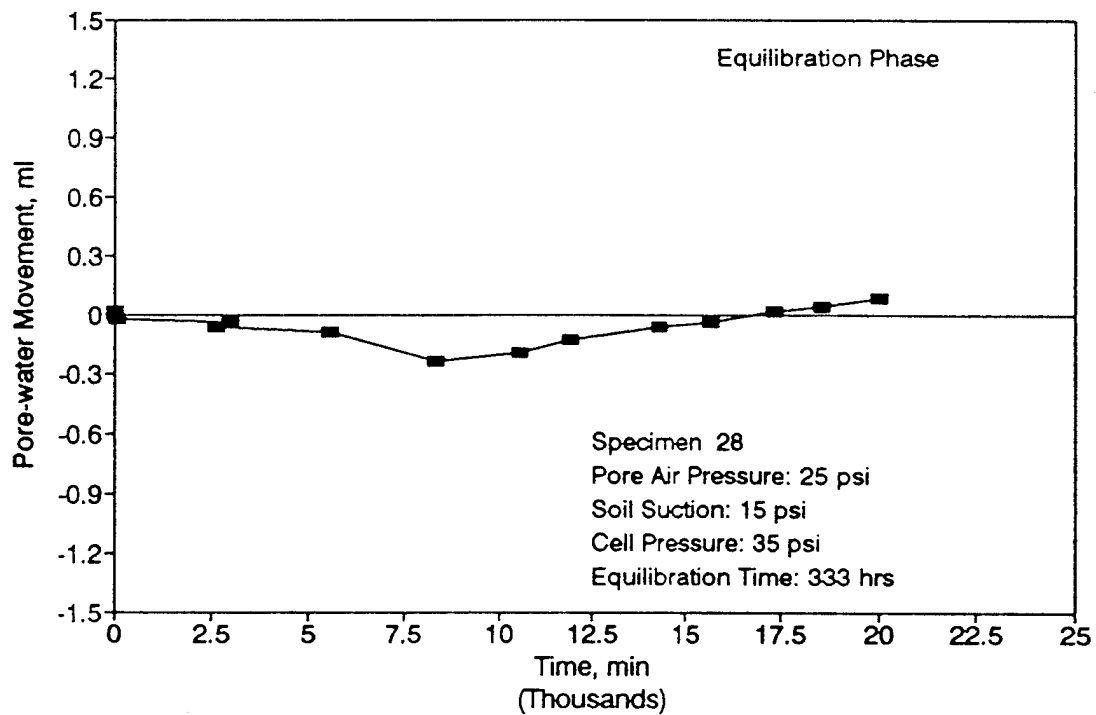
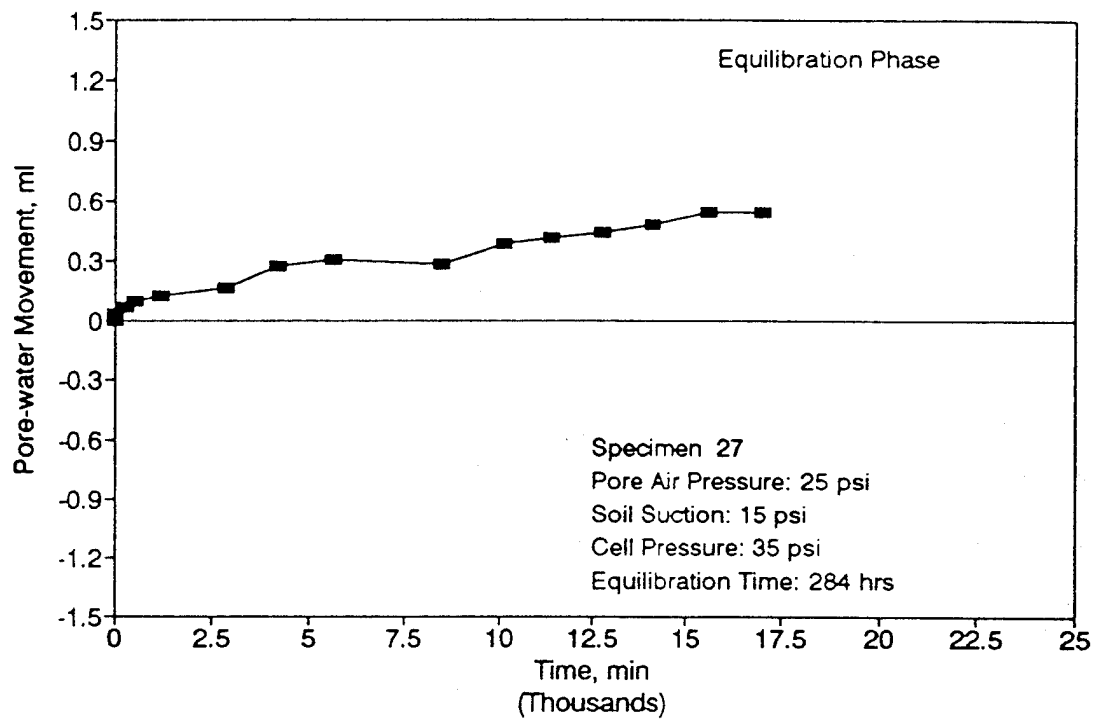


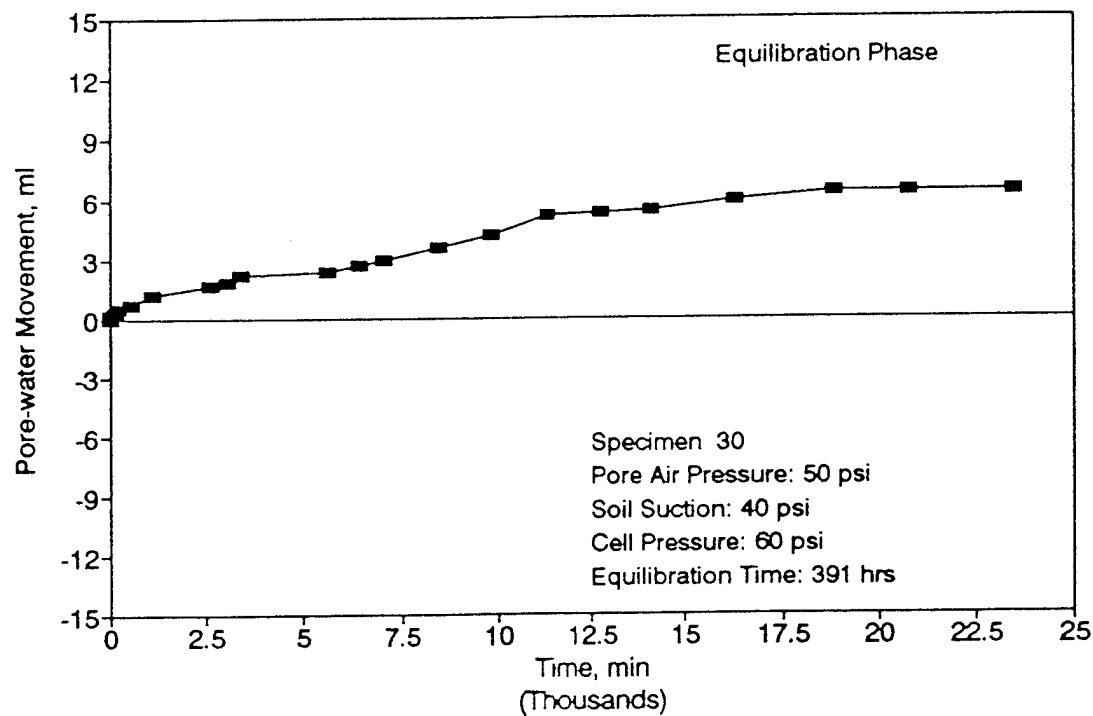
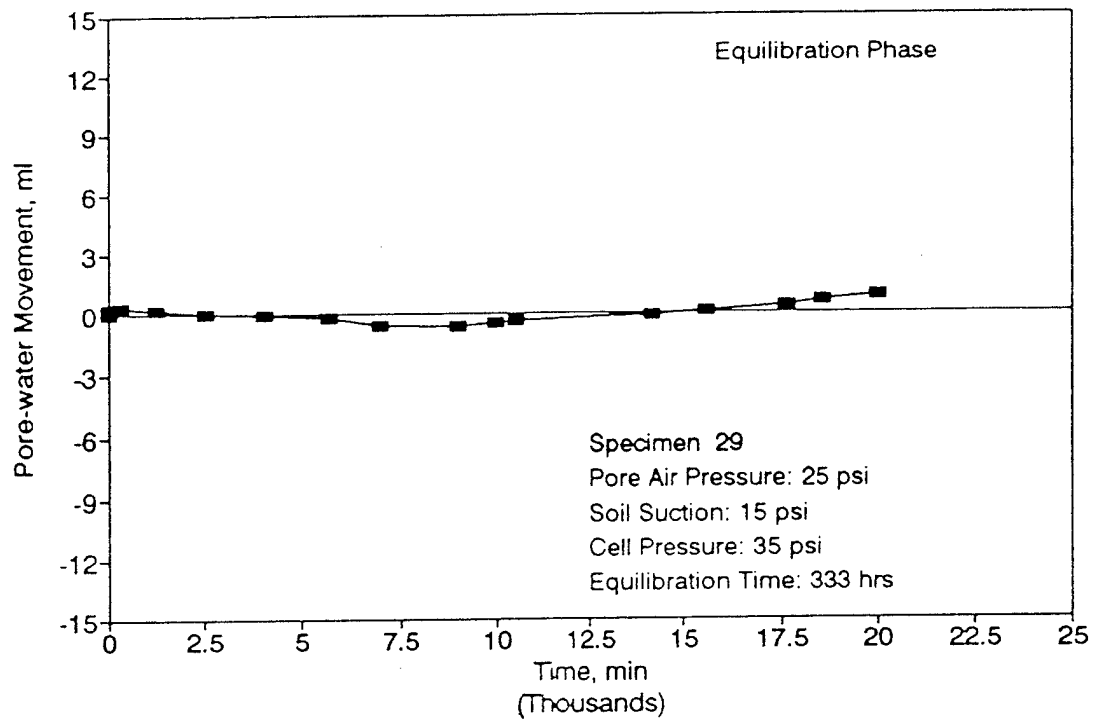


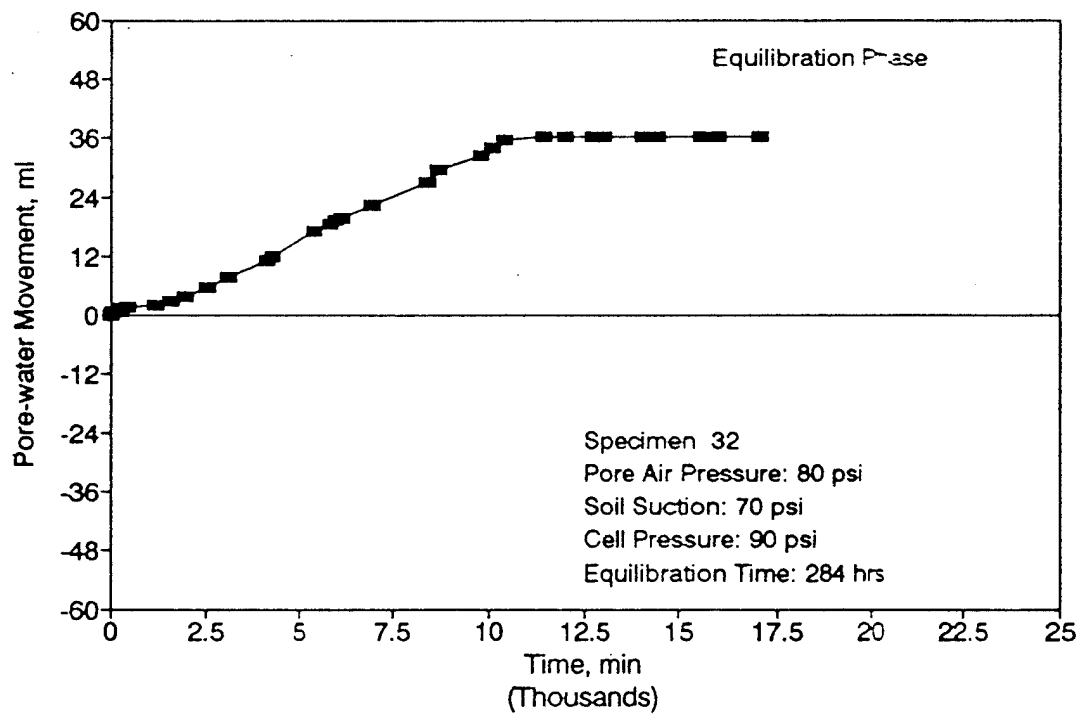
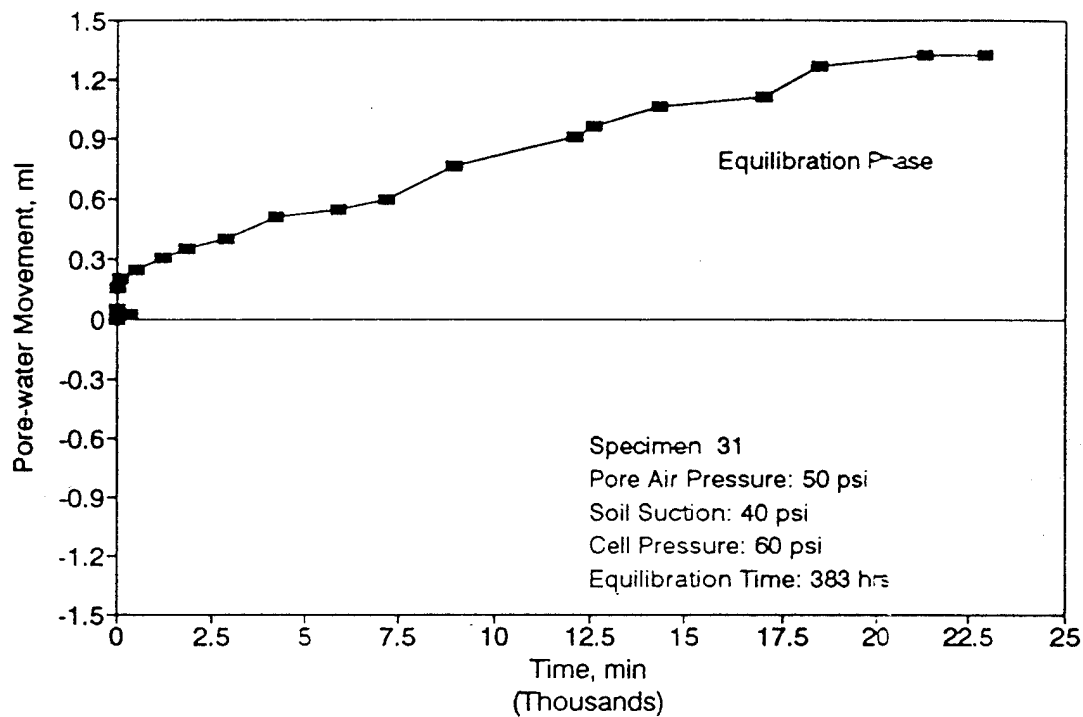


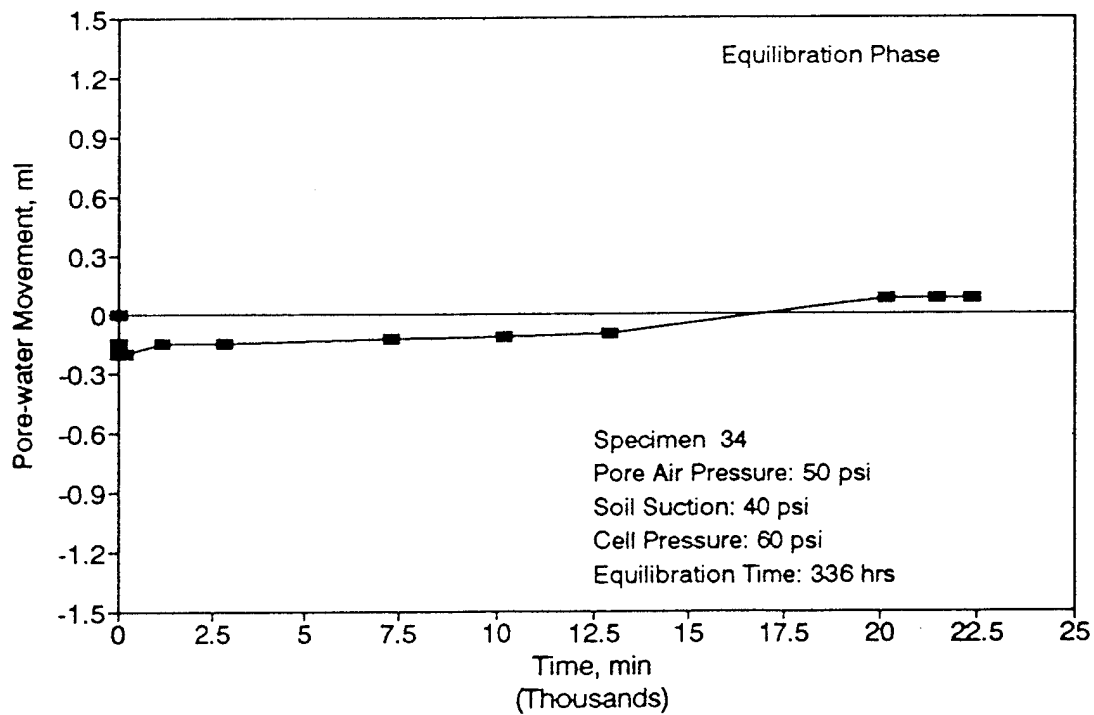
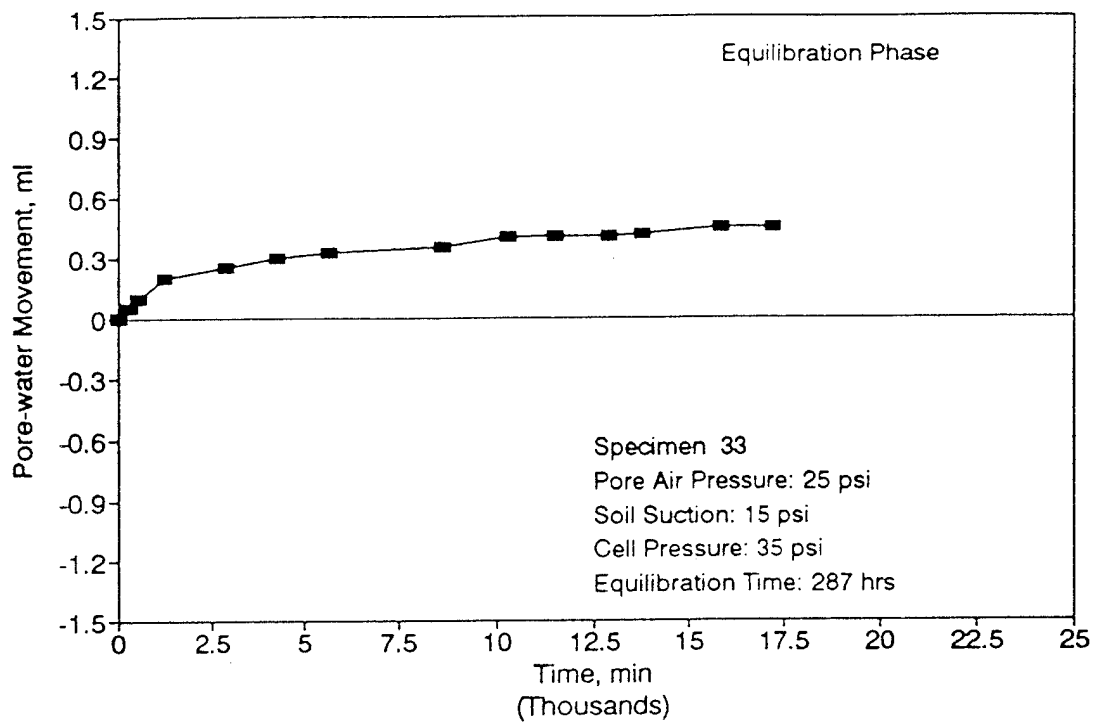


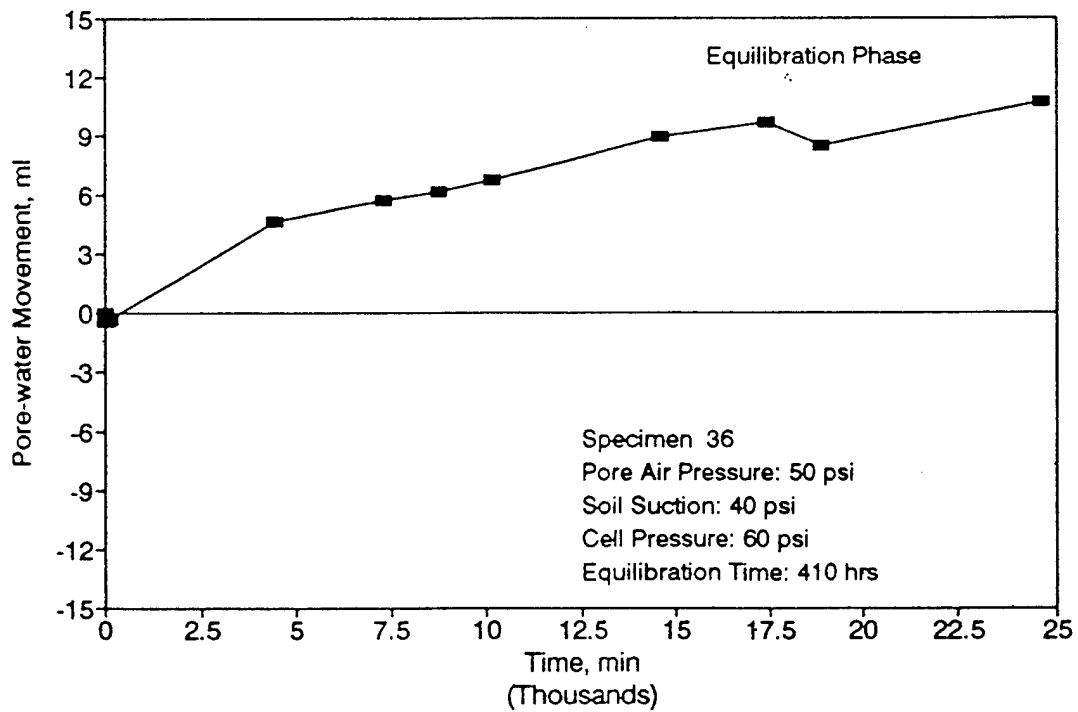
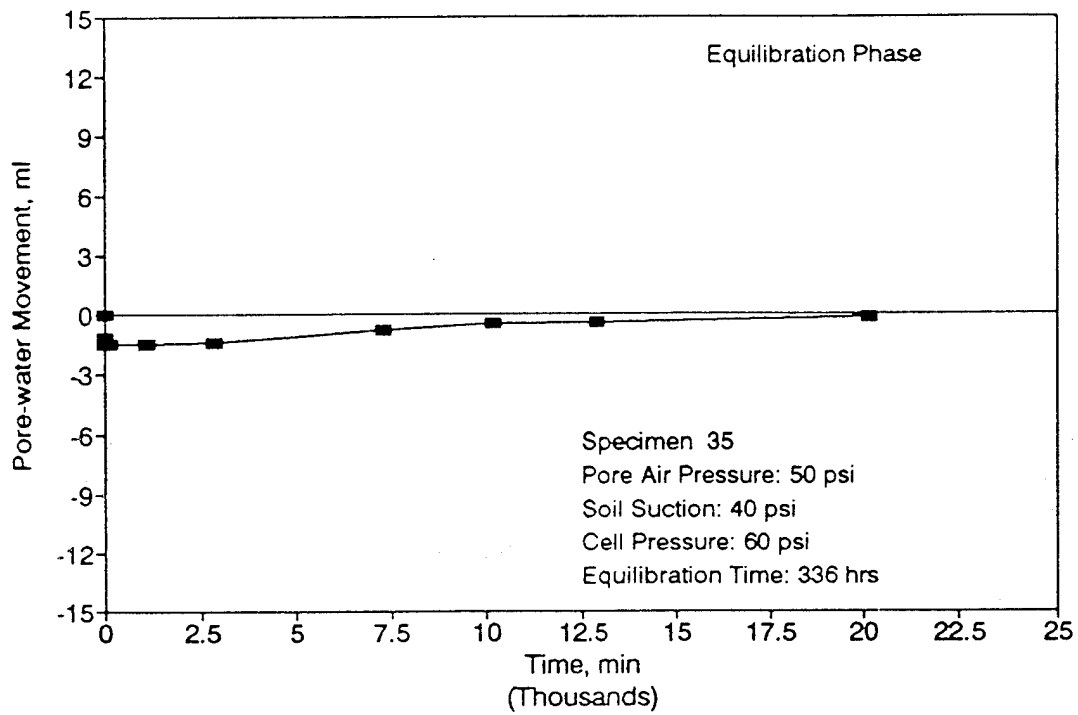


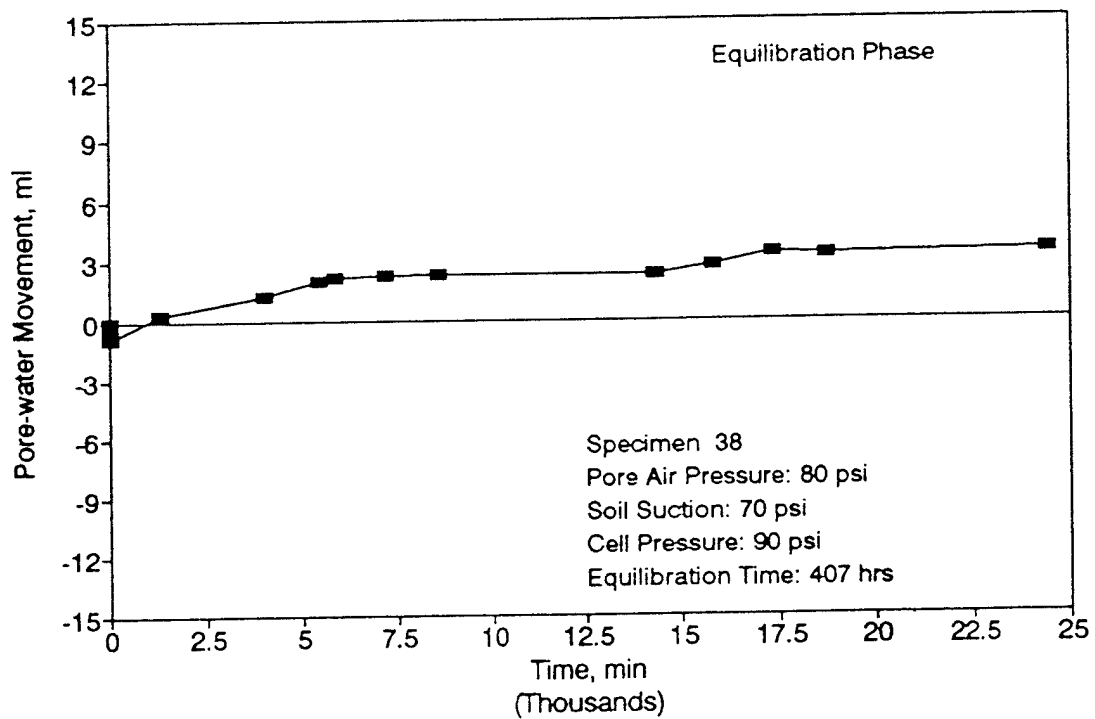
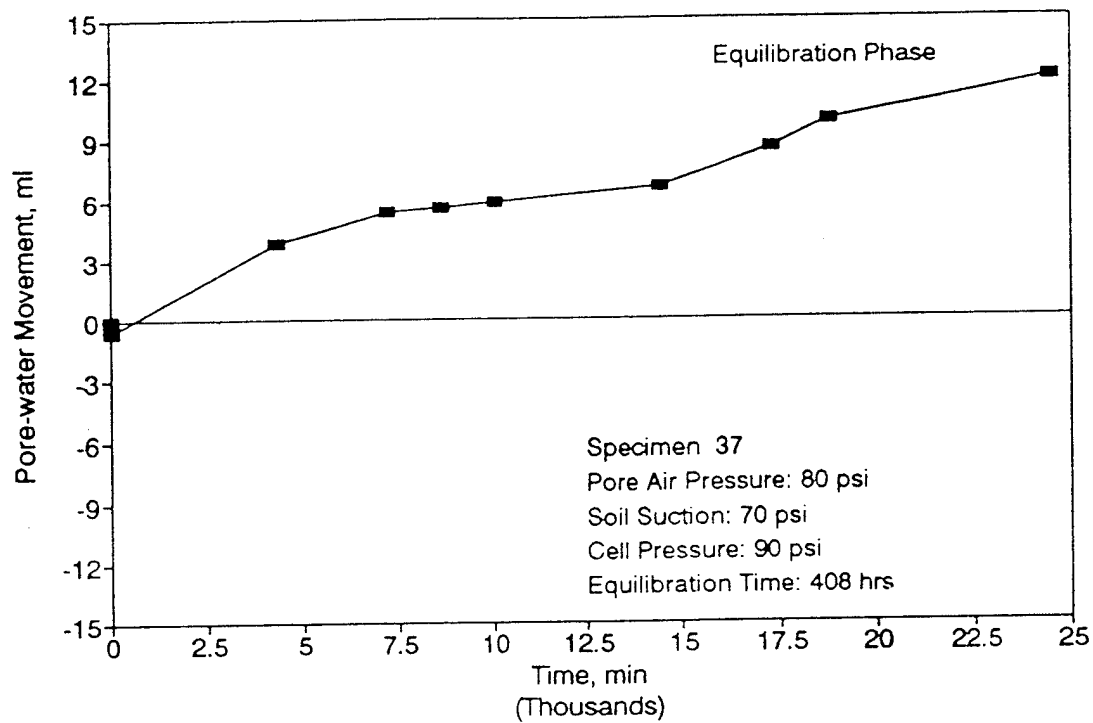


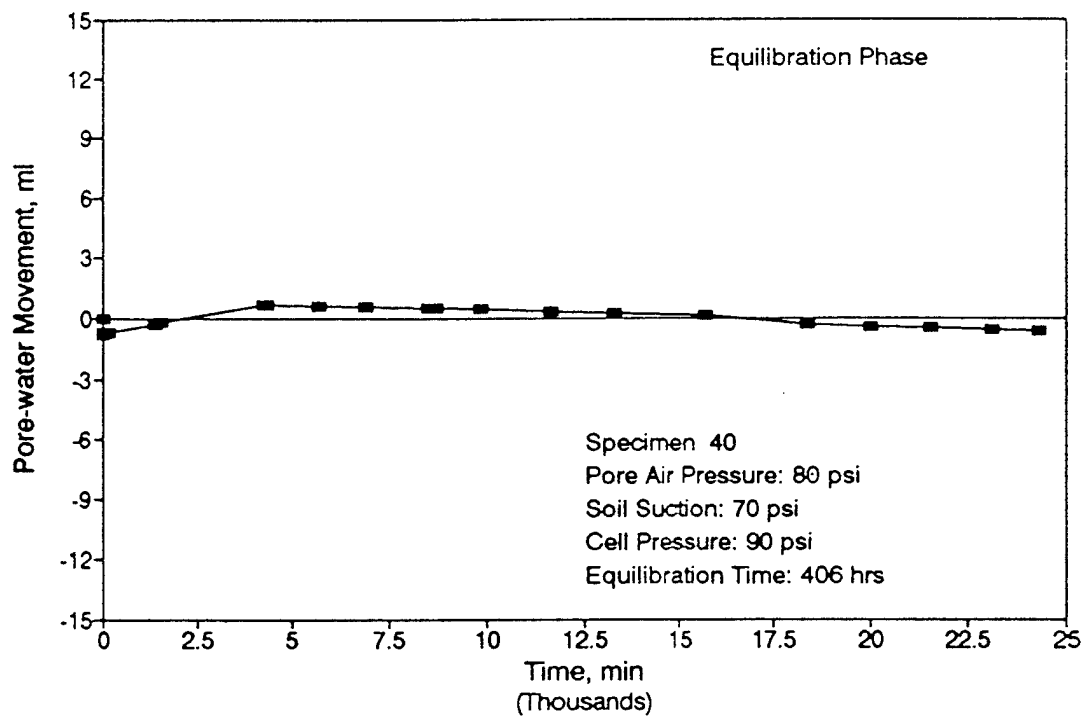
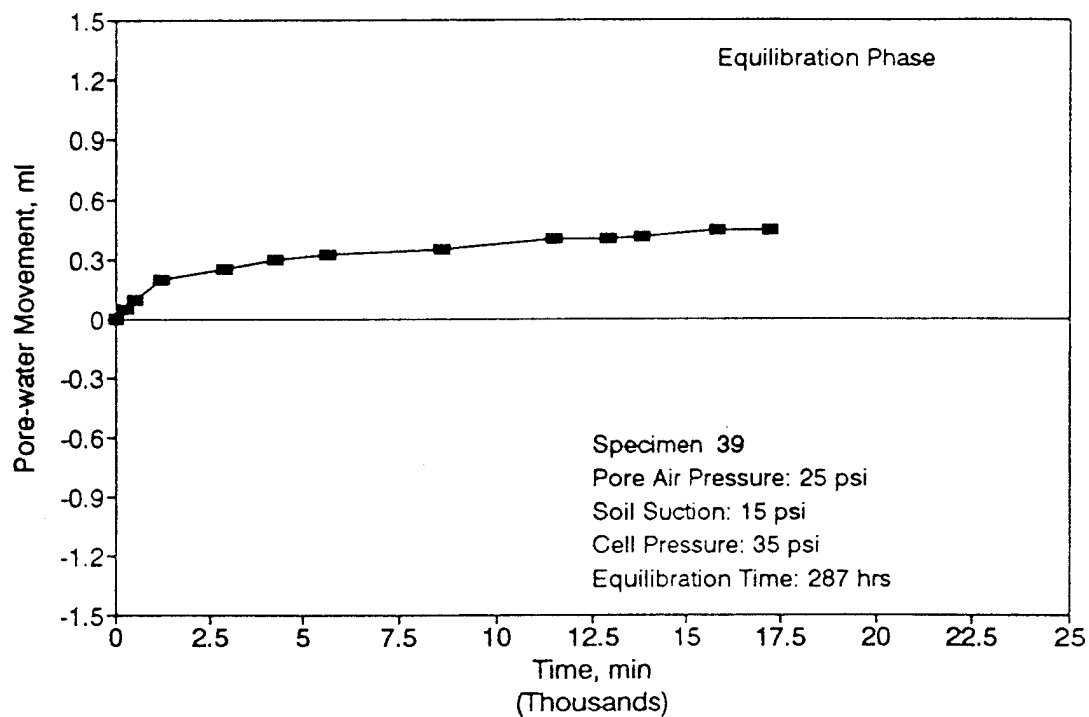


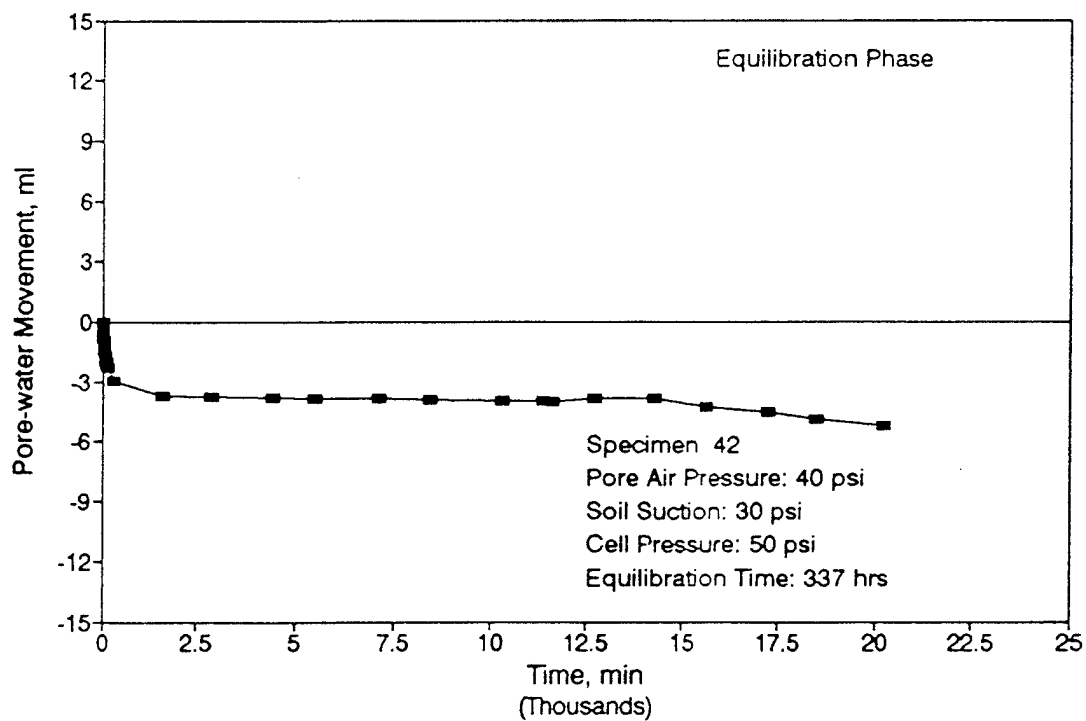
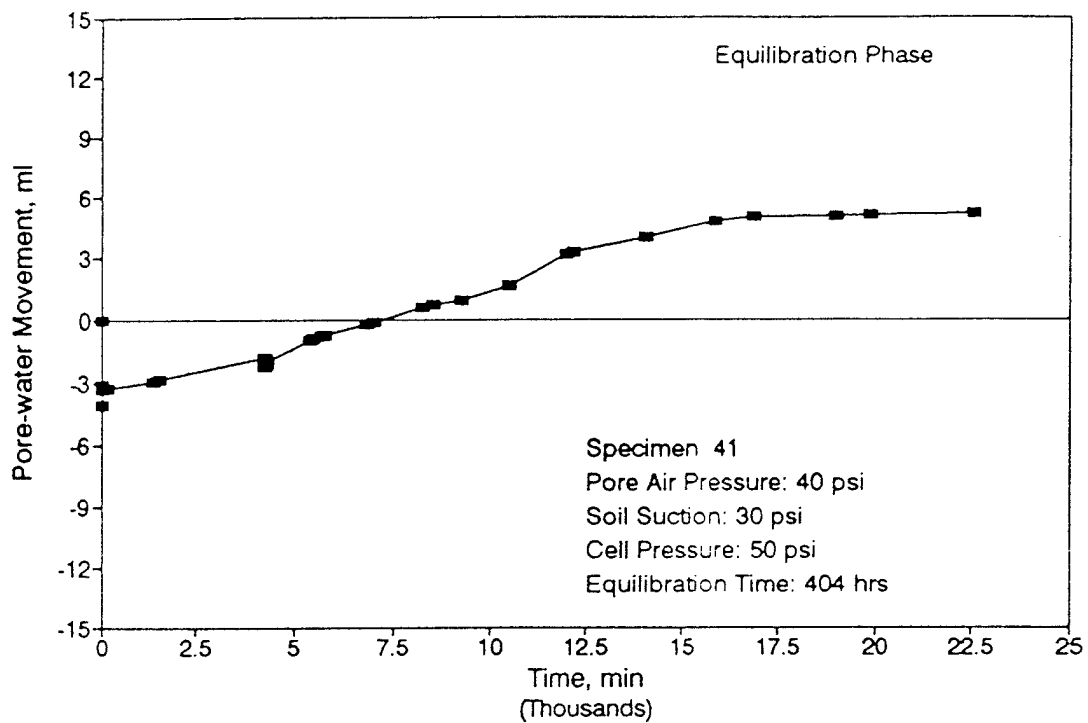




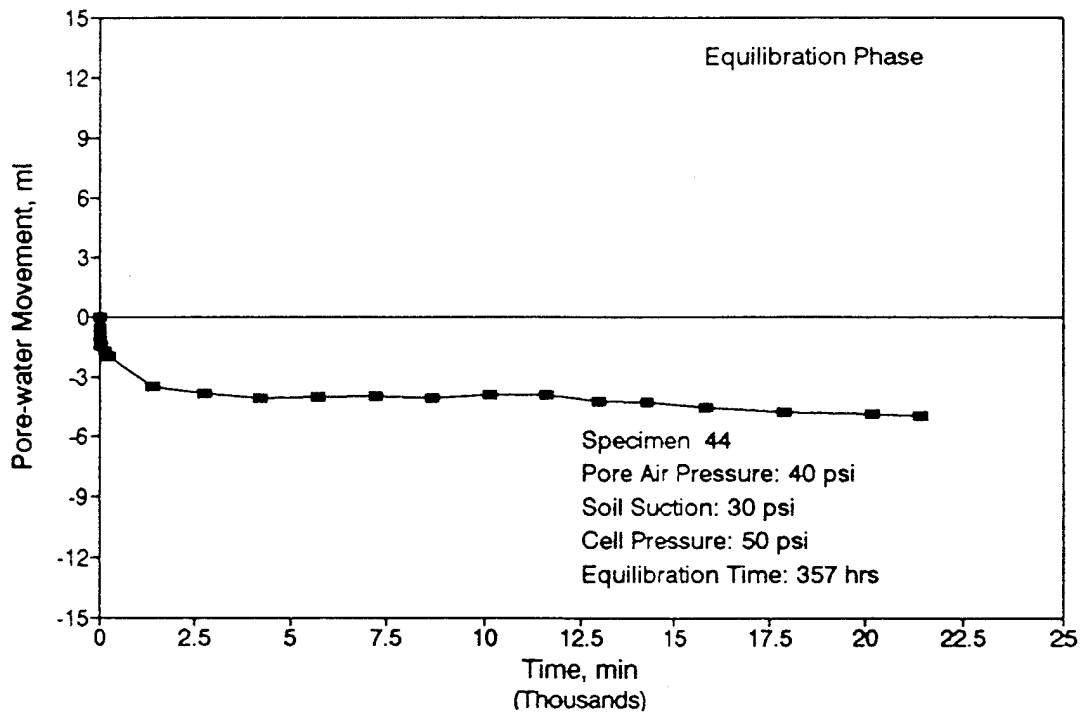
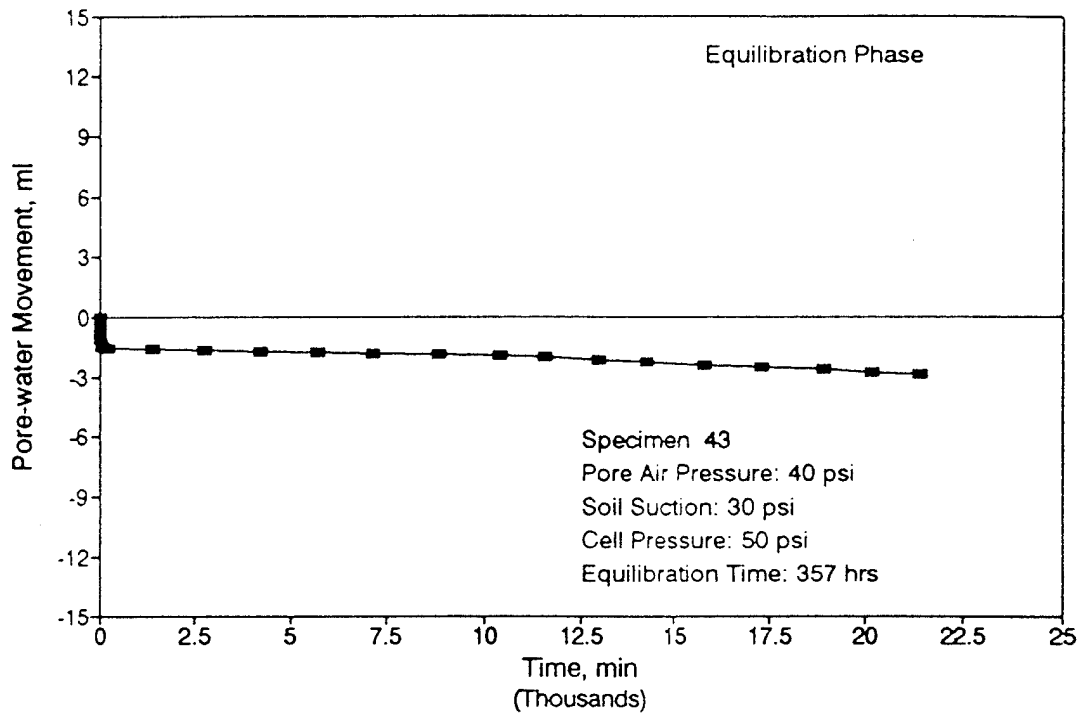


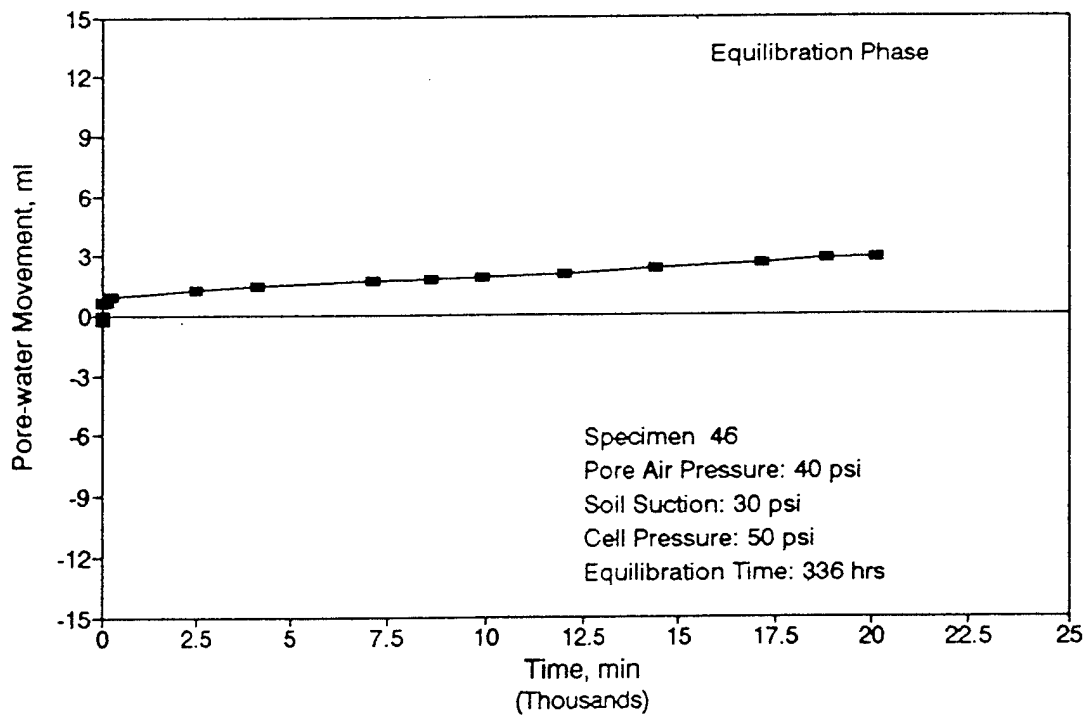
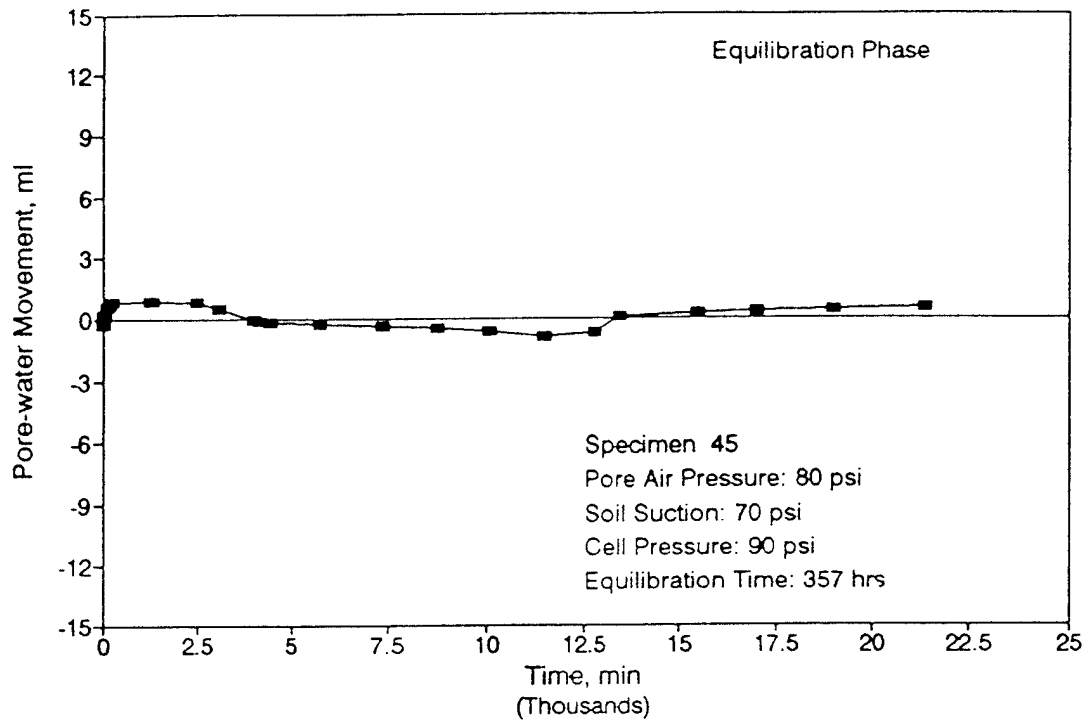


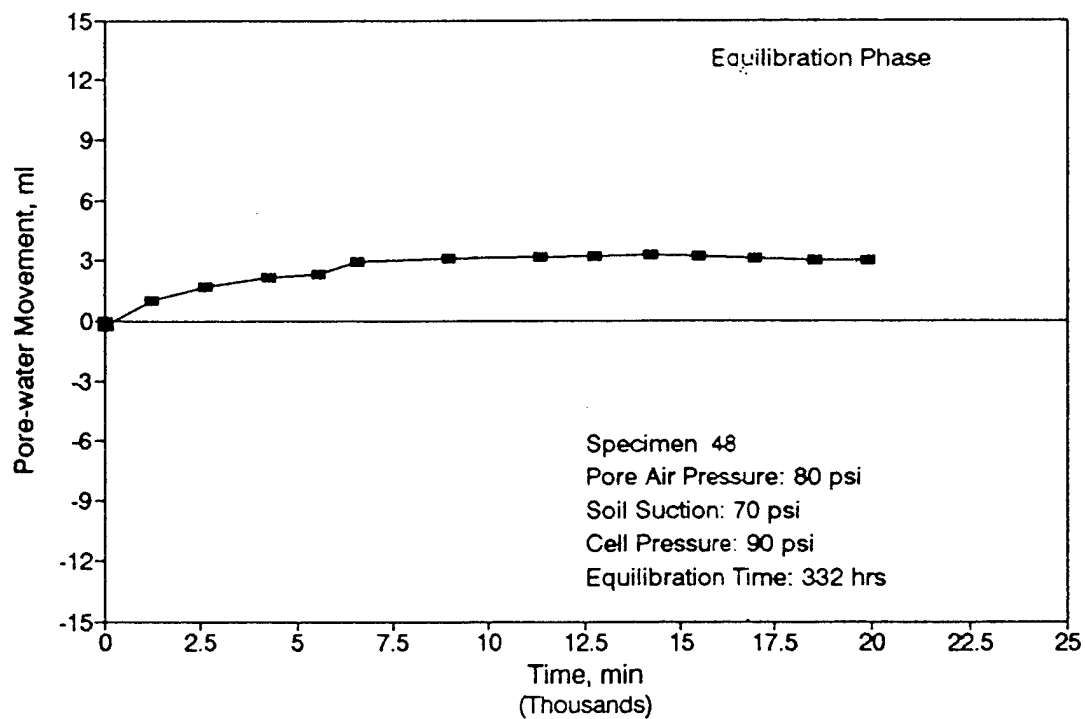
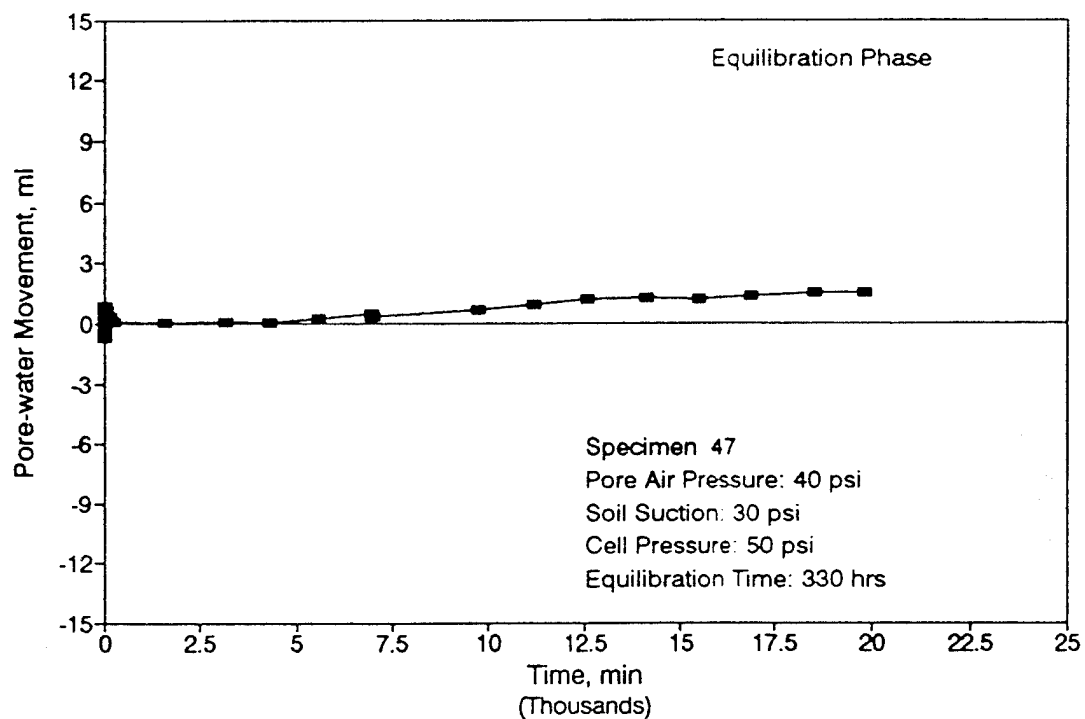


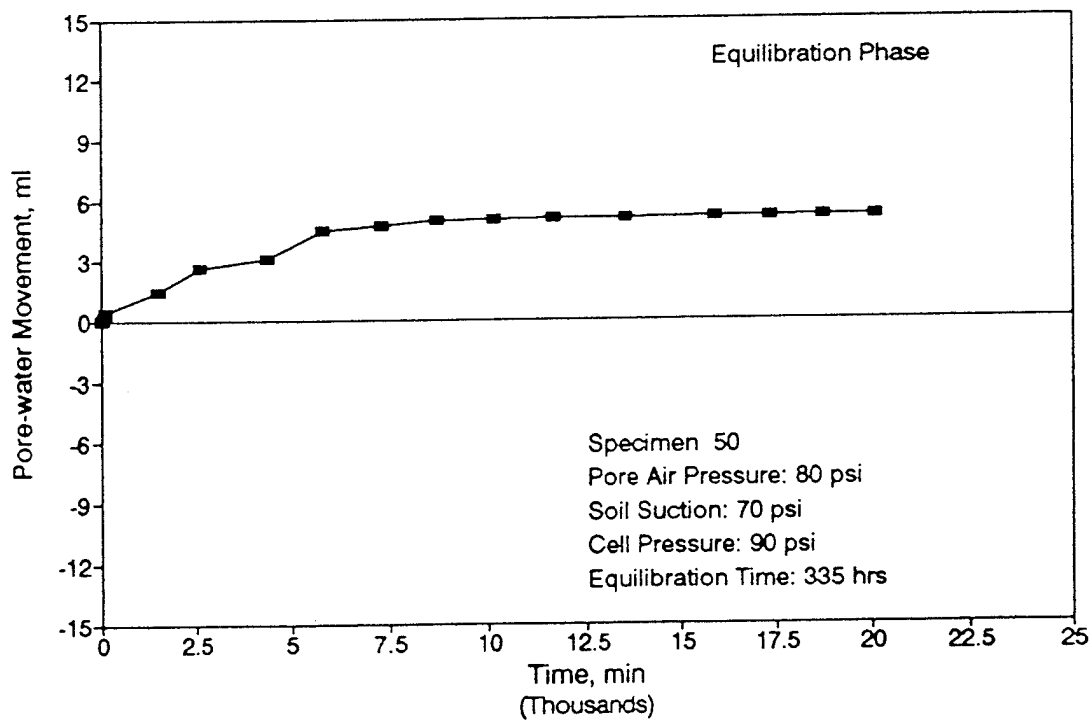
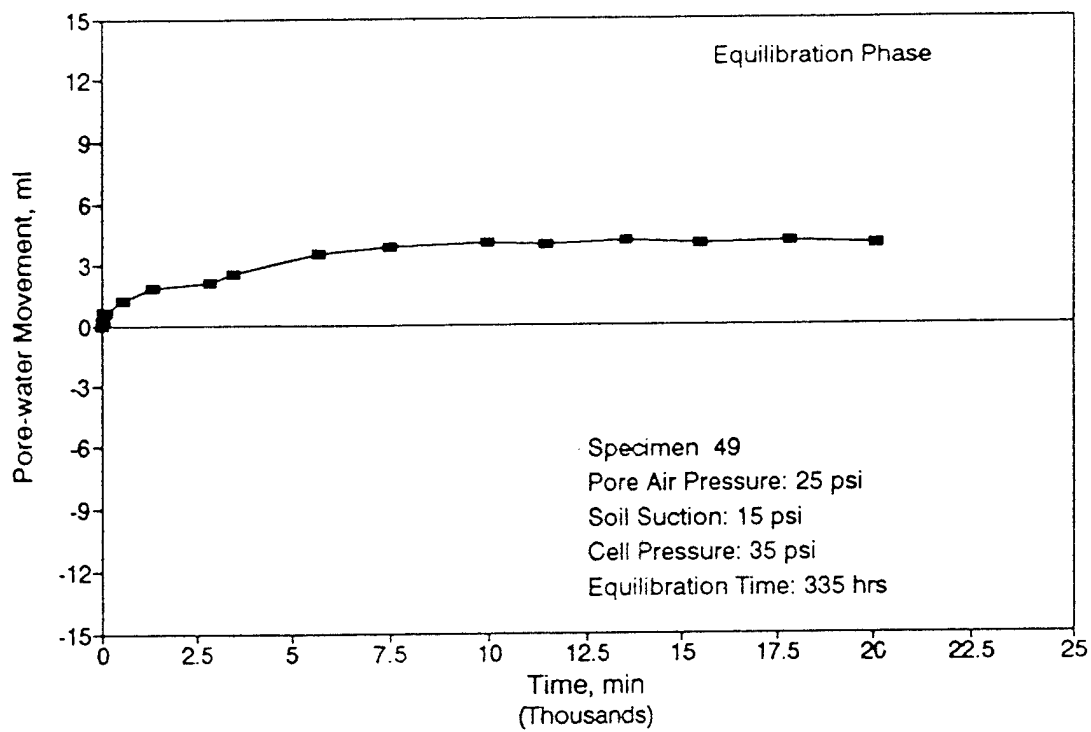


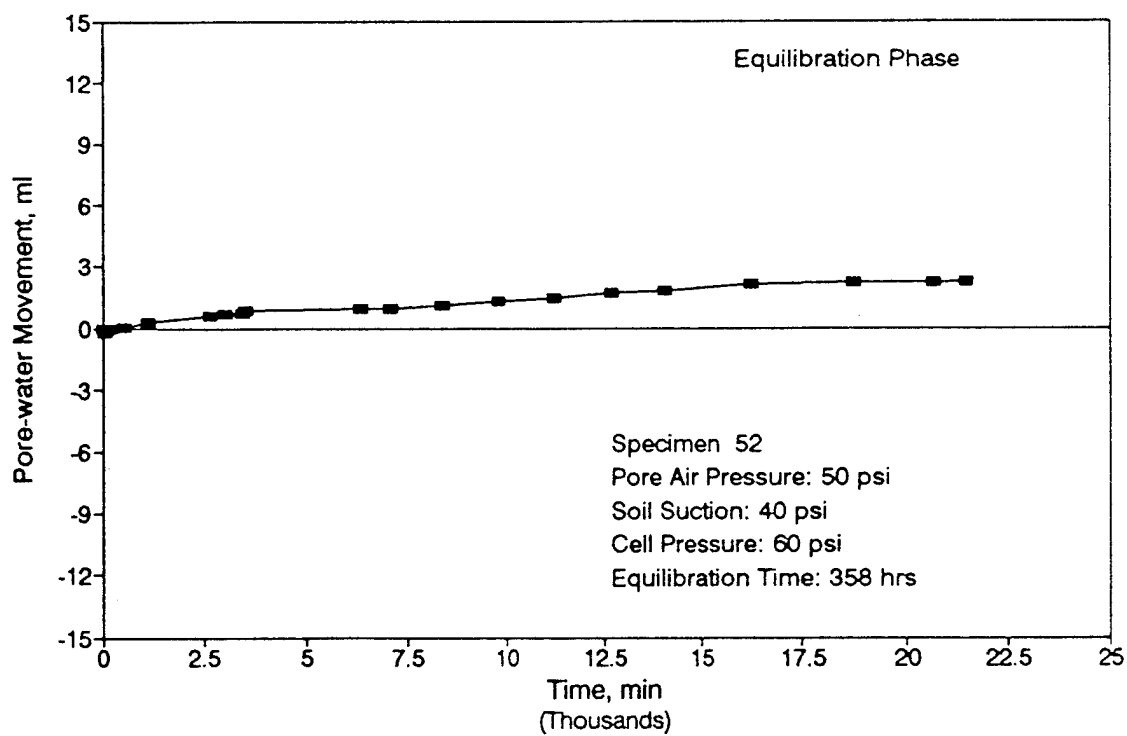
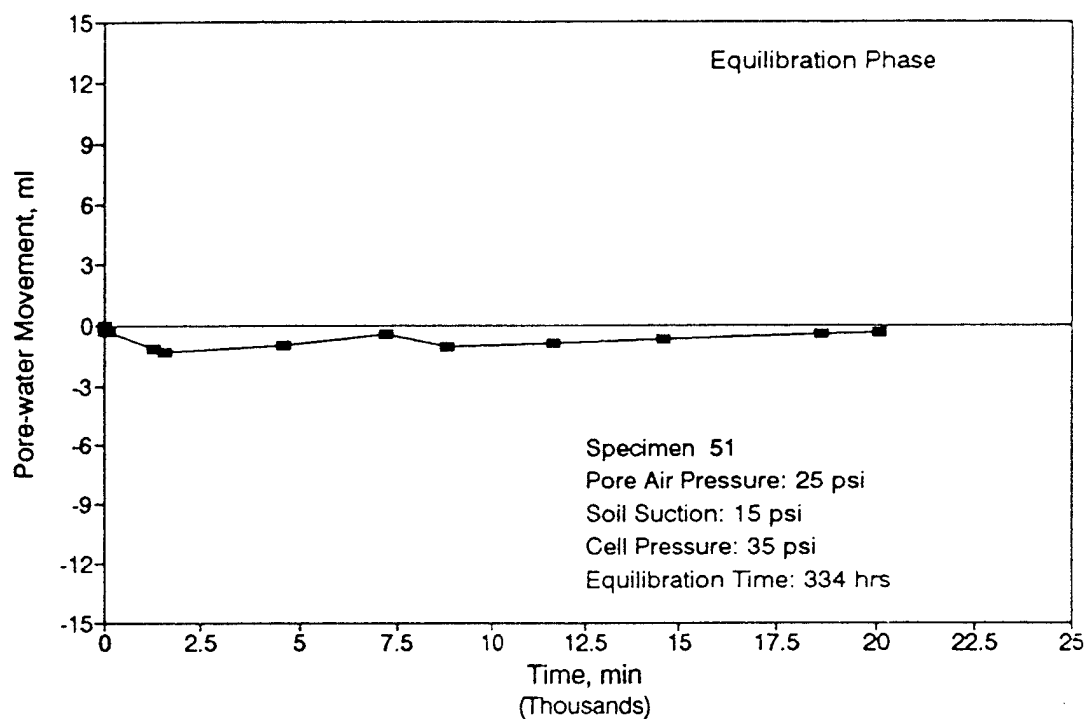


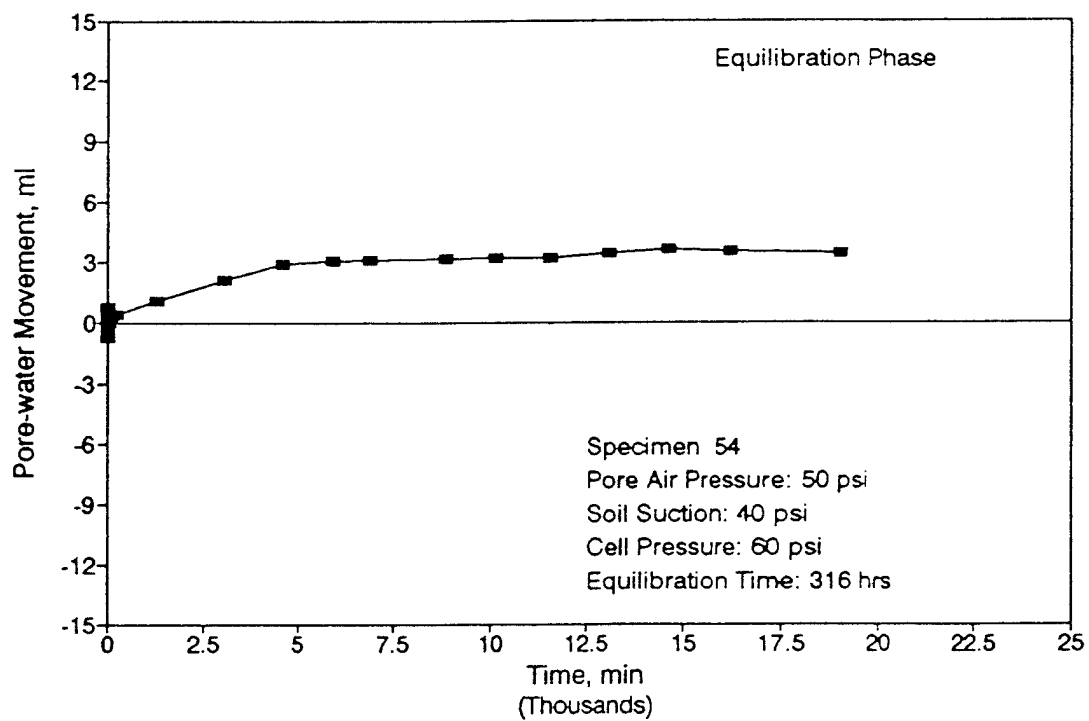
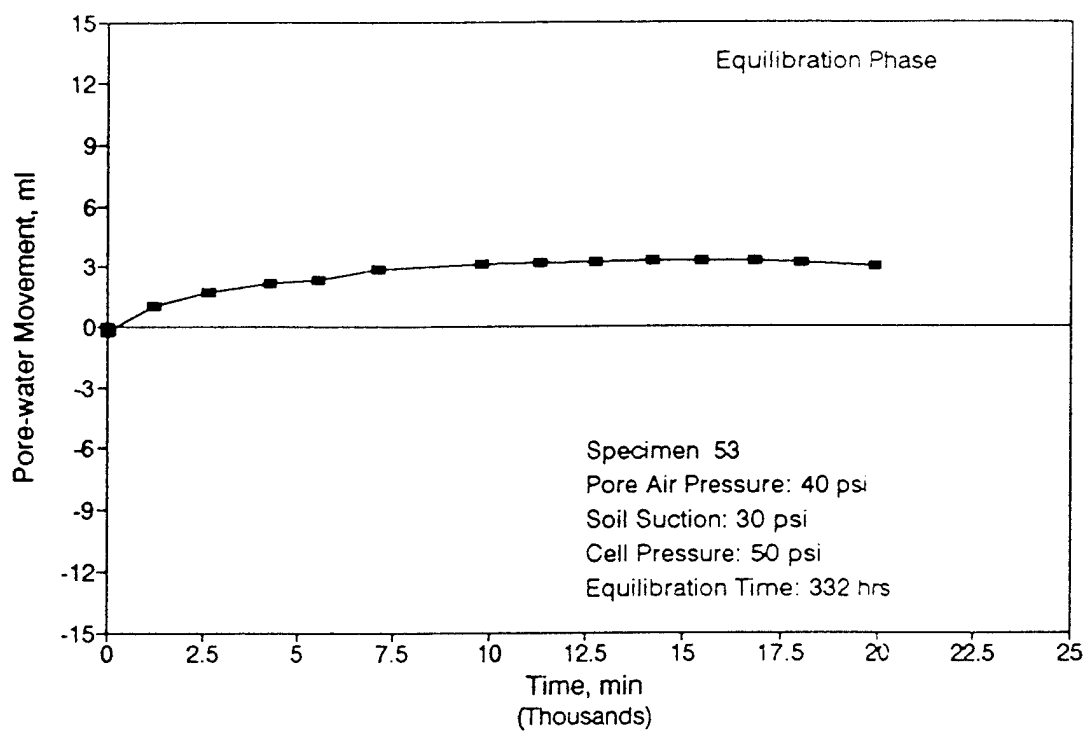


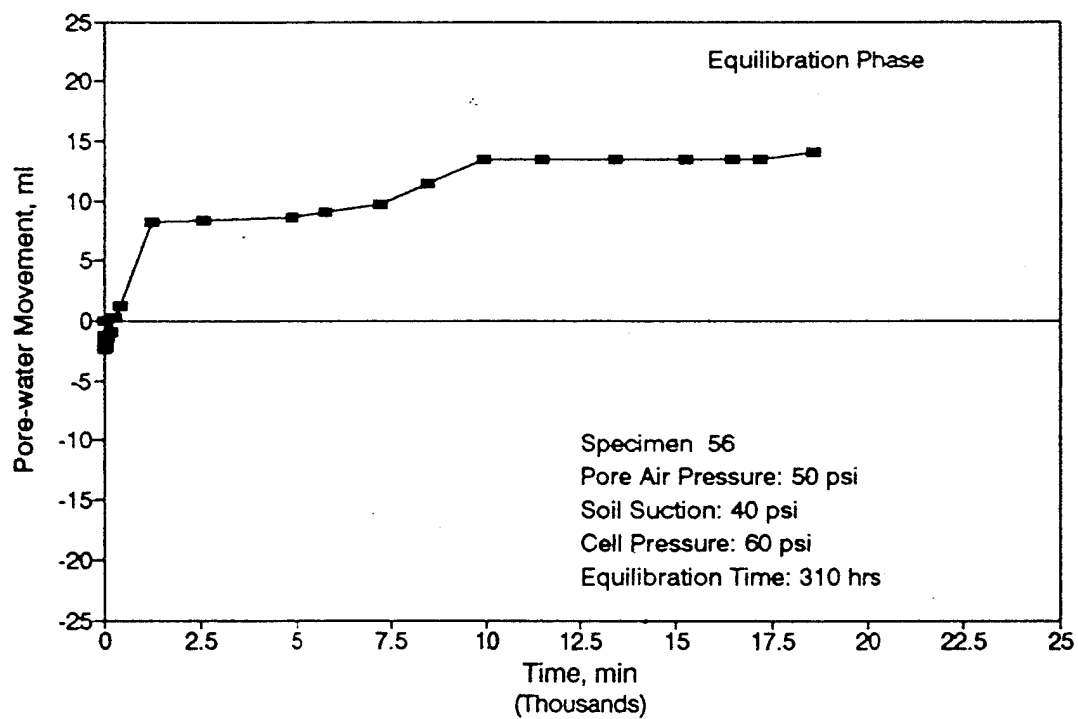
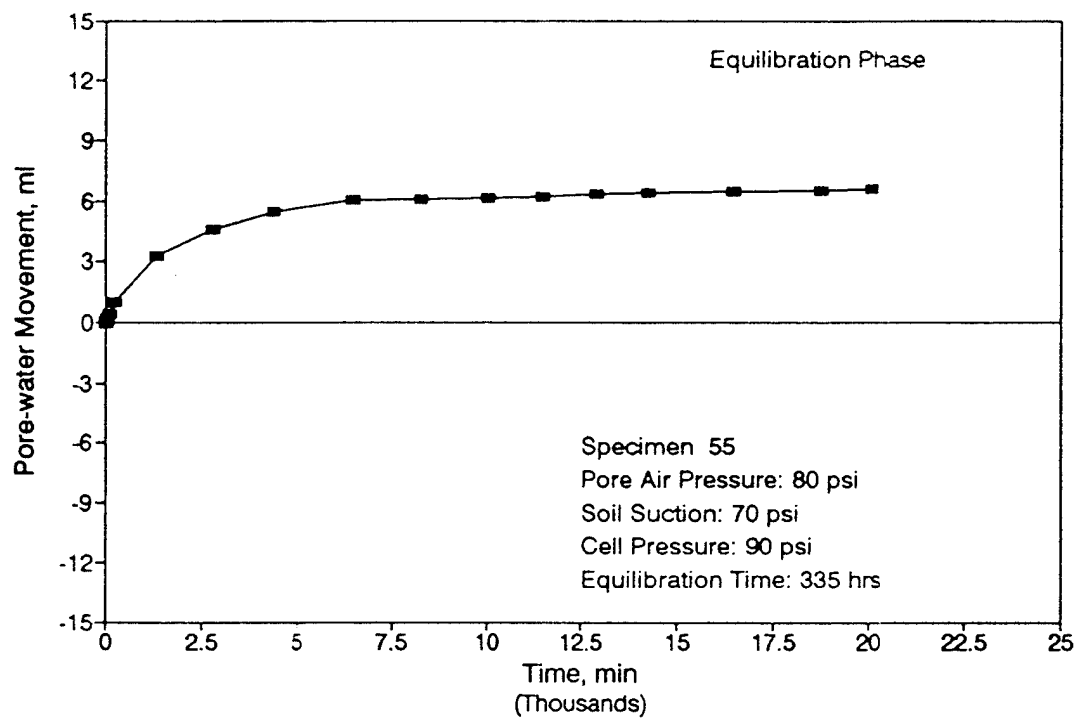


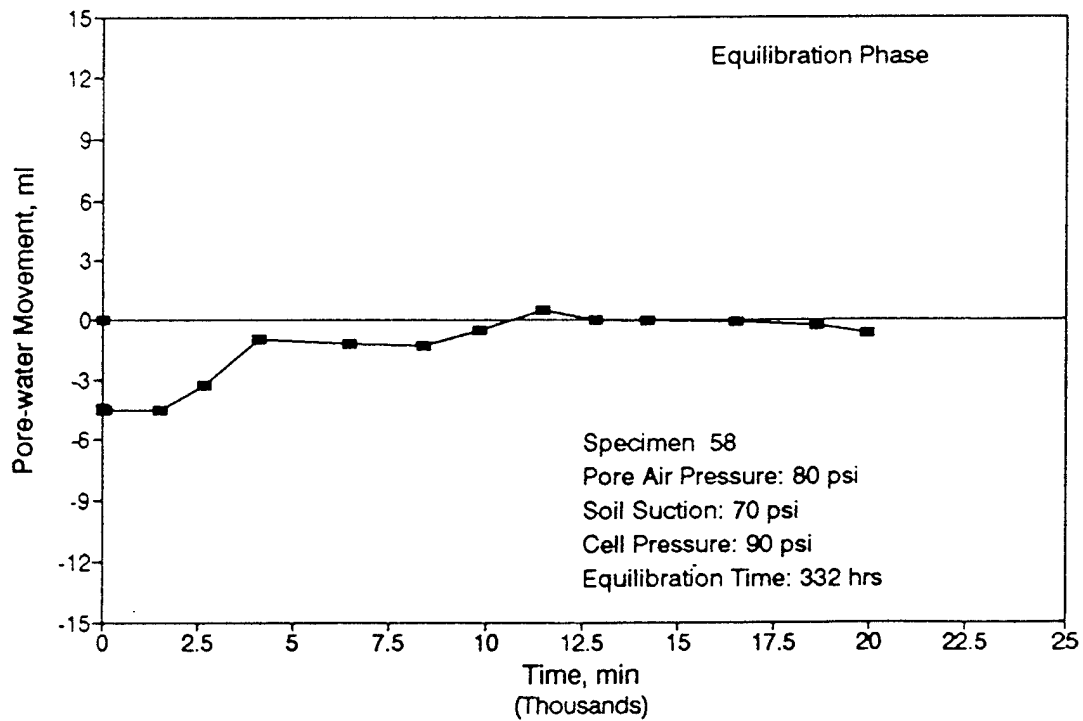
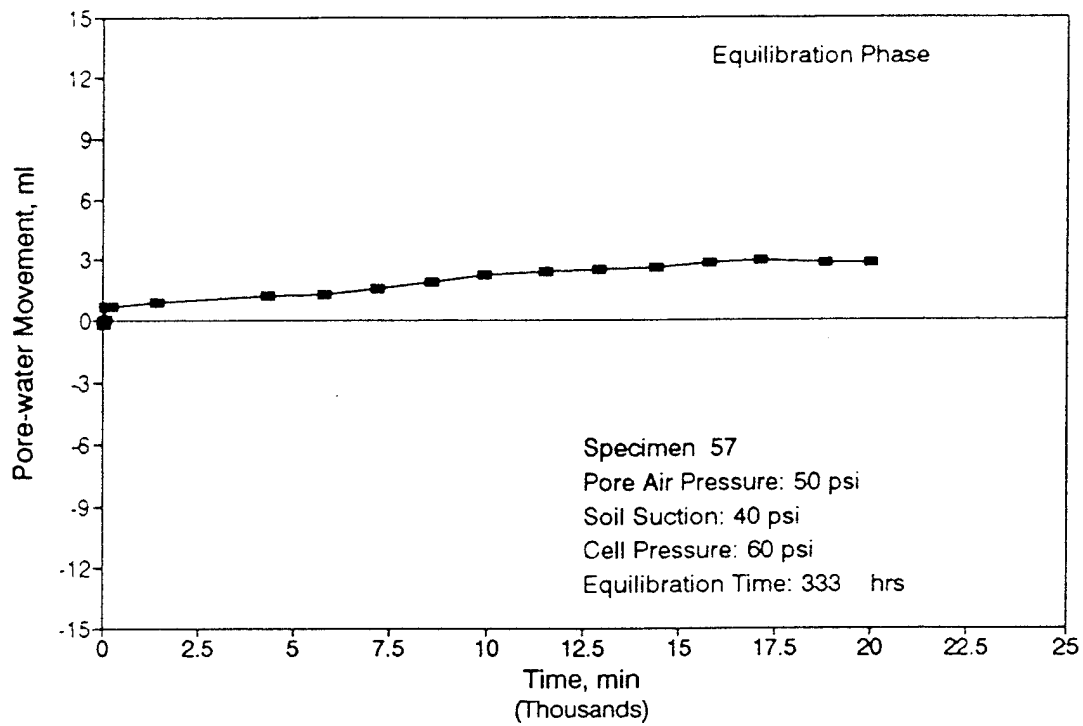




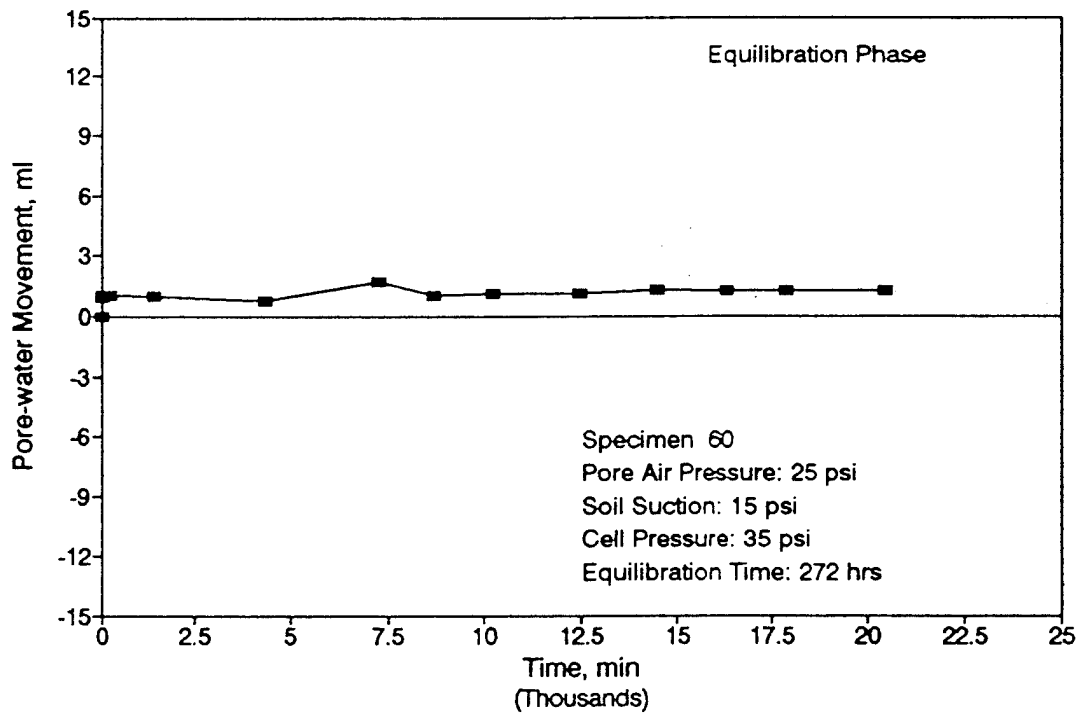
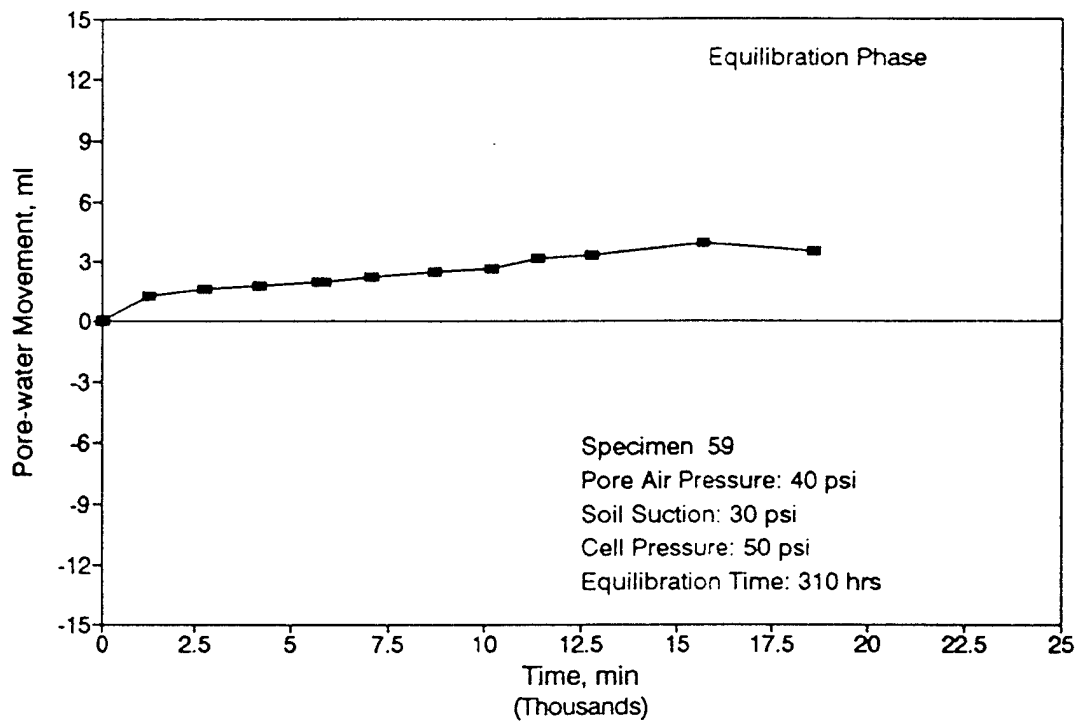


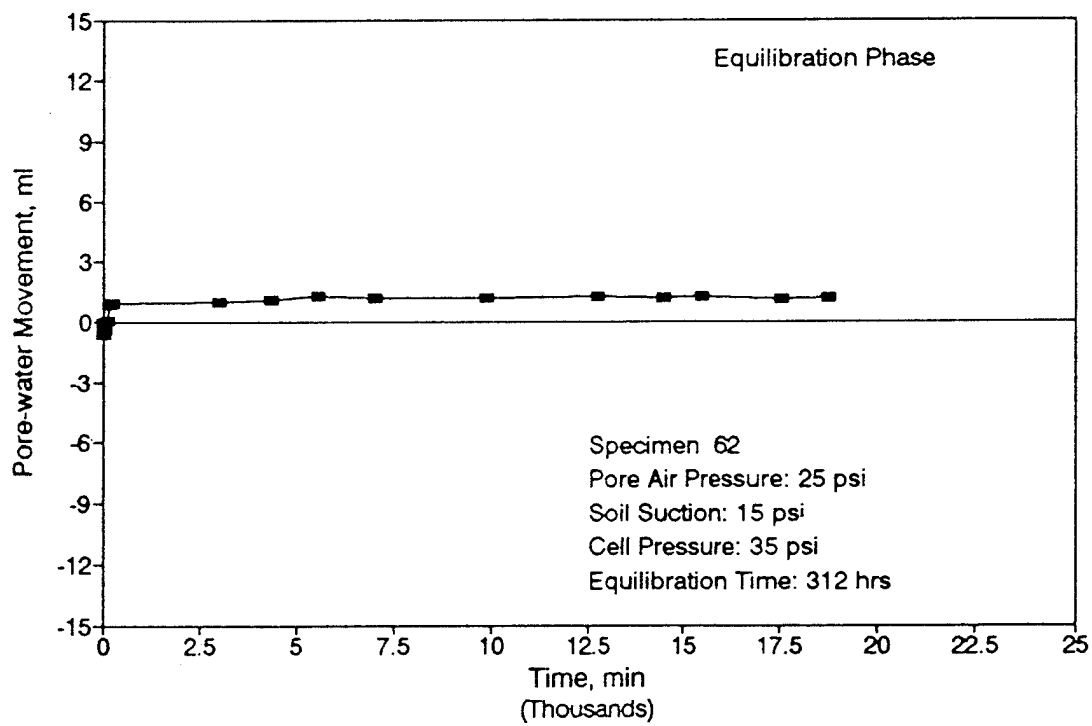
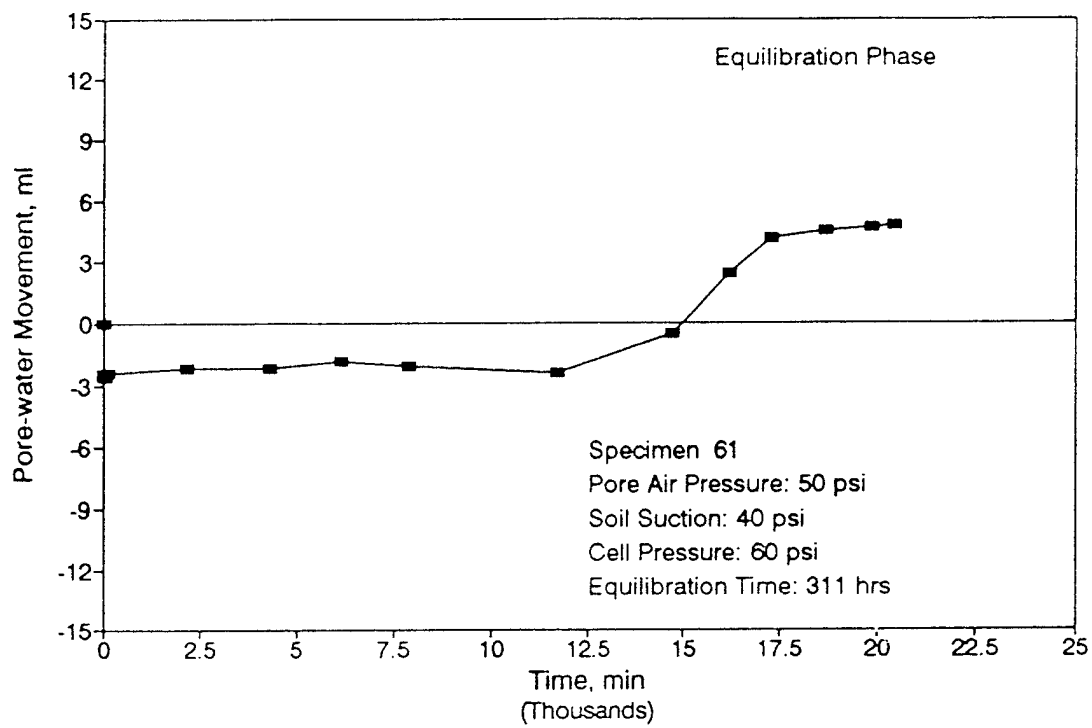


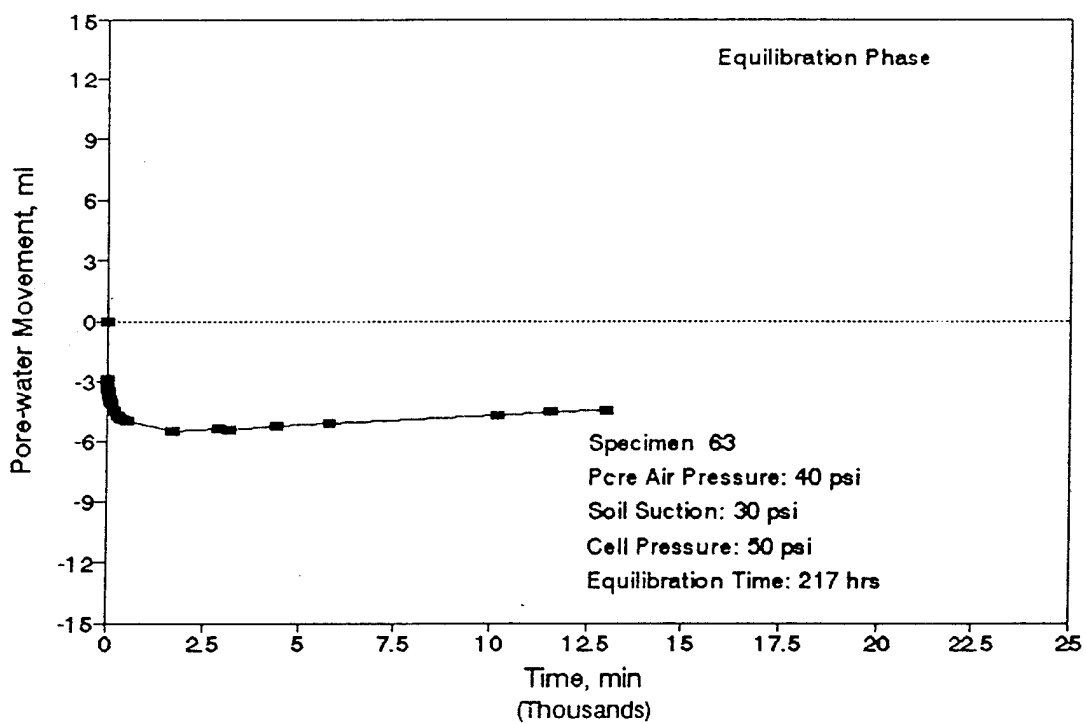
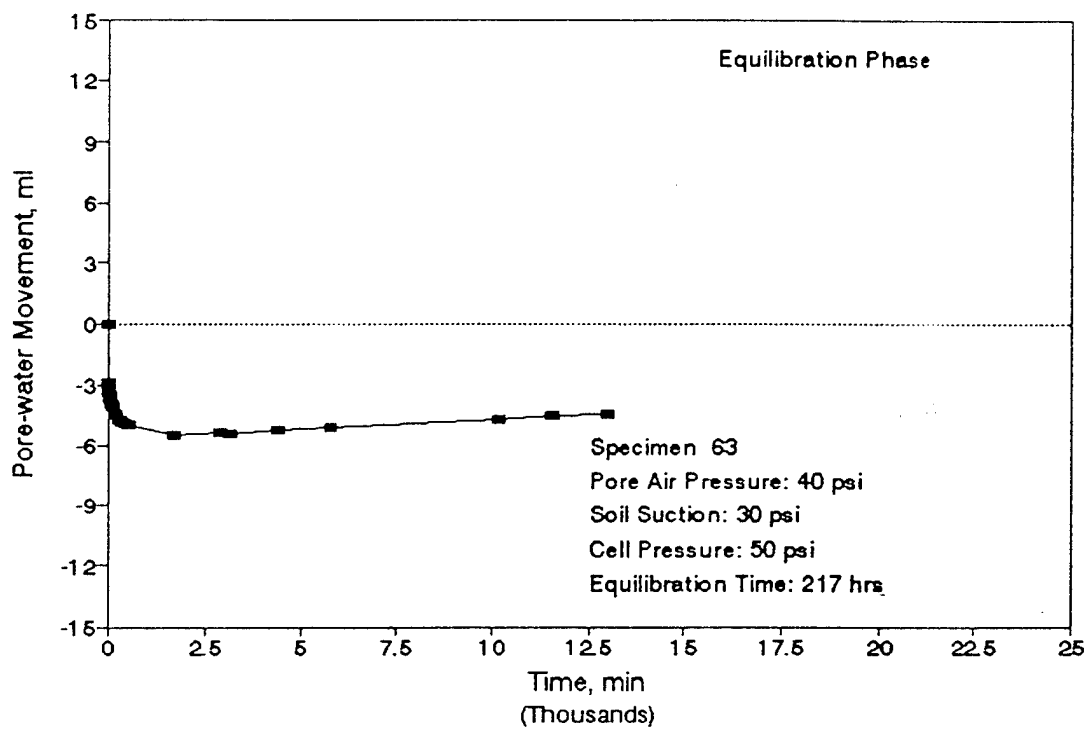


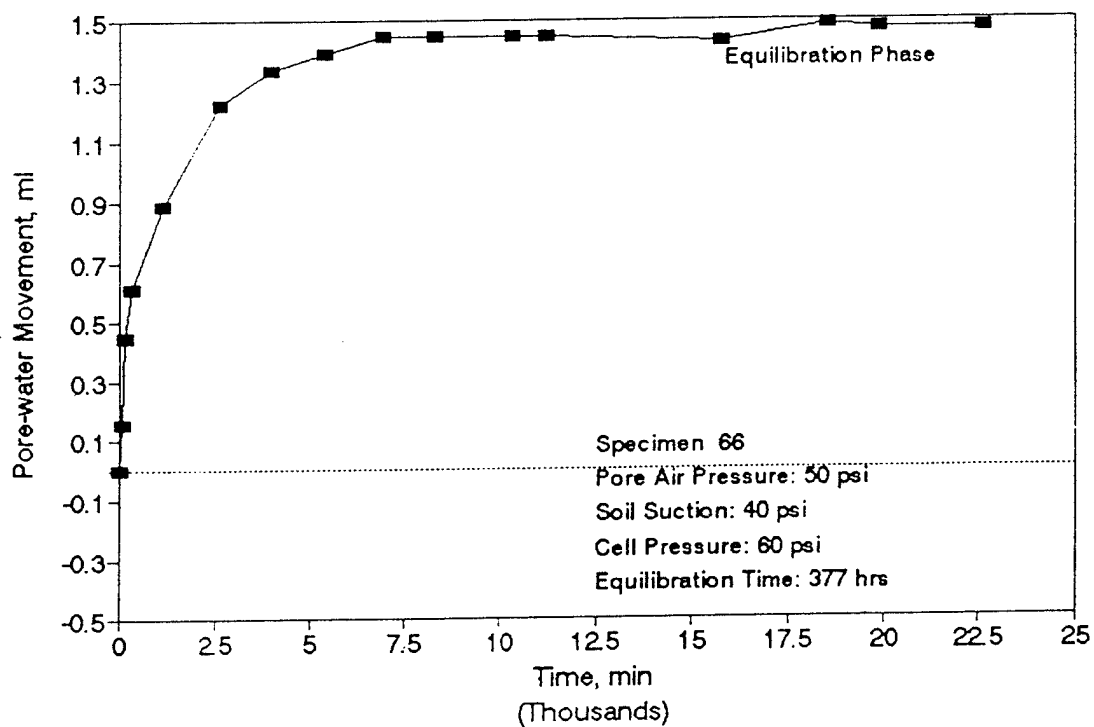
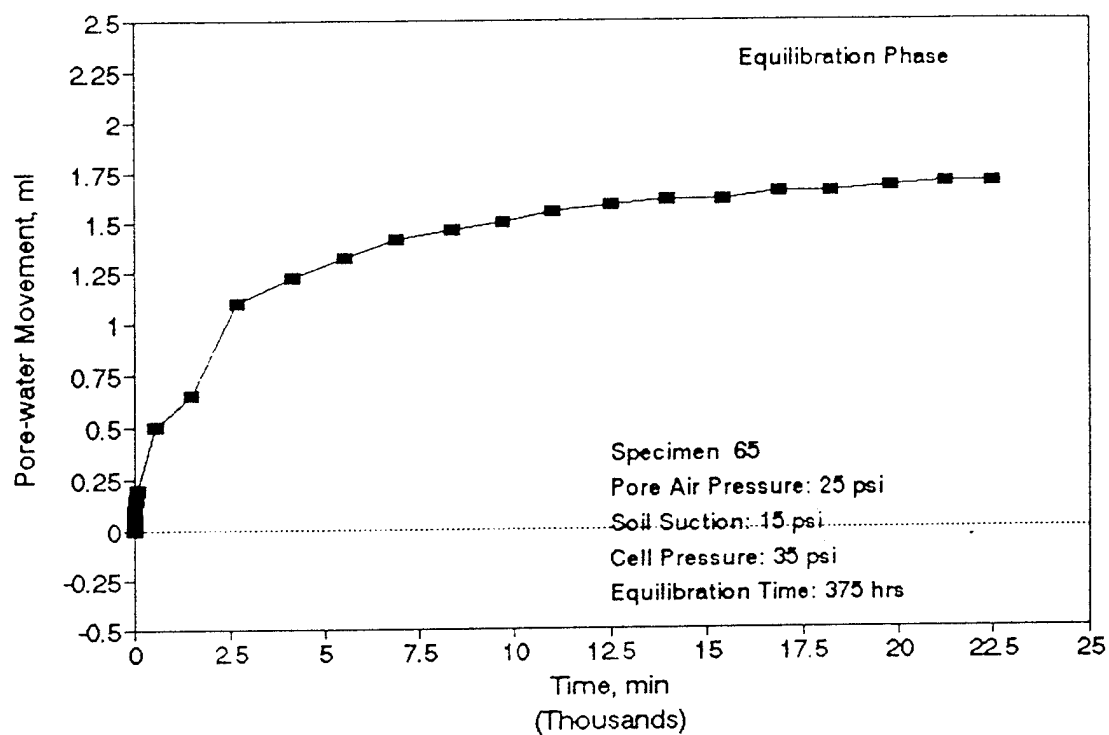


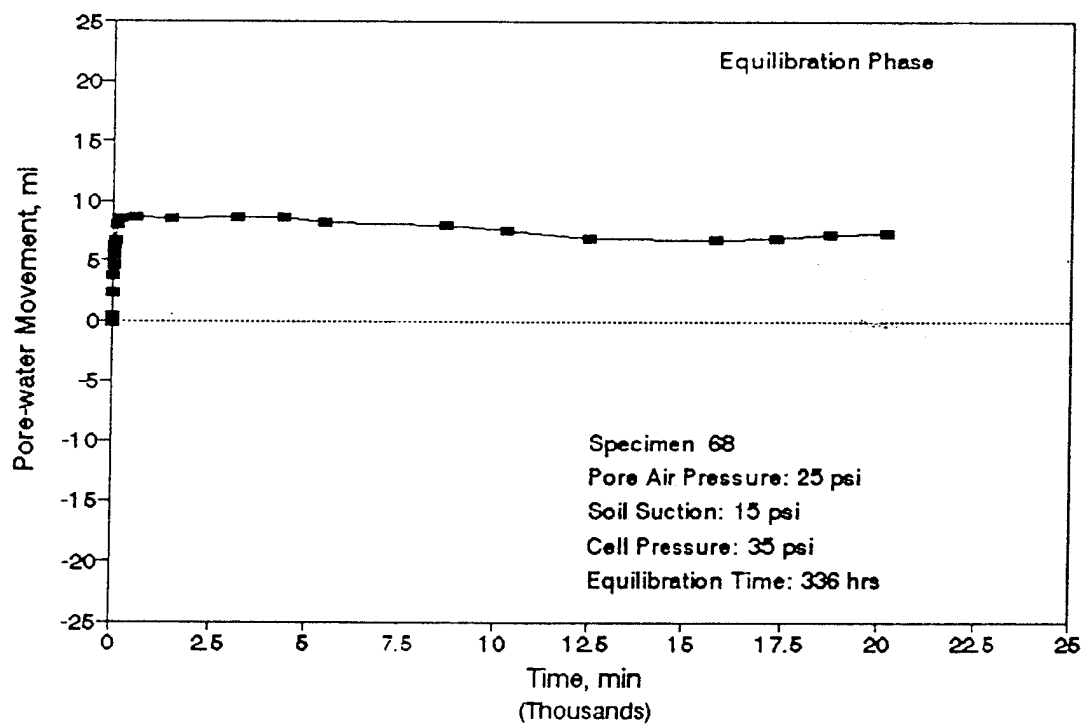
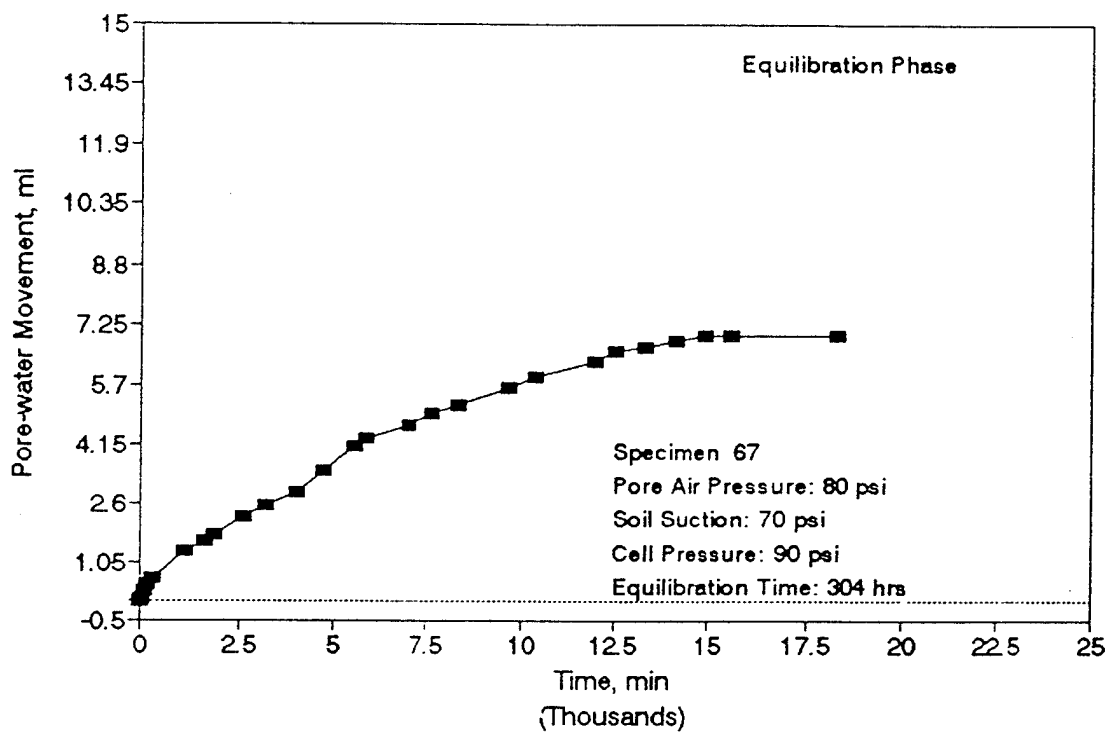




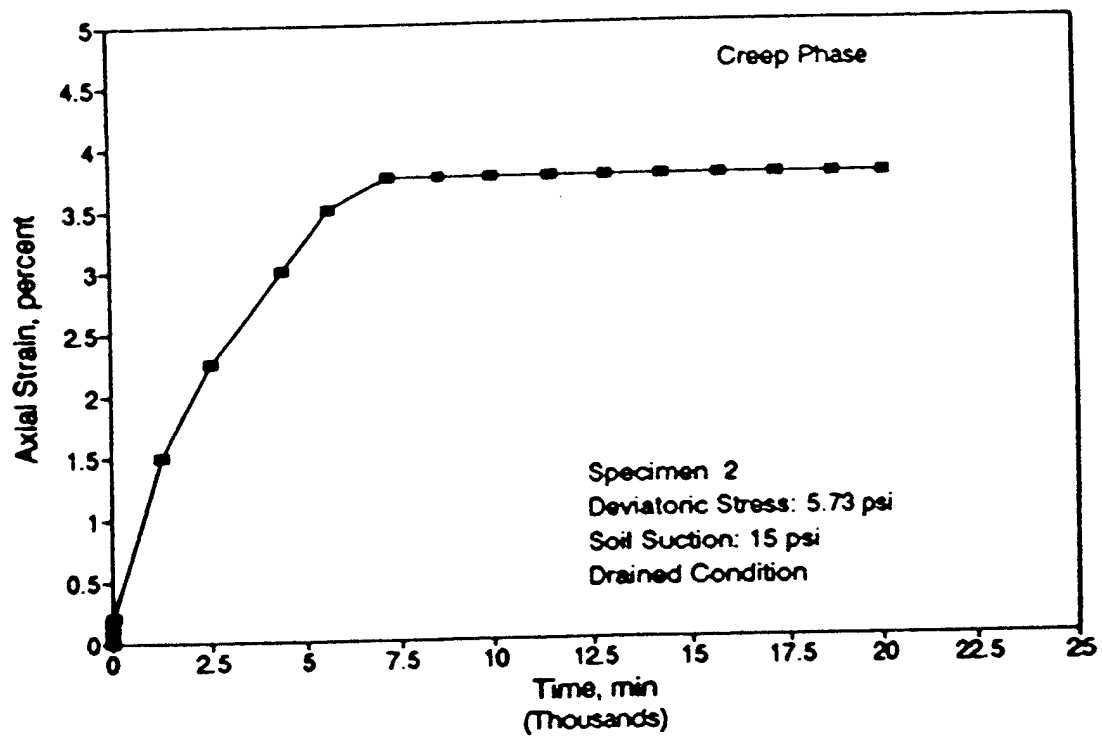
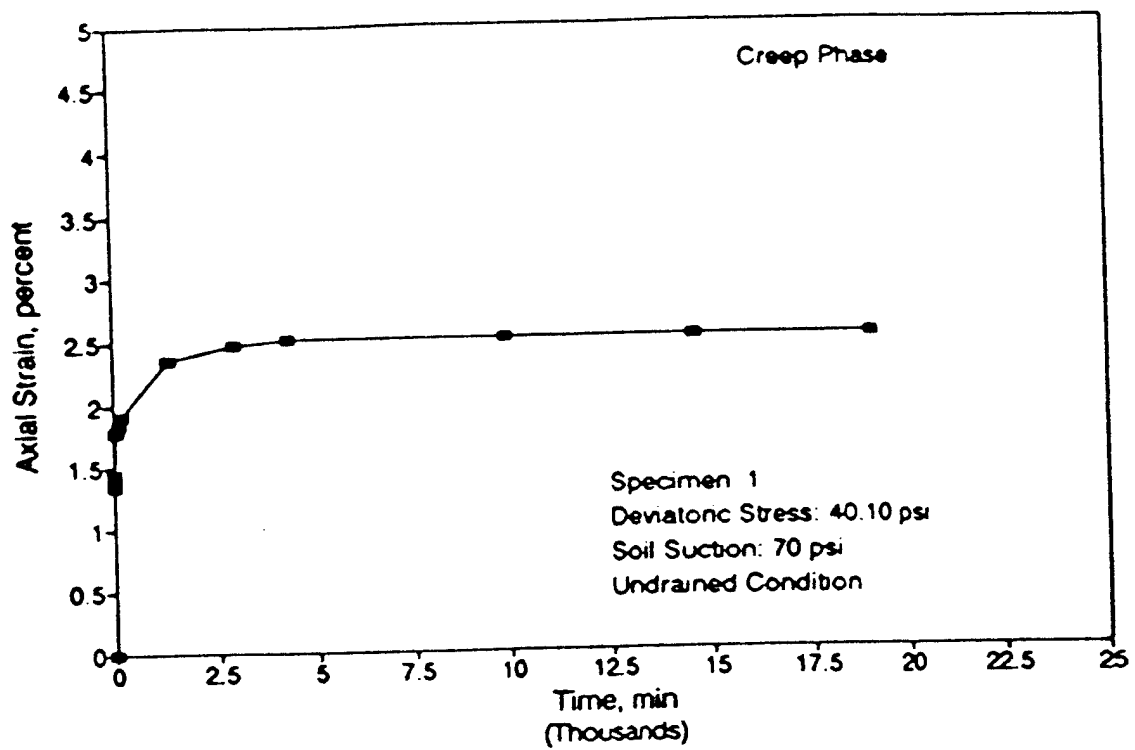


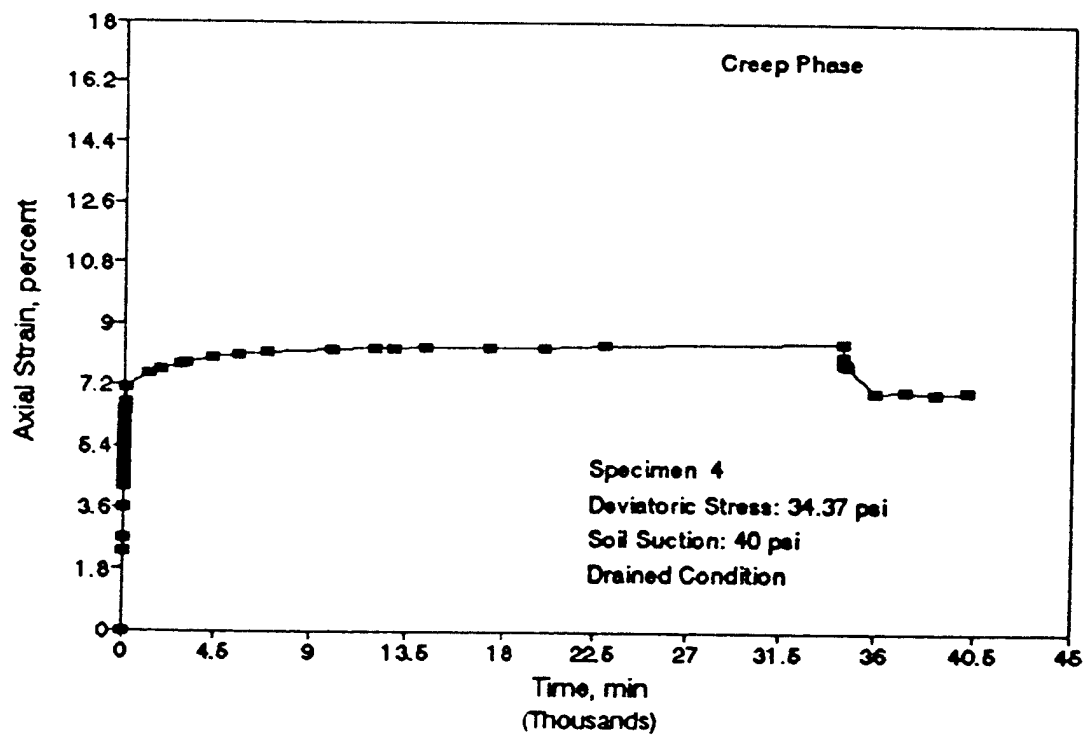
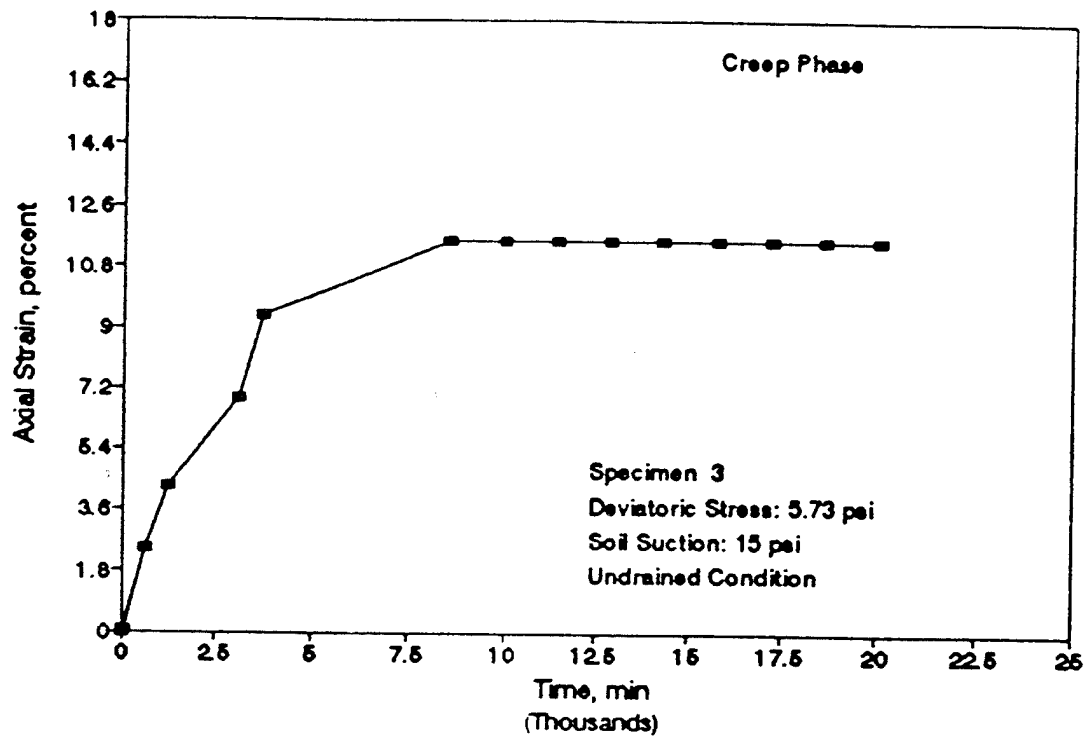




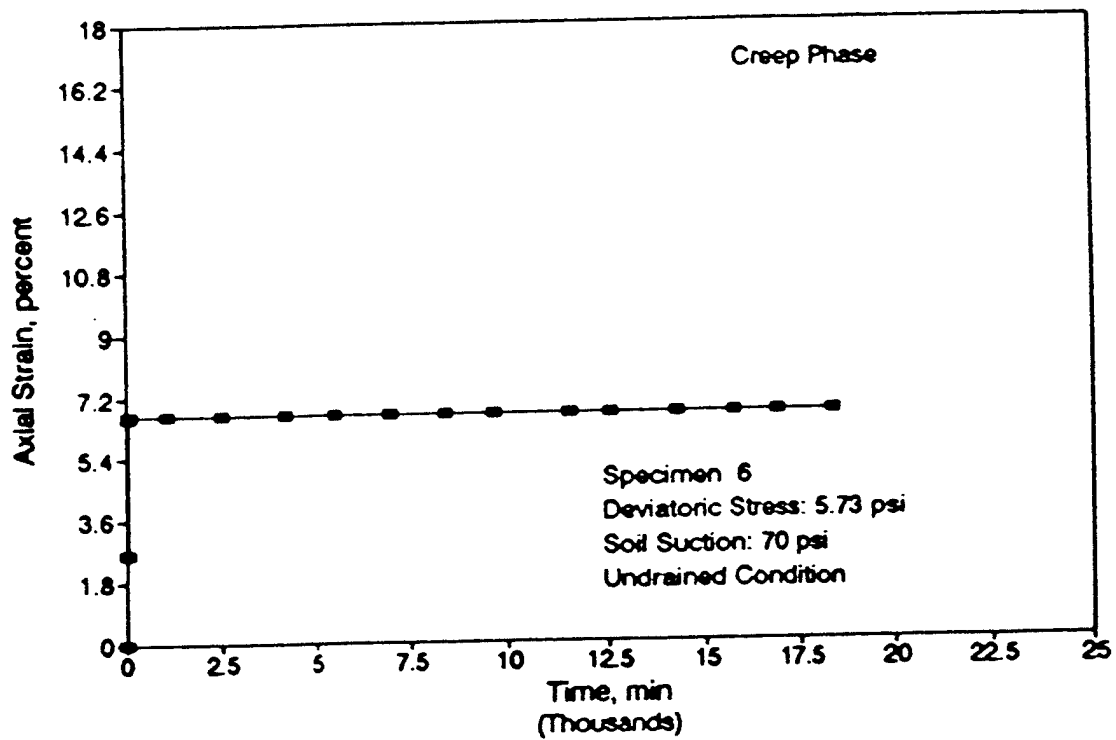
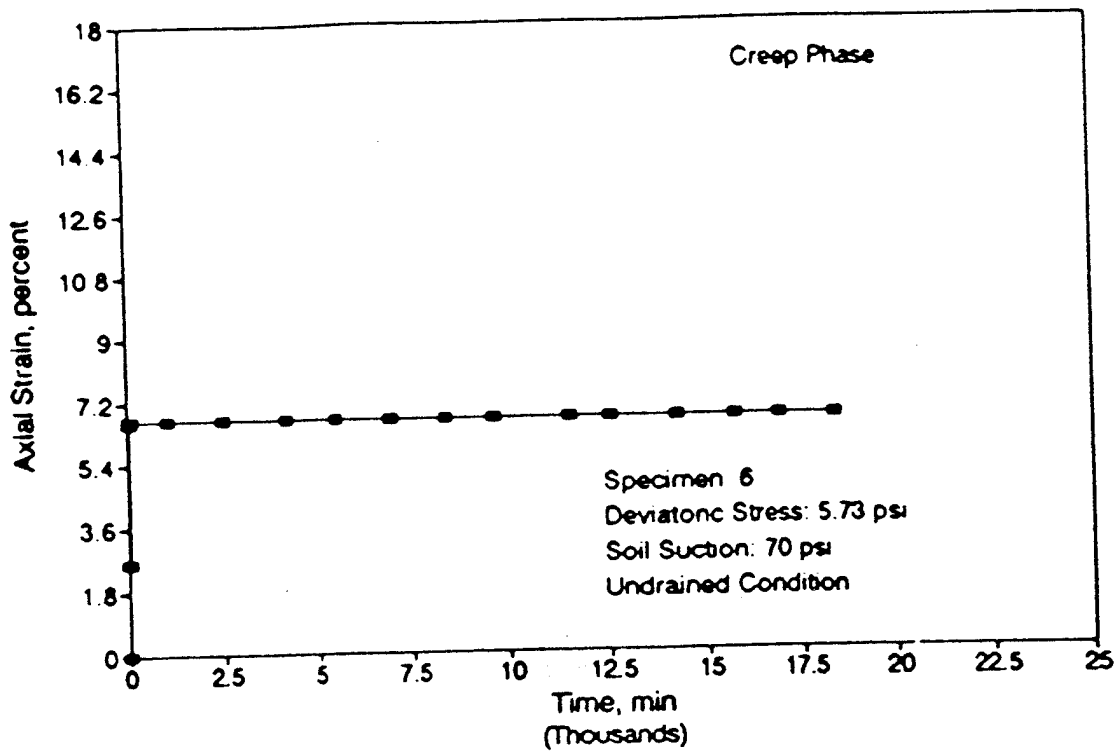


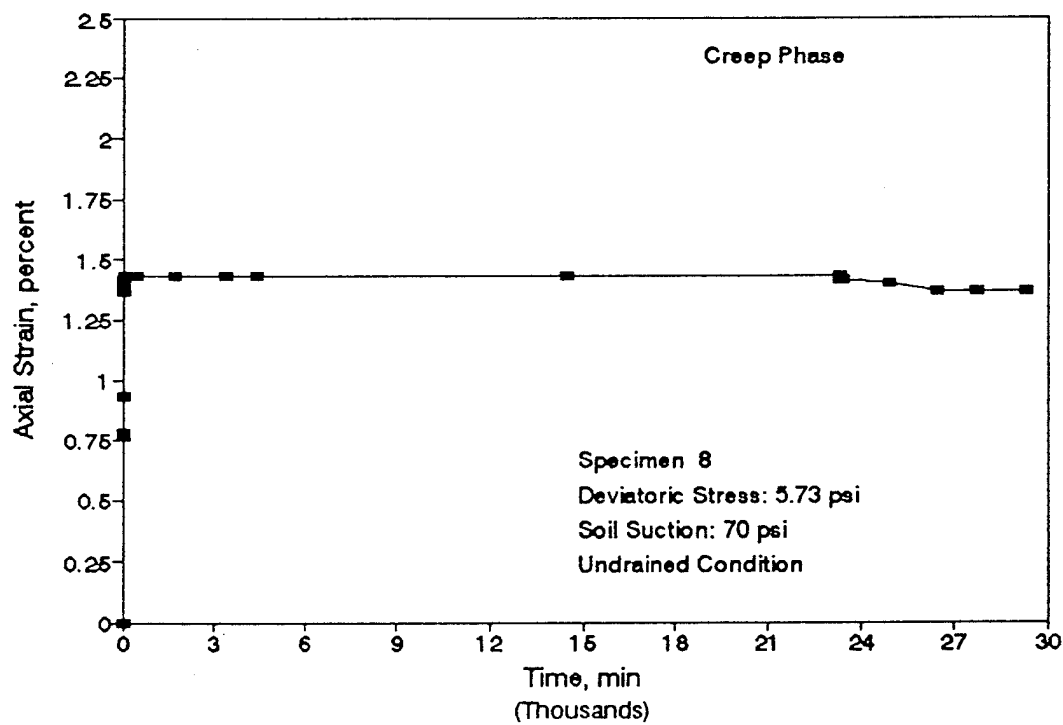
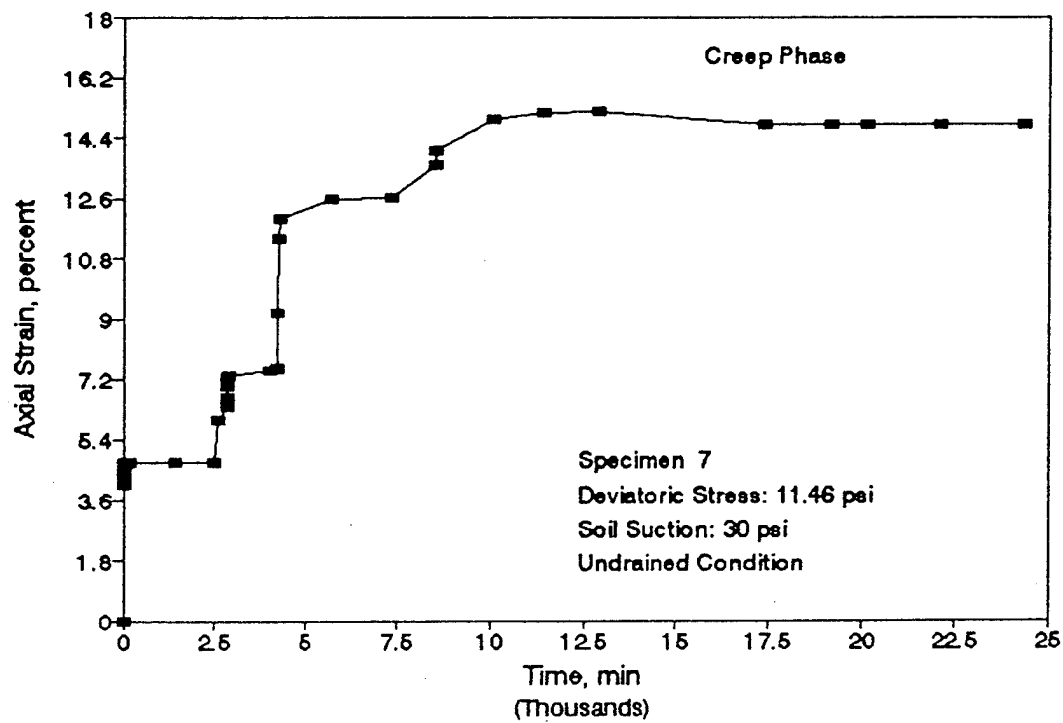
**APPENDIX C**  
**RECORDS OF CREEP/RECOVERY TESTS**

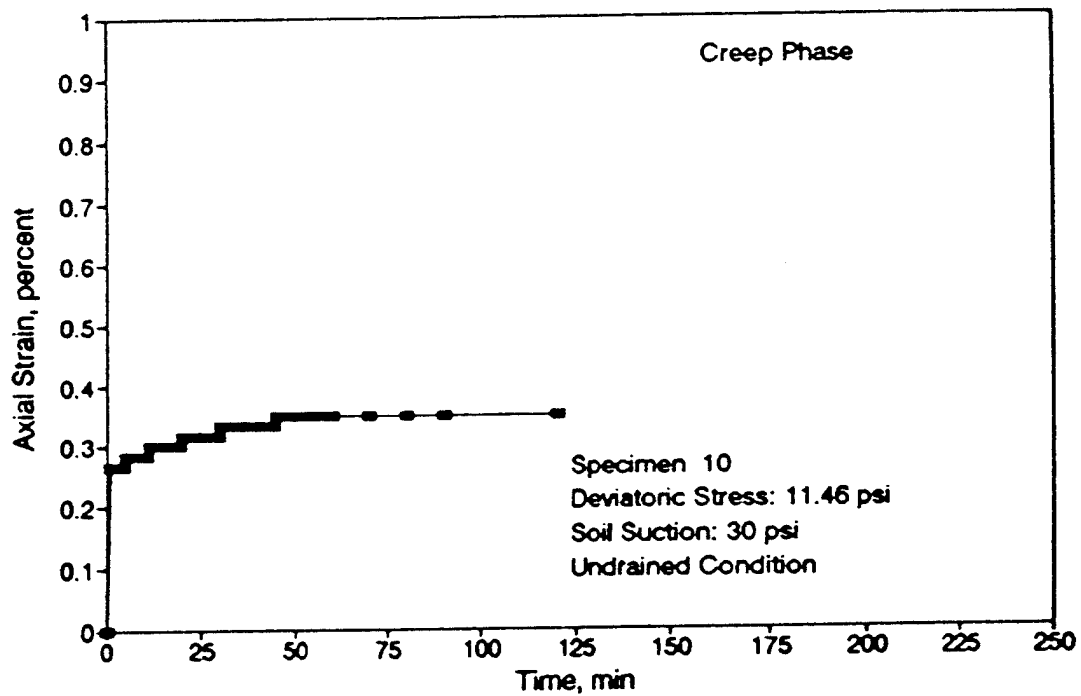
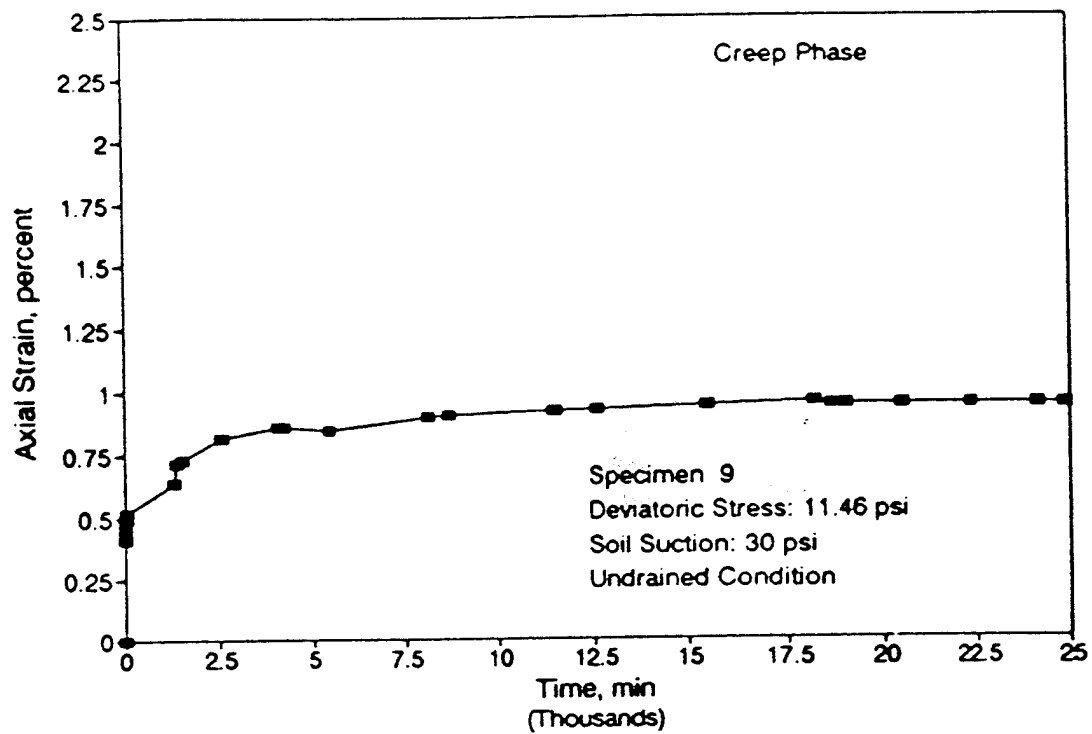


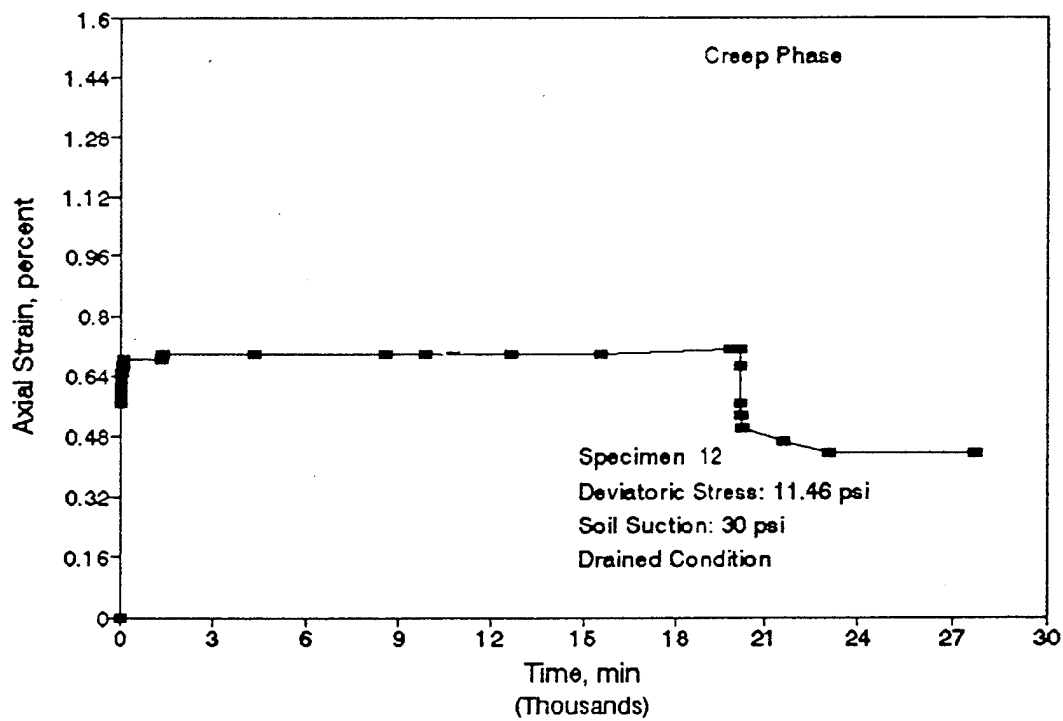
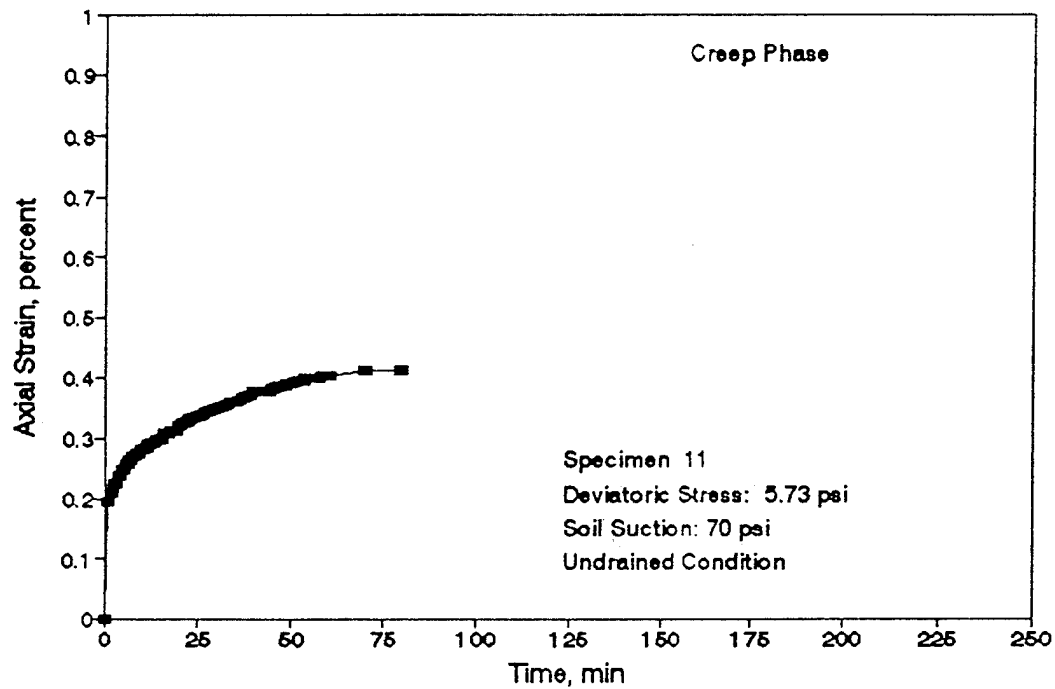


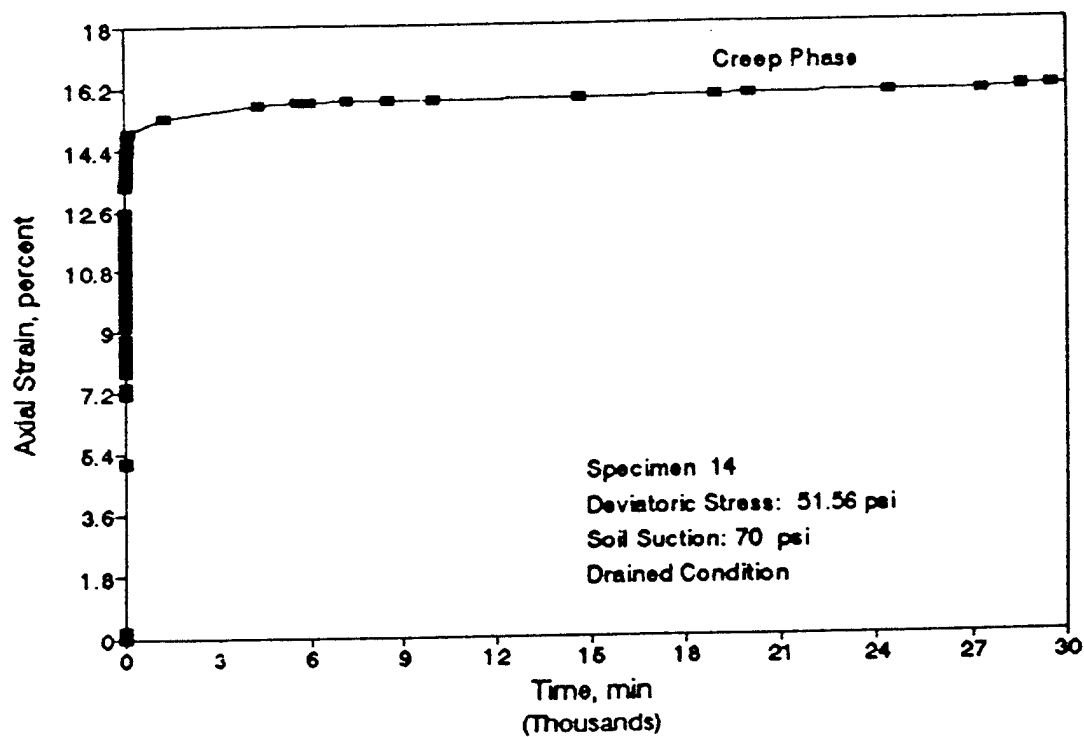
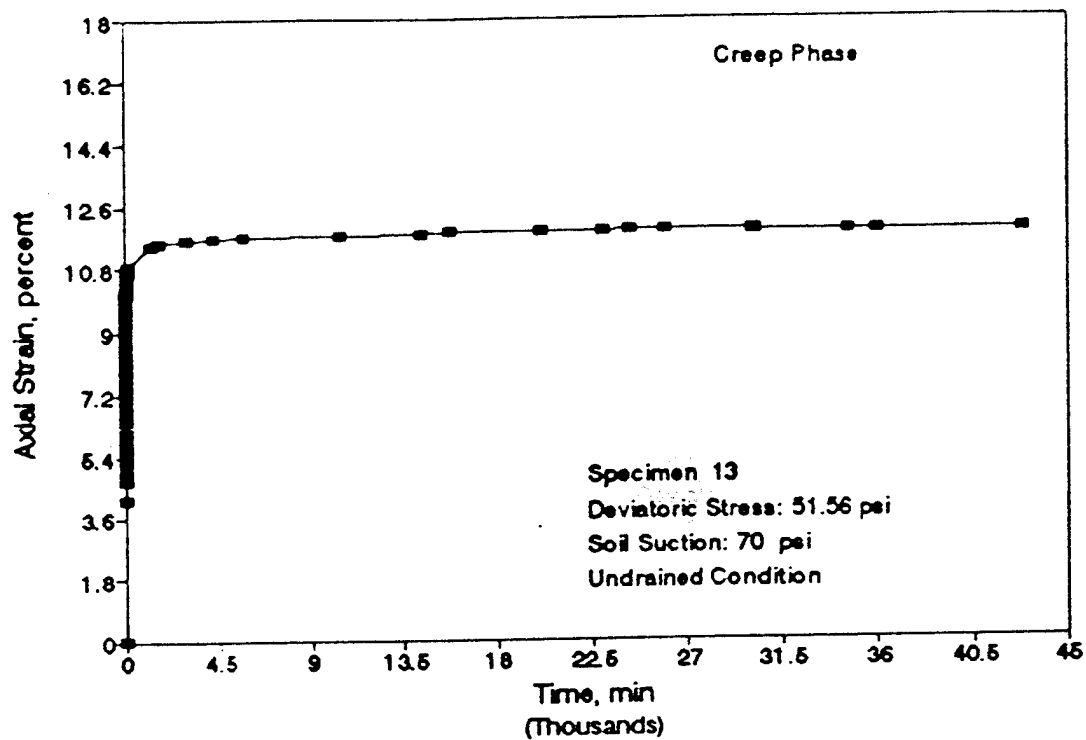


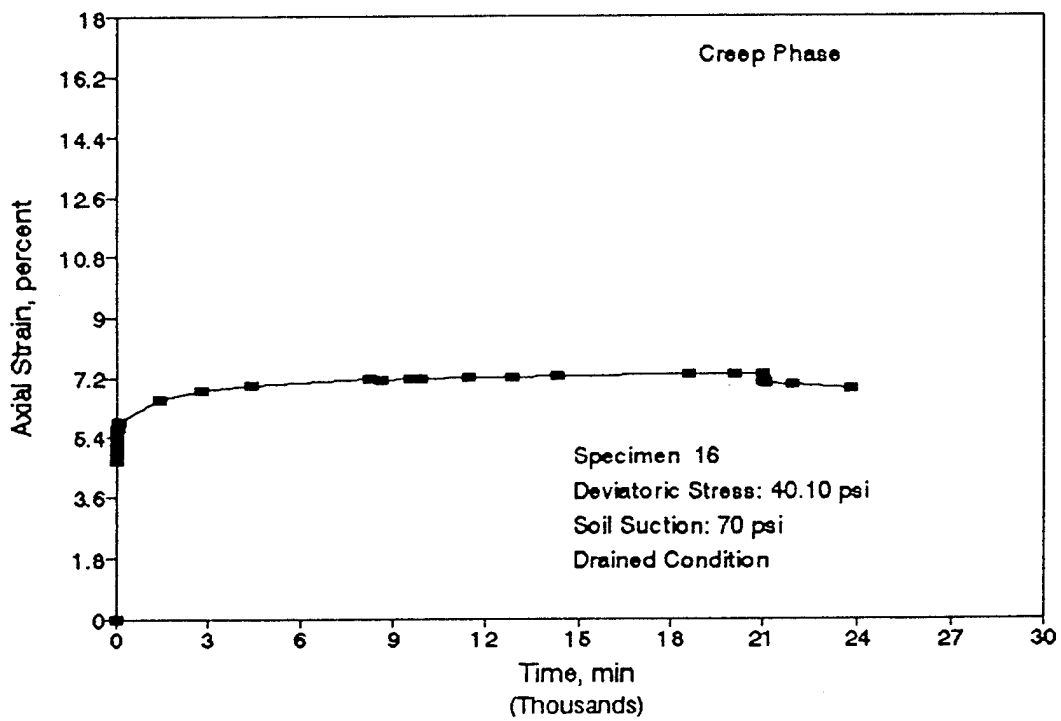
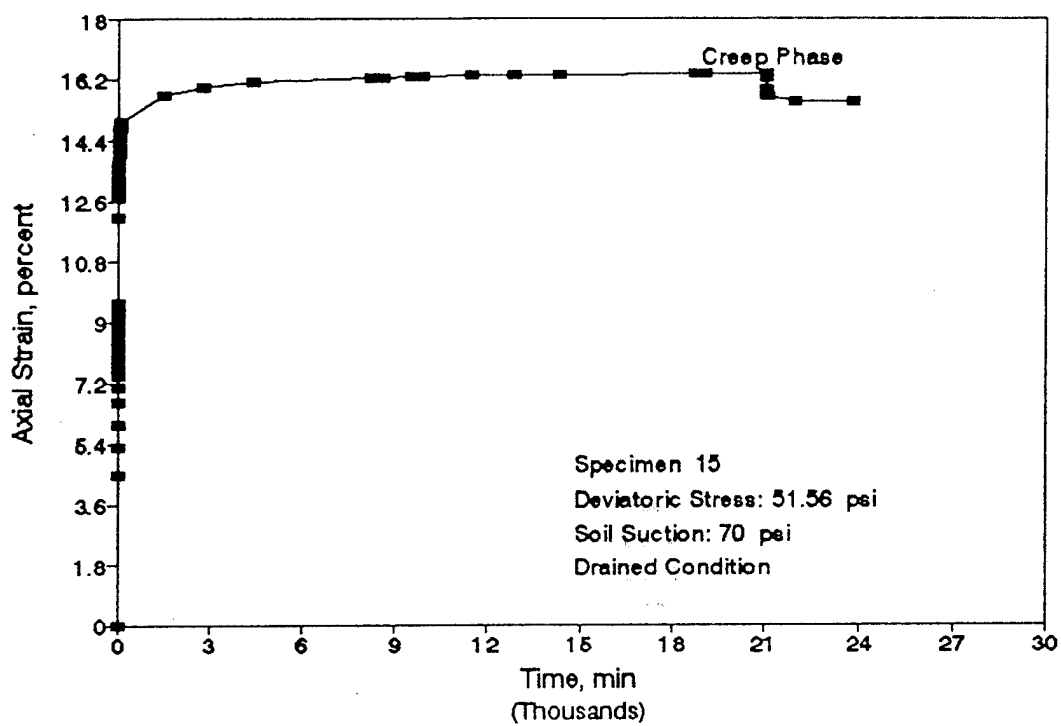


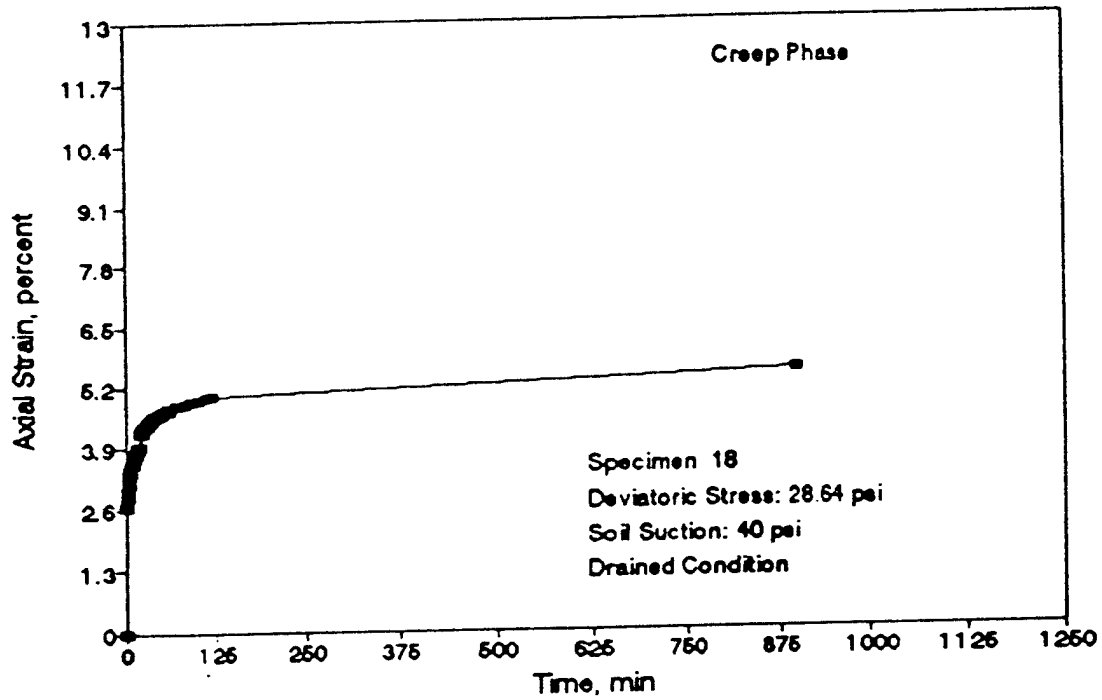
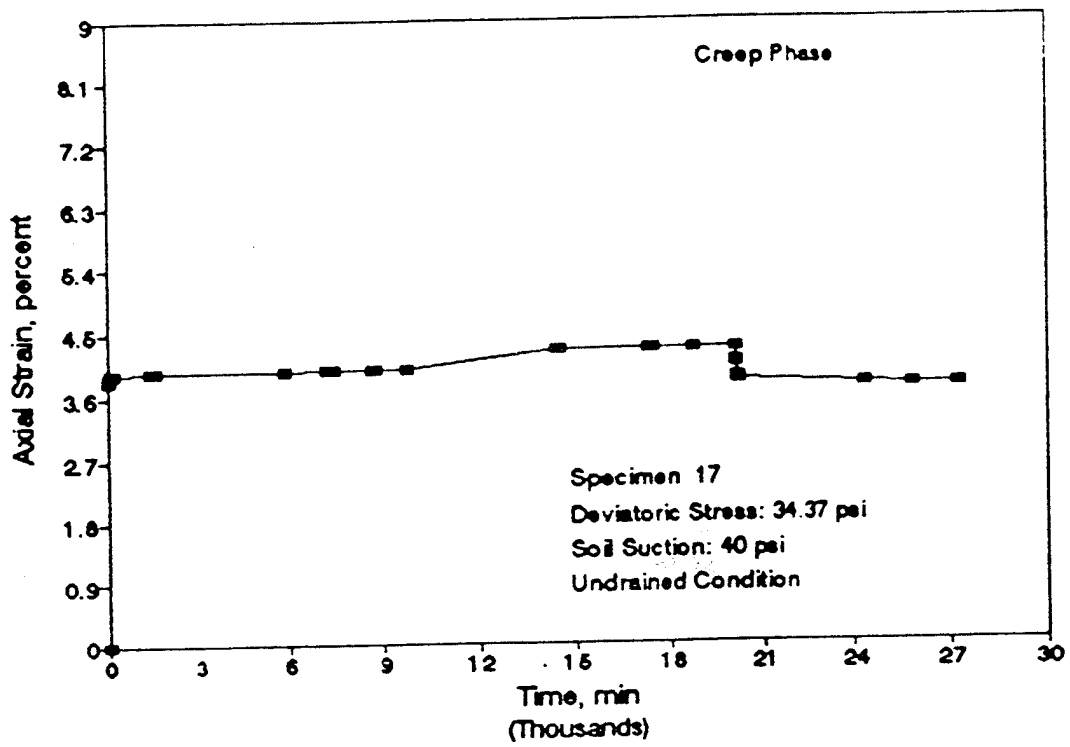


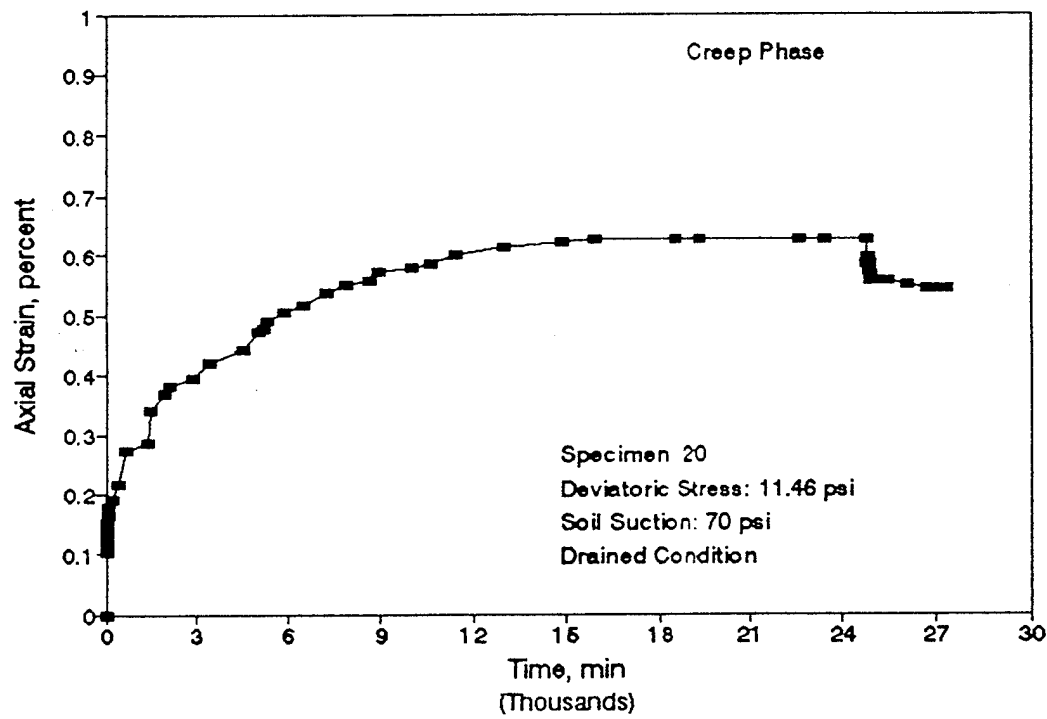
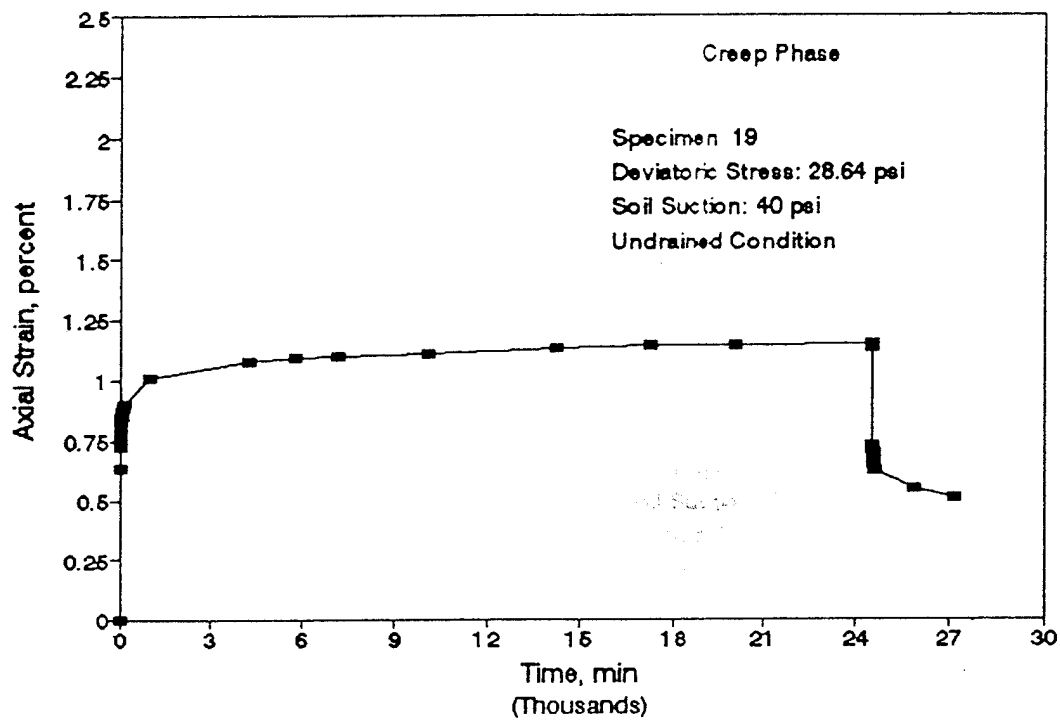




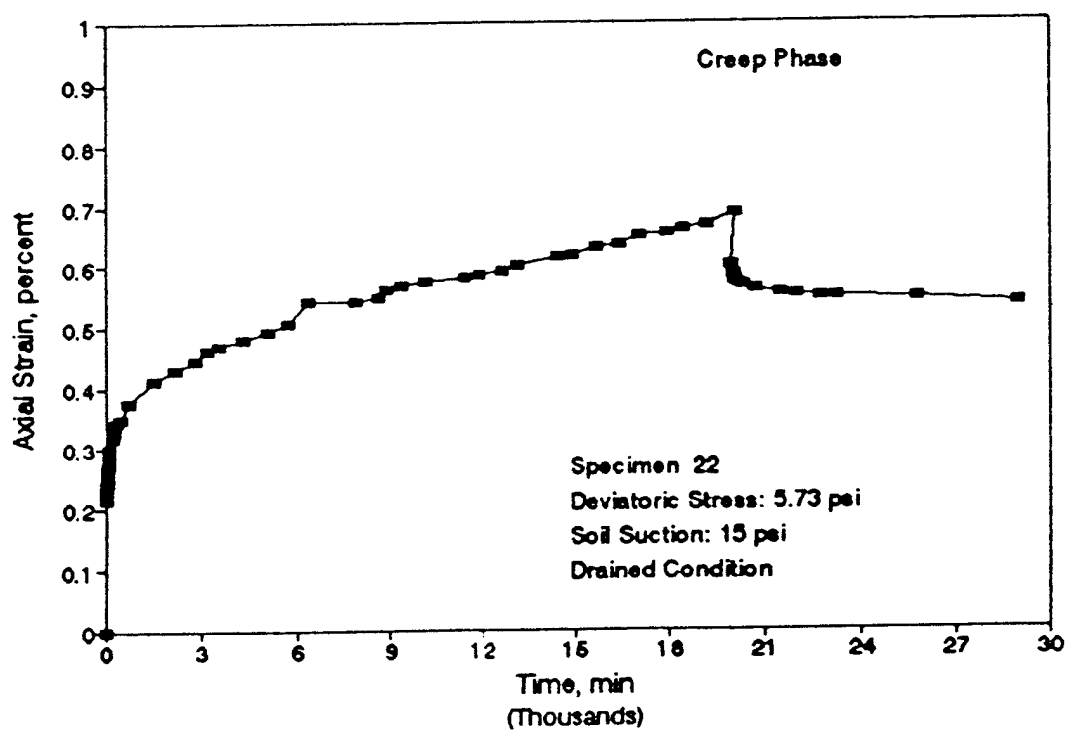
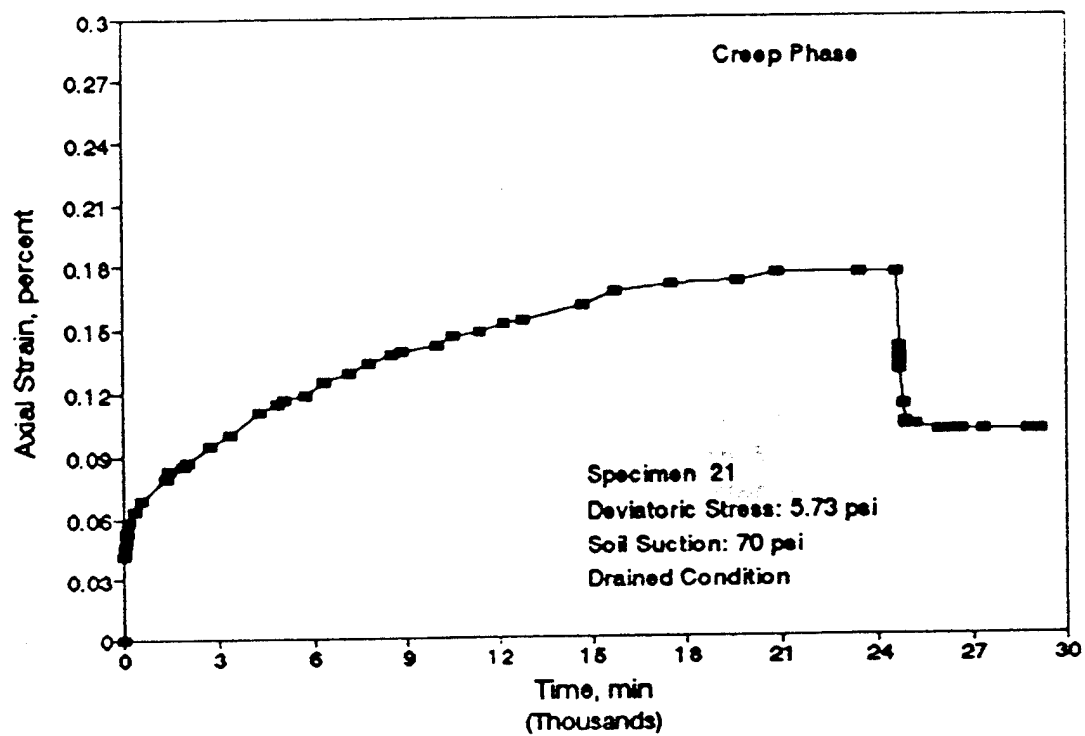


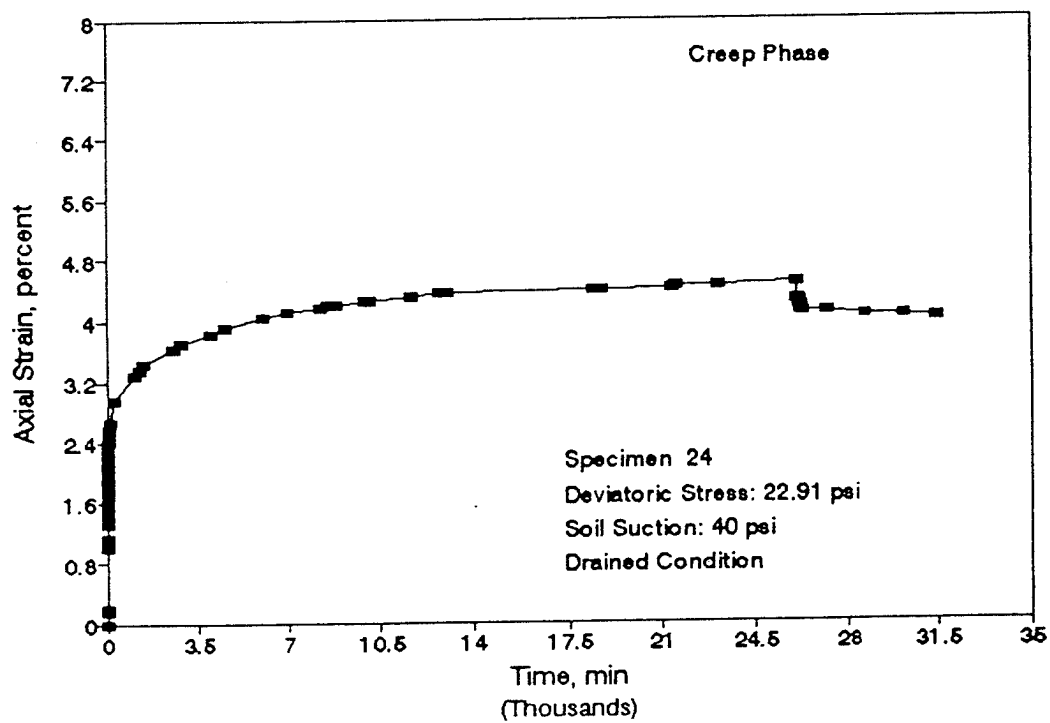
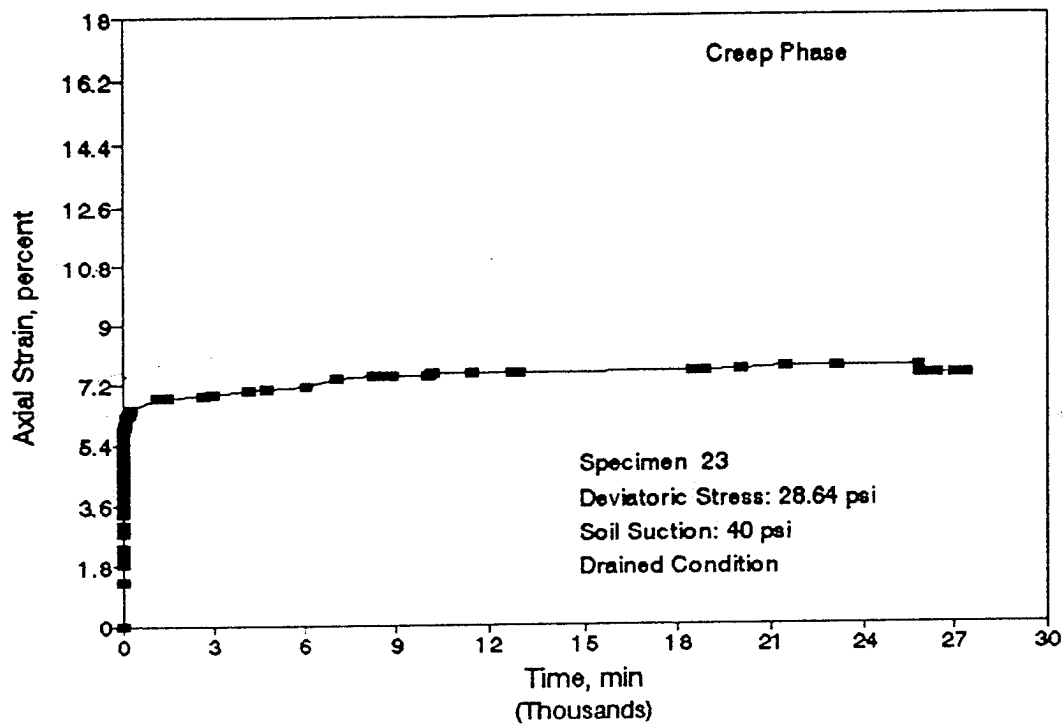


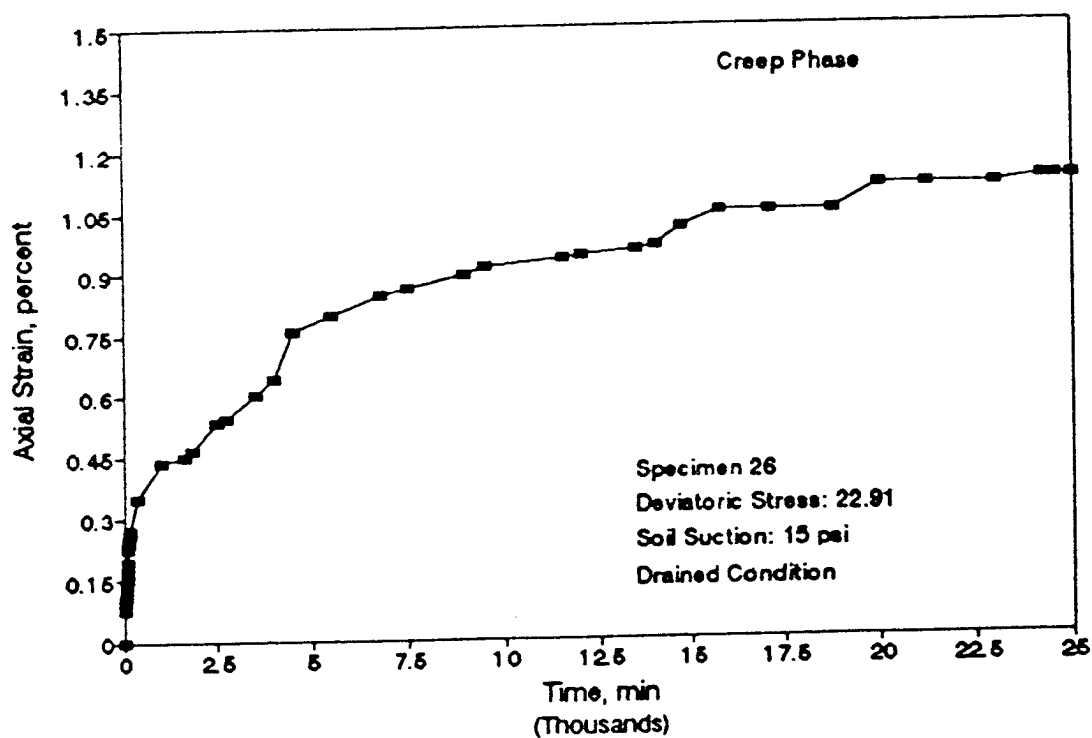
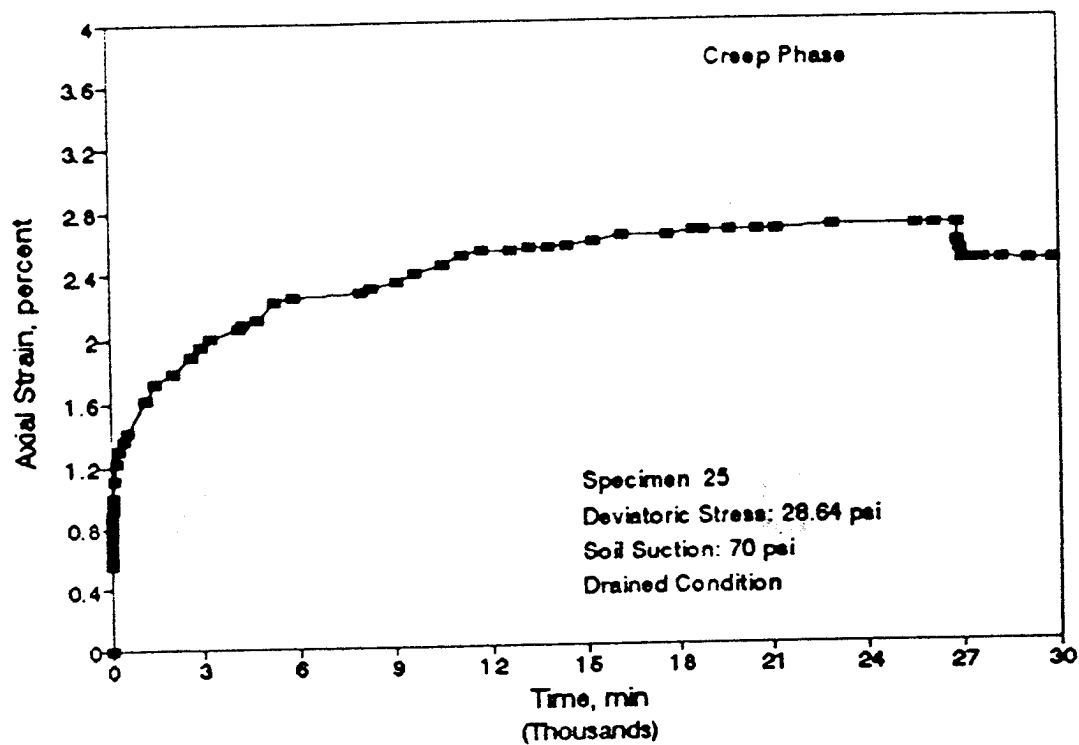


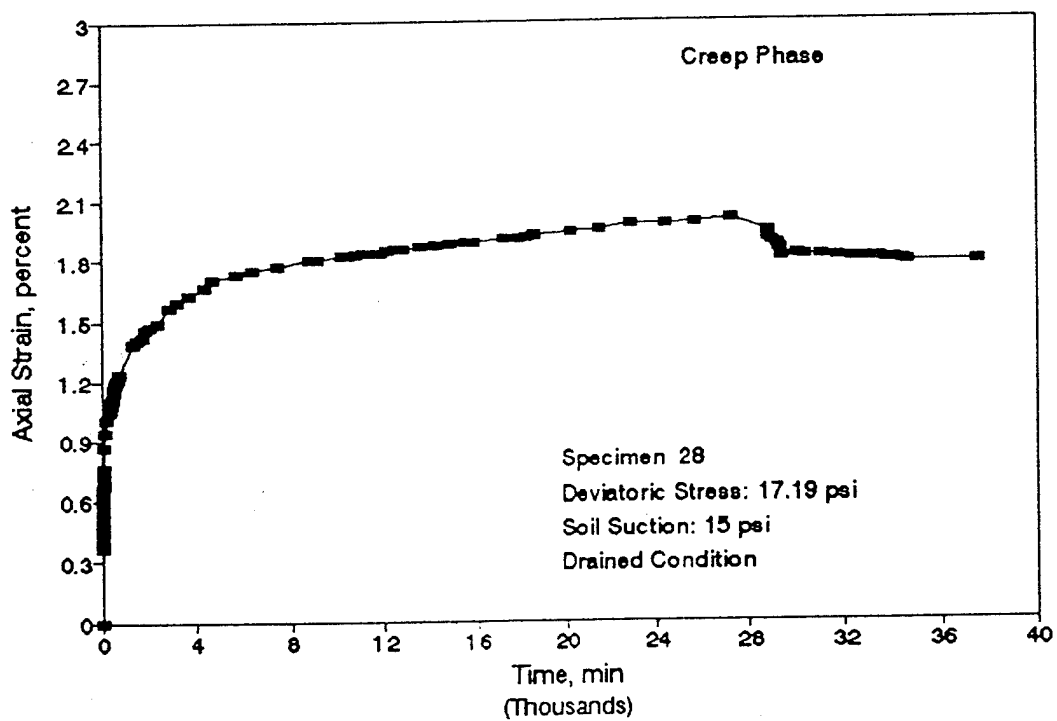
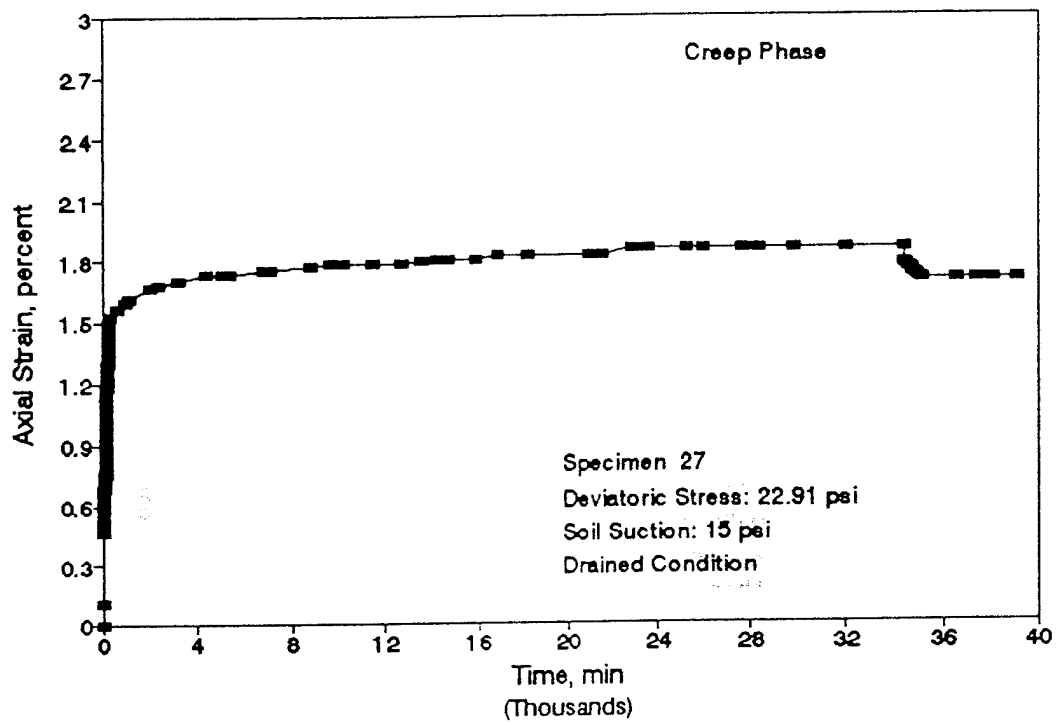


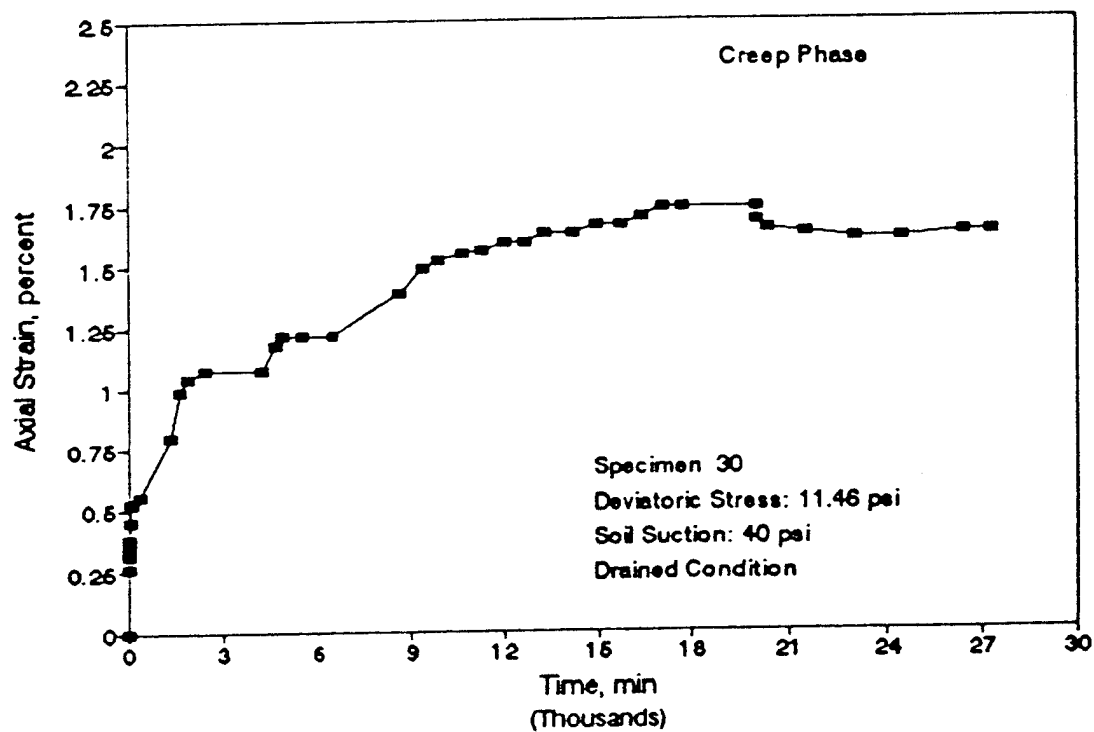
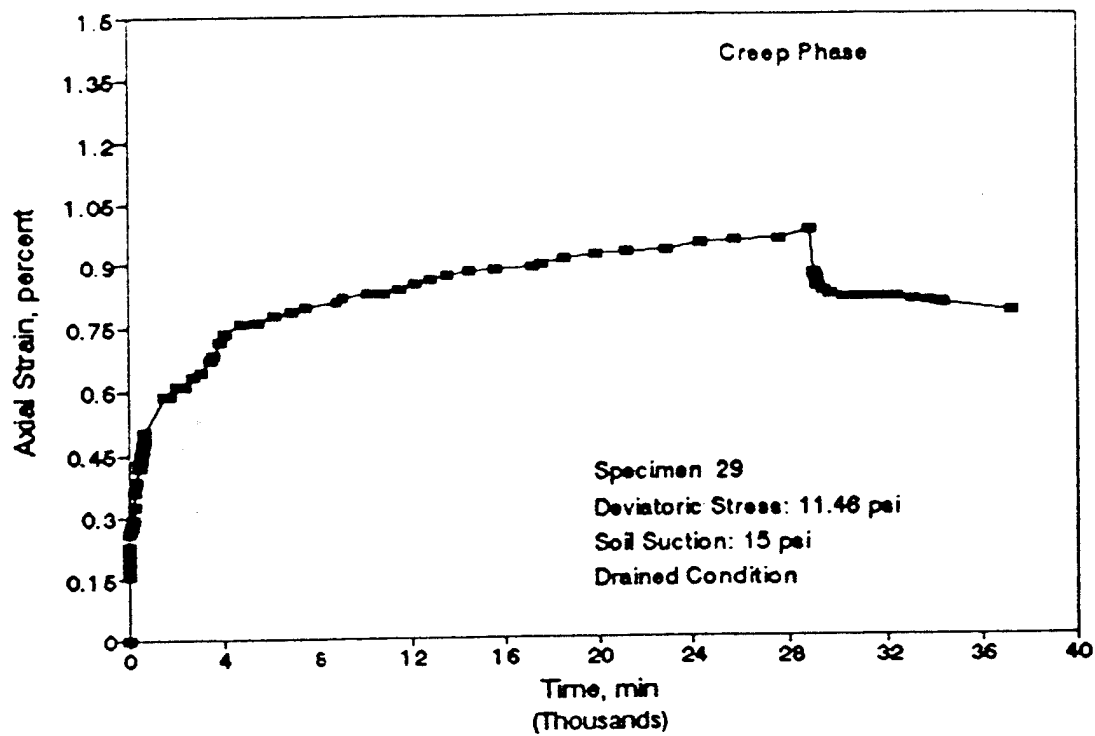


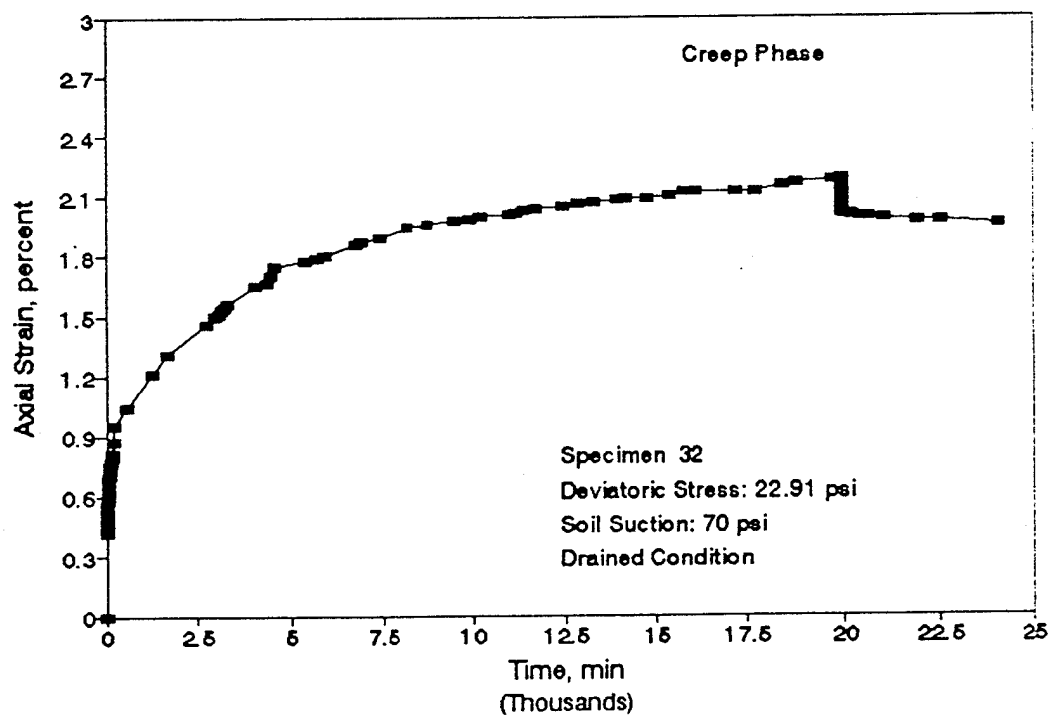
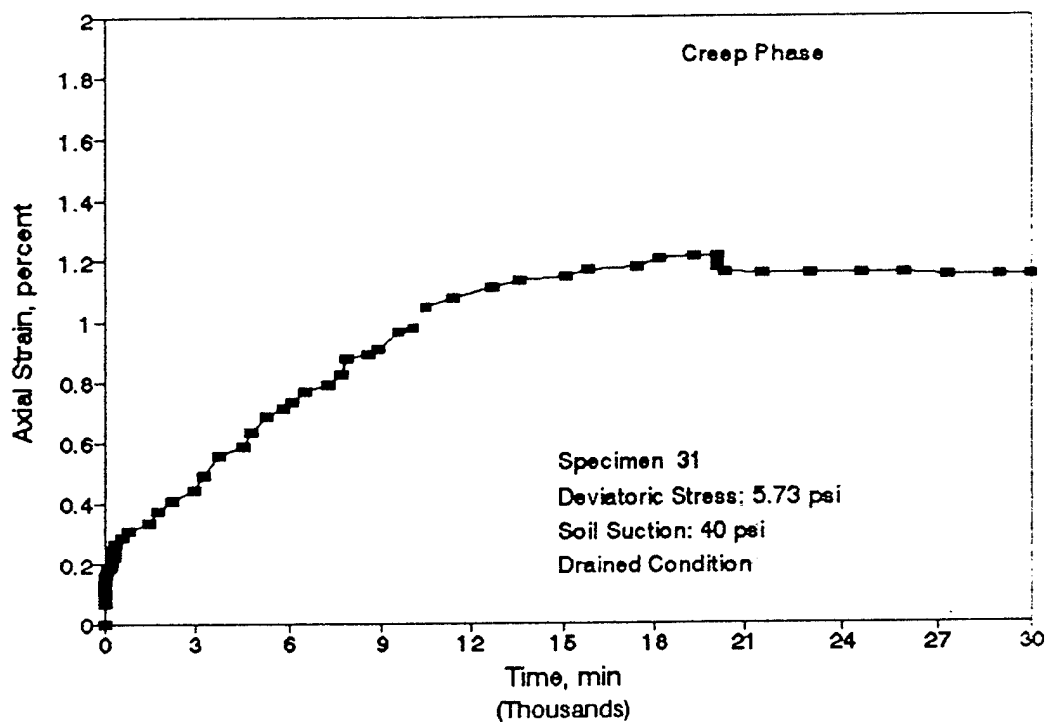


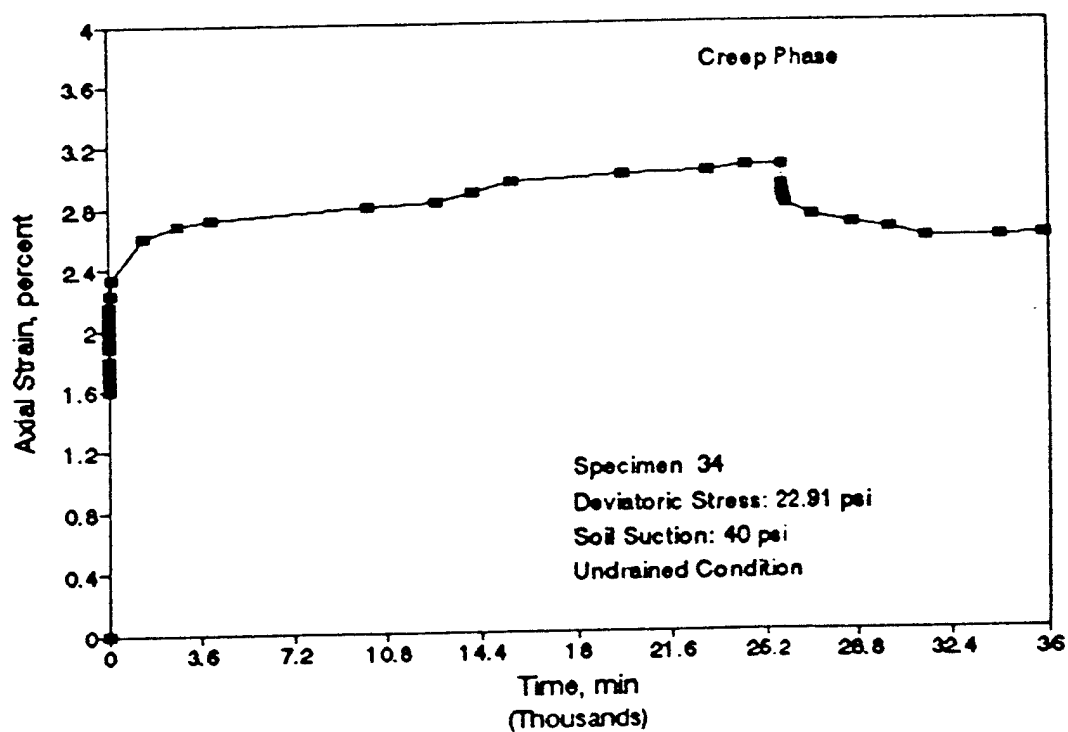
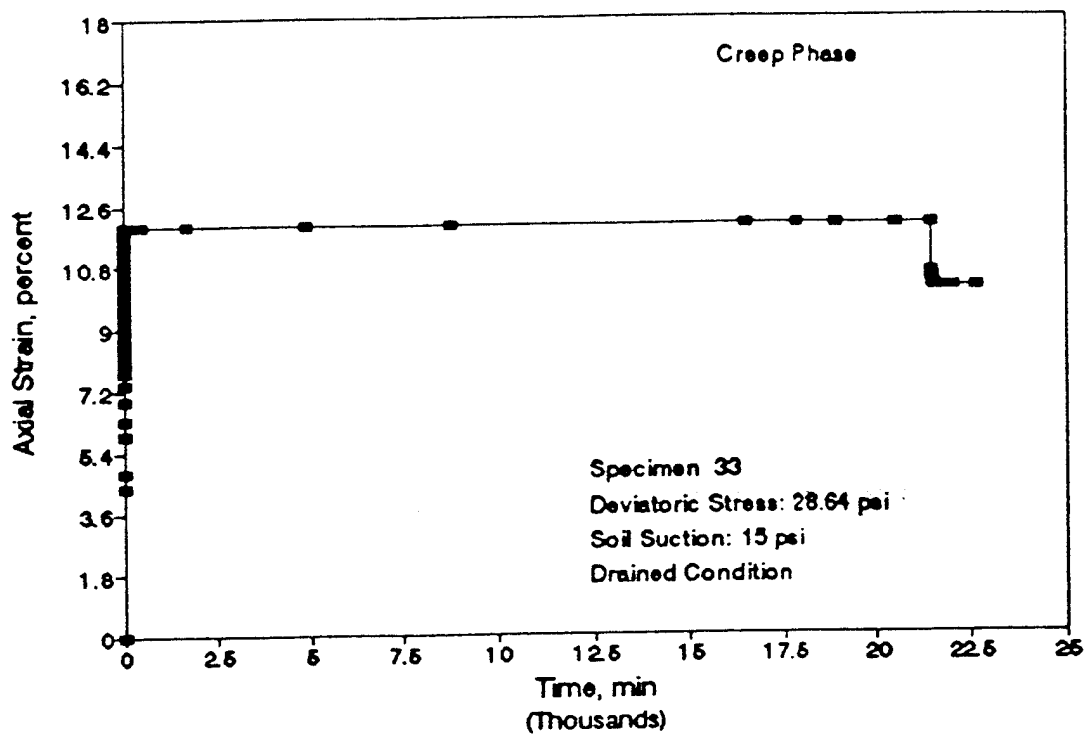


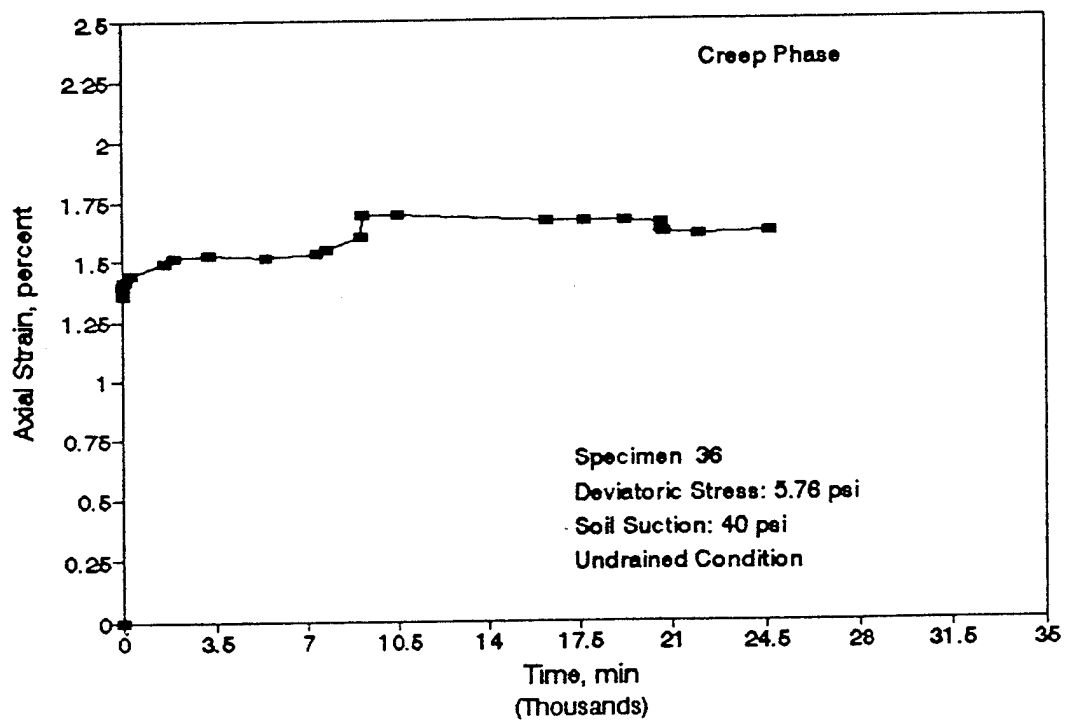
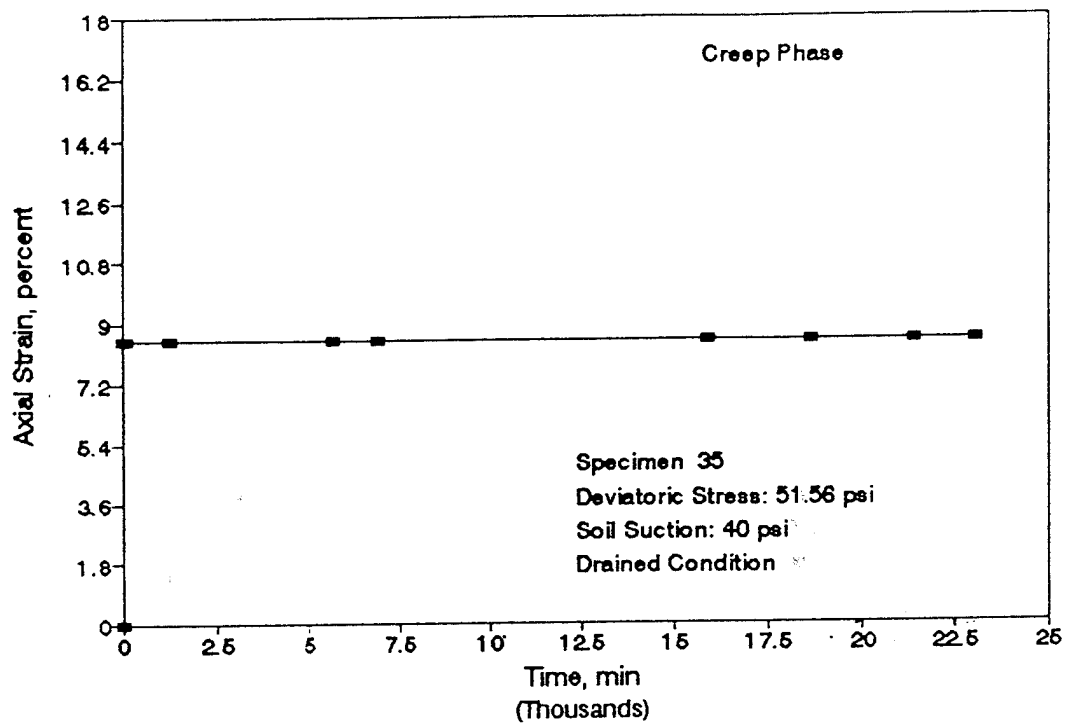




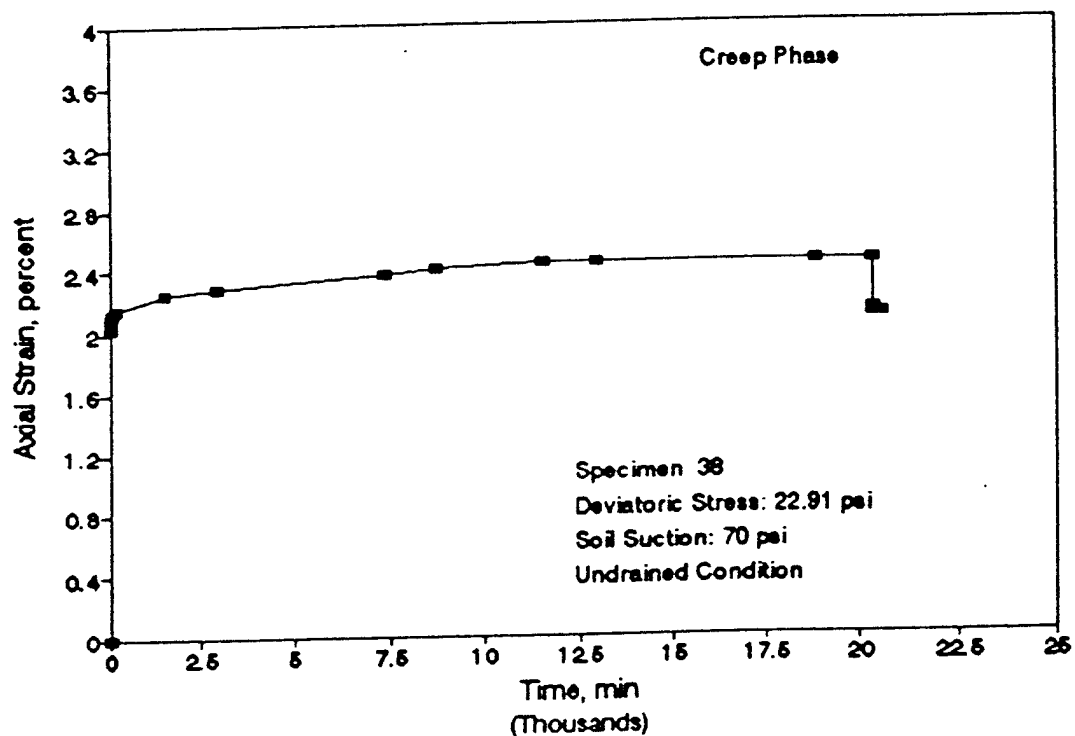
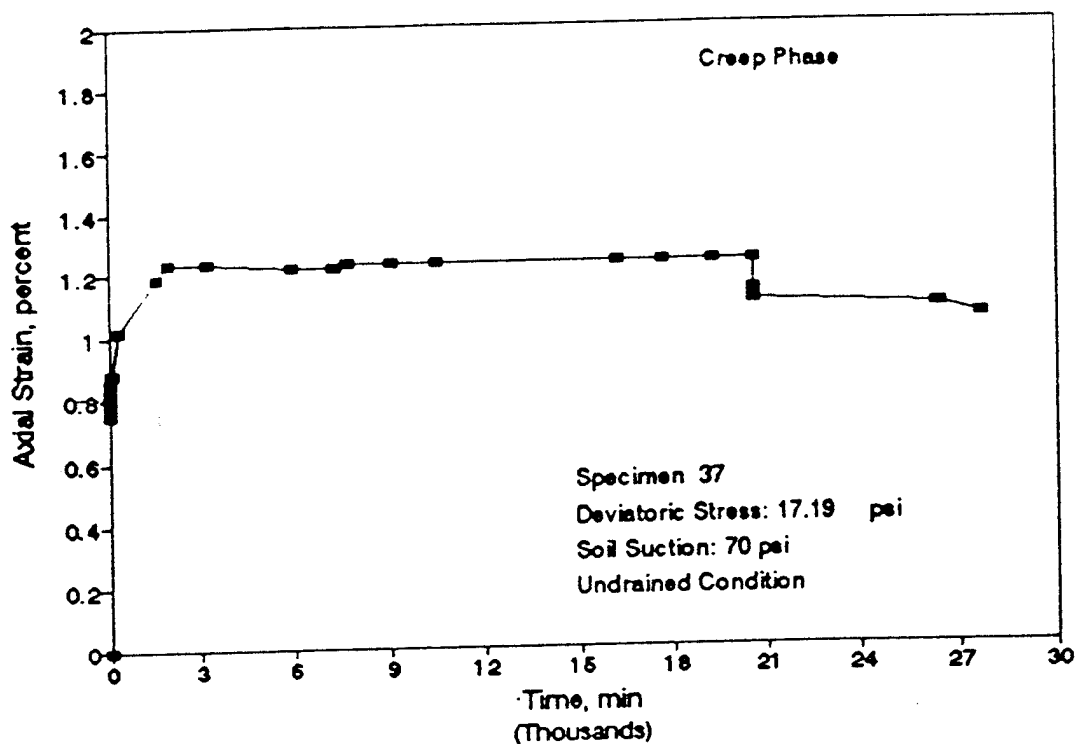


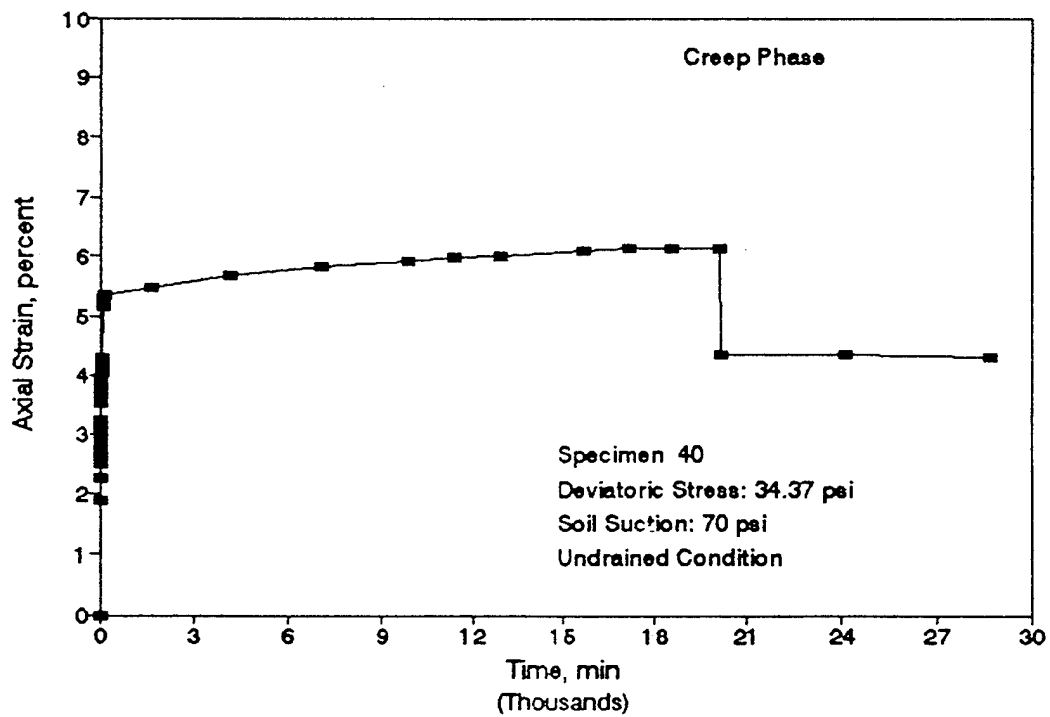
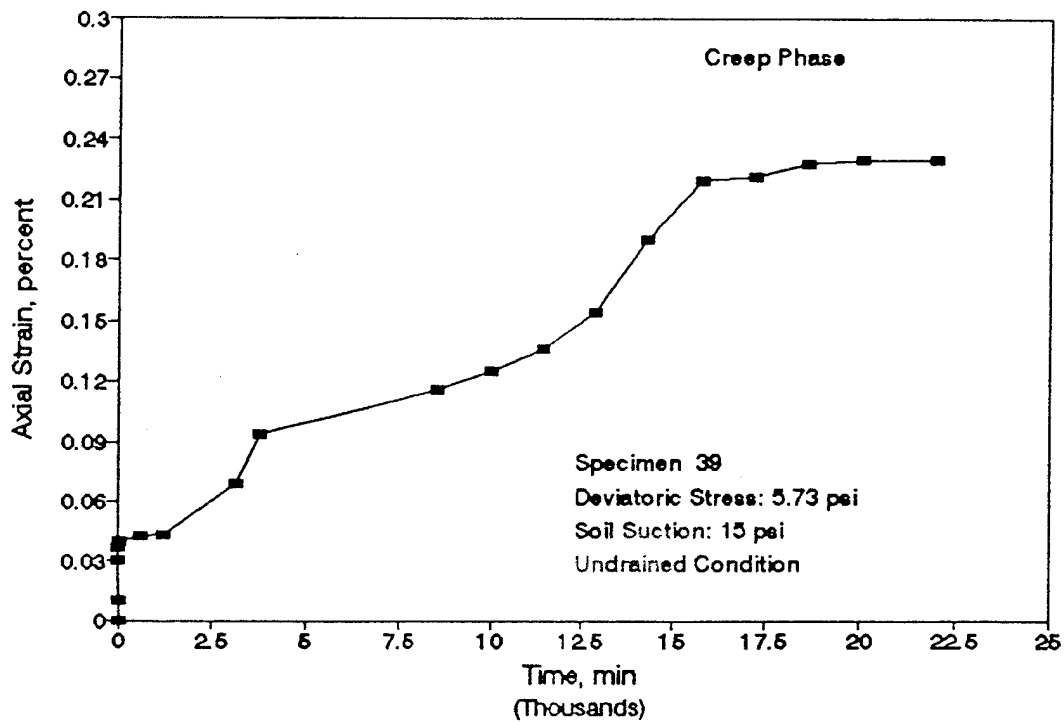


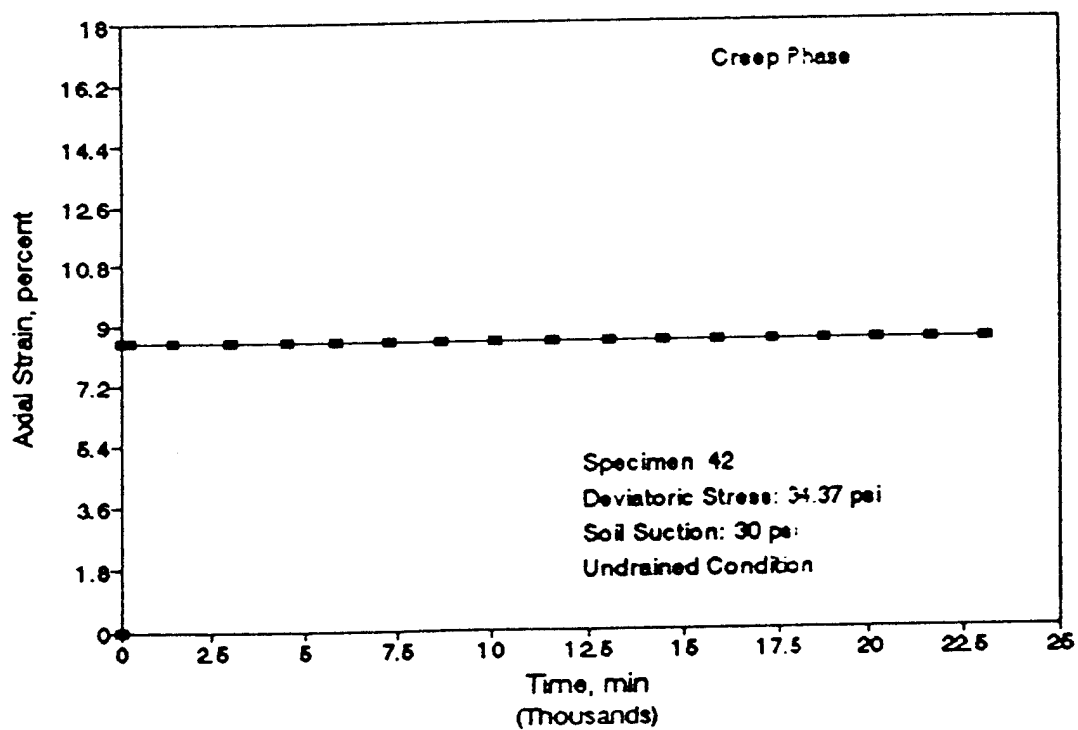
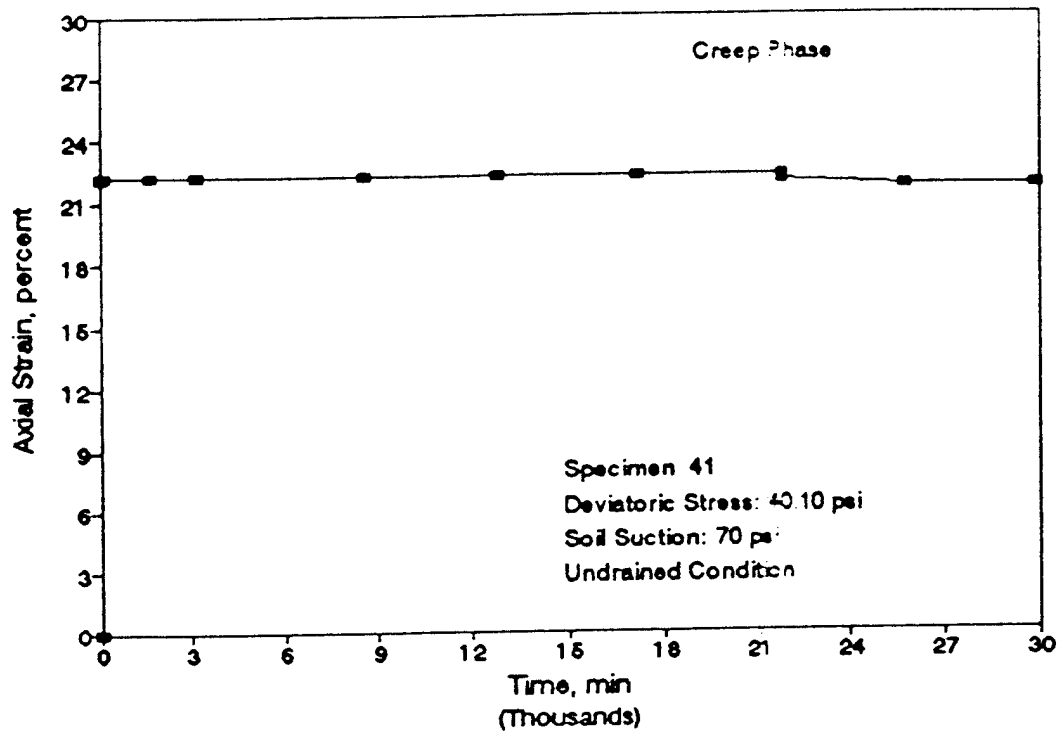


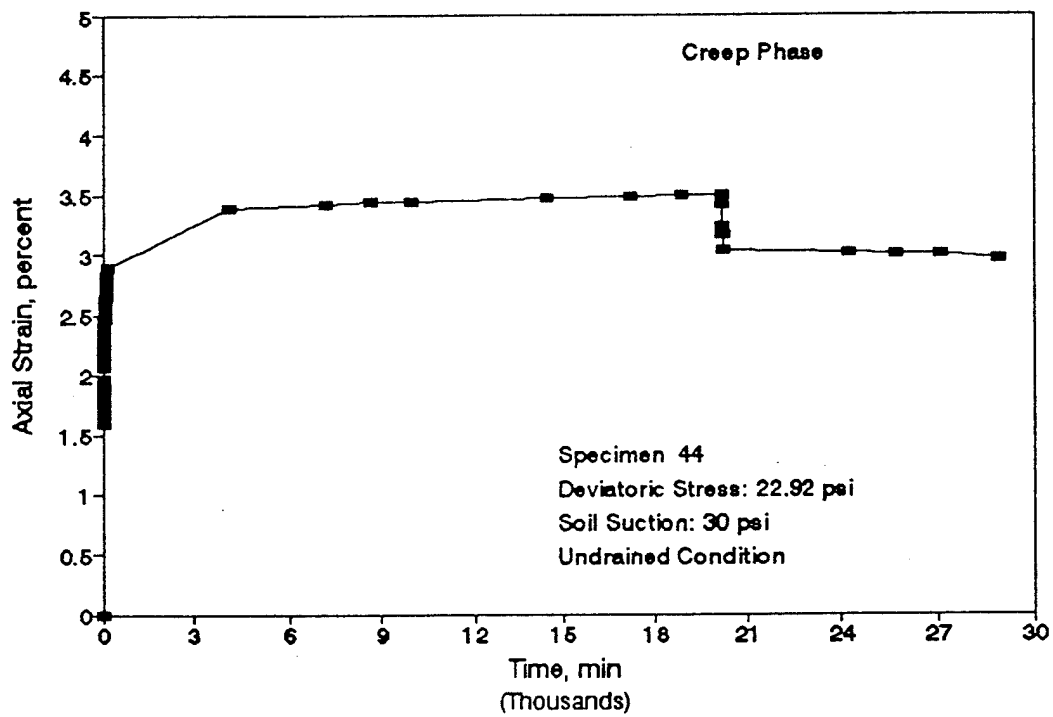
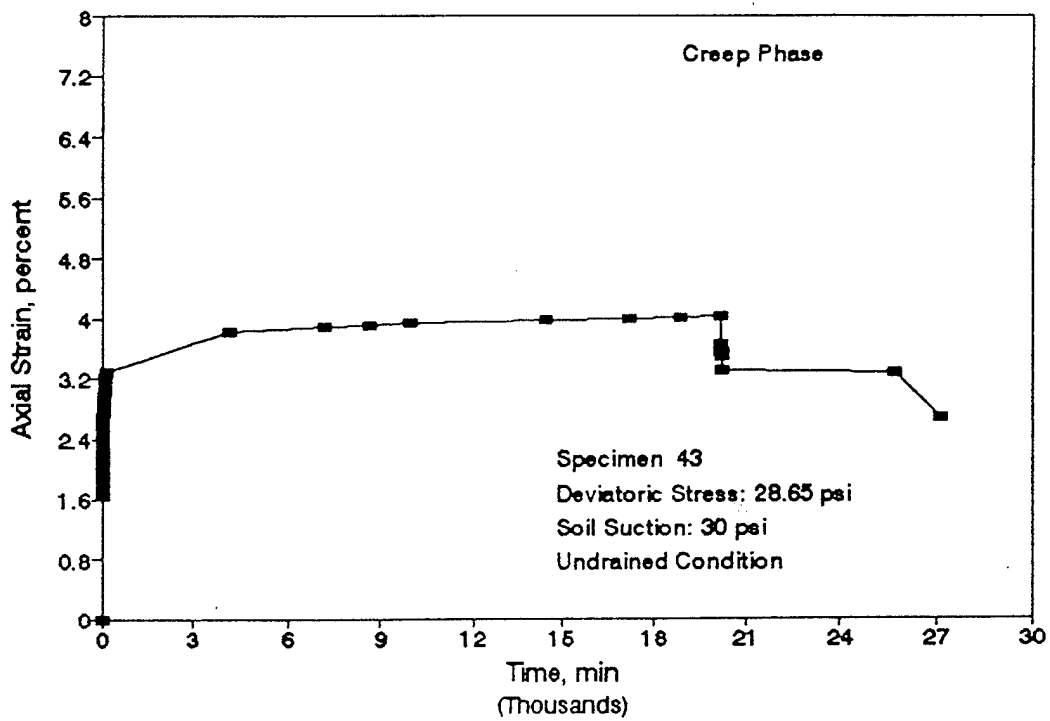


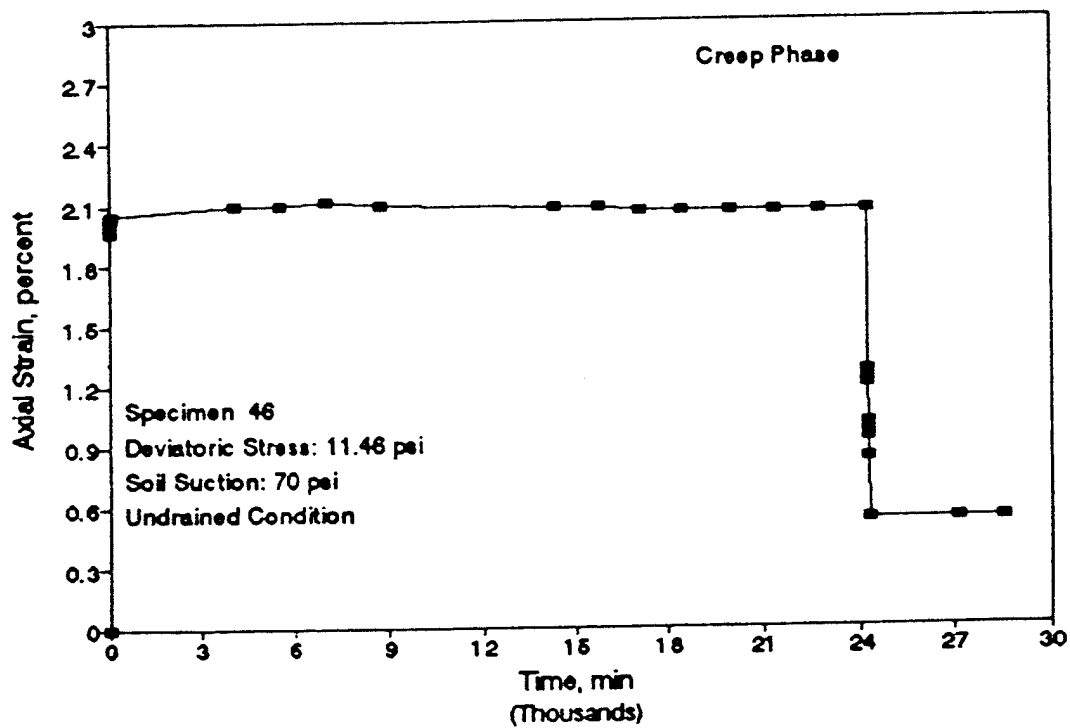
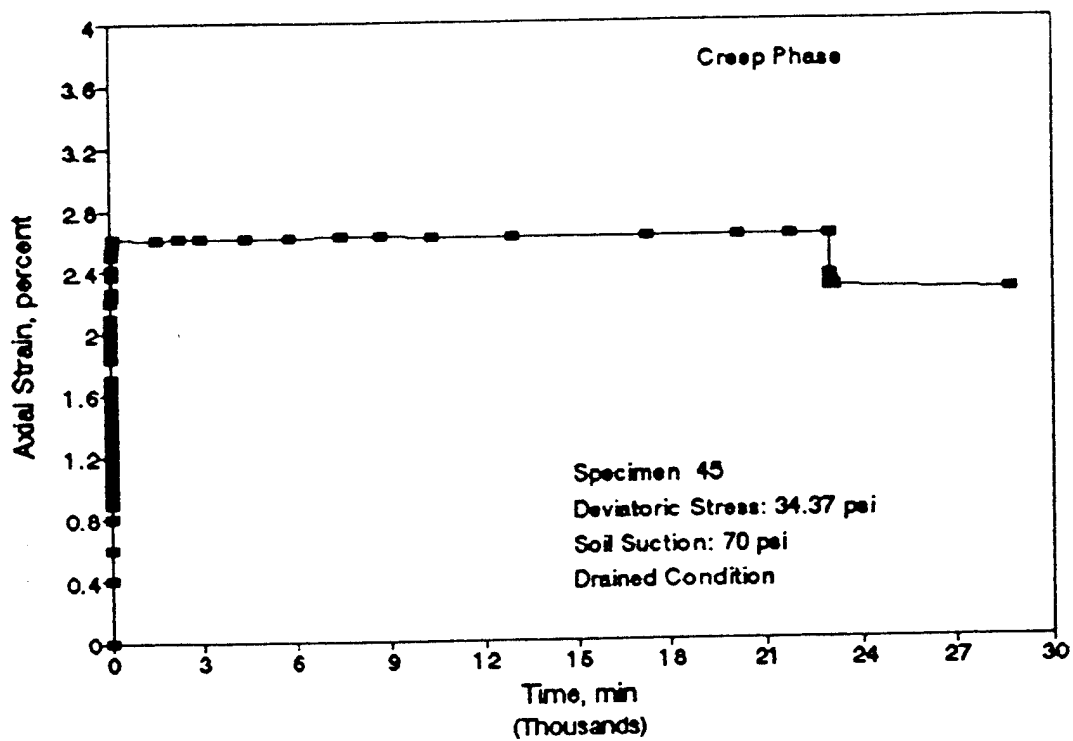


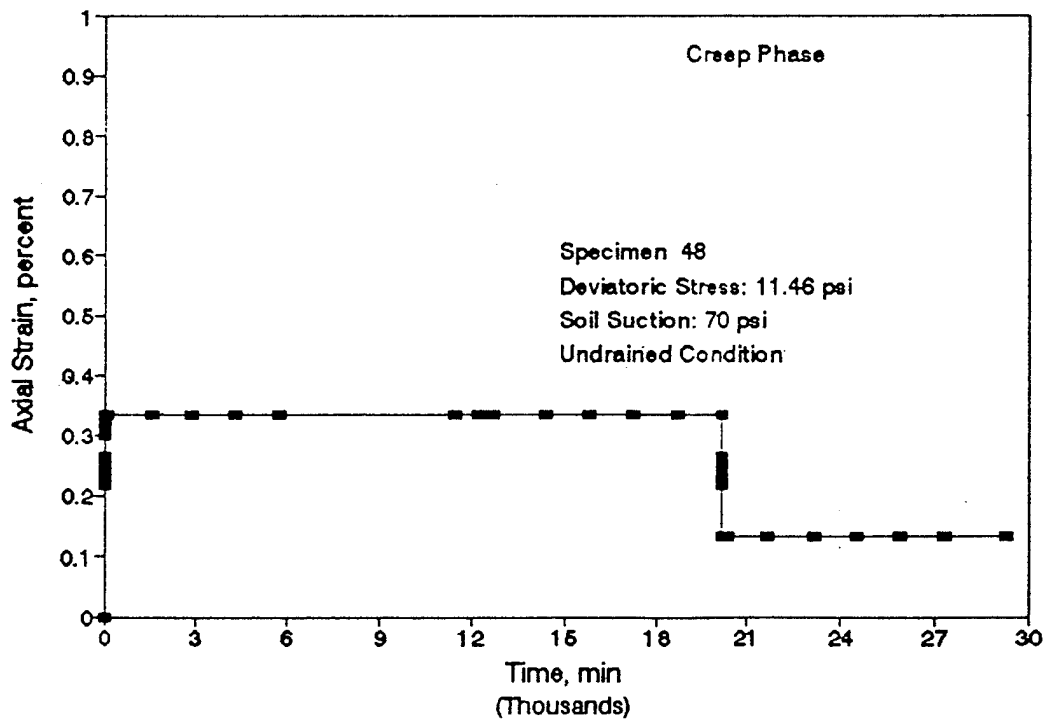
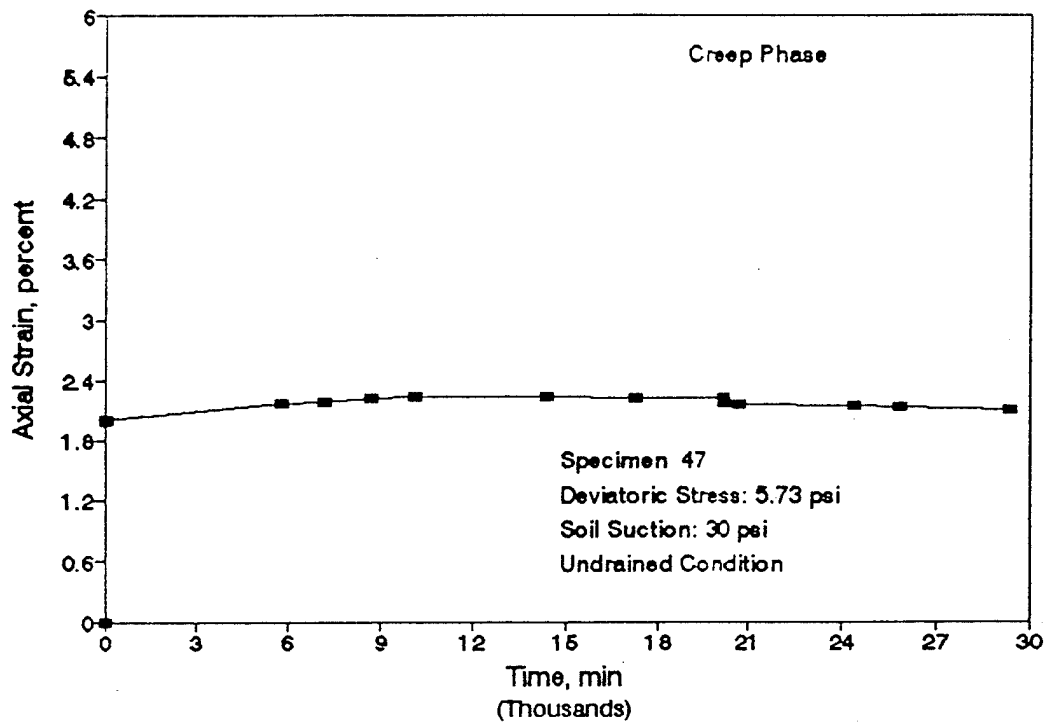


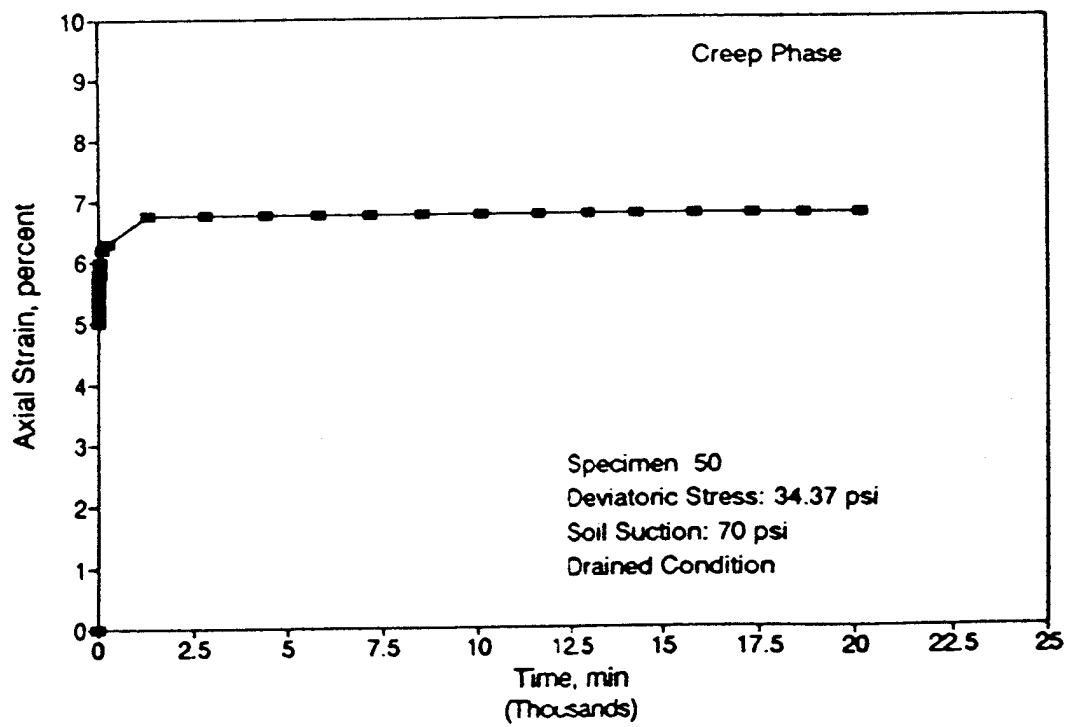
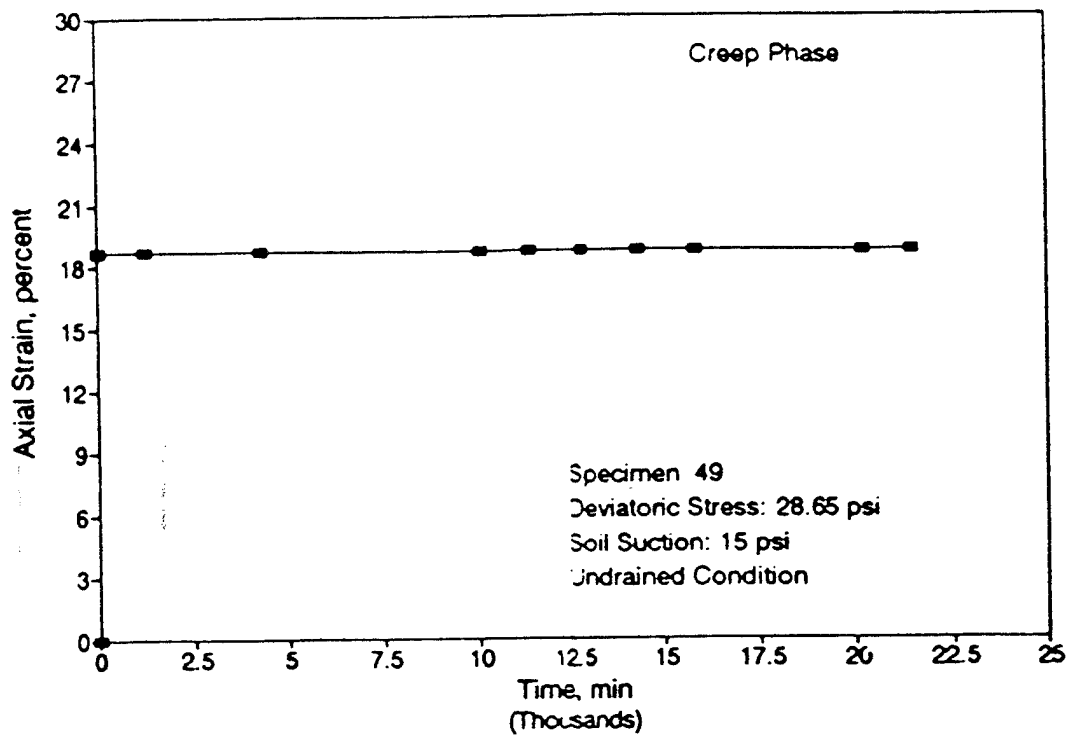


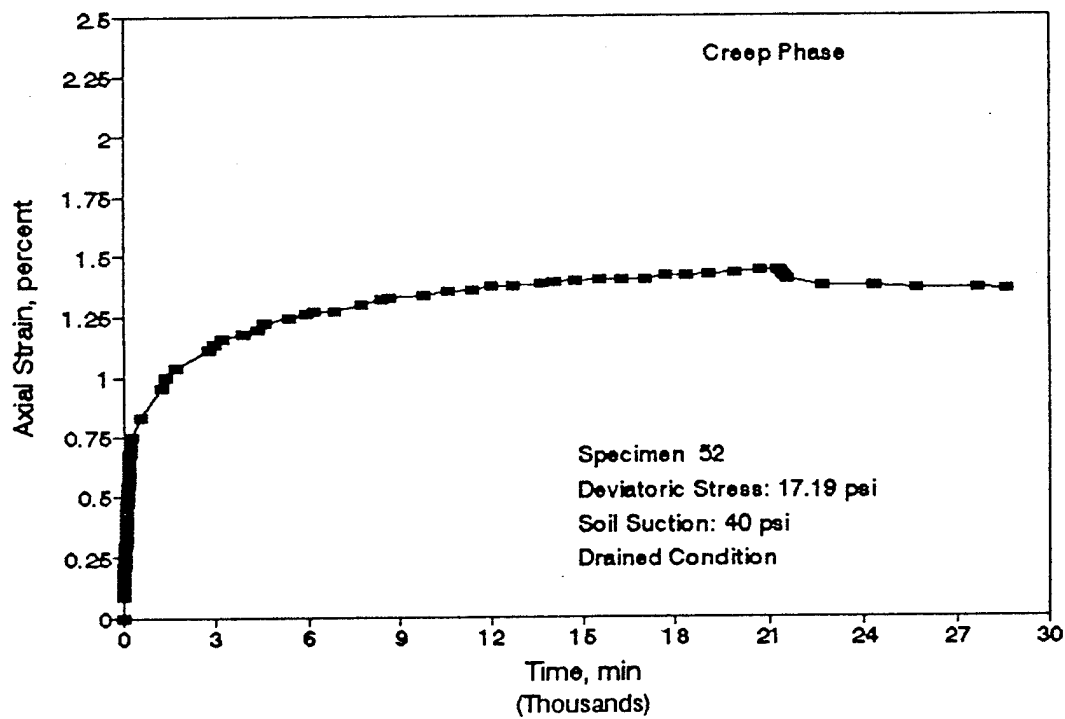
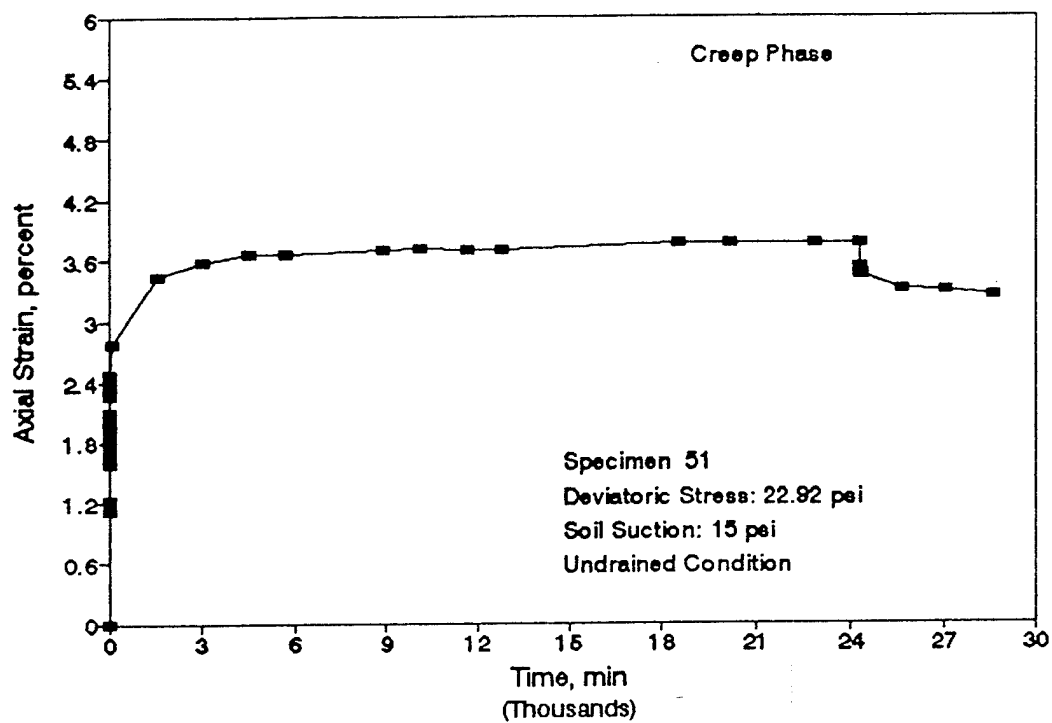




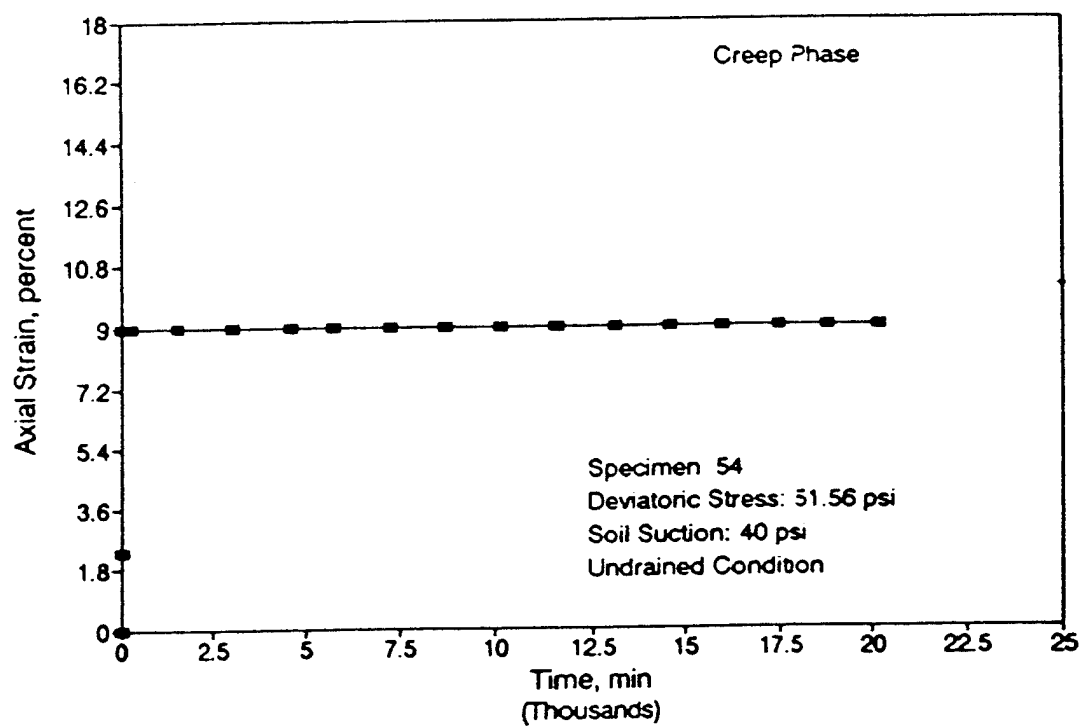
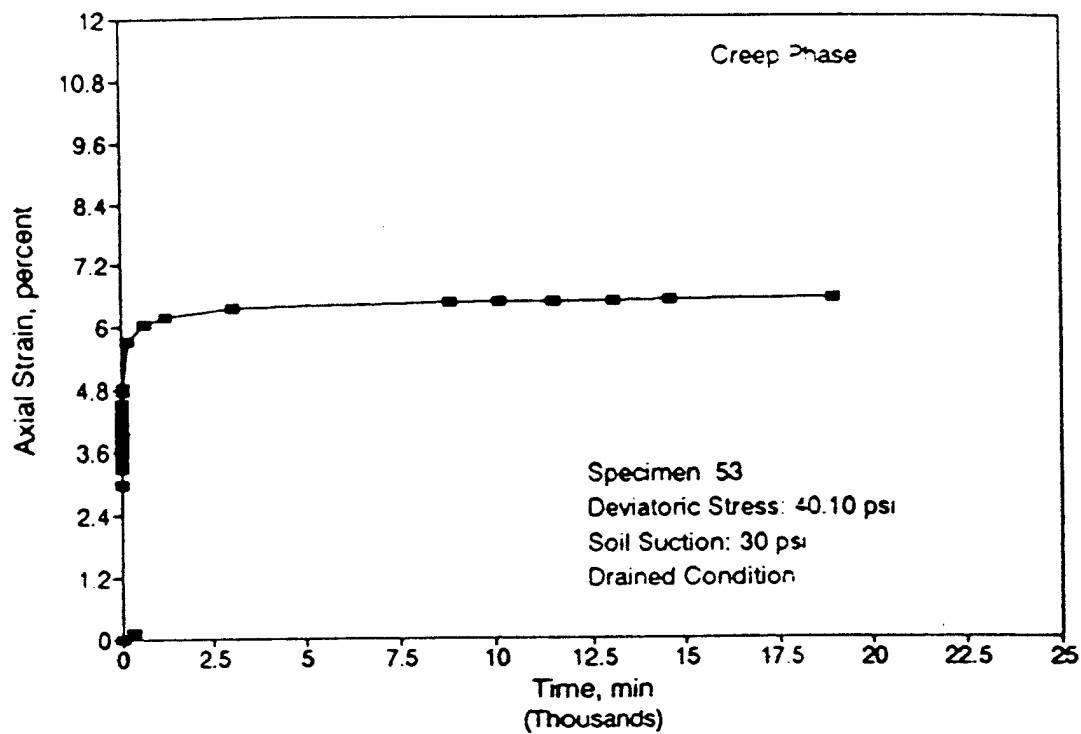


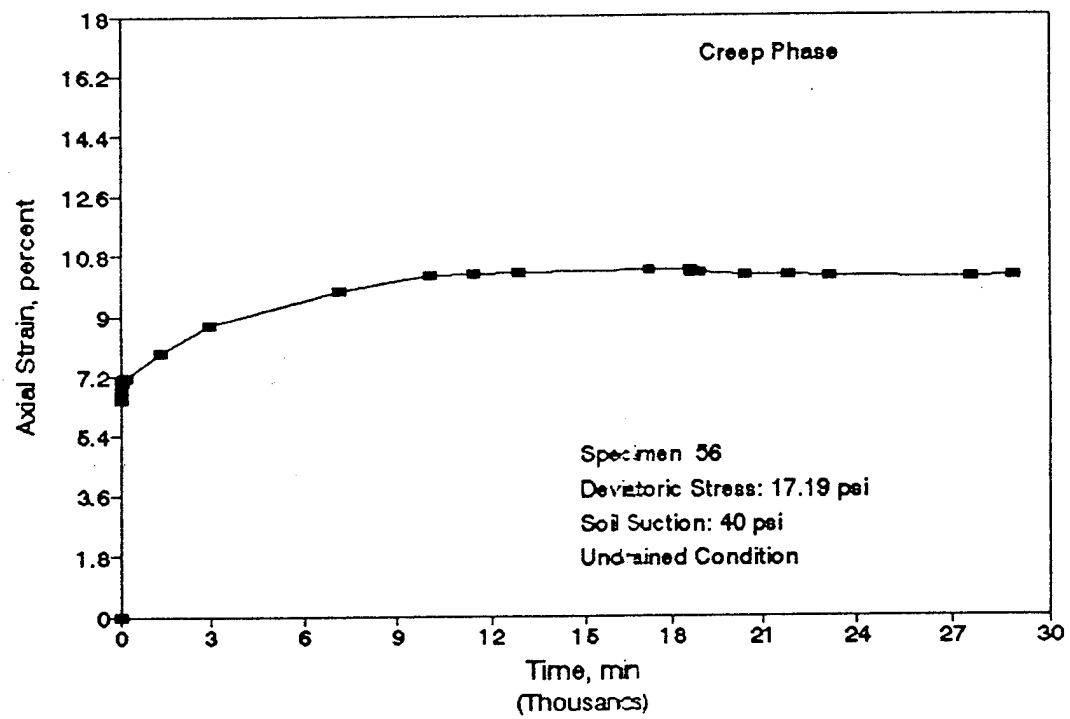
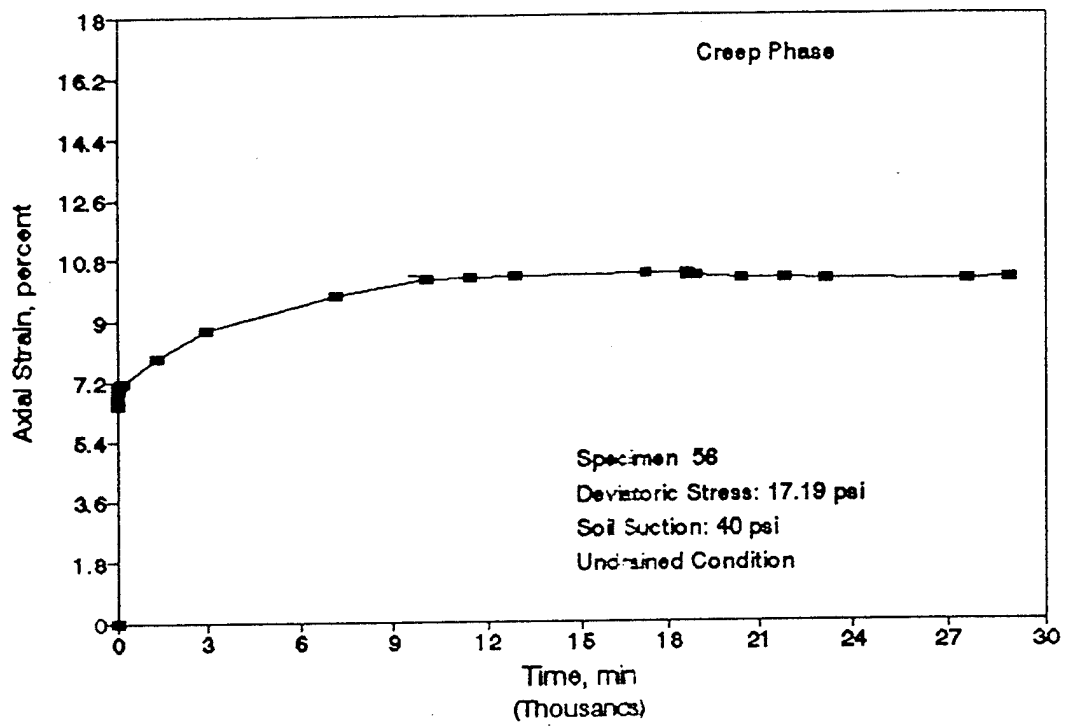


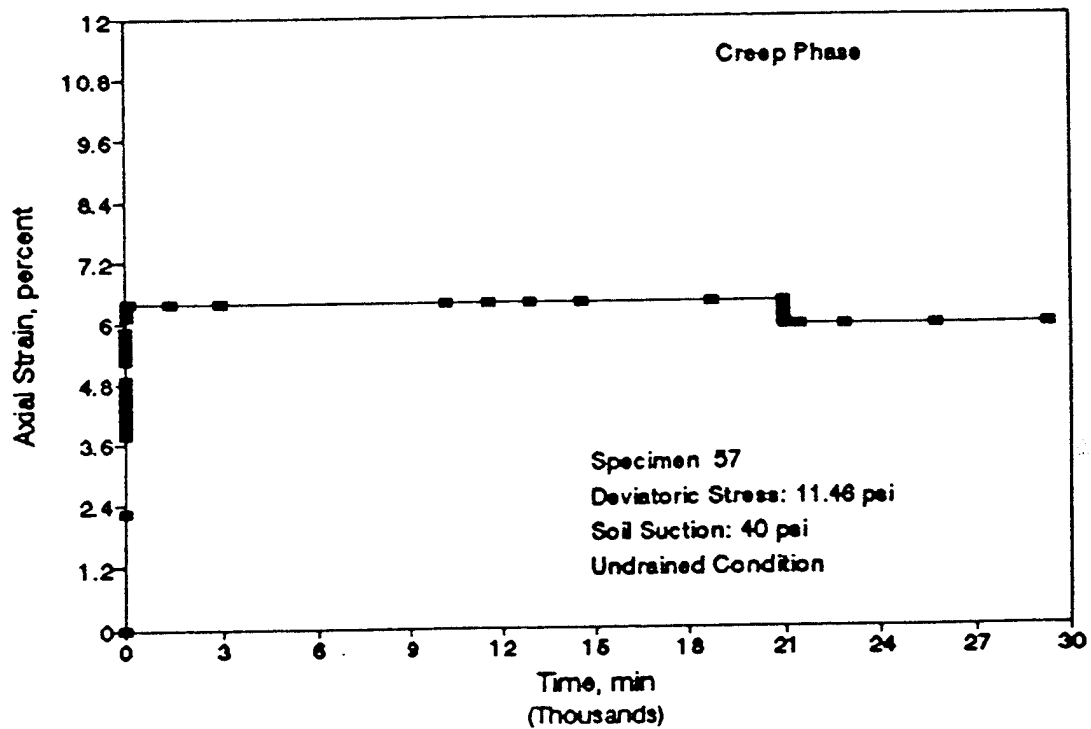
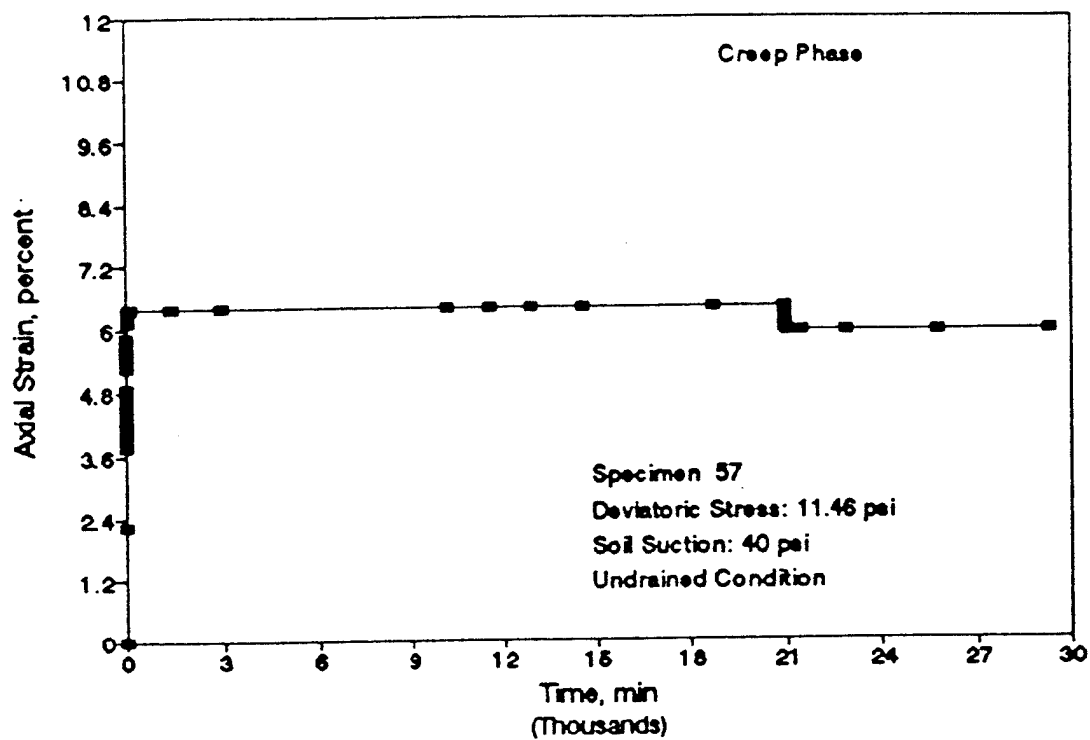


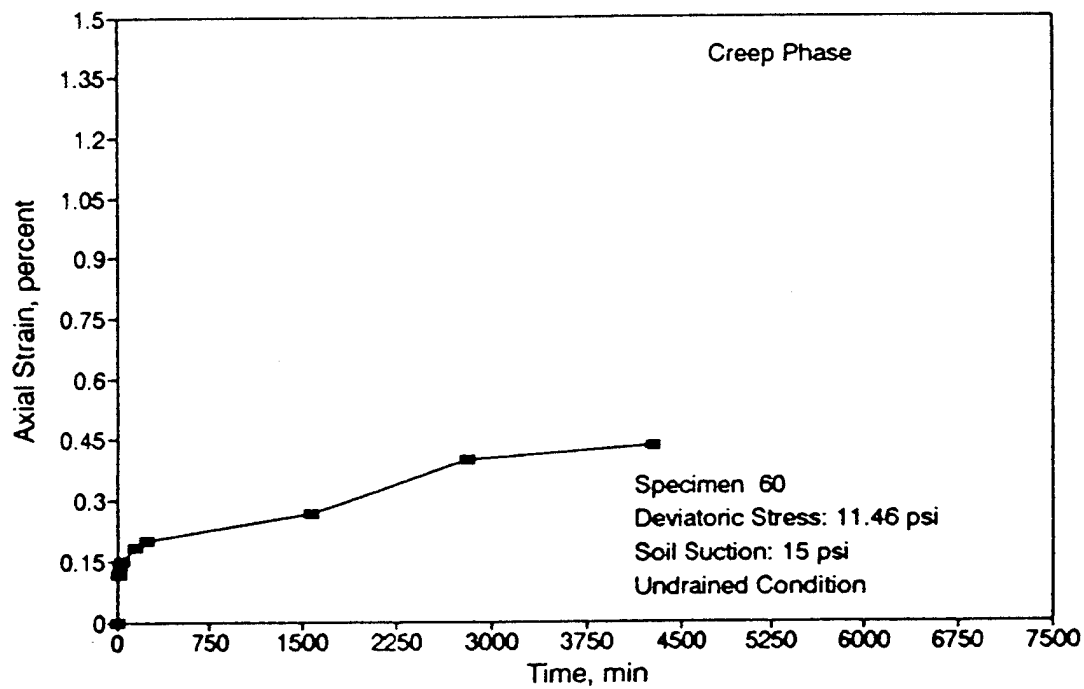
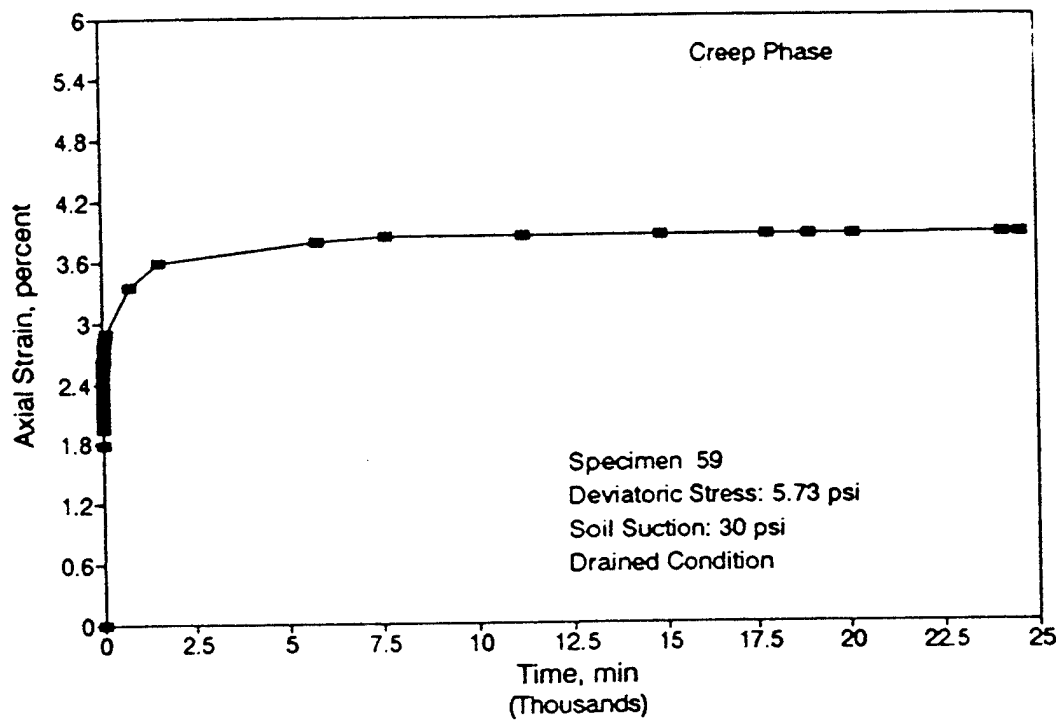


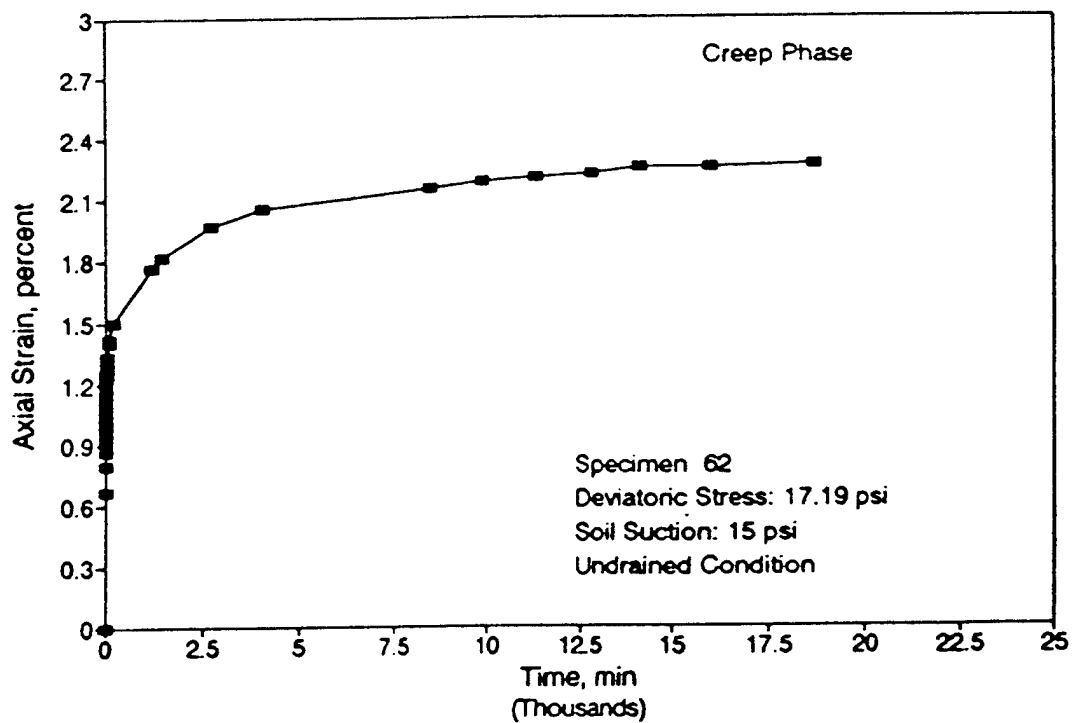
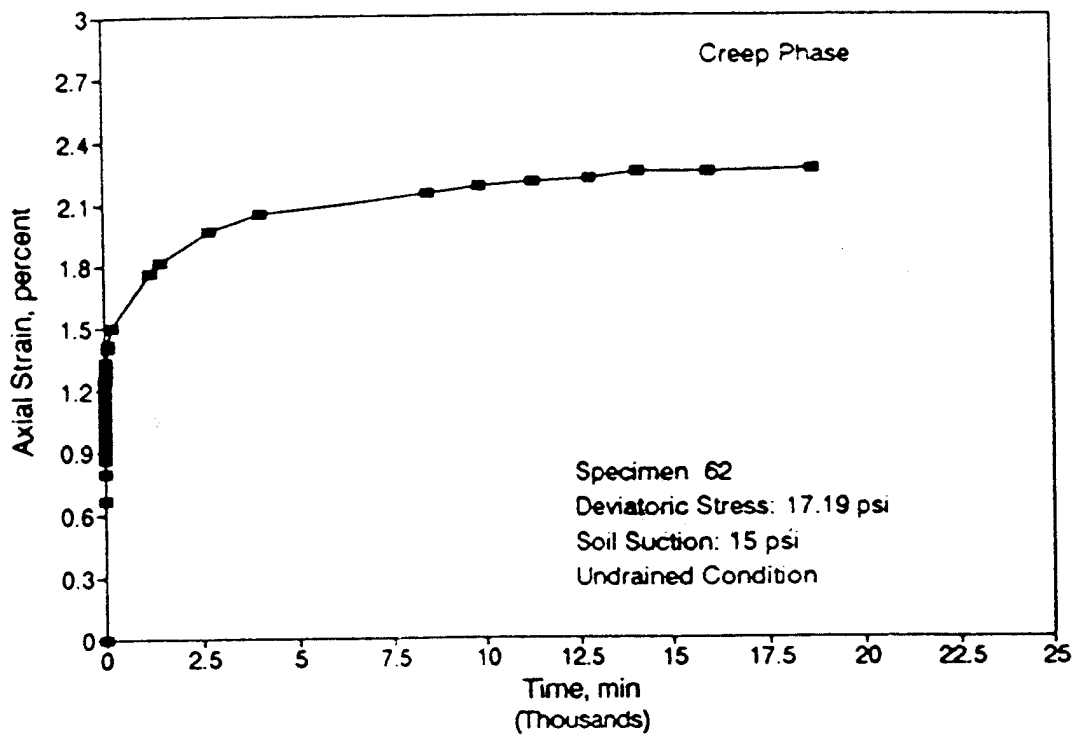




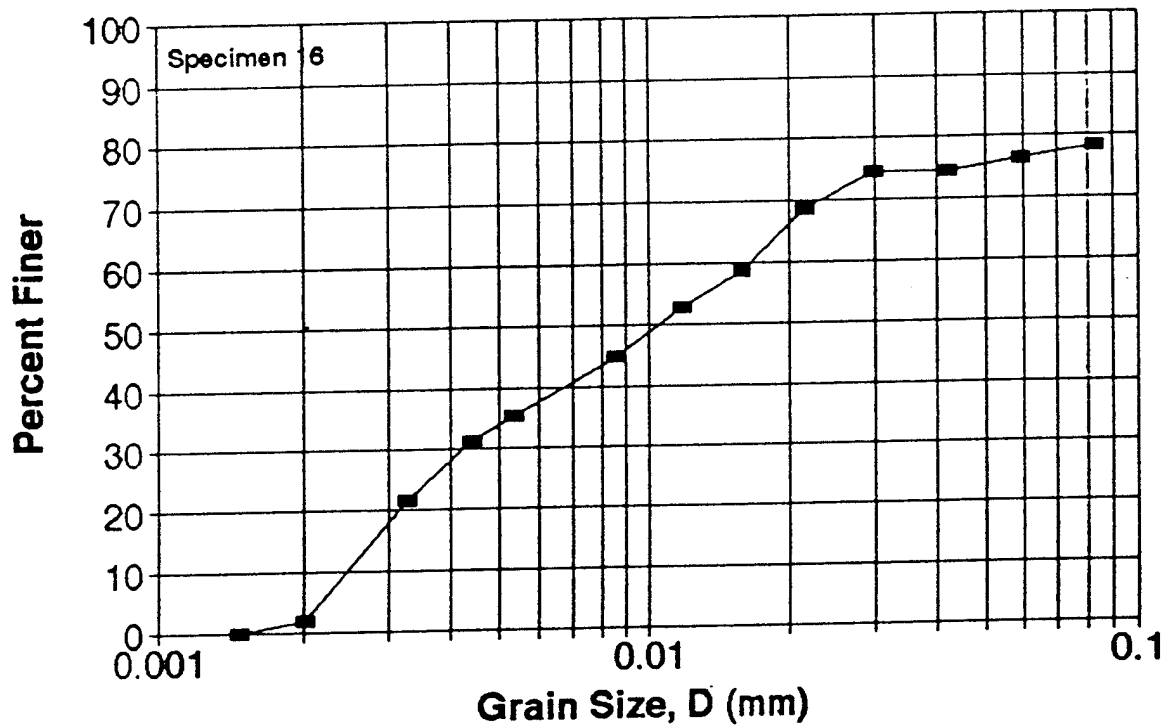
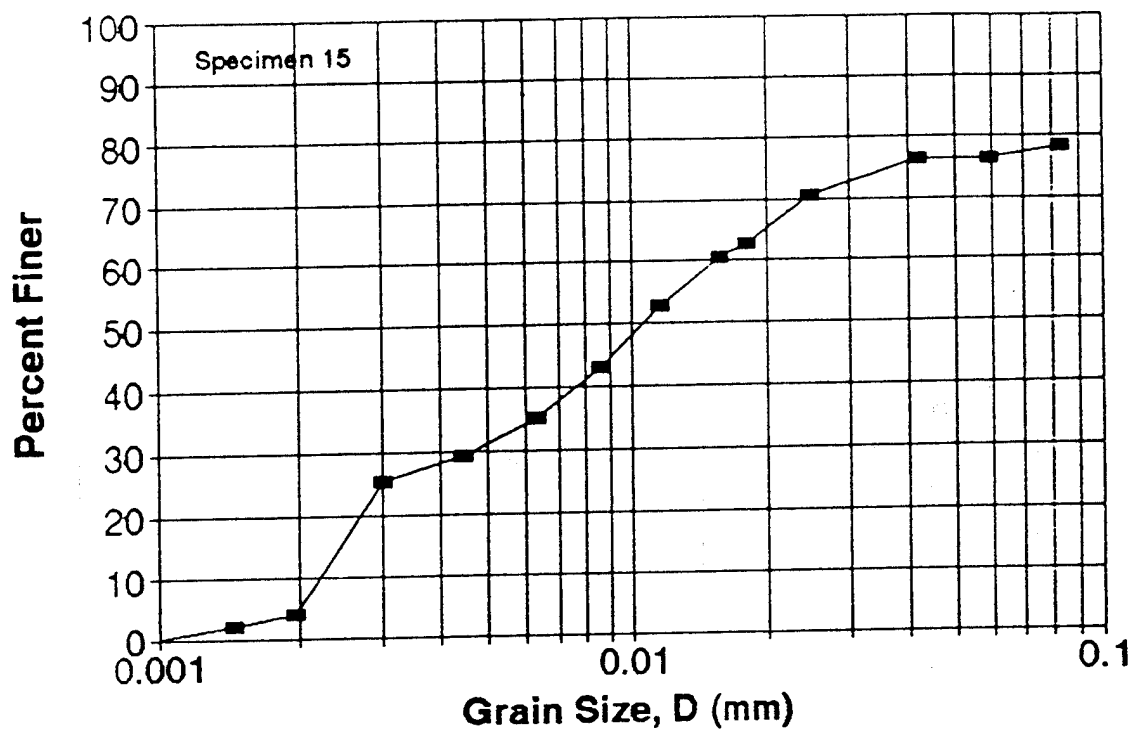


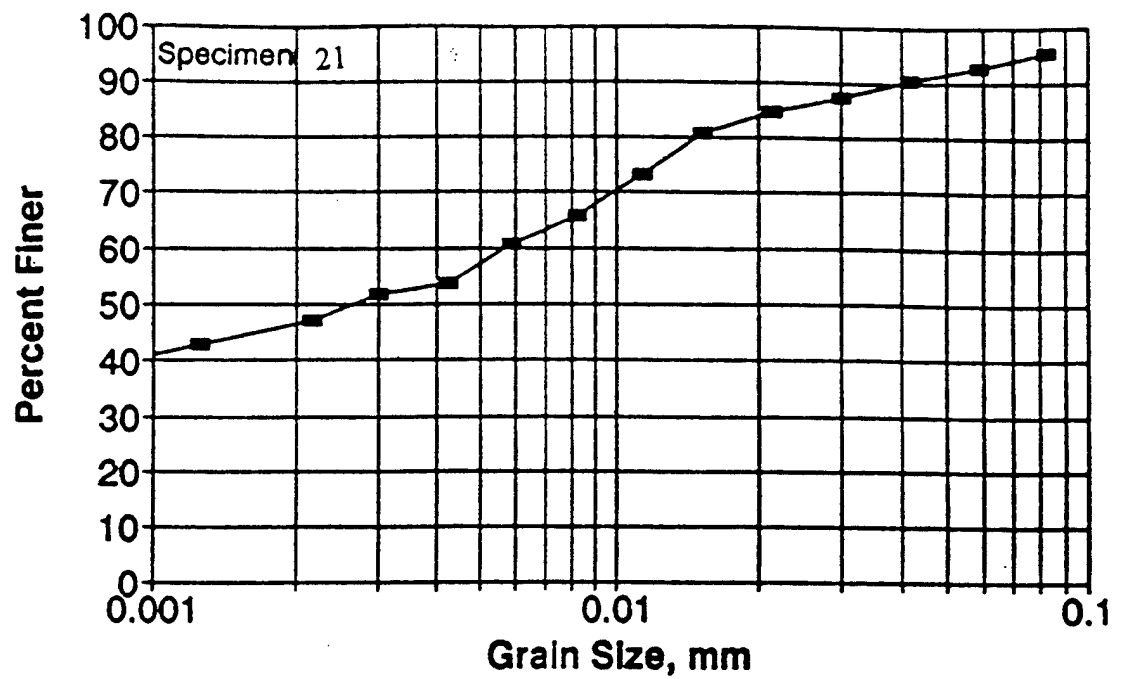
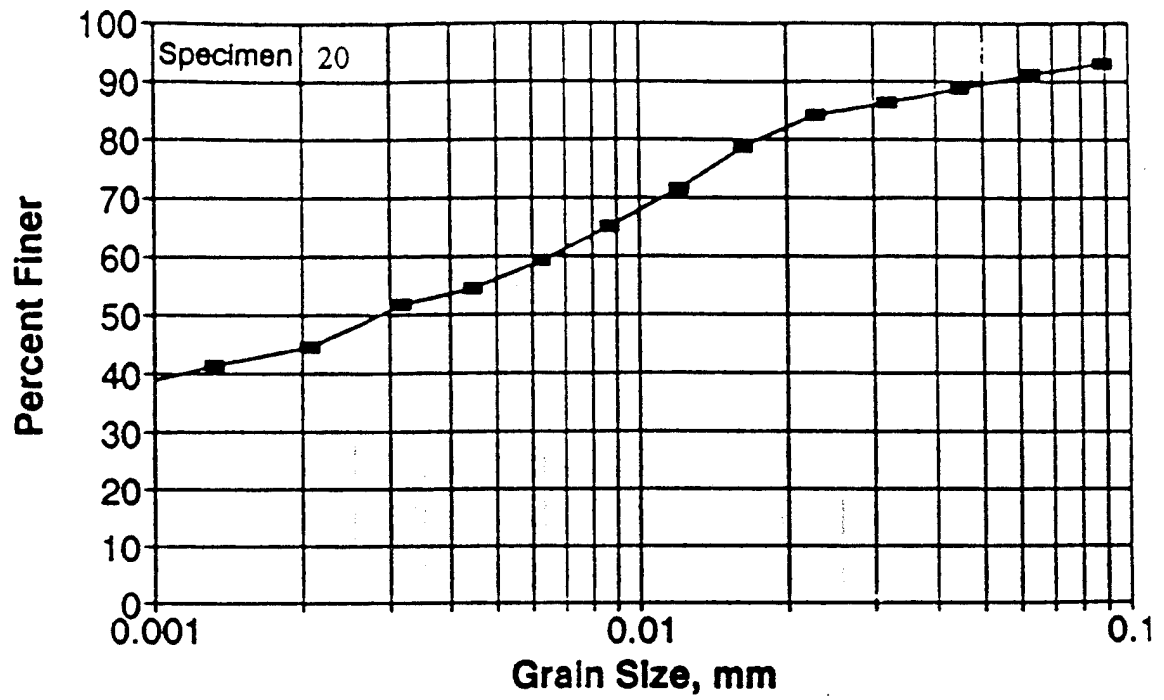




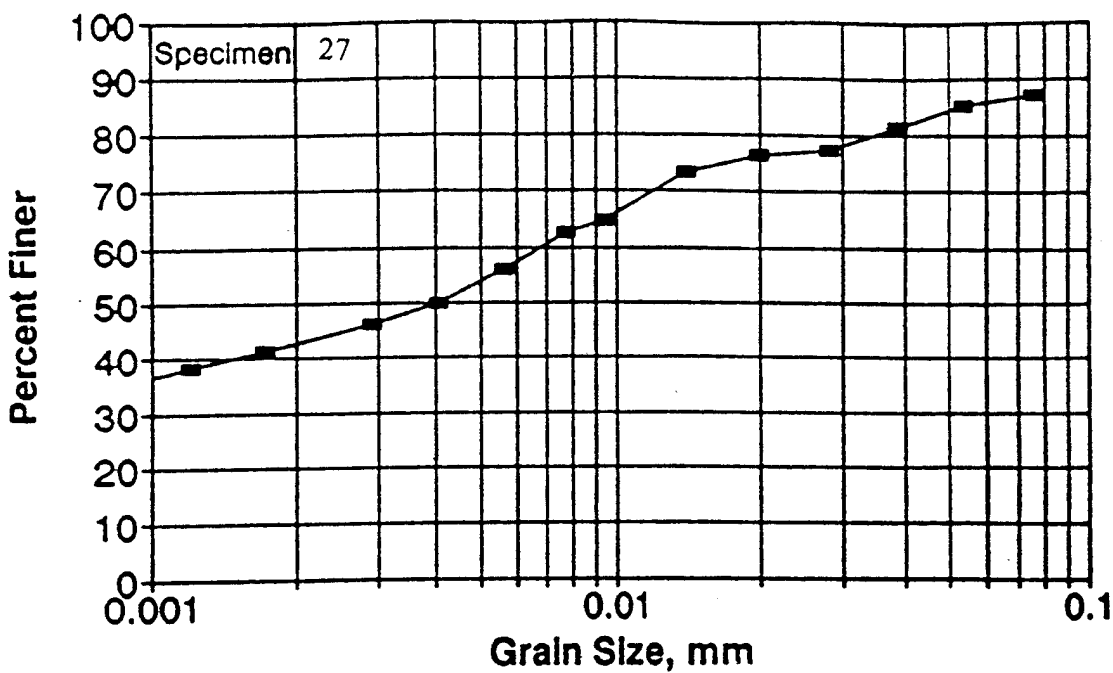
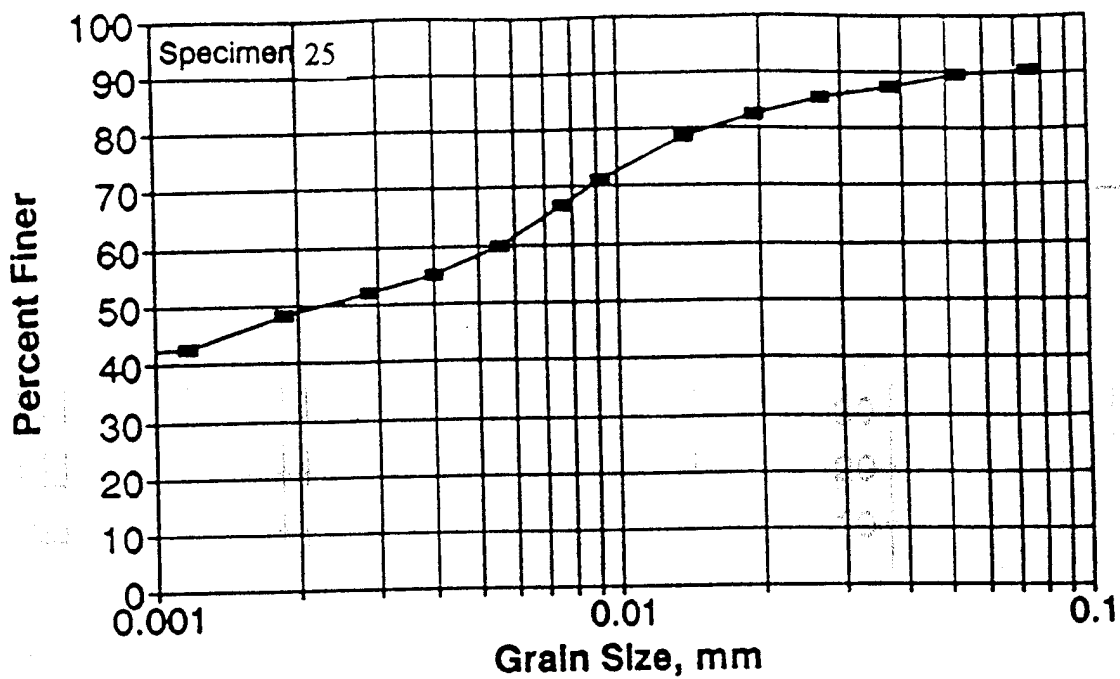


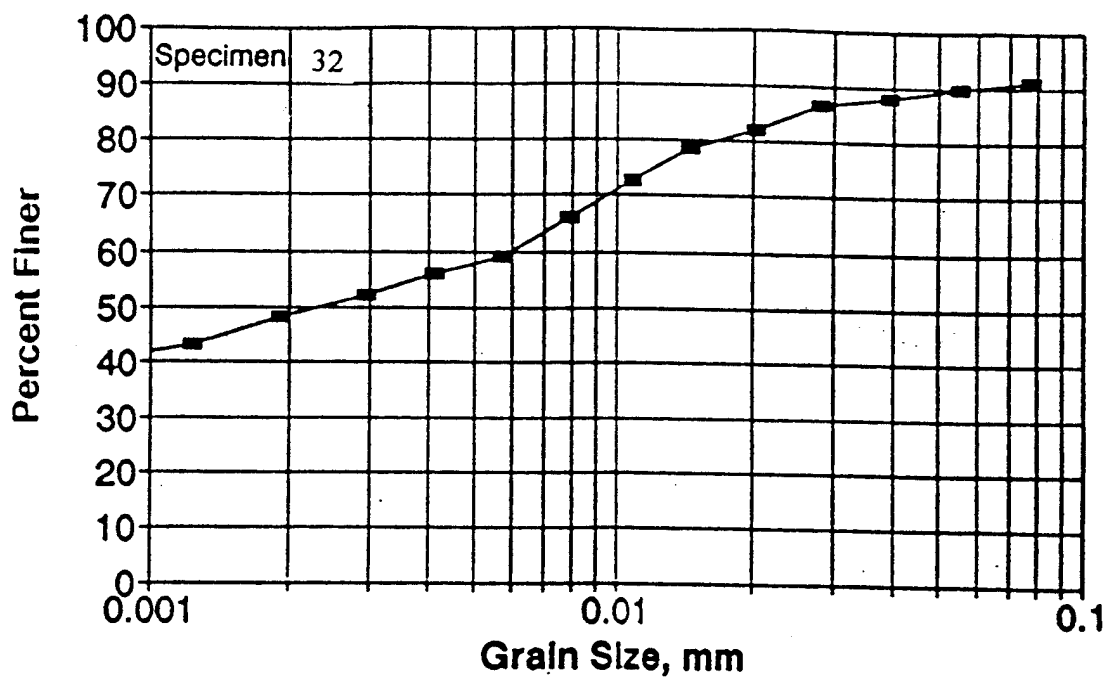
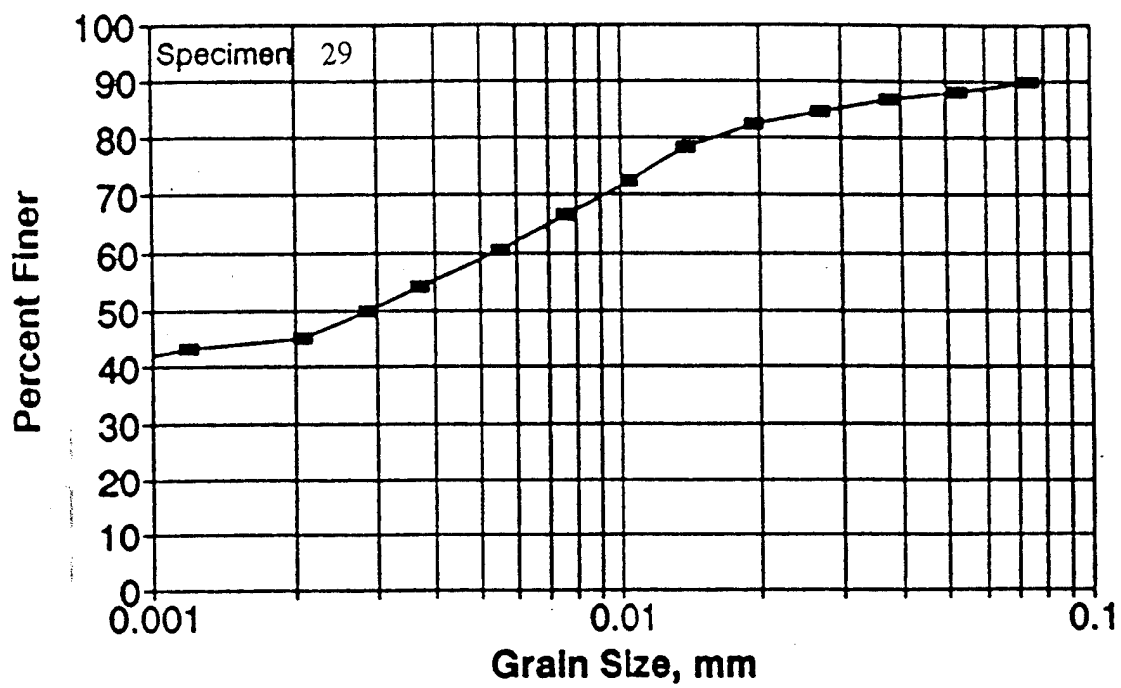
**APPENDIX D**  
**RESULTS OF GRAIN SIZE ANALYSIS**

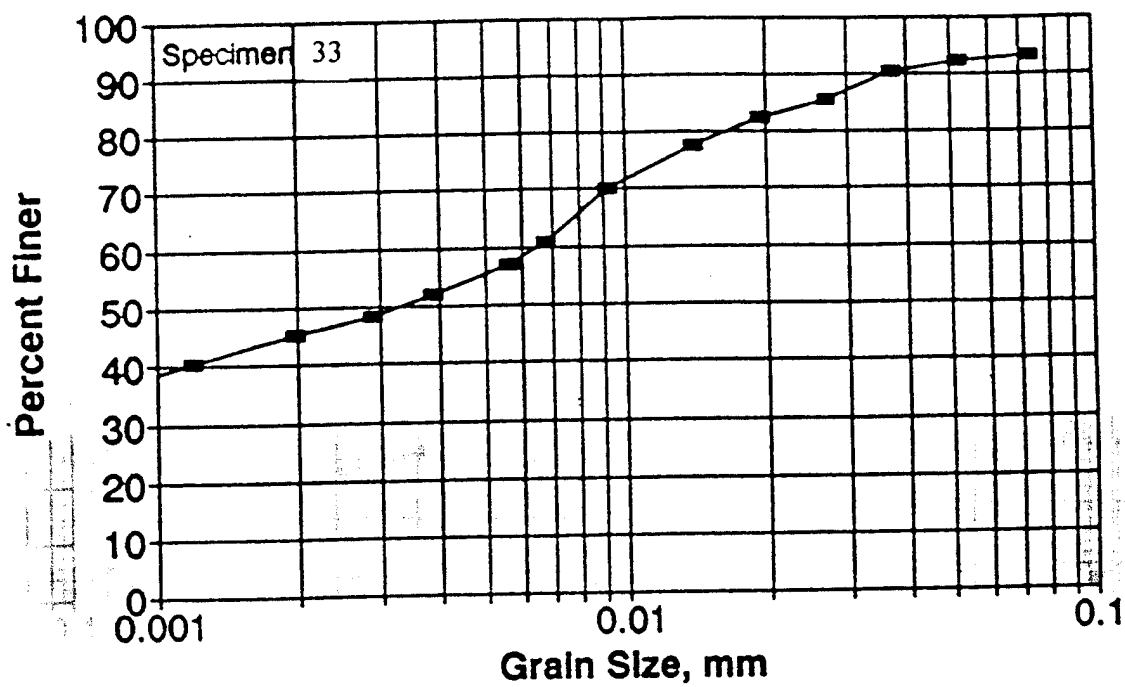














**APPENDIX E**

**DATA OF EXTERNAL VERSUS INTERNAL LOAD CELL READINGS FOR**

**SYNTHETIC SPECIMENS**

# Load Cell Readings

## External vs. Internal

Initial Readings are 10.0 lb for External and 17.7 lb for Internal

MTS Program No.	Programmed Peak Load lb	Final Cell Reading		Corrected Reading	
		External	Internal	External	Internal
		lb	lb	lb	lb
75	20	30.2	37.8	20.2	20.1
76	40	49.4	56.9	39.4	39.2
77	60	69.9	77.2	59.9	59.5
78	80	89.6	96.7	79.6	79
79	100	109	116	99	98.3
80	150	157.9	164.4	147.9	146.7
81	200	206.5	212.5	196.5	194.8
82	250	254.1	259.8	244.1	242.1
83	300	300.3	305.7	290.3	288
84	350	345.8	350.7	335.8	333
85	400	394.2	398.3	384.2	380.6
86	450	442.7	446.7	432.7	429
75	20	29.2	36.8	19.2	19.1
76	40	49.3	56.9	39.3	39.2
77	60	69.7	76.8	59.7	59.1
78	80	89.3	96.7	79.3	79
79	100	108.9	115.7	98.9	98
80	150	157.6	164	147.6	146.3
81	200	206.1	212	196.1	194.3
82	250	254.5	260.3	244.5	242.6
83	300	300.1	305.4	290.1	287.7
84	350	346.2	351.1	336.2	333.4
85	400	392.05	396.5	382.05	378.8
86	450	441.1	445.1	431.1	427.5

### Notes:

- (1) Young modulus of specimen, 2430 psi.
- (2) Confining pressure applied, 0 psi.
- (3) Corrected readings obtained by subtracting the initial reading from the final reading.

Load Cell Readings  
External vs. Internal

Initial Readings are 98.65 lb for External and 41.6 lb for Internal

MTS Program No.	Programmed Peak Load lb	Final Cell Reading		Corrected Reading	
		External	Internal	External	Internal
		lb	lb	lb	lb
75	20	118.25	64.1	19.6	22.5
76	40	137.35	84.7	38.7	43.1
77	60	157.05	99.8	58.4	58.2
78	80	176.25	118.7	77.6	77.1
79	100	195.95	138.1	97.3	96.5
80	150	245.55	186.3	146.9	144.7
81	200	295.4	249	196.75	207.4
82	250	345	265.6	246.35	224
83	300	394.5	308.3	295.85	266.7
84	350	443.5	360.7	344.85	319.1
85	400	493.5	403	394.85	361.4
86	450	542.7	454.3	444.05	412.7
75	20	117.95	64.4	19.3	22.8
76	40	137.35	82.4	38.7	40.8
77	60	156.9	103.2	58.25	61.6
78	80	176	120.3	77.35	78.7
79	100	196	142	97.35	100.4
80	150	246.15	185.7	147.5	144.1
81	200	295.8	227.9	197.15	186.3
82	250	345.2	263.5	246.55	221.9
83	300	394.55	329.8	295.9	288.2
84	350	443.55	362.4	344.9	320.8
85	400	492.8	405.7	394.15	364.1
86	450	542.45	455.6	443.8	414

Notes:

- (1) Young modulus of specimen, 2430 psi.
- (2) Confining pressure applied, 50 psi.
- (3) Corrected readings obtained by subtracting the initial reading from the final reading.

Load Cell Readings  
External vs. Internal

Initial Readings are 116.9 lb for External and 99.4 lb for Internal

MTS Program No.	Programmed Peak Load lb	Final Cell Reading		Corrected Reading	
		External	Internal	External	Internal
		lb	lb	lb	lb
75	20	135.65	121.1	18.75	21.7
76	40	155.9	140.6	39	41.2
77	60	175.3	159.2	58.4	59.8
78	80	194.9	178.9	78	79.5
79	100	214.35	195.6	97.45	96.2
80	150	263.6	246.5	146.7	147.1
81	200	313.2	289.7	196.3	190.3
82	250	361.9	334.8	245	235.4
83	300	411.8	380.1	294.9	280.7
84	350	460.85	425.4	343.95	326
85	400	510.1	467.6	393.2	368.2
86	450	560	507.5	443.1	408.1
75	20	136.15	119.9	19.25	20.5
76	40	155.9	142	39	42.6
77	60	175.4	158.8	58.5	59.4
78	80	195.05	176.1	78.15	76.7
79	100	214.55	197.5	97.65	98.1
80	150	264.35	246.3	147.45	146.9
81	200	313.6	295.4	196.7	196
82	250	362.45	335	245.55	235.6
83	300	411.7	379.6	294.8	280.2
84	350	461.1	426.1	344.2	326.7
85	400	510.25	467.2	393.35	367.8
86	450	559.25	508.8	442.35	409.4

Notes:

- (1) Young modulus of specimen, 2430 psi.
- (2) Confining pressure applied, 100 psi.
- (3) Corrected readings obtained by subtracting the initial reading from the final reading.

Load Cell Readings  
External vs. Internal

Initial Readings are 161.8 lb for External and 146.0 lb for Internal

MTS Program No.	Programmed Peak Load lb	Final Cell Reading		Corrected Reading	
		External	Internal	External	Internal
		lb	lb	lb	lb
75	20	181.3	167.1	19.5	21.1
76	40	200.9	189.5	39.1	43.5
77	60	220.3	204.9	58.5	58.9
78	80	239.85	230.1	78.05	84.1
79	100	260	242.4	98.2	96.4
80	150	308.9	288.7	147.1	142.7
81	200	358.05	336.6	196.25	190.6
82	250	407.95	379.2	246.15	233.2
83	300	456.55	431.7	294.75	285.7
84	350	505.55	475.5	343.75	329.5
85	400	555	516.6	393.2	370.6
86	450	604.45	562.4	442.65	416.4
75	20	181.15	167.2	19.35	21.2
76	40	200.95	189.2	39.15	43.2
77	60	220.25	205.4	58.45	59.4
78	80	239.9	227.6	78.1	81.6
79	100	259.7	243.9	97.9	97.9
80	150	308.8	295.8	147	149.8
81	200	357.95	332.5	196.15	186.5
82	250	407.3	380.9	245.5	234.9
83	300	457.05	428.6	295.25	282.6
84	350	505.5	475.4	343.7	329.4
85	400	555.2	521.8	393.4	375.8
86	450	603.9	568.1	442.1	422.1

Notes:

- (1) Young modulus of specimen, 2430 psi.
- (2) Confining pressure applied, 150 psi.
- (3) Corrected readings obtained by subtracting the initial reading from the final reading.



Load Cell Readings  
External vs. Internal

Initial Readings are 185.45 lb for External and 171.4 lb for Internal

MTS Program No.	Programmed Peak Load lb	Final Cell Reading		Corrected Reading	
		External lb	Internal lb	External lb	Internal lb
75	20	204.5	190.6	19.05	19.2
76	40	224.7	211.8	39.25	40.4
77	60	244.05	228.1	58.6	56.7
78	80	263.6	242.4	78.15	71
79	100	283.2	263.5	97.75	92.1
80	150	332.5	309.7	147.05	138.3
81	200	381.65	360.8	196.2	189.4
82	250	430.85	405	245.4	233.6
83	300	479.9	446.6	294.45	275.2
84	350	529.05	493.5	343.6	322.1
85	400	578.55	539.4	393.1	368
86	450	626.95	584.5	441.5	413.1
75	20	204.6	190.3	19.15	18.9
76	40	224.65	210.7	39.2	39.3
77	60	244	233.4	58.55	62
78	80	263.6	244.6	78.15	73.2
79	100	283.2	265.1	97.75	93.7
80	150	332.3	313.2	146.85	141.8
81	200	381.9	356.8	196.45	185.4
82	250	431.1	399	245.65	227.6
83	300	479.9	448.1	294.45	276.7
84	350	528.95	498.2	343.5	326.8
85	400	577.95	539.3	392.5	367.9
86	450	626.9	589.7	441.45	418.3

Notes:

- (1) Young modulus of specimen, 2430 psi.
- (2) Confining pressure applied, 200 psi.
- (3) Corrected readings obtained by subtracting the initial reading from the final reading.

# Load Cell Readings

## External vs. Internal

Initial Readings are 10.0 lb for External and 17.7 lb for Internal

MTS Program No.	Programmed Peak Load lb	Final Cell Reading		Corrected Reading	
		External	Internal	External	Internal
		lb	lb	lb	lb
75	20	29.2	36.6	19.2	18.9
76	40	48	55.6	38	37.9
77	60	67.7	74.5	57.7	56.8
78	80	86.5	93.4	76.5	75.7
79	100	105.95	112.4	95.95	94.7
80	150	154.75	161.2	144.75	143.5
81	200	203	208.9	193	191.2
82	250	250.75	256.2	240.75	238.5
83	300	298.9	304	288.9	286.3
84	350	347.9	352.5	337.95	334.8
85	400	395.95	400.5	385.95	382.8
86	450	448.4	452.2	438.4	434.5
75	20	28	35.6	18	17.9
76	40	47.4	55	37.4	37.3
77	60	66.8	74.1	56.8	56.4
78	80	86.4	93.8	76.4	76.1
79	100	105.7	113	95.7	95.3
80	150	154.45	161.4	144.45	143.7
81	200	203.25	209.8	193.25	192.1
82	250	251.9	258	241.9	240.3
83	300	300.35	306	290.35	288.3
84	350	348.9	354	338.9	336.3
85	400	397.45	402.2	387.45	384.5
86	450	447.95	451.7	437.95	433.9

### Notes:

- (1) Young modulus of specimen, 10070 psi.
- (2) Confining pressure applied, 0 psi.
- (3) Corrected readings obtained by subtracting the initial reading from the final reading.

# Load Cell Readings

## External vs. Internal

Initial Readings are 56.3 lb for External and 73.6 lb for Internal

MTS Program No.	Programmed Peak Load lb	Final Cell Reading		Corrected Reading	
		External	Internal	External	Internal
		lb	lb	lb	lb
75	20	75.75	95.1	19.45	21.5
76	40	95.6	109.5	39.3	35.9
77	60	115.2	131.5	58.9	57.9
78	80	135.55	149.6	79.25	76
79	100	154.85	166.7	98.55	93.1
80	150	204.5	208.4	148.2	134.8
81	200	254.1	263.3	197.8	189.7
82	250	304.6	310.4	248.3	236.8
83	300	353.95	360.5	297.65	286.9
84	350	402.3	401.5	346	327.9
85	400	452.9	448.2	396.6	374.6
86	450	501.2	487	444.9	413.4
75	20	76.05	88.9	19.75	15.3
76	40	95.45	115.1	39.15	41.5
77	60	115.65	134.3	59.35	60.7
78	80	135.35	150.8	79.05	77.2
79	100	155.2	167.6	98.9	94
80	150	205.3	211.8	149	138.2
81	200	253.75	256.7	197.45	183.1
82	250	303.2	307.5	246.9	233.9
83	300	353.3	357.6	297	284
84	350	403.15	405.8	346.85	332.2
85	400	451.95	443.6	395.65	370
86	450	501.4	439	445.1	365.4

### Notes:

- (1) Young modulus of specimen, 10070 psi.
- (2) Confining pressure applied, 50 psi.
- (3) Corrected readings obtained by subtracting the initial reading from the final reading.

Load Cell Readings  
External vs. Internal

Initial Readings are 69.9 lb for External and 116.7 lb for Internal

MTS Program No.	Programmed Peak Load lb	Final Cell Reading		Corrected Reading	
		External	Internal	External	Internal
		lb	lb	lb	lb
75	20	89.15	136	19.25	19.3
76	40	109.5	154.4	39.6	37.7
77	60	129.3	180.7	59.4	64
78	80	149.1	191.7	79.2	75
79	100	169.05	209	99.15	92.3
80	150	218.45	256.4	148.55	139.7
81	200	267.7	306.6	197.8	189.9
82	250	317	352.4	247.1	235.7
83	300	366.5	396.1	296.6	279.4
84	350	415.5	439.9	345.6	323.2
85	400	464.7	484.2	394.8	367.5
86	450	511.05	514.7	441.15	398
75	20	89.4	135	19.5	18.3
76	40	109.45	155.4	39.55	38.7
77	60	129.4	173.8	59.5	57.1
78	80	149	187.4	79.1	70.7
79	100	168.7	209.7	98.8	93
80	150	218.35	253.4	148.45	136.7
81	200	267.35	283.8	197.45	167.1
82	250	320.95	360.3	251.05	243.6
83	300	366.7	399.4	296.8	282.7
84	350	415.3	433.2	345.4	316.5
85	400	464.65	476	394.75	359.3
86	450	511.3	526.7	441.4	410

Notes:

- (1) Young modulus of specimen, 10070 psi.
- (2) Confining pressure applied, 100 psi.
- (3) Corrected readings obtained by subtracting the initial reading from the final reading.

# Load Cell Readings

## External vs. Internal

Initial Readings are 129 lb for External and 130.3 lb for Internal

MTS Program No.	Programmed Peak Load lb	Final Cell Reading		Corrected Reading	
		External	Internal	External	Internal
		lb	lb	lb	lb
75	20	147.75	145.5	18.75	15.2
76	40	168.3	167.6	39.3	37.3
77	60	187.75	188.6	58.75	58.3
78	80	207.4	204	78.4	73.7
79	100	227.15	222	98.15	91.7
80	150	276.05	266.3	147.05	136
81	200	325.5	315.9	196.5	185.6
82	250	374.5	361.1	245.5	230.8
83	300	423.25	413.9	294.25	283.6
84	350	471.95	462.1	342.95	331.8
85	400	521.15	504.9	392.15	374.6
86	450	569.2	545.3	440.2	415
75	20	148.5	149.9	19.5	19.6
76	40	168.2	169.6	39.2	39.3
77	60	187.8	189.3	58.8	59
78	80	207.3	204.6	78.3	74.3
79	100	227	227.1	98	96.8
80	150	276.2	267.3	147.2	137
81	200	325.05	316.5	196.05	186.2
82	250	374.4	364.4	245.4	234.1
83	300	423.35	410.1	294.35	279.8
84	350	471.9	448.8	342.9	318.5
85	400	520.9	501	391.9	370.7
86	450	568.65	548.3	439.65	418

### Notes:

- (1) Young modulus of specimen, 10070 psi.
- (2) Confining pressure applied, 150 psi.
- (3) Corrected readings obtained by subtracting the initial reading from the final reading.

# Load Cell Readings

## External vs. Internal

Initial Readings are 153.7 lb for External and 133.2 lb for Internal

MTS Program No.	Programmed Peak Load lb	Final Cell Reading		Corrected Reading	
		External lb	Internal lb	External lb	Internal lb
75	20	171.4	146.7	17.7	13.5
76	40	192.3	171.8	38.6	38.6
77	60	212.3	190.6	58.6	57.4
78	80	232.6	202.8	78.9	69.6
79	100	251.95	228.7	98.25	95.5
80	150	301.4	270.9	147.7	137.7
81	200	350.25	326.9	196.55	193.7
82	250	399.4	361.4	245.7	228.2
83	300	448	421.2	294.3	288
84	350	496.75	463.2	343.05	330
85	400	545.75	501.8	392.05	368.6
86	450	594.65	552.5	440.95	419.3
75	20	174.35	152.8	20.65	19.6
76	40	193.3	172.8	39.6	39.6
77	60	213.45	189.2	59.75	56
78	80	232.35	205	78.65	71.8
79	100	252.1	225.2	98.4	92
80	150	301.4	272.9	147.7	139.7
81	200	350.6	329.1	196.9	195.9
82	250	399.25	363.1	245.55	229.9
83	300	448.3	414.7	294.6	281.5
84	350	496.85	452.9	343.15	319.7
85	400	545.8	498.8	392.1	365.6
86	450	594.65	556.6	440.95	423.4

Notes:

- (1) Young modulus of specimen, 10070 psi.
- (2) Confining pressure applied, 200 psi.
- (3) Corrected readings obtained by subtracting the initial reading from the final reading.

# Load Cell Readings

## External vs. Internal

Initial Readings are 10.0 lb for External and 17.7 lb for Internal

MTS Program No.	Programmed Peak Load lb	Final Cell Reading		Corrected Reading	
		External	Internal	External	Internal
		lb	lb	lb	lb
75	20	28.35	35.9	18.35	18.2
76	40	48.1	55.8	38.1	38.1
77	60	67.85	75.6	57.85	57.9
78	80	87.5	95.1	77.5	77.4
79	100	107.45	114.9	97.45	97.2
80	150	156.2	163.3	146.2	145.6
81	200	205.2	212	195.2	194.3
82	250	254.45	260.9	244.45	243.2
83	300	303.1	308.9	293.1	291.2
84	350	351.75	357.1	341.75	339.4
85	400	401	405.8	391	388.1
86	450	452.5	456.4	442.5	438.7
75	20	28.4	35.9	18.4	18.2
76	40	48.5	56.2	38.5	38.5
77	60	67.95	75.6	57.95	57.9
78	80	87.6	95.2	77.6	77.5
79	100	107.35	114.9	97.35	97.2
80	150	156.35	163.6	146.35	145.9
81	200	205.4	211.6	195.4	193.9
82	250	254.05	260.4	244.05	242.7
83	300	303.25	309.2	293.25	291.5
84	350	352.2	357.5	342.2	339.8
85	400	400.5	405.2	390.5	387.5
86	450	449.6	453.5	439.6	435.8

### Notes:

- (1) Young modulus of specimen, 52000 psi.
- (2) Confining pressure applied, 0 psi.
- (3) Corrected readings obtained by subtracting the initial reading from the final reading.

Load Cell Readings  
External vs. Internal

Initial Readings are 28.95 lb for External and 28.3 lb for Internal

MTS Program No.	Programmed Peak Load lb	Final Cell Reading		Corrected Reading	
		External	Internal	External	Internal
		lb	lb	lb	lb
75	20	48.65	48	19.7	19.7
76	40	68.05	48.4	39.1	20.1
77	60	87.55	48.8	58.6	20.5
78	80	107.15	56.1	78.2	27.8
79	100	126.55	69.5	97.6	41.2
80	150	175.85	121.1	146.9	92.8
81	200	224.55	169.8	195.6	141.5
82	250	272.8	217.6	243.85	189.3
83	300	320.9	261.8	291.95	233.5
84	350	368.65	303.9	339.7	275.6
85	400	416.25	349.6	387.3	321.3
86	450	463.95	395.8	435	367.5
75	20	48.65	46.8	19.7	18.5
76	40	68.7	68.9	39.75	40.6
77	60	87.65	28.5	58.7	0.2
78	80	108.5	115	79.55	86.7
79	100	127.95	128.3	99	100
80	150	177.85	184.9	148.9	156.6
81	200	226.85	213.7	197.9	185.4
82	250	275.05	276.3	246.1	248
83	300	324	269.7	295.05	241.4
84	350	370.8	371.6	341.85	343.3
85	400	418.9	415.4	389.95	387.1
86	450	466.8	438.7	437.85	410.4

Notes:

- (1) Young modulus of specimen, 52000 psi.
- (2) Confining pressure applied, 50 psi.
- (3) Corrected readings obtained by subtracting the initial reading from the final reading.



# Load Cell Readings

## External vs. Internal

Initial Readings are 37.8 lb for External and 64.1 lb for Internal

MTS Program No.	Programmed Peak Load lb	Final Cell Reading		Corrected Reading	
		External	Internal	External	Internal
		lb	lb	lb	lb
75	20	57.15	80.8	19.35	16.7
76	40	77.15	115.1	39.35	51
77	60	97.1	131	59.3	66.9
78	80	117.1	166.3	79.3	102.2
79	100	137.4	195.3	99.6	131.2
80	150	186.4	254.1	148.6	190
81	200	235.75	313.1	197.95	249
82	250	285.25	345	247.45	280.9
83	300	334.4	396.3	296.6	332.2
84	350	384.2	481.7	346.4	417.6
85	400	432.2	483.1	394.4	419
86	450	480.75	533.1	442.95	469
75	20	57.45	93.6	19.65	29.5
76	40	77.1	116.2	39.3	52.1
77	60	96.75	142.1	58.95	78
78	80	116.7	162.1	78.9	98
79	100	136.5	186.2	98.7	122.1
80	150	185.8	246.8	148	182.7
81	200	235.75	303.6	197.95	239.5
82	250	284.1	314.3	246.3	250.2
83	300	334.25	425.3	296.45	361.2
84	350	382.95	486	345.15	421.9
85	400	431.9	546.7	394.1	482.6
86	450	481.05	599.6	443.25	535.5

### Notes:

- (1) Young modulus of specimen, 52000 psi.
- (2) Confining pressure applied, 100 psi.
- (3) Corrected readings obtained by subtracting the initial reading from the final reading.

Load Cell Readings  
External vs. Internal

Initial Readings are 133.3 lb for External and 101.0 lb for Internal

MTS Program No.	Programmed Peak Load lb	Final Cell Reading		Corrected Reading	
		External	Internal	External	Internal
		lb	lb	lb	lb
75	20	152.9	116.66	19.6	15.66
76	40	172.4	141.1	39.1	40.1
77	60	192.2	164.3	58.9	63.3
78	80	211.95	190.3	78.65	89.3
79	100	231.45	218.3	98.15	117.3
80	150	280.35	274.9	147.05	173.9
81	200	333.1	265.2	199.8	164.2
82	250	378.3	361.2	245	260.2
83	300	427.7	408.7	294.4	307.7
84	350	476.95	455.9	343.65	354.9
85	400	525.8	505.6	392.5	404.6
86	450	574.5	556	441.2	455
75	20	152.6	120.1	19.3	19.1
76	40	172.45	146.2	39.15	45.2
77	60	191.9	164.1	58.6	63.1
78	80	211.75	190.2	78.45	89.2
79	100	231.25	217.9	97.95	116.9
80	150	280.4	275	147.1	174
81	200	329.35	305.6	196.05	204.6
82	250	378.65	357.7	245.35	256.7
83	300	427.35	411.7	294.05	310.7
84	350	476.8	452.8	343.5	351.8
85	400	525.55	510.8	392.25	409.8
86	450	575.1	560	441.8	459

Notes:

- (1) Young modulus of specimen, 52000 psi.
- (2) Confining pressure applied, 150 psi.
- (3) Corrected readings obtained by subtracting the initial reading from the final reading.

**Load Cell Readings  
External vs. Internal**

Initial Readings are 182.9 lb for External and 115.2 lb for Internal

MTS Program No.	Programmed Peak Load lb	Final Cell Reading		Corrected Reading	
		External	Internal	External	Internal
		lb	lb	lb	lb
75	20	202.45	137.2	19.55	22
76	40	223.2	162.3	40.3	47.1
77	60	241.6	183.5	58.7	68.3
78	80	261.4	206.1	78.5	90.9
79	100	281.1	224.7	98.2	109.5
80	150	330	283.1	147.1	167.9
81	200	378.95	331.1	196.05	215.9
82	250	428	375.9	245.1	260.7
83	300	476.75	435	293.85	319.8
84	350	526.35	469.4	343.45	354.2
85	400	575.35	517.3	392.45	402.1
86	450	624.45	564.4	441.55	449.2
75	20	203.05	140.2	20.15	25
76	40	222.3	160.6	39.4	45.4
77	60	241.75	183.5	58.85	68.3
78	80	261.4	207.7	78.5	92.5
79	100	281.35	233.2	98.45	118
80	150	330.3	279.6	147.4	164.4
81	200	379.2	325.6	196.3	210.4
82	250	428	378.1	245.1	262.9
83	300	476.9	425.7	294	310.5
84	350	525.95	470.2	343.05	355
85	400	575	517.4	392.1	402.2
86	450	624.6	565.6	441.7	450.4

**Notes:**

- (1) Young modulus of specimen, 52000 psi.
- (2) Confining pressure applied, 200 psi.
- (3) Corrected readings obtained by subtracting the initial reading from the final reading.

APPENDIX F  
FORTRAN LISTING OF PROGRAM "HSTRAIN"

```

$LARGE
$NOTRUNCATE
C*****C
C
C          PROGRAM HSTRAIN2.FOR
C
C  THIS PROGRAM REDUCES THE COLLECTED DATA BY 2063 FOURIER ANALYSER
C  FOR THE PROJECT 'UNSATURATED CLAYEY SOILS BEHAVIOR UNDER HIGH
C  STRAIN RATES'. THE TESTS ARE PERFORMED ON STRESS CONTRAL USING MTS
C  FACILITY. THREE CHAMNLE DATA WERE COLLECTED.
C
C  IFILE--INPUT DATA FILE NAME;
C  FILELOAD--OUTPUT DATA FILE NAME FOR STRESS-TIME RELATION;
C  FILEDIS--OUTPUT DATA FILE NAME FOR STRAIN-TIME RELATION;
C  STRESS--DIMENSION FOR STRESS DATA;
C  STRAIN--DIMENSION FOR STRAIN DATA;
C  VOLT--DIMENSION FOR MICROPROFILE WAVEFORM DATA;
C  TSTRESS--DIMENSION FOR TIME DATA WITH STRESS;
C  TSTRAIN--DIMENSION FOR TIME DATA WITH STRAIN;
C  BEGINVOLT--BEGINING POINT OF UP-RAMP CURVE FOR MICROPROFILE
C             WAVEFORM;
C  BEGINSTRESS--BEGINING POINT OF UP-RAMP CURVE COLLECTED BY
C              LOAD CELL;
C  BEGINSTRAIN--BEGINING POINT OF STRAIN-TIME CURVE;
C*****C
C          CHARACTER IFILE*20,FILELOAD*20,FILEDIS*20,IFILE1*20,FILELOAD1*20,
C          &          FILEDIS1*20
C          COMMON /STRAIN1/ STRAIN
C          COMMON /STRESS1/ STRESS
C          COMMON /VOLT1/ VOLT
C          COMMON /TSTRESS1/TSTRESS
C          COMMON /TSTRAIN1/TSTRAIN
C          INTEGER BEGINVOLT,BEGINSTRESS,BEGINSTRAIN
C          DIMENSION STRAIN(4100),STRESS(4100),VOLT(4100),TSTRESS(4100),
C          &          TSTRAIN(4100)
C
C  BEGIN TO READ DATA FROM SCREEN
C  WRITE(*,*)'ENTER THE DATA POINTS FOR EACH CHANNEL'
C  READ(*,*)NUMPTS
C  WRITE(*,*)'ENTER THE TIME LENTH OF COLLECTING DATA (milisec.)'
C  READ(*,*)TIMELEN
C  WRITE(*,*)'ENTER THE VALUE OF DISPLACEMENT CARTRIDGE (in)'
C  READ(*,*)CAR1
C  WRITE(*,*)'ENTER THE VALUE OF LOAD CARTRIDGE (lb)'
C  READ(*,*)CAR2
C  WRITE(*,*)'ENTER THE FIRST FILE NUMBER IN THE SET'
C  READ(*,*)NSTART
C  WRITE(*,*)'ENTER THE NUMBER OF FILE IN THE SET'
C  READ(*,*)NFILES
C  WRITE(*,*)'ENTER THE INPUT DATA FILE NAME IN THE SET'
C  READ(*,10)IFILE
C  WRITE(*,*)'ENTER THE OUTPUT STRESS DATA FILE NAME IN THE SET'
C  READ(*,10)FILELOAD
C  WRITE(*,*)'ENTER THE OUTPUT STRAIN DATA FILE NAME IN THE SET'
C  READ(*,10)FILEDIS
10  FORMAT(A20)
C
C          OPEN(UNIT=41,FILE='POINT.OUT',STATUS='NEW')
C

```

```

DO 2000 IT=NSTART, (NSTART+NFILES-1)
WRITE(*,*) 'FILE NUMBER=', IT
KK=IT*4
WRITE(41,*) '*****'
&*****'
WRITE(41,*) 'FILE NUMBER=', IT, '      APPLIED LOAD(kg)=' , KK
WRITE(41,*) '*****'
&*****'
C
WRITE(*,*) 'CALLING SUBROUTINE GET_FILE_NAME'
CALL GET_FILE_NAME(IFILE, FILELOAD, FILEDIS, IFILE1, FILELOAD1,
& FILEDIS1, IT)
IFILE1=IFILE1
FILELOAD1=FILELOAD1
FILEDIS1=FILEDIS1
C
C
C
WRITE(*,*) 'CALLING SUBROUTINE READ_DATA_FILE'
CALL READ_DATA_FILE(IFILE1, NUMPTS, CAR1, CAR2)
C
C
C
WRITE(*,*) 'CALLING SUBROUTINE SMOOTH_DATA'
CALL SMOOTH_DATA(NUMPTS)
C
C
C
WRITE(*,*) 'CALLING SUBROUTINE FIND_BEGIN_POINTS'
CALL FIND_BEGIN_POINTS(NUMPTS, BEGINVOLT, BEGINSTRESS,
& BEGINSTRAIN)
BEGINVOLT=BEGINVOLT
BEGINSTRESS=BEGINSTRESS
BEGINSTRAIN=BEGINSTRAIN
C
C
C
WRITE(*,*) 'CALLING SUBROUTINE INITIALIZE_DATA'
CALL INITIALIZE_DATA(BEGINVOLT, BEGINSTRESS, BEGINSTRAIN, NUMPTS)
C
C
C
WRITE(*,*) 'CALL SUBROUTINE VARIATION WITH TIME'
CALL VARIATION_WITH_TIME(NUMPTS, BEGINSTRESS, BEGINSTRAIN,
& TIMELEN, FILELOAD1, FILEDIS1)
C
C
C
WRITE(*,*) 'CALLING SUBROUTINE FIND_MAXIMUM_POINTS'
CALL FIND_MAXIMUM_POINTS(NUMPTS, TIMELEN, BEGINVOLT, BEGINSTRESS,
& BEGINSTRAIN)
C
C
C
2000 CONTINUE
STOP
END
C
C*****C
C      THE SUBROUTINE FOLLOWED      C
C*****C
C
C*****C
C      SUBROUTINE GET_FILE_NAME      C
C      THIS SUBROUTINE GENERATES THE INPUT AND OUTPUT DATA FILE NAMES      C
C*****C
C

```







```

C
SUBROUTINE FIND_BEGIN_POINTS (NUMPTS, BEGINVOLT, BEGINSTRESS,
    & BEGINSTRAIN)
INTEGER BEGINVOLT, BEGINSTRESS, BEGINSTRAIN
COMMON /VOLT1/VOLT
COMMON /STRESS1/STRESS
COMMON /STRAIN1/STRAIN
DIMENSION VOLT(4100), STRESS(4100), STRAIN(4100)

C
BEGINVOLT=0
TEMP=0.0
C>>>>FIND THE INITIAL AVERAGE VALUE FROM FIRST 200 POINTS
DO 400 I=1,200
TEMP=TEMP+VOLT(I)
400 CONTINUE
BEGINAVG=TEMP/200.0
C>>>>FIND THE BEGINING POINT OF UP-RAMP WAVEFORM
DO 410 I=1,NUMPTS
IF (VOLT(I).GE.BEGINAVG) THEN
IF ((VOLT(I+1)-BEGINAVG).GE.(VOLT(I)-BEGINAVG)) THEN
INDEX1=I
DO 420 J=(INDEX1+1), (INDEX1+550)
IF ((VOLT(J)-BEGINAVG).LT.0.0) THEN
GO TO 410
ENDIF
420 CONTINUE
BEGINVOLT=I
WRITE(*,*) 'BEGINVOLT=', BEGINVOLT
GO TO 430
ENDIF
ENDIF
410 CONTINUE
430 CONTINUE
C>>>>FIND THE BEGINING POINT OF UP-RAMP LOAD CUTVE
DO 440 K=BEGINVOLT+1, NUMPTS
IF (STRESS(K).GE.STRESS(BEGINVOLT)) THEN
IF (STRESS(K+1).GE.STRESS(K)) THEN
INDEX2=K
DO 450 KK=INDEX2+1, INDEX2+550
IF (STRESS(KK).LE.STRESS(INDEX2)) THEN
GO TO 440
ENDIF
450 CONTINUE
BEGINSTRESS=K
WRITE(*,*) 'BEGINSTRESS=', BEGINSTRESS
GO TO 460
ENDIF
ENDIF
440 CONTINUE
460 CONTINUE
C>>>>FIND THE BEGIN POINT OF STRAIN
DO 470 J=BEGINSTRESS+1, NUMPTS
IF (STRAIN(J).GE.STRAIN(BEGINSTRESS)) THEN
IF (STRAIN(J+1).GE.STRAIN(J)) THEN
INDEX3=J
DO 480 JJ=INDEX3+1, INDEX3+550
IF (STRAIN(JJ).LE.STRAIN(INDEX3)) THEN
GO TO 470
ENDIF
480 CONTINUE

```



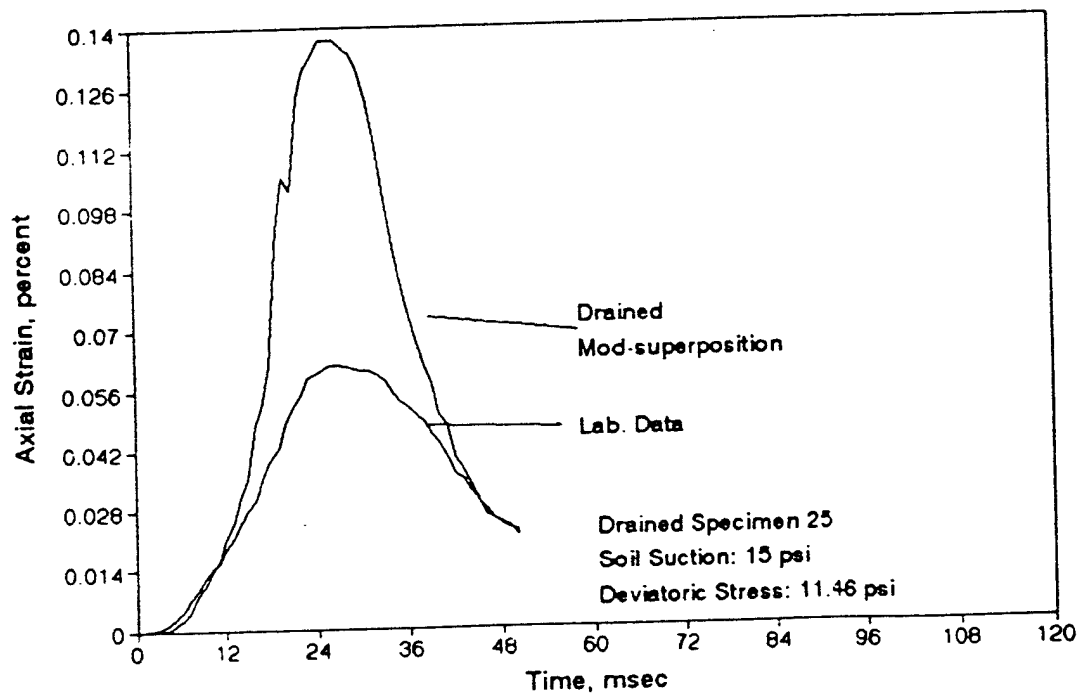
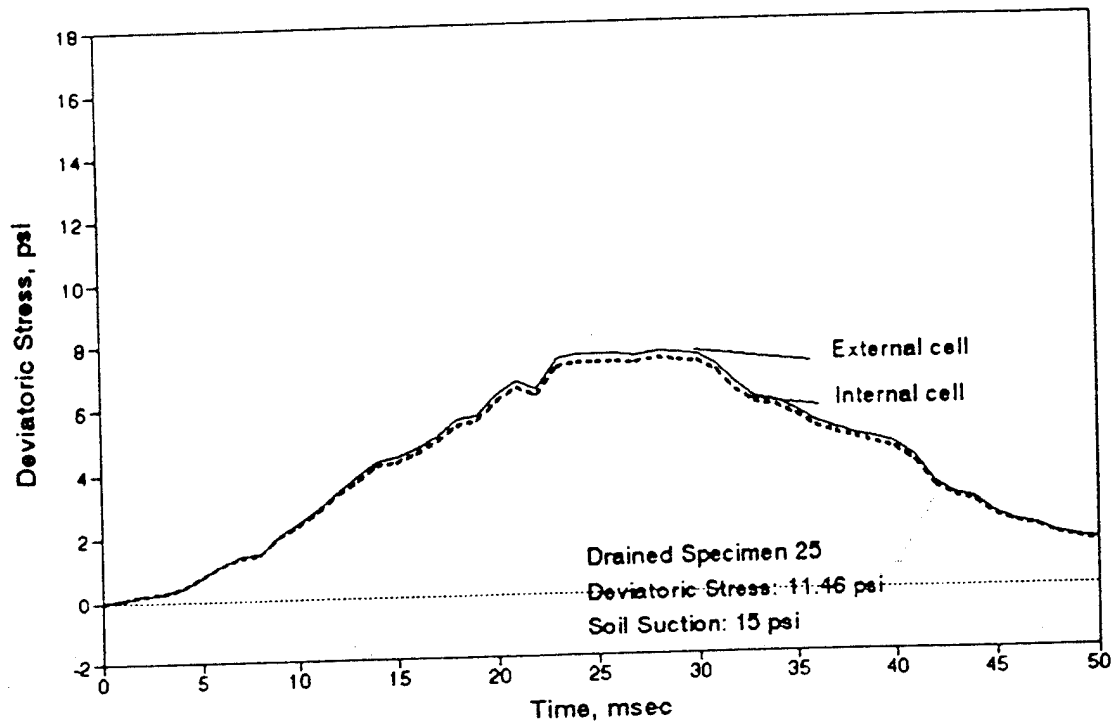


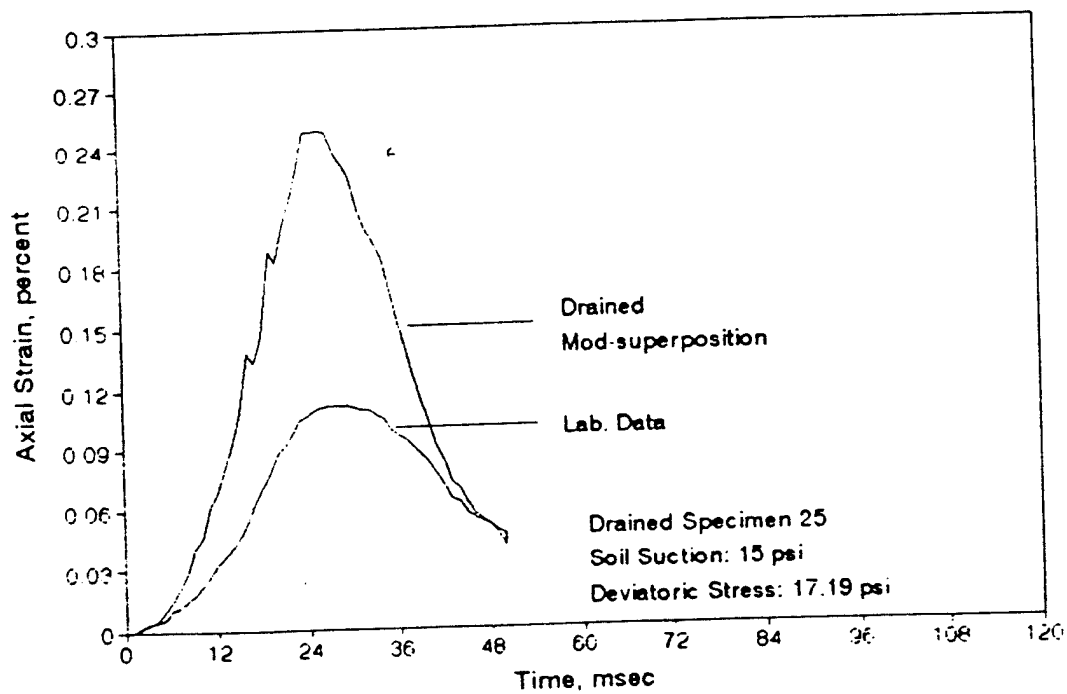
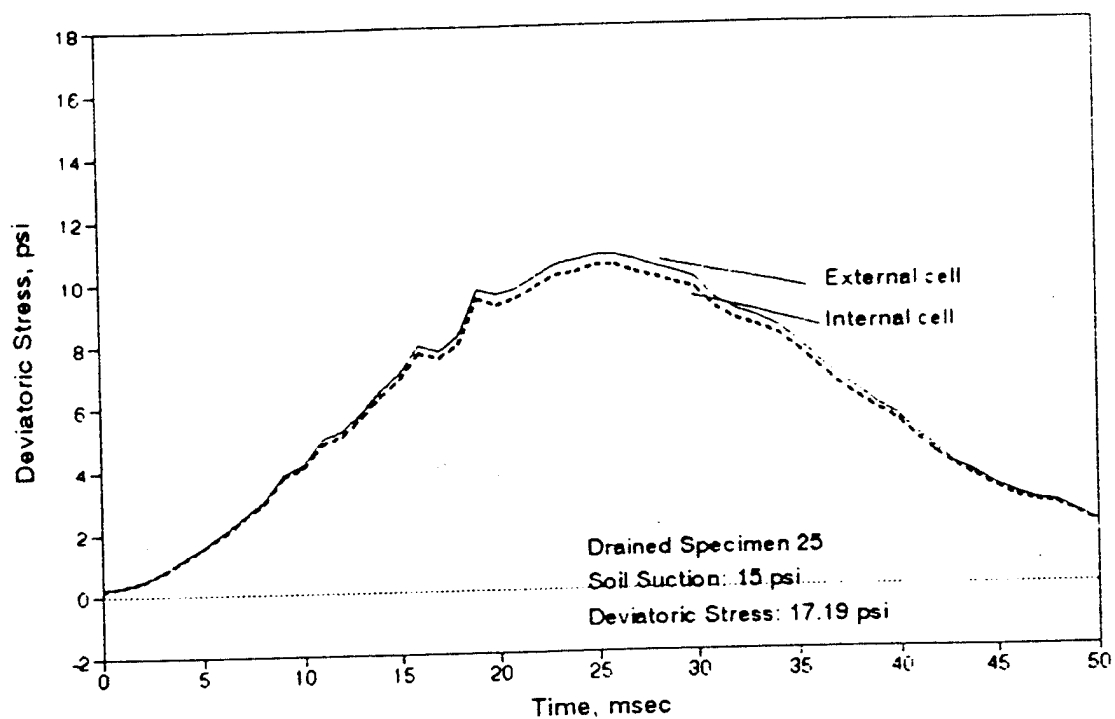
```

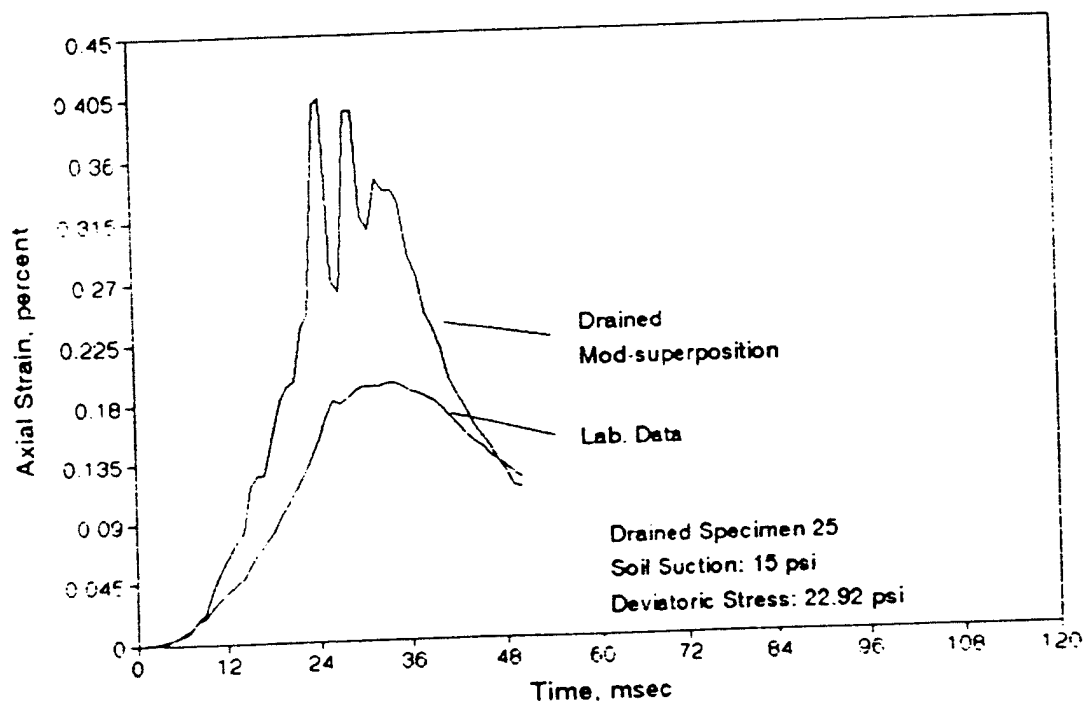
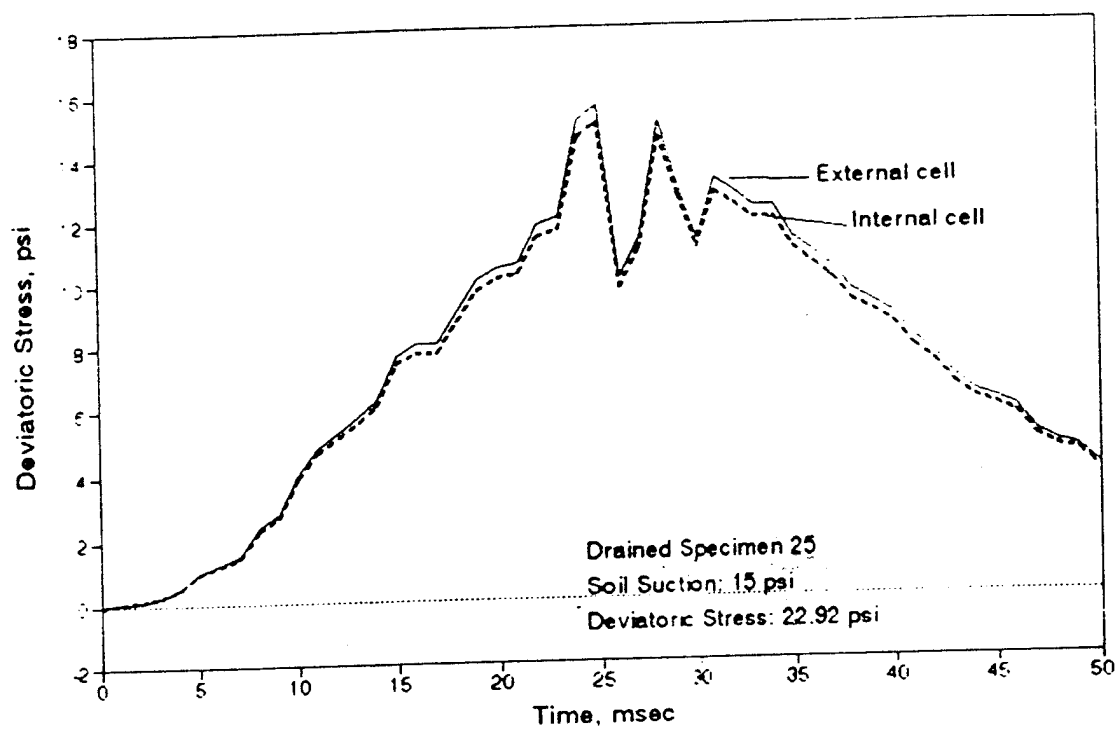
C*****C
C
      SUBROUTINE FIND_MAXIMUM_POINTS(NUMPTS,TIMELEN,BEGINVOLT,
&BEGINSTRESS,BEGINSTRAIN)
      INTEGER BEGINVOLT,BEGINSTRESS,BEGINSTRAIN
      COMMON /STRAIN1/ STRAIN
      COMMON /STRESS1/ STRESS
      COMMON /VOLT1/ VOLT
      DIMENSION STRAIN(4100),STRESS(4100),VOLT(4100)
C
C>>>>FIND MAXIMUM VALUE OF STRAIN CURVE
      MAXSTRAIN=0
      STRAINMAX=0.0
      DO 710 I1=BEGINSTRAIN,2500
      IF (STRAIN(I1).GE.STRAINMAX) THEN
      STRAINMAX=STRAIN(I1)
      MAXSTRAIN=I1
      ENDIF
710   CONTINUE
C
C>>>>FIND MAXIMUM VALUE OF STRESS CURVE
      MAXSTRESS=0
      STRESSMAX=0.0
      DO 720 I2=BEGINSTRESS,2500
      IF (STRESS(I2).GE.STRESSMAX) THEN
      STRESSMAX=STRESS(I2)
      MAXSTRESS=I2
      ENDIF
720   CONTINUE
C
C>>>>FIND MAXIMUM VALUE OF VOLT CURVE
      MAXVOLT=0
      VOLTMAX=0.0
      DO 730 I3=BEGINVOLT,2500
      IF (VOLT(I3).GE.VOLTMAX) THEN
      VOLTMAX=VOLT(I3)
      MAXVOLT=I3
      ENDIF
730   CONTINUE
C
      STRAINMAXTIME=(MAXSTRAIN-BEGINSTRAIN)*(TIMELEN/FLOAT(NUMPTS))
      STRESSMAXTIME=(MAXSTRESS-BEGINSTRESS)*(TIMELEN/FLOAT(NUMPTS))
      VOLTMAXTIME=(MAXVOLT-BEGINVOLT)*(TIMELEN/FLOAT(NUMPTS))
C
C>>>>WRITE OUTPUT DATA
      WRITE(41,*)'                               MAX. TIME, millisec.'
      WRITE(41,*)'-----'
      WRITE(41,*)STRAINMAXTIME,STRESSMAXTIME,VOLTMAXTIME
      WRITE(41,*)' '
      WRITE(41,*)'                               MAX. VALUES'
      WRITE(41,*)'-----'
      WRITE(41,*)STRAINMAX,STRESSMAX,VOLTMAX
      WRITE(41,*)' '
      WRITE(41,*)' '
      RETURN
      END

```

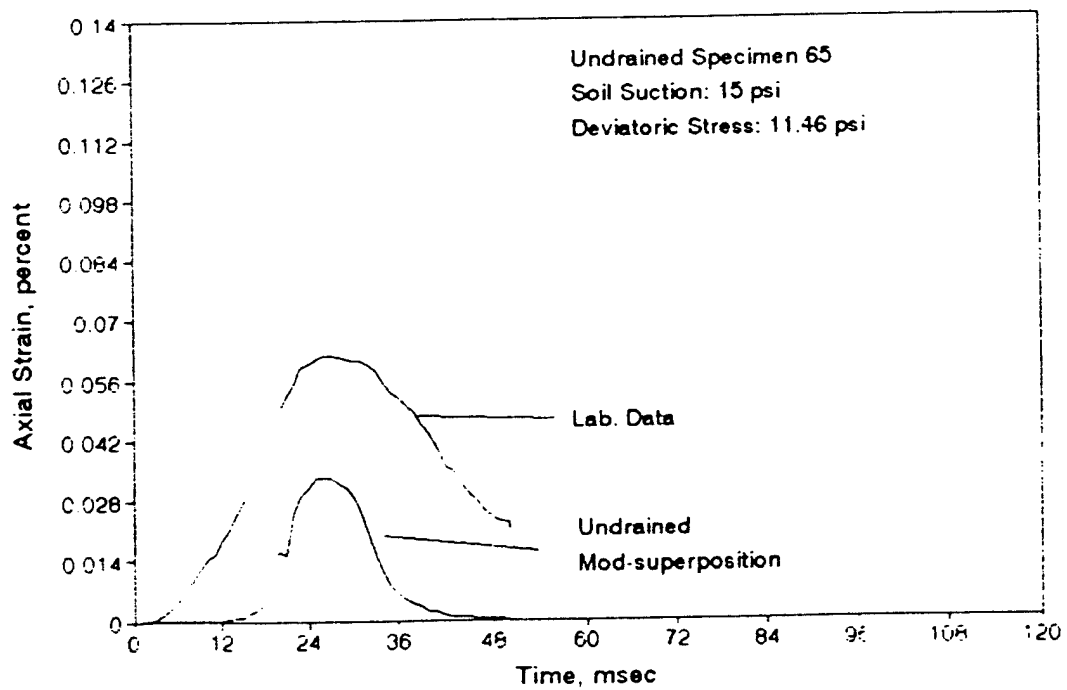
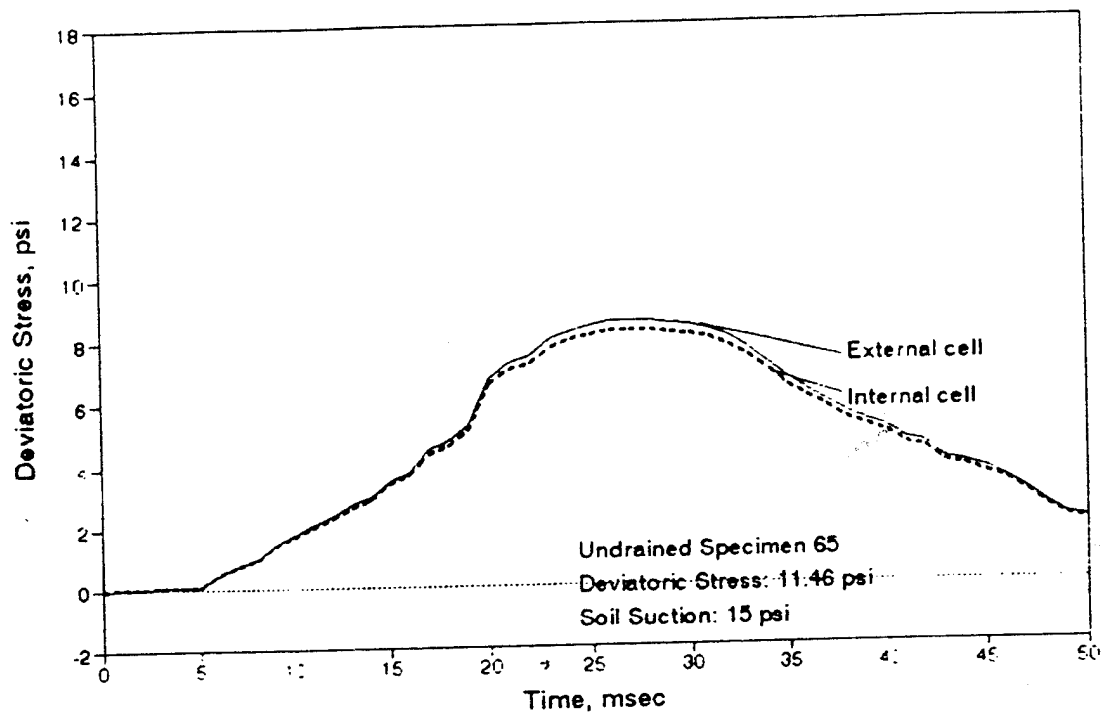
**APPENDIX G**  
**SELECTED RESULTS OF DYNAMIC TESTS ON SPECIMENS AT 15 PSI SOIL**  
**SUCTION**

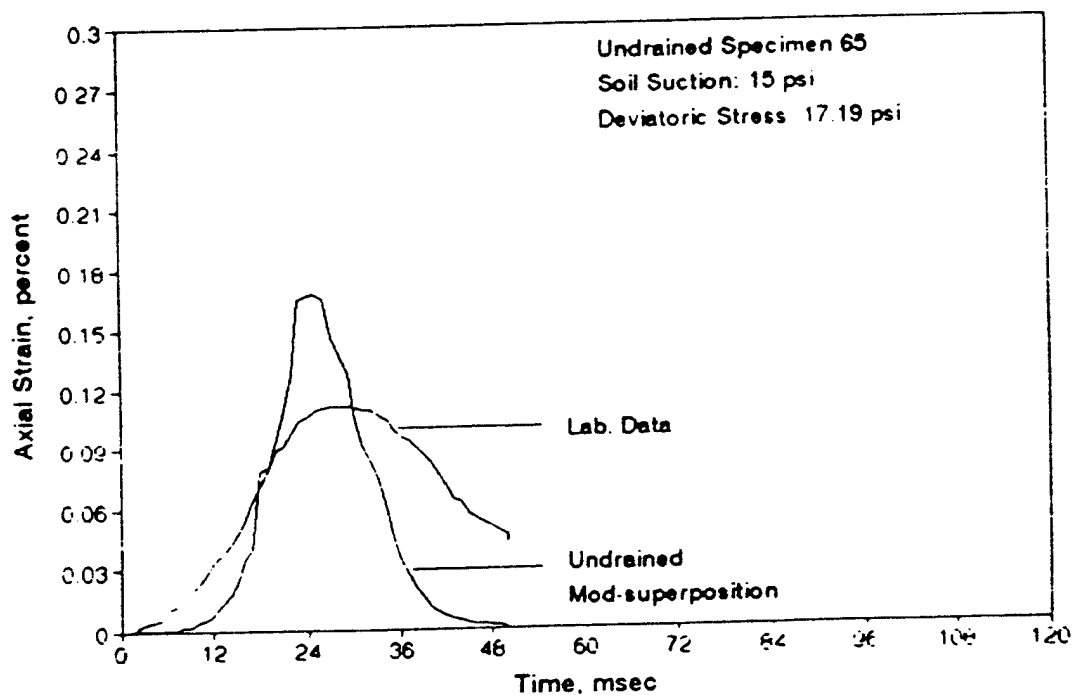
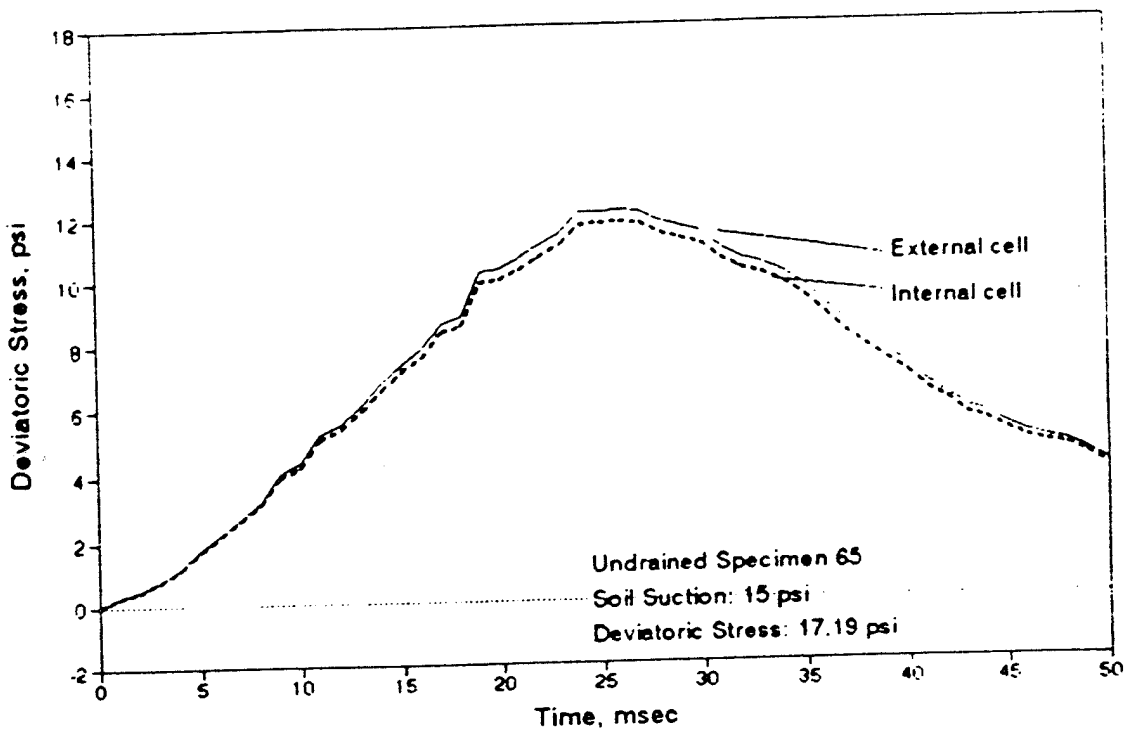


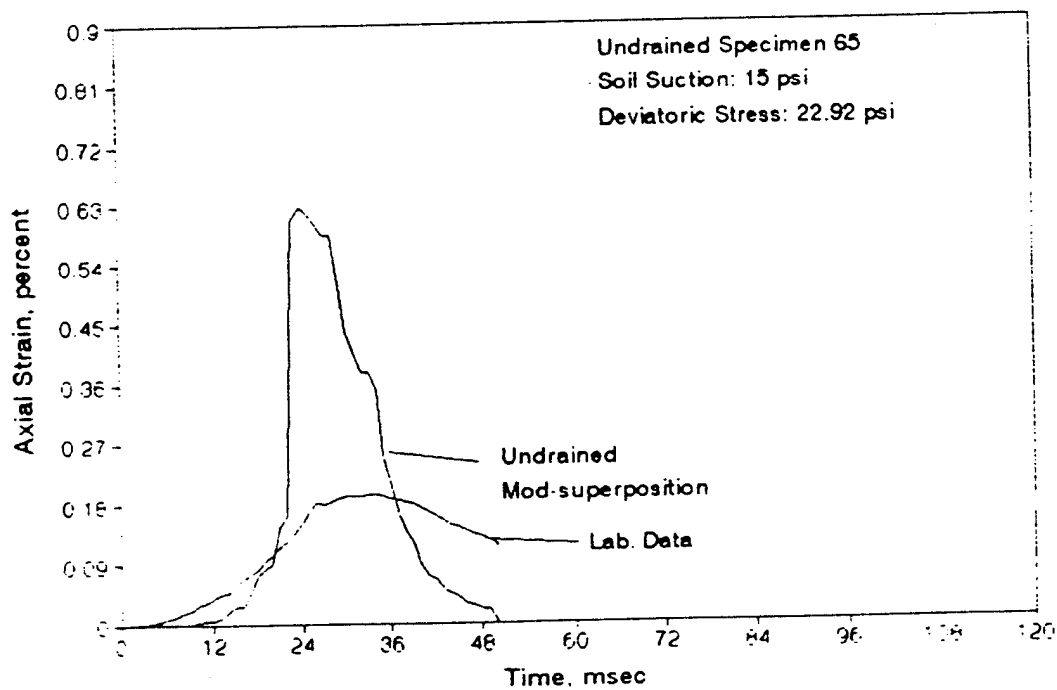
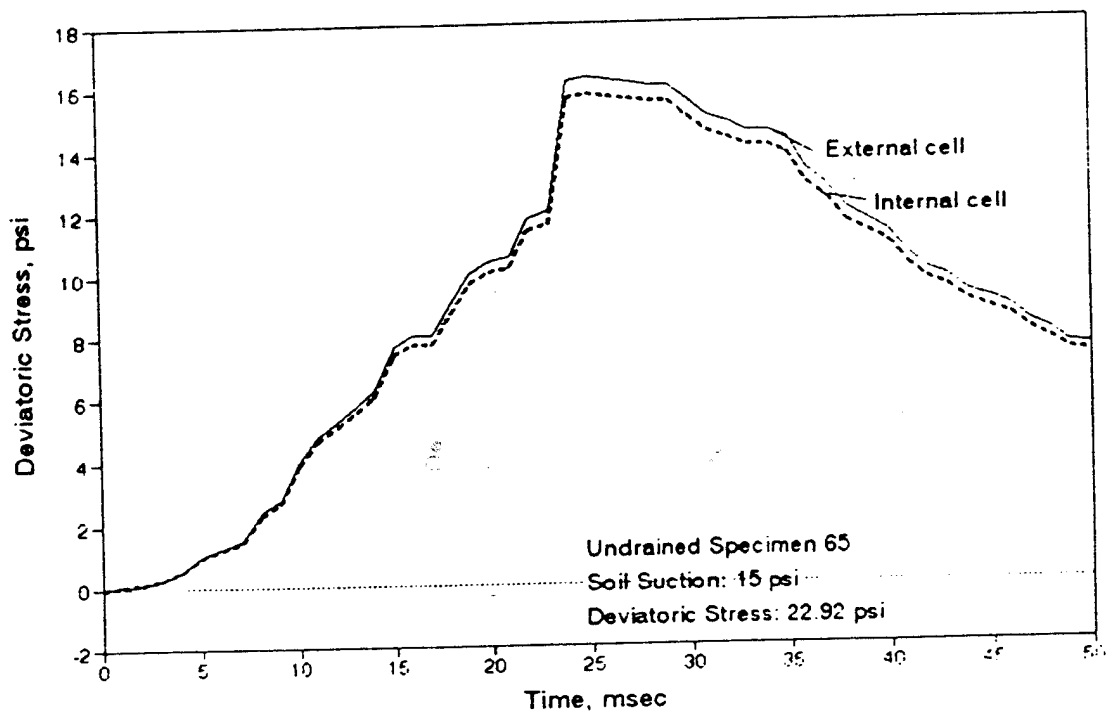








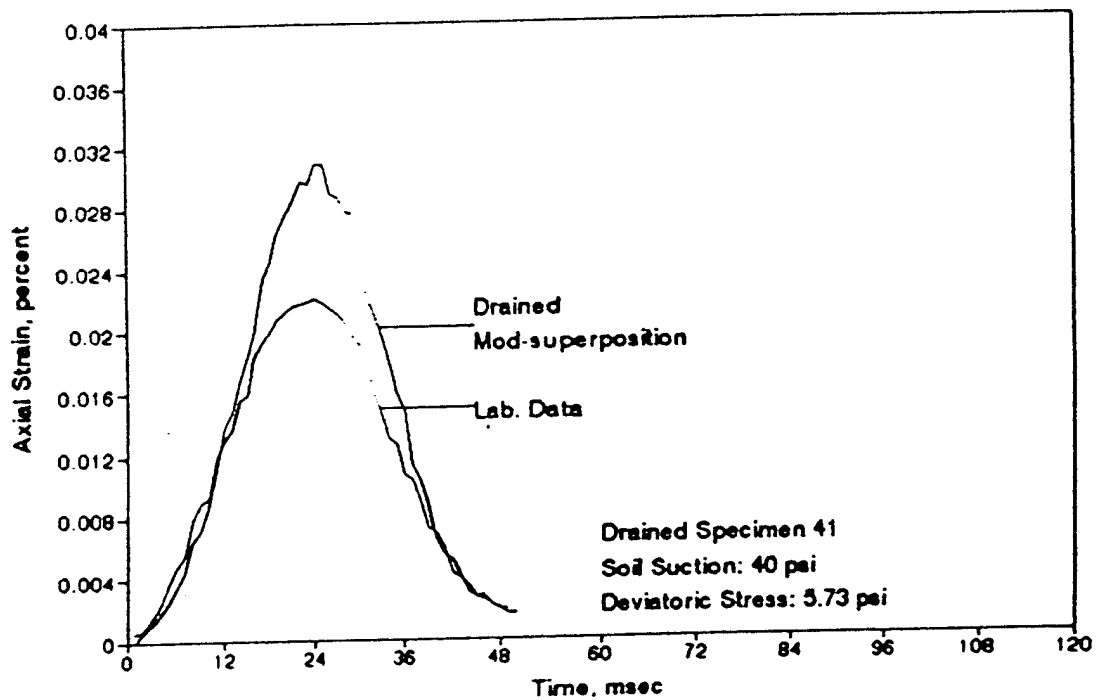
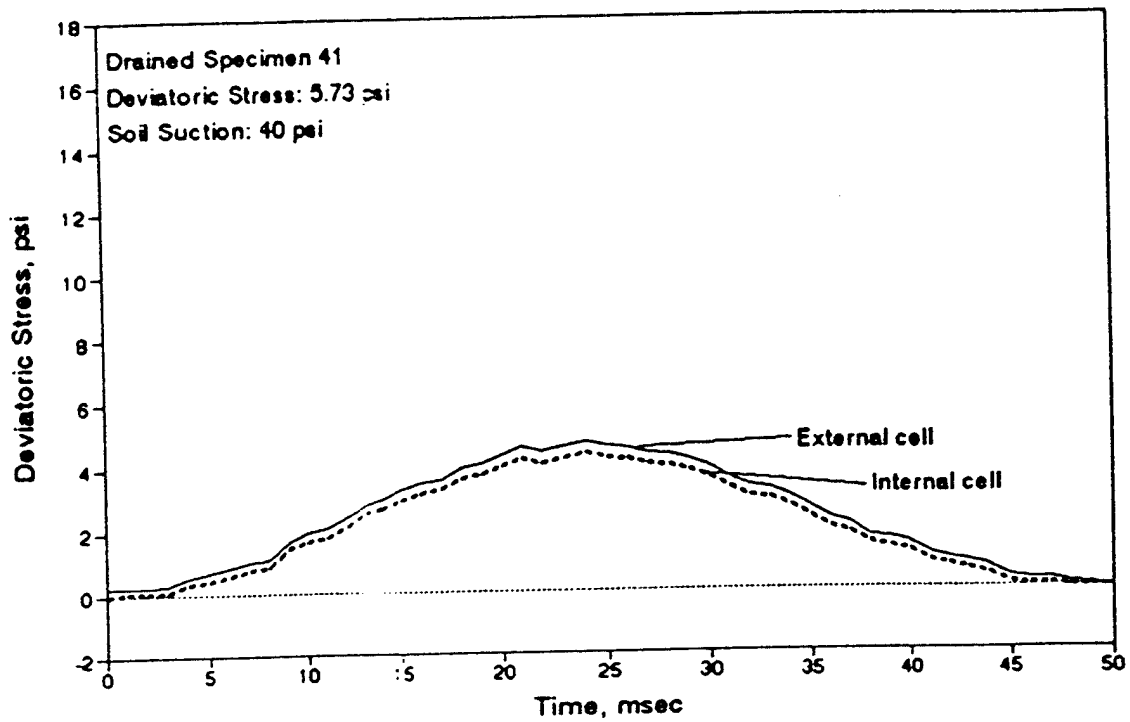


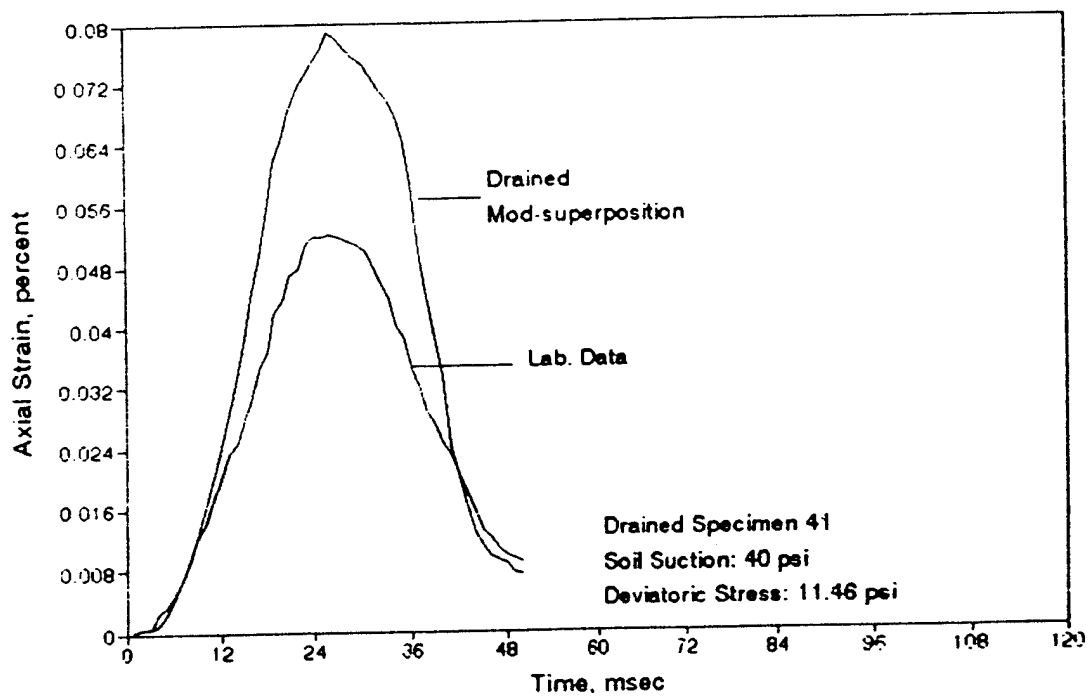
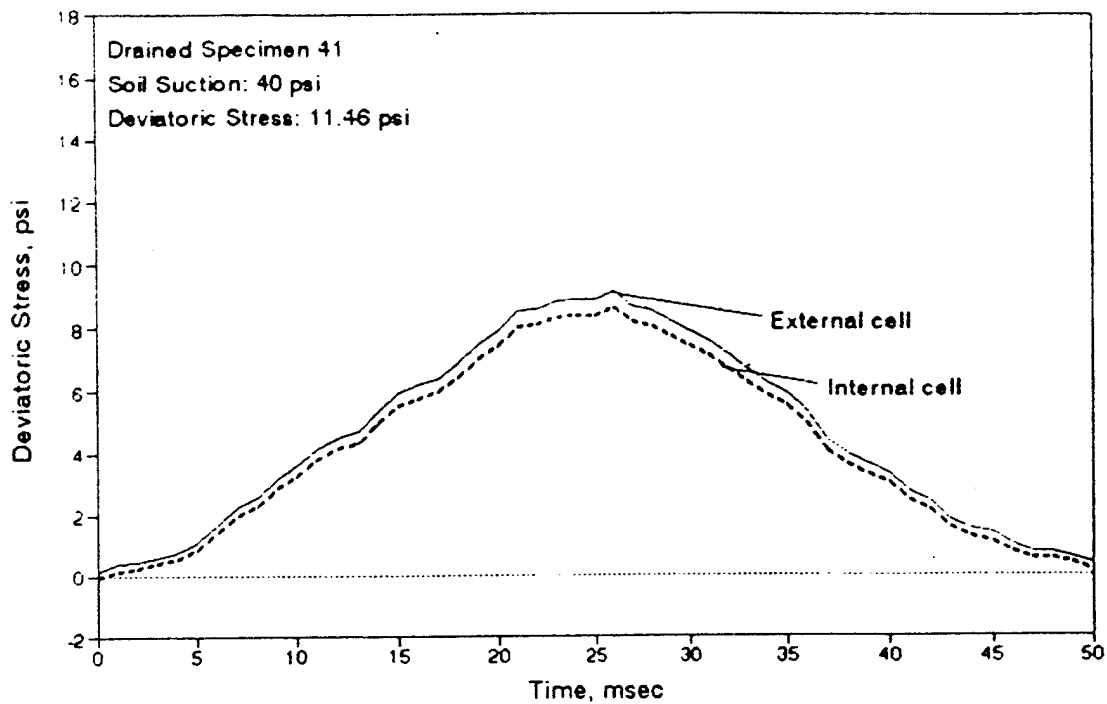


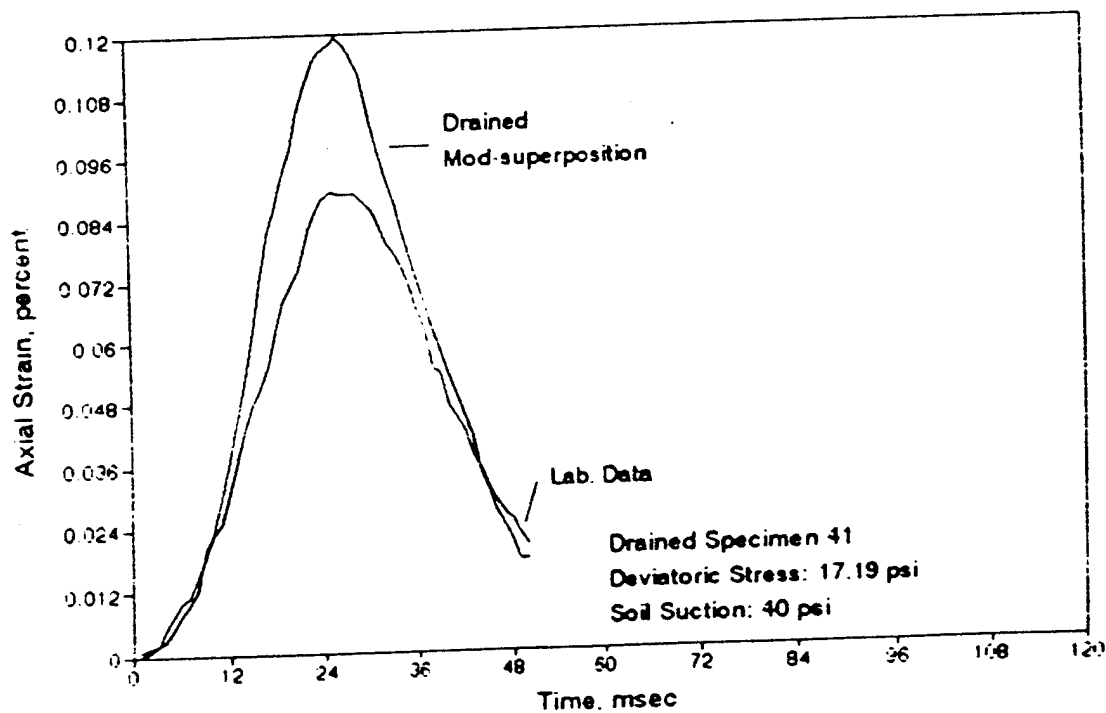
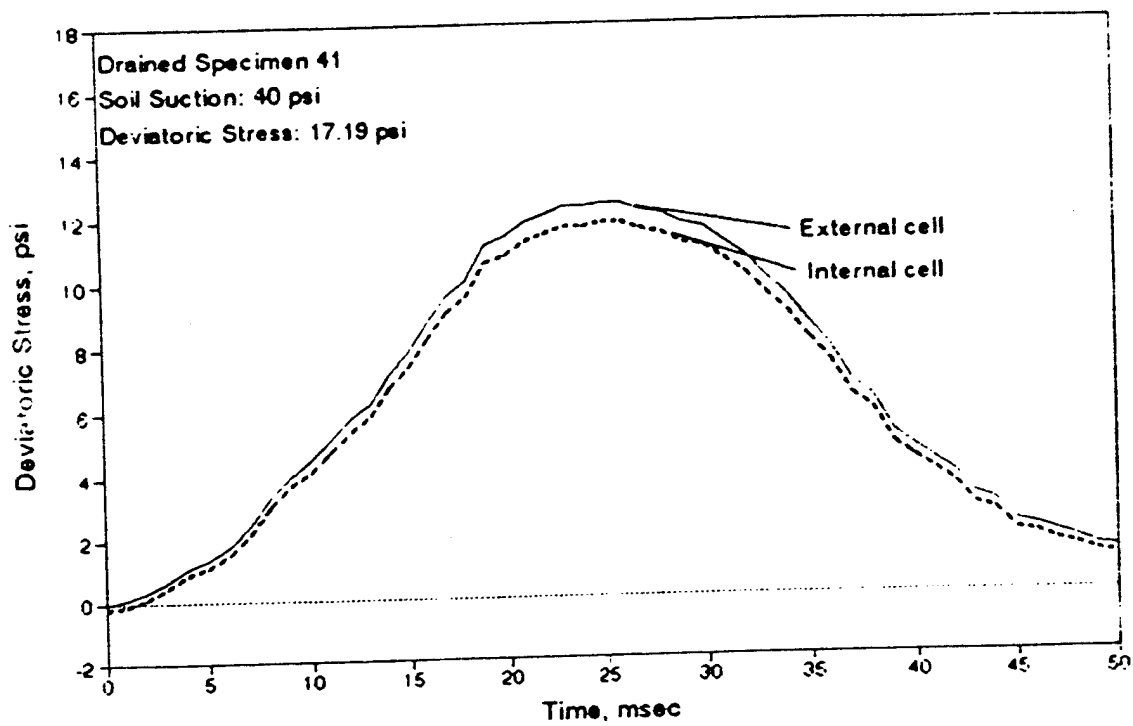
**APPENDIX H**

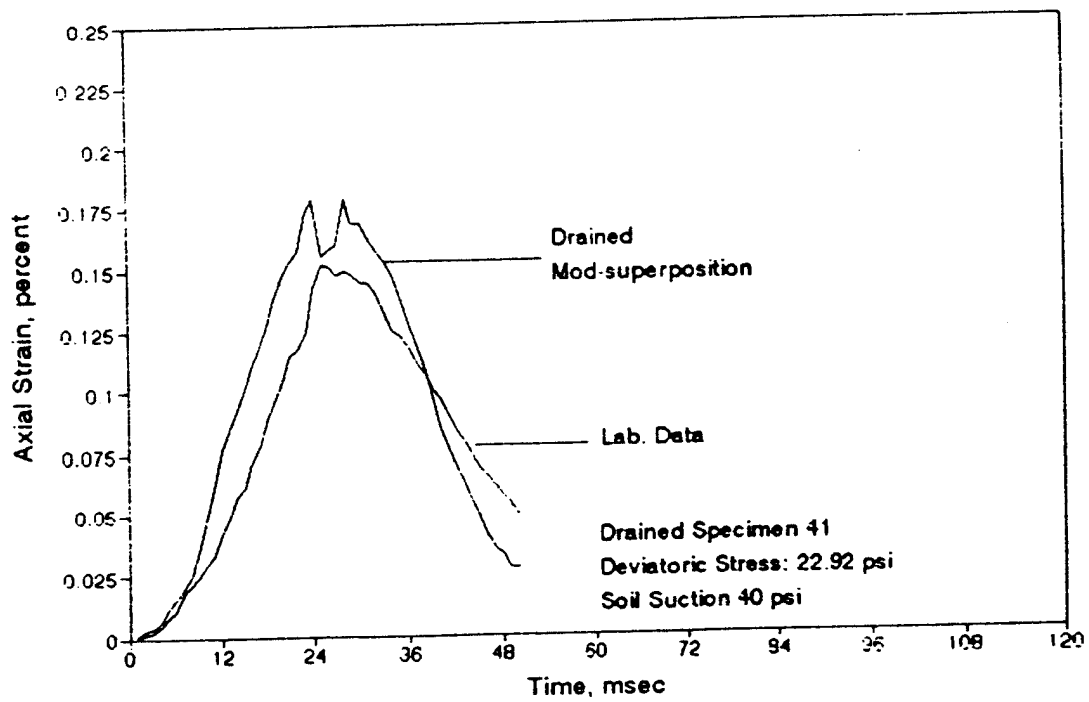
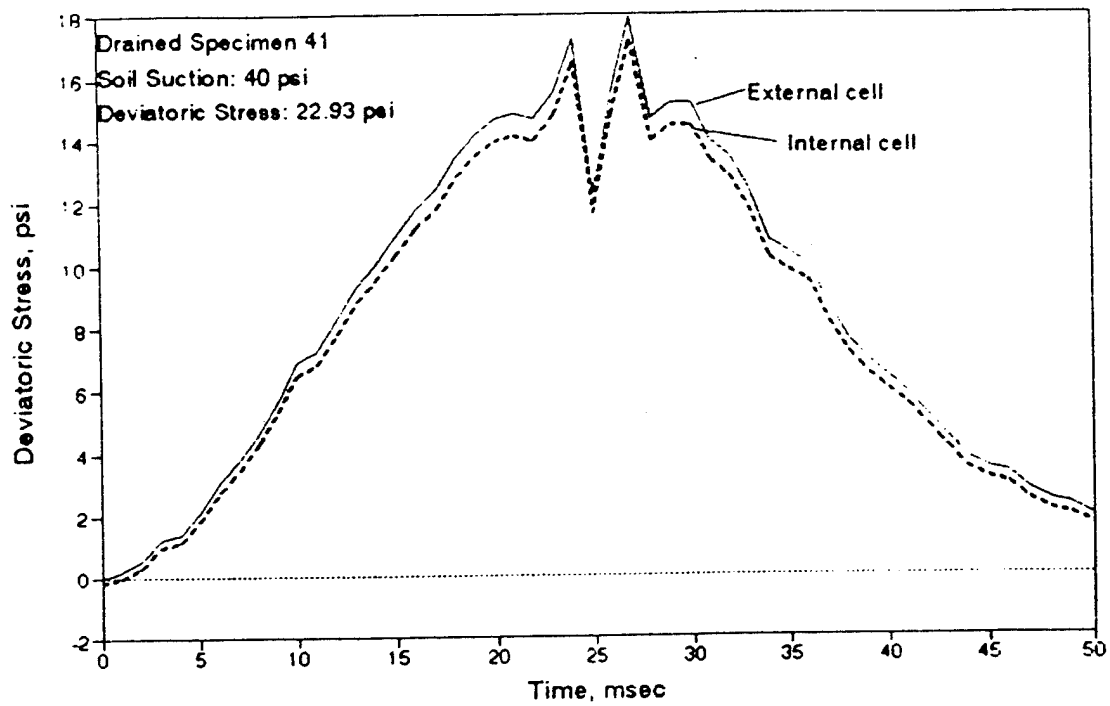
**SELECTED RESULTS OF DYNAMIC TESTS ON SPECIMENS AT 40 PSI SOIL**

**SUCTION**

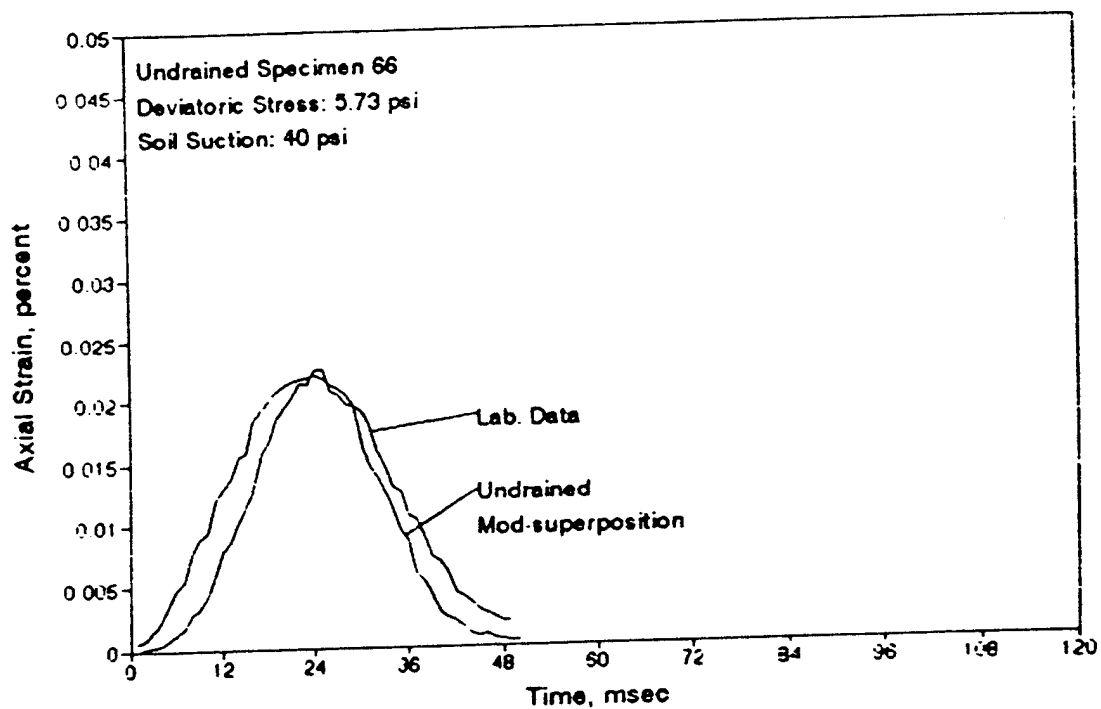
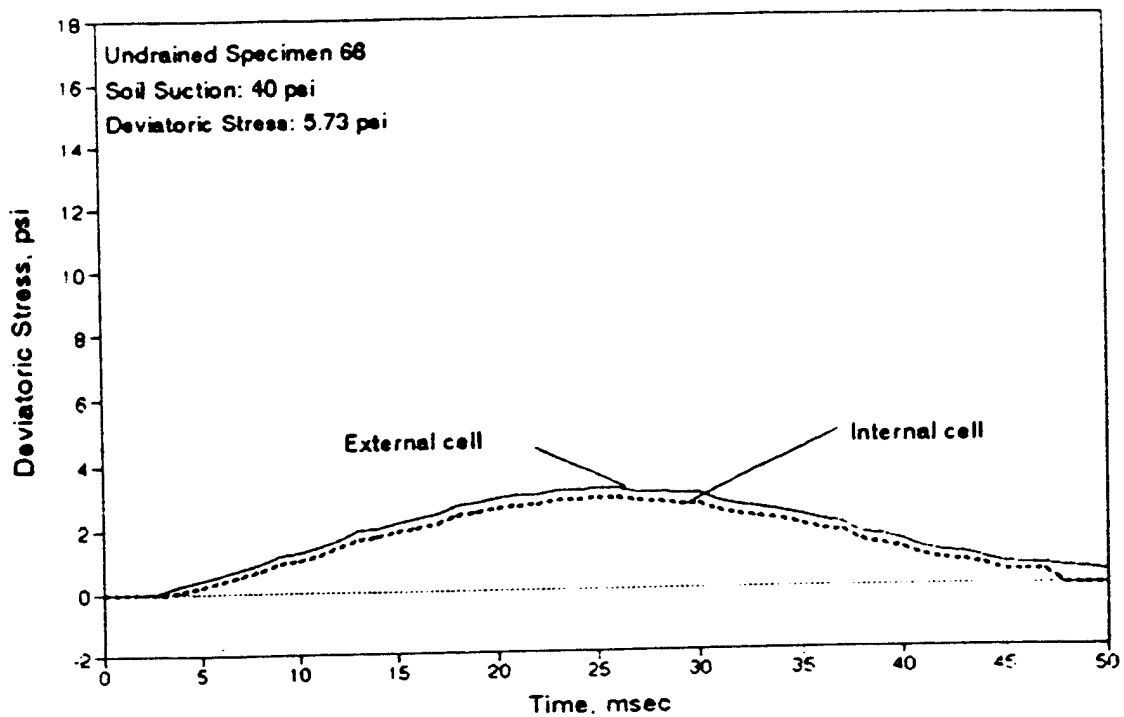


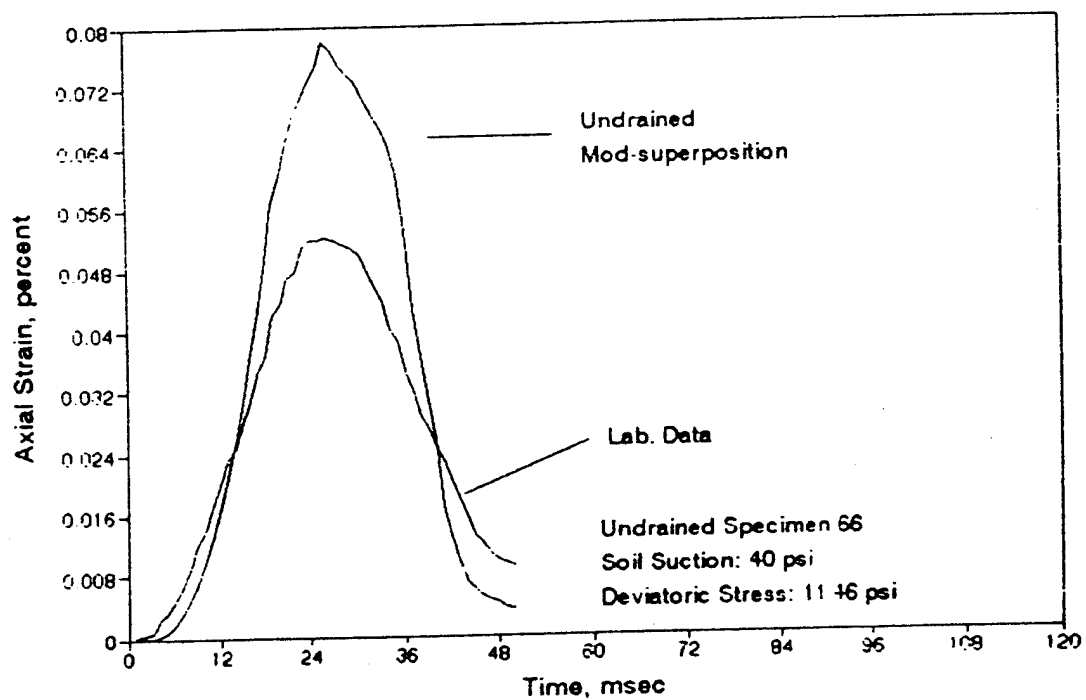
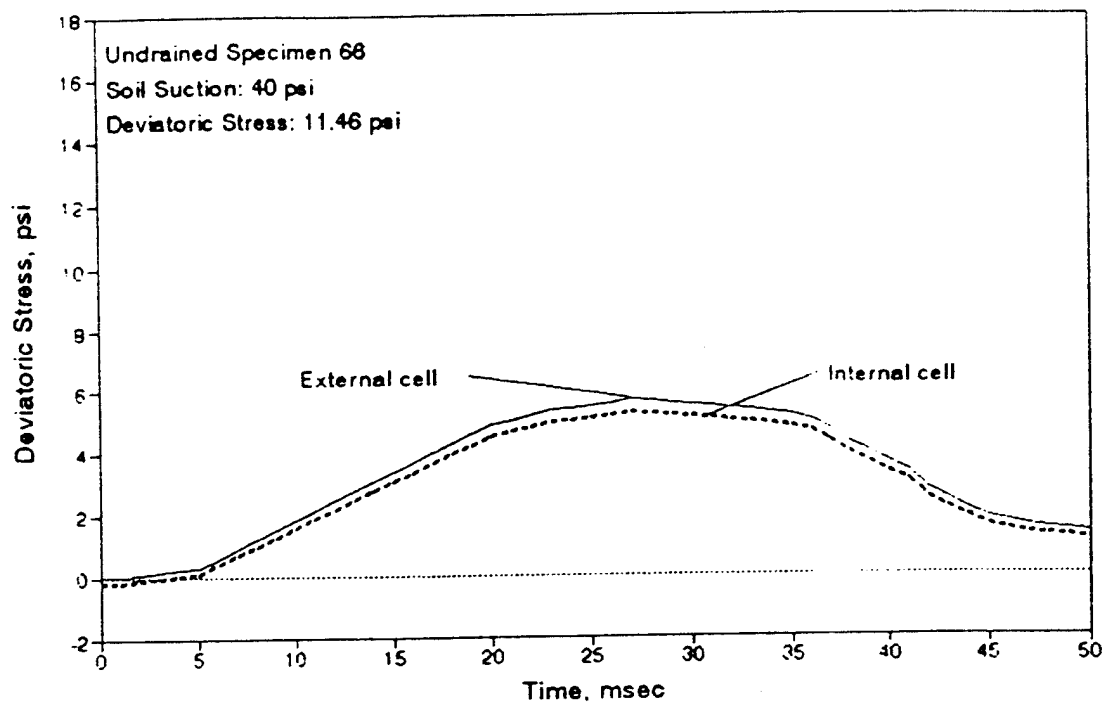


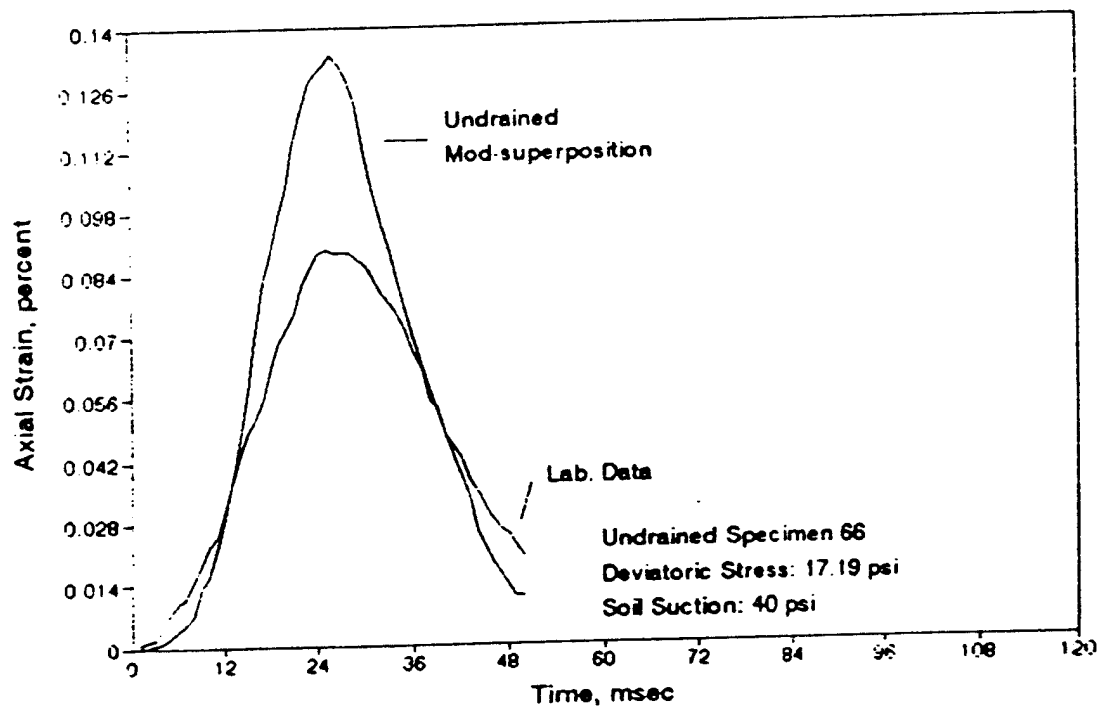
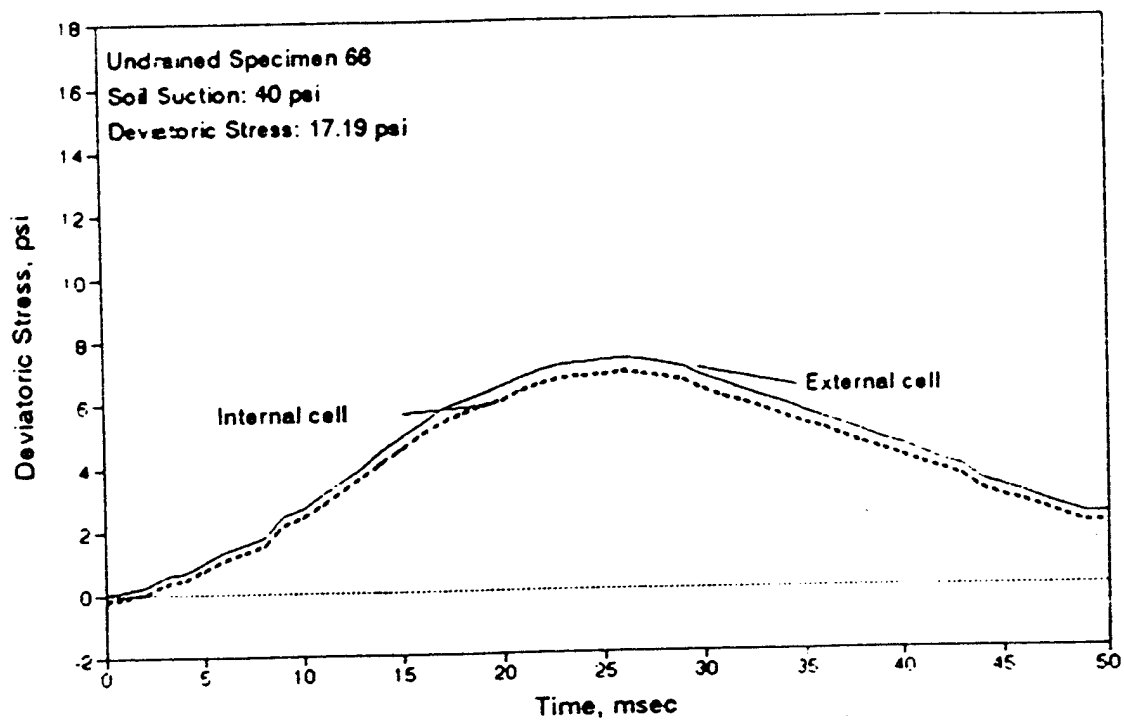


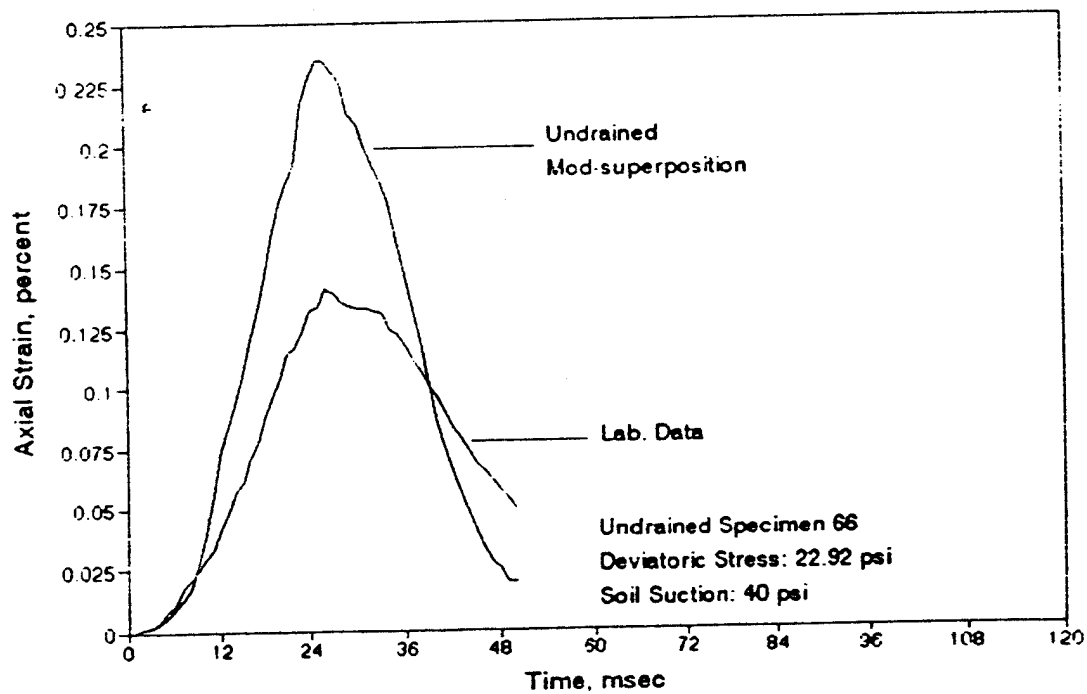
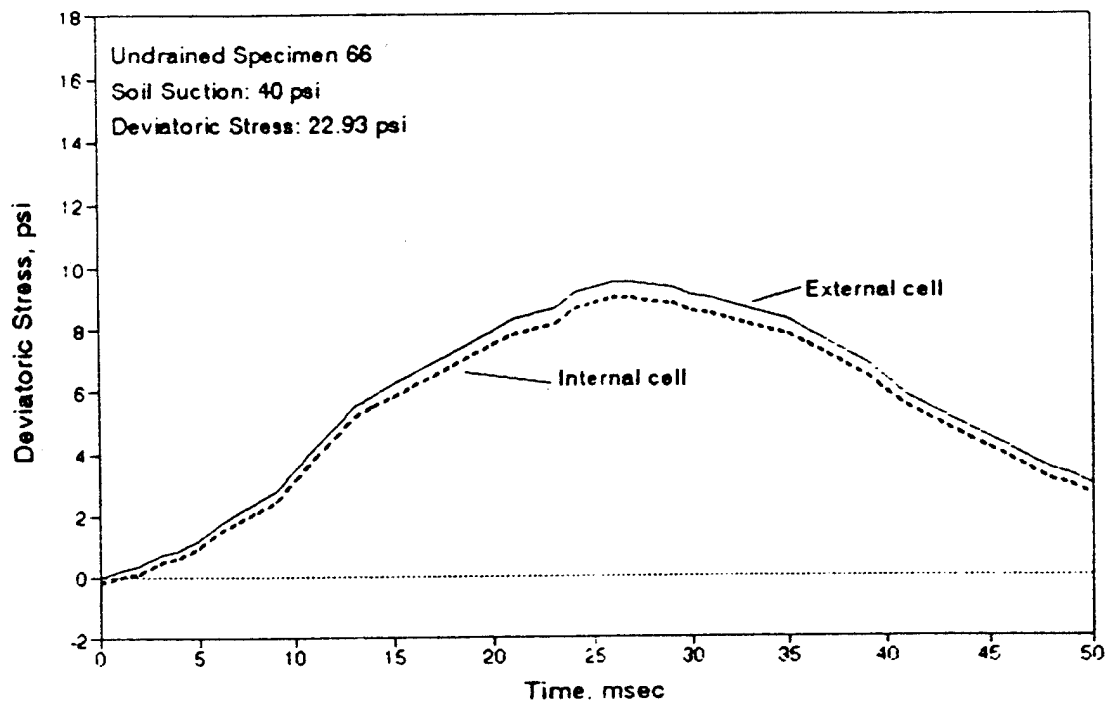












**APPENDIX I**

**SELECTED RESULTS OF DYNAMIC TESTS ON SPECIMENS AT 70 PSI SOIL**

**SUCTION**

